

CONTENTS

VOLUME I - SYSTEMS TECHNOLOGY

PREFACE	iii	1/A7
1. LARGE SPACE SYSTEMS TECHNOLOGY OVERVIEW	1	1/A13
Robert L. James, Jr.		

SUPPORTING ACTIVITIES

2. LSST CONTROL TECHNOLOGY	9	1/B7
A. F. Tolivar		
3. ADVANCED CONTROL TECHNOLOGY FOR LSST ANTENNAS	19	1/C3
Y. H. Lin		
4. ADVANCED CONTROL TECHNOLOGY FOR LSST PLATFORM	31	1/D1
R. S. Edmunds		
5. CONTROL TECHNOLOGY DEVELOPMENT	49	1/E5
G. Rodriguez		
6. INTEGRATED ANALYSIS CAPABILITY (IAC) DEVELOPMENT	65	1/F7
J. P. Young		
7. INTEGRATED ANALYSIS CAPABILITY PILOT COMPUTER PROGRAM	73	1/G1
R. G. Vos		
8. AN ECONOMY OF SCALE SYSTEM'S MENSURATION OF LARGE SPACECRAFT	87	2/A4
L. J. DeRyder		
9. RADIATION EXPOSURE OF SELECTED COMPOSITES AND THIN FILMS	105	2/B8
Wayne S. Slomp and Beatrice Santos		
10. THERMAL EXPANSION OF COMPOSITES: METHODS AND RESULTS	119	2/C8
David E. Bowles and Darrel R. Tenney		

SPACE PLATFORMS

11. SPACE PLATFORM REFERENCE MISSION STUDIES OVERVIEW	129	2/D4
James K. Harrison		
12. ADVANCED SCIENCE AND APPLICATIONS SPACE PLATFORM	133	2/D8
Jack White and Fritz Runge		

13. STRUCTURAL REQUIREMENTS AND TECHNOLOGY NEEDS OF GEOSTATIONARY PLATFORMS	149 2/E10
G. R. Stone	
14. SUMMARY OF LSST SYSTEMS ANALYSIS AND INTEGRATION TASK FOR SPS FLIGHT TEST ARTICLES	167 2/F14
H. S. Greenberg	
15. ERECTABLE CONCEPTS FOR LARGE SPACE SYSTEM TECHNOLOGY	183 3/A5
W. E. Agan	
16. SPACE ASSEMBLY METHODOLOGY	199 3/B7
J. W. Stokes and H. H. Watters	
17. CONSTRUCTION ASSEMBLY AND OVERVIEW	217 3/C11
Lyle M. Jenkins	
18. SPACE PLATFORM ADVANCED TECHNOLOGY STUDY	229 3/D9
G. C. Burns	
19. A DOCUMENT DESCRIBING SHUTTLE CONSIDERATIONS FOR THE DESIGN OF LARGE SPACE STRUCTURES	243 3/E9
John A. Roebuck, Jr.	

SPACE ANTENNAS

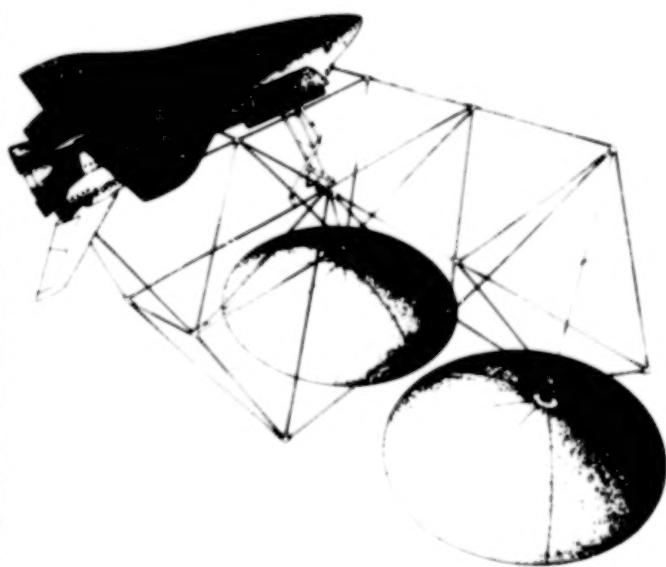
20. ELECTROSTATIC MEMBRANE ANTENNA CONCEPT STUDIES	259 3/F11
J. W. Goslee	
21. ELECTROSTATIC ANTENNA SPACE ENVIRONMENT INTERACTION STUDY	271 3/G9
Ira Katz	
22. ENVIRONMENTAL EFFECTS AND LARGE SPACE SYSTEMS	279 4/A6
H. B. Garrett	
23. JPL ANTENNA TECHNOLOGY DEVELOPMENT	287 4/A14
R. E. Freeland	
24. OFFSET WRAP RIB ANTENNA CONCEPT DEVELOPMENT	295 4/B8
A. A. Woods, Jr.	
25. ANALYTICAL PERFORMANCE PREDICTION FOR LARGE ANTENNAS	325 4/D10
M. El-Raheb	
26. JPL SELF-PULSED LASER SURFACE MEASUREMENT SYSTEM DEVELOPMENT	339 4/E10
Martin Berdahl	
27. ANTENNA SYSTEMS REQUIREMENTS DEFINITION STUDY	349 4/F6
C. T. Golden	

28. HOOP/COLUMN ANTENNA TECHNOLOGY DEVELOPMENT SUMMARY	357	4/F14
Thomas G. Campbell		
29. DEVELOPMENT OF THE MAYPOLE (HOOP/COLUMN) DEPLOYABLE REFLECTOR CONCEPT FOR LARGE SPACE SYSTEMS APPLICATIONS	365	4/G8
D. C. Montgomery		
30. RADIO FREQUENCY PERFORMANCE PREDICTIONS FOR THE HOOP/COLUMN POINT DESIGN	407	5/C11
Thomas G. Campbell		
31. OFFSET FED UTILIZATION OF FOUR QUADRANTS OF AN AXIALLY SYMMETRICAL ANTENNA STRUCTURE	431	5/E7
P. Foldes		
32. SURFACE ACCURACY MEASUREMENT SENSOR FOR DEPLOYABLE REFLECTOR ANTENNAS	439	5/F1
R. B. Spiers, Jr.		
SECOND ANNUAL TECHNICAL REVIEW ATTENDEES	449	5/F11

NASA Conference Publication 2168

Large Space Systems Technology - 1980

Volume I - Systems Technology



ORIGINAL
COMPLETED

*Second Annual Technical Review
held at NASA Langley Research Center
Hampton, Virginia
November 18-20, 1980*

NASA

NASA Conference Publication 2168

Large Space Systems Technology - 1980

Volume I - Systems Technology

Compiled by
Frank Koprivier III
Systems Management Associates
Hampton, Virginia

Second Annual Technical Review
held at NASA Langley Research Center
Hampton, Virginia
November 18-20, 1980

NASA

National Aeronautics
and Space Administration

**Scientific and Technical
Information Office**

1980

BLANK PAGE

BLANK PAGE

PREFACE

This publication is a compilation of the papers presented at the Second Annual Large Space Systems Technology (LSST) Technical Review conducted at NASA Langley Research Center on November 18-20, 1980. The Review provided personnel of government, university, and industry with an opportunity to exchange information, to assess the present status of technology developments on the LSST Program, and to plan the development of new technology for large space systems.

The papers describe technological or developmental efforts that were accomplished during Fiscal Year 1980 in support of the LSST Program and were prepared by those in government, university, and industry who performed the work. These papers were divided into three major areas of interest: (1) technology pertinent to large antenna systems, (2) technology related to large space systems, and (3) activities that support both antenna and platform systems.

This publication is divided into two volumes. Volume I, entitled "Systems Technology", includes research activities sponsored through the LSST Program Office. Volume II, entitled "Base Technology", covers research activities sponsored through the Materials and Structures Section, Research and Technology Division, of the Office of Aeronautics and Space Technology.

This compilation provides the participants and their organizations with the papers presented at the Review in a referenceable format. Also, users of large space systems technology can follow the development progress with this document along with proceedings of previous and future LSST Technical Reviews. (See NASA CP-2118, 1980.) The LSST Program Office, Langley Research Center, which hosted the Review, will use this information as an aid in measuring performance and in planning future tasks. The historical background of the LSST Program is given in the introduction to NASA CP-2035, 1978, which covers a NASA/industry seminar that provided ideas and plans to the Program Office for its initial year of operation.

This publication was expedited and enhanced through the efforts of the staff of the Scientific and Technical Information Programs Division, Langley Research Center.

The use of trade names or manufacturer's names in this publication does not constitute endorsement, either expressed or implied, by the National Aeronautics and Space Administration.

BLANK PAGE

BLANK PAGE

CONTENTS

VOLUME I - SYSTEMS TECHNOLOGY

PREFACE	iii
-------------------	-----

1. LARGE SPACE SYSTEMS TECHNOLOGY OVERVIEW	1
Robert L. James, Jr.	

SUPPORTING ACTIVITIES

2. LSST CONTROL TECHNOLOGY	9
A. F. Tolivar	
3. ADVANCED CONTROL TECHNOLOGY FOR LSST ANTENNAS	19
Y. H. Lin	
4. ADVANCED CONTROL TECHNOLOGY FOR LSST PLATFORM	31
R. S. Edmunds	
5. CONTROL TECHNOLOGY DEVELOPMENT	49
G. Rodriguez	
6. INTEGRATED ANALYSIS CAPABILITY (IAC) DEVELOPMENT	65
J. P. Young	
7. INTEGRATED ANALYSIS CAPABILITY PILOT COMPUTER PROGRAM	73
R. G. Vos	
8. AN ECONOMY OF SCALE SYSTEM'S MENSURATION OF LARGE SPACECRAFT	87
L. J. DeRyder	
9. RADIATION EXPOSURE OF SELECTED COMPOSITES AND THIN FILMS	105
Wayne S. Slomp and Beatrice Santos	
10. THERMAL EXPANSION OF COMPOSITES: METHODS AND RESULTS	119
David E. Bowles and Darrel R. Tenney	

SPACE PLATFORMS

11. SPACE PLATFORM REFERENCE MISSION STUDIES OVERVIEW	129
James K. Harrison	
12. ADVANCED SCIENCE AND APPLICATIONS SPACE PLATFORM	133
Jack White and Fritz Runge	

13. STRUCTURAL REQUIREMENTS AND TECHNOLOGY NEEDS OF GEOSTATIONARY PLATFORMS	149
G. R. Stone	
14. SUMMARY OF LSST SYSTEMS ANALYSIS AND INTEGRATION TASK FOR SPS FLIGHT TEST ARTICLES	167
H. S. Greenberg	
15. ERECTABLE CONCEPTS FOR LARGE SPACE SYSTEM TECHNOLOGY	183
W. E. Agan	
16. SPACE ASSEMBLY METHODOLOGY	199
J. W. Stokes and H. H. Watters	
17. CONSTRUCTION ASSEMBLY AND OVERVIEW	217
Lyle M. Jenkins	
18. SPACE PLATFORM ADVANCED TECHNOLOGY STUDY	229
G. C. Burns	
19. A DOCUMENT DESCRIBING SHUTTLE CONSIDERATIONS FOR THE DESIGN OF LARGE SPACE STRUCTURES	243
John A. Roebuck, Jr.	

SPACE ANTENNAS

20. ELECTROSTATIC MEMBRANE ANTENNA CONCEPT STUDIES	259
J. W. Goslee	
21. ELECTROSTATIC ANTENNA SPACE ENVIRONMENT INTERACTION STUDY	271
Ira Katz	
22. ENVIRONMENTAL EFFECTS AND LARGE SPACE SYSTEMS	279
H. B. Garrett	
23. JPL ANTENNA TECHNOLOGY DEVELOPMENT	287
R. E. Freeland	
24. OFFSET WRAP RIB ANTENNA CONCEPT DEVELOPMENT	295
A. A. Woods, Jr.	
25. ANALYTICAL PERFORMANCE PREDICTION FOR LARGE ANTENNAS	325
M. El-Raheb	
26. JPL SELF-PULSED LASER SURFACE MEASUREMENT SYSTEM DEVELOPMENT	339
Martin Berdahl	
27. ANTENNA SYSTEMS REQUIREMENTS DEFINITION STUDY	349
C. T. Golden	

28. HOOP/COLUMN ANTENNA TECHNOLOGY DEVELOPMENT SUMMARY	357
Thomas G. Campbell	
29. DEVELOPMENT OF THE MAYPOLE (HOOP/COLUMN) DEPLOYABLE REFLECTOR CONCEPT FOR LARGE SPACE SYSTEMS APPLICATIONS	365
D. C. Montgomery	
30. RADIO FREQUENCY PERFORMANCE PREDICTIONS FOR THE HOOP/COLUMN POINT DESIGN	407
Thomas G. Campbell	
31. OFFSET FED UTILIZATION OF FOUR QUADRANTS OF AN AXIALLY SYMMETRICAL ANTENNA STRUCTURE	431
P. Foldes	
32. SURFACE ACCURACY MEASUREMENT SENSOR FOR DEPLOYABLE REFLECTOR ANTENNAS	439
R. B. Spiers, Jr.	
SECOND ANNUAL TECHNICAL REVIEW ATTENDEES	449

VOLUME II - BASE TECHNOLOGY*

PREFACE	iii
1. BASE TECHNOLOGY OVERVIEW	1
Michael F. Card	

SUPPORTING ACTIVITIES

2. OPTIMUM DAMPER LOCATIONS FOR A FREE-FREE BEAM	5
G. C. Horner	
3. CONTROL THEORETICS FOR LARGE STRUCTURAL SYSTEMS	17
Raymond C. Montgomery	
4. BUCKLING AND VIBRATION OF PERIODIC LATTICE STRUCTURES	35
Melvin S. Anderson	
5. STRUCTURAL SIZING CONSIDERATIONS FOR LARGE SPACE STRUCTURES	45
Walter L. Heard, Jr., Harold G. Bush, and Joseph E. Walz	
6. DEPLOYMENT TESTS OF A 36-ELEMENT TETRAHEDRAL TRUSS MODULE	59
R. W. Herr and G. C. Horner	

*Contents of Volume II is included for convenience.

SPACE PLATFORMS

7. AUTOMATED INSTALLATION OF LARGE PLATFORM UTILITIES 71
R. M. Vernon
8. FREE-FLYING SOLAR REFLECTOR SPACECRAFT 89
John M. Hedgepeth

SPACE ANTENNAS

9. DESIGN CONCEPTS FOR LARGE ANTENNA REFLECTORS 103
John M. Hedgepeth
10. A MODULAR APPROACH TOWARD EXTREMELY LARGE APERTURES 121
A. A. Woods, Jr.
11. MODULAR REFLECTOR CONCEPT STUDY 145
D. H. Vaughan
12. ELECTROMAGNETIC ANALYSIS FOR LARGE REFLECTOR ANTENNAS 171
M. C. Bailey
- SECOND ANNUAL TECHNICAL REVIEW ATTENDEES 185

LARGE SPACE SYSTEMS TECHNOLOGY OVERVIEW

Robert L. James, Jr.
NASA Langley Research Center

Large Space Systems Technology - 1980
Second Annual Technical Review
November 18-20, 1980

THE LSST PROGRAM

In order to provide a base of systems technology to enable this new class of spacecraft, the NASA Office of Aeronautics and Space Technology (OAST) established the Large Space Systems Technology (LSST) Program. The multicenter LSST Program is managed by the NASA Langley Research Center (LaRC). The program is developing fundamental systems technology which will provide a basis for the design of large Shuttle-era spacecraft. Ongoing and planned activities will ensure that important initial design choices are made on a sound basis of technical knowledge and experience.

OBJECTIVE:

TO DEVELOP TECHNOLOGY TO ENABLE AND ENHANCE SHUTTLE - COMPATIBLE
LARGE SPACE SYSTEMS

- SPONSORING PROGRAM OFFICE:

OFFICE OF AERONAUTICS AND SPACE TECHNOLOGY (OAST)

- LEAD CENTER AND PROGRAM MANAGEMENT OFFICE:

LANGLEY RESEARCH CENTER

LARGE SPACE SYSTEMS TECHNOLOGY (LSST) PROGRAM OFFICE

- PARTICIPATING NASA CENTERS:

GODDARD SPACE FLIGHT CENTER

JET PROPULSION LABORATORY

JOHNSON SPACE CENTER

LANGLEY RESEARCH CENTER

LEWIS RESEARCH CENTER

MARSHALL SPACE FLIGHT CENTER

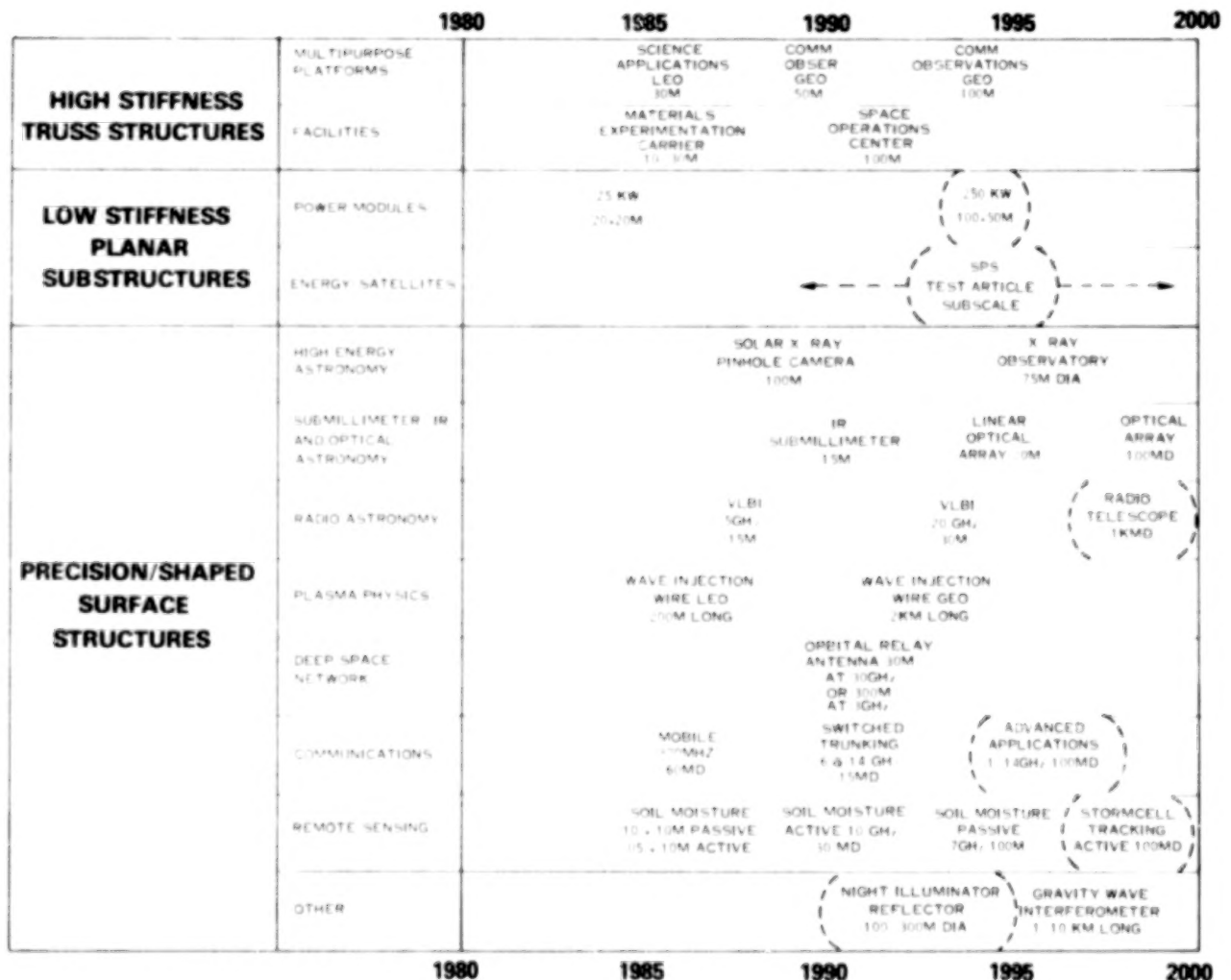
ELEMENTS OF THE LSST PROGRAM

The LSST Program is currently subdivided into the elements shown below. These elements comprise the primary technology needs of near-term Shuttle-era large space structural systems. Included are the structural systems and related technologies. Program activities are also undertaken to define the interfaces of the other subsystems to the structure.

- LARGE ANTENNAS
- SPACE PLATFORMS
- ASSEMBLY EQUIPMENT AND DEVICES
- SURFACE SENSING AND CONTROL
- CONTROL AND STABILIZATION
- INTEGRATED ANALYSIS AND DESIGN

POTENTIAL LARGE SPACE SYSTEMS MISSIONS

For the past several years, OAST has periodically surveyed the NASA program offices to identify future space missions which will require large space systems. The results of the most recent survey are shown here. This mission model includes potential missions derived from many sources. Individual missions cover a wide spectrum in level of definition and program office support. However, the compilation gives an overall indication of the strong potential requirements for this class of space vehicle.



REFERENCE MISSIONS OF THE LSST PROGRAM

The identified potential missions fall primarily in two classes: large antennas and platforms. In order to provide an integrating focus to the technology development, the LSST Program has selected a set of reference missions which collectively represent the technology challenges. These missions are studied to define technology requirements and to identify subsystem interfaces.

● LARGE ANTENNAS

● MOBILE COMMUNICATIONS

- 60 - 100 M (180 - 300 FT)
- 0.8 - 14.0 GHz ($\lambda/20$ SURFACE ACCURACY)

● VERY LONG BASELINE INTERFEROMETER (VLBI)

- 40 - 80 M (120 - 240 FT)
- 1.4 - 14.0 GHz ($\lambda/10$ SURFACE ACCURACY)

● ORBITING DEEP SPACE RELAY STATION (ODSRS)

- 20 - 50 M (60 - 150 FT)
- 3.0 - 30.0 GHz ($\lambda/30$ SURFACE ACCURACY)

● RADIOMETERS

- 30 - 100 M (90 - 300 FT)
- 1.4 - 10.0 GHz ($\lambda/50$ SURFACE ACCURACY)

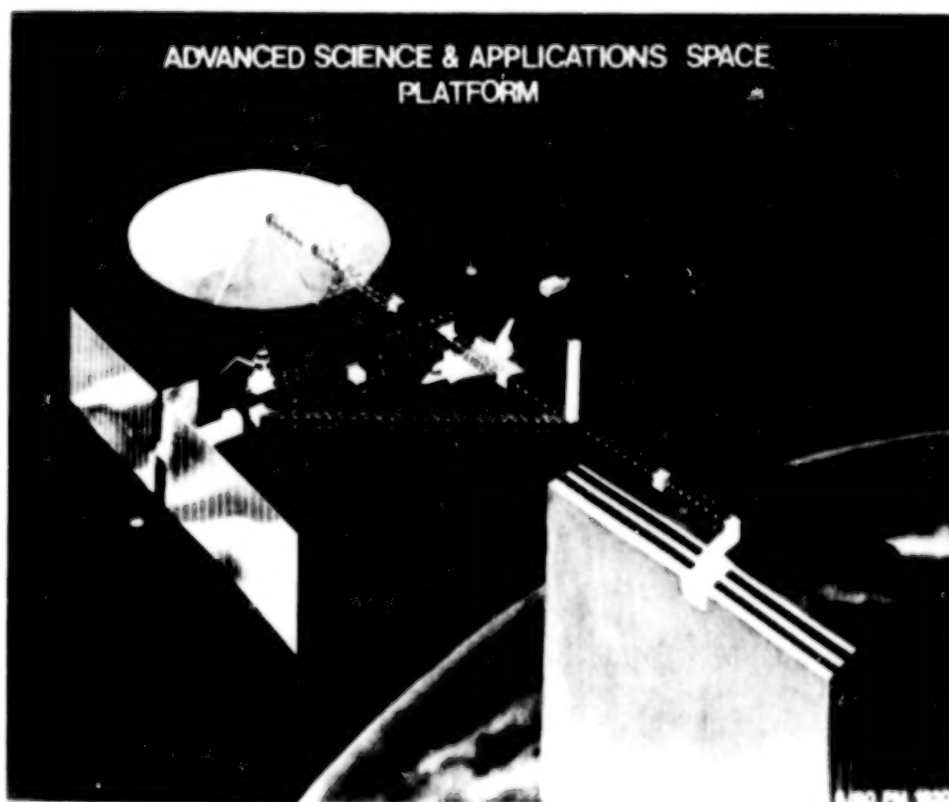
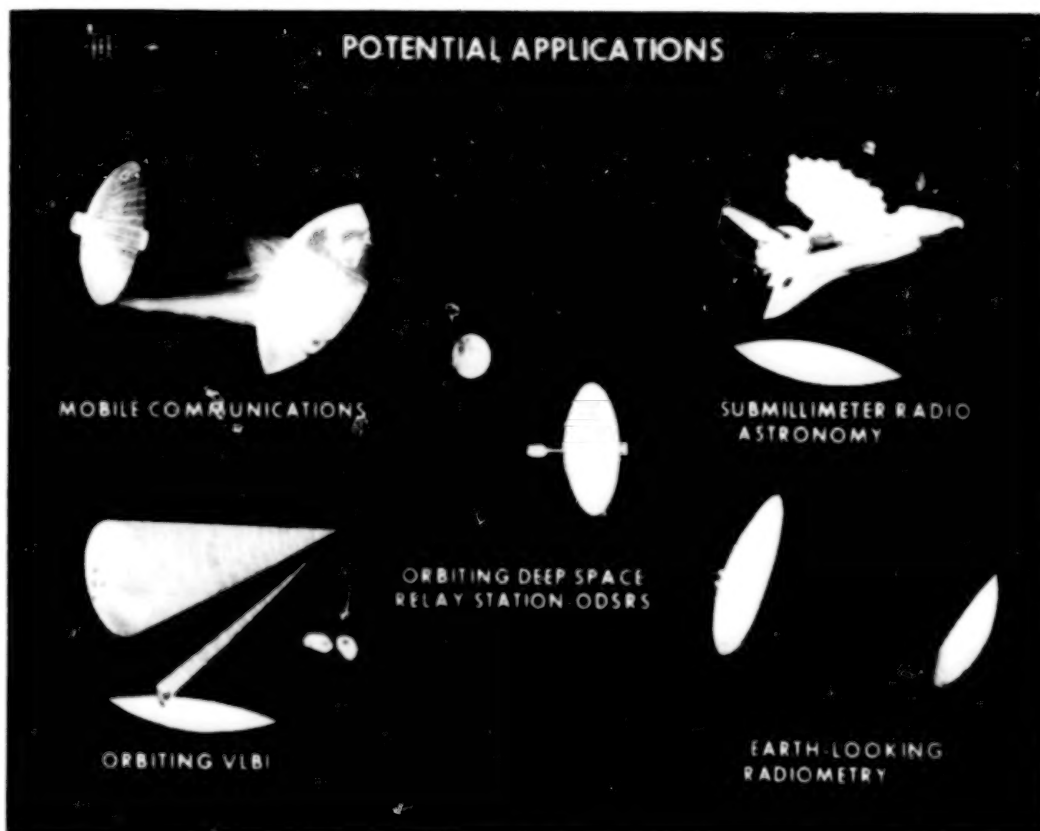
● PLATFORMS

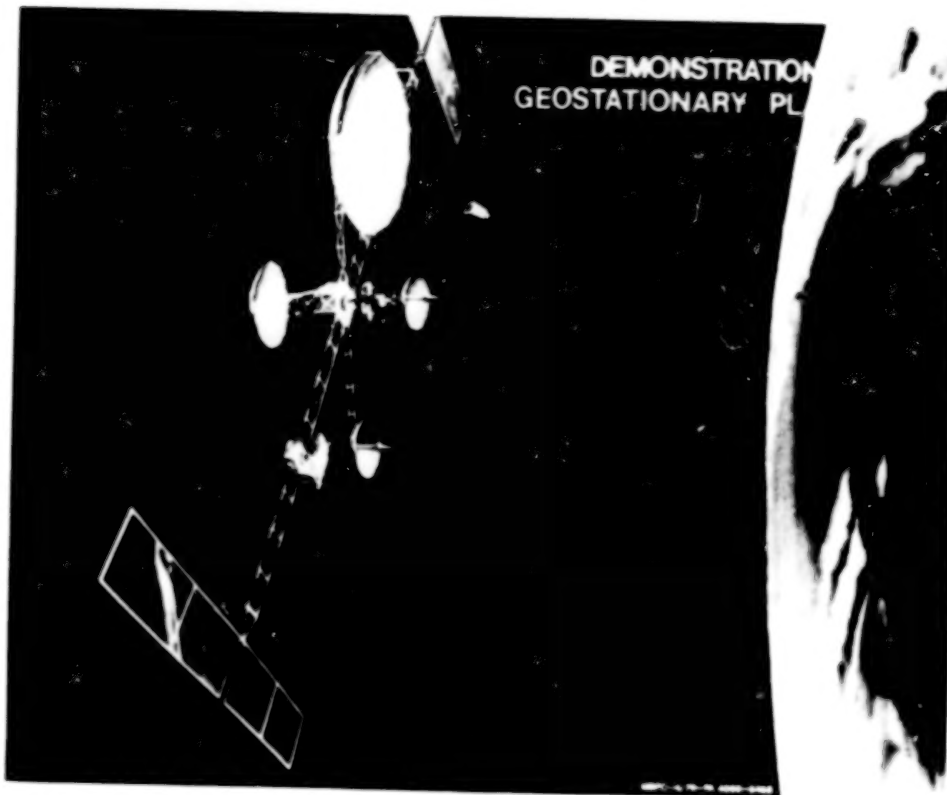
● ADVANCED SCIENCE/APPLICATIONS PLATFORM

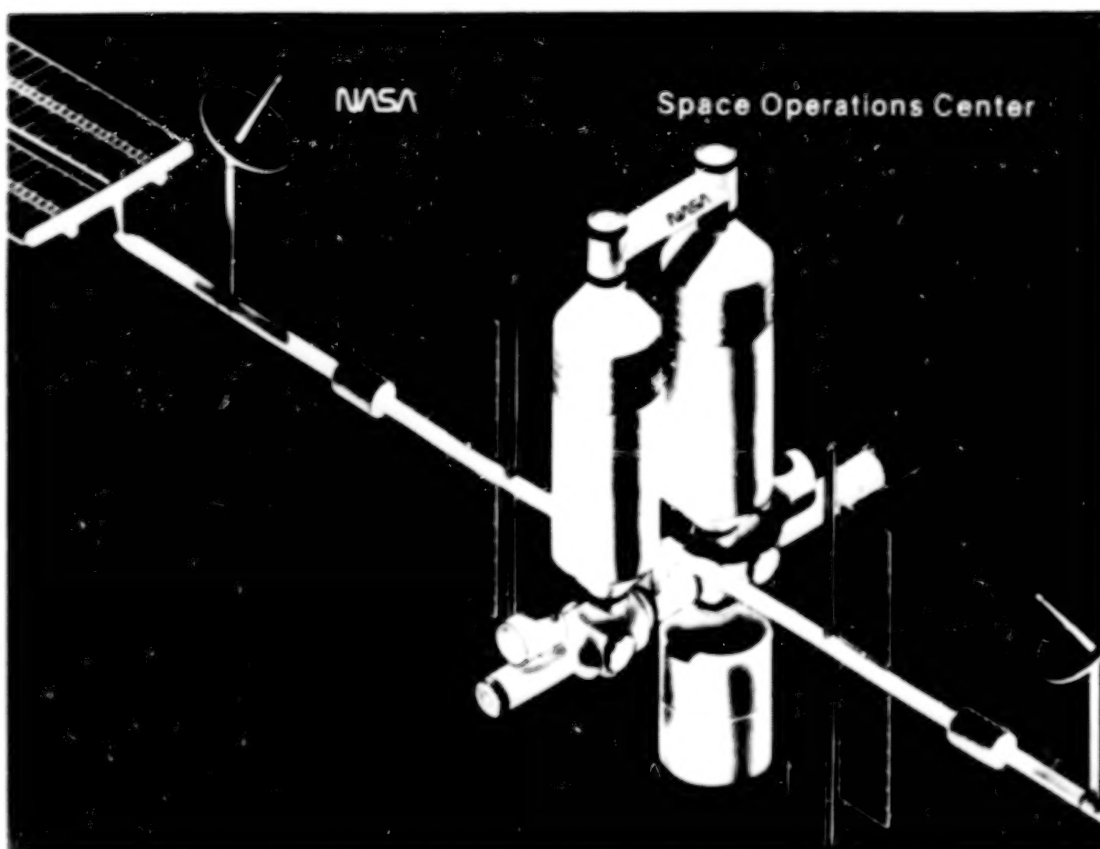
● OPERATIONAL GEOSYNCHRONOUS COMMUNICATIONS/OBSERVATIONS PLATFORM

● SATELLITE POWER SYSTEM (SPS) ENGINEERING TEST ARTICLE

● SPACE OPERATIONS CENTER (SOC)







CONCLUDING REMARKS

- LARGE SIZE WILL MAKE SIGNIFICANT CONTRIBUTIONS TO THE PERFORMANCE AND UTILITY OF SPACE SYSTEMS
- SHUTTLE CAPABILITIES WILL ENABLE THESE SYSTEMS
- TECHNOLOGY ADVANCEMENTS ARE NEEDED TO REDUCE THE COST AND RISK
- THE LSST PROGRAM IS PROVIDING TECHNOLOGY WHICH WILL ACCELERATE THE TECHNICAL AND ECONOMIC FEASIBILITY

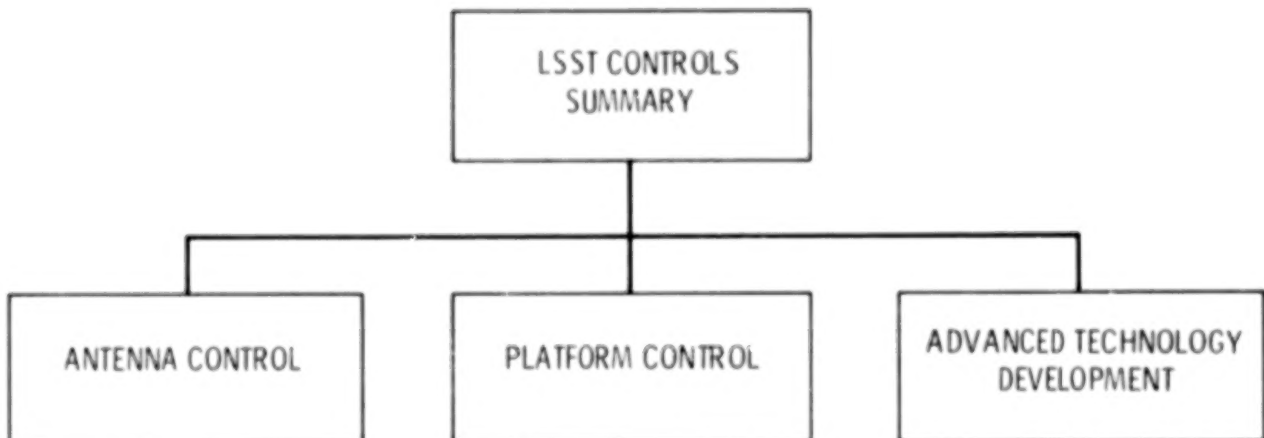
LSST CONTROL TECHNOLOGY

A. F. TOLIVAR
JET PROPULSION LABORATORY
PASADENA, CALIFORNIA

LARGE SPACE SYSTEMS TECHNOLOGY - 1980
SECOND ANNUAL TECHNICAL REVIEW
NOVEMBER 18-20, 1980

LSST CONTROLS PRESENTATION

The presentation on LSST Controls will be given by a total of 4 speakers. I shall begin by giving a brief summary of the overall LSST controls program at JPL. The next three speakers, Y. H. Lin, R. S. Edmunds, and G. Rodriguez will then present specific reports on each of the three main elements of the program: Antenna Control, Platform Control, and Advanced Technology Development, respectively.



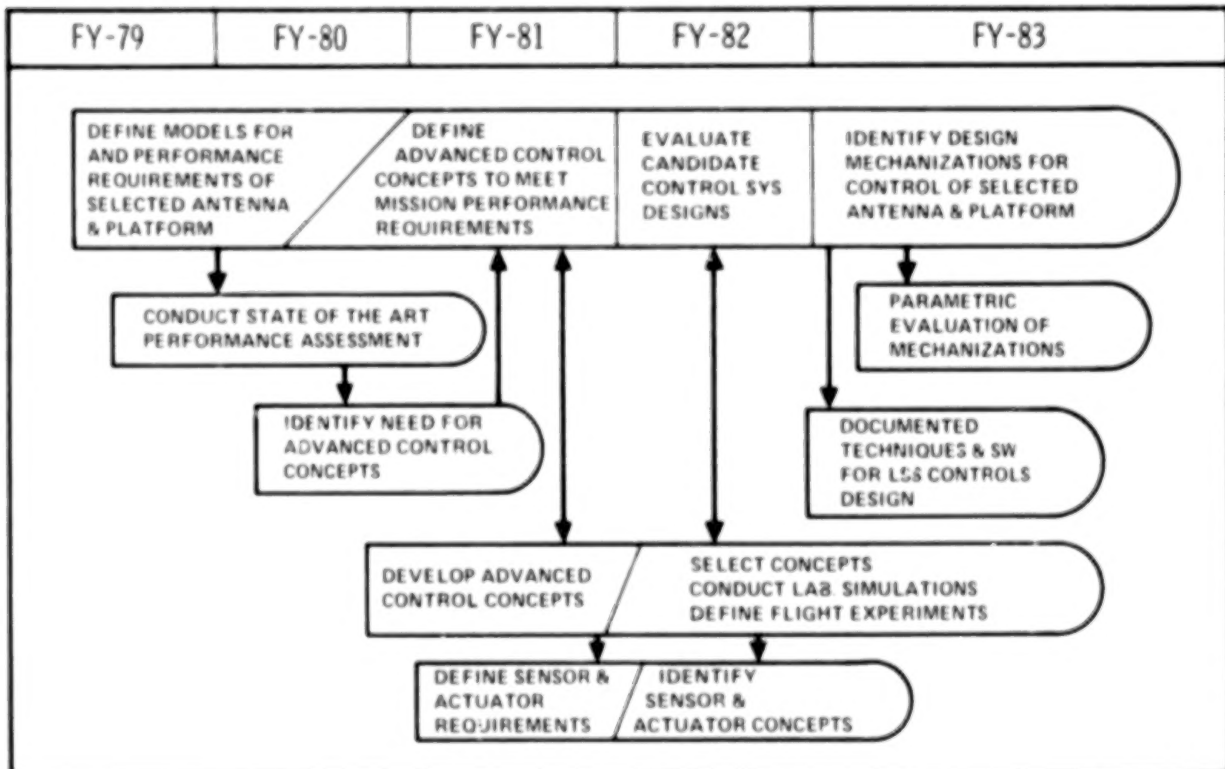
LSST CONTROLS TECHNOLOGY DEVELOPMENT PLAN

The broad objective of LSST controls is to define and develop the necessary controls technology required for precise attitude, shape, and pointing control of large space systems.

The major controls tasks are summarized in the development plan shown below. During FY-80, the main thrust has been in (1) the selection of typical antenna and platform configurations, and the definition of models and performance requirements, (2) evaluating the applicability of state-of-the-art control techniques to the control of large antennas and platforms, and (3) identifying the need for and initiating the development of advanced control concepts required for LSS.

During FY-81/82 the plan shows (1) the continued development of advanced control concepts, (2) the definition and evaluation of specific advanced control system designs for the antenna and platform, and (3) the definition of sensor, actuator, and software requirements.

During FY-82/83 the plan calls for (1) the identification of sensor and actuator concepts, (2) the selection and evaluation of preferred mechanizations, (3) ground demonstration of control technology, and (4) the definition of flight experiments required for verification.



LSST CONTROLS - FY'80 OBJECTIVES

The objectives during FY'80 have been to:

- (1) Select typical antenna and platform configurations, and to define the corresponding models and performance requirements.
- (2) Evaluate the applicability - or limitations - of current flight demonstrated control technology to those large antennas and platforms.
- (3) Identify control problems and potential solutions.
- (4) Identify and develop advanced control technologies critical to LSS.

- ANTENNA AND PLATFORM CONTROL
 - DEFINE CONFIGURATIONS, MODELS, CONTROL REQUIREMENTS
 - ASSESS APPLICABILITY/LIMITATIONS OF CURRENT TECHNOLOGY
 - IDENTIFY CONTROL PROBLEMS AND POTENTIAL SOLUTIONS
- IDENTIFY AND DEVELOP ADVANCED CONTROL TECHNOLOGIES CRITICAL TO LSS

FY'80 ACCOMPLISHMENTS
ANTENNA AND PLATFORM CONTROL

The FY'80 accomplishments can be summarized as follows:

- (1) Defined Reference Antenna and Platform Configurations based on a typical communications mission using an offset-feed wrap-rib antenna, and on a typical large platform, respectively. Established control requirements and developed Dynamic/Control models.
- (2) Identified control problems.
- (3) Established that there are limitations in current control technology in meeting LSST needs.
- (4) Identified potential solutions.

The control problems, current technology limitations, and potential solutions are the following:

ANTENNA CONTROL. The main control problem of the reference antenna is the performance degradation due to dynamic interactions between the feed, the boom, and the reflector dish. These dynamic interactions result in attitude errors as well as surface deformations which, ultimately result in RF performance degradation (pointing, gain loss, etc.). The problem exists for either the center or the offset-feed configuration, although it is somewhat aggravated by the offset-feed configuration. (Continued)

- DEVELOPED DYNAMIC/CONTROL MODELS FOR LARGE PLATFORM AND ANTENNA
- IDENTIFIED CONTROL PROBLEMS
- ESTABLISHED LIMITATIONS OF CURRENT CONTROL TECHNOLOGY IN MEETING LSST NEEDS
- IDENTIFIED POTENTIAL SOLUTIONS

FY'80 ACCOMPLISHMENTS
ANTENNA AND PLATFORM CONTROL (CONTINUED)

Various antenna control systems based on current communication satellite control technology were investigated with the same consistent result: lumped controllers fail to meet pointing and shape accuracy requirements for typical communication missions.

A number of potential solutions to this problem were identified which involve sensing the feed/dish displacements and using this information in the control decisions.

PLATFORM CONTROL. The main control problem of the reference platform is due to the severe disturbances/interaction among multiple independent controllers and pointing systems. To further complicate matters, gross parameter and configuration changes can occur depending upon how many experiments are installed on the platform and their location.

Several attitude and pointing control schemes based on technology currently used in geostationary and planetary spacecraft were investigated with the result that they fail to meet the stability requirements for typical applications. Two potential solution paths were identified. One involves attitude and pointing control system designs based on disturbance isolation techniques. The second would exploit additional information exchange among the various control systems.

	ANTENNA	PLATFORM
PROBLEM	<ul style="list-style-type: none"> • PERFORMANCE LOSS DUE TO DISH-BOOM DYNAMIC INTERACTIONS <ul style="list-style-type: none"> • ATTITUDE ERRORS • SURFACE DEFORMATION • RF POINTING/GAIN LOSS • PROBLEM FOR CENTER OR OFFSET FEED 	<ul style="list-style-type: none"> • SEVERE DISTURBANCES/INTERACTION AMONG MULTIPLE CONTROLLERS <ul style="list-style-type: none"> • SIMULTANEOUS PALLET ARTICULATION • VARIABLE CONFIGURATION • PROBLEM EVEN IF PERFECTLY RIGID
CURRENT TECHNOLOGY ASSESSMENT	<ul style="list-style-type: none"> • SINGLE POINT CONTROLLERS FAIL TO MEET POINTING AND SHAPE ACCURACY REQUIREMENTS FOR TYPICAL COMMUNICATIONS MISSIONS 	<ul style="list-style-type: none"> • STABILITY REQUIREMENTS NOT MET FOR TYPICAL APPLICATIONS
POTENTIAL SOLUTION	<ul style="list-style-type: none"> • SENSE FEED/DISH DISPLACEMENTS AND USE INFORMATION IN CONTROL DECISIONS 	<ul style="list-style-type: none"> • CONTROL SYSTEM DESIGNS USING <ul style="list-style-type: none"> • DISTURBANCE ISOLATION TECHNIQUES • INCREASED INFORMATION EXCHANGE

FY'80 ACCOMPLISHMENTS
CONTROL TECHNOLOGY

Four problem areas in the control of large structures have been isolated. FY'80 development in these areas has led to important results for:

- (1) Shape estimation and control of a structure, e.g. maintaining the parabolic shape of a reflector.
- (2) Distributed control for vibration and command control, e.g. the stabilization and slew response of a spacecraft.
- (3) Modeling of very high order dynamic systems, e.g. how many and which structural modes need be retained for control design.
- (4) Ground demonstration of advanced control technology. A hardware flexible beam facility was completed to experimentally demonstrate and verify advanced control concepts.

- IDENTIFIED AND DEVELOPED CRITICAL BASE TECHNOLOGY FOR LSS IN
 - STATIC SHAPE ESTIMATION AND CONTROL
 - ACTIVE DISTRIBUTED CONTROL
 - SYSTEMATIC MODEL ORDER REDUCTION TECHNIQUES
 - EXPERIMENTAL FACILITY FOR ADVANCED TECHNOLOGY DEMONSTRATION

FY'81 OBJECTIVES

ANTENNA CONTROL

Major objectives during FY'81 will be to develop the Feed/Dish motion compensation concept for the reference offset-feed wrap-rib antenna, to establish through simulation the pointing and surface accuracy enhancements achieved with that concept, and to establish the sensitivity and impact of antenna boom dynamic characteristics on control complexity.

In addition, a new area to be addressed in FY'81 will be the control of the Hoop/Column antenna. Its main objective will be the definition and assessment of candidate control methodologies for a typical Hoop/Column antenna system.

WRAP-RIB

- DEVELOP FEED-DISH MOTION COMPENSATION CONCEPT BASED ON MULTIPLE SENSING
- ESTABLISH CONTROL SENSITIVITY TO FLEXIBLE-BOOM TORSION AND BENDING STIFFNESS
- EVALUATE POINTING AND SURFACE ACCURACY ENHANCEMENTS ACHIEVED WITH MULTIPOINT CONTROLLER DESIGNS
- ASSESS INTEGRATED CONTROL/STRUCTURE/RF PERFORMANCE

HOOP-COLUMN

- CONDUCT CONTROL/STRUCTURE MODELING AND PERFORMANCE EVALUATIONS

FY'81 OBJECTIVES
PLATFORM CONTROL

A major FY'81 objective will be to define, develop, and evaluate multi-point pallet/bus controller designs which account for and reduce system sensitivity to combined control and dynamic interactions. One approach is to add additional sensors and/or actuators to individual experiment controllers. A second approach is to allow increased information exchange among the various controllers.

An additional objective will be to assess the impact of structural parameters and configuration variations on system performance.

- DEVELOP AND VERIFY ATTITUDE AND POINTING CONTROLLER DESIGNS TO MINIMIZE CONTROL INTERACTION
- DEVELOP CONTROLLER DESIGNS WHICH UTILIZE INFORMATION EXCHANGE
- PERFORM PARAMETRIC ANALYSIS OF CONTROL COMPLEXITY VS. VEHICLE STIFFNESS
- EVALUATE ATTITUDE AND POINTING CONTROL PERFORMANCE

FY'81 OBJECTIVES
CONTROL TECHNOLOGY

FY'81 Control Technology objectives will be:

(1) Continue development of shape determination and control for multidimensional continuum and discrete systems; evaluate application to 100m parabolic reflector model.

(2) Develop design and analysis tools needed to specify, design, and evaluate the performance of antenna control systems in terms of RF parameters.

(3) Extend FY'80 model order reduction results to include unavoidable system and parameter uncertainties.

(4) Extend model error estimation results to adaptive estimation and control.

(5) Experimental verification of advanced control technology by means of Flexible Beam Experiment demonstrations. Specific demonstrations of shape and vibration estimation and control.

- DEVELOP BASIC SHAPE DETERMINATION AND CONTROL TECHNOLOGY FOR DISTRIBUTED SYSTEMS AND EVALUATE APPLICATION TO 100m PARABOLIC REFLECTOR MODEL
- DEVELOP ANALYSIS KNOW-HOW TO DETERMINE CONTROLLER DESIGNS BASED ON RF PERFORMANCE
- DEVELOP MODEL ORDER REDUCTION SOFTWARE FOR AUTOMATED ITERATION OF TRUNCATED CONTROLLER MODELS
- DEVELOP MODEL ERROR ESTIMATION TECHNIQUES FOR USE IN ADAPTIVE CONTROL DESIGNS
- DEMONSTRATE PERFORMANCE OF SHAPE CONTROL AND ESTIMATION DESIGNS BY MEANS OF HARDWARE/SOFTWARE SIMULATIONS AND FLEXIBLE BEAM EXPERIMENTS

ADVANCED CONTROL TECHNOLOGY
FOR LSST ANTENNAS

Y. H. LIN
JET PROPULSION LABORATORY
PASADENA, CALIFORNIA

LARGE SPACE SYSTEMS TECHNOLOGY - 1980
SECOND ANNUAL TECHNICAL REVIEW
NOVEMBER 18-20, 1980

FY'80 LSST WRAP-RIB ANTENNA CONTROL TECHNOLOGY OBJECTIVES

The long range objective of this program is to identify and develop control technology for the realization of LSST antenna systems. During FY'80, emphasis was directed at the control of LSST wrap-rib offset-feed antenna. Specifically FY'80 objectives were to (1) evaluate overall dynamic and control performance of offset-feed antenna, (2) provide quantitative definitions of control problems, and (3) identify enabling control concepts for future development.

- EVALUATE OVERALL DYNAMIC AND CONTROL PERFORMANCE OF ANTENNA
- PROVIDE QUANTITATIVE DEFINITIONS OF CONTROL PROBLEMS
- IDENTIFY ENABLING CONTROL CONCEPTS

FY'80 APPROACH

The specific FY'80 approach for the offset-feed wrap-rib antenna control study is as follows: selection of an antenna system configuration, definition of functional requirements, acquisition and validation of structural finite-element (F.E.) models of antenna reflectors, coupling of F.E. models with dynamic models of boom structure and spacecraft, development of disturbance models, controller designs, overall system performance evaluation by simulation, analysis of simulation results and definition of enabling control concepts.

- DEVELOP DYNAMIC MODELS OF ANTENNA SYSTEMS
- DESIGN CONTROLLERS
- ASSESS CONTROL PERFORMANCE
- DEFINE ENABLING CONTROL OPTIONS

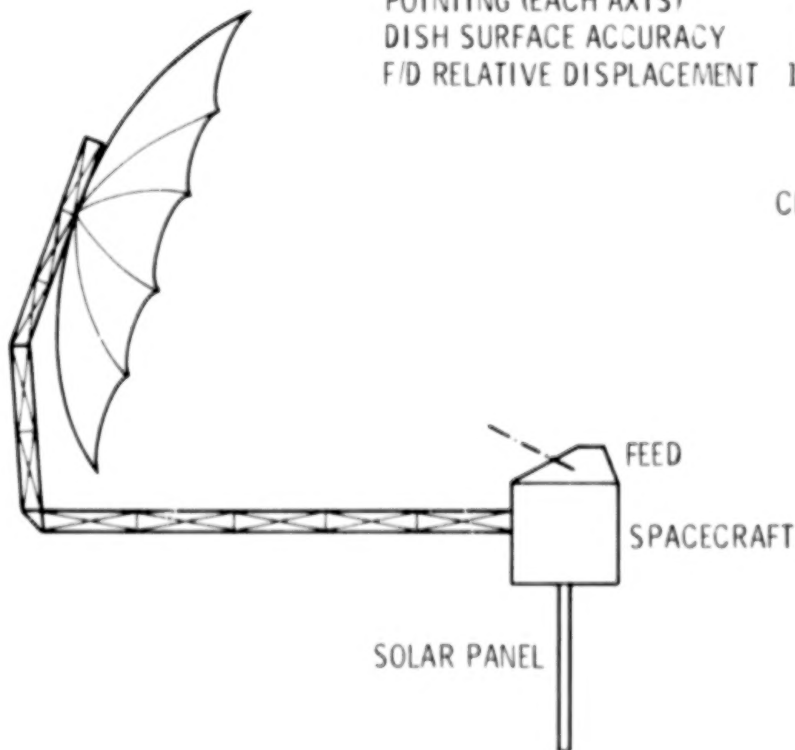
SELECTED CONFIGURATION

The selected configuration has antenna feed mounted on spacecraft to which a solar panel is attached. For communications missions at 2.5GHz, the typical control requirements are given in this viewgraph. This configuration is characterized by the unique dynamic features as follows:

- 1 Dynamic coupling due to imbalanced configuration
- 2 Low frequencies of boom due to large moments of inertia of dish and spacecraft/solar panel
- 3 Feed/dish relative displacement due to physical separation of feed and dish
- 4 Dish vibrations causing dish surface error and spacecraft attitude error.

TYPICAL REQUIREMENTS AT 2.5 GHz

POINTING (EACH AXIS)	0.6 mrad (0.035°)
DISH SURFACE ACCURACY	6 mm ($\lambda/20$)
F/D RELATIVE DISPLACEMENT	12 mm ($\lambda/10$)



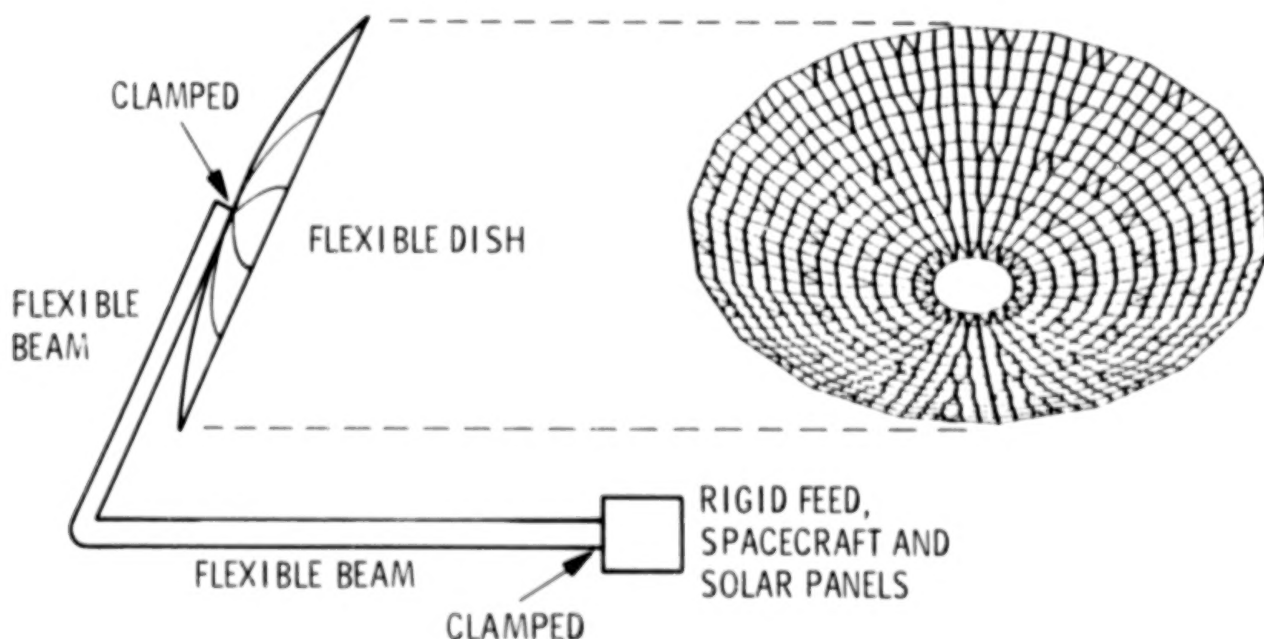
CHARACTERISTICS :

- IMBALANCED CONFIGURATION
- LOW FREQUENCIES OF BOOM
- F/D RELATIVE DISPLACEMENT
- DISH VIBRATIONS

DYNAMIC MODELS FOR CONTROL STUDY

The overall dynamic model for the antenna was generated by combining individual dynamic models for the dish, boom, spacecraft and solar panel. Disturbances are also modeled as external torques applied to the antenna system. The lowest frequencies for either 15-meter or 100-meter system are due to boom torsion or bending. A number of subroutines were developed for the overall dynamic models to compute, print and plot antenna performance parameters such as dish surface RMS errors, dish pointing errors, feed/dish relative displacement errors, etc. Graphic subroutines were also developed for visual display of dish distortions as functions of time. Model parameter changes are easy to implement. Therefore, these models are useful for system/sensitivity performance analysis. In this presentation, inherent damping of LSST antenna was assumed at 0.5%.

- 15-METER DISH - LOWEST VIBRATION FREQUENCY 0.0133 HZ
- 100-METER DISH - LOWEST VIBRATION FREQUENCY 0.0016 HZ



- USEFUL FOR SYSTEM/SENSITIVITY PERFORMANCE EVALUATION

CONTROLLERS FOR PERFORMANCE EVALUATION

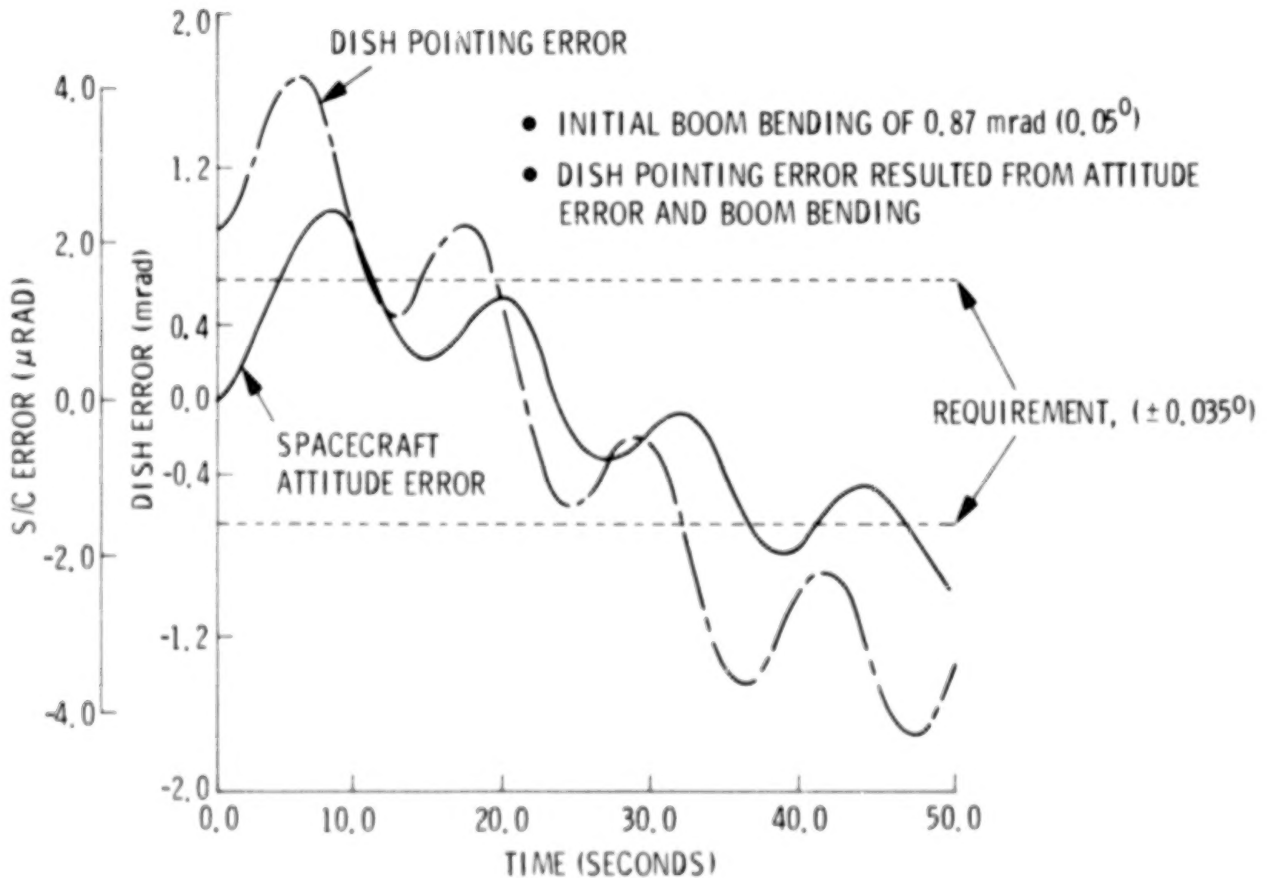
Current attitude controllers refer to those designed for current geostationary communication satellites. In particular, 3-axis stabilization and control designs employing attitude rate and error feedback are typical of today's non-spinning spacecraft attitude control. A number of such controllers were designed for the LSST antenna system covering a bandwidth range from 0.001Hz to 0.1Hz. To consider the control of flexible LSST antenna systems, the standard optimal controllers were also designed. The designs assumed attitude error sensing only, and the attitude as well as flexible mode information were estimated. Based on the estimated attitude and flexible dynamics, control was performed at spacecraft. A number of these optimal controllers were designed covering a bandwidth range of 0.003Hz - 0.03Hz.

- CURRENT ATTITUDE CONTROLLERS
 - ATTITUDE RATE AND ERROR FEEDBACK
 - RIGID BODY MODES ONLY
 - BANDWIDTH: 0.001 Hz - 0.1 Hz

- OPTIMAL CONTROL
 - ATTITUDE ERROR SENSING
 - ESTIMATION OF FLEXIBLE MODES
 - BANDWIDTH: 0.003 Hz - 0.03 Hz

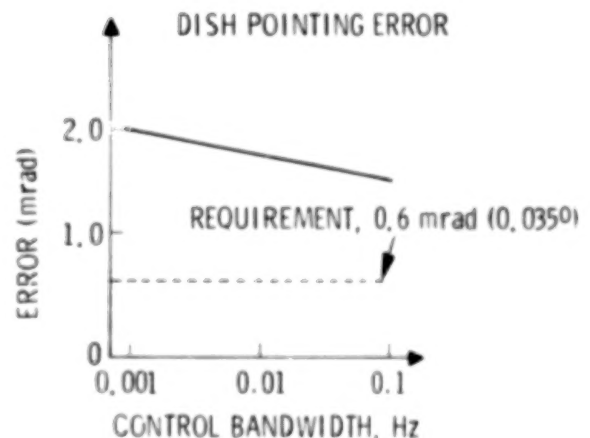
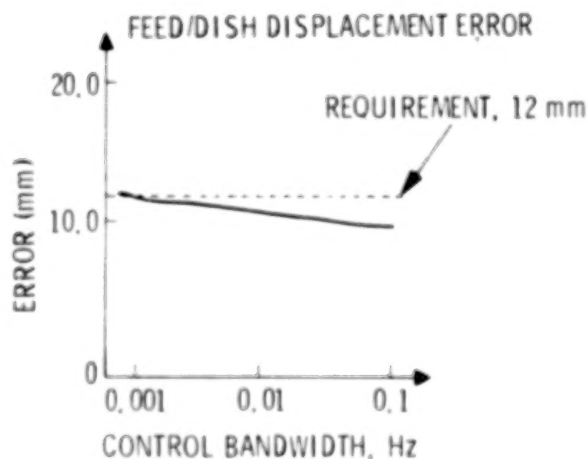
TYPICAL RESULTS

This is a 15-meter system simulation result, displaying both spacecraft attitude error and dish pointing error as functions of time. The system was under the control of a current attitude controller corresponding to a bandwidth of 0.1Hz. The only initial conditions were boom bending of 0.87 mrad (0.05°) about each of 3 axes. This chart shows that spacecraft attitude of good accuracy can not guarantee a dish pointing meeting the requirement. The reason is that dish pointing error is a result of both attitude error and boom bending. Two boom bending frequencies evident in both spacecraft attitude error and dish pointing error indicate coupling of boom, spacecraft, and dish dynamics.



CONTROL PERFORMANCE ASSESSMENT (15-METER SYSTEM)

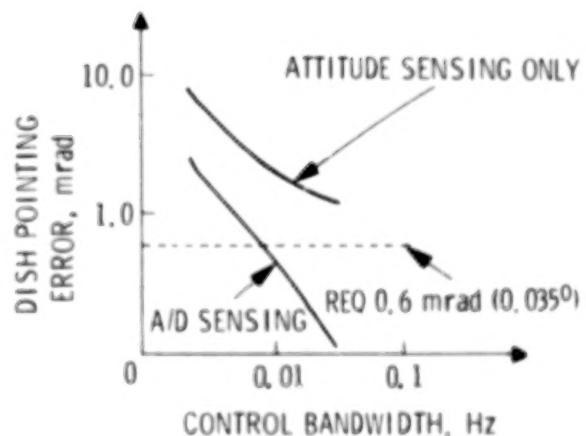
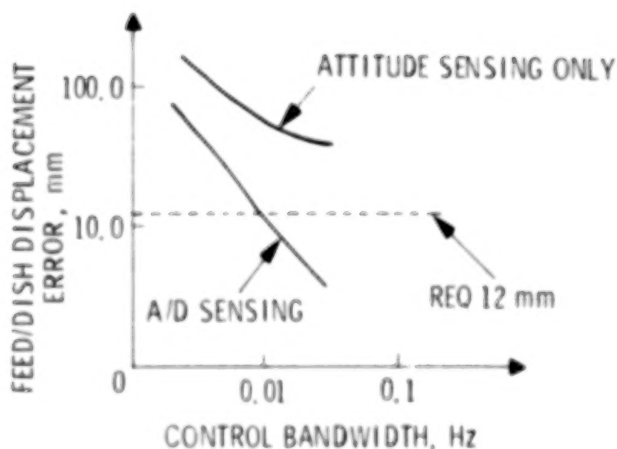
This chart is a summary of antenna dynamic performance with current attitude controllers of different bandwidths. In each case, stability was achieved and dish surface error was within requirement (with inherent damping of flexible modes at 0.5%). However, pointing requirement was not met and feed/dish relative displacement error was only marginally acceptable. Slight improvement in dish pointing and feed/dish relative stability over two decades of control bandwidth indicate that current attitude controllers with attitude-rate and error feedback only are not adequate for LSST antenna.



- STABILITY ACHIEVED
- DISH SURFACE ERROR MEETS REQUIREMENT
- POINTING REQUIREMENT IS NOT MET
- ATTITUDE RATE AND DISPLACEMENT FEEDBACK APPROACH NOT EFFECTIVE FOR BCCM VIBRATION SUPPRESSION

CONTROL PERFORMANCE ASSESSMENT (100-METER SYSTEM)

This is a summary of antenna dynamic performance with optimal controllers of different bandwidths. Performance is sensitive to model errors. Although performance requirement was not met with attitude sensing only, the performance improvement as control bandwidth increased was significant relative to the previous chart. The reason is that flexible dynamics was not ignored as in the previous case. This chart also indicates that required performance can be achieved by using the same control approach with additional feed/dish relative displacement sensing.



- REQUIREMENT IS NOT MET WITH ATTITUDE SENSING ONLY
- ATTITUDE AND DISH SENSING IMPROVED NOT ONLY FEED/DISH STABILITY BUT ALSO DISH POINTING, THUS MEETING REQUIREMENTS
- PERFORMANCE SENSITIVE TO MODEL ERRORS

CONCLUSIONS

Based on overall dynamic models of antenna systems developed in FY'60, current controllers studied were found to be incapable of meeting all typical requirements. Major problems were identified and quantified. In general, problems arose as a result of imbalanced antenna configuration and flexibility of vehicle. In particular, dynamics of boom structure connecting the dish and the feed was found to be a critical factor determining antenna performance. "Feed/Dish Motion Compensation" scheme has been identified as a candidate enabling control concept to be studied further next year.

- IMBALANCED OFFSET CONFIGURATION RESULTS IN
 - DYNAMIC COUPLING
 - CONTROL/STRUCTURE DYNAMICS INTERACTION
- DYNAMICS OF BOOM STRUCTURE CONNECTING THE DISH AND THE FEED IS CRITICAL TO
 - ANTENNA DISH POINTING
 - FEED/DISH RELATIVE DISPLACEMENT
- CURRENT CONTROLLERS STUDIED DO NOT MEET ALL REQUIREMENTS
- POTENTIAL SOLUTION IDENTIFIED: FEED/DISH MOTION COMPENSATION CONTROLLER

FY'81 LSST ANTENNA CONTROL TASKS

In a previous chart, it was demonstrated that a version of feed/dish motion compensation (F/DMC) scheme could enable the required antenna performance. However, this F/DMC scheme needs to be further developed and improved to achieve objectives listed below. Major tasks involve: sensor/actuator placement tradeoff, definition of sensing strategy, definition and development of control design approach, assessment of hardware requirement, performance evaluation and tradeoff.

New areas to be addressed in FY'81 are the control of Hoop/column antenna and antenna control/RF performance interactions. Approach similar to that for FY'80 wrap-rib antenna control task will be taken for the Hoop/column antenna. Emphasis will be directed at the assessment of its unique control mechanism and its control design.

The objective of control/RF performance interaction task is to develop design and analysis tools needed to specify and evaluate the performance of LSST antenna systems in terms of RF parameters. The activities will be directed toward: (1) development of control/structure/RF models to define their relations, and (2) development of control designs for representative systems (e.g. offset feed wrap-rib antenna) that maximize antenna gain by reducing losses due to control/structure/RF interactions.

- FEED/DISH MOTION COMPENSATION (F/D MC) CONCEPT FOR WRAP-RIB ANTENNA

OBJECTIVES:

- COMPENSATION FOR BOOM BENDING AND TORSION
- REAL-TIME STABILIZATION OF FEED/DISH RELATIVE DISPLACEMENT
- REDUCTION OF BOOM DYNAMIC UNCERTAINTIES

ISSUES:

- SENSING STRATEGY
- CONTROL DESIGN APPROACH
- HARDWARE REQUIREMENT
- CONTROL OF HOOP/COLUMN ANTENNA
 - ASSESS CAPABILITIES OF CONTROL STRINGERS
 - DEVELOP PRELIMINARY CONTROL DESIGNS TO IDENTIFY CRITICAL PROBLEMS
- ANTENNA CONTROL/RF PERFORMANCE INTERACTIONS
 - DETERMINE CONTROL/STRUCTURE/RF RELATIONS
 - DEVELOP CONTROL DESIGNS TO MAXIMIZE RF PERFORMANCE

BLANK PAGE

BLANK PAGE

ADVANCED CONTROL TECHNOLOGY
FOR LSST PLATFORM

R. S. EDMUNDS
JET PROPULSION LABORATORY
PASADENA, CALIFORNIA

LARGE SPACE SYSTEMS TECHNOLOGY - 1980
SECOND ANNUAL TECHNICAL REVIEW
NOVEMBER 18-20, 1980

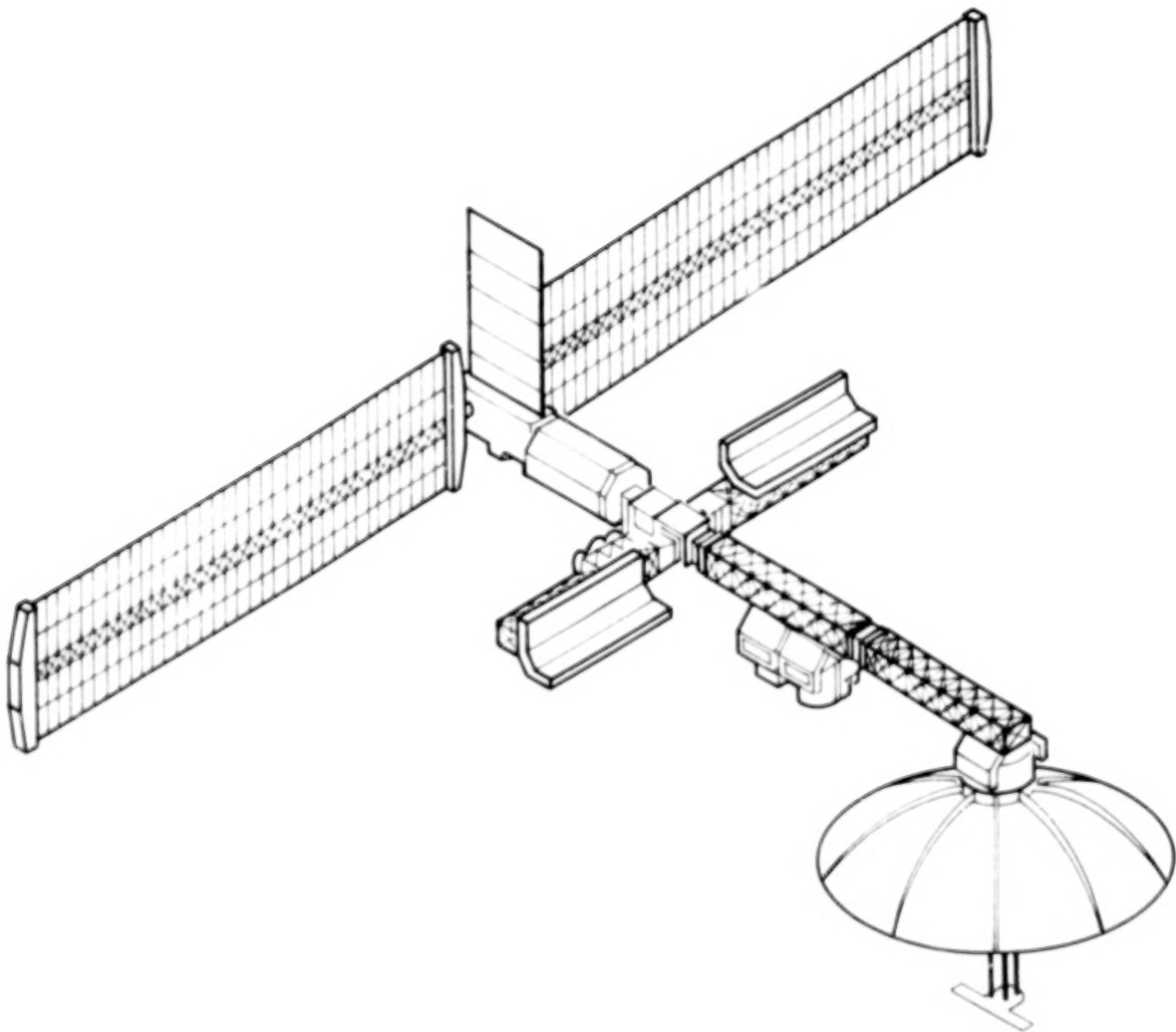
FY'80 LSST PLATFORM CONTROL TECHNOLOGY OBJECTIVES

The long range objective of this task is to develop basic technology in the design, mechanization, and analysis of control systems for large flexible space structures. The focus of the FY'80 platform control effort was on pointing control. The reason for this emphasis was because of the unique problems in this area posed by multiple independent experiment packages operating simultaneously on a single platform. Attitude control and stationkeeping will be addressed in future years.

- ESTABLISH POINTING CONTROL REQUIREMENTS
- DEVELOP STRUCTURAL/CONTROL MODELS
- PROVIDE QUANTITATIVE DEFINITION OF CONTROL PROBLEMS
- PROVIDE CONCEPTUAL DEFINITION AND ASSESSMENT OF ADVANCED CONTROL SYSTEM CONCEPTS

LSST PLATFORM CONFIGURATION

The LSST platform consists of solar panels, a central bus (with associated power, telemetry, and control systems), and platform arms with mounting pads on which various experiments can be attached. The actual configuration for the platform arms might vary widely depending on experiment requirements for physical separation and viewing angles. The tip to tip dimension of the solar panels is approximately 100 meters, and the weight of the combined solar panels and central bus is approximately 13,000 kg.



POINTING CONTROL PROBLEMS

Perhaps the most important control problem for the LSST Reference Platform identified in FY'80 is the interaction of multiple independent control systems. The mass of a single articulated experiment may be as much as 1/4 the total platform mass so that motion of an experiment can create large disturbance inputs to the platform. This interaction would exist even if the platform were completely rigid, so that stiffening up structural members of the platform is not a viable solution to this problem. The simplest solution might be to restrict the magnitude of the disturbance inputs which any experiment can input to the platform. Advanced control system designs are required, however, to minimize the severity of any such constraints.

- INTERACTION OF MULTIPLE INDEPENDENT CONTROL SYSTEMS
 - THIS PROBLEM WOULD EXIST FOR A RIGID PLATFORM AND IS AGGRAVATED BY FLEXIBILITY
 - EXPERIMENT COMPATIBILITY WILL BE AN IMPORTANT OPERATIONAL CONSIDERATION
 - ADVANCED CONTROLLERS WILL BE NEEDED TO MINIMIZE COMPATIBILITY CONSTRAINTS

POINTING CONTROL PROBLEMS (CONT.)

The design of experiment controllers is hindered by the potential for large uncertainty in the structural model parameters. Gross parameter changes can occur depending upon how many experiments are installed on the platform and their location. A second, related problem is that structural vibration frequencies will occur within the controller bandwidths. Results show that controller bandwidth cannot be reduced below the structural frequencies without unacceptable performance degradation in the presence of disturbances created by experiment motion. These two problems will require advanced controller design techniques for their solution.

- VARIATION IN STRUCTURAL PARAMETERS AS FUNCTION OF EXPERIMENTS INSTALLED
- STRUCTURAL VIBRATION FREQUENCIES IN SAME BANDWIDTH AS CONTROLLERS

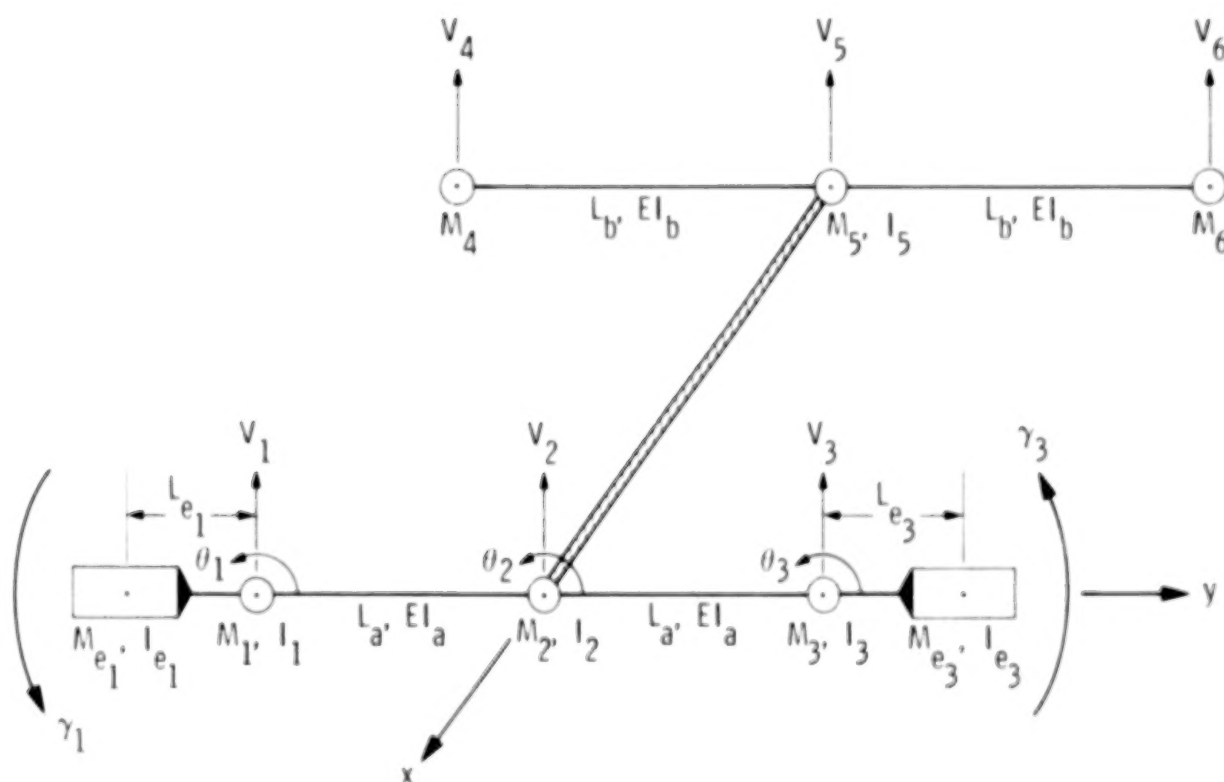
POINTING CONTROL REQUIREMENTS

The requirements listed below are representative of the most stringent specified by potential platform users. The numbers presented were taken from a payload data base provided by the Office of Space Science and the Office of Space and Terrestrial Applications. The Shuttle Infrared Test Facility (SIRTF) has accuracy and stability requirements in this range and the Materials Experiment Module has acceleration requirements in this range. Only the stability and acceleration requirements will be addressed in what follows.

ACCURACY	0.485 TO 48.5 μ rad (0.1 TO 10 arc sec)
STABILITY	0.0243 TO 0.485 μ rad (0.005 TO 0.1 arc sec)
ACCELERATION	0.098 TO 9.8 mm/s ² (10 ⁻⁵ TO 10 ⁻³ g)

SIMPLIFIED STRUCTURAL MODEL

This figure shows the structural model used in the studies conducted. It has 6 linear degrees of freedom (V_1 through V_6) and 5 angular degrees of freedom (θ_1 , θ_2 , θ_3 , γ_1 , and γ_3). The masses M_2 and M_5 represent the central bus structure and are rigidly connected. M_1 and M_3 are associated with the platform arm mounting pads, and M_{e1} and M_{e3} with two experiment packages. I_1 , I_2 , I_3 , I_5 , I_{e1} and I_{e3} are inertias. All masses are assumed to be connected by massless beams. The beams connecting M_4 , M_5 , M_6 and M_1 , M_2 , M_3 are assumed elastic. All other beams are assumed to be rigid.



NATURAL VIBRATION FREQUENCIES

The first four elastic mode frequencies for the platform are shown below:

Data used for the Solar Panels was:

$$EI_b = 0.01 \times 10^6 \text{ N} - \text{m}^2, M_4 = M_6 = 500 \text{ kg}, L_b = 20 \text{ m}.$$

Data used for the central bus was:

$$M_2 = M_5 = 6000 \text{ kg}, I_2 = I_5 = 25000 \text{ kg} - \text{m}^2.$$

Data used for the platform arms was:

$$EI_a = 20 \times 10^6 \text{ N} - \text{m}^2, M_1 = M_3 = 300 \text{ kg}, I_1 = I_3 = 100 \text{ kg} - \text{m}^2.$$

Data used for the experiment packages was:

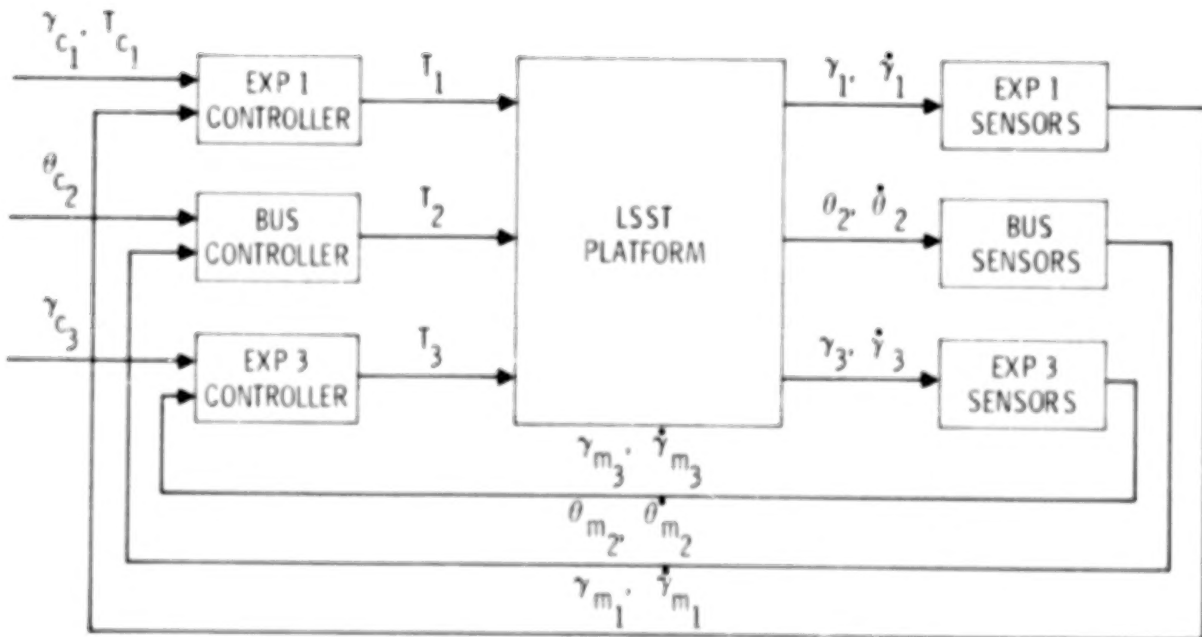
$$L_{e1} = L_{e3} = 3.6 \text{ m}, M_{e1} = M_{e3} = 3300 \text{ kg}, I_{e1} = I_{e3} = 48000 \text{ kg} - \text{m}^2.$$

Two different arm lengths, 15m and 6m, were used to demonstrate the effect of different structural parameters on control performance. It should be noted that a more complete solar panel model would result in vibration frequencies between and above the frequencies tabulated below.

	MODE	ARM LENGTH	
		15m	6m
1-5	RIGID BODY	0	0
6	1ST SOLAR PANEL SYMMETRIC	0.0471 Hz	0.0471 Hz
7	1ST SOLAR PANEL ANTISYMMETRIC	0.0639	0.0984
8	1ST ARM SYMMETRIC	0.912	3.59
9	1ST ARM ANTISYMMETRIC	2.18	4.54

CONTROL SYSTEM CONFIGURATION

A block diagram for the control system studied is shown below. It consists of three independent controllers. Altogether there are four inputs and six outputs for this system. The sensors and actuators for each of the three control loops are assumed to be colocated. Ideal sensors are assumed and torquer dynamics are not included. The controllers use rate plus position feedback, without compensation, to generate torque commands (T_1, T_2, T_3). Experiment controller 1 also uses a commanded torque in a feed forward loop (T_{C1}) to influence its output torque command (T_1). Feedback gains for each controller were selected independently using rigid body platform models.



PERFORMANCE RESULTS

Performance results were obtained from time domain simulation runs. The results of six representative runs are shown below. The disturbance input for each run was a 88 mrad slew of Exp. 1 using a commanded torque (T_{C1}) of 20 N-m. The bus controller bandwidth (W_{n2}) was 0.01 Hz for all runs. Structural damping of 0.5% was assumed. The platform arm length was varied from 6 to 15 m. Controller bandwidth for Exp. 1 (W_{n1}) was set at 1.0 Hz for some runs, and for others open loop torquing was used. Controller bandwidth for Exp. 3 (W_{n3}) was set at 1.0 and 0.1 Hz. The peak pointing errors for Exp. 3 (γ_3) and the central bus (θ_2) are tabulated as are the peak linear acceleration levels (\ddot{V}_2) at Exp. 2 located on the bus structure. It can be seen that the pointing requirements stated earlier cannot be easily met using controllers of the type considered here.

$$\gamma_{c1} = 88 \text{ mrad}, T_{c1} = 20 \text{ N-m}, W_{n2} = 0.01 \text{ Hz}$$

RUN	ARM LENGTH (m)	CONTROL BANDWIDTH		PEAK RESPONSE		
		W_{n1} (Hz)	W_{n3} (Hz)	γ_3 (μ rad)	θ_2 (mrad)	\ddot{V}_2 (mm/s ²)
F12	15.0	*	1.0	56.00	5.11	3.000
F10	15.0	1.0	1.0	7.59	3.27	0.964
F13	15.0	1.0	0.1	357.00	3.25	0.608
F17	6.0	*	1.0	12.20	3.10	0.848
F18	6.0	1.0	1.0	3.13	2.28	0.819
F19	6.0	1.0	0.1	254.00	2.26	0.819

*OPEN LOOP TORQUING

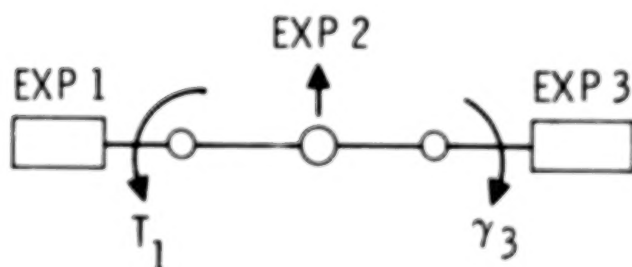
PERFORMANCE TRENDS

A comparison of the six representative simulation runs illustrates several clear trends. It should be kept in mind that Exp. 1 is creating the disturbance, and Exp. 2 (fixed to the bus) and Exp. 3 are feeling the influence of the disturbance. Using a closed loop controller for Exp. 1 (compare runs F10 & F12) results in a smoother disturbance torque profile, and as such improves pointing stability for both γ_3 and θ_2 . It also reduces acceleration levels at the bus (\ddot{V}_2). Increasing Exp. 3 bandwidth (compare runs F10 & F13) increases γ_3 stability, but has an adverse affect on \ddot{V}_2 . Increasing the arm stiffness (compare runs F10 & F18) increases pointing stability of both γ_3 and θ_2 and in most cases decreases acceleration levels (\ddot{V}_2).

- A SMOOTHER TORQUE PROFILE AT EXP 1 RESULTS IN
 - INCREASED POINTING STABILITY (γ_3 AND θ_2)
 - DECREASED ACCELERATION LEVELS (\ddot{V}_2)
- INCREASED EXP 3 BANDWIDTH RESULTS IN
 - INCREASED POINTING STABILITY (γ_3)
 - INCREASED ACCELERATION LEVELS (\ddot{V}_2)
- INCREASED ARM STIFFNESS RESULTS IN
 - INCREASED POINTING STABILITY (γ_3 AND θ_2)
 - DECREASED ACCELERATION LEVELS (\ddot{V}_2)

EXP. 2 AND EXP. 3 RESPONSE TO 20 N-M EXP. 1 CONTROL ACTION

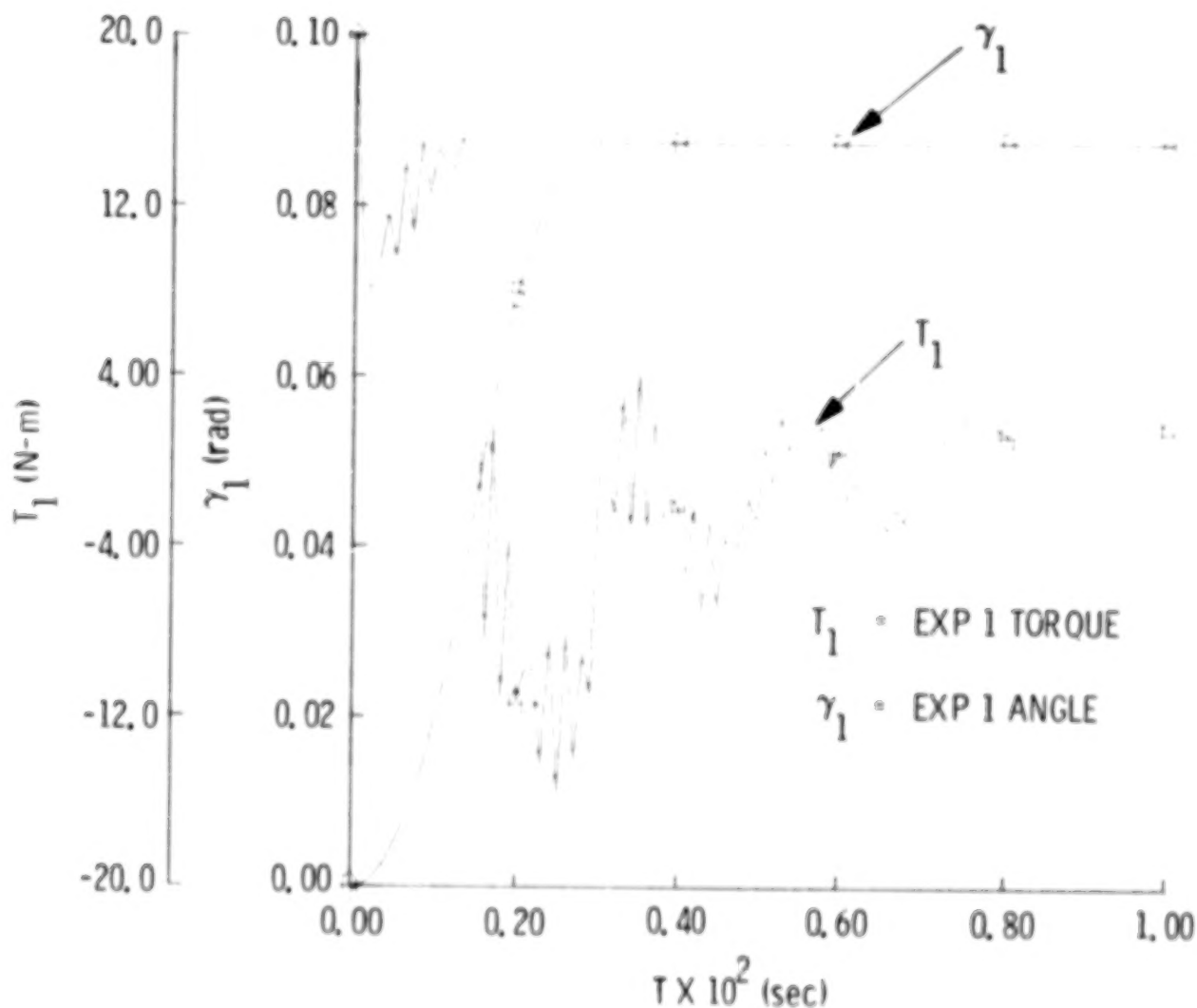
The absolute performance of the control systems considered here was poor compared to the requirements stated earlier. The pointing requirements are very tight and the disturbance torques considered are relatively large (but well within the torque capabilities of pointing systems being considered for space platforms). The results demonstrate clearly the magnitude of the control system design problem for platforms having more than one independently articulated experiment package.



- STABILITY PERFORMANCE (EXP 3)
 - 6 TO 100 TIMES WORSE THAN $0.5 \mu\text{rad}$ REQUIREMENT
 - 120 TO 2000 TIMES WORSE THAN $0.025 \mu\text{rad}$ REQUIREMENT
- ACCELERATION LEVELS (EXP 2)
 - WITHIN THE 10 mm/s^2 REQUIREMENT
 - 8 TO 30 TIMES WORSE THAN 0.1 mm/s^2 REQUIREMENT

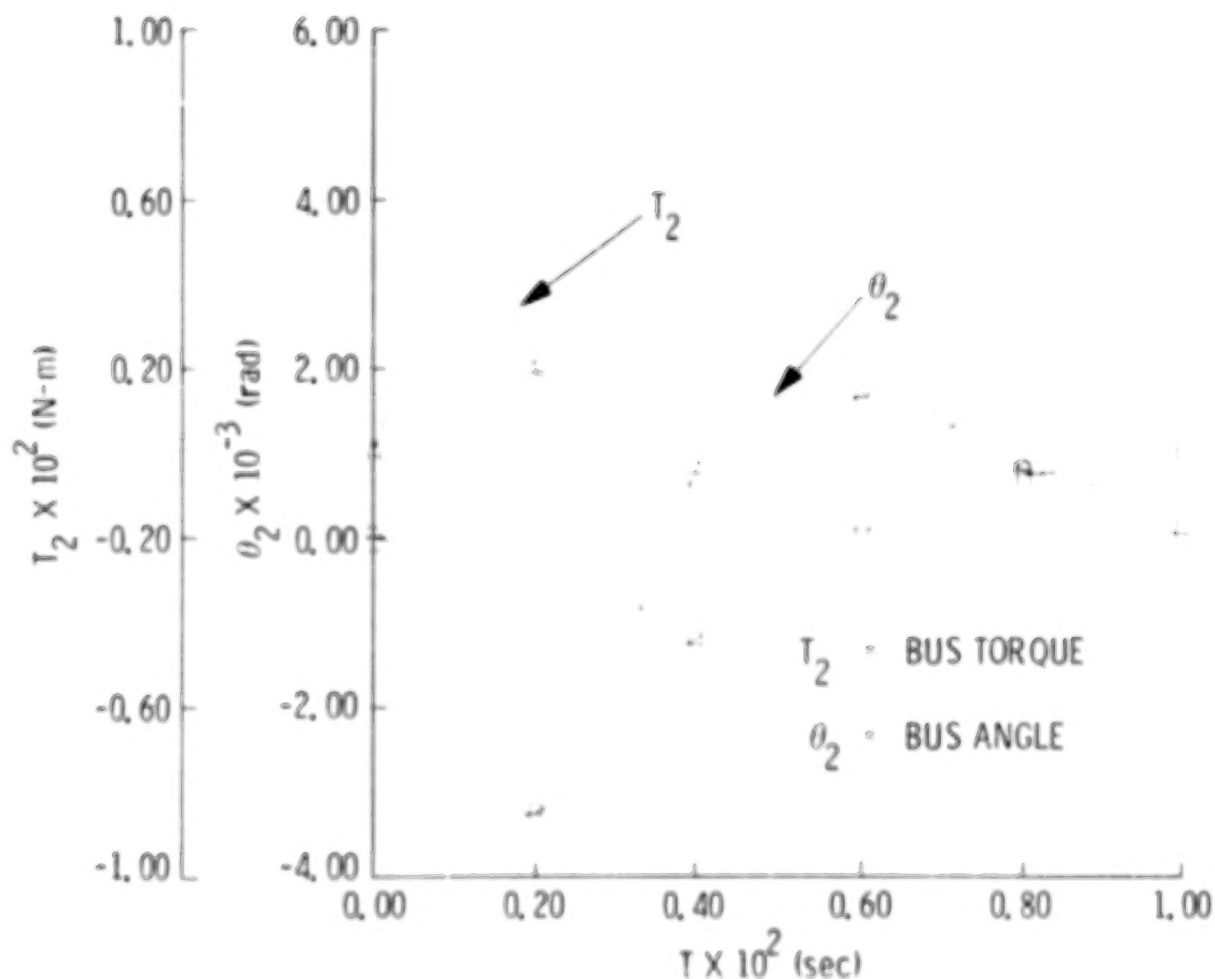
ACTUATOR TORQUE AND ANGULAR RESPONSE FOR EXPERIMENT 1, RUN F10

The actuator torque (T_1) and angular response (γ_1) for experiment 1 are shown below for a representative run. The commanded torques (T_{C1}) for this run was +20 N-m for the first 14 seconds, -20 N-m for the next 14 seconds, and zero thereafter. The commanded angle (γ_{C1}) was consistent with this. The actual torque applied shows the strong influence of the structural elastic response fed back to the controller by the rate and position sensor.



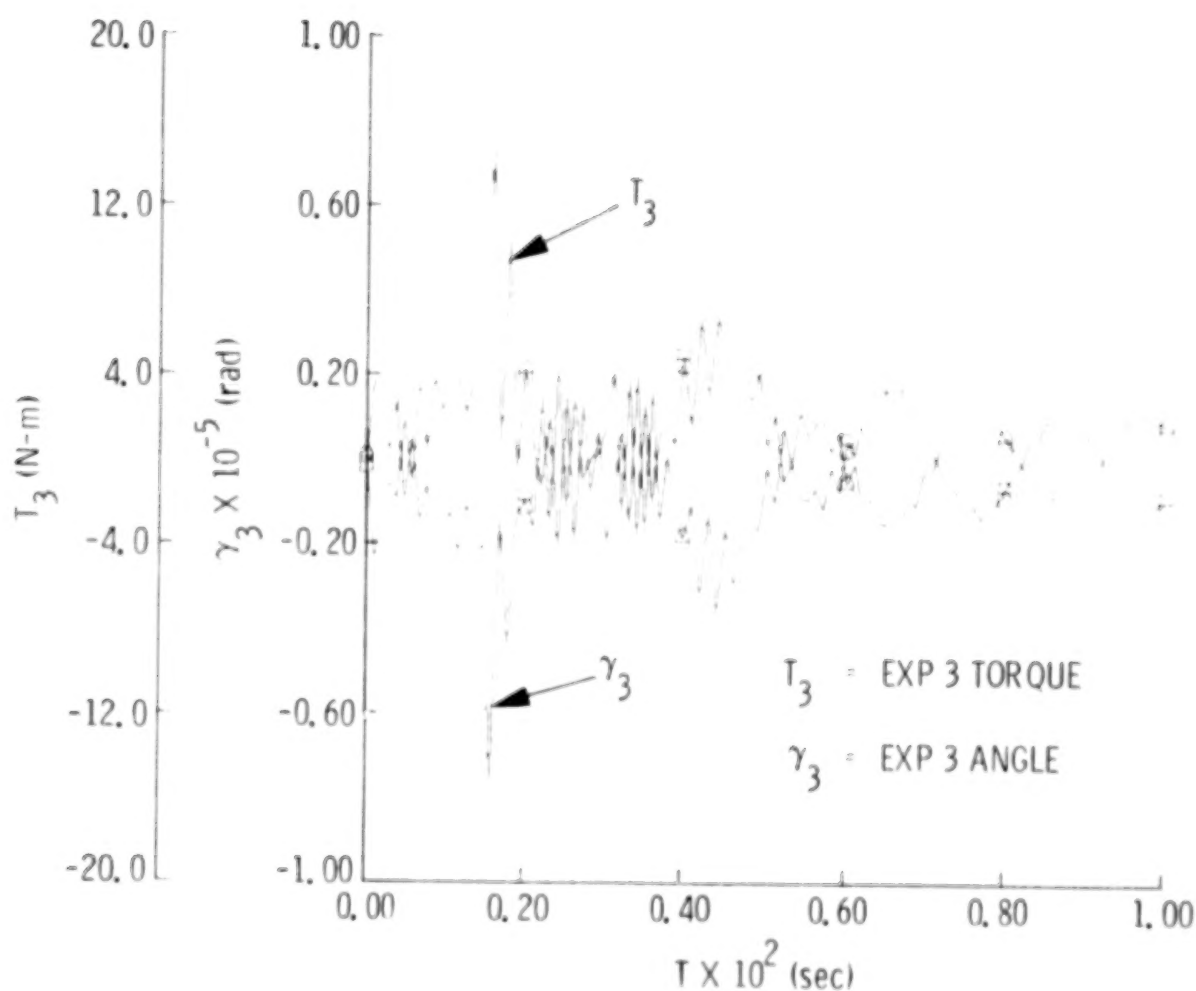
ACTUATOR TORQUE AND ANGULAR RESPONSE FOR THE CENTRAL BUS, RUN F10

The actuator torque (T_2) and angular response (θ_2) are shown below for a representative run. The commanded angle (θ_{c2}) was zero. The primary response is a rigid body rotation which occurs because the bus controller frequency is low (0.01 Hz) compared to the frequency of the disturbance input. Some structural oscillations are evident, however.



ACTUATOR TORQUE AND ANGULAR RESPONSE FOR EXPERIMENT 3, RUN F10

The actuator torque (T_3) and angular response (γ_3) are shown below for a representative run. The commanded angle (γ_{C3}) was zero. The frequency content of T_3 is very similar to that of T_1 for this run. In fact, after about 40 seconds, the two torques are almost identical. Notice that the damping is very poor, indicating a low stability margin.



ADDITIONAL FACTORS WHICH CAN AFFECT PERFORMANCE

There are many factors not considered in this study which could have a major influence on the absolute performance of the LSST reference platform. Imperfect sensors and actuators, gimbal friction and flexibility, and more complex structural dynamics could all result in poorer performance than that presented here. On the other hand improved controller gain selection or more sophisticated controllers could improve the performance results. For example, base motion compensation could be added using an additional sensor for each experiment package (an accelerometer), and image motion compensation could be implemented for some types of experiment packages by the addition of another actuator (a secondary mirror drive for example).

FACTORS WHICH CAN DEGRADE PERFORMANCE

- IMPERFECT SENSORS AND ACTUATORS
- GIMBAL FRICTION OR FLEXIBILITY
- MORE COMPLEX STRUCTURAL DYNAMICS

FACTORS WHICH CAN IMPROVE PERFORMANCE

- IMPROVED CONTROLLER GAIN SELECTION
- MORE SOPHISTICATED CONTROLLERS
 - BASE MOTION COMPENSATION
 - IMAGE MOTION COMPENSATION

SUMMARY

During FY'80 several control problems for the LSST Reference Platform have been identified and quantified. Perhaps the most important of these is that operation of multiple independent control systems on a single platform presents a major problem when high performance is required. Experiment compatibility will be an important operational consideration. Control system design is complicated by large shifts in structural parameters which occur as a result of variations in the number and location of experiments mounted on the platform. Structural vibration frequencies in the controller bandwidth further complicate the design problem. It has been found that conventional controllers miss performance requirements by a wide margin when these factors are taken into account.

- INTERACTION OF MULTIPLE INDEPENDENT CONTROL SYSTEMS IS A MAJOR PROBLEM
- EXPERIMENT COMPATIBILITY WILL BE AN IMPORTANT OPERATIONAL CONSIDERATION
- CONTROL SYSTEM DESIGN IS COMPLICATED BY LARGE VARIATIONS OF STRUCTURAL PARAMETERS AND BY VIBRATION FREQUENCIES IN CONTROLLER BANDWIDTHS
- CONVENTIONAL CONTROLLERS DO NOT MEET PERFORMANCE REQUIREMENTS BY WIDE MARGINS

FUTURE WORK IN LSST PLATFORM AREA

Two controls approaches have been identified for future study. The first approach is to add additional sensors and/or actuators to individual experiment controllers. Base motion and image motion compensation fall in this category. The second approach is to allow information exchange between controllers, particularly one way exchange from the bus controller to the experiment controllers. The challenge is to develop controllers which can significantly reduce the controller interaction problem and at the same time reduce controller sensitivity to structural parameter variations.

- INVESTIGATE IMPROVED INDEPENDENT CONTROLLER DESIGNS USING ADDITIONAL SENSORS AND ACTUATORS
- DEVELOP DESIGNS WHICH UTILIZE INFORMATION EXCHANGE FROM BUS TO EXPERIMENT CONTROLLERS
- VERIFY EFFECTIVENESS OF ABOVE DESIGNS IN REDUCING CONTROLLER INTERACTIONS AND SENSITIVITY TO PARAMETER VARIATIONS

CONTROL TECHNOLOGY DEVELOPMENT

G. RODRIGUEZ
JET PROPULSION LABORATORY
PASADENA, CALIFORNIA

LARGE SPACE SYSTEMS TECHNOLOGY - 1980
SECOND ANNUAL TECHNICAL REVIEW
NOVEMBER 18-20, 1980

FY'80 OBJECTIVES

The FY'80 objectives were primarily concerned with developing static and dynamic control design approaches for distributed parameter systems. In addition to this analytical work, a hardware flexible beam facility was completed to experimentally demonstrate and verify the theoretical control concepts. Work in the area of model order reduction and error estimation for control of systems with uncertain or time varying parameters was continued. A part of the modeling work was done by contract to Purdue University, and contract work in the area of non colocated sensors and actuators was begun at Stanford University.

- DEVELOP CONCEPTS FOR STATIC SHAPE ESTIMATION AND CONTROL
- DEVELOP TECHNOLOGY FOR DISTRIBUTED CONTROL OF DYNAMIC SYSTEMS
- DERIVE MODEL ORDER REDUCTION TECHNIQUES
- PERFORM SELECTED CONTROL TECHNOLOGY DEMOS USING EXPERIMENTAL FACILITY

LSST CONTROL PROBLEMS

As spacecraft become larger and more flexible, they begin to take on more characteristics of continuously distributed systems than of lumped parameter systems. For example, rather than an attitude control system being solely concerned with the rigid body behavior of a spacecraft, it also must deal with the many flexible body modes that now lie within the controller bandwidth. Four problem areas in the control of large structures have been isolated. They are: the shape control of a structure (e.g. maintenance of a reflector's parabolic shape), vibration and command control (e.g. the stabilization and slew response of any satellite), modeling of the high order dynamic model (e.g. how many and which structural modes must be retained for control design) and, finally, verification of newly developed control concepts (e.g. analysis, computer simulation, and hardware verification).

STATIC SHAPE CONTROL

- DEDUCE CONTINUOUS SHAPE FROM DISCRETE MEASUREMENTS
- APPLY DISCRETE LOADS TO OBTAIN DESIRED SHAPE
- OPTIMIZE SENSOR/ACTUATOR NUMBER, TYPE, AND LOCATION

DYNAMIC CONTROL

- SOLVE ABOVE PROBLEMS FOR DYNAMIC SYSTEMS
- STABILIZE STRUCTURE IN DISTURBANCE ENVIRONMENT
- DESIGN FOR COMMAND INPUT RESPONSE
- OVERCOME BANDWIDTH LIMITATIONS OF SENSORS/ACTUATORS/ CONTROLLERS

MODELS

- PRODUCE "BEST" LOW ORDER CONTROLLER
- DESIGN PARAMETER INSENSITIVE CONTROLLERS

VERIFICATION

- ANALYSIS AND SIMULATION MAY OMIT IMPORTANT FEATURES
- COMPUTER RESULTS ARE SATISFYING ONLY TO A CERTAIN EXTENT

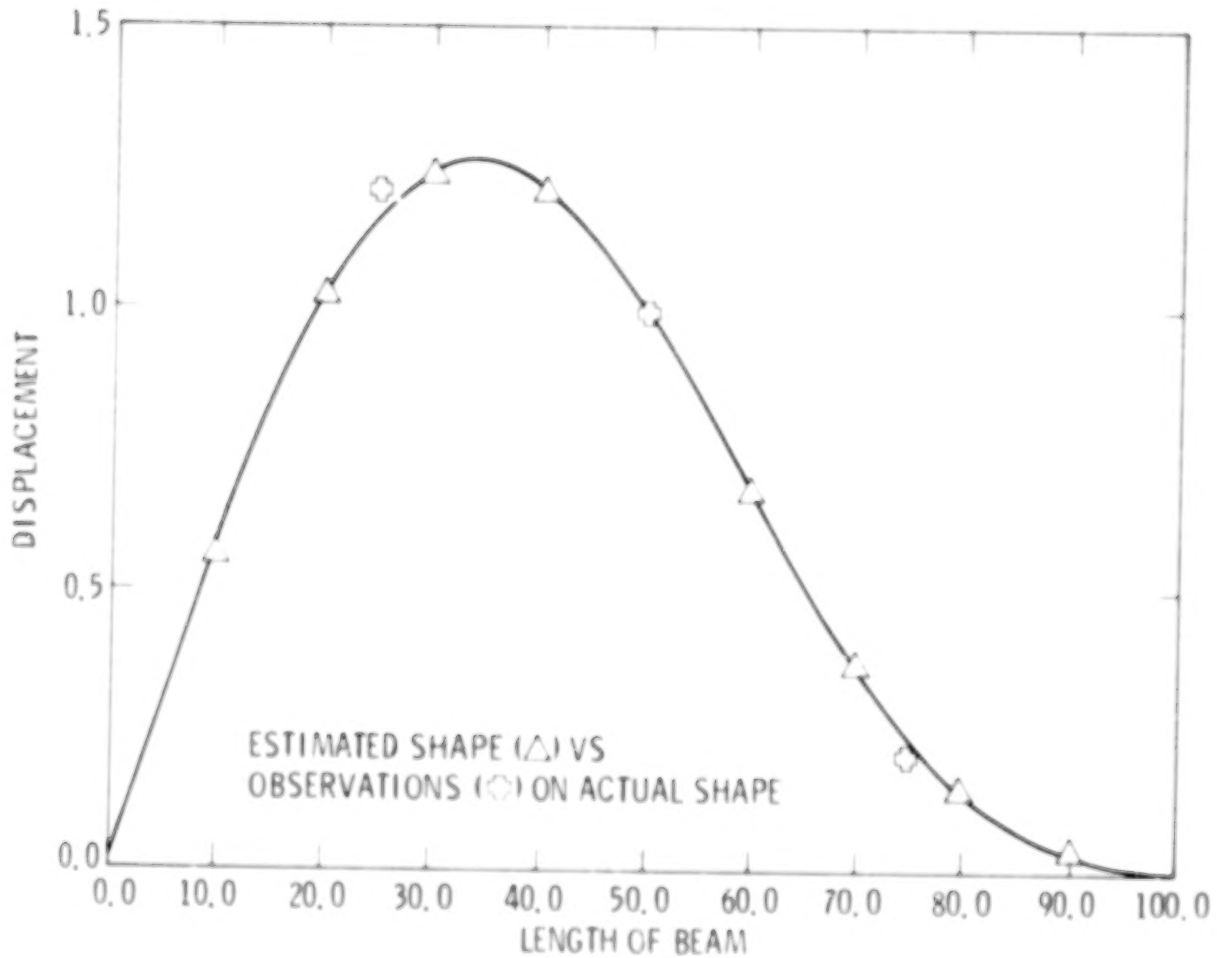
STATIC SHAPE CONTROL

The problem of static shape estimation and control of a spatially continuous infinite dimensional structure with a finite number of spatially discrete sensors and actuators has been studied. Using partial differential equations (pde) to model the continuous shape, so-called Green's functions are employed to handle the continuous/discrete mixture of the problem, and the appropriate boundary conditions. The rationale behind the use of pde models, in both this area and the area of dynamic control, is to retain as full a model as is possible through the control design process. Although it is certainly possible to work with truncated models, a great deal of insight can be gained by working directly with the continuous case. Additionally, virtually no additional computational complexity is required with pde's, and, a single pde is usually much less burdensome for the control analyst than the approximating high order set of ordinary differential equations. Results have been obtained for several simple systems, including the simply supported beam, a pinned-free beam (which retains a rigid body mode), a flexible plate, and a circular membrane; and the general theory has been developed for application to arbitrary systems.

- PROBLEM: ESTIMATE AND CONTROL A CONTINUOUS STATIC SHAPE USING DISTRIBUTED SENSING AND ACTUATION
- APPROACH: USE PDE FOR STRUCTURAL MODELING AND DERIVE GREEN'S FUNCTION TO INCORPORATE THE CONTINUOUS/DISCRETE MIX AND BC'S
- FY '80 ACHIEVEMENTS: THE GENERAL THEORY FOR SHAPE CONTROL HAS BEEN DEVELOPED AND ANALYTIC RESULTS HAVE BEEN OBTAINED FOR:
- 1) A SIMPLY SUPPORTED BEAM
 - 2) A PINNED-FREE BEAM
 - 3) A TWO DIMENSIONAL FLEXIBLE PLATE
 - 4) A TWO DIMENSIONAL CIRCULAR MEMBRANE

SHAPE CONTROL RESULTS

Using sensors located at three stations along the beam, it is desired to estimate the beam's actual shape. There are an infinite number of shapes that will coincide exactly with the sensor outputs at a finite number of locations. The shape estimation procedure is used for determining that one shape which optimally trades off the sensor accuracy with the model accuracy. Although the estimation approach is general (independent of the number of sensors, their location, and the dynamic system) results are shown on the viewgraph for a greatly simplified system to convey the essential ideas.



DISTRIBUTED CONTROL

The problem of estimating and controlling a spatially continuous (i.e. infinite dimensional) dynamic system has been studied. As with the problem of static shape control, formulation of the dynamic problem is in the general framework of partial differential equations (pde) of motion. This allows for replication of the results obtained using optimal control theory and ordinary differential equations (ode), plus the derivation of powerful new results that could only be obtained using pde's. These new results demonstrate the optimality of local controllers for any high gain system, and a computation of the feedback laws for any low gain system in terms of Green's functions.

- PROBLEM: ESTIMATE AND CONTROL SPATIALLY CONTINUOUS DYNAMIC SYSTEM USING DISTRIBUTED SENSING AND ACTUATION
- APPROACH: USE PARTIAL DIFFERENTIAL EQUATIONS OF MOTION AND DIFFERENTIAL OPERATOR APPROACH TO DERIVE RESULTS ANALOGOUS TO THOSE OBTAINED FOR LUMPED PARAMETER SYSTEMS
- FY '80 ACHIEVEMENTS: THE GENERAL THEORY FOR THE DISTRIBUTED CONTROL OF ARBITRARY DYNAMIC SYSTEMS HAS BEEN DEVELOPED AND ANALYTIC RESULTS HAVE BEEN OBTAINED FOR A STRING IN TENSION

DISTRIBUTED CONTROL RESULTS

Although the approach is general, control results are shown on the viewgraph for a simple system: a string in tension. Explicit formulas for the continuous position and velocity control gains obtained using an infinite dimensional approach are given. These results are graphically compared at a few points with the results obtained by discretizing the continuous system and applying existing know-how to derive the control laws. The control, $u(x)$, is formed by weighting the position, $y(\xi)$, and velocity, $v(\xi)$, with the appropriate control gains. Specifically

$$u(x) = \int_0^1 (K_y(x, \xi) y(\xi) + K_v(x, \xi) v(\xi)) d\xi$$

K_y is defined as the Green's function for the structure while the operator K_v is the (somewhat more obscure) square root of the Green's function. Very close agreement between the two approaches is evident; however, the infinite dimensional results can be obtained in closed analytical form while the discretized results require extensive numerical computations.

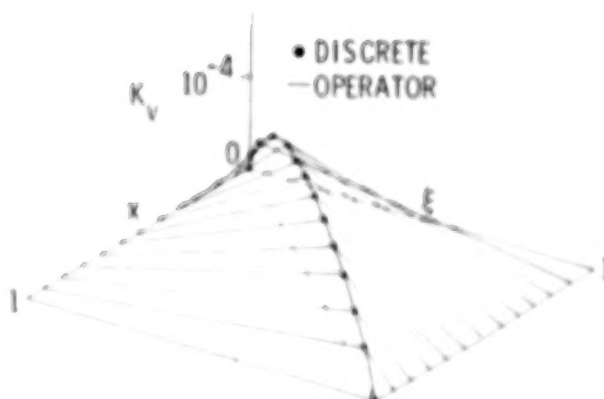
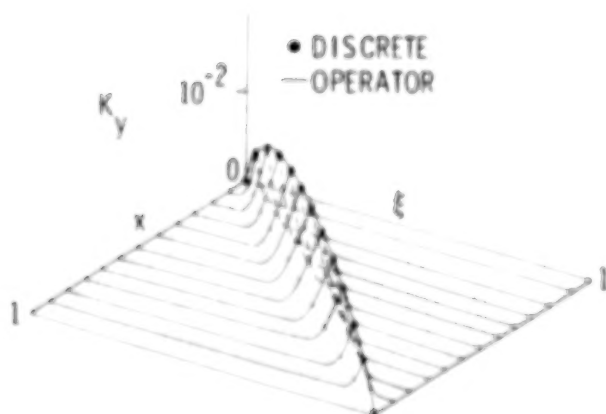
SPATIAL CONTROL GAINS FOR A FLEXIBLE STRING

POSITION GAIN

$$K_y \sim \frac{1}{\pi} \log \left| \frac{\sin \frac{\pi(x+\xi)}{2}}{\sin \frac{\pi(x-\xi)}{2}} \right|$$

VELOCITY GAIN

$$K_v \sim \begin{cases} x(1-\xi) & x < \xi \\ \xi(1-x) & x > \xi \end{cases}$$



MODEL ORDER REDUCTION

The model reduction and controller design research at Purdue seeks to develop a systematic approach to reduce the effects of model order errors in the design of structure controls. The approach which has been developed at Purdue is called Component Cost Analysis (CCA), and descriptions of this procedure are about to appear in several journals. Basically, component cost analysis determines the contribution of each component of the system in the overall performance metric. The contribution of each component is called the "component cost" and if one component (such as a sensor, actuator or flexible solar panel) has a much higher component cost than other components it might be redesigned for better "cost-balancing" (item 1) within the system. Component cost analysis can also be used to find the best distribution and number of sensors and actuators (item 2). The original application of component cost analysis was for model reduction. This method truncates those mathematical components of the system which have the smallest component costs (item 3). By adding a sensitivity term in the quadratic performance metric, the model reduction can be performed with due consideration of parameter uncertainty (item 4). In order to reduce the controller to meet the constraints of the flight software limitation, the "controller reduction" takes into account the coupling due to control feedback loops (item 5).

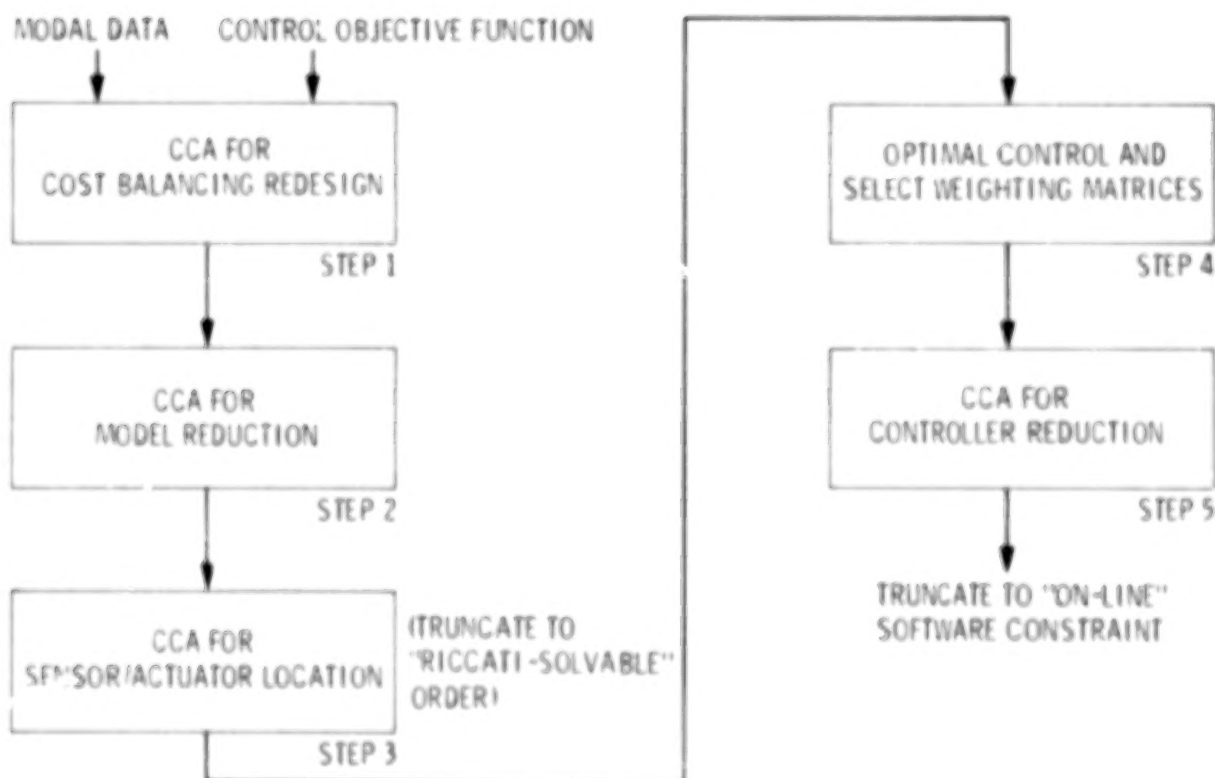
- PROBLEM: REDUCE THE EFFECTS OF MODEL ORDER ERRORS IN THE CONTROL OF LSS
- APPROACH: DEVELOP THE THEORY OF COMPONENT COST ANALYSIS (CCA) TO ASSIGN RELATIVE WEIGHTS TO THE VARIOUS CONTROL SYSTEM COMPONENTS
- FY '80 ACHIEVEMENTS: THE CCA ALGORITHM HAS BEEN PARTITIONED INTO SEVERAL BLOCKS. THE BLOCKS ARE SEQUENTIALLY BEING MECHANIZED FOR FUTURE DESIGN WORK. CCA HAS PROVIDED A UNIFIED THEORY FOR:
1. STRUCTURE REDESIGN
 2. SENSOR/ACTUATOR LOCATION
 3. MODEL REDUCTION CRITERIA
 4. PARAMETER SENSITIVITY REDUCTION
 5. DYNAMIC CONTROLLER REDUCTION

MODEL ORDER REDUCTION RESULTS

Under construction this year is an operational computer program which automates some of the design features of component cost analysis.

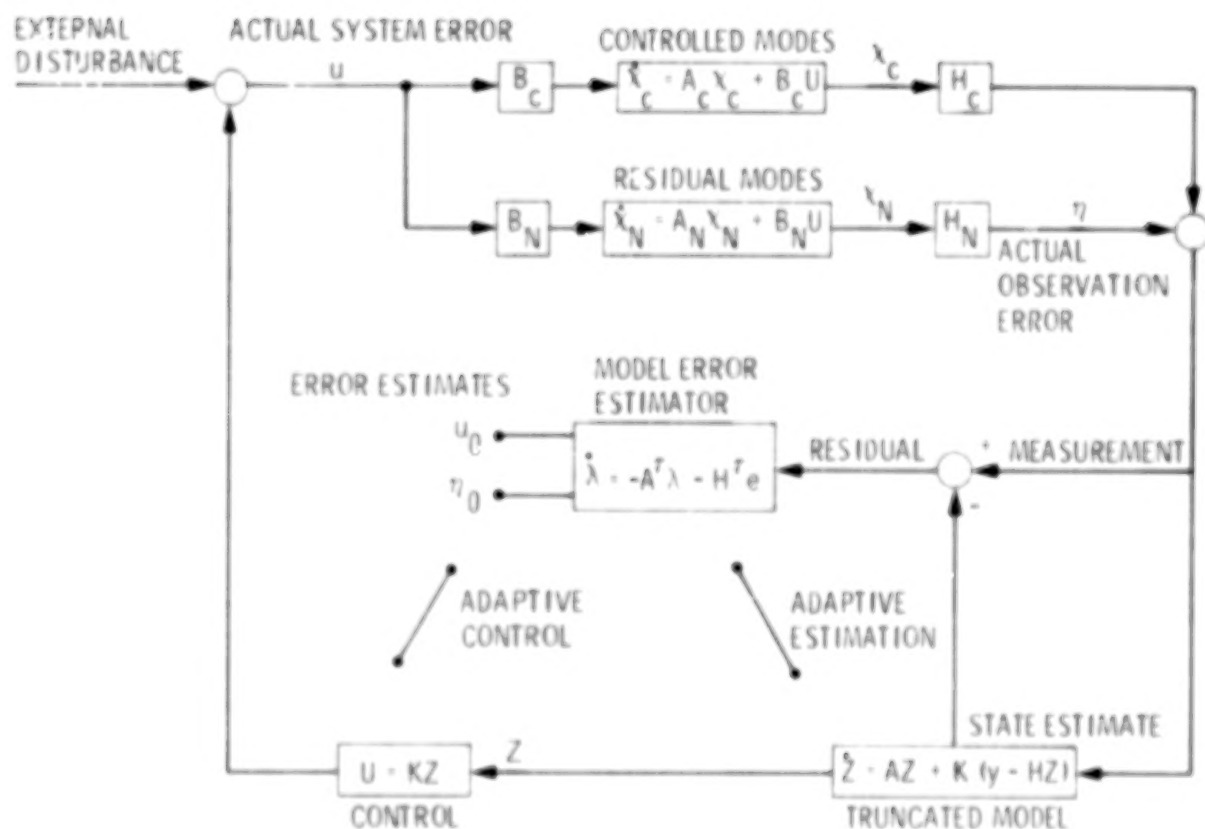
- Step 1 Can be utilized only when a specific mission is at hand. This slide illustrates the methodology.
- Step 2 Reduces the model order to the size that can be used in control design calculations.
- Step 3 Locates the sensor and actuators.
- Step 4 Solves the optimal control problem for a dimension that is still too large for on-line use.
- Step 5 Reduces the controller to acceptable on-line dimensions.

This step produces better controllers than can be obtained by simply reducing the model in Step 2 all the way down to on-line controller dimension. This is true because the open loop reduction schemes all ignore the coupling effects of the control feedback terms - whereas Step 5 does not ignore these terms in the reduction of the controller.



MODEL ERROR ESTIMATION WITH TRUNCATED MODEL

The process of model error estimation determines the errors inherent in the truncated dynamical models used for large structure controller designs. The truncated model shown on the lower portion of the viewgraph is based on the so-called controlled modes which constitute only a subset of the upper model describing the system dynamics. This truncation leads to inevitable errors (labeled system and observation) that can lead to degraded performance and at worst to potential instabilities. The model error estimation provides for autonomous detection and evaluation of these errors and therefore can be used to prevent system performance degradation. It can also be used as a foundation to develop adaptive control and estimation schemes. The FY'80 objectives were: 1) to develop the basic estimation know-how to determine model errors, 2) to conduct a model error estimate analysis for comparison of actual vs. estimated errors, and 3) to apply and verify the general analysis to systems typical of a flexible multibody spacecraft and a large platform-like structure.



MODEL ERROR ESTIMATION
FY'80 ACHIEVEMENTS

The major achievements included: 1) development of a new model error estimation scheme and detailed computation method that constitutes a state-of-the-art advance in estimation know-how, 2) development of error analysis techniques that establish that the error estimates retain the significant dynamics of the actual errors, 3) development of analysis software to automate estimator design and performance evaluation for arbitrary flexible multibody systems, 4) generation of model error analysis software to compare actual and estimated errors, and 5) verification of estimator performance for a representative flexible spacecraft and a platform structure. Future activities will be intended toward development of numerical methods required for on board implementation and extension of the model error estimation results to adaptive estimation and control.

- DEVELOPED NEW MODEL ERROR ESTIMATION SCHEME
- ESTABLISHED METHOD FOR DETAILED COMPUTATION OF MODEL ERROR ESTIMATES
- DEVELOPED MODEL ERROR ANALYSIS TECHNIQUES TO COMPARE ACTUAL AND ESTIMATED ERRORS
- DEVELOPED ANALYSIS SOFTWARE TO SIMULATE PERFORMANCE OF ERROR ESTIMATION PROCESS FOR ARBITRARY FLEXIBLE MULTIBODY SYSTEMS
- DEVELOPED COMPUTER PROGRAMS FOR EVALUATION OF RELATIONSHIPS BETWEEN ACTUAL AND ESTIMATED ERRORS
- VERIFIED ESTIMATOR PERFORMANCE FOR FLEXIBLE MULTIBODY SPACECRAFT AND PLATFORM-LIKE LARGE STRUCTURE

HARDWARE DEMONSTRATION

The hardware flexible beam facility construction was begun in FY'79, and completed during FY'80. Preliminary control system designs were implemented in FY'80. The facility consists of a hanging pinned-free flexible beam 3.8 m (12 1/2 feet) long, 150 mm (6 inches) wide, and 0.8 m (1/32 inches) thick. Four eddy current position sensors and three brushless d.c. motors are used for sensing and actuation. A microprocessor completes the control loop by sampling the sensor through the A/D converter, and by outputting the control command through the D/A converter. A chart recorder is used for recording results, and a tape recorder has been interfaced to store the control system parameters.

PROBLEM:

DEVELOP A FACILITY FOR DEMONSTRATING
AND VERIFYING

- SHAPE CONTROL
- DISTRIBUTED CONTROL
- ADAPTIVE CONTROL
- ROBUST CONTROL
- NON CO-LOCATED SENSORS/ACTUATORS

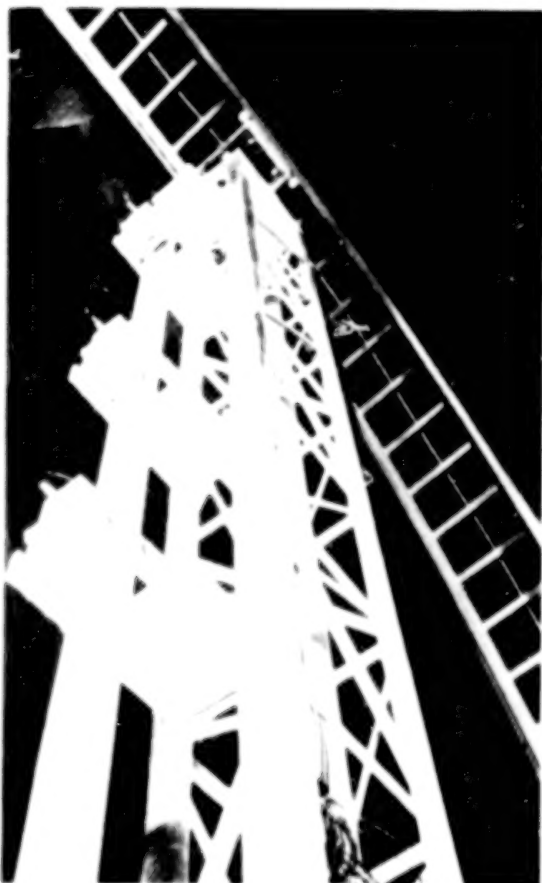
APPROACH:

DESIGN AND CONSTRUCT A PINNED FREE FLEXIBLE
BEAM EXPERIMENT WITH MULTIPLE SENSORS AND
ACTUATORS, AND AN UPGRADED MICROPROCESSOR
CONTROLLER

FY '80 ACHIEVEMENTS: THE FACILITY HAS BEEN COMPLETED AND CONTROL
SYSTEM DESIGN APPROACHES HAVE BEEN
IMPLEMENTED

PERFORMANCE EVALUATION - LABORATORY VERIFICATION

This viewgraph shows a photograph of the laboratory experimental facility developed at JPL. The experiment consists of a hanging pinned-free 3.8 m (12-1/2 foot) long stainless steel beam (150 mm (6") wide, 0.8 mm (1/32") thick). This configuration results in modal frequencies of 0.30, 0.74, 1.32, 2.00, 3.22, 5.72... hertz, and easily observed mode shapes. Four non-contacting eddy current position sensors and three brushless d.c. motor force actuators may be mounted at any station along the length of the beam. A microprocessor controller implements the estimation and control algorithms by sampling the sensors, updating the state estimates, and outputting the control command. The sample rate for a six state controller is 20 hertz.



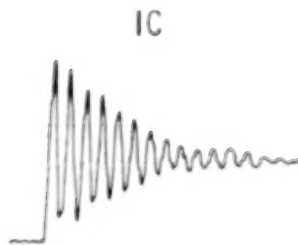
LABORATORY VERIFICATION

- VIBRATION SUPPRESSION
- STATIC SHAPE CONTROL
- DISTRIBUTED CONTROL
- ADAPTIVE CONTROL
- NON COLOCATED SENSORS AND ACTUATORS

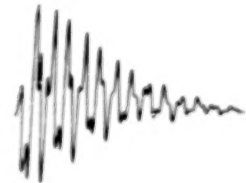
HARDWARE DEMONSTRATION RESULTS

Control system results are shown for a sixth-order estimator and controller, which uses only a single sensor and actuator located at the free end of the beam. First, the open-loop free-end responses to an initial condition and to an impulsive force are shown. The small amount of open loop damping is primarily due to atmospheric drag. Next, the same disturbances are repeated with the control system activated. Notice the more highly damped response. The residual oscillation in both cases is due to a small amount of spillover into the first unmodeled mode. By increasing the control gain just slightly, the first unmodeled mode is destabilized by the controller due to this spillover. With no input, the free end response can be seen to be growing exponentially.

OPEN LOOP
TIP RESPONSE



IMPULSE



CLOSED LOOP
TIP RESPONSE
(LOW GAIN)



CLOSED LOOP
TIP RESPONSE
(HIGH GAIN)



FUTURE WORK

In the future, the results of static shape control, and distributed control, will be generalized to include those systems modeled with finite elements. The flexible beam facility will be fully characterized to precisely determine the dynamic system to be studied, and extensive implementation of the various control system concepts will be performed. The model order reduction technique studied during FY'80 will be extended to include the case of uncertain parameters. Adaptive control laws will be developed to provide precise control in lieu of the uncertainty of the structural models before flight. The various components of the control system will then be integrated, and the numerical details for on board implementation studied. Finally, ground and flight experiments will be identified to show the capability of these extended control concepts.

- EXTEND CONTROL CONCEPTS TO FINITE ELEMENT MODELS - 1981
- CHARACTERIZE FLEXIBLE BEAM CONTROL FACILITY AND INITIATE EXTENSIVE EXPERIMENTATION WITH DISTRIBUTED AND SHAPE CONTROL - 1981
- EXTEND 1980 MODEL ORDER REDUCTION RESULTS TO INCLUDE PARAMETER UNCERTAINTIES - 1981
- DEVELOP SELF CONTAINED ADAPTIVE CONTROL DESIGN TECHNIQUES - 1981
- IDENTIFY LSS CONTROL SENSOR AND ACTUATOR REQUIREMENTS AND TECHNOLOGIES - 1981
- INTEGRATE SHAPE/ACTIVE CONTROL LAWS WITH SENSORS/ACTUATORS - 1982
- DEVELOP NUMERICAL METHODS FOR ON BOARD IMPLEMENTATION OF CONTROL SYSTEM - 1983
- DEFINE GROUND AND FLIGHT EXPERIMENTS - 1982/83

BLANK PAGE

BLANK PAGE

INTEGRATED ANALYSIS CAPABILITY (IAC) DEVELOPMENT

J. P. Young
NASA/Goddard Space Flight Center
Greenbelt, Maryland

Large Space Systems Technology--1980
Second Annual Technical Review
November 18-20, 1980

INTEGRATED ANALYSIS CAPABILITY (IAC)

Since reporting last year, there has been a maturing of thought during the FY 1980 period on the technical and programmatic aspects of this activity. For example the initial belief was that the Integrated Analysis Capability (IAC) use would be focused only on supporting the early to late preliminary design phase. After further consideration, it was realized that depending on the user's skill and experience, characteristics of the particular design task, analysis modules residing in the system, and complexity of the data base, applicability of the IAC can range from the definition phase to the final verification phase. This point of view is also supported in part by the recent requirement that the IAC must be capable of functioning in conjunction with IPAD. Another change in the development thrust has been to eliminate the consideration of mainframe computers as host machines for the IAC and concentrate entirely on use of super minicomputer systems as possibly augmented by array processors. From a programmatic point, the IAC development plan has been structured as a series of staged deliverables with the Level 1 system targeted for completion by the end of FY 1982.

OBJECTIVE

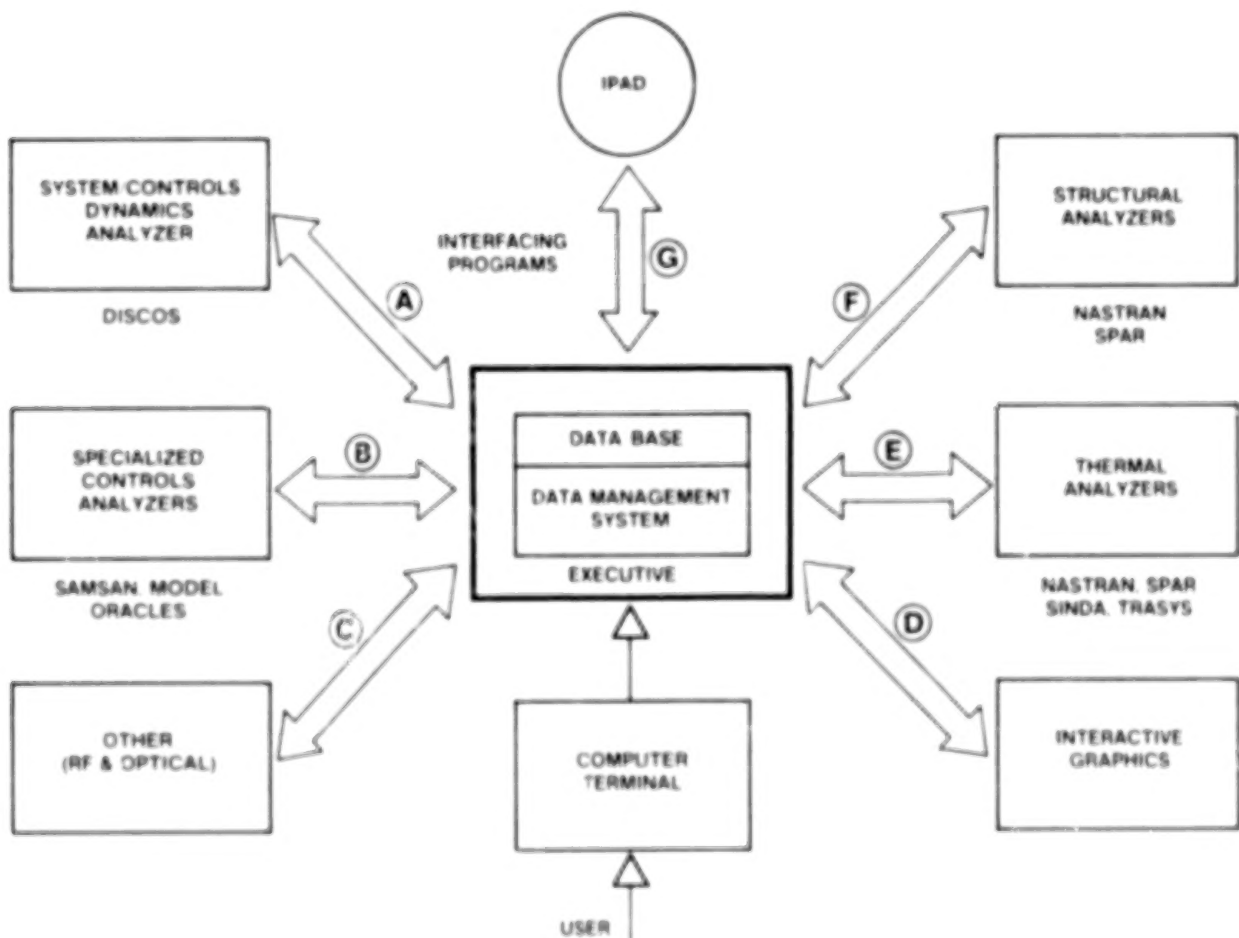
- **INTERDISCIPLINARY ANALYSIS SYSTEM CONTAINING WIDE RANGE OF GENERAL PURPOSE ANALYSIS PROGRAMS INTERFACED VIA A COMMON DATA BASE AND UNIFIED EXECUTIVE**
- **SYSTEM WILL BE DESIGNED WITH SIGNIFICANT INTERACTIVE CAPABILITY**
- **CAPABILITY WILL SUPPORT ENTIRE RANGE OF DESIGN PHASES FROM DEFINITION PHASE TO VERIFICATION PHASE**
- **SYSTEM TO FUNCTION EITHER STANDALONE OR INTERFACED WITH IPAD**
- **DEVELOPMENT ORIENTED TO USE OF SUPER MINICOMPUTERS**

GOAL

- **LEVEL 1 IAC SYSTEM DELIVERED BY END OF FY 1982**
- **STAGED DELIVERY OF ENHANCED LEVELS EACH OF FOLLOWING 3-YEARS**

IAC ARCHITECTURE

The IAC design has an architecture not too unlike any common data base based software system with a data handling capability and unified system executive command encircled by application programs and a key supportive interactive graphics module. The diagram also shows the required interface to IPAD. A very important aspect of the IAC system, as indicated by the "OTHER" module block, is that specific attention is being given to making the system "open ended" by facilitating the effort necessary to add other analysis capabilities. One design criterion for the early IAC release levels is to incorporate, where possible, analysis modules that are considered "industry standard." The most notable exceptions to this criterion are the SAMSAN and MODEL control system analysis related programs which are currently being developed at the Goddard Space Flight Center. Creation of the INTERFACE PROGRAMS, shown as the broad arrows A - G, constitutes a major part of the total IAC development activity. The bulk of the remaining task centers around building up the total data handling and executive systems.



IAC END PRODUCT

The IAC development plan can be viewed as composed of two phases - next five years (near term) and beyond (long range). The focus for the next five years will be to produce an end product that will support thermal, structures, and controls interdisciplinary/interactive analyses together with RF radiation and optical performance analyzers. With the basic interdisciplinary analysis capability well established, attention can then be given to adding other discipline analysis capabilities (e.g., contamination, formal structural design optimization methods, specialized analysis capability unique to systems whose geometric form is time varying, and modern control theory analysis techniques).

NEAR TERM (2-5 YEARS)

- **THERMAL/STRUCTURAL COUPLED ANALYSIS-SEQUENTIAL MODE**
- **STRUCTURAL/CONTROL SYSTEM COUPLED ANALYSIS**
- **QUASI-STATIC THERMAL/STRUCTURAL/CONTROL SYSTEM COUPLED ANALYSIS — A PRIORI DEFINED TEMPERATURES**
- **CLOSED LOOP THERMAL/STRUCTURAL/CONTROL SYSTEM ANALYSIS VIA USE OF THERMAL MODE CONCEPT**
- **RF RADIATION ANALYSIS**
- **OPTICAL PERFORMANCE ANALYSIS**

LONG RANGE

- **DESIGN ANALYSIS OPTIMIZATION METHODS**
- **CONTAMINATION ANALYSIS**
- **VARIABLE GEOMETRY ANALYSIS METHODS**
- **MODERN CONTROL THEORY ANALYSIS METHODS**

IAC DEVELOPMENT PLAN

This figure gives a picture of the projected staged level delivery schedule of the IAC through FY 1985. In addition, a FY 1980 accomplishment is shown as the completion of Phase I and delivery of a pilot program. The Level 1 through Level 4 IAC systems are shown as being completed on 1 year intervals starting the latter part of FY 1982. Each level will successively incorporate the additional capability as briefly noted in the chart. For definition of the solution paths (S/P) I-V as shown, refer to the following paper by R. G. Vos (Boeing Aerospace Company). The first host computer (H/C) will be the DEC VAX 11/780 super minicomputer manufactured by Digital Equipment Corporation. The second H/C has not yet been selected. Selection will be delayed as long as possible to allow the super minicomputer user market to further develop. Since a significant class of large space structures appear to be of a complex tension stiffened (T/S) member type of construction, the Level 3 IAC is projected to contain solution algorithms unique for such structures. The need for improved capability to analyze for geometric nonlinearities is anticipated and is projected for incorporation into the Level 4 IAC.

		FY					
MILESTONES		1980	1981	1982	1983	1984	1985
PHASE I COMPLETED PILOT PROGRAM		▼					
PHASE II LEVEL 1 IAC	NASTRAN BASED S/P I-IV, 1ST H/C SAMPLED DATA CONTROL		▬	▼			
PHASE II LEVEL 2 IAC	REDUNDANT THERMAL RF & OPTICS PERFORMANCE ENVIRONMENTAL LOADS			▬	▼		
PHASE II LEVEL 3 IAC	FULL REDUNDANCY COMPLEX T/S STRUCTURES IPAD LINK, 2ND H/C				▬	▼	
PHASE II LEVEL 4 IAC	S/P V GEOMETRIC NONLINEARITY					▬	▼

BOEING AEROSPACE COMPANY IAC CONTRACT STATUS

In July 1980, the Boeing Aerospace Company was awarded a contract for a detailed system definition of the IAC. The contract was for a 12-month Phase I effort to result in a system definition for the IAC and a proof-of-concept pilot program. In addition, the contract contained a pre-negotiated Phase II option for actual design and delivery of an operational IAC system. The Phase I activity was completed and the deliverables received July 1980. The Phase II option was also exercised in July 1980. The option specifies the delivery of a Level 1 IAC capability.

- **PRIME CONTRACTOR TO PRODUCE IAC SYSTEM**
- **PHASE I COMPLETED JULY 1980**
 - **DETAIL SYSTEM DEFINITION**
 - **PILOT PROGRAM**
- **PHASE II INITIATED JULY 1980**
 - **LEVEL 1 CAPABILITY**

GSFC IN-HOUSE IAC SUPPORT ACTIVITIES

During FY 1980, GSFC in-house accomplishments to support the IAC development were largely in the control system analysis discipline. Two of the accomplishments, as listed below, are uniquely related to analysis of sampled data control systems. The first item deals with the problem of formalistically setting up the mathematical equations required to define the dynamics of a sampled data feedback control system. The net result is a set of state variable equations compatible with standard follow-on analysis procedures. The outcome of the second item is a summary of a large body of relevant numerical error analysis literature in a language understandable to non-specialists. This information is principally related to eigenvalue problem solution of a general nature. The third item is an outgrowth of the second where it was recognized that there is a need for an algorithm which can be used to reduce the order of the full set of dynamic equations in such a manner that engineering insight into the problem is enhanced. Specifically, the output is a detail definition of a software program called BLOCK IT which implements the recently developed algorithm. As implied by the program title, the algorithm is based on the block diagonalization technique.

- **METHOD COMPLETED TO DEFINE SAMPLED DATA CONTROL SYSTEMS COMPATIBLE WITH IAC SYSTEM NEEDS**
- **ASSESSMENT COMPLETED OF INHERENT NUMERICAL ERROR CHARACTERISTICS OF ALGORITHMS TO BE USED FOR SYSTEM FREQUENCY RESPONSE**
- **ALGORITHM DEVELOPED FOR "ALMOST" DECOUPLING THE EQUATIONS OF MOTION OF A LINEAR MULTI-BODY SYSTEM SUBJECT TO LINEAR SAMPLED DATA FEEDBACK CONTROL**

BLANK PAGE

BLANK PAGE

INTEGRATED ANALYSIS CAPABILITY
PILOT COMPUTER PROGRAM

R. G. Vos
Boeing Aerospace Company
Seattle, Washington

Large Space Systems Technology - 1980
Second Annual Technical Review
November 18-20, 1980

IAC PILOT COMPUTER PROGRAM - SUMMARY

This paper describes some of the activities and software resulting from NASA Contract NAS5-25767, "Integrated Analysis Capability (IAC) for Large Space Systems". This contract is part of the NASA LSST program effort, with direction by the NASA Goddard Space Flight Center.

The end product of this work is to be an IAC computer software package for design analysis and performance evaluation of large space systems. The IAC will aid users in coupling the required technical disciplines (initially structures, thermal and controls), providing analysis solution paths which reveal critical interactive effects in order to study loads, stability and mission performance. Existing technical software modules, having a wide existing user community, will be combined with new interface software to bridge between the different technologies and mathematical modeling techniques. The package will be supported by executive, data management and interactive graphics software, with primary development within the super-minicomputer environment.

The Pilot Program software was developed during the IAC Phase I contract effort, in conjunction with a plan for the fully operational IAC system. The purpose of this software was to provide proof-of-concept for the IAC plan, and to serve as a testbed for further development. In addition to satisfying its intended purpose, the Pilot Program has been in successful operation at GSFC and BAC supporting actual project analyses.

The paper introduces a brief background of the IAC design, discusses the Pilot Program in this context, and concludes with a statement of the currently defined ongoing IAC contract activities. A summary of the topics covered is shown in Figure 1.

- IAC BACKGROUND
 - REQUIRED CAPABILITIES
 - TECHNICAL MODULES
 - INTEGRATION PHILOSOPHY
- PILOT PROGRAM
 - GENERAL ARCHITECTURE
 - EXECUTIVE FUNCTIONS
 - DATA HANDLING
 - SOLUTION PATHS
 - DEMO PROBLEM
- CURRENT DEVELOPMENT

Figure 1

IAC - REQUIRED CAPABILITIES

Much of the required technical capability of the IAC can be described as being part of one or more distinct "solution paths". Each path is actually a class of solutions, which consists of a number of selectable options and variations, rather than a rigidly predefined and automated process. An engineer-in-the-loop mode of operation is therefore possible and, in fact, emphasized. Currently, five such solution paths, as shown in Figure 2, have been defined. Paths I-III have been implemented to some degree within the Pilot Program. The dashed lines of Paths IV-V indicate capabilities which have not yet been initiated. The standalone (uncoupled) operation of each technology or major technical module is defined to be Solution Path I. Paths II through V involve an increasing degree of interdisciplinary coupling and corresponding greater complexity. Solution Path II provides thermal deformations via the coupling of a thermal analyzer such as SINDA or NASTRAN with a structural analyzer such as NASTRAN or SPAR. Obviously, a major coupling task is to handle the generally incompatible thermal and structural models. Path III accomplishes a structural/control analysis, in either the frequency or time domain, by providing required modal data from a structural analyzer to the DISCOS system dynamics module. Solution Path IV provides a time domain structural/control analysis, including a time varying but quasi-static thermal loading, i.e., thermal loads are unaffected by the dynamic motions. Finally, Path V provides a fully coupled analysis in the frequency domain, and is directed at problems such as thermal flutter of long spacecraft members. This last solution path requires development and verification of new analysis technology.

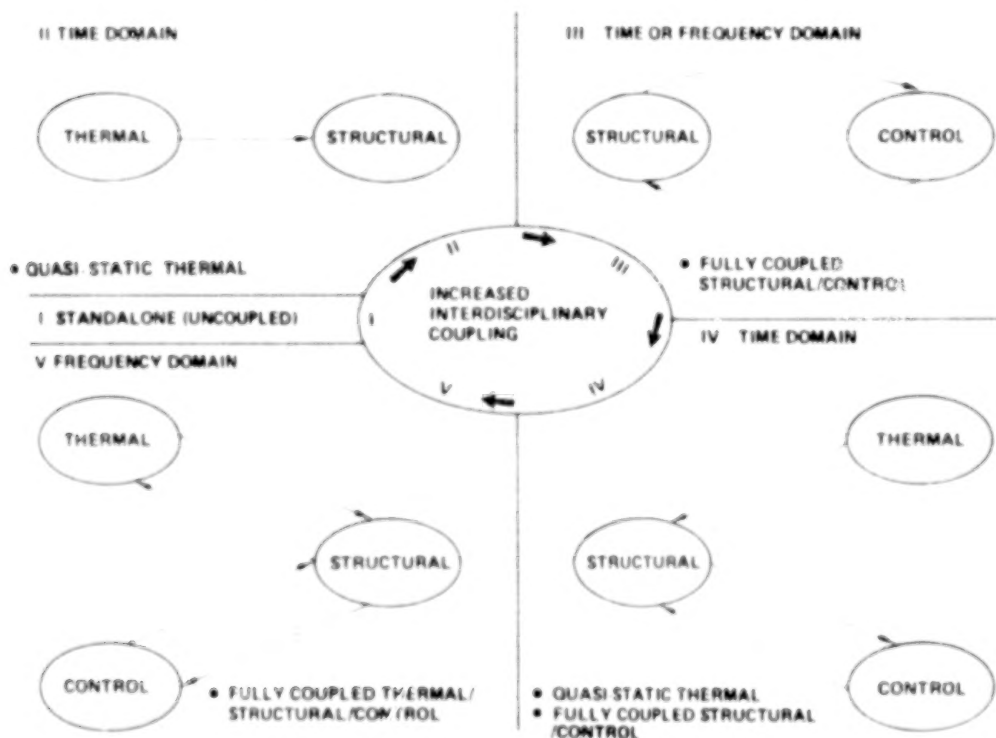


Figure 2

SELECTED TECHNICAL MODULES

The technical modules currently defined for implementation within the IAC are shown in Figure 3. These modules are classified into four technical groups - system dynamics, structural, thermal and controls. The solid lines indicate capabilities which have been incorporated into the Pilot Program. Dashed lines indicate capabilities which have been planned for the IAC, but not yet implemented. DISCOS (Dynamic Interaction Simulation of Controls and Structures) is an important computational backbone of the IAC system. The selected thermal and structural modules are generally well known within the technical community. ORACLS (Optimal Regulator Algorithms for the Control of Linear Systems) is a modern control theory design package. SAMSAN (SAMPled System ANalysis capability) is a package currently under development at GSFC.

It will be readily apparent to those familiar with the designated structural and thermal modules that there is some duplication of capability, e.g., NASTRAN/SPAR and SINDA/NASTRAN. This is due in part to a Phase I study and conclusion that both finite difference and finite element thermal codes should be available within the IAC. More importantly, it is the result of a conscious effort to provide alternate technical modules within several areas of the IAC, in order to support as wide an existing user community as practical.

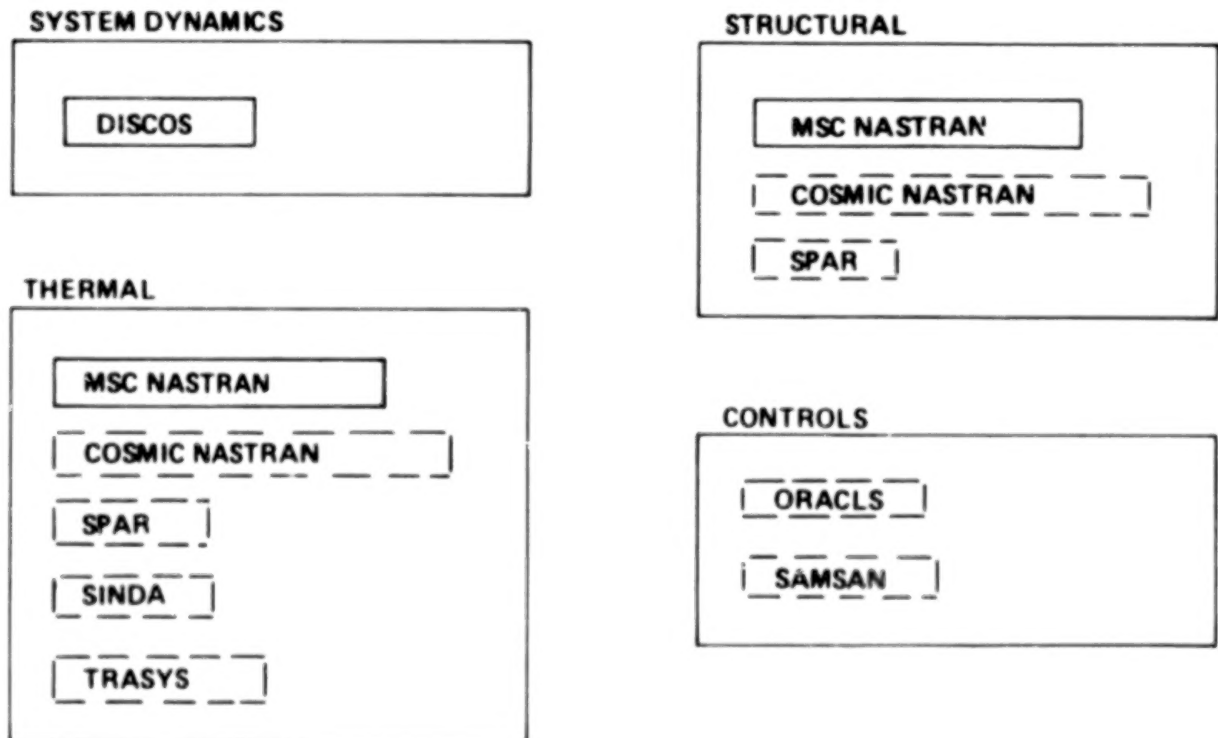


Figure 3

SYSTEM INTEGRATION PHILOSOPHY

The solution paths already discussed define the basic technical requirements of the IAC system. The selected technical modules provide major components for supporting the individual technologies represented within these paths, and required interdisciplinary couplings will be largely implemented via new interface software which bridges between the different technologies and mathematical modeling techniques.

At the overall system level, Figure 4 summarizes the philosophy for integration of the entire IAC package. Key characteristics required of the IAC are shown on the right, and components of the supporting software and hardware, as designed for the IAC and implemented within the Pilot Program, are given on the left. First, the computational complexities inherent in most LSS problems led to an early decision that the IAC must operate in an engineer-in-the-loop fashion, rather than in a highly automated "button pushing" mode of operation. A specialized executive program was designed to make all capabilities available to the engineer, in a modular but consistent and engineer-friendly manner. Second, in order to accomplish in-depth analyses with the selected technical modules, in a reasonably efficient and natural manner, it was concluded that a file oriented data management system would be essential. In order to provide effective user access to data, some enhancements to the file oriented system, relative to data identification and display, are planned. For the same reason, considerable emphasis will be given to interactive graphics. The modern super-minicomputers already offer many advantages for the IAC system, and their further improvement and widespread usage is expected. These machines will be used as the primary hardware environment for the IAC development.

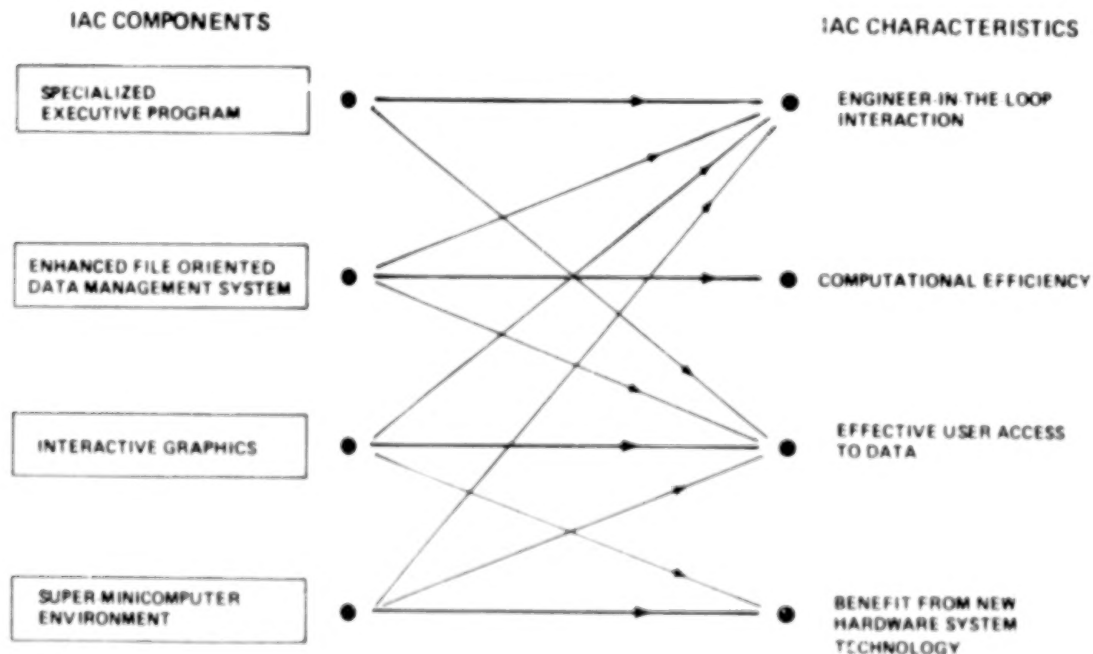


Figure 4

IAC PILOT PROGRAM ARCHITECTURE

A schematic of the Pilot Program architecture is shown in Figure 5. The executive provides the user with a common interface to all capabilities of the system. It contains a command interpreter and drivers for the system modules. Three data storage areas are provided by the Pilot Program. These consist of (1) a file oriented database; (2) a user workspace contained within the executive; and (3) the host file system. Utilities are provided to move data structures between these areas as required. Two major technical modules have been implemented within the Pilot Program. DISCOS provides system dynamics and controls capabilities; MSC NASTRAN provides general capabilities, with emphasis on structural statics and normal modes, and thermal steady state and transient analyses. Several interface modules have also been provided to establish necessary linkages between DISCOS and NASTRAN, and between NASTRAN thermal and structural capabilities. The Pilot Program provides basic ingredients of the IAC solution Paths I, II and III.

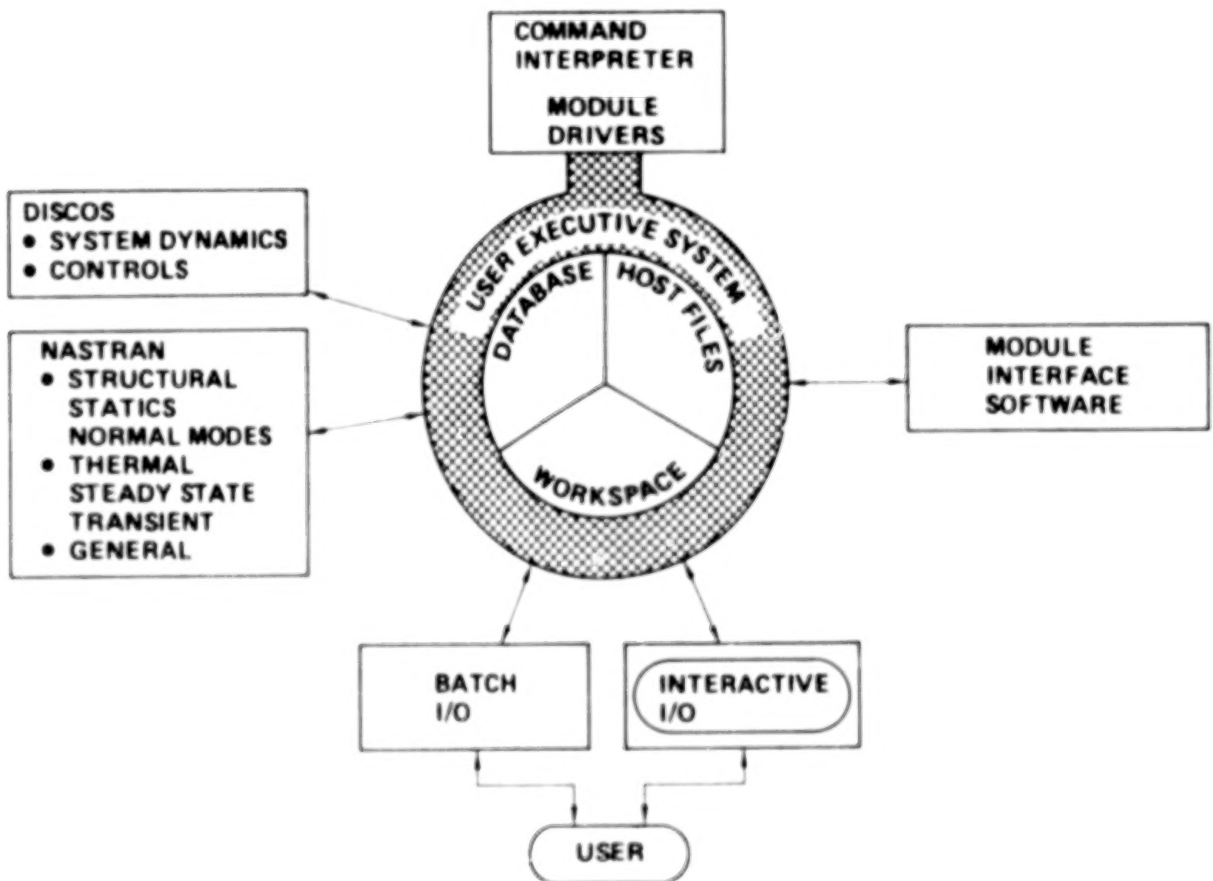


Figure 5

EXECUTIVE

The Pilot Program executive integrates other components of the system into a unified package, and provides the primary interface between the IAC and the user. A schematic of executive functions is shown in Figure 6. The executive provides a command language for executing both interactive and batch tasks. The emphasis is on interactive commands, however, modules are often executed in essentially a batch mode. The user accomplishes the mainstream of his tasks within the IAC "primary job". Within this job he may request the executive to execute a module with user specified parameters, under direct control of the host operating system. He may also request that a sequence of commands (including module executions) be initiated as a separate "secondary job", in a batch mode concurrently with the primary job. Computed secondary results can later be obtained from the printer or from storage. The user may also execute many general commands, to accomplish the identification or transfer of data structures, and to call special purpose executive routines for display of data or textual information.

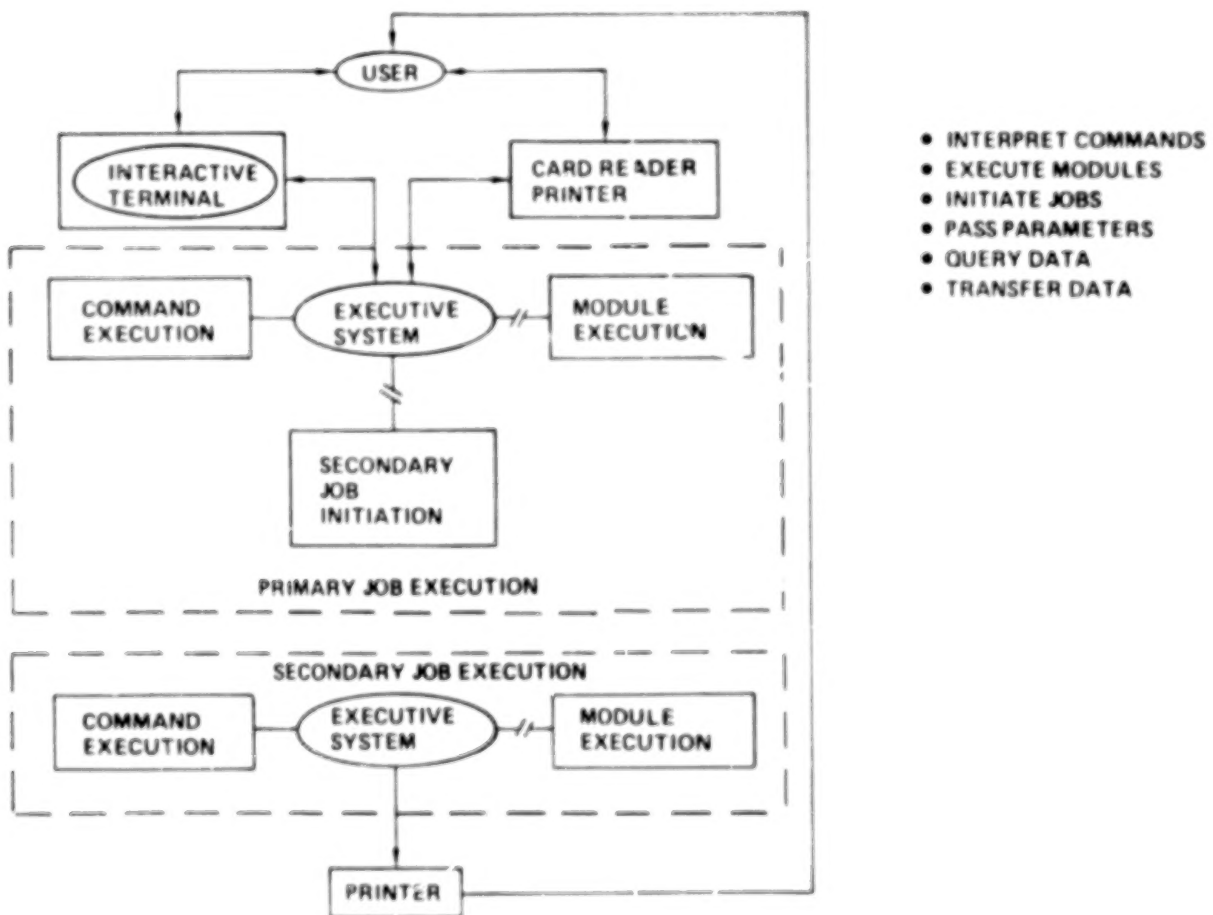


Figure 6

PILOT PROGRAM DATA HANDLING

A file oriented data handling approach has been designed for the IAC and implemented within the Pilot Program. Each file (also called "data structure") consists of one or more logical groups of information, which are stored in essentially a physically contiguous manner. The file oriented approach was chosen because of the primarily computational nature of the IAC system, and the need to achieve efficient data access for computational modules. The Pilot Program scheme for accessing and organizing files is represented in Figure 7. A database table of contents is shown on the left. Each row corresponds to a particular data structure, and contains attributes of, and a pointer to, that structure. The user may display and verify the identity of data structures prior to their use in computations. For example, a user might ask for display of the attributes of all data structures created by SMITH via the DISCOS module, subsequent to August 1980. The files themselves may reside either in the database, in a user workspace, or on the host file system. Each structure contains a small identifying header, an optional module- or user-generated textual definition, and the actual data itself. Textural definitions and data can be separately displayed using special purpose routines within the executive.

• FILE ORIENTED APPROACH DESIGNED FOR COMPUTATIONAL EFFICIENCY

* STORAGE/ACCESS VIA DATABASE, WORKSPACE, HOST FILES

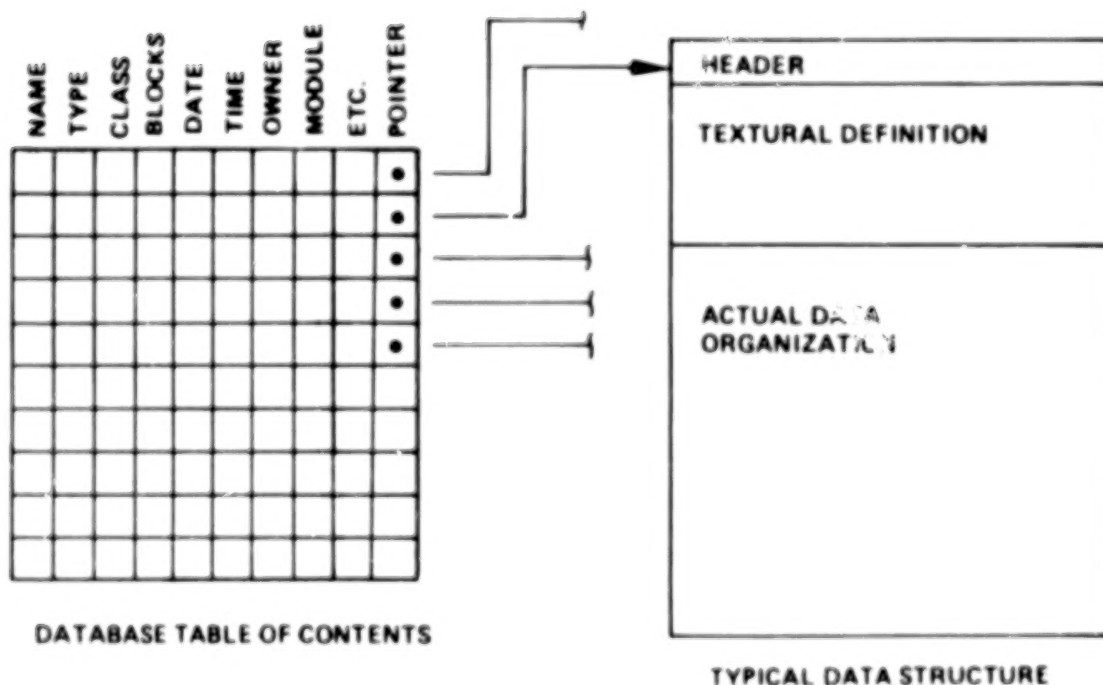


Figure 7

DATA STRUCTURES

The IAC planning effort concluded that three types of structured data are required by the IAC: arrays, tables and hierarchies. Hierarchical data are such that they can be represented in a tree type of structure. An example is the DISCOS state vector, where at each timewise integration point several levels of data are computed, associated with body, hinge or control system configuration and characteristics. Tables are 2-dimensional structures having a specified attribute (name and format) for each column. An example might be a table of gridpoint definitions, containing node ID, coordinate system, and x-y-z coordinate values. For computational purposes, emphasis has been placed on array type structures. These include vectors and matrices as special cases. Arrays are of arbitrary dimension (2-D and 3-D arrays have been used within the Pilot Program), and data access may be accomplished via either integer indices or integer/real/alphabetic labels. A simple example is shown in Figure 8 for the case of computed transient temperature data. Temperature values are stored in the 2-dimensional array, while gridpoint ID's and time values are stored in the vertical and horizontal labels, respectively. The array is a natural structure for this data, and many user queries may be satisfied via trivial search of only the labels. For example, a user might ask for display of temperatures corresponding to time 5.0, including all gridpoint ID's between 75 and 100. Display of maximum and minimum temperatures would be accomplished via search of the array itself.

- MAJOR IAC DATA TYPES: ARRAYS, TABLES, HIERARCHIES
- EMPHASIS ON ARRAYS (INCLUDES VECTOR/MATRIX DATA)

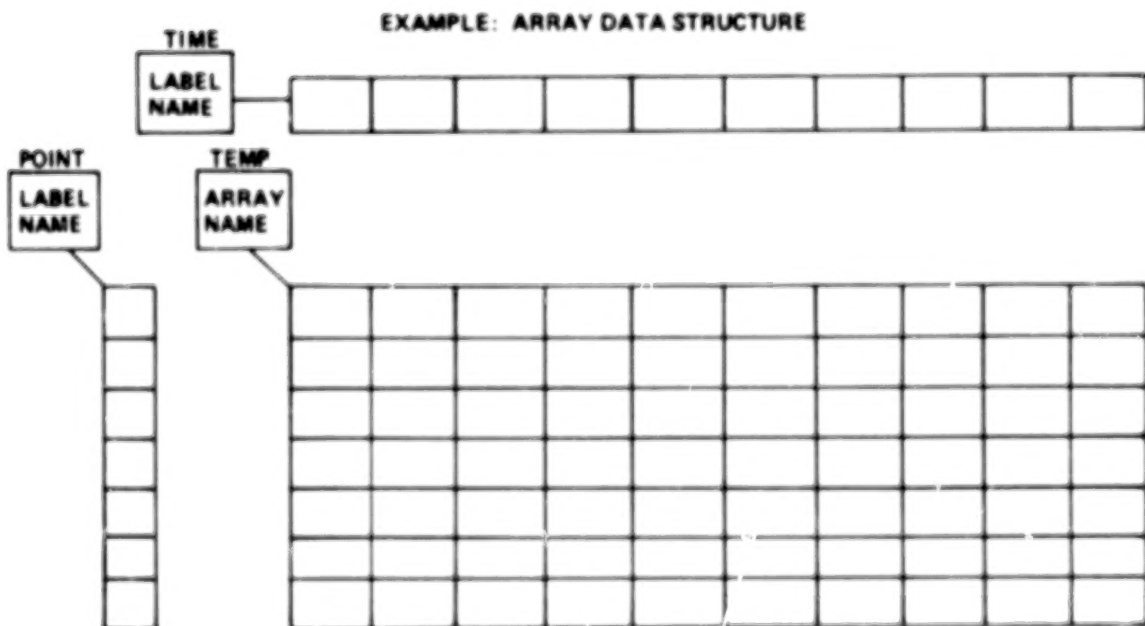


Figure 8

PILOT PROGRAM THERMAL/STRUCTURAL SOLUTION PATH

A schematic of the IAC thermal/structural solution path, as implemented within the Pilot Program, is given in Figure 9. This solution path involves a steady-state or transient thermal analysis to compute nodal temperatures, followed by a statics analysis to determine thermal deformations. The hexagons in the center column represent major technical or interface modules. Associated input/output data structures are shown on the left and right hand sides. User input commands, including required parameters, for executing each of the respective modules are listed at the bottom of the figure. The Pilot Program data-structure naming convention is defined by a two-part name.type specification. For example, an INSA module parameter F=TRUSS would cause the input file TRUSS.DAT to be read by INSA. The solution path begins by executing the NASTRAN thermal analyzer using a special IAC NASTRAN DMAP sequence (IACDMAP2), in order to output a file of gridpoint/time/temperature data. The INTA (Interface to NASTRAN Thermal Analyzer) module is then executed to put this data into a standard IAC format and store it in the database for possible intermediate examination by the user. The INSA (Interface to NASTRAN Static Analyzer) is run to take temperatures at user selected times, along with a partial NASTRAN input file, and generate a completed input file which includes thermal load sets and associated data control. The statics analyzer can then be run to obtain thermal deformations. Note that in this solution path a capability to accommodate different thermal and structural models is a major task which has not yet been implemented.

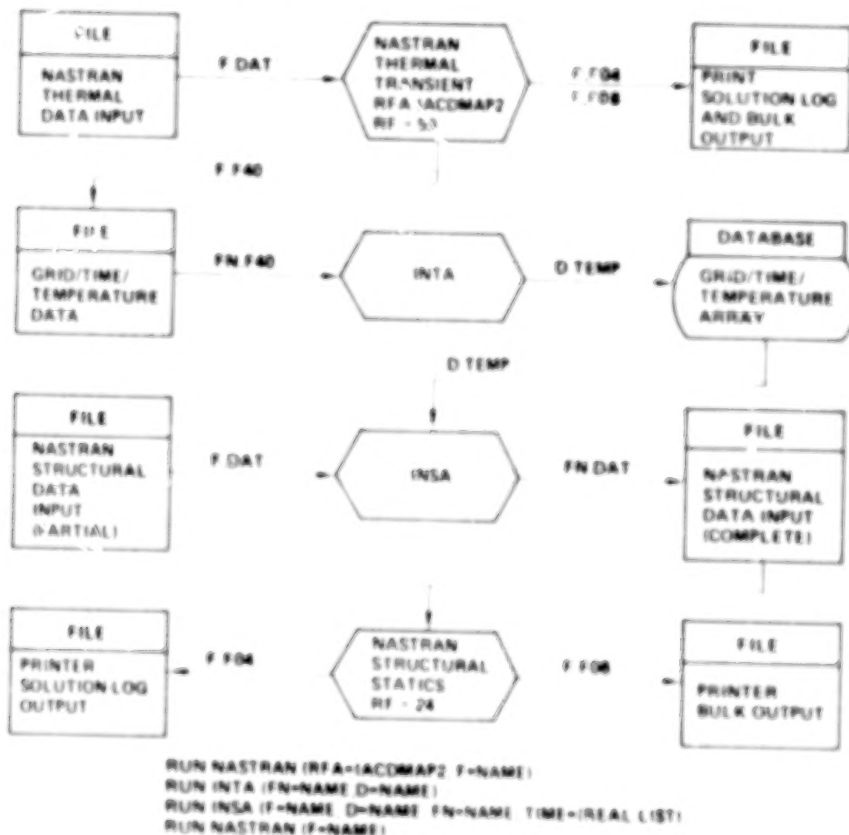


Figure 9.

PILOT PROGRAM STRUCTURAL/CONTROL SOLUTION PATH

A schematic of the Pilot Program structural/control solution path is given in Figure 10. This path provides either a time domain or frequency domain analysis for a multiple-flexible-body spacecraft, using modal data computed by a structural dynamics analyzer. Module execution commands and data structure handling follows the general approach already described for the thermal/structural path. The NASTRAN structural dynamics analyzer is run with a special DMAP sequence to output a variety of modal data (mass definitions, mode shapes, stiffness matrix, etc.). The INDA (Interface to NASTRAN Dynamics Analyzer) is run to place some or all of this data, corresponding to a user selected list of mode numbers, into the database. There the data is available for intermediate examination and verification. The DISCOS module is executed using an input file which contains references to required data types in the database. The DISCOS EXE parameter allows execution of a special version of DISCOS containing user defined subroutines. A DISCOS plot file is generated to provide for detailed interactive review of the computed results.

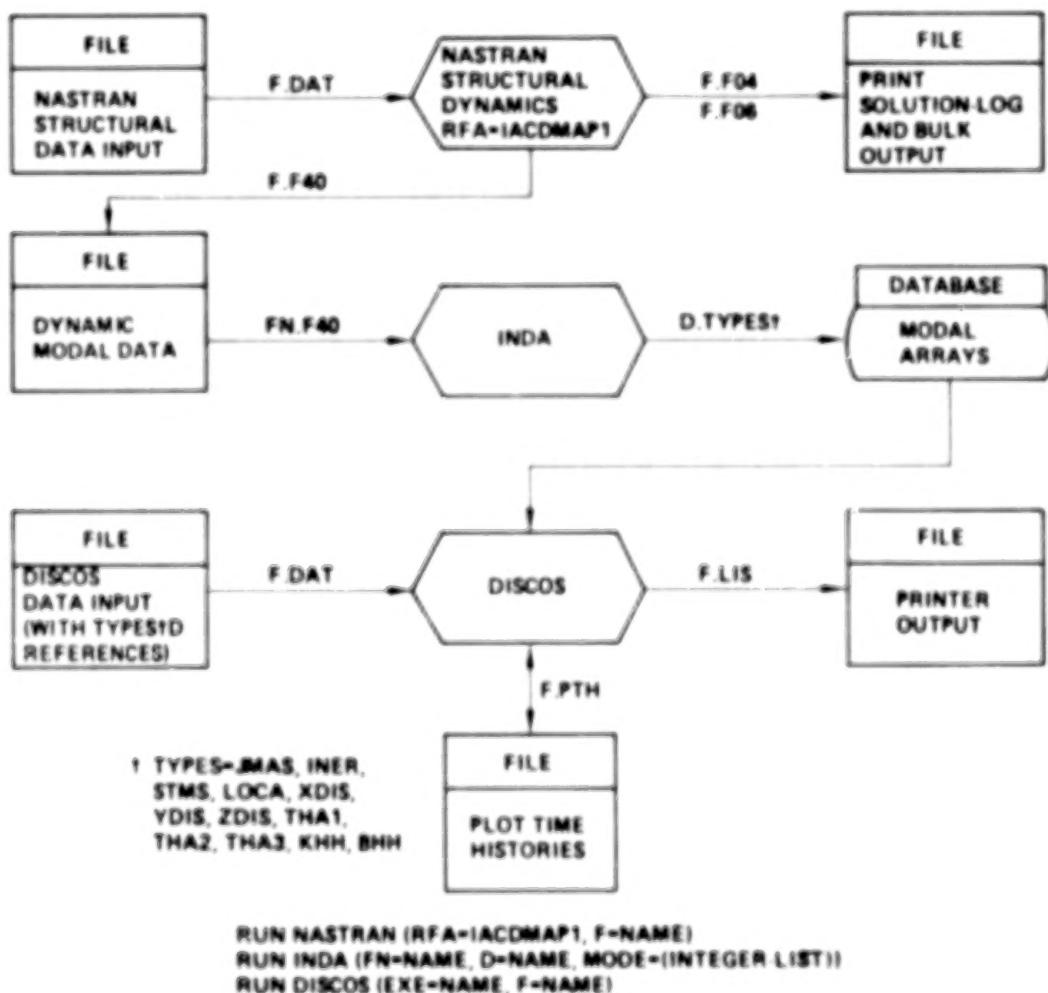


Figure 10

PILOT PROGRAM DEMONSTRATION PROBLEM

A 30-meter antenna demonstration problem was selected for the Phase I IAC effort, and was analyzed by the Pilot Program. The basic geometry and structural model for this antenna were defined by JPL. Two solution paths, thermal/structural and structural/control, were accomplished. In the thermal/structural path both steady-state and transient thermal analyses were performed, using heat loads determined for a geosynchronous orbit. These analyses included NASTRAN heat boundary elements and computed radiation exchange factors between surfaces. Thermal deformations were determined as an end result. In the structural/control path, both frequency domain and time domain analyses were performed. NASTRAN and DISCOS models are shown in Figure 11. The structural models contained 300+ degrees of freedom. The DISCOS model consisted of three bodies - the dish and feed tubes, the support structure, and the bus. DISCOS input modal characteristics were defined via NASTRAN dynamic analysis. A DISCOS 6-DOF hinge, with specified stiffnesses, was defined between the dish and support structure. A 1-DOF gimbal angle was defined between the bus and support structure, under the influence of a linear control system. Eigenvalue solutions were obtained for the entire NASTRAN model, for a NASTRAN dish and feed tube combination, and for the entire 3-body DISCOS model. The latter case included both fixed and controlled gimbal angle solutions. The DISCOS time domain analysis was performed based on an initial step command for altering the controlled gimbal freedom. Results of the demonstration analyses are available in the IAC Phase I final report.

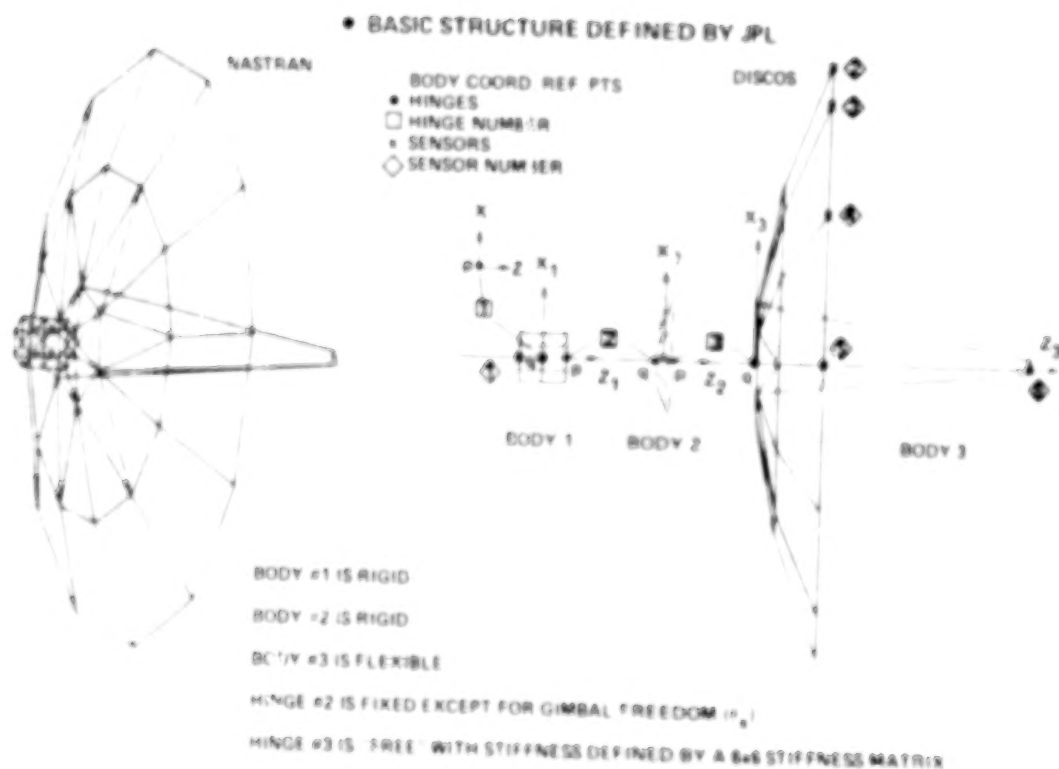


Figure 11

CURRENT DEVELOPMENT ACTIVITY

IAC Phase I contract activity, including the Pilot Program, was completed in June 1980. Current IAC development activity is summarized in Figure 12. Recognition of the Pilot Program as a simple but useful production level tool led to its use as a starting point for the development. The modules listed are those which will be incorporated in at least a standalone manner into an initial IAC software package. They will provide what is considered to be a non-redundant set of modules, i.e., without significant overlap in capability. Solution Path II is being further enhanced, primarily in the area of thermal/structural modeling integration (mesh compatibility) techniques. Path IV will be developed to a rudimentary but useful level in order to support analysis of time domain thermal/structural/control coupled problems. Executive, graphics and data management tools will be developed where necessary to support the required solution paths. In addition to deliverable software, an IAC functional specifications document and user manual will be developed.

- PILOT PROGRAM IS DEVELOPMENT STARTING POINT
- SOLUTION PATH I CAPABILITY, INCORPORATING
 - MSC NASTRAN
 - DISCOS
 - TRASYS
 - SINDA
 - INPUTB
 - ORACLS
- SOLUTION PATH II USING NASTRAN
- PARTIAL SOLUTION PATH IV
- EXECUTIVE, GRAPHICS, DATA MANAGEMENT TOOLS TO SUPPORT SOLUTION PATHS
- SOFTWARE, USER MANUAL, FUNCTIONAL SPECS

Figure 12

BLANK PAGE

BLANK PAGE

CONTENTS

VOLUME I - SYSTEMS TECHNOLOGY

PREFACE	iii	1/A7
1. LARGE SPACE SYSTEMS TECHNOLOGY OVERVIEW	1	1/A13
Robert L. James, Jr.		

SUPPORTING ACTIVITIES

2. LSST CONTROL TECHNOLOGY	9	1/B7
A. F. Tolivar		
3. ADVANCED CONTROL TECHNOLOGY FOR LSST ANTENNAS	19	1/C3
Y. H. Lin		
4. ADVANCED CONTROL TECHNOLOGY FOR LSST PLATFORM	31	1/D1
R. S. Edmunds		
5. CONTROL TECHNOLOGY DEVELOPMENT	49	1/E5
G. Rodriguez		
6. INTEGRATED ANALYSIS CAPABILITY (IAC) DEVELOPMENT	65	1/F7
J. P. Young		
7. INTEGRATED ANALYSIS CAPABILITY PILOT COMPUTER PROGRAM	73	1/G1
R. G. Vos		
8. AN ECONOMY OF SCALE SYSTEM'S MENSURATION OF LARGE SPACECRAFT	87	2/A4
L. J. DeRyder		
9. RADIATION EXPOSURE OF SELECTED COMPOSITES AND THIN FILMS	105	2/B8
Wayne S. Slomp and Beatrice Santos		
10. THERMAL EXPANSION OF COMPOSITES: METHODS AND RESULTS	119	2/C8
David E. Bowles and Darrel R. Tenney		

SPACE PLATFORMS

11. SPACE PLATFORM REFERENCE MISSION STUDIES OVERVIEW	129	2/D4
James K. Harrison		
12. ADVANCED SCIENCE AND APPLICATIONS SPACE PLATFORM	133	2/D8
Jack White and Fritz Runge		

13. STRUCTURAL REQUIREMENTS AND TECHNOLOGY NEEDS OF GEOSTATIONARY PLATFORMS	149 2/E10
G. R. Stone	
14. SUMMARY OF LSST SYSTEMS ANALYSIS AND INTEGRATION TASK FOR SPS FLIGHT TEST ARTICLES	167 2/F14
H. S. Greenberg	
15. ERECTABLE CONCEPTS FOR LARGE SPACE SYSTEM TECHNOLOGY	183 3/A5
W. E. Agan	
16. SPACE ASSEMBLY METHODOLOGY	199 3/B7
J. W. Stokes and H. H. Watters	
17. CONSTRUCTION ASSEMBLY AND OVERVIEW	217 3/C11
Lyle M. Jenkins	
18. SPACE PLATFORM ADVANCED TECHNOLOGY STUDY	229 3/D9
G. C. Burns	
19. A DOCUMENT DESCRIBING SHUTTLE CONSIDERATIONS FOR THE DESIGN OF LARGE SPACE STRUCTURES	243 3/E9
John A. Roebuck, Jr.	

SPACE ANTENNAS

20. ELECTROSTATIC MEMBRANE ANTENNA CONCEPT STUDIES	259 3/F11
J. W. Goslee	
21. ELECTROSTATIC ANTENNA SPACE ENVIRONMENT INTERACTION STUDY	271 3/G9
Ira Katz	
22. ENVIRONMENTAL EFFECTS AND LARGE SPACE SYSTEMS	279 4/A6
H. B. Garrett	
23. JPL ANTENNA TECHNOLOGY DEVELOPMENT	287 4/A14
R. E. Freeland	
24. OFFSET WRAP RIB ANTENNA CONCEPT DEVELOPMENT	295 4/B8
A. A. Woods, Jr.	
25. ANALYTICAL PERFORMANCE PREDICTION FOR LARGE ANTENNAS	325 4/D10
M. El-Raheb	
26. JPL SELF-PULSED LASER SURFACE MEASUREMENT SYSTEM DEVELOPMENT	339 4/E10
Martin Berdahl	
27. ANTENNA SYSTEMS REQUIREMENTS DEFINITION STUDY	349 4/F6
C. T. Golden	

28. HOOP/COLUMN ANTENNA TECHNOLOGY DEVELOPMENT SUMMARY	357	4/F14
Thomas G. Campbell		
29. DEVELOPMENT OF THE MAYPOLE (HOOP/COLUMN) DEPLOYABLE REFLECTOR CONCEPT FOR LARGE SPACE SYSTEMS APPLICATIONS	365	4/G8
D. C. Montgomery		
30. RADIO FREQUENCY PERFORMANCE PREDICTIONS FOR THE HOOP/COLUMN POINT DESIGN	407	5/C11
Thomas G. Campbell		
31. OFFSET FED UTILIZATION OF FOUR QUADRANTS OF AN AXIALLY SYMMETRICAL ANTENNA STRUCTURE	431	5/E7
P. Foldes		
32. SURFACE ACCURACY MEASUREMENT SENSOR FOR DEPLOYABLE REFLECTOR ANTENNAS	439	5/F1
R. B. Spiers, Jr.		
SECOND ANNUAL TECHNICAL REVIEW ATTENDEES	449	5/F11

AN ECONOMY OF SCALE
SYSTEM'S MENSURATION OF LARGE SPACECRAFT

L. J. DeRyder
NASA, Langley Research Center
Hampton, Virginia

Large Space Systems Technology - 1980
Second Annual Technical Review
November 18-20, 1980

An Economy of Scale - System's Mensuration of Large Spacecraft

Previous generalized studies (Ref. 1) have indicated that there are economic advantages of a large multifunctional platform system over a set of smaller customized special purpose spacecraft buses. The economy of scale has relied on the premise of accrued savings due to the sharing of common subsystem utility resources such as power, stability and control, orbit maintenance, structure, information systems, and navigation, as well as the premise that certain traffic model scenarios would produce lower transportation costs. However, the specific economic advantage of a particular platform design supporting a particular set of experiments has not been shown. A recent systems' study was performed at the NASA Langley Research Center to take a measured look at some of the technology developments and economic considerations involved in evaluating the two concepts, given the same set of mission objectives.

Spacecraft Economy of Scale Study

Specifically, the purpose of the study was to gain insight into the systems technology and cost particulars of using multipurpose platforms versus several sizes of bus-type free-flyer spacecraft to accomplish the same space experiment missions. A set of NASA Office of Space Science (OSS) and Office of Space and Terrestrial Applications (OSTA) experiment missions compatible with a Rockwell International (RI) science and application platform design (Ref. 2) were selected to size several spacecraft bus designs. Computer models of these spacecraft bus designs were created to obtain data relative to size, weight, power, performance, and cost. To answer the question of whether or not large scale does produce economy, the dominant cost factors had to be determined and the programmatic effect on individual experiment costs had to be evaluated.

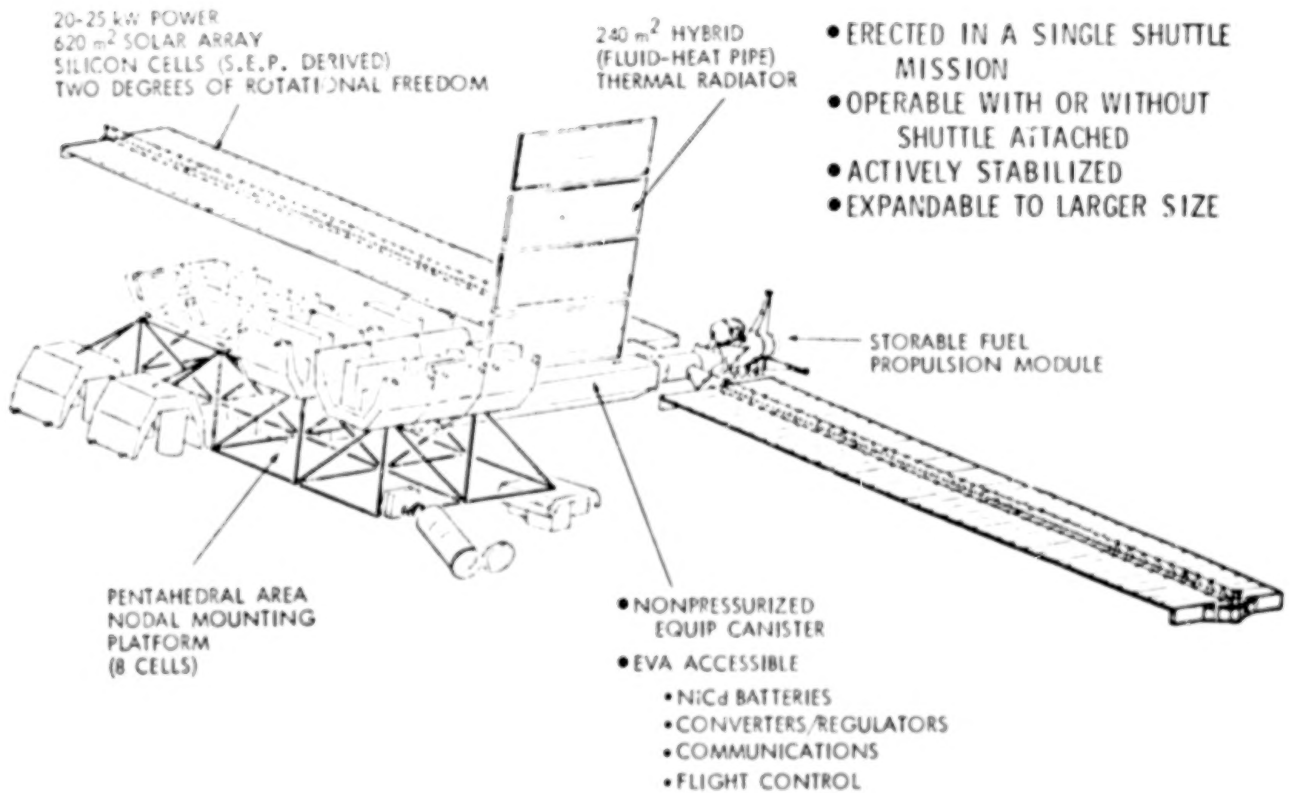
PURPOSE : TO GAIN INSIGHT INTO THE SYSTEM / SUBSYSTEM TECHNOLOGY
AND COST PARTICULARS OF USING MULTIPURPOSE SPACE PLATFORMS
VERSUS SEVERAL SIZES OF BUS-TYPE FREE-FLYER SPACECRAFT TO
ACCOMPLISH THE SAME SPACE EXPERIMENT MISSIONS.

APPROACH : A SET OF OSS / OSTA EXPERIMENT MISSIONS COMPATIBLE WITH A
ROCKWELL DESIGNED SCIENCE AND APPLICATIONS PLATFORM WERE
SELECTED TO SIZE SEVERAL SPACECRAFT BUS DESIGNS. COMPUTER
MODELS OF THE SPACECRAFT BUS DESIGNS AND THE ROCKWELL P-2
PLATFORM WERE CREATED TO OBTAIN DATA RELATIVE TO SIZE,
WEIGHT, POWER, PERFORMANCE, AND COST.

Baseline Configuration - Platform 2

Rockwell produced three platform system designs for the NASA Large Space System Technology (LSST) program as part of a 1979 study on Erectable Space Platforms for science and applications. For economy of scale analysis, the second Rockwell design, designated as P-2, was chosen from which a computer design and cost model was created. P-2 was chosen on the basis that its higher orbital inclination created the more difficult design and transportation requirement. The P-2 platform weighs 25,000 kilograms and consists of a 7,000 kilogram utility module and a 1,000 kilogram payload accommodation platform structure upon which 17,000 kilograms of payload equipment is housed.

(8 Payload Cells - Pentahedral Area Nodal Mounting)



Flight Experiments for Science and Applications Platform

The P-2 platform accommodates seven science experiments: Solar Physics I (SP 1), Solar Physics II (SP 2), Landsat D (LAND D), System 85 Operational Polar Satellite (SYS 85), Solar Optical Telescope (SOT, National Oceanic Satellite System (NOSS), High Energy Pallet II (HEP II), whose mission objectives include Earth surveillance, solar terrestrial observation, astronomy and cosmology and space physics. Specifically the seven experiments had the following objectives:

- | | |
|---|---|
| 1. Solar Physics 1 | Measure solar spectral and magnetic characteristics |
| 2. Solar Physics 2 | Solar gamma ray measurements from solar flares |
| 3. Landsat D | Earth resource agricultural observations |
| 4. Systems 85 Operational Polar Satellite | Operational weather satellite for climatology and water budget estimation |
| 5. Solar Optical Telescope | High spatial resolution studies using 1.25m UV/IR spectroscopy |
| 6. National Oceanic Satellite System | Provide global observation of ocean surface conditions |
| 7. High Energy Pallet II | Cosmic ray instrument to measure isotropic composition of solar F_{10} nuclei |

EXPERIMENT TITLE	SIZE (EQUIV. PALLETS)	WEIGHT (KILOGRAMS)	POWER (WATTS)
SOLAR PHYSICS 1 (SP 1)	1 / 2	1000	500
SOLAR PHYSICS 2 (SP 2)	1 / 2	1000	50
LANDSAT D (LAND D)	1	2131	500
SYSTEMS 85 OPERATIONAL POLAR SATELLITE (SYS 85)	1	1000	500
SOLAR OPTICAL TELESCOPE (SOT)	3	3820	1800
NATIONAL OCEANIC SATELLITE SYSTEM (NOSS)	3	6599	2500
HIGH ENERGY PALLET II (HEP 2)	3	3000	200
TOTALS	12	18550	6050

Multi-Mission Modular Spacecraft (MMS)

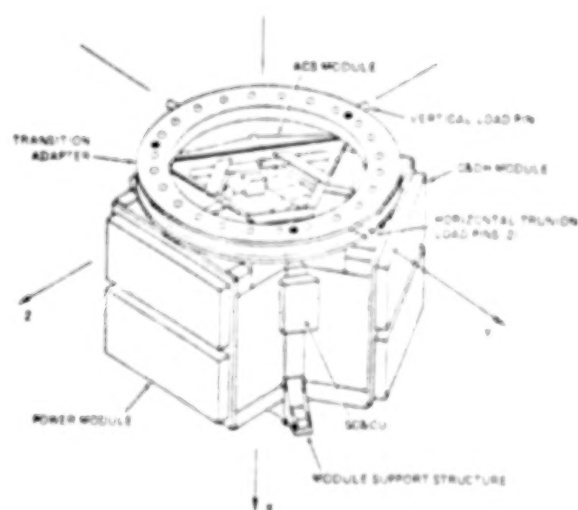
The various free-flyer spacecraft used for analyses were designed and priced against a state-of-the-art design represented by the Multi-Mission Modular Spacecraft (MMS).¹ As each spacecraft was designed to accommodate a particular experiment mission, individual subsystem capability was adjusted to meet the experiment payloads performance requirements. In terms of size, as related to equivalent space Shuttle orbiter pallets, the individual experiments volumetric requirements ranged in size from one-half a pallet to three pallets.

MMS subsystem component technical and cost characteristics were provided from the Planning Research Corporation (PRC).² In addition, PRC subsystem cost models were used to independently verify the computer model of the baseline MMS design. As the subsystem capability was adjusted upward to meet the individual payload mission requirements, individual subsystem costs were adjusted using cost estimating relationships (CER) that take into account weight, power, and performance.

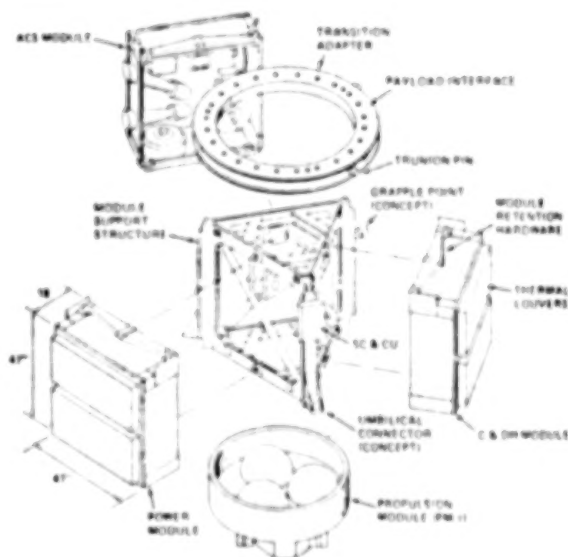
¹Goddard Space Flight Center, specifications unpublished.

²NASA Contract NAS1-15109.

ASSEMBLED VIEW

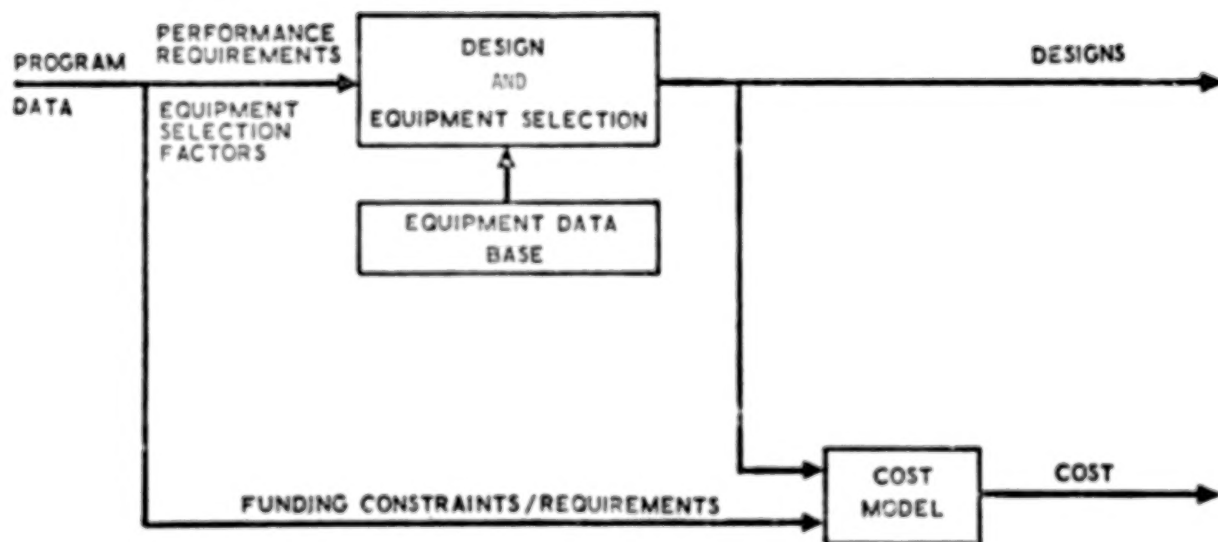


EXPLODED VIEW OF SUBSYSTEMS



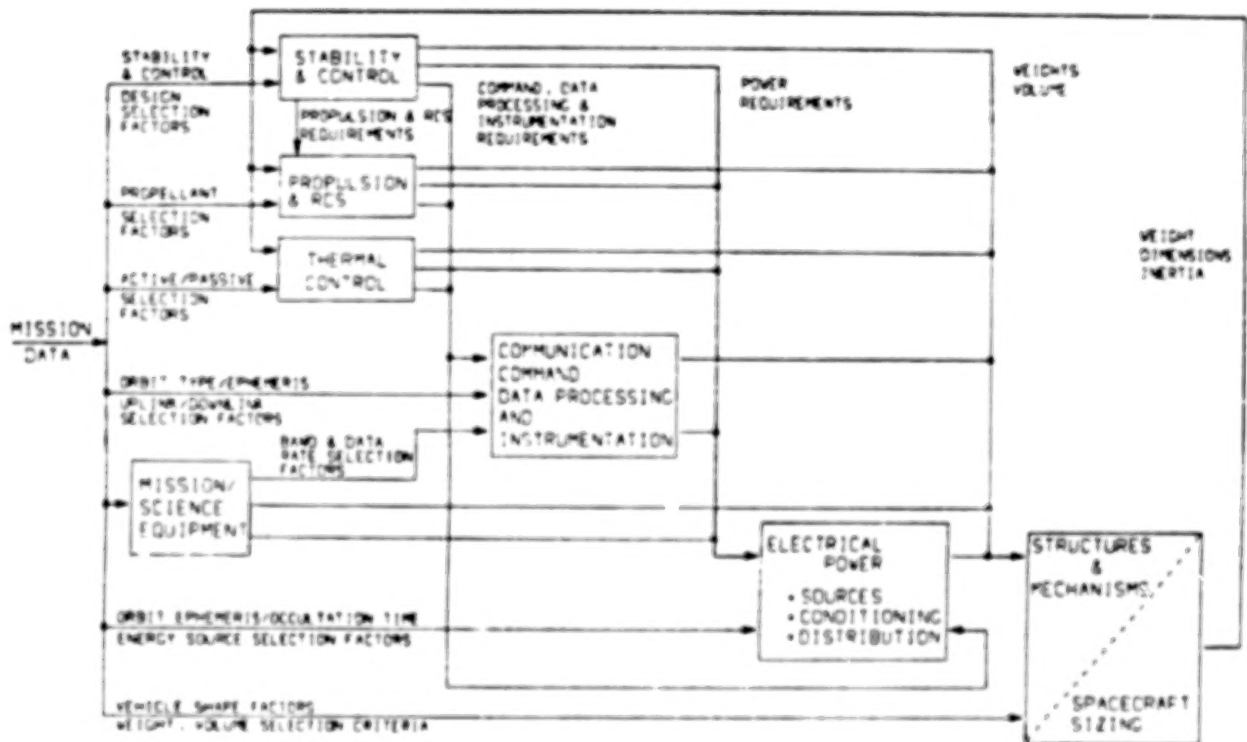
Space Systems Computer-Aided Design and Cost

Over the past 2 1/2 years, the NASA Langley Research Center has compiled several major sets of computer software which have been brought together to provide a spacecraft computer-aided design and costing capability. This capability is used to evaluate and trade-off design concepts and to evaluate the effects of systems technology advancements for new and existing spacecraft designs. The basic tool used for this study was the Spacecraft Design and Cost Model (SDCM), (Ref. 3). This tool is an interactive computer program which allows analysts to create spacecraft designs sized to meet specific missions and performance requirements. Spacecraft descriptions produced by this technique include subsystem selection, sizing, reliability, redundancy, and most importantly for this study, spacecraft cost. As shown, the program performs design calculations for each of the spacecraft subsystems, then sorts through a data base of prestored spacecraft components, selecting appropriate equipment to satisfy the performance requirements.



Spacecraft Subsystem Design

System designs created by the process of matching performance requirements to data base capability, in the first execution cycle of the program, are refined during subsequent program iterations on the basis of performance, reliability, and cost. The design process is performed on a subsystem-by-subsystem basis until a system level design and cost convergence is achieved.



Free-Flyer Mission Scenarios

Four flight programs consisting of seven flights each were modeled as a family of free-flyer mission scenarios. Parametric spacecraft bus designs were created for each experiment. The number of spacecraft designed and the number of recurring units for each spacecraft procured were logically varied for each flight program. Since each flight program required seven flights to accomplish its objectives, spacecraft designs were created by setting up four design modeling cases which correspond to the four flight programs.

FOUR PROGRAMS WITH SEVEN FLIGHTS EACH

PROGRAM 1 - SEVEN UNIQUE SPACECRAFT DESIGNS, ONE EACH FOR SP 1, SP 2, SYS 85, LAND D, HEP 2, NOSS, SOT

PROGRAM 2 - FOUR UNIQUE SPACECRAFT DESIGNS :

- 1 - SOT
- 2 - NOSS
- 3 - HEP 2
- 4 - SP 1, SP 2, SYS 85, LAND D

PROGRAM 3 - TWO UNIQUE SPACECRAFT DESIGNS :

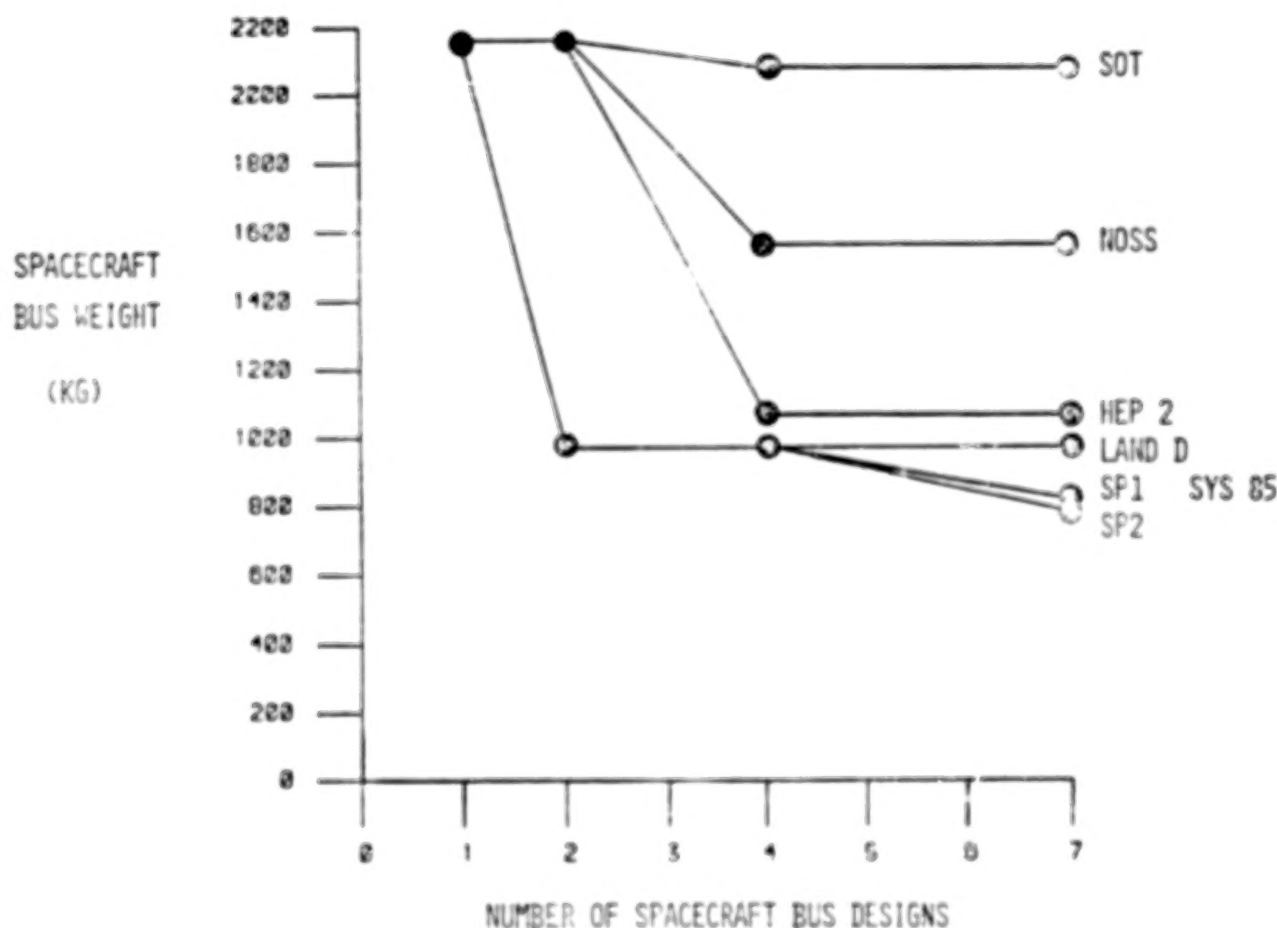
- 1 - SOT, NOSS, HEP 2
- 2 - SP 1, SP 2, SYS 85, LAND D

PROGRAM 4 - ONE SPACECRAFT DESIGN

Spacecraft Bus Scaling

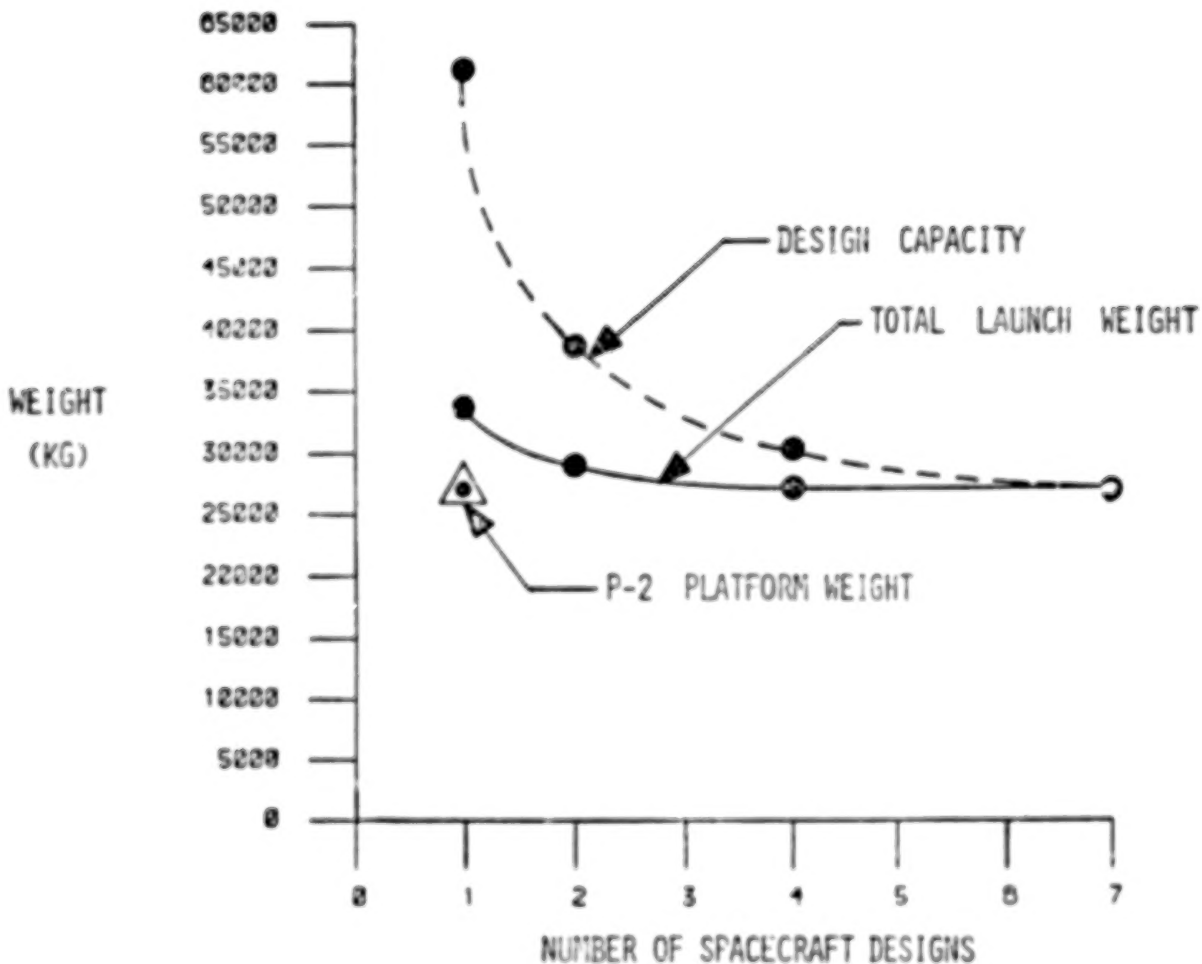
As the number of bus designs decreased from seven unique designs, one for each of the individual payload flights, to one common bus design, the spacecraft system performance had to be expanded to satisfy the composite set of seven experiment requirements which increased as the number of bus designs decreased. The overall spacecraft bus system weight growth depicted shows that the single bus design converges at a bus weight of 2,200 kg which is only slightly larger than the 2,100 kg spacecraft design individually tailored to meet the Solar Optical Telescope requirements.

The MMS subsystem performance specifications were considered to be the minimum acceptable for free-flyer computer design convergence. However, only three payloads, SP 1, SP 2, and SYS 85, were accommodated by the baseline MMS requirements. All other payloads required subsystem performance adjustments upward resulting in upward growth in overall bus weight varying from the 680-kilogram MMS baseline to the 2,100-kilogram bus designed for the SOT payload.



Total Mass to Orbit

The significance of upgraded performance capability with respect to system weight growth can be shown by observing the growth characteristics of common bus designs which occur as systems capabilities are increased to satisfy the composite set of experiments. The graph shows how the total mass to orbit is affected as the performance is increased for each bus design. The larger number of spacecraft designs represents the smaller spacecraft individually tailored to its unique payload, whereas the single spacecraft design represents the larger spacecraft which is individually tailored to accommodate the larger payload. As the number of spacecraft designs decreases from seven to four, to two, and finally to one spacecraft, the bus capabilities are under-utilized for specific experiment missions. The smaller experiment payloads are flown on the larger buses with excess capability. A measure of this capability is shown by the dashed line. Because of off-loading, the capacity or total mass to orbit possible if the spacecraft and transportation system were fully loaded would be almost twice the required mass. Also, when total mass to orbit is considered with respect to transportation system utilization, the platform is almost identical with the total mass of the seven flights/seven designs mass optimized scenario of the free-flying bus program.



Economy of Scale Cost Elements (\$ Millions)

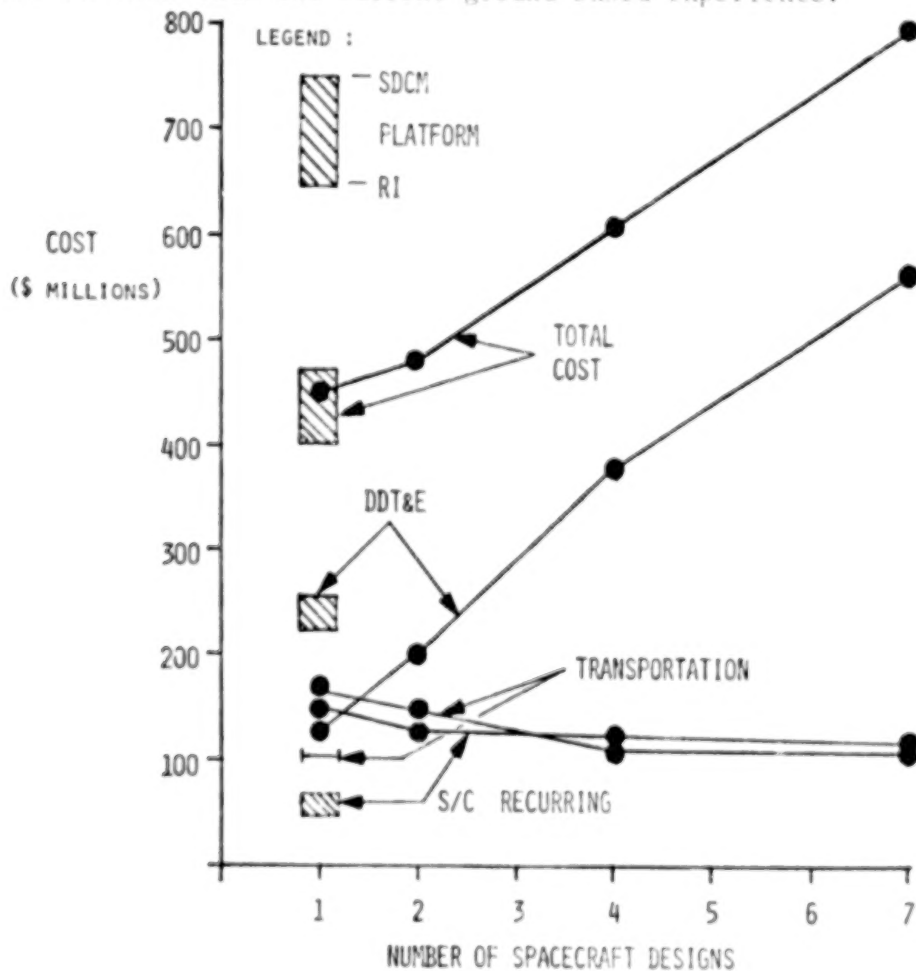
As the parametric bus designs were created, the attendant costs were accumulated in the categories of design, development, test, and engineering (DDT&E); recurring spacecraft; transportation; and total program cost. All costs are adjusted to 1980 dollars and the costs for the payloads and the pallets were assumed to be zero. For the four free-flyer programs, the computer model costing algorithms were set up such that the DDT&E costs included the cost of a qualification vehicle one of which was required for each spacecraft bus design. For the P-2 platform, the costing algorithms were set up for two cases: one with a qualification vehicle and one which only developed a so-called protoflight platform. Rockwell's rough-order-of-magnitude costs generated during their design study priced only a protoflight case which did not include a qualification vehicle.

FLIGHT PROGRAMS	NUMBER OF SPACECRAFT DESIGNS	DDT&E	SPACECRAFT RECURRING	TRANSPORTATION AND OPERATIONS	TOTAL PROGRAM
<u>FREE FLYER</u>					
NUMBER 1	7	561	117	112	790
NUMBER 2	4	376	119	114	609
NUMBER 3	2	198	132	148	478
NUMBER 4	1	124	154	168	446
<u>P-2 PLATFORM</u>					
ROCKWELL	1	224	71	110	405
COMPUTER MODEL A (N/O QUAL)	1	250	55	110	415
COMPUTER MODEL B (W/QUAL)	1	305	55	110	469

Program Cost Elements

The dominant cost of the free-flyer programs which utilize the larger number of smaller spacecraft designs is the DDT&E cost element. The total program cost is reduced by almost one-half by reducing the number of spacecraft designed, developed and tested. When spacecraft designs were used for more than one experiment payload, the DDT&E was amortized over the entire flight program. For the seven experiment set, the utilization of the larger common bus design reduces the development cost below both the transportation cost and the spacecraft recurring cost. Also due to the reduction in transportation cost and the spacecraft recurring cost, the platform total cost is comparable to the single spacecraft design case.

In this study, the computer cost model assumes that all of the DDT&E costs for each spacecraft including the platform is accomplished on the ground prior to launch. In the case of the platform, the upper limit for program cost is taken to be the case that models the flight platform and a qualification platform. However, the final spacecraft assembly, payload integration and checkout is envisioned by current mission planners to be accomplished in orbit. No cost data exists for this eventuality. A substantial advancement in technology must be achieved in order to reduce the orbital integration and checkout to less than the current ground-based experience.



Spacecraft and Launch Costs Proportioned by Weight (\$ Millions)

Experiment programs in the past have had to contend with absorbing the full per-copy spacecraft cost as well as payload integration costs as the overhead for using a particular bus. An examination of the programmatic impact on a single user clearly indicates that the larger bus and the platform are more cost effective. Shown here is the cost variation of each flight experiment parametrically with program and spacecraft scenarios. The spacecraft costs were distributed to each experiment by the weight carried to orbit rather than a per-copy cost of the last spacecraft. Such a charge plan is consistent with the Shuttle program cost philosophy as opposed to a per-copy cost philosophy that is characteristic of past spacecraft bus programs. Per-copy costs favor the larger payloads and the weight distribution costs favor the smaller payloads. In either case, however, the major conclusions remain unchanged.

PROGRAM	SP 1	SP 2	LAND D	SYS 85	NOSS	SOT	HEP 2	TOTAL COST	AVG. BUS & LAUNCH
<u>FREE FLYER</u> (7 FLIGHTS)									
7 S/C DESIGNS	93	91	105	93	133	163	112	790	113
1 S/C DESIGN	49	49	59	49	74	98	66	446	63
<u>P-2 PLATFORM</u>									
ROCKWELL	22	22	46	22	83	144	66	405	
COMPUTER MODEL A (W/O QUAL)	22	22	48	22	22	148	67	415	
COMPUTER MODEL B (W/QUAL)	25	24	54	25	97	167	75	469	

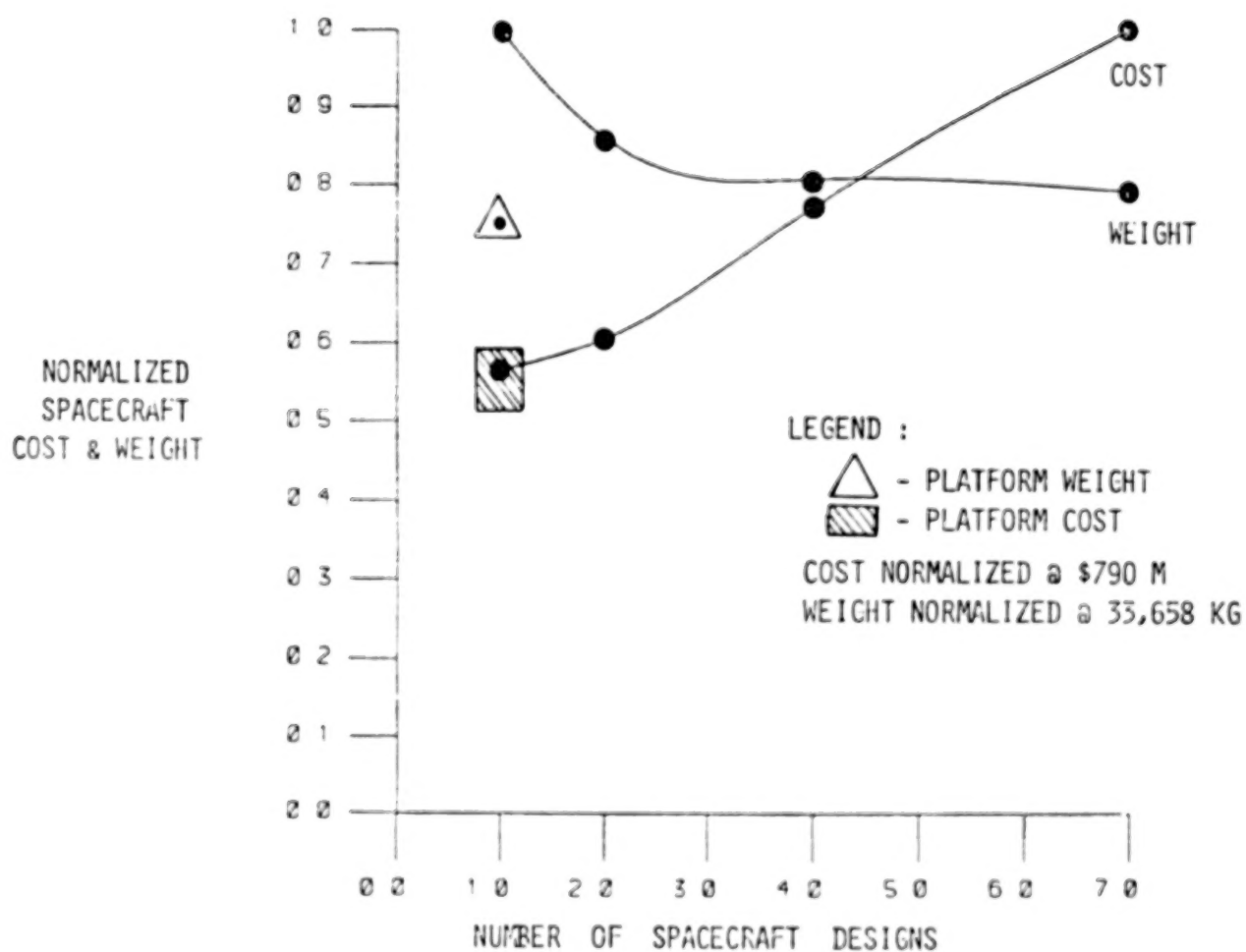
Economy of Scale Summary

For the selected set of OSTA/OSS science and application missions selected for study, analysis has shown that there is economy associated with large scale, as graphically shown by the normalized weight and cost summary curves. As has been shown, the larger multimission bus gains its cost advantages over the smaller special purpose spacecraft due to amortization of its larger development cost over several flights. The platform is cost competitive with the multimission bus for the same reasons, that is, DDT&E amortization, and not so much for on-orbit sharing of utility resources. In this case, any economics associated with on-orbit resource sharing is a direct function of the transportation cost of getting the experiment to the platform. It may also be seen that the platform offers a transportation cost advantage potential over the large multimission bus because it requires less total mass to orbit to support the equivalent experiment set.

In addition, any future achievement of reducing on-orbit test and check-out below the current ground based experience can be a significant plus for space platforms. The programmatic effect on individual experiment cost can be even more significant than currently shown to be by this study.

- o LARGE SCALE DOES PRODUCE ECONOMY
- o DDT & E COST IS THE DOMINANT FACTOR
- o PLATFORM OFFERS GREATER TRANSPORTATION COST ADVANTAGE DUE TO LESS TOTAL MASS TO ORBIT
- o NO DATA EXIST ON THE COST OF TEST AND CHECK-OUT IN ORBIT
- o PROGRAMMATIC EFFECT ON INDIVIDUAL EXPERIMENT COST SIGNIFICANT

Normalized Weight and Cost Summary Curves for Economy of Scale Study



References

1. Cuneo, William J., Jr., and Williams, Dell P., III, "Space Platforms for NASA - Opportunity or Pitfall?" Space - The Best is Yet to Come, Proceedings of the 16th Space Congress, Cocoa Beach, Florida, April 25-27, 1979.
2. "Erectable Space Platform for Science and Applications," Final Report, SSD-79-0074, Rockwell International, 1979.
3. "Systems Cost/Performance Analysis (Study 2.3), Final Report," ATR-75-(7363)-3, Aerospace Corporation, 1975.

BLANK PAGE

BLANK PAGE

RADIATION EXPOSURE OF SELECTED COMPOSITES AND THIN FILMS

Wayne S. Slomp and Beatrice Santos
Langley Research Center

LSST Second Annual Technical Review
November 18-20, 1980

Materials for Advanced Space Systems

Graphite fiber reinforced polymeric matrix composite materials have emerged as prime candidate materials for structural applications in large space systems because of good strength, high stiffness, low density and high dimensional stability. However, the performance of these composites in the space radiation environment for long-term missions is unknown. Because most polymeric materials are known to undergo changes in physical and/or mechanical properties when exposed to electron and proton radiation found in the Earth's trapped radiation belts, a program designed to evaluate the effect of this radiation on selected candidate composite materials was initiated by the Langley Research Center. This paper presents some of the initial significant results from this research program.

The major studies included in the Radiation Effects on Materials for Advanced Space Systems program are outlined in figure 1 with the results expected from these studies. Because of equipment limitations, the radiation effects studies have used single parameter (electron or proton) radiation exposure for evaluation for polymeric films and composite materials. One study, performed by TRW, also evaluated the effects of in-situ (during irradiation), in vacuum (radiation off, specimens maintained in vacuum) and in air (radiation off, vacuum chamber bled up to air) testing on tensile properties of composites before and after irradiation.

The major studies during FY-81 and FY-82 will be combined (electron and proton) and sequential radiation exposure of films and composites, identification of radiation damage mechanisms and measurement of the coefficient of thermal expansion (CTE) of composite materials.

<u>MAJOR STUDIES</u>	<u>EXPECTED RESULTS</u>
SINGLE PARAMETER RADIATION EXPOSURE OF FILMS AND COMPOSITES	ASSESSMENT OF SPACE DURABILITY OF COMPOSITES
POST-RADIATION EVALUATION (IN-SITU, VACUUM, DRY-AIR)	ACCELERATED EXPOSURE TEST METHODOLOGY
COMBINED AND SEQUENTIAL RADIATION EXPOSURE OF FILMS AND COMPOSITES	ASSESSMENT OF γ , e^- AND p^+ RADIATION DAMAGE TO COMPOSITES
CTE MEASUREMENT OF COMPOSITES	DIMENSIONALLY STABLE COMPOSITES FOR SPACE STRUCTURES
PHYSICAL/CHEMICAL ANALYSIS OF RADIATION DAMAGE IN POLYMERS AND COMPOSITES	IDENTIFICATION OF RADIATION DAMAGE MECHANISMS

Figure 1

Major Radiation Effects Contracts

Two major contracts were active during FY-80 to support and augment the Langley in-house radiation effects program. In the first contract, Langley supplied specimens and Boeing performed the irradiation. These specimens were shipped back to Langley for evaluation. Miniature (6.3 mm x 31.8 mm) flexure composite specimens and polymeric films were exposed to 1 MeV electrons with doses from 1×10^8 rads to 1×10^{10} rads.

The second contract was with TRW. Langley also supplied these specimens to TRW's specifications but TRW performed the irradiation and testing. The tensile specimens used in these studies were ($\pm 45^\circ/\mp 45^\circ$) 4-ply, 9.5 mm wide x 50.8 mm long with tapered tabs bonded on each end leaving a 25.4 mm gage length. These specimens were exposed in a configuration allowing 18 specimens to be irradiated simultaneously. The specimens were irradiated with 700 keV electrons to doses from 1×10^9 to 1×10^{10} rads.

Some of the significant results from these irradiations are presented in the following figures, starting with the studies of the effects of radiation on polysulfone films.

RADIATION EXPOSURE OF COMPOSITES
AND POLYMERIC FILMS - NAS1-15606

BOEING AEROSPACE

- o 1.0 MeV ELECTRONS
- o MINIATURE FLEXURE SPECIMENS
- o TESTING PERFORMED IN AIR AT
LANGLEY RESEARCH CENTER

RADIATION TESTING OF COMPOSITE MATERIALS
IN-SITU VERSUS EX-SITU EFFECTS
NAS1-15848

TRW-DEFENSE AND SPACE SYSTEMS GROUP

- o 700 KeV ELECTRONS
- o MINIATURE TENSILE SPECIMENS
- o TESTING PERFORMED IN AIR AND
IN VACUUM AT TRW

Figure 2

Preparation of Polysulfone Films for Radiation Testing

Figure 3 shows the molecular structures of the four polysulfones studied. Solutions of each polymer were made in concentrations between 5 and 10% in the solvents indicated in the figure. Films of each polysulfone were cast in a dust free, low humidity box by coating a mechanically driven glass plate with the polymer-solvent solution. The glass plate was moved at constant velocity underneath a Gardner knife edge which was set to obtain a film thickness no greater than $2.54 (10)^{-5}$ m (one mil). After air-drying in the dry box, the films were removed from the glass plate and placed in an oven to remove residual solvent. The drying conditions used are as follows: 12 hours at 200°C in vacuum for Radel 5000; 1 hour at 150°C in nitrogen for P-1700; 12 hours at 225°C in vacuum for Polyethersulfone; and 12 hours at 200°C in vacuum for Bisphenol-A Hydroquinone. Verification of the solvent removal process was obtained by thermogravimetric analysis. The solvent-free films were then cut into 5.4 cm squares with slits of various widths corresponding to sizes needed for different characterization techniques. These squares were examined for thickness uniformity and did not exceed a thickness of $2.54 (10)^{-5}$ m. The films were then packaged and sent to Boeing Aerospace and irradiated at various dose rates and dose levels, using a 4 MeV Dynamitron in the electron or proton modes. Following irradiation, all films were stored at room temperature in a vacuum chamber to prevent moisture absorption. The following graphs show only the 1 MeV electron irradiation effects data.



Figure 3

Effect of Electron Radiation on the Glass Transition Temperature of Polysulfones

The effect of total electron dose on the glass transition temperature (T_g) of the four polysulfones is shown in figure 4. The values of T_g were obtained using a Dupont Model 994 Thermal Mechanical Analyzer in the tensile mode. The value on the y-axis represents the T_g for the unirradiated film. Total electron radiation doses between 10^8 and 10^{10} rads at $2(10)^8$ rad/hr were obtained for each polymer film.

All of the polymers exhibited a change in T_g following irradiation, particularly at 10^{10} rad total dose. An increase in T_g of about 15% above the unirradiated value was generally observed at 10^{10} rad for all polysulfones. This increase, with the exception of the Radel 5000 curve, was preceded by a lowering of the T_g between 10^8 and 10^9 rad. The observed two-stage change, T_g decrease between 10^8 and 10^9 rad and T_g increase between 10^9 and 10^{10} rad, may suggest that electron radiation interacts with polysulfones through two mechanisms: degradation (chain-scission) and crosslinking. Degradation could result in a T_g decrease, while crosslinking could cause a T_g increase. Of the four polysulfones studied in this investigation, Radel 5000 appears to have the highest threshold before a change in T_g is observed.

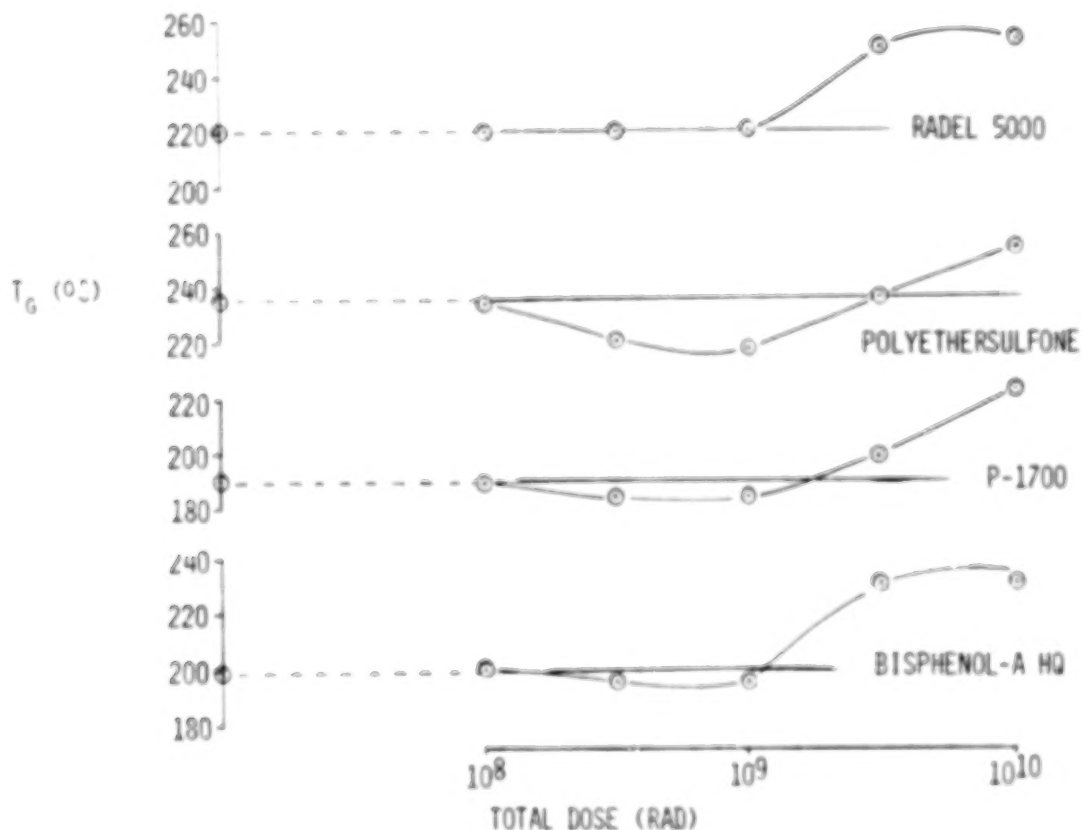


Figure 4

Effect of Electron Radiation on the Modulus of Polysulfones

The effect of total electron dose on the observed modulus of polysulfone films following irradiation between 10^8 and 10^{10} rad at $2(10)^8$ rad/hr is shown in figure 5. The modulus of the unirradiated film is given on the y-axis. Modulus values were obtained using an automated Rheovibron, with all data obtained at a frequency of 3.5 Hz.

When determining a modulus value, the film was inserted in the Rheovibron, several readings were taken, and the film was removed completely from the clamps and re-mounted. Several readings were again taken. This was done to attempt to eliminate sample mounting effects. All modulus values obtained for that particular film were then averaged.

For all materials, the modulus increased as dose level increased, and the threshold value for a major change in modulus appears to be near 10^9 rad. The percent increase ranges from about 24% for P-1700, to 58% for Radel 5000. This increase with higher dose suggests that crosslinking is occurring in all materials, particularly after 10^9 rad.

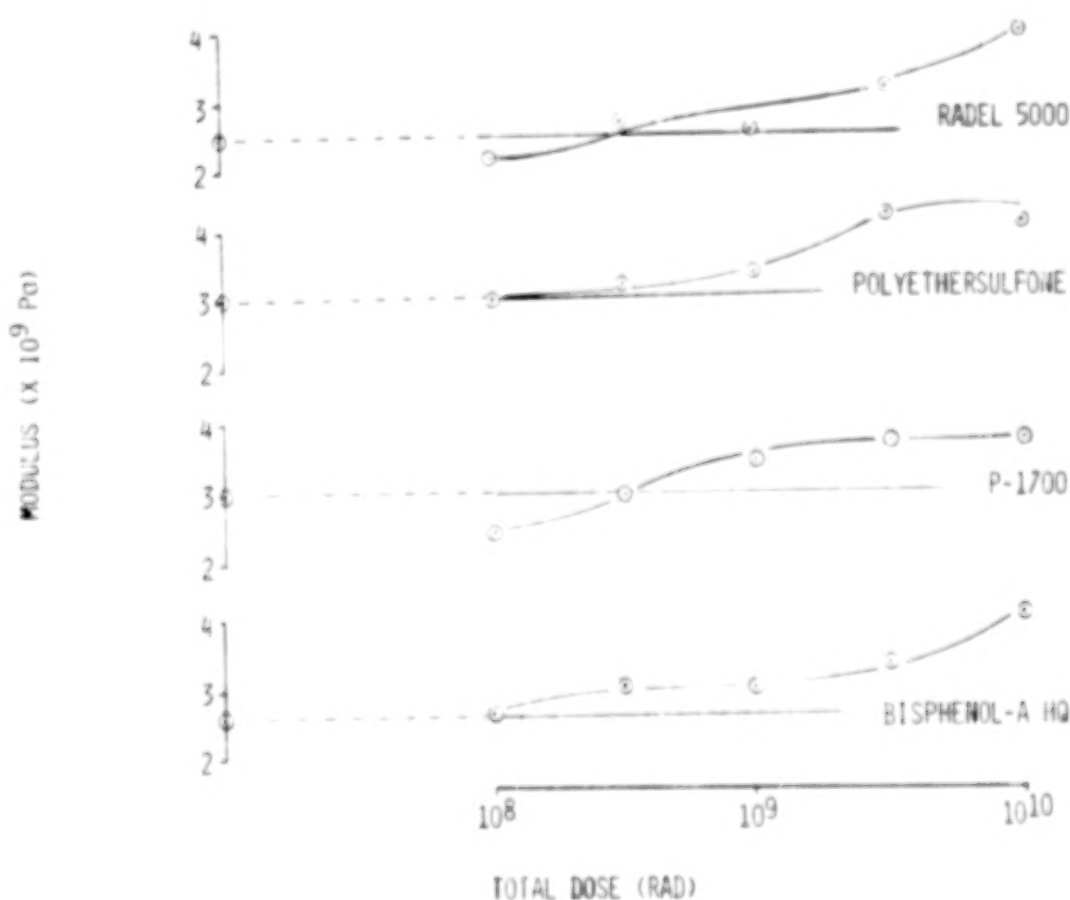


Figure 5

The Effect of Electron Radiation on the Thermal Stability of a Polysulfone

Shown in figure 6 is a thermogravimetric analysis of Polyethersulfone. The data were obtained using approximately 3 mg of film heated from room temperature to 700°C at 3°C/min in a nitrogen atmosphere. The graph shows data for the unirradiated film sample along with the curves from samples irradiated from 10^8 to 10^{10} rad at $2(10)^8$ rad/hr. It appears that the thermal stability of Polyethersulfone generally decreased with increasing electron total dose. This is shown by the trend at approximately 450°C toward greater percent weight loss with increasing total dose. This suggests that, as the dose increased, the molecular weight of the fragments produced decreased. However, there appear to be two mechanisms taking place, i.e., degradation and crosslinking. This second mechanism is suggested by the behavior of the polymer at the higher temperatures (600°C and above), where a greater quantity of residue is observed for film samples exposed to the 10^{10} rad dose. The crosslinked material should have greater thermal stability than both the unirradiated and degraded polymer, as is shown.

There appears to be almost no crosslinking occurring at the 10^8 rad dose level, which would indicate that only the degradation mechanism was taking place. At the 10^9 rad dose level, perhaps there is slight crosslinking, but at the 10^{10} rad level, there is a substantial increase in the quantity of residual material. All of the polysulfones exhibited the same general trend as shown for Polyethersulfone. The suggested crosslinking at high dose level in these materials is also supported by previously shown data for modulus and T_g changes following irradiation.

The following figures will show results from the irradiation studies on composite materials.



Figure 6

Effect of Radiation on Modulus

Figure 7 presents data on the effect of radiation on the modulus of two composite materials. The circles represent specimens made of Union Carbide Thornel 300 PAN fiber impregnated with Fiberite 934 epoxy resin. The squares represent specimens made of Celanese Celion 6000 fiber impregnated with Union Carbide Udel P1700 polysulfone resin. The open symbols represent data taken in vacuum while the closed symbols represent data taken in air before and after irradiation in vacuum. Each data point represents the average of a minimum of 3 test specimens. These data were generated by TRW using the tensile test specimens described earlier in this paper.

There is substantial scatter in these data but a trend of increasing modulus with increasing radiation dose is indicated. Also, the materials tested in air gave higher values than those tested in vacuum, which was used for the in vacuum and in air measurements. A logical reason for this difference has not been found, especially for the prior to irradiation measurements.

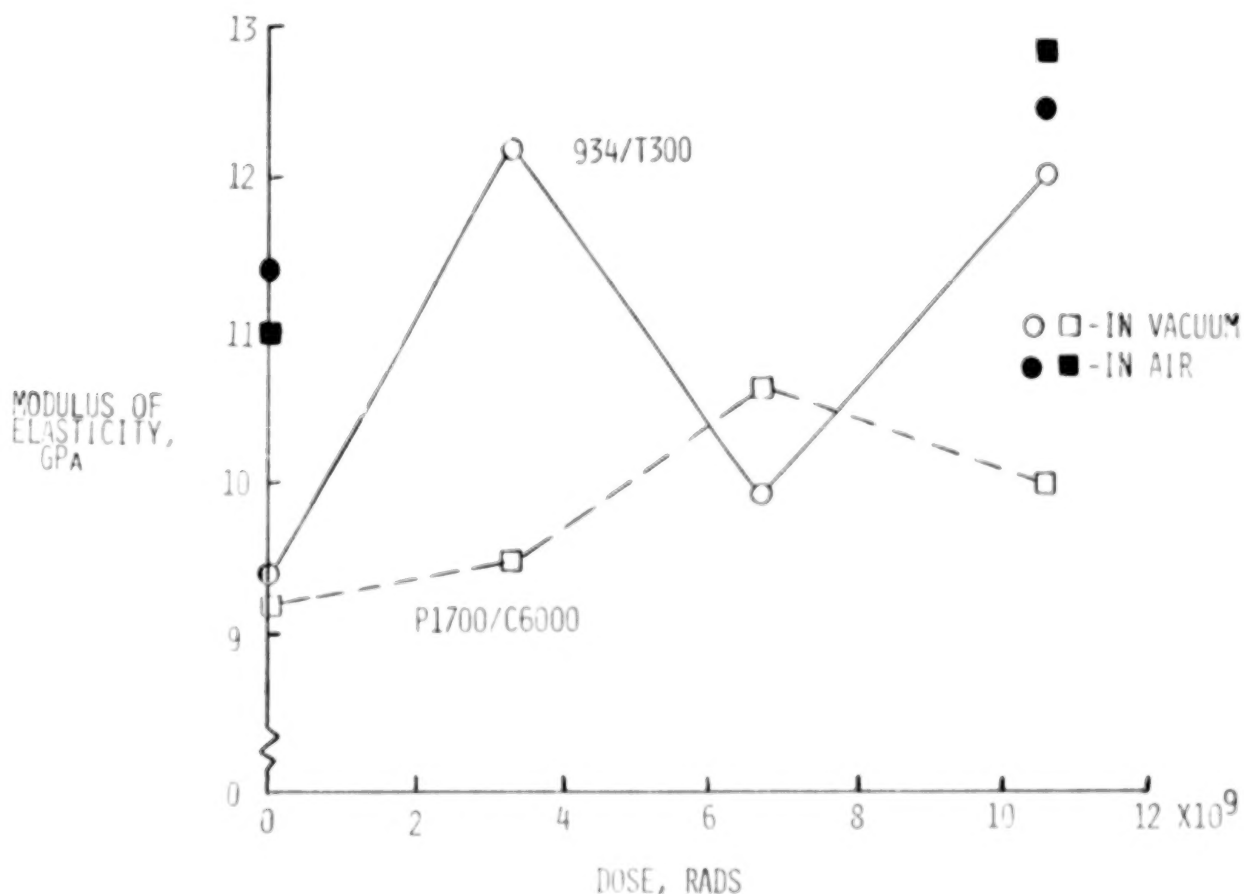


Figure 7

Effect of Radiation on Ultimate Tensile Strength

The effect of radiation on the ultimate tensile strength of these composites is presented in figure 8 using the same symbols as figure 7. The 934/T300 epoxy composite increases in tensile strength with increasing radiation dose from the unirradiated condition to 6.5×10^9 rads dose, but levels-off from 6.5×10^9 to 1×10^{10} rads. The increase in tensile strength was approximately 19%. The P1700/C6000 composite increased in tensile strength as the radiation dose increased. The increase in tensile strength was approximately 10%. The scatter in these data is $\pm 5\%$.

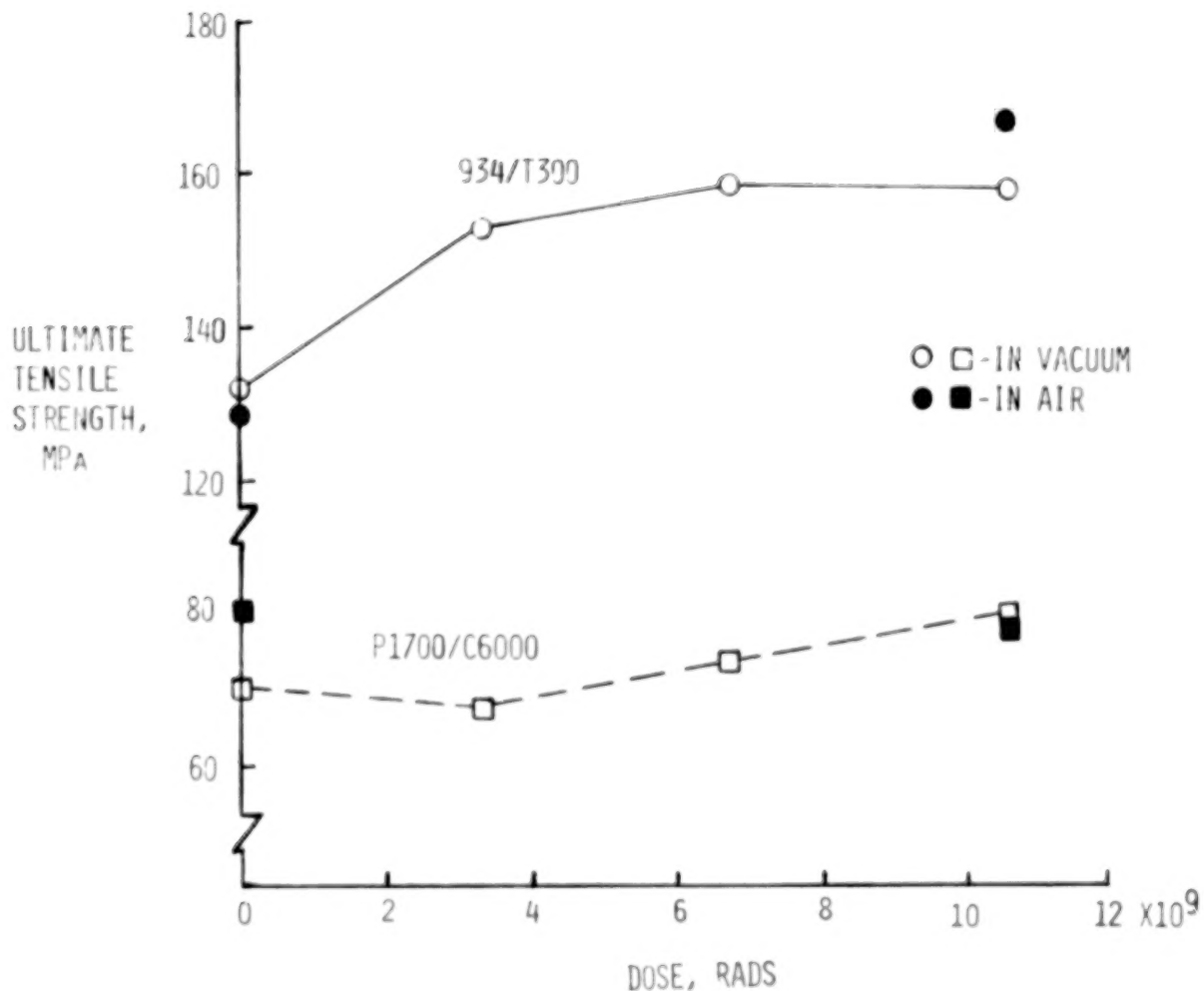


Figure 8

Effect of Radiation on Flexural Modulus

The following 3 figures show data generated in-house at Langley on materials irradiated with 1.0 MeV electrons under the Boeing Aerospace contract. The composite materials used in this study are: (1) Union Carbide Thornel 300 PAN fiber impregnated with Narmco 5208 epoxy resin; (2) Union Carbide Thornel 300 PAN fiber impregnated with Fiberite 934 epoxy resin; (3) a PAN 50 graphite (6 K tows) woven with S-glass end rovings and impregnated by Fiberite using Union Carbide Udel P1700 polysulfone resin. This material was consolidated at Convair Division of General Dynamics and supplied to this program by the Johnson Space Center. The first two materials were fabricated as 4-ply unidirectional composites with a nominal thickness of 0.635 mm (0.025 in.). Material 3 was a single ply with nominal thickness of 0.813 mm (0.032 in.). The flexure test specimens used in this program were 6.35 mm (0.25 in.) wide and 31.75 mm (1.25 in.) long. This small size allowed 30 specimens to be irradiated simultaneously in the Boeing facility.

Figure 9 was plotted using data taken at $2, 3$ and 6×10^9 rads and 1×10^{10} rads. Generally, eight specimens were tested for each data point. These data show that the 934 and 5208 epoxies behave similarly and that all three materials have little change in flexural modulus after a total dose of 1×10^{10} rads of 1.0 MeV electrons.

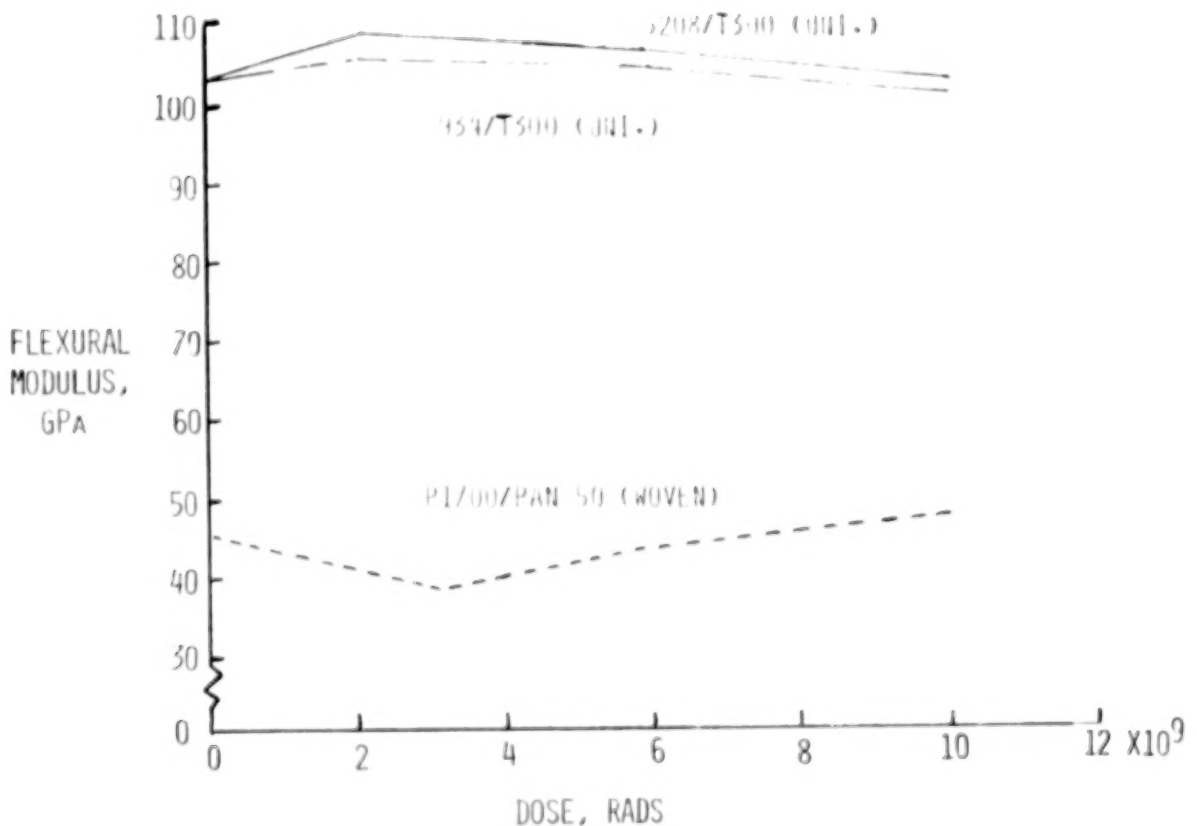


Figure 9

Effect of Radiation on Ultimate Flexure Strength

The 5208 and 934 epoxy composites increase in ultimate flexure strength from the unirradiated condition to a dose of 6×10^9 rads of electrons, but then decreased in strength at 1×10^{10} rads. The change is approximately $\pm 5\%$ from the unirradiated specimen value. The P1700/PAN 50 composite decreased in ultimate flexure strength from the unirradiated condition to a dose of 6×10^9 rads and then increased in strength at 1×10^{10} rads. The nominal change in ultimate flexure strength is also $\pm 5\%$ in this case. The changes of $\pm 5\%$ are within the reproducibility of these data.

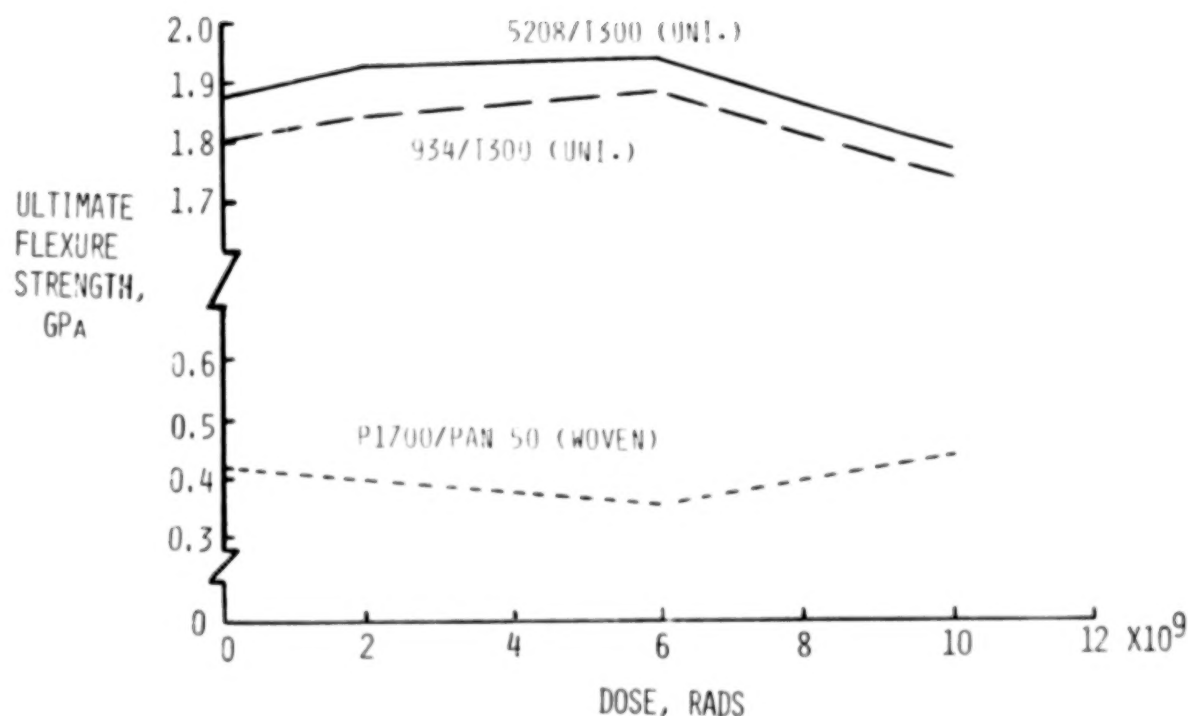


Figure 10

Effect of Radiation on Glass Transition Temperature

Figure 11 shows the effect of radiation dose on the glass transition temperature (T_g) of three composite materials. The apparent glass transition temperatures were obtained using probe penetration by a thermal mechanical analyzer. The 5208 and 934 epoxy composites had a substantial decrease in glass transition temperature from the unirradiated condition to a dose of 6×10^9 rads. At 1×10^{10} rads the temperature increased to within 5°C of the unirradiated T_g . The P1700/PAN 50 composite had a low initial T_g of 136°C but this increased to 154°C with a dose of 6×10^9 rads. When the dose was increased to 1×10^{10} rads the T_g was even higher at 204°C . These data indicate that substantial crosslinking is occurring after 6×10^9 rads of radiation in each of these materials.

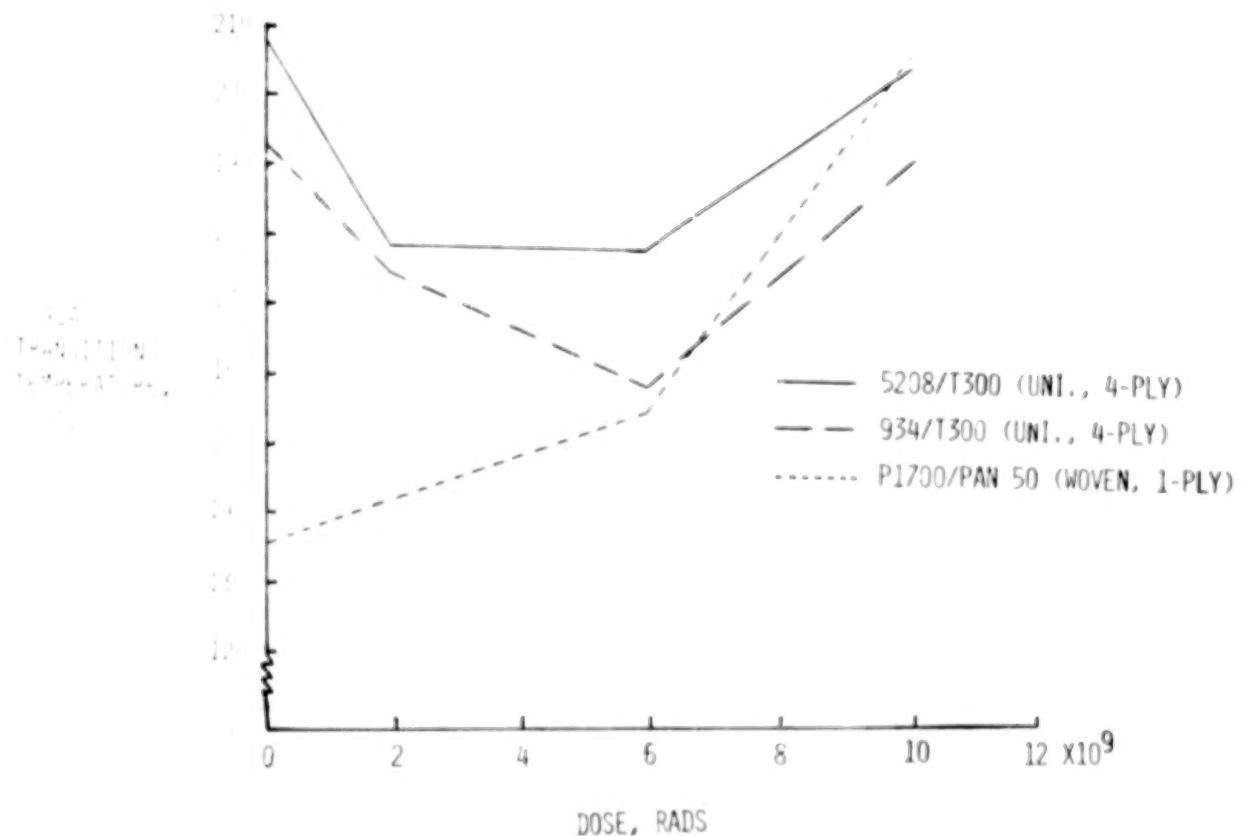


Figure 11

Concluding Remarks

Although data presented in this paper were obtained from a limited number of tests conducted under accelerated (5,000X) space electron flux exposure conditions, some conclusions on the stability of these materials to radiation can be made. The threshold for major physical and mechanical property changes in the polysulfone films and in the polysulfone and epoxy composites is in excess of 1×10^9 rads of electrons. Based upon these data, the 5208 and 934 epoxies and the P1700 polysulfone composites would be acceptable for 5- to 10-year geosynchronous Earth environment missions receiving $< 1 \times 10^9$ rads of electron radiation.

Future studies must include the effects of radiation on the coefficient of thermal expansion (CTE) of composites and longer-term tests to evaluate the effects of acceleration rate on these data.

- o THE THRESHOLD FOR MAJOR PROPERTY CHANGES IN POLYSULFONE FILMS AND COMPOSITES IS IN EXCESS OF 1×10^9 RADS
- o BASED UPON THESE DATA, THE 5208 AND 934 EPOXIES AND THE P1700 POLYSULFONE WOULD BE ACCEPTABLE FOR MISSIONS RECEIVING 1×10^9 RADS
- o OTHER TESTING REQUIRED IN FUTURE:
 - EFFECTS OF RADIATION ON CTE
 - EFFECTS OF ACCELERATED EXPOSURE ON MECHANICAL PROPERTIES

Figure 12

1

BLANK PAGE

BLANK PAGE

THERMAL EXPANSION OF COMPOSITES: METHODS AND RESULTS

DAVID E. BOWLES AND DARREL R. TENNEY

LANGLEY RESEARCH CENTER

LARGE SPACE SYSTEMS TECHNOLOGY - 1980
SECOND ANNUAL TECHNICAL REVIEW
NOVEMBER 18-20, 1980

DIMENSIONAL STABILITY OF SPACE STRUCTURES

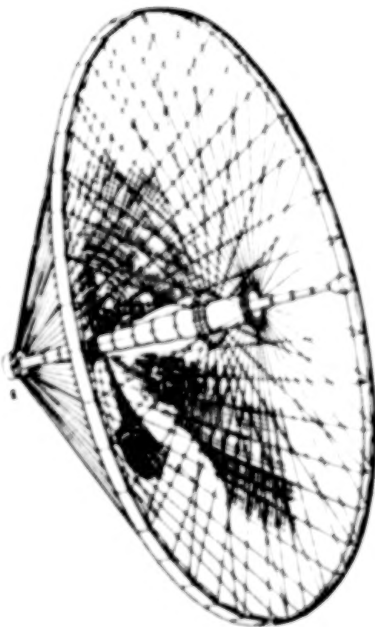
The performance characteristics of many large space structures are dependent upon their dimensional stability. An example of this is a space communications antenna in which small dimensional changes may cause a defocusing of the antenna and a corresponding loss in efficiency. In the Hoop/Column antenna (Harris design, fig. 1), the major structural components are a telescoping mast and hoop constructed with graphite/epoxy tubular members, and a network of quartz or graphite cables. In order to predict dimensional changes that the structure will experience in its space environment, the factors controlling the dimensional stability of the various components must be well understood.

The primary factors controlling the dimensional stability of cables are cyclic thermal and mechanical loading which can result in permanent residual strains. For organic matrix composites, such as graphite/epoxy, these factors include moisture desorption in the space environment, thermal expansion as the structure moves from sunlight to shadow in its orbit, mechanical loading, and microyielding of the material caused by microcracking of the matrix material.

The present research focuses on the thermal expansion of composites and in particular the development and testing of a new method for its measurement.

FACTORS CONTROLLING DIMENSIONAL STABILITY

- o CABLES -
 - o DIMENSIONAL CHANGES DUE TO:
 - o THERMAL CYCLING
 - o MECHANICAL LOADING
- o ORGANIC MATRIX COMPOSITES -
 - o DIMENSIONAL CHANGES DUE TO:
 - o MOISTURE DESORPTION
 - o THERMAL EXPANSION
 - o MECHANICAL LOADING
 - o MICROYIELDING (CAUSED BY MATRIX MICROCRACKING)



HOOP/COLUMN ANTENNA

Figure 1.

COMMON METHODS OF MEASUREMENT

There is a wide variety of existing techniques for measuring thermally induced strains in materials. Resolution capabilities range from 10^{-6} m to fractions of a wavelength of light ($<10^{-8}$ m). Wolff (ref. 1) presents a comprehensive discussion of the available methods commenting on the advantages and disadvantages of each. Some of the more commonly used methods are described in figure 2. Strain gages offer the advantages of being easy to use and not limiting the specimen geometry. Their ability to accurately measure small strains is questionable however, as will be discussed later. Quartz tube or rod dilatometers are widely used to measure the thermal expansion of materials. In this method the expansion is determined from the displacement of one end of the specimen relative to the other, which somewhat limits the specimen geometry. In conventional engineering materials this technique does not cause any problems; however, the isotropic behavior of composites can cause problems. End distortions can develop in certain laminates due to a mismatch of CTE's in adjacent plies, and can produce errors in the measurement. These errors can be significant especially for small gage lengths. The interferometric techniques offer the highest resolution, which is of prime importance when examining composites designed for "near zero" expansion, but suffer from the same limitations as the dilatometers.

The moiré method of strain analysis, although not previously applied to thermal expansion measurements, offers a resolution approaching that of two-beam interferometry without relying on the expansion determined from the ends of the specimen.

ELECTRICAL RESISTANCE STRAIN GAGES:

- o EASY TO USE
- o SPECIMEN GEOMETRY NOT LIMITED
- o GIVES POINT MEASUREMENT

QUARTZ TUBE OR ROD DILATOMETERS:

- o EXPANSION DETERMINED FROM SPECIMEN ENDS
- o SPECIMEN GEOMETRY LIMITED

TWO-BEAM INTERFEROMETRY

- o EXPANSION DETERMINED FROM SPECIMEN ENDS
- o SPECIMEN GEOMETRY LIMITED
- o ELABORATE OPTICAL SETUP REQUIRED

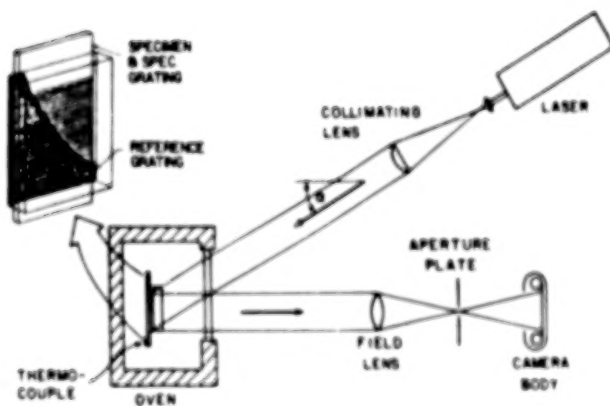
Figure 2.

MOIRÉ INTERFEROMETRY

A method based on moiré strain analysis was selected as the measurement technique for determination of the CTE's of composites. Reasons for the selection of this method rather than some of the more conventional techniques described earlier are listed in figure 3. Moiré interferometry differs from conventional methods of moiré strain analysis in that a fringe multiplication phenomenon (ref. 2) is employed. This allows for the use of a relatively coarse grating on the specimen and a much finer grating for the reference. By observing selected diffraction orders, the resolution is dependent upon the frequency of the reference grating, and not that of the coarse specimen grating. Details of the method may be found in reference 3.

In the present application a reference grating with 1200 lines/mm (30,000 lines/in) on a fused silica blank was purchased from Bausch and Lomb. A RTV silicone rubber (General Electric RTV 615) grating is replicated onto the specimen surface using a 600 lines/mm (15,000 lines/in) grating on a photographic plate as the master. The specimen grating is approximately 0.025 mm (0.001 in) thick and its modulus of elasticity is three to four orders of magnitude lower than that of the composite; thus, any reinforcement is considered negligible. As shown in figure 3, the specimen and reference grating are illuminated with a collimated beam from a 5 mW He-Ne laser and are mounted in an environmental chamber capable of cycling between 422 K (300°F) and 116 K (-250°F). Measurements are made by counting interference fringes between gage marks cast in the specimen grating.

EXPERIMENTAL APPARATUS



ADVANTAGES ARE:

- o PURELY GEOMETRICAL MEASUREMENT
- o RESOLUTION OF ≤ 5 MICROSTRAIN
- o ELIMINATE SPECIMEN END EFFECTS
- o FULL FIELD OBSERVATION PERMITS DETERMINATION OF NON-HOMOGENEOUS STRAIN FIELDS
- o APPLICABLE TO VARIOUS LOADING CONDITIONS (THERMAL AND MECHANICAL)
- o NO ELABORATE EQUIPMENT NEEDED

Figure 3.

EXPERIMENTAL PROGRAM

The objective of the experimental program undertaken in this investigation was to determine the feasibility of applying moiré interferometry to the measurement of thermally induced strains in composites. A secondary aim was to assess the accuracy of electrical resistance strain gages in the same application. Measurements were performed on four graphite/epoxy laminates. This particular material system was selected because of its potential widespread use in space structures. The four laminates investigated were the [0], [90], and two quasi-isotropic configurations. The [0] and [90] orientations provided data on the lamina CTE values, which can be used in an analysis to predict laminate response, and also give the extreme values of expansion which might be encountered. The quasi-isotropic laminates provide expansion typical of many structural composites.

As outlined in figure 4, this program consisted of first calibrating the moiré interferometry apparatus to account for the thermal expansion of the reference grating. Apparent strain data were also collected for later use in strain gage measurements and to provide data on the variability in strain gage response. After calibration procedures had been completed, length change versus temperature data were collected between room temperature and 422 K (300°F). Efforts are underway to extend the moiré method for making measurements down to 116 K (-250°F).

OBJECTIVES:

- o ASSESS THE FEASIBILITY OF USING MOIRÉ INTERFEROMETRY FOR CTE MEASUREMENTS OF COMPOSITES
- o DETERMINE THE ACCURACY OF STRAIN GAGES FOR CTE MEASUREMENTS

APPROACH:

- o MATERIALS -
[0], [90], [0/±45/90]_s, [0/90/±45]_s GRAPHITE EPOXY
- o CALIBRATION -
DETERMINE EXPANSION OF REFERENCE GRATING
COLLECT APPARENT STRAIN DATA
- o COLLECT $\Delta L/L$ VERSUS TEMPERATURE DATA FOR SPECIMENS CYCLED BETWEEN
297 K (75°F) AND 422 K (300°F)
- o APPLY MOIRÉ METHOD FOR MEASUREMENTS IN THE RANGE 297 K (75°F)
TO 116 K (-250°F)

Figure 4.

STRAIN GAGE RESULTS

Single back-to-back gages (Micro-Measurements WK Series) were bonded to a block of titanium silicate and subjected to repeated thermal cycling between 279 K (75°F) and 422 K (300°F), to determine the apparent strain characteristics of the gages. Results were obtained for two different gage lengths designated as Type I (6.35 mm) and Type II (3.175 mm). The results shown in figure 5 represent the average response of the back-to-back gages during several thermal cycles. These data show the large variability in strain gage response. This includes variability from supposedly identical back-to-back gages, as well as from cycle to cycle for the same gage. For a one standard deviation scatter band, the variability may be expressed as $+0.175 \mu\epsilon/K$ ($+0.097 \mu\epsilon/^\circ F$) for the Type I gage and $+0.007 \mu\epsilon/K$ ($+0.039 \mu\epsilon/^\circ F$) for the Type II gage. The manufacturers supplied apparent strain curves are also given in figure 5. Again, these curves are based on an average response with a variability of $\pm 0.23 \mu\epsilon/K$ ($\pm 0.13 \mu\epsilon/^\circ F$) for a one standard deviation error band (ref. 4).

These results show that gage response variability can introduce significant errors when this variability is a large percentage of the expansion of the specimen.

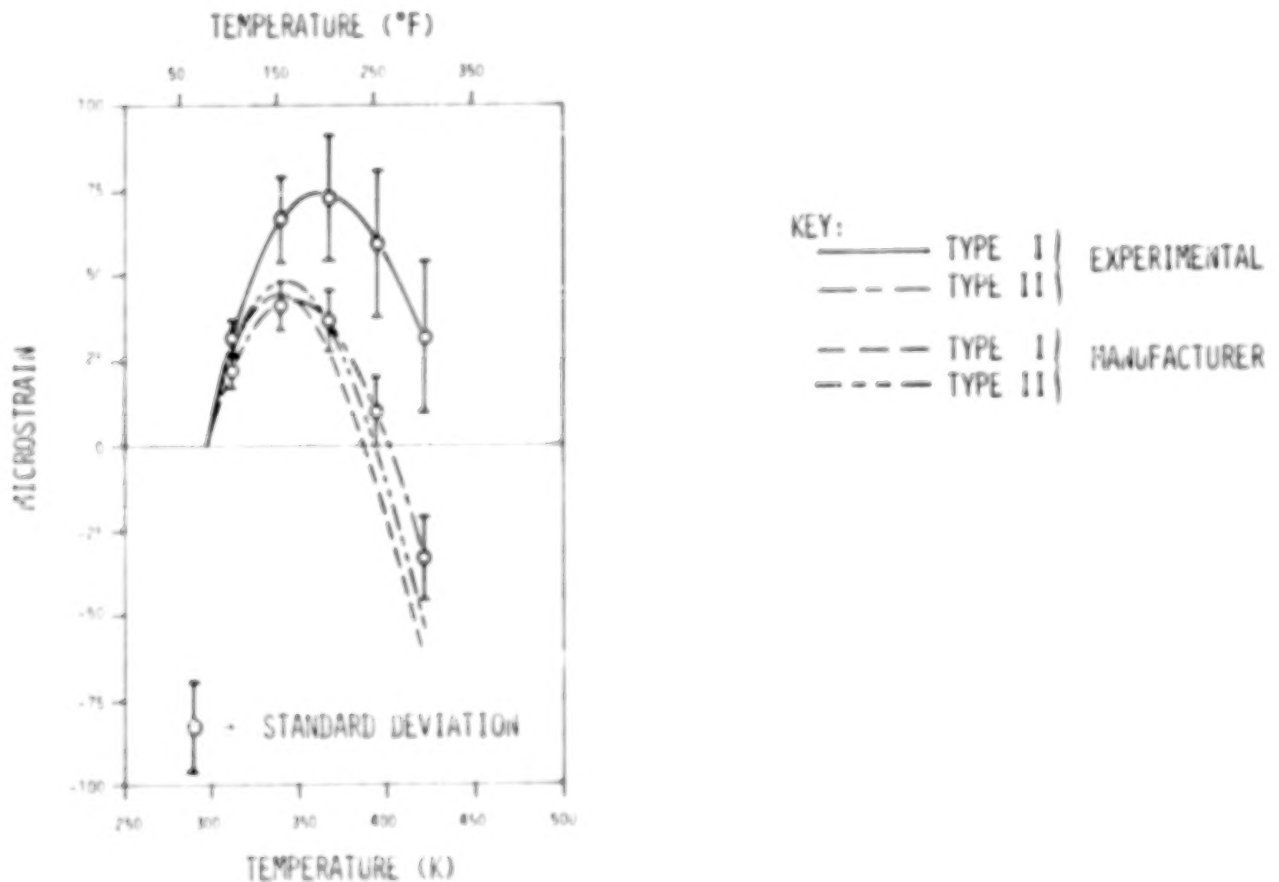


Figure 5.

MOIRÉ INTERFEROMETRY RESULTS

Strain versus temperature curves for the four laminates examined in this investigation are shown in figure 6. The composite specimens were dried prior to testing to remove any moisture that might be present. In a specimen that was not dried, the entrapped moisture significantly altered the thermal response resulting in hysteresis as the specimen dried out during testing. The results shown below represent a least squares polynomial fit of the data obtained from two thermal cycles between room temperature and 422 K (300°F). A second order polynomial was fit to the [90] and two quasi-isotropic laminates, while a first order curve best fit the data for the [0] laminate. The standard deviation of the experimental data is also shown beside each curve. It is interesting to note that the results for the two quasi-isotropic laminates fall on top of one another as classical lamination theory would predict. Instantaneous CTE values were obtained by differentiating the polynomial expressions obtained from the least-squares analysis. The [0] laminate had a constant CTE over the temperature range while the CTE's for the [90] and quasi-isotropic laminates increased linearly with temperature. Uncertainty limits on the CTE values were computed from the systematic error in the calibration along with a one standard deviation random error. These are listed below with the CTE values computed at 360 K (188°F).

The above results demonstrate that moiré interferometry is an effective and precise method for measuring the CTE's of composites. Preliminary results on extending the method for making measurements down to 116 K (-250°F) indicate that the brittle point of the silicone rubber grating material, 213 K (-75°F), places a lower temperature limit on the usefulness of the moiré method. Research is underway to find an alternate grating material.

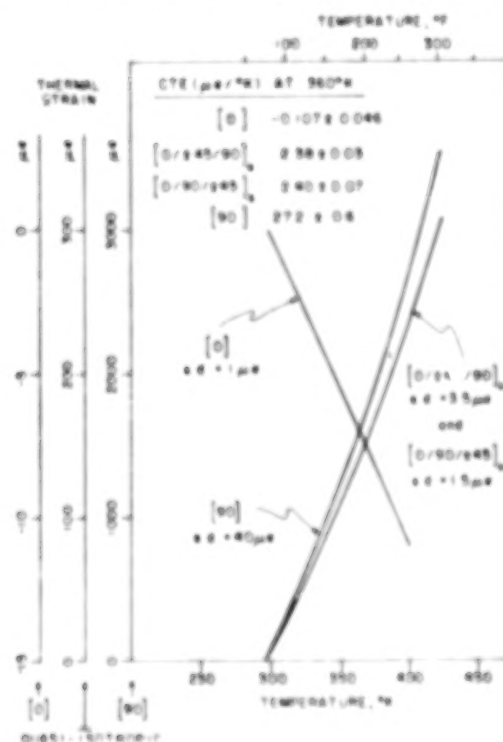
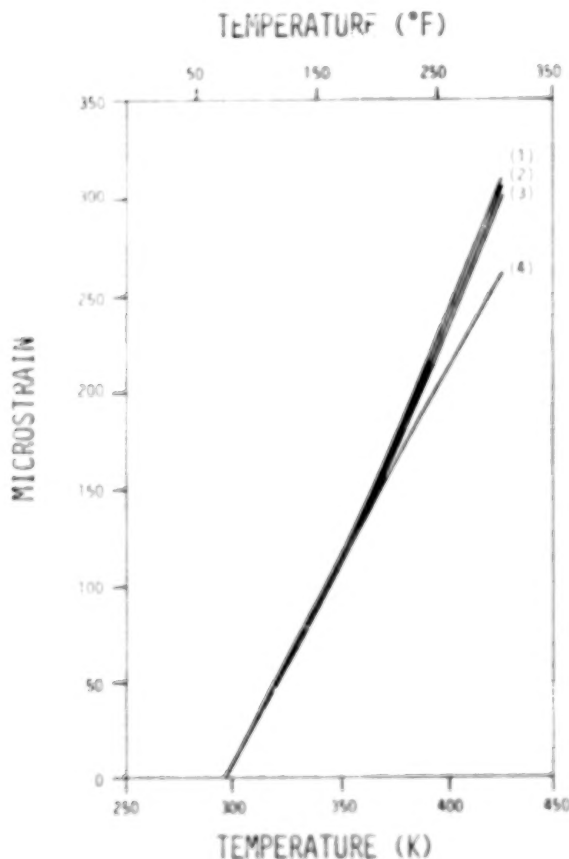


Figure 6.

ANALYTICAL PREDICTIONS

An analysis based on classical lamination theory was used to predict the thermal response of a quasi-isotropic laminate and compare it with experimental results. Two cases were examined. First, the lamina CTE's (α_1, α_2) were allowed to vary with temperature while the lamina elastic properties were assumed to be constant with temperature, Case I. For Case II, all of the lamina material properties were allowed to vary with temperature. The lamina thermal properties used in both cases were those obtained experimentally from the [0] and [90] laminates. Information was readily available in the literature on the room temperature elastic properties, but information concerning their temperature dependence was scarce.

As shown in figure 7, the Case I analysis compares well with the experimental results. The Case II analysis compares less favorably; however it should be noted that the temperature dependence of the elastic properties used as input in the analysis was based on a very limited amount of data. From these results it may be concluded that laminate analysis is capable of predicting the thermal response of composites based on room temperature elastic properties. More data on the temperature dependence of elastic properties are needed to assess their influence on predicting the thermal response.



ANALYSIS: CLASSICAL LAMINATION
THEORY WITH TEMPERATURE DEPENDENT
LAMINA ELASTIC PROPERTIES

o CASE I -

$$(\alpha_1, \alpha_2) = F(T)$$

$$(E_1, E_2, \nu_{12}, G_{12}) \neq F(T)$$

o CASE II -

$$(\alpha_1, \alpha_2, E_1, E_2, \nu_{12}, G_{12}) = F(T)$$

KEY:

(1) $[0/\pm 45/90]_s$ EXPERIMENTAL

(2) $[0/90/\pm 45]_s$ EXPERIMENTAL

(3) CASE I ANALYSIS

(4) CASE II ANALYSIS

Figure 7.

SUMMARY

The results of this research may be summarized as follows:

- o MOIRÉ INTERFEROMETRY IS A PRECISE AND EFFECTIVE METHOD FOR DETERMINING THE THERMAL EXPANSION OF COMPOSITE LAMINATES IN THE RANGE 297 K (75°F) TO 422 K (300°F).
- o THE BRITTLE POINT OF THE SILICONE RUBBER GRATING MATERIAL PLACES A LOWER TEMPERATURE LIMIT OF 213 K (-75°F) ON THE MOIRÉ INTERFEROMETRY TECHNIQUE.
- o VARIABILITY IN APPARENT STRAIN RESPONSE IS A MAJOR UNCERTAINTY IN STRAIN GAGE DATA.
- o LAMINATE ANALYSIS, BASED ON ROOM TEMPERATURE ELASTIC PROPERTIES, IS CAPABLE OF PREDICTING THE THERMAL EXPANSION OF COMPOSITES.

REFERENCES

1. Wolff, E. F.: Measurement Techniques for Low Expansion Materials, Materials and Processes--In Service Performance. National SAMPE Tech. Conf., vol. 9, Oct. 1977.
2. Post, D.: Moiré Fringe Multiplication With a Non-Symmetrical Doubly-Blazed Reference Grating. Applied Optics, vol. 11, no. 9, Sept. 1971, pp. 408-413.
3. Bowles, D. E.; Post, D.; Herakovich, C. T.; Tenney, D. R.: Thermal Expansion of Composites Using Moiré Interferometry. NASA TM-80788; VPI-E-80-19, August 1980.
4. Micro-Measurements Tech. Note: Temperature-Induced Apparent Strain and Gage Factor Variation in Strain Gages. TN-128-2.

SPACE PLATFORM REFERENCE MISSION
STUDIES OVERVIEW

James K. Harrison
George C. Marshall Space Flight Center
Huntsville, Alabama

Large Space Systems Technology - 1980
Second Annual Technical Review
November 18-20, 1980

MISSIONS SELECTED

The initial step in the program to develop the necessary technology for building deployable space platforms was the identification of the design requirements. These requirements were based on three major systems that were in a Phase A development stage. The three were the Science and Applications Space Platform (SASP), the Geostationary Platform (GSP), and the Satellite Power System (SPS). Because the SASP and GSP were assumed to require no advanced technology for their development an advanced version of each was selected on which to base the design requirements. The SPS represented the opposite development state hence a nearer term test article was selected on which to base the requirements. The development period for these missions is depicted in figure 1. These particular missions were chosen because their development will involve space deployable structures, LEO and GEO orbit locations, linear and area structures, and variations in overall size, shape, stiffness, and mission objectives.

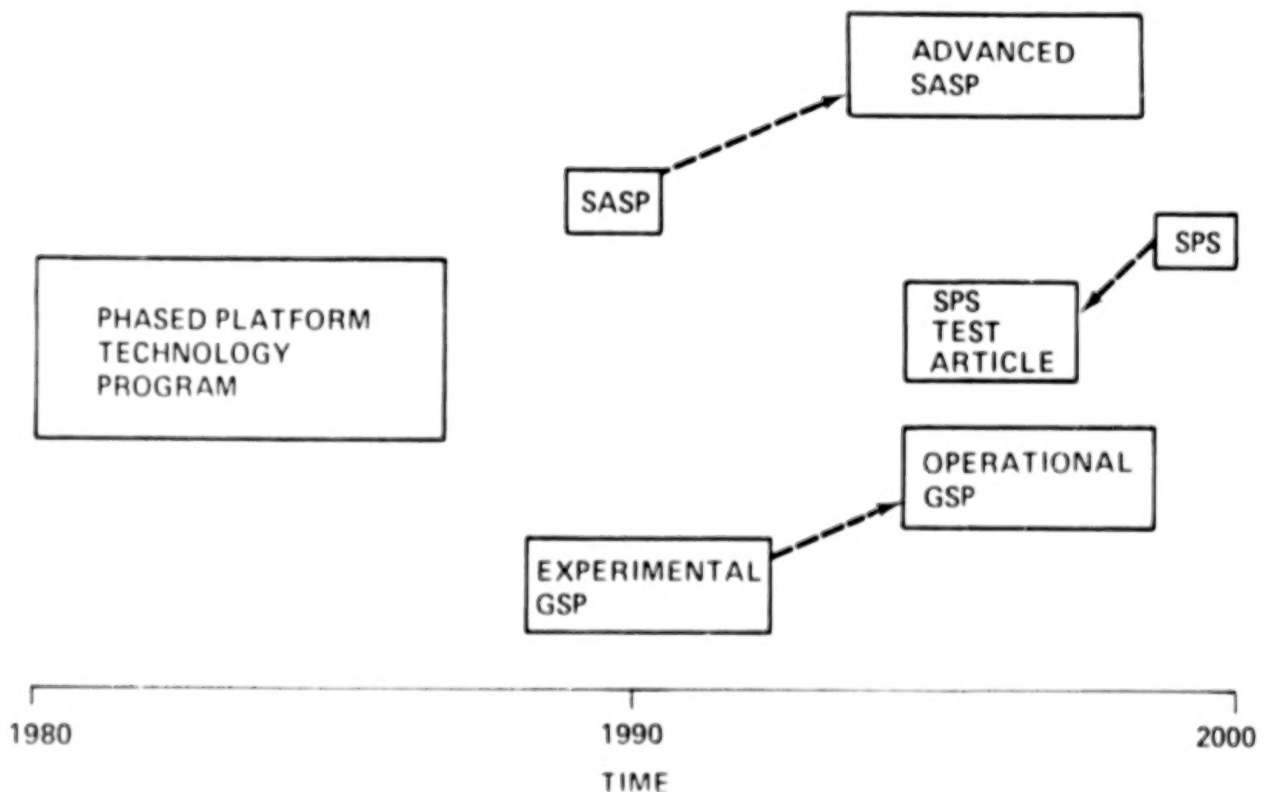


Figure 1

PLATFORM REQUIREMENTS OUTLINE

An outline of the platform design requirements that were developed using these three reference missions as a base are shown in figure 2. A brief summary of the requirements for each mission is given in the following three papers.

PLATFORM REQUIREMENTS

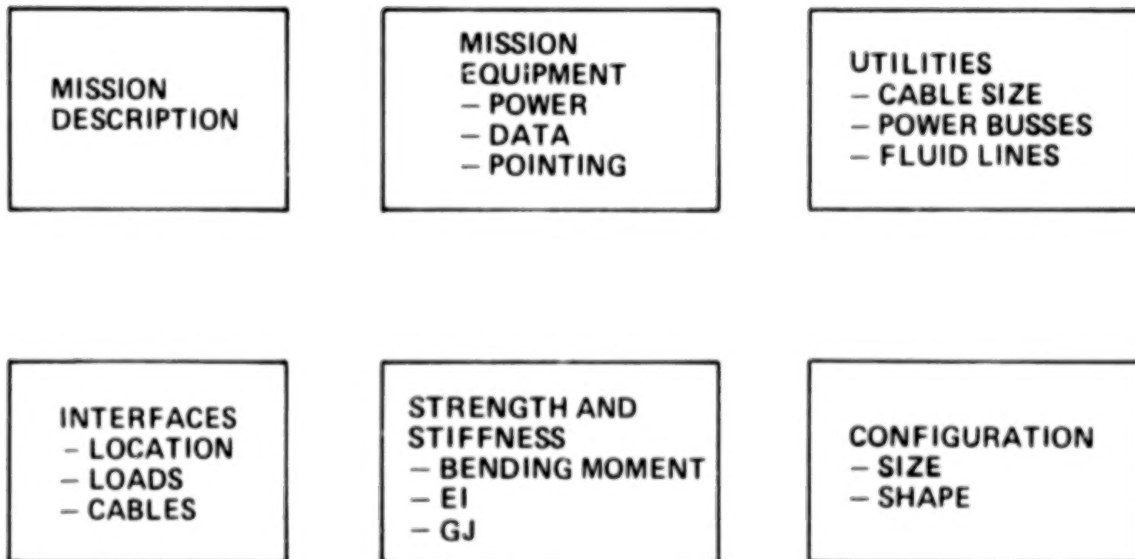


Figure 2

LONG RANGE PLAN AND PURPOSE

The requirements that were developed in the initial step will be the basis for a five year step-by-step deployable platform development program. The program purpose is to develop the technology needed to design, fabricate, and deploy linear and area space platforms by the mid-1980's. The steps to be taken are outlined in figure 3 along with a forecast by year for their accomplishment.

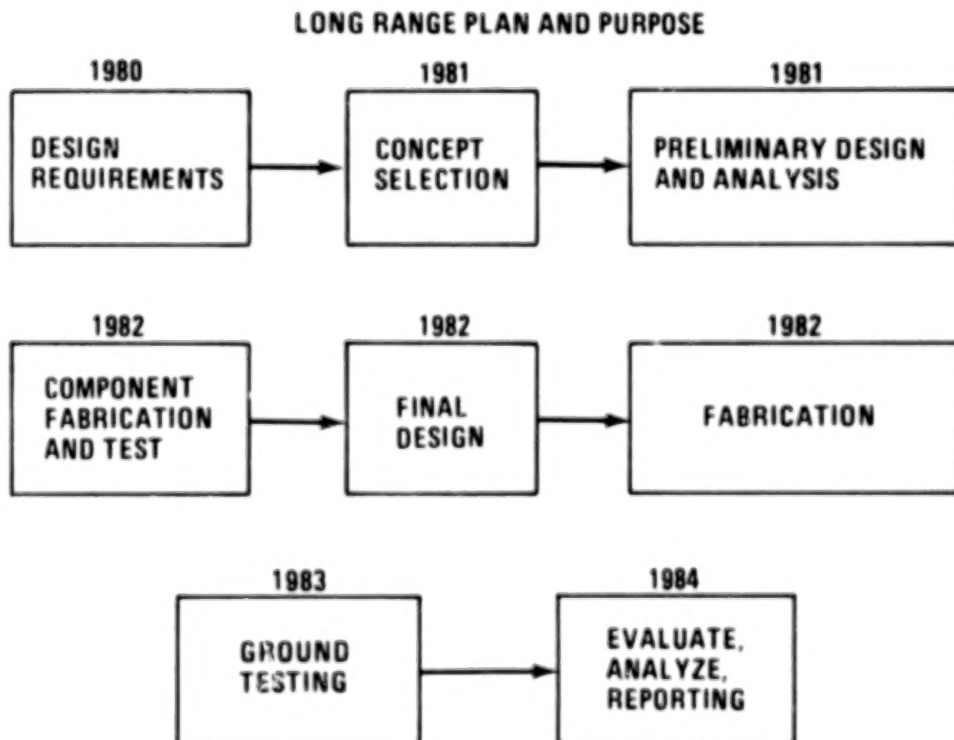


Figure 3

ADVANCED SCIENCE AND
APPLICATIONS SPACE PLATFORM

Jack White and Fritz Runge
McDonnell Douglas Astronautics Company
Huntington Beach, California

Contract NAS8-33592(L)

Large Space Systems Technology - 1980
Second Annual Technical Review
November 18-20, 1980

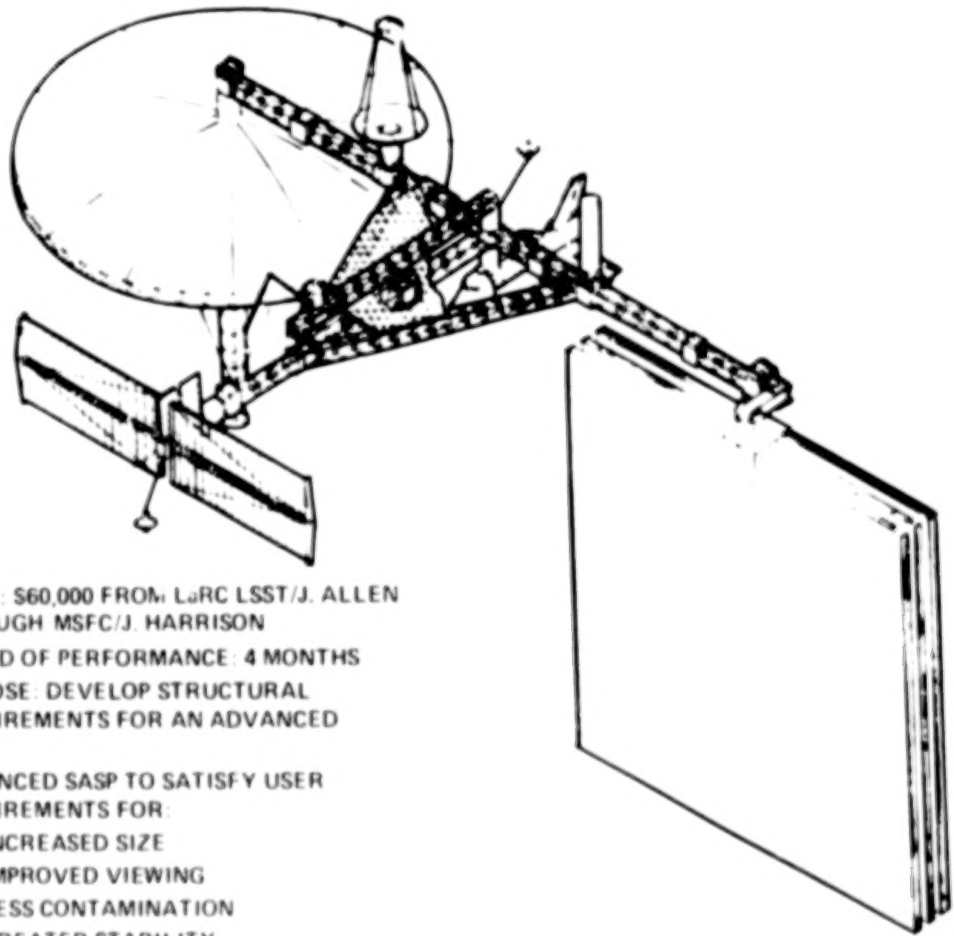
ADVANCED SCIENCE AND APPLICATIONS SPACE PLATFORM

The purpose of this LSST study was to develop requirements for and descriptions of the mission equipment, subsystems, configuration, utilities, and interfaces for an Advanced Science and Applications Space Platform (ASASP) using large space structure technology. Structural requirements and attitude control system concepts were emphasized. The results were later to be used by NASA for deployable structure development criteria.

To support the development of ASASP requirements, a mission was described that would satisfy the requirements of a representative set of payloads requiring large separation distances selected from the Science and Applications Space Platform data base.

Platform subsystems were defined which would support the payload requirements and a physical platform concept was developed. Structural system requirements which included utilities accommodation, interface requirements, and platform strength and stiffness requirements were developed. An attitude control system concept was also described by Bendix, a subcontractor.

The resultant ASASP concept was analyzed and technological developments deemed necessary in the area of large space systems were recommended.



- SCOPE: \$60,000 FROM LARC LSST/J. ALLEN
THROUGH MSFC/J. HARRISON
- PERIOD OF PERFORMANCE: 4 MONTHS
- PURPOSE: DEVELOP STRUCTURAL
REQUIREMENTS FOR AN ADVANCED
SASP
- ADVANCED SASP TO SATISFY USER
REQUIREMENTS FOR:
 - INCREASED SIZE
 - IMPROVED VIEWING
 - LESS CONTAMINATION
 - GREATER STABILITY

Figure 1.

ADVANCED SCIENCE AND APPLICATIONS SPACE PLATFORM STUDY SCHEDULE

The first task was to develop a mission description and the equipment requirements to support a compliment of Science and Applications Payloads to be flown in the 1990's, which would require a space platform significantly larger than that currently envisioned to support the payload needs of the late 1980's. Using the results from this task, the second task described the major platform subsystems and developed a representative advanced platform concept in terms of size and shape. The third task developed the structural system requirements including utilities accommodation, interface descriptions, and strength and stiffness requirements of the overall platform structural system. Task four developed control system concepts with regard to dynamic stability and control of the Platform. The fifth and final task analyzed the descriptions and definitions of the previous study tasks with respect to their technology needs in the area of Large Space Systems.

The study was performed concurrently with the basic Science and Applications Platform designed to accommodate payloads with dimensions of less than 15 meters.

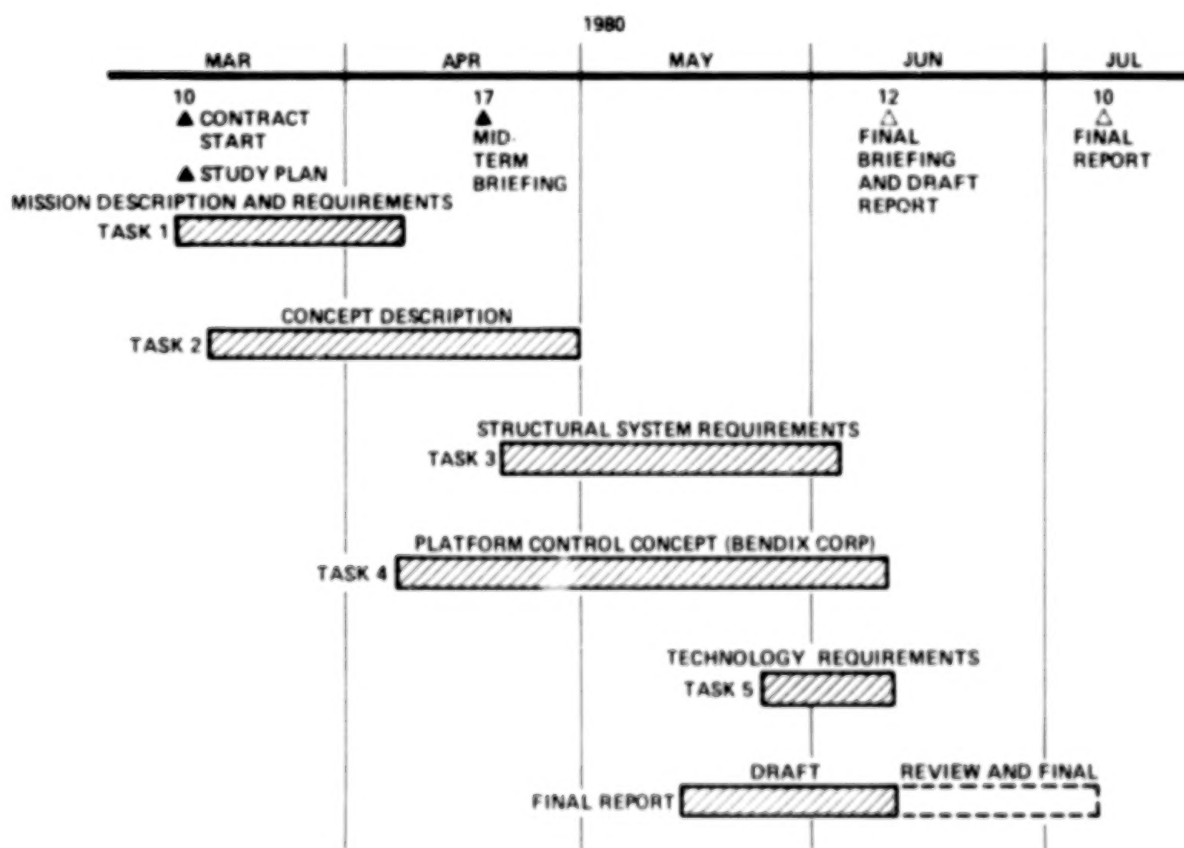


Figure 2.

ADVANCED SCIENCE AND APPLICATIONS SPACE PLATFORM CONCEPT

The mission objective was to conduct scientific experiments from a space platform which will accommodate the needs of advanced (1990's) science and applications payloads requiring large separation of scientific instruments.

The payloads accommodated were a 100 meter diameter Atmospheric Gravity Wave Antenna (AGWA); a 100 meter by 100 meter Particle Beam Injection Experiment (PBI); a 2 meter diameter, 18 meter long Astrometric Telescope (AST/TEL), and a 15 meter diameter, 35 meter long Large Ambient Deployable IR Telescope (IR TEL). A low earth orbit at 500 km altitude and 56° inclination was selected as being the best compromise for meeting payload requirements.

It is anticipated that Orbiter revisits will normally occur twice per year for the purpose of payload servicing, payload and platform systems maintenance, payload changeout, and providing the Platform with sufficient propellant for station keeping purposes. Platform station keeping will be maintained by a self-contained platform propulsion system. The large area payloads will be positioned in minimum drag attitudes whenever practical to minimize orbital decay and station keeping propellant requirements. However, the Platform must be able to maintain attitude control and function normally for all possible payload orientations. Orbital parameters were selected to be 56° inclination and 500 km altitude.

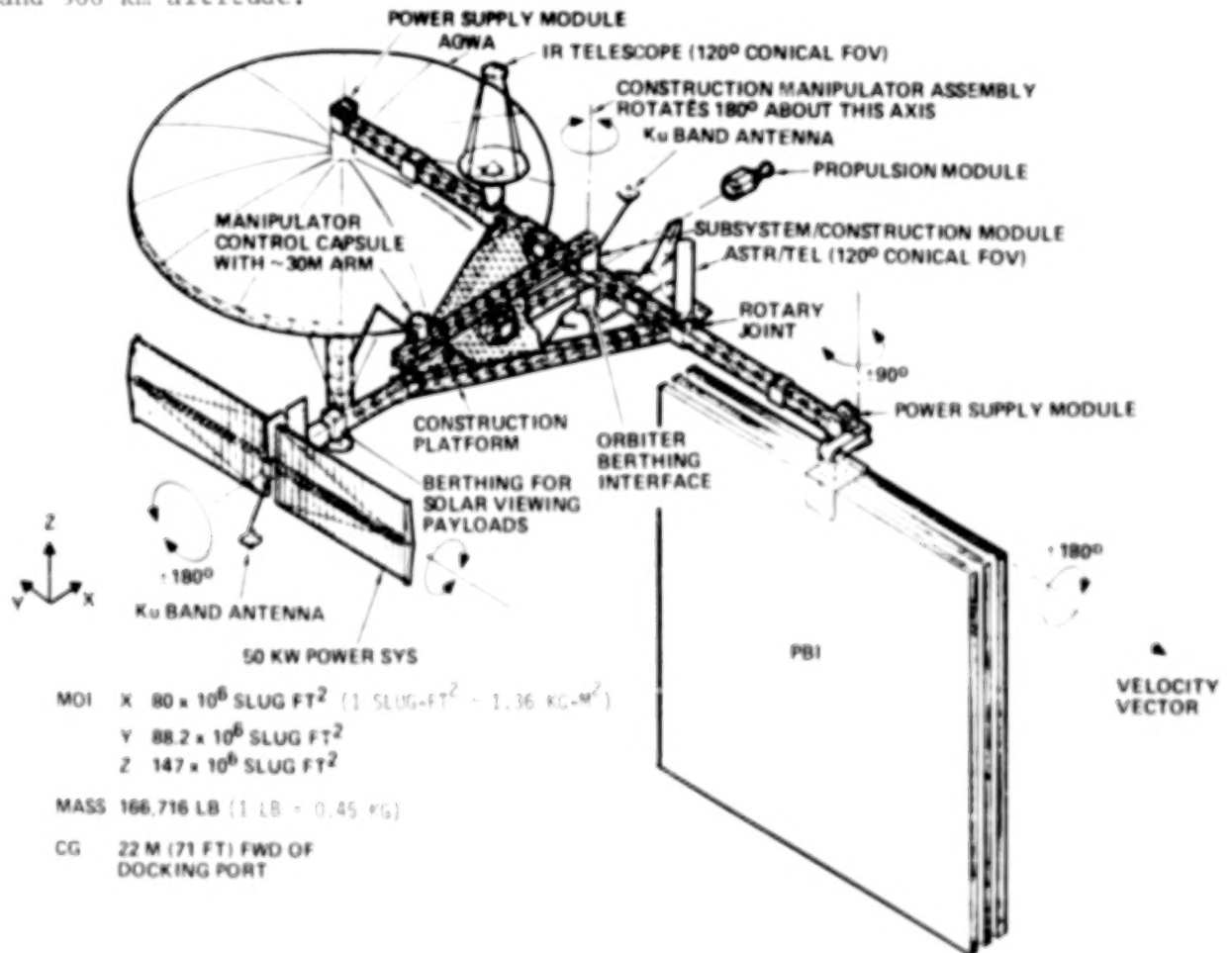


Figure 3

ADVANCED SCIENCE AND APPLICATIONS SPACE PLATFORM STRUCTURAL CONFIGURATION

A platform configuration using a central planar area with long linear appendages for attachment of large payloads and solar arrays was selected as the best configuration for incorporating the desired platform features. The Platform is oriented with the principal Z axis in a local vertical position to minimize control momentum storage requirements. The velocity vector would nominally be along the Y axis.

The triangular central area provides a more rigid structure for the attachment of payloads requiring greater pointing accuracy and stability. This area might also be used as a platform to aid in the space construction of large payloads. The size of the construction portion of the triangular area would be dependent on construction requirements. Three structural appendages are attached to the central triangular area via a rotary joint to aid in the positioning of the large payloads and solar array wings. The rotary joint provides a second degree of freedom for the solar array to give improved solar orientation.

Due to the large size and mass of the Platform and payloads, a construction manipulator assembly will be required to support deployment and servicing of payloads and platform subsystems. This construction manipulator assembly must be capable of reaching all areas of the Platform and the Orbiter cargo bay.

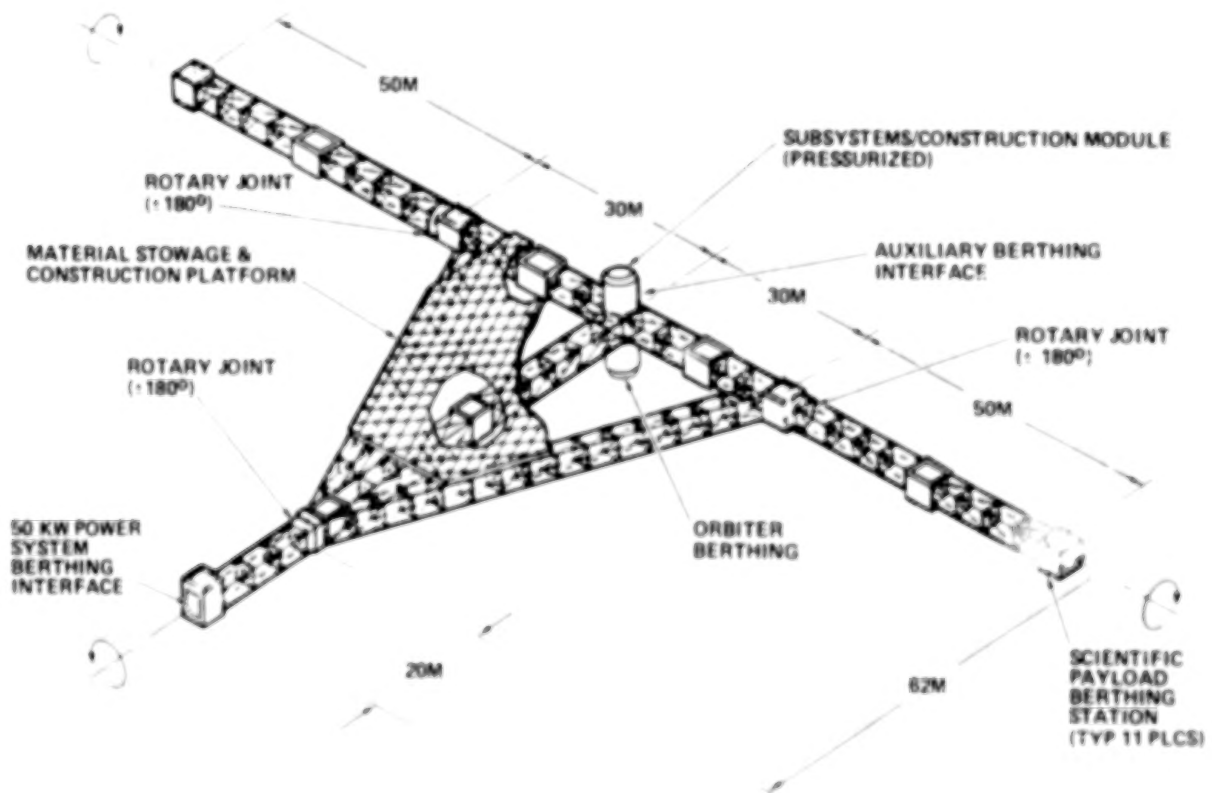


Figure 4.

ASASP CONSTRUCTION SEQUENCE

To support development of the attitude control system concept, a construction sequence for the ASASP was developed and is illustrated. The actual number of Orbiter flights required to place the platform hardware into earth orbit will be dependent on the structure concept selected and the capability of packaging this structure in the cargo bay.

The subsystems/construction module was located near the overall platform center of gravity so that the Orbiter docking could be accomplished at the module with minimal effect on the overall platform attitude control. The construction module must be large enough to accommodate the platform subsystem hardware and to support EVA crew operations. This module should be capable of being pressurized to support crew habitability but would operate unpressurized during manned platform operations.

Due to the large power demands of the Particle Beam Injection experiment and of the Atmospheric Gravity Wave Antenna, separate power supply modules containing banks of Nickel-Hydrogen batteries were located in close proximity to the payload at the extremities of the platform arms. Ku band antennas were positioned on both sides of the Platform, one outboard of the solar arrays and one outboard of the subsystems/construction module, to provide uninterrupted line-of-sight communications with the Tracking and Data Relay Satellite (TDRS). A self-contained propulsion module will interface at the subsystems/construction module to provide station keeping impulse to the ASASP.

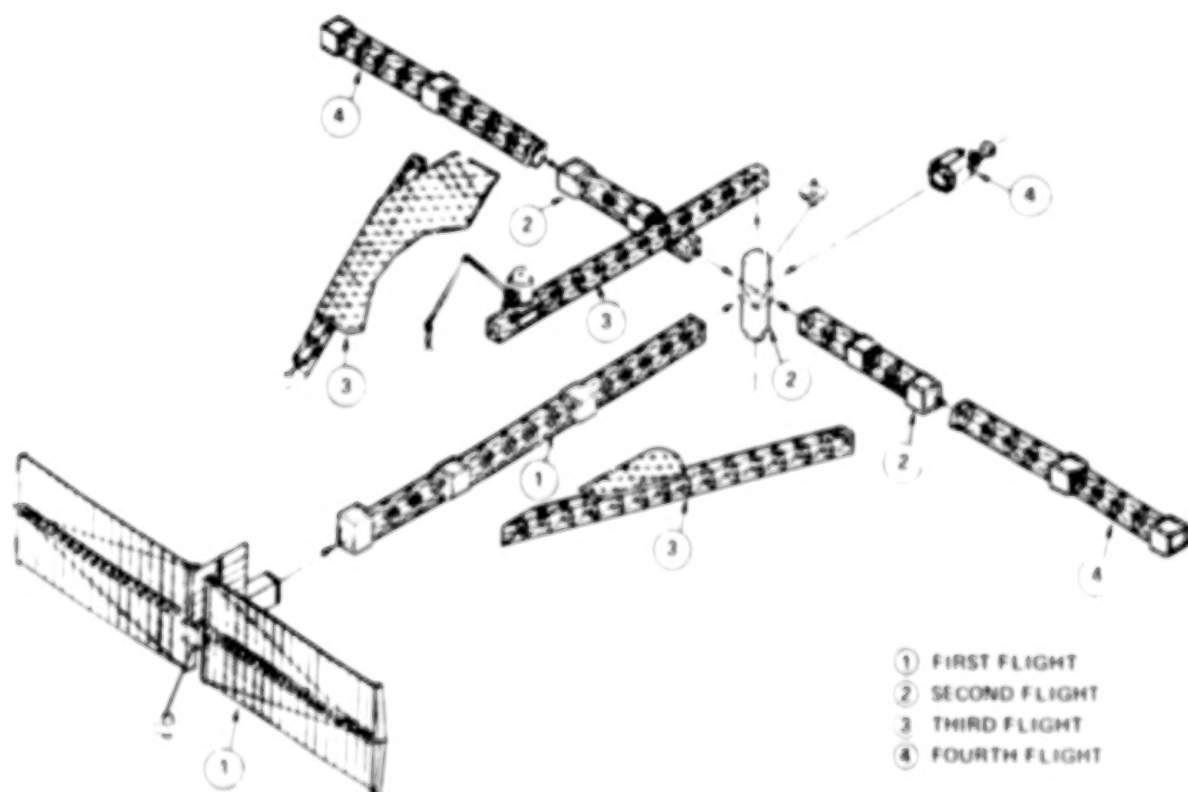


Figure 5.

ASASP POWER DISTRIBUTION WIRE SIZES*/WEIGHT

Electrical power distribution requirements were developed to transfer electrical power between the platform subsystems and the payload interfaces. unregulated high voltage (124-164 VDC) power will be provided to each payload interface for high power usage of up to 20 kW. The unregulated high voltage will also be provided to the ASASP subsystems module where power regulators will provide a regulated 30 VDC power to each payload interface where 4 kW will be available for payload usage. In addition, 400 Hz inverters will be located in the subsystems module to provide 115/200 VAC 3 Ø 400 Hz power to each payload interface.

Given the electrical voltage and power requirements, the power distribution wiring requirements were developed. The numbers and sizes of all wires required to distribute electrical power to the various interfaces are illustrated. The largest wiring size was limited to #0 gauge wire as this is the largest size in use with space-qualified connectors. Wiring was sized to limit distribution loss to an orbital average of 7.5% or less with a resistance corresponding to 366 K (200°F) maximum wire temperature. Wiring outside diameters for the various wire sizes used are shown in the small table at the bottom. These diameters are based on the use of multistranded small-gauge rope lay cable with Teflon TFE tape insulation.

	UNREGULATED HIGH VOLTAGE DC		REGULATED 30 VDC MAINS		REGULATED 30 VDC P/L SUBSYSTEMS		115/200 VAC 3Ø 400 Hz	
	CIRCUIT CONFIG	WIRE WEIGHT	CIRCUIT CONFIG	WIRE WEIGHT	CIRCUIT CONFIG	WIRE WEIGHT	CIRCUIT CONFIG	WIRE WEIGHT
PS TO ASASP SUBSYSTEMS MODULE	3 BUSES 2 CCTS/BUS 2 #2 GA/CCT	768 POUNDS 12 WIRES						
SUBSYSTEMS MODULE TO P/L INTERFACES	3 BUSES 1 CCT/BUS 2 #0 GA/CCT	1665 POUNDS 6 WIRES	3 BUSES 2 CCTS/BUS 2 #2 GA/CCT	2294 POUNDS 12 WIRES	1 BUS 2 CCTS 2 #2 GA/CCT	765 POUNDS 4 WIRES	1 BUS 1 CCT 4 #14 GA	43 POUNDS 4 WIRES
SUBSYSTEMS MODULE TO ORBITER I/F			3 BUSES 2 CCTS/BUS 2 #0 GA/CCT	113 POUNDS 12 WIRES				
SUBSYSTEMS MODULE TO REBOOST MODULE I/F			2 BUSES 1 CCT/BUS 2 #12 GA/CCT	1 POUND 4 WIRES				
SUBSYSTEMS MODULE TO CONSTRUCTION MANIPULATOR I/F			2 BUSES 1 CCT/BUS 2 #2 GA/CCT	116 POUNDS 4 WIRES				

(1 LB = 0.45 KG; 1 IN = 2.54 CM)

* WIRE SIZE (GAGE)	#0	#2	#12	#14
WIRE OD (INCHES)	0.47	0.37	0.18	0.08

Figure 6.

ASASP FIBER OPTIC DATA CABLES

Data distribution on board the ASASP was based on the data subsystem requirement to provide the following data services to each of eleven payload berthing ports:

- Scientific data acquisition ≤ 20 Mbps peak.
- Housekeeping data acquisition ≤ 50 Kbps peak.
- Command capability ≤ 25 Kbps peak.
- TV/Analog data acquisition ≤ 4.2 MHz.
- Total data rates (all payloads) not to exceed 25 kW ref P/S capability.

Two options for data distribution were considered, both based on the use of fiber optic data paths. Fiber optics was selected because of its advantages over copper cable in data capacity, weight, size, and EMI susceptibility, and its expected cost advantage in the late 1980's. The data bus option offers advantages associated with less total cable, i.e., lower weight, installation ease. However, the dedicated link option was chosen for the ASASP because (1) its implementation does not depend on the development of optical bus couplers, and (2) it represents a more stressing condition for structural design. For purposes of bundle sizing, it is assumed that five separate fiber optic channels are required between the central data subsystem and each payload port. The figure shows the resulting number of channels at each segment of the Platform and the estimated OD of the bundle along each platform segment.

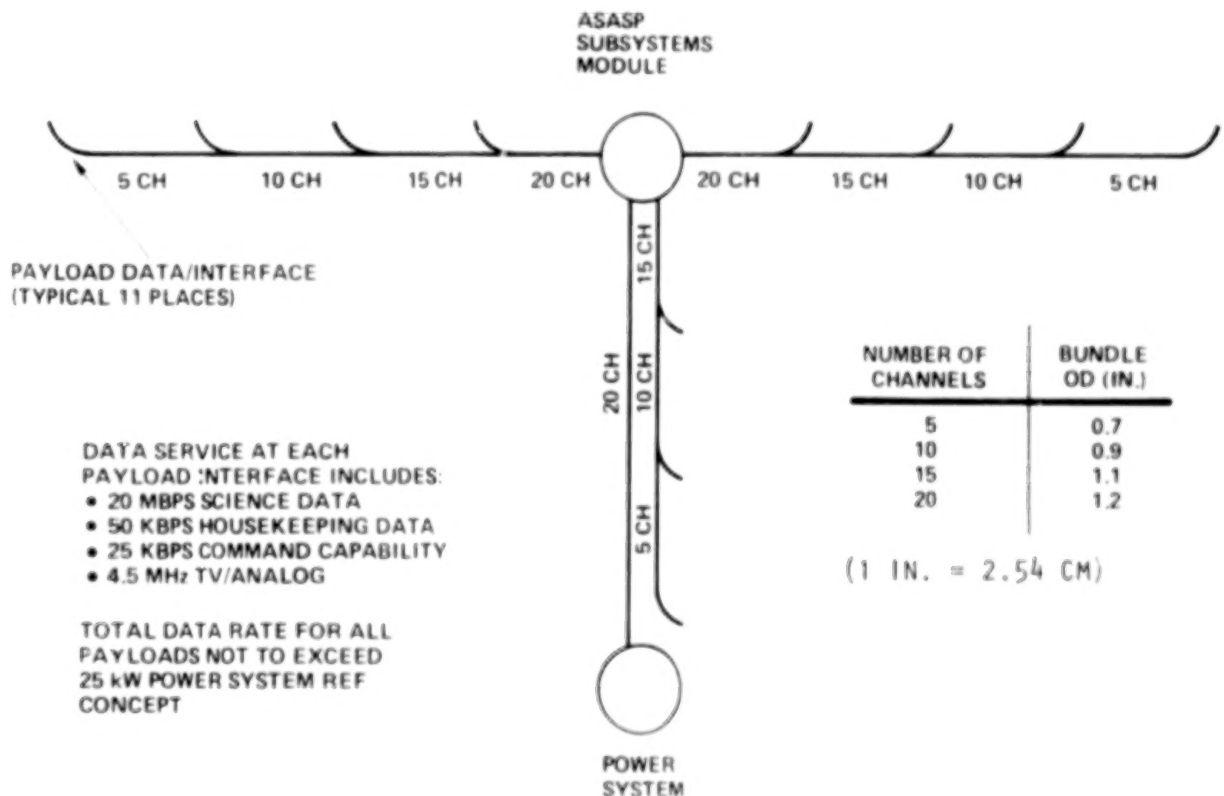


Figure 7.

PRELIMINARY ESTIMATE OF MAXIMUM ALLOWABLE BASE ACCELERATION FOR AGS GIMBAL SYSTEM (STRUCTURAL RESPONSE REQUIREMENT)

For payloads with a pointing system, a preliminary estimate of the maximum allowable base acceleration was made. The analysis is based upon the AGS pointing system acceleration disturbance model and a simplified disturbance controller model summarized on Figures A and B respectively.

The basis of the analysis and results are shown on Figure C which plots allowable base acceleration perpendicular to line-of-sight (A LOS) versus frequency for a pointing stability requirement of 0.1 sec LOS error. The results indicate that base acceleration levels must be held to 10^{-4} to 10^{-3} g's to meet the noted stability requirement.

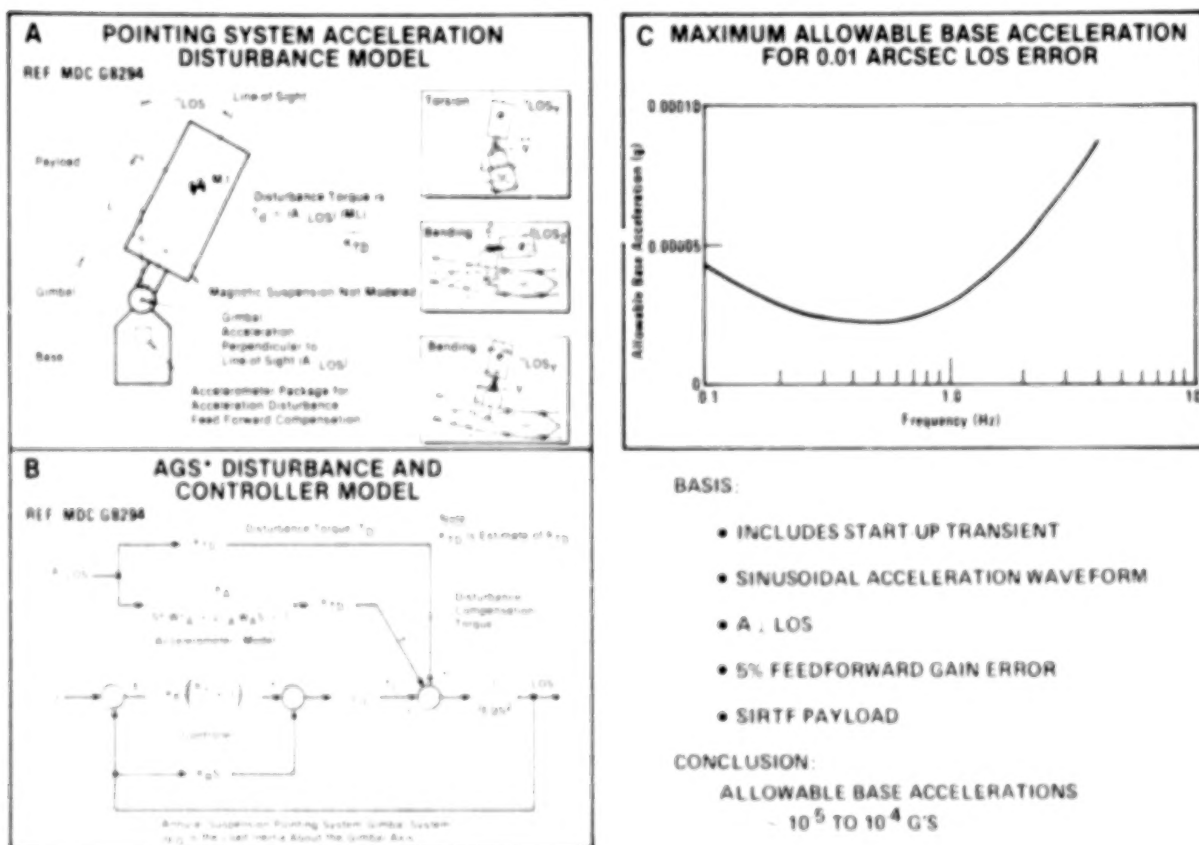


Figure 8.

ADVANCED SASP STRUCTURAL STRENGTH AND STIFFNESS REQUIREMENTS (SUMMARY)

Structural strength and stiffness requirements were developed for an Advanced SASP Platform. These requirements were based upon considerations of (1) Orbiter to Platform docking, (2) lower bound structural vibration frequencies for platform overall attitude control and minimum impact on IPS and AGS pointing systems currently being developed, (3) platform structural response requirements based upon considerations of payload pointing and stability accuracy requirements for payloads with and without pointing systems, and (4) platform accelerations during reboost, roll, pitch, and yaw maneuvers.

The docking loads and stiffness requirements were based upon the noted constraints. The Orbiter closing conditions were selected based upon results of Orbiter docking simulations conducted at JSC. The maximum allowed Orbiter bending moment of 162 698 J (120 000 ft-lb) was selected as 50% of the Orbiter longeron limit strength capabilities and the maximum allowable platform rigid body acceleration consistent with this assumption is .02g. The maximum allowable Orbiter c.g./platform relative travel was selected as 0.61 m (2 ft) which requires that the platform rigid body acceleration be greater than .001g.

- DOCKING LOADS AND STIFFNESS REQUIREMENTS (HARD DOCK) (1 ft = 0.305 m; 1 ft-lb = 1.36 J)
 - ORBITER CLOSING CONDITIONS - $v_z = 0.5 \text{ FT/SEC}$, $\theta_y = 0.2 \text{ DEG/sec}$
 - MAXIMUM ALLOWED ORBITER BENDING MOMENT - $M_y \text{ MAX} = 120,000 \text{ FT-LB}$
 - MAXIMUM ALLOWED ORBITER CG/PLATFORM RELATIVE TRAVEL - 2 FT
 - MAXIMUM ALLOWED PLATFORM ACCELERATION - 0.02 g (RIGID BODY)
 - PLATFORM STRENGTH AND STIFFNESS REQUIREMENTS (SEE CHART)
- LOWER BOUND STRUCTURAL VIBRATION FREQUENCIES
 - OVERALL ATTITUDE CONTROL - $f_1 \geq 0.1 \text{ Hz}$
 - MINIMUM IMPACT ON IPS OR AGS SYSTEMS NOW BEING DEVELOPED - $f_1 \geq 4 \text{ Hz}$
- STRUCTURAL RESPONSE
 - (PAYLOADS WITH POINTING SYSTEM)
 - MAXIMUM ALLOWABLE BASE ACCELERATION (SINUSOIDAL WAVE) - $10^{-4} \text{ TO } 10^{-3} \text{ g's}$
(THERMAL AND MECHANICAL LOAD INPUTS)
 - (PAYLOADS WITHOUT POINTING SYSTEM)
 - STABILITY
 - MAXIMUM ALLOWED DYNAMIC ROTATIONAL RESPONSE - 0.25 DEG/SEC (0.5 DEG MAX)
(THERMAL AND MECHANICAL LOAD INPUTS)
 - ACCURACY
 - MAXIMUM QUASI-STATIC THERMAL ROTATION DISTORTION - 1 DEG
- MANEUVER ACCELERATIONS
 - REBOOST - $X = 0.0015 \text{ g's}$; $y = 0.00015 \text{ g's}$; $Z = 0.00015 \text{ g's}$
 - ROLL, PITCH, YAW - $1.5 \times 10^{-5} \text{ RAD/SEC}^2$; $1.4 \times 10^{-5} \text{ RAD/SEC}^2$; $8.1 \times 10^6 \text{ RAD/SEC}^2$

Figure 9.

ADVANCED SASP STRUCTURAL STRENGTH AND STIFFNESS REQUIREMENTS (SUMMARY)

Structural response requirements were estimated for payloads requiring pointing systems and the results indicate that allowable sinusoidal payload base accelerations must be held to 10^{-4} to 10^{-3} g's to meet a payload pointing stability requirement of .1 sec LOS error.

For payloads without a pointing system, a maximum dynamic rotational response rate of .25 deg/sec is required along with a maximum response of .5 deg to meet the stability requirements of the PBI and AGWA experiments, respectively. This requirement is the maximum allowed due to combined thermal and mechanical dynamic excitation response.

A quasi-static thermal distortion maximum accuracy requirement of 1 deg was selected to allow for the possibility of future experiments without pointing systems but with more demanding accuracy requirements than the AGWA or PBI.

For reboost, using a minimum platform mass and reboost propulsion thrust load of 890 N (200 lb), the maximum X axis translational rigid body acceleration expected is .0015 g's. Considering the $\pm 6^\circ$ gimbale angle, the maximum Y and Z axis acceleration levels will be approximately 10% of this value, or .00015g.

Using 10 Skylab type CMG's and the ASASP mass properties, the roll, pitch, and yaw rigid body angular acceleration levels are found to be 1.5×10^{-6} , 1.4×10^{-5} , and 8.1×10^{-6} rad/sec², respectively.

- DOCKING LOADS AND STIFFNESS REQUIREMENTS (HARD DOCK) (1 ft = 0.305; 1 ft-lb = 1.36 J)
 - ORBITER CLOSING CONDITIONS $\sim v_z = 0.5$ FT/SEC, $\dot{\theta}_y = 0.2$ DEG/sec
 - MAXIMUM ALLOWED ORBITER BENDING MOMENT $\sim M_y \text{ MAX} = 120,000$ FT-LB
 - MAXIMUM ALLOWED ORBITER CG/PLATFORM RELATIVE TRAVEL ~ 2 FT
 - MAXIMUM ALLOWED PLATFORM ACCELERATION ~ 0.02 g (RIGID BODY)
 - PLATFORM STRENGTH AND STIFFNESS REQUIREMENTS (SEE CHART)
- LOWER BOUND STRUCTURAL VIBRATION FREQUENCIES
 - OVERALL ATTITUDE CONTROL $\sim f_1 \geq 0.1$ Hz
 - MINIMUM IMPACT ON IPS OR AGS SYSTEMS NOW BEING DEVELOPED $\sim f_1 \geq 4$ Hz
- STRUCTURAL RESPONSE
 - (PAYLOADS WITH POINTING SYSTEM)
 - MAXIMUM ALLOWABLE BASE ACCELERATION (SINUSOIDAL WAVE) $\sim 10^{-4}$ TO 10^{-3} g's
(THERMAL AND MECHANICAL LOAD INPUTS)
 - (PAYLOADS WITHOUT POINTING SYSTEM)
 - STABILITY
 - MAXIMUM ALLOWED DYNAMIC ROTATIONAL RESPONSE ~ 0.25 DEG/SEC (0.5 DEG MAX)
(THERMAL AND MECHANICAL LOAD INPUTS)
 - ACCURACY
 - MAXIMUM QUASI-STATIC THERMAL ROTATION DISTORTION ~ 1 DEG
- MANEUVER ACCELERATIONS
 - REBOOST $\sim X = 0.0015$ g's; $Y = 0.00015$ g's; $Z = 0.00015$ g's
 - ROLL, PITCH, YAW $\sim 1.5 \times 10^{-5}$ RAD/SEC²; 1.4×10^{-5} RAD/SEC; 8.1×10^{-6} RAD/SEC²

Figure 10.

APPLICATION OF MODULAR CONTROL TO ASASP

With sensors and actuators distributed throughout the vehicle, it is easy to visualize the ACS as shown in Figure 11, where structure N is the AGWA, PBI, manipulator capsule and Orbiter ($N=3,4,5,6$). In general, a control module is included on each structure. Stabilization sensors and actuators may be mounted on each structure, along with all auxiliary hardware. A processor may also be included for processing of sensor data, actuator commands and for communication with a main or coordinator processor. Outputs from each control module could be sensor and momentum storage data. Inputs from the coordinator processor could be the short term feedbacks, long term attitude commands, and momentum management commands.

The ACS design will also be faced with the stabilization of two or more connected structures and with self-contained attitude control sensors and actuators. The attitude stabilization problem with vehicles of this type is caused by the compliance between adjacent structures. Bodies 1 and 2 would be the PS and construction platform, respectively.

- Design goal for stiffness of the construction platform section should have no structural natural frequencies less than 4-5 Hz.
- Beam coupling between the construction platform and the AGWA, PBI, and PS will result in cantilever and torsional modes above 0.1 Hz.
- Largest possible passive damping of beams connecting the construction platform to the PS, AGWA, and PBI would be advantageous for distributed actuation and experiment pointing.

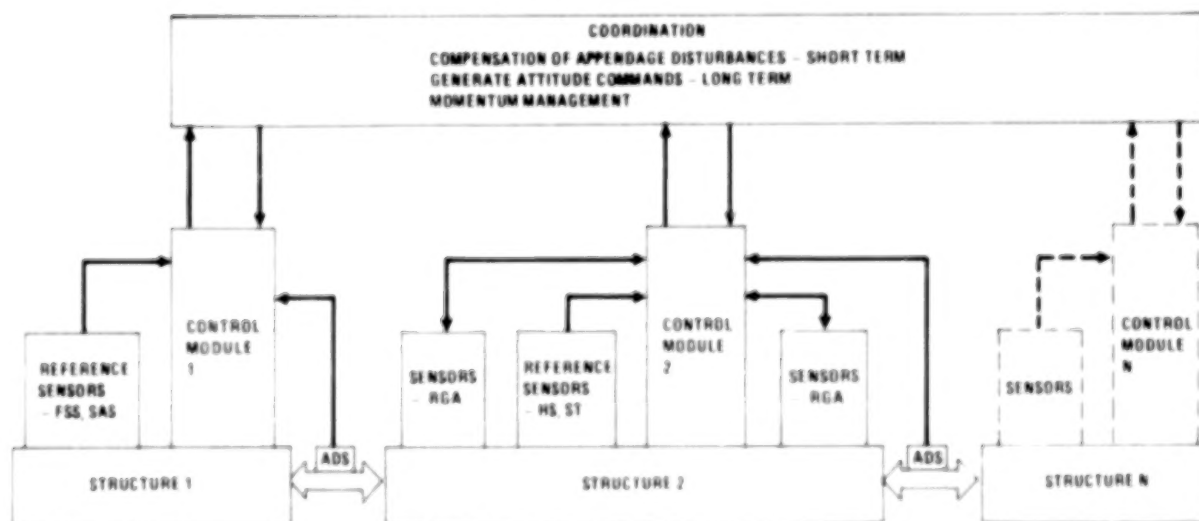


Figure 11.

TECHNOLOGY REQUIREMENTS TO SUPPORT ASASP DEVELOPMENT

For those large pointing instruments, such as the IR Astrometric Telescopes where extreme pointing accuracies are required, the stability of the instrument base becomes critical. A stable instrument base can be provided by any combination of platform structural stiffness, platform structure control systems, and instrument pointing systems. Future technology development is required in one or all of these areas to obtain the required instrument pointing accuracies. Solving this problem primarily through improved structural stiffness would result in the least complex overall system.

Should Orbiter hard docking to the Platform become the desired mode of operation, as assumed in this study, then detailed analysis and preliminary design concepts of a docking mechanism should be initiated. Should a berthing operation be selected in lieu of docking, then berthing mechanisms capable of maneuvering the large masses involved need development.

- DEVELOP CAPABILITY FOR HIGH ACCURACY INSTRUMENT POINTING FROM LARGE SPACE STRUCTURES
 - STRUCTURAL TECHNOLOGY DEVELOPMENT TO PROVIDE HIGH STRUCTURAL STIFFNESS WITH RESULTANT HIGH STRUCTURAL FREQUENCIES
 - CONTROL SYSTEM TECHNOLOGY DEVELOPMENT TO PROVIDE STRUCTURAL STABILITY THROUGH CONTROL/FEEDBACK SYSTEMS
 - INSTRUMENT POINTING SYSTEM DEVELOPMENT TO ALLOW FOR ACCURATE POINTING FROM A RELATIVELY FLEXIBLE PLATFORM BASE
- DEVELOP (ANALYSIS AND DESIGN) AN ORBITER TO PLATFORM DOCKING MECHANISM

Figure 12.

TECHNOLOGY REQUIREMENTS TO SUPPORT ASASP DEVELOPMENT (CONTINUED)

Due to the long distances required for transfer of large quantities of electrical power to support payload operations, power transfer at high voltages becomes necessary. Use of the lower 28-30 DC voltage common today results in excessive power transfer losses and excessive weight involved in the larger size power conductors. The development of space qualified high voltage electrical components in all areas of power conditioning, transfer, and utilization is necessary.

Maintaining the altitude of large space structures in low earth orbit requires significant station keeping impulse due to the large aerodynamic drag forces involved. Use of the relatively low efficiency chemical propulsive systems common today results in a significant mass of propellant to be delivered to the Platform at the expense of useful payload. This large mass of propellant also contributes to undesirable contamination effects when expended. Development of more efficient low thrust chemical propulsion systems or electrical propulsion systems is recommended.

Methods for minimizing the effects of undesirable chemical propulsion exhaust contamination of sensitive payload surfaces needs attention. Very large expansion nozzles installed in orbit by EVA may prove very desirable for minimizing contamination.

The development of construction aids and a means of supporting extended crew stay times to accomplish this significant stay-time construction is recommended.

- DEVELOPMENT OF SPACE QUALIFIED HIGH VOLTAGE ELECTRICAL COMPONENTS IS REQUIRED FOR EFFICIENT ELECTRICAL POWER TRANSFER OVER LONG DISTANCES
- DEVELOP HIGH EFFICIENCY LOW THRUST PROPULSION SYSTEMS FOR PLATFORM STATION KEEPING (THE PERIODIC AVAILABILITY OF EXCESS ELECTRICAL POWER SUGGESTS THE POTENTIAL USE OF ELECTRICAL PROPULSION)
- DEVELOP MEANS FOR MINIMIZING PAYLOAD CONTAMINATION EFFECTS FROM STATION KEEPING AND ORBITER PROPULSION SYSTEMS
- DEVELOP CONSTRUCTION AIDS AND MEANS OF SUPPORTING EXTENDED CREW STAY TIME REQUIRED FOR PAYLOAD AND PLATFORM ON-ORBIT CONSTRUCTION

Figure 13.

RECOMMENDED ACS STUDIES

There is much development work required in the area of attitude control of large space structures. A summary list of recommended attitude control system studies is listed.

- **CONTROL DYNAMICS**
 - DESIGN AND SIMULATION OF DISTRIBUTED ACTUATION SYSTEM
 - STUDY THE EFFECTS OF ROTATIONAL OSCILLATION OF ONE OR MORE CMG SETS AND ITS COMPENSATION
 - DESIGN AND SIMULATION OF "ACTIVE DECOUPLING" OF EXPERIMENT MOTION
 - DESIGN AND SIMULATE IPS CONTROL SYSTEM COMPLETE WITH FEED-FORWARD COMPENSATION, EVALUATE PERFORMANCE WHEN COUPLED WITH ACS-CONTROLLED VEHICLE
 - DOCKING PROCEDURE
- **ATTITUDE DETERMINATION AND MEASUREMENT**
 - STAR TRACKERS VS SCANNERS
 - BLENDING OF EPHEMERIS DATA
 - RATE GYRO UPDATE, CORRELATION BETWEEN ASSEMBLIES
- **MOMENTUM MANAGEMENT**
 - FURTHER DEVELOPMENT OF GRAVITY GRADIENT DESATURATION USING VARIATION ABOUT Y AXIS; MAY FUNCTIONS OTHER THAN SINUSOIDAL BE UTILIZED TO REDUCE GENERATED CYCLIC MOMENTUM
 - FEASIBILITY OF VARIABLE SURFACE CONTROL TO AERODYNAMICALLY TRIM THE VEHICLE ABOUT Y AND Z AXES
 - RCS FEASIBILITY, RESUPPLY, CONTAMINATION
- **STRUCTURAL**
 - ADS SENSOR SYSTEM SELECTION (OPTICS, INERTIAL, STRAIN DEVICES)
 - METHOD OF PASSIVE DAMPING FOR AGWA AND PBI BEAMS TO ASSIST POINTING STABILITY
 - GENERATE VEHICLE DYNAMIC MODEL FOR FUTURE ACS STUDIES

Figure 14.

BLANK PAGE

BLANK PAGE

STRUCTURAL REQUIREMENTS AND TECHNOLOGY NEEDS
OF
GEOSTATIONARY PLATFORMS

G. R. Stone
General Dynamics Convair Division
San Diego, California

Large Space Systems Technology - 1980
Second Annual Technical Review
November 18-20, 1980

GEOSTATIONARY PLATFORM STRUCTURAL REQUIREMENTS STUDY (LSST)

In today's world of expanding space communications services, the geostationary orbit is rapidly becoming an extremely valuable and limited earth resource. At geostationary altitude, independent satellites operating at the same frequency must be separated by about 4 degrees of longitude to prevent RF interference, dictated by the large beamwidths of the small affordable ground antennas now in use. About 90 "slots" therefore exist around the world, with about 12 over the U.S. and our northern and southern neighbors. The frequency spectrum is also a valuable and limited resource which is rapidly approaching saturation, particularly in those regions of low noise and freedom from atmospheric attenuation.

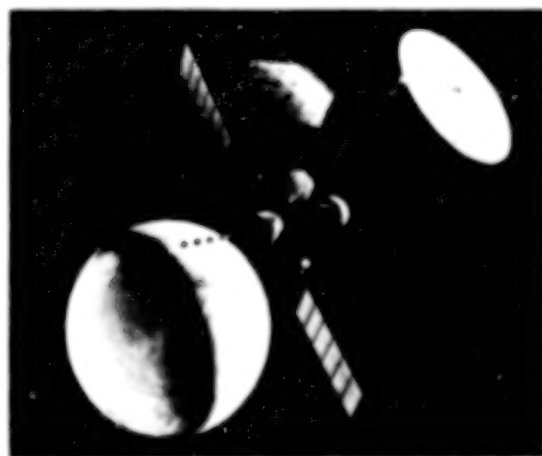
An attractive technical and economic solution to this orbital arc and frequency spectrum saturation problem is the aggregation of many transponders, large antennas, and connectivity switches on board a small number of large orbital space facilities, or "Geostationary Platforms". Under the direction of NASA's George C. Marshall Space Flight Center, an Initial Phase A Study was completed in July of this year (1980), directed toward conceptual definition of Operational Geostationary Platforms of the 1990s. A Follow-On Study is now in progress, and includes a specific task (Task 11) to identify Platform structural requirements and technology needs in the area of Large Space Systems Technology. Task 11 has been completed and is the subject of this summary report.

<u>OBJECTIVE</u>	PROVIDE GEOSTATIONARY PLATFORM REQUIREMENTS TO THE NASA LARGE SPACE SYSTEMS TECHNOLOGY (LSST) PROGRAM. THESE WILL BE USED BY NASA TO IDENTIFY THE STRUCTURAL SYSTEMS TECHNOLOGIES THAT SHOULD BE DEVELOPED FOR FUTURE MISSIONS, INCLUDING GEOPLATFORM.
<u>SCOPE</u>	REQUIREMENTS DEFINITION IS BASED ON REPRESENTATIVE PLATFORM CONCEPTS DEVELOPED IN INITIAL STUDY TASK 3.
<u>LIMITATIONS</u>	GEOSTATIONARY PLATFORM DEFINITION IS CURRENTLY IN AN ITERATIVE CYCLE. PAYLOAD INFORMATION, ON WHICH UTILITY REQUIREMENTS ARE BASED, IS "PRELIMINARY". CONSEQUENTLY, THE STRUCTURAL REQUIREMENTS GENERATED BY THIS ANALYSIS MUST BE CONSIDERED AS <u>REPRESENTATIVE</u> .

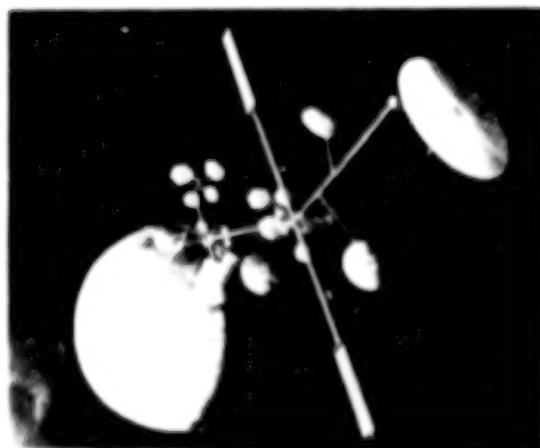
TASK APPROACH

Two of the four platform concepts defined in the Initial Study were selected for further analysis in this study, LSST Task 11, as representative of the probable configurations which could evolve in the next decade or so. Alternative 1 is comprised of 6,800 kg (15,000 lb) platform modules, each delivered to low earth orbit (LEO) with an attached OTV in a single Shuttle flight, deployed, and transferred to a geostationary constellation of platforms. Alternative 4 is made up of 16,800 kg (37,000 lb) platform modules, each delivered to LEO, deployed, mated to a 2-stage OTV (delivered to LEO in two additional Shuttle flights) and transferred to GEO for docking with other modules to form a single large platform.

To identify structural requirements and technology needs of the geostationary platforms, Alternatives 1 and 4 were analyzed with respect to utilities accommodation, interface, and strength and stiffness requirements. Results for the two platform concepts were nearly identical. Differences existed only in the quantitative values of specific design details, and Alternative 4 had the added requirement for docking between modules to form the single large platform.



**INITIAL STUDY
ALTERNATIVE 1**
THREE
REPRESENTATIVE
SINGLE-SHUTTLE-
LAUNCHED
PLATFORMS



**INITIAL STUDY
ALTERNATIVE 4**
SINGLE
REPRESENTATIVE
MULTIPLE-SHUTTLE-
LAUNCHED
PLATFORM

FURTHER DEFINE AND
ANALYZE, WITH EMPHASIS
ON STRUCTURAL ASPECTS:

- UTILITIES
ACCOMMODATION
- INTERFACE
DESCRIPTION
- STRENGTH AND
STIFFNESS
- IDENTIFY LSST
TECHNOLOGY
NEEDS

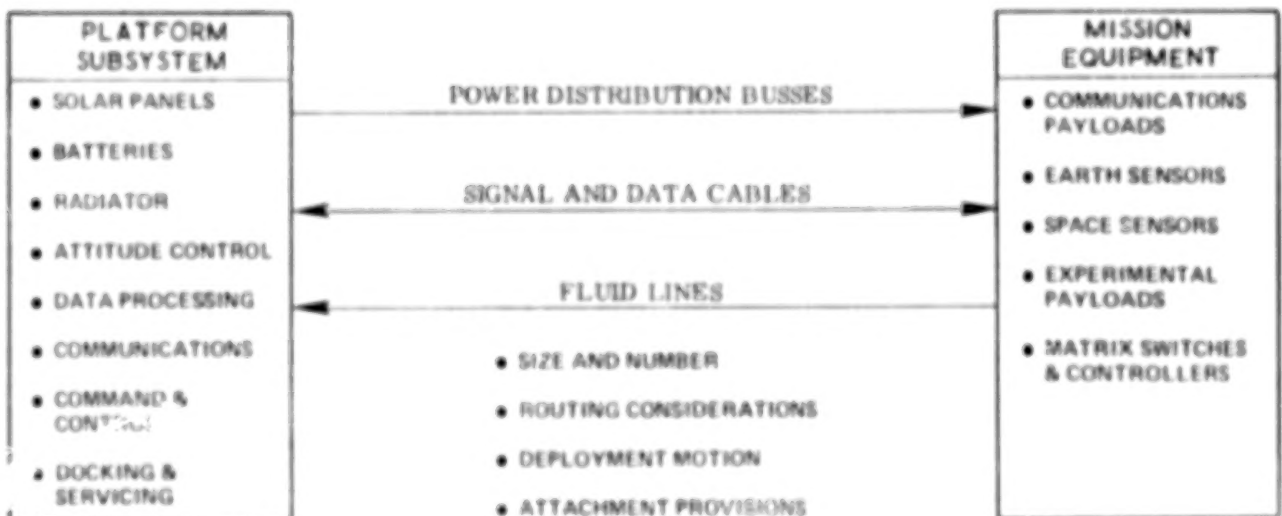
UTILITIES ACCOMMODATION

Large deployable space structures such as the platform concepts require packaging or folding to fit within the dimensional constraints of the Orbiter cargo bay. Utility lines such as those shown here for power, data, and fluid transfer therefore become an integration consideration in the design of the structure.

If the platform is completely deployable with expandable or telescoping structural elements and rotating or geniculate joints, the utility lines must be designed to permit full deployment of the structure without hindering deployment motions or jeopardizing the integrity and effectiveness of the lines.

For each platform or platform module analyzed in this study, the payload utility requirements for power, data, and fluid transfer between platform subsystems and mission equipment were calculated and line routings selected within the structure to accommodate the requirements. The combined utilities requirements for each structural element were defined in terms of service functions, utilities weight and cross-sectional area, and deployment motion involved. The most stringent routings with respect to weight, area, and motion were then analyzed in greater detail to identify feasible design solutions, and the resultant data tabulated for each structural element involved.

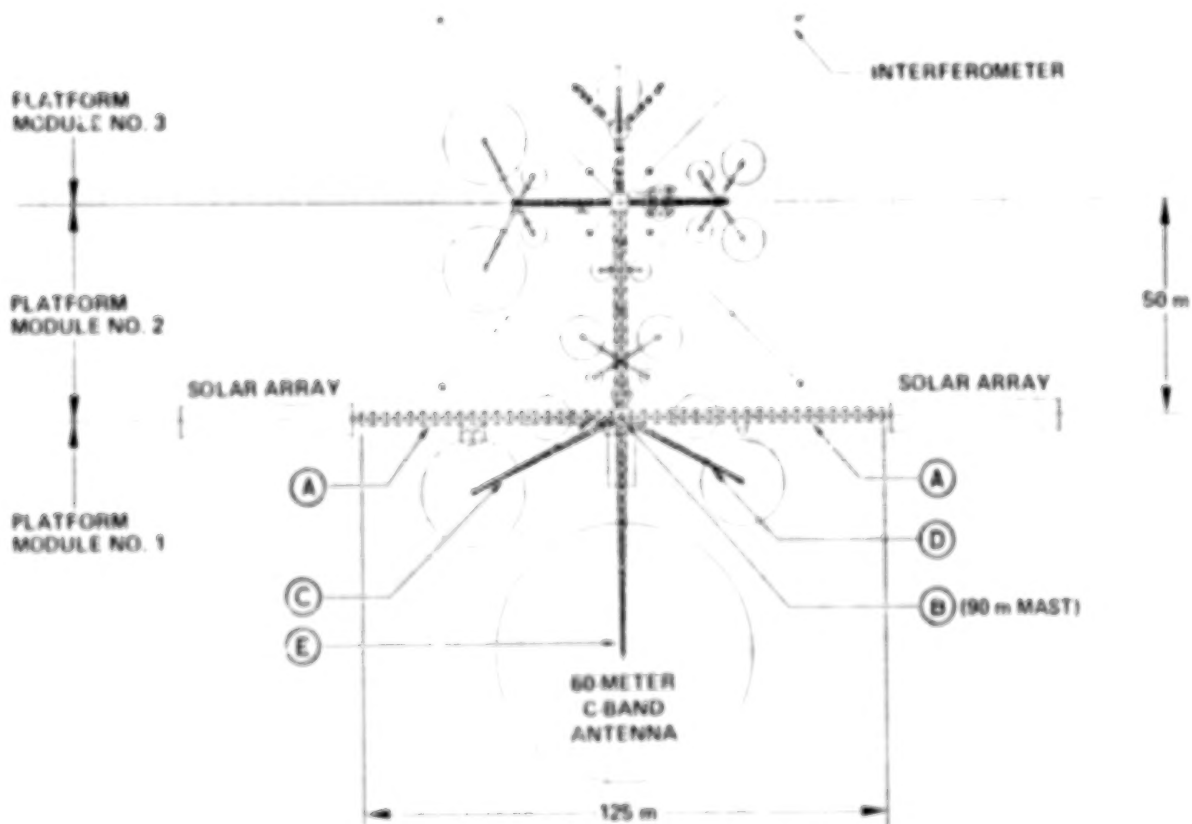
DEFINE REQUIREMENTS FOR DISTRIBUTING UTILITIES (THOSE WHICH MUST BE CONNECTED TO OR INTEGRATED INTO THE STRUCTURAL SYSTEM) BETWEEN PLATFORM SUBSYSTEMS AND MISSION EQUIPMENT.



PLATFORM ALTERNATIVE 4

Shown here are the structural elements of Platform Alternative 4, made up of three modules docked together at GEO to form a single platform with a gross weight of over 50,000 kg (110,000 lb) and a power generation capability of 100 Kw. Predominantly a communications platform, it provides a 60-meter C-band antenna for high-volume trunking service, but also provides an RF interferometer science payload with 120 meter (265 ft) separation arms. The utilities accommodation and distribution considerations involved here are significant.

To identify and quantify the utilities requirements, each structural element was analyzed separately - expandable truss mast "A", for example. Results were tabulated on utilities data sheets for each structural element, and on a summary sheet for the complete platform.



TASK II DATA SHEETS - LSST UTILITIES

Alternative 4, Platform Module No. 1

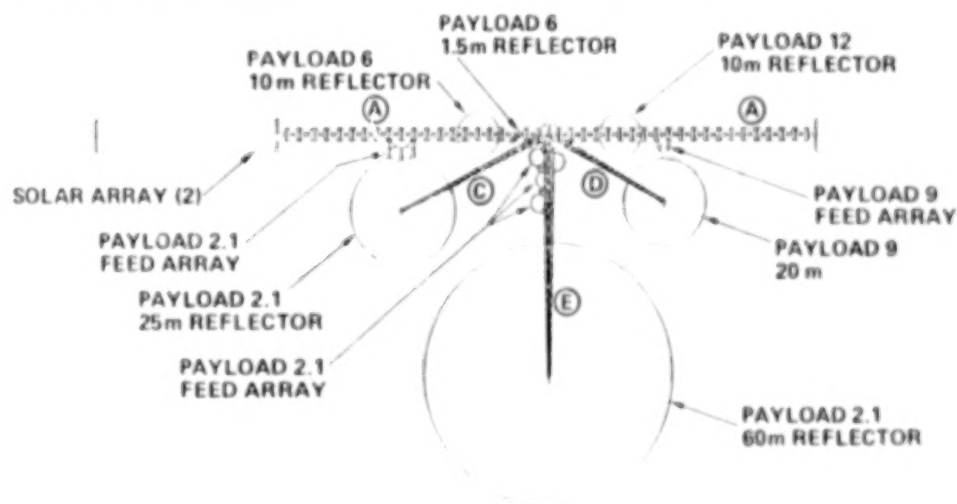
This utilities data sheet for expanding mast "A" is typical of those for the structural elements in each platform. Payloads supported by the arm are identified in the table heading (payloads 6 and 12, feeds for payloads 2.1 and 9), and are located on the figure showing their relationship to other components of the payloads (antennas for payloads 2.1 and 9) and to other payloads and structure.

Power and data distribution lines and cables, radiator fluid lines, and ACS propellant feed lines are tabulated by number and size. Joint accommodation in number of joints and degrees of angular rotation, and required expansion or extension of utility lines in meters are tabulated to identify requirements which must be investigated for viable design solutions.

POWER: 400 VAC/400 VDC

STRUCTURAL ELEMENT: EXPANDING ARMS (A)
PAYLOADS SUPPORTED: PAYLOAD 6, 12, FEEDS FOR 2.1, 9

Utility Requirements									Utility Combined Weight (kg/m)	Services Routing						
Power Distribution		Qty of 22 AWG TSP	Qty of 26 AWG TSP	Fiber Optic or Coax Data		Other Services				Pivoted Support		Rotating Joint		Telescoping Strut		Expand Mast
Qty	AWG			Type	Qty	Function	Qty	Size (cm)		Qty	Deg	Qty	Deg	Qty	ΔL (m)	ΔL (m)
20	18	34	58	FO	144	FLUID LINES	6	2.5	6.2			3	±5		60	
4	13					ACS FEED	4	1.0							60	
6	3														60	

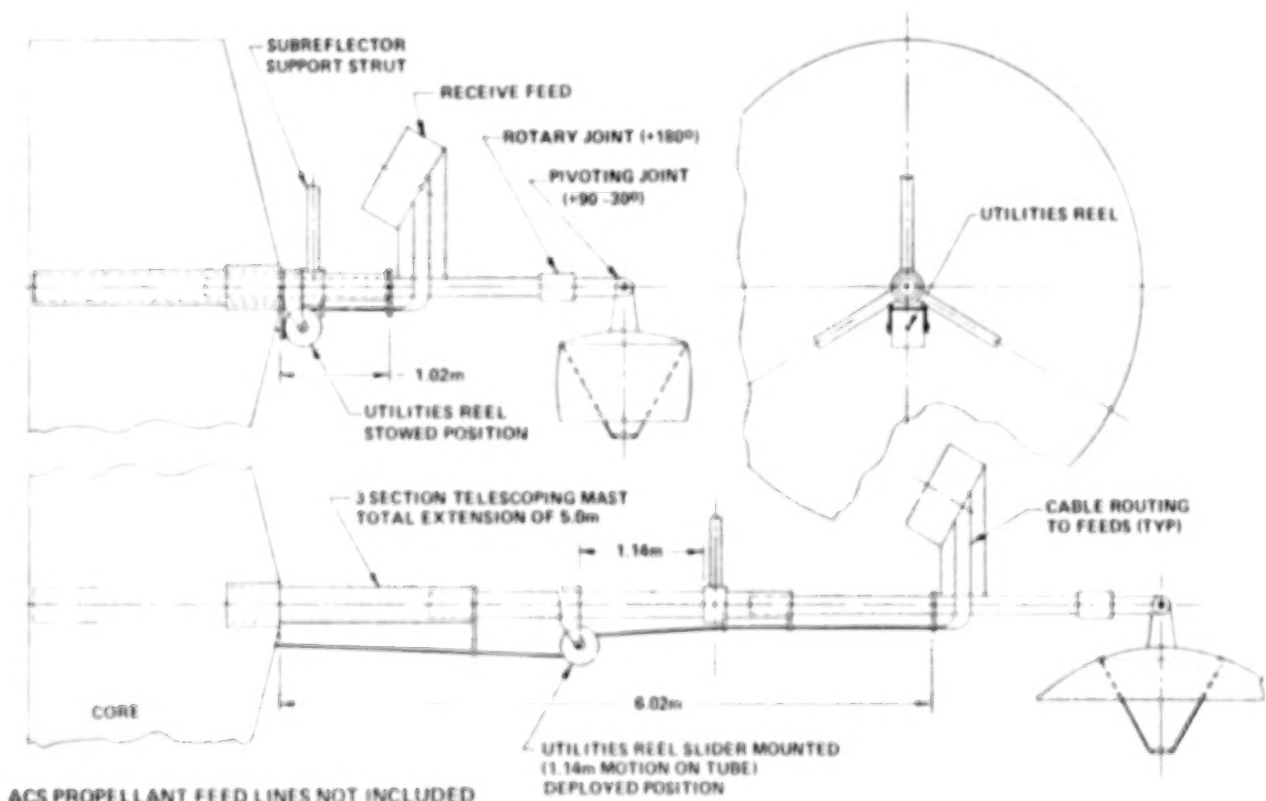


TELESCOPING MAST Utilities Accommodation Concept

Wherever unique or unusual utilities accommodation requirements were identified, designs were developed to determine the feasibility of the basic concept. One such concept is shown here for structural element A₁, Platform No. 6 of Alternative 1. A traveling utilities reel using a flat-ribbon single umbilical floats on one section of the mast, free to slide as the umbilical deploys in both directions to accommodate a 6-meter extension of the deployable mast.

Concepts such as this and others developed during the study are not intended to imply optimized design solutions. They are intended only to show that solutions to the utilities accommodations requirements are possible, and may require innovative designs in some instances.

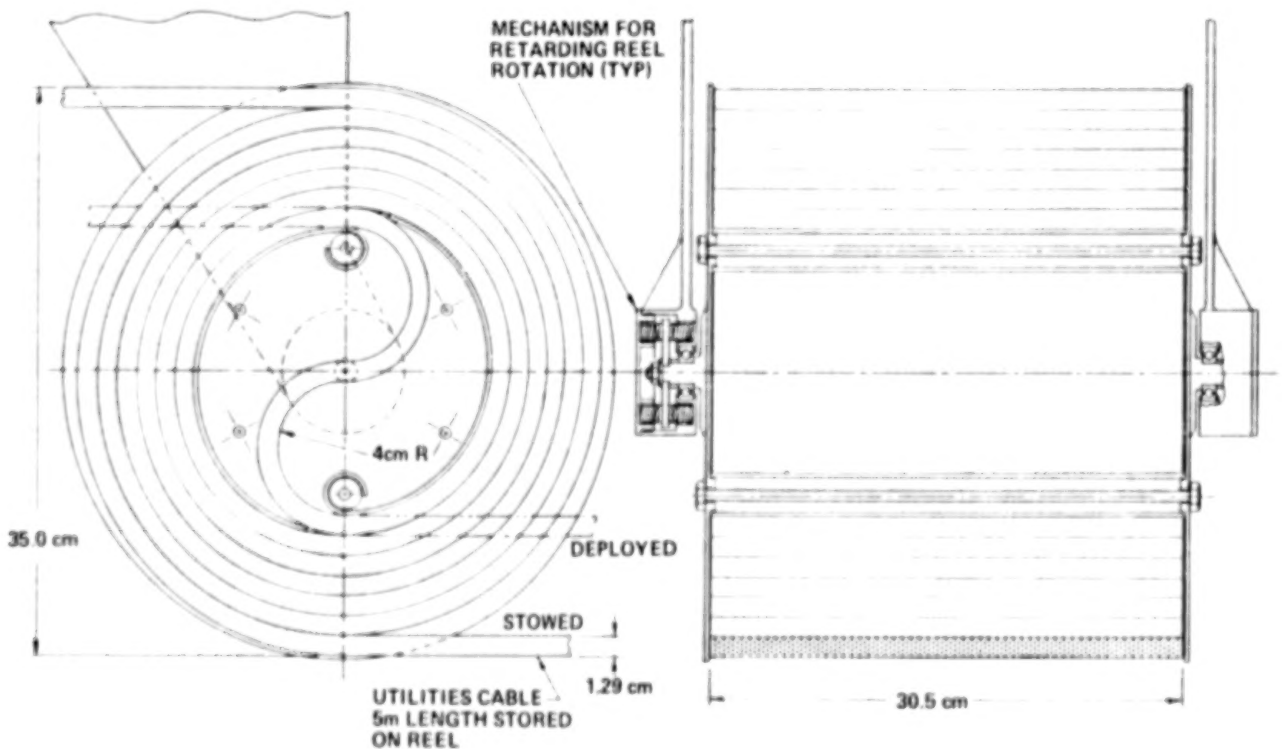
ALTERNATIVE 1, PLATFORM NO. 6, ELEMENT A₁



UTILITIES REEL CONCEPT

The reel concept shown in the previous figure is given in more detail here. A 1/2" by 12" flat umbilical is double-wound on the reel; there are no umbilical "ends" on the reel. A retarding mechanism is used on the reel as it deploys, to prevent free-wheeling. This same spring-loaded mechanism permits rewinding of the umbilical during mast retraction and repackaging, if there is a mission abort resulting from failure to attain proper checkout after deployment.

ALTERNATIVE 1, PLATFORM NO. 6, ELEMENT A₁



ALTERNATIVE 1, PLATFORM NO. 1 UTILITIES SUMMARY

The utilities requirements for all structural elements of each Platform were summarized in the final report for all platform subsystems and payloads, detailing cable and line sizes, functions, and joint and element descriptions. Here, the utilities for Platform No. 1 of Alternative 1 are summarized in short form for each structural element. The combined cross-sectional area of the umbilicals to be carried on each element is given to identify flexibility and volume requirements. The combined utilities weight in kg/meter was used as input to the strength analysis task, to determine the impact of utilities accommodation on strength and weight requirements for each platform structural element.

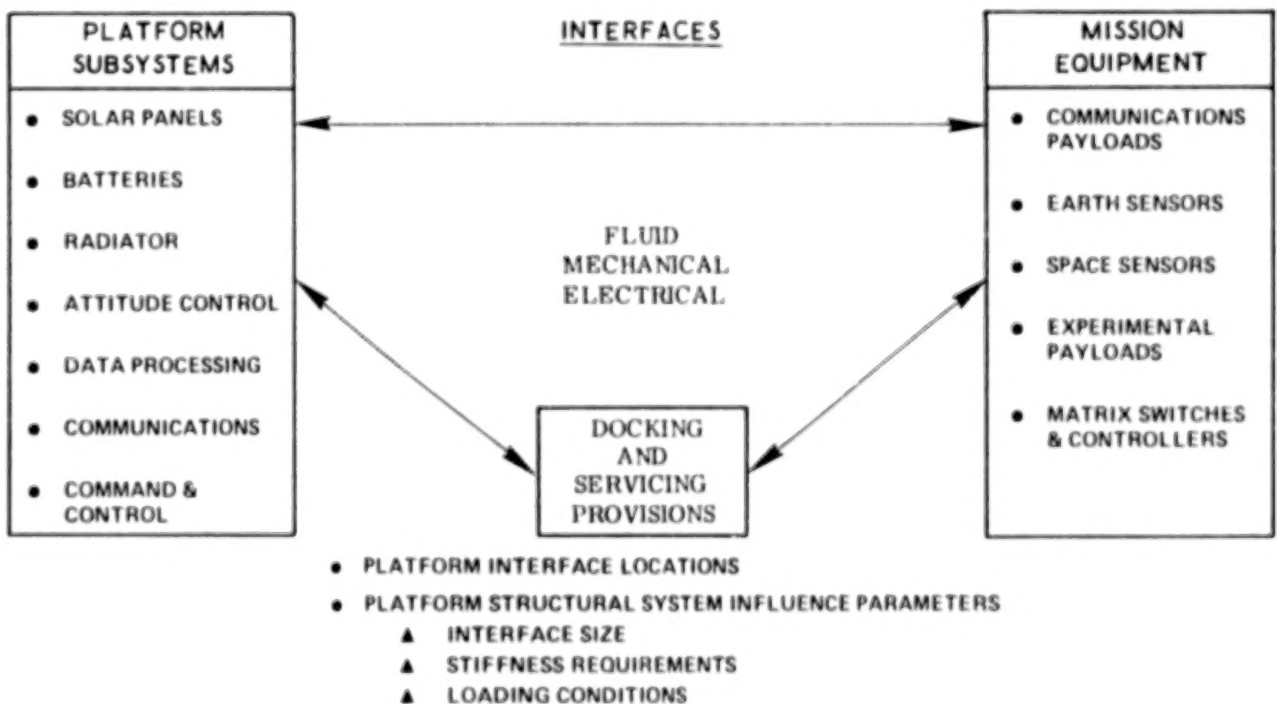
STRUCTURAL ELEMENT	UTILITY REQUIREMENTS (QTY)				ROUTING REQUIREMENTS (QTY)				COMBINED UTILITIES WEIGHT (kg/m)	COMBINED CROSS SECTION AREA (cm ²)
	POWER WIRES	DATA WIRES (TSP)	OPTICAL FIBERS	FLUID LINES	PIVOT	ROTATE	TELESCOPE	EXPAND ΔL (m)		
A	4	97	4	2	-	-	-	17.3	3437	12.20
B	-	24	-	-	1	1	-	14.9	0.707	2.52
C	-	24	-	-	1	1	-	11.8	0.707	2.52
D	4	35	4	-	1	1	-	3.7	1.066	4.31
FEED	4	32	65	-	2	1	-	-	1.231	16.39
E	22	86	150	2	3	1	9	-	4.696	31.99
F	10	64	1	4	1	-	-	-	3.648	14.46
G	6	16	-	-	1	1	-	-	1.592	5.39
RAD	-	23	-	2	10	-	-	-	1.349	12.07

INTERFACE REQUIREMENTS

Interfaces to be considered on the Geostationary Platforms are summarized here. Since interface requirements between payload mission equipment and platform subsystems are existing state-of-the-art in current communications satellites, only the interfaces concerned with docking and servicing were investigated.

"Docking" refers here to the joining of platform modules to create a single large platform in geostationary orbit. "Servicing" refers to the periodic maintenance and resupply of expendables aboard a platform every other year or so to provide extended lifetime. Servicing at this time is envisioned as unmanned automated visits by an Orbit Transfer Vehicle (OTV) carrying a servicing module such as the Teleoperator Maneuvering System (TMS) or equivalent. The servicing module will be equipped to add or replace black boxes and batteries, and replenish propellants for stationkeeping and attitude control either by tank replacement or liquid transfer. Payload replacement or addition is a further possibility, to increase communications services and improve performance.

DESCRIBE MECHANICAL AND ELECTRICAL INTERFACES FOR PLATFORM SUBSYSTEMS, MISSION EQUIPMENT, AND DOCKING/SERVICING OPERATIONS.

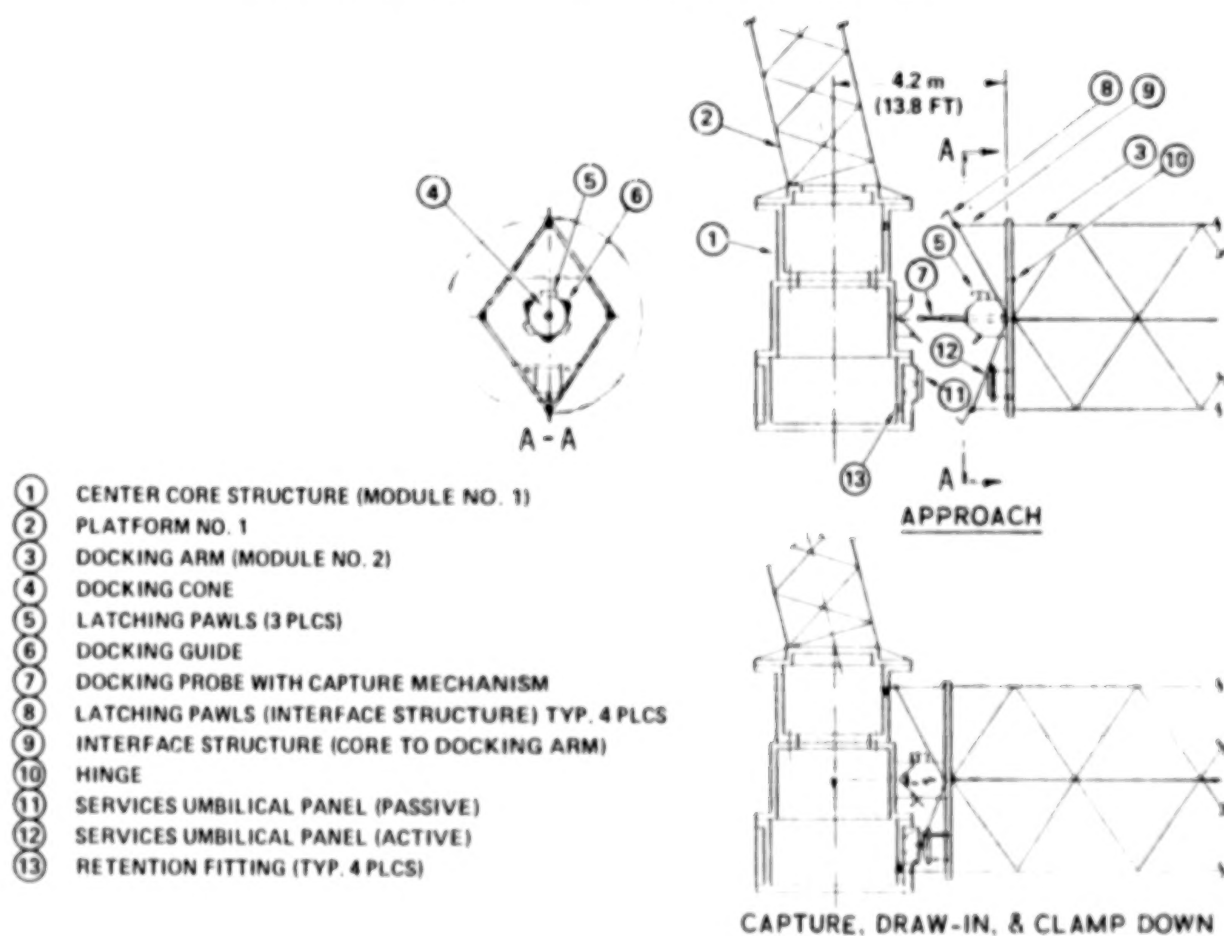


DOCKING CONCEPT

A single-point docking system has evolved in our studies as an optimum method for joining large structures in space. It minimizes risk, technology development, and structural loading, which also obviates the need for a complex damping system. The concept incorporates a utilities panel interface with the docking structure.

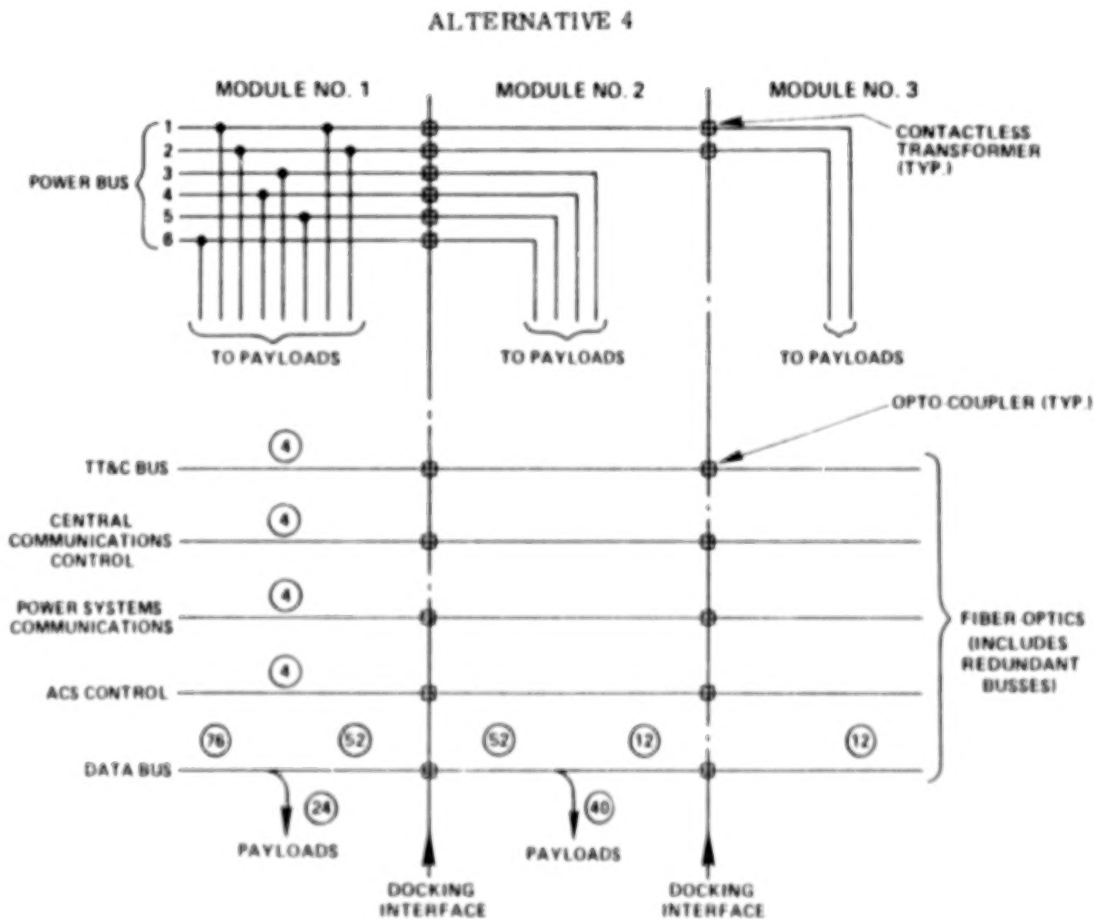
As shown here for Platform Modules 1 and 2 of Alternative 4, Module #2 is the active module and incorporates a steerable probe and docking latches. In the final approach position (approximately 1.5 m separation), the steerable probe is engaged by the passive docking port in Module #1. The steerable probe is retracted, drawing the two modules together. Docking guides are provided on the docking port and receptacle that orient or clock the two modules as the draw-in progresses. Once the draw-in is complete, perimeter latches on the active probe are actuated, structurally joining the two halves of the docking mechanism. To accommodate utilities across the interface, the powered half of the interface panel is driven forward to engage the passive half of the interface panel.

ALTERNATIVE NO. 4 - PLATFORM MODULE NOS. 1 & 2



DOCKING INTERFACE SCHEMATIC - SUPPORT SERVICES

A typical docking interface schematic, for Alternative #4, is shown here, identifying the service utilities that are required across the interfaces between the modules that make up the platform. For simplicity, utilities are combined by function into separate disconnects, as shown by the 52 fiber optic data line disconnects between modules #1 and #2. Circled numbers indicate the number of leads in each bundle.

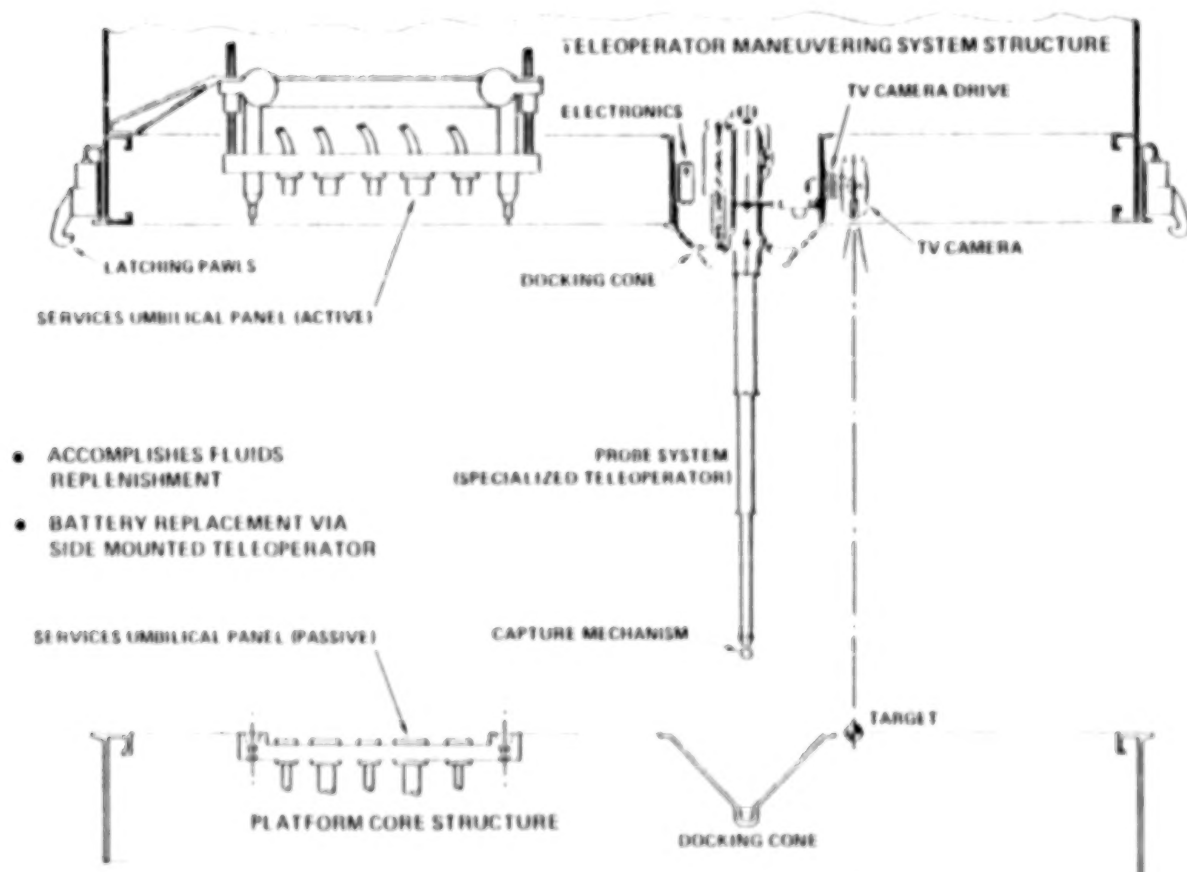


ALTERNATIVE TMS ON-ORBIT SERVICING INTERFACE CONCEPT

To extend the useful life of geostationary platforms, servicing in geostationary orbit is needed. Our platform conceptual designs are based on a central core structure which contains the major components of the support subsystems. This central core interfaces with the OTV for platform transfer from LEO to GEO, and can also serve as the interface for the TMS, for servicing. Advantages of this concept are:

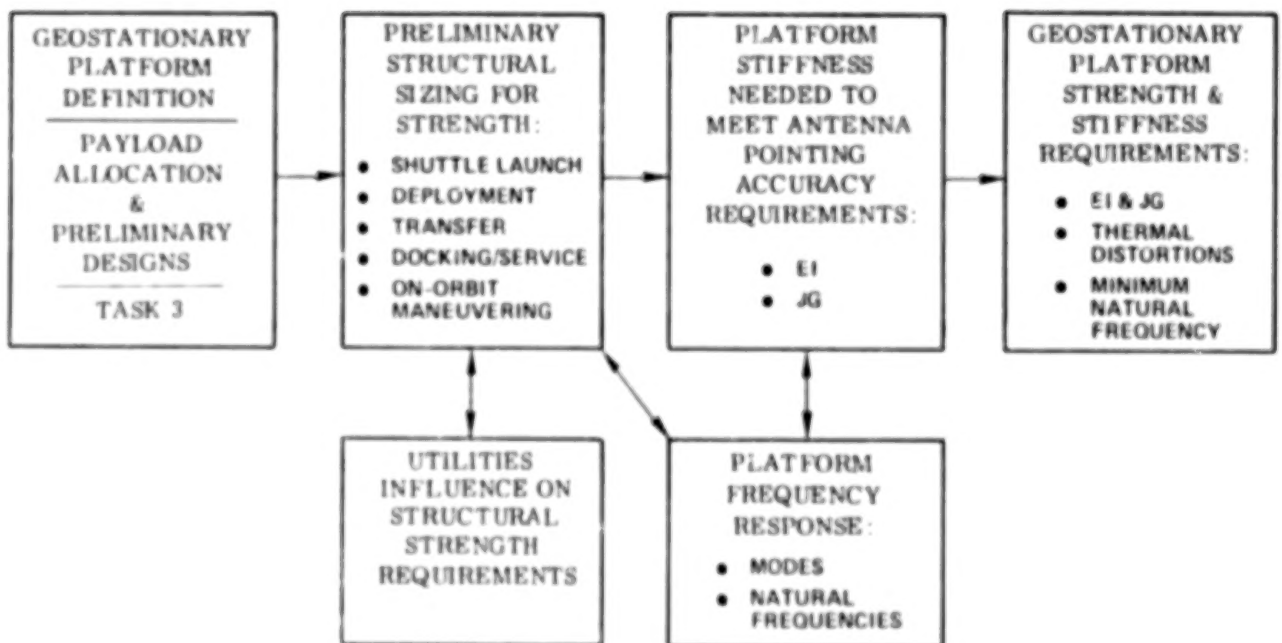
- It provides a common OTV and TMS interface for all platforms.
- Replaceable components and platform expendables are contained in a centralized location within reach of the TMS manipulator arms.
- A soft docking technique can be used for the TMS with unobstructed access to the platform during approach and docking.

The central core system can also include a servicing panel with a matching one on the TMS. This servicing interface concept is shown here, incorporating the same umbilical panels and docking mechanisms as the platform-to-platform docking concept.



STRENGTH AND STIFFNESS APPROACH

The platform configurations considered in this study were all sized on a preliminary basis for strength, to withstand the major load conditions shown here. The structures were then iterated for effect of the utilities accommodation requirements, dynamic response, and stiffness requirements.



UTILITIES INFLUENCE ON STRENGTH REQUIREMENTS

From a strength standpoint, the effect of the utility distribution system on the structural mass of the platforms proved to be minimal. The weight penalties associated with even the most critical structural supports such as those for the cantilevered subsystems were on the order of 2 to 4 percent increase in structural mass for each structural element.

- ANALYZED EFFECT OF DISTRIBUTED SERVICE LINES ON STRUCTURAL MEMBERS FOR T/W BETWEEN 0.035 & 0.10 G.
- WEIGHT PENALTIES OF 2 TO 4 PERCENT FOR MOST CRITICAL STRUCTURAL ELEMENTS (CANTILEVERED BEAMS).

MINIMAL EFFECT

DYNAMIC ANALYSIS

NASTRAN finite element models were generated for the platforms, based first on strength requirements, and later for the effect of resizing for stiffness.

For Platform Alternative 4, shown here, the model was comprised of 65 grid points, 64 structural elements, and 390 structural degrees of freedom, total. Natural modes and corresponding natural frequencies were determined for the system, listed here. The fundamental natural frequency of the system based on strength requirements is 0.019 Hz, mode 7. Resized to comply with stiffness requirements, the natural frequencies were somewhat higher, as expected.

To ensure that the lower frequency vibrational modes do not interact with the attitude control system and cause instability, advanced modern control techniques such as ACOSS (Active Control of Space Structures) are necessary, and will be incorporated in the platform subsystem designs.

ALTERNATIVE 4 PLATFORM SIZED FOR STRENGTH

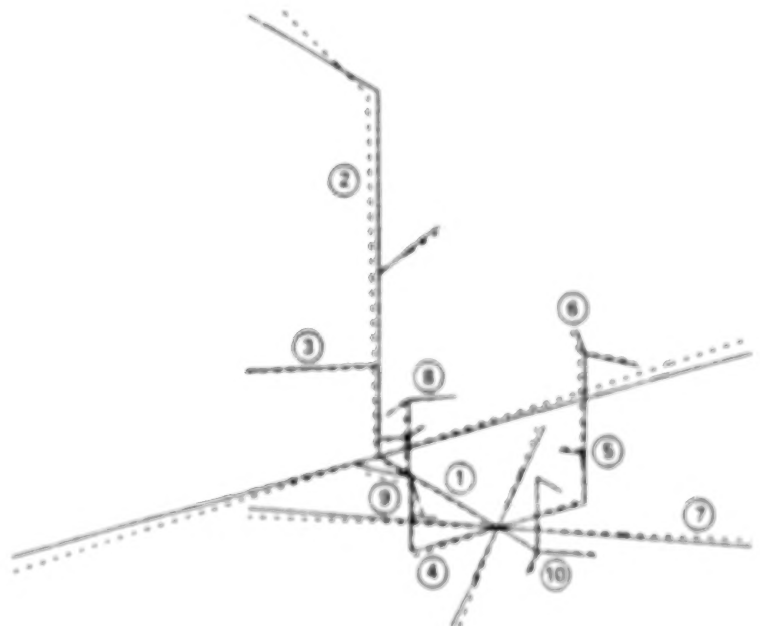
DYNAMIC MODEL

- 65 GRID POINTS
- 64 STRUCTURAL ELEMENTS
- 390 STRUCTURAL DEGREES OF FREEDOM

MODE	FREQUENCY (Hz)	DESCRIPTION OF MODE SHAPES
1-6	—	RIGID BODY MODES
7	0.019	② MAST TORSION
8	0.023	④ ARM TORSION
9	0.030	⑧ MAST TORSION
10	0.043	⑨ & ⑩ MASTS, COUPLED TORSION
11	0.044	① BEAM TORSION
12	0.046	
↓	↓	
23	0.098	

MODE SHAPE

STRUCTURAL VIBRATION MODE 7
NATURAL FREQUENCY = 0.019 Hz



STRUCTURAL RESIZING FOR STIFFNESS

Stiffness requirements for platform structural elements are dependent on the variations in relative position geometry that payloads and payload components can tolerate and still maintain the required quality of performance during on-orbit operations. Attitude control impulse is the primary loading condition that affects feed assembly/antenna reflector geometry. Secondary distortions, caused by infrequent docking and servicing loads, are minimized by soft-docking design techniques.

The strength requirements for orbit transfer and the stiffness requirements for ACS firing are summarized here for Platform Alternative #4 supporting structure, with acceleration parameters for analysis as noted.

Antenna position requirements proved to have a more pronounced effect on total platform structure than any other payload components. For elements B, E, and I, (supporting the largest antenna reflectors), stiffness sizing overrode the strength requirements. For the other structural elements, the design was governed by strength (orbit transfer) requirements.

The weight penalty associated with satisfying stiffness requirements over and above the strength requirements was 22% of the structural weight for this platform concept, or 2.7% of the total platform weight.

ALTERNATIVE 4

ELEMENT NUMBER	REQUIREMENT	DEPTH OF SECTION***	EI_{xx} (Nm ²)	JG (Nm ²)
(B & E)	STRENGTH*	2.29 m	5.83×10^7	2.47×10^6
	STIFFNESS**	3.31 m	2.55×10^8	1.00×10^7
(C)	STRENGTH*	0.93 m	3.10×10^6	1.68×10^5
	STIFFNESS**	(ABOVE SECTION ADEQUATE)		
(A)	STRENGTH*	5.00 m	7.35×10^8	2.36×10^7
	STIFFNESS**	(ABOVE SECTION ADEQUATE)		
(I)	STRENGTH*	0.62 m	6.31×10^5	5.02×10^4
	STIFFNESS**	0.91 m	2.90×10^6	2.31×10^5
(J)	STRENGTH*	0.76 m	1.36×10^6	9.15×10^4
	STIFFNESS**	(ABOVE SECTION ADEQUATE)		

*ORBIT TRANSFER ACCELERATIONS ARE 0.035 G IN PRIMARY DIRECTION AND 0.005 G IN TRANSVERSE DIRECTIONS. DYNAMIC FACTOR = 2.0.

**ACCELERATIONS PRODUCED BY ACS FIRING ARE APPROXIMATELY 0.0003 G IN EACH OF THE 3 PRINCIPAL DIRECTIONS. DYNAMIC FACTOR = 2.0.

***ALL SECTIONS ARE GRAPHITE EPOXY OOA TYPE TRUSSES.

TASK 11 RESULTS

Results of the Geostationary Platform LSST study are summarized here. All have been discussed in the previous charts with the exception of the two major technology needs dealing with component materials.

The two top candidates for deployable structure elements are the expandable truss beam and the Astromast.

The beam, fabricated of graphite/epoxy with a designed coefficient of thermal expansion of zero, provides good packaging density and high strength and stiffness per unit weight. The Astromast as now configured provides the best packaging density, but lacks the strength and stiffness required for the platform payloads and has not been produced in low CTE materials. A graphite/epoxy mast with the Astromast packaging density is an advancement in technology needed for optimizing the Geostationary Platform designs.

Further advances are also needed in space-qualified, extended-life composite materials and components, such as compression-molded graphite/epoxy strut end fittings.

UTILITIES ACCOMMODATIONS

- NO SIGNIFICANT STRUCTURAL INFLUENCE.
- UMBILICAL STOWAGE & DEPLOYMENT IMPLEMENTATION WILL REQUIRE INNOVATIVE APPROACHES — NO INSURMOUNTABLE OBSTACLES IDENTIFIED.

INTERFACE DESCRIPTION

- INCORPORATE DOCKING AND ON-ORBIT SERVICING PROVISIONS AT OTV INTERFACE.

STRENGTH AND STIFFNESS

- MOST STRUCTURAL MEMBERS MUST BE SIZED FOR STIFFNESS.
- INITIAL CONCEPTUAL DESIGNS AND WEIGHTS VERIFIED.

MAJOR TECHNOLOGY NEEDS IDENTIFIED

- GRAPHITE-EPOXY MAST WITH "ASTROMAST" PACKAGING CAPABILITY
- ADVANCED DOCKING, UMBILICAL PANEL, AND DEPLOYMENT MECHANISM CONCEPTS.
- SPACE-QUALIFIED, EXTENDED-LIFE COMPOSITE MATERIALS AND COMPONENTS.

SUMMARY OF LSST SYSTEMS ANALYSIS
AND INTEGRATION TASK FOR
SPS FLIGHT TEST ARTICLES

H. S. Greenberg
Space Operations and
Satellite Systems Division
Rockwell International
Seal Beach, California

Large Space Systems Technology - 1980
Second Annual Technical Review
November 18-20, 1980

STUDY OBJECTIVES

The objective of this study was the establishment of the structural requirements for the two SPS test articles listed below which are fundamental structures and intermediate design steps in the SPS development cycle. Directing the establishment of these requirements was the philosophy that they would be used for future studies of deployable, erectable, and space-fabricated construction options.

The concept and mission of SPS Test Article I were first proposed by Rockwell to NASA/MSFC on December 19, 1979 and subsequently documented in reference 1. The test article mission requirements, configuration, and detailed equipment requirements were derived in this study.² For SPS Test Article II, the detailed data developed in the Space Construction System Study by Rockwell for NASA/JSC³ were directly applicable.

The two test articles, having vastly different size, shape, loading, and dimensional stability requirements, provide a dramatic illustration of the significance of mission-induced structural requirements variations on the design requirements.

ESTABLISHMENT OF THE SIGNIFICANT STRUCTURAL REQUIREMENTS (FROM MISSION, MISSION EQUIPMENT, AND REQUIREMENTS)

- HEXAGONAL FRAME STRUCTURE FOR SPS TEST ARTICLE I
(ROCKWELL BRIEFING TO MSFC, DEC. 19, 1979)
- SOLAR BLANKET SUPPORT STRUCTURE FOR SPS TEST ARTICLE II
(SPACE CONSTRUCTION SYSTEM ANALYSIS, NAS9-15718 (JSC))

DOCUMENTATION OF THESE REQUIREMENTS TO PERMIT FUTURE DEFINITION, COMPARISON, OF THE DESIGN AND CONSTRUCTION CHARACTERISTICS OF

- DEPLOYABLE
- ERECTABLE
- SPACE-FABRICATED STRUCTURES

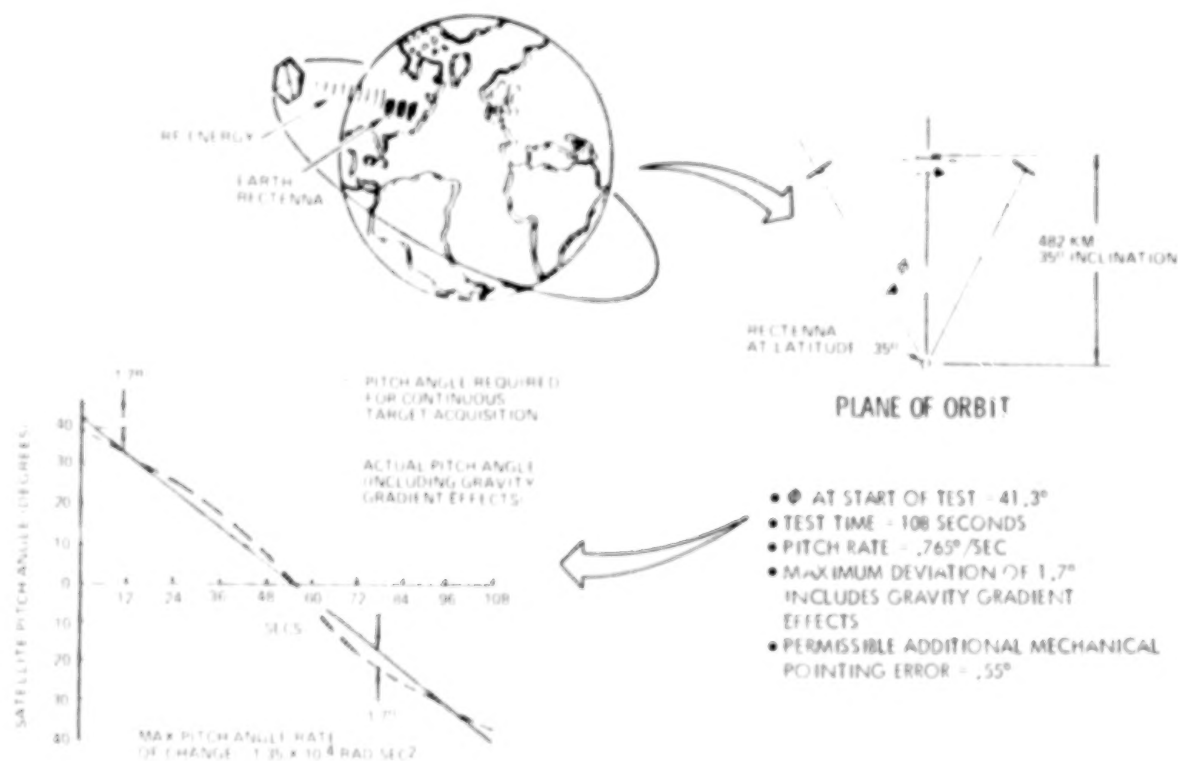
WITH RECORDING OF STRUCTURES TECHNOLOGY REQUIREMENTS

ARTICLE I DEMONSTRATION TEST/MANEUVER

The demonstration concept is based on a LEO satellite which converts energy from the sun into microwave energy and transmits it to an earth-based rectenna. Batteries are used to store the dc power generated by a set of photovoltaic panels. The dc battery power is converted to microwave power by solid-state oscillator/amplifier modules operating at 2450 MHz. These devices excite two crossed dipole arrays whose orthogonal beams are focused on the rectennas as the satellite passes over its site.

At an altitude of 482 km (260 nmi) and inclination of 35° , the satellite completes exactly 15 orbits each day and thus will make one appearance per day over a rectenna located at 35°N latitude. Variations in received power levels will be experienced as functions of elevation angles and slant range; however, since the exact positions of those will be known, actual measurements can be correlated with the calculated performance specifications.

An additional factor that must be accounted for is satellite pitch angle. The results of a computer simulation illustrate the deviation between the pitch angle required for continuous target acquisition and a constant induced pitch rate for the satellite. Providing the beam deviation is not too large, correction can be achieved by electronic beam pointing created by phase control of individual subarrays. If subarray size is 1 m by 1 m, then electronic beam steering through $\pm 2.25^\circ$ is possible at the expense of up to 1.6 dB loss in antenna gain. The 2.25° allowable deviation is the sum of 1.7° and an allowance of 0.55° for mechanical pointing error.

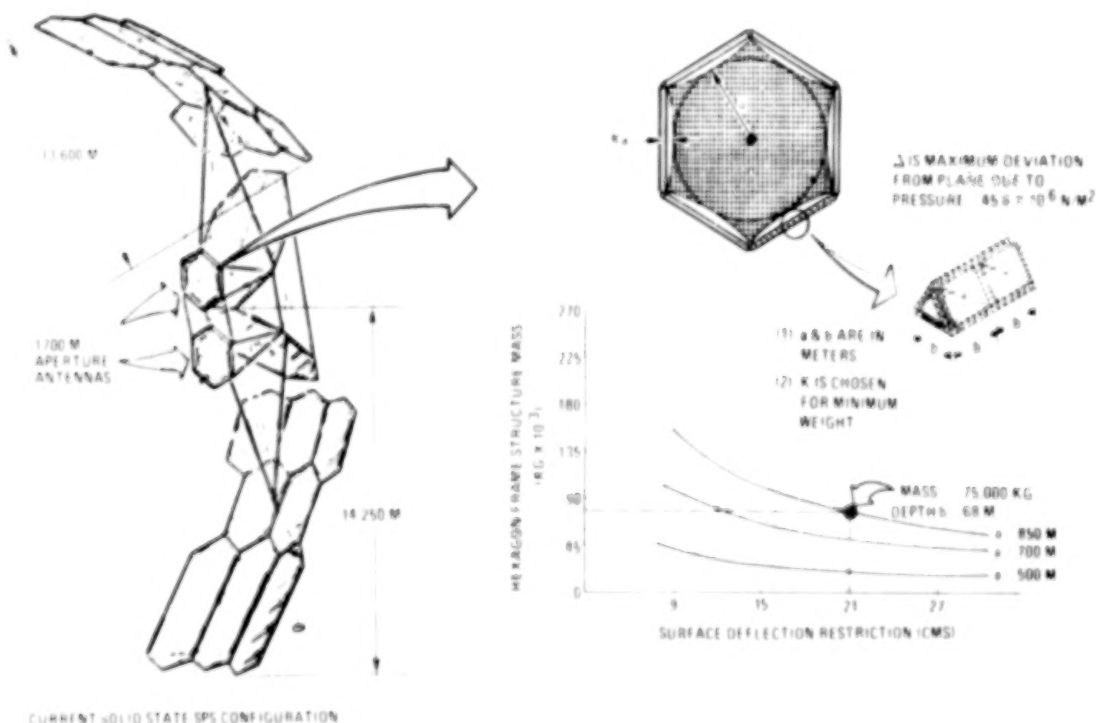


PROTOTYPE SPS HEXAGONAL FRAME CHARACTERISTICS FOR ARTICLE I

The SPS prototype design analysis⁴ is based on the use of two 1700 m aperture diameter antennas in the solid-state configuration shown. In this concept, the solid-state amplifiers are structurally integral with the solar cell array and are referred to as a *solid-state sandwich design*. The microwave surface is directed toward earth with the solar cells mounted on the back face and illuminated by a system of primary and secondary reflector surfaces as shown. An orthogonal array of cables, tension-stabilized by the peripheral compression-carrying frame, provides a primary structural support system with no encroachment on either surface. The electronics studies conducted have established the microwave surface flatness requirements to be maintained within 21 cm. The frame weight versus the surface flatness requirement is shown. For a tri-beam construction, a depth of 68 m and a frame mass of 75,000 kg are required for the flatness requirement of 21 cm.

Other constructions such as a pentahedral truss (essentially a statically determinate structure) comprised of either dixe-cup struts and unions or designs using the machine-made beams developed by Grumman, McDonnell-Douglas, or General Dynamics will have different mass, EI, and GJ characteristics based on the results of construction versus weight tradeoffs.

Of concern to the construction operation is the minimum modal frequency of the frame during construction in the free-drift mode. In its weakest configuration (just prior to frame closure) the modal frequency is 0.0018 Hz which is five times the frequency of earth orbit gravity-gradient disturbances and feasible since there is no target acquisition.



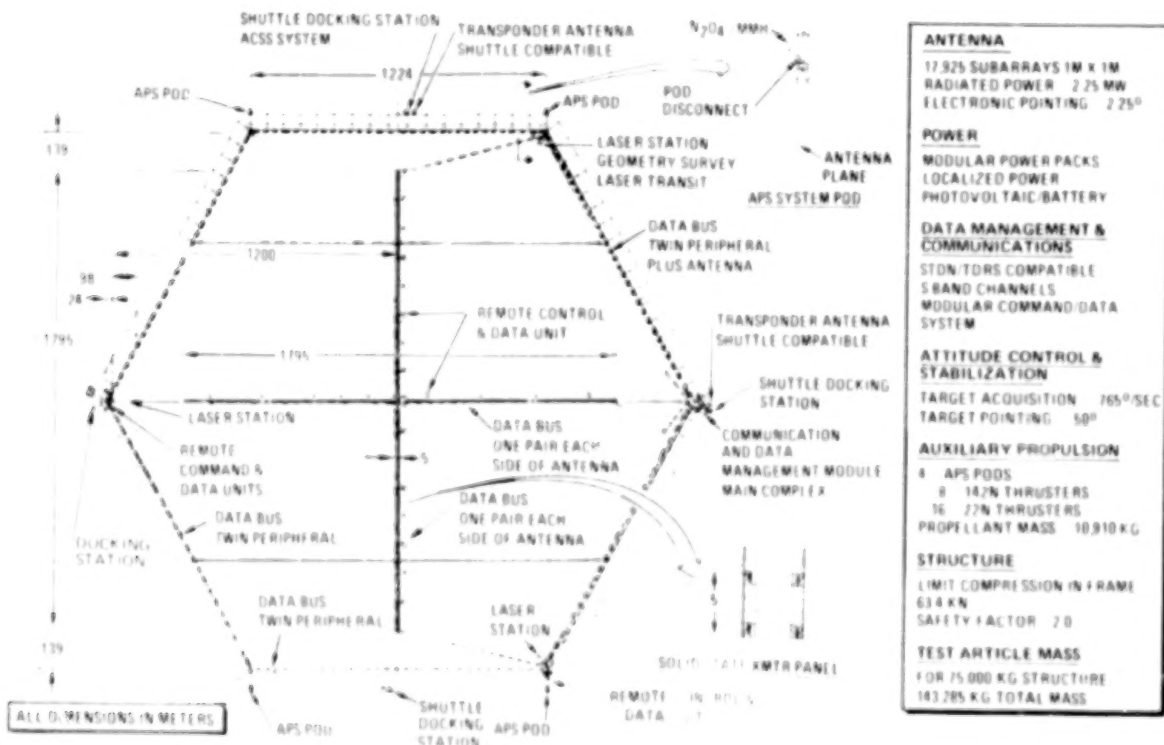
ARTICLE I CONFIGURATION

The test article uses a hexagonal frame structure to stabilize the array of primary tension cables configured to support a Mills Cross antenna containing 17,925 subarrays composed of dipole radiating elements and solid-state power amplifier modules. Nickel hydrogen battery packs mounted on the back face provide power storage capability compatible with the mission power requirements. The total antenna/solar-cell/battery structure distributed mass is 2.5 kg/m^2 . Electronic beam steering is provided by phase control of the individual sub-array to within $\pm 2.25^\circ$ which is compatible with the attitude control and structural systems.

For minimum propellant usage the test article continuously rotates about the axis of minimum mass moment of inertia at $0.765^\circ/\text{sec}$. The attitude control and stabilization system uses four APS pods containing $\text{N}_2\text{O}_4/\text{mmH}$ bipropellant for control. The control system features a precision attitude reference system, coarse alignment system, flight computer, and interface unit. Its output provides the command signals to an active three-axis APS. The communication system utilizes S-band transceivers compatible with existing ground-based (STDN) networks, orbiter channels, and the TDRSS links.

The hexagonal frame structure supports the primary array of tension cables upon which the solid-state panels are mounted. A secondary array of tension cables reduces (to small values) the in-plane bending moments resulting from the article spin. Appropriate constant tension devices are used to maintain the primary cable load tensions.

A total of eight docking ports is provided at the four APS pods and at the four stations as shown.



ARTICLE 1 MISSION DESCRIPTION

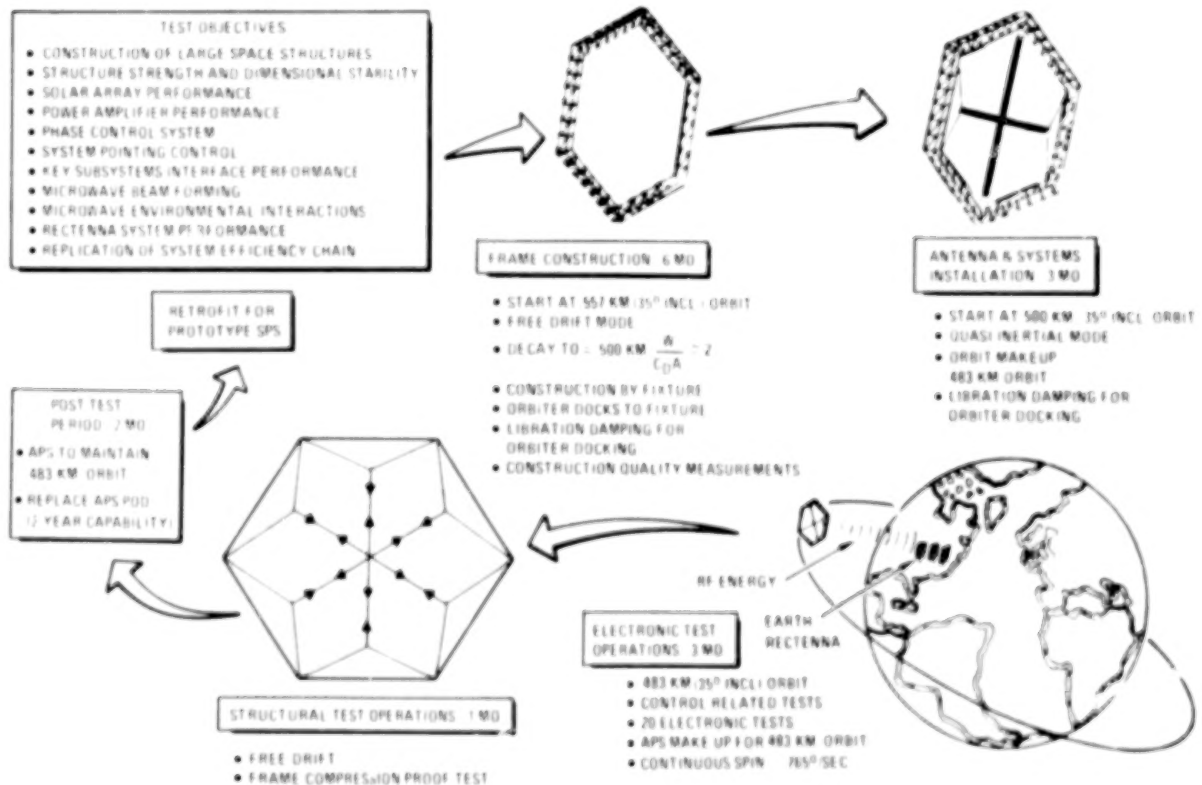
The SPS test article mission objectives and scenario are shown. The highlights of each mission phase are discussed below.

Frame construction is from an orbiter constructed fixture. Data from the Space Construction Study³ indicated a total structure construction time of 36 hours to fabricate (one beam machine) the tri-beam structure. For this tri-beam hexagonal frame, extrapolation indicated a construction time of 112 days. Use of more than one beam machine can reduce this value; however, it is estimated that other constructions could require additional time—hence, a six-month construction period was estimated.

The antenna and systems installation time is three months and is based on the requirement to make the 17,925 subarrays monitor and control electrical connections. This will allow about seven minutes per connection which is expected to be adequate. To accommodate delivery and installation of the antenna solid-state panels, orbiter docking ports are provided.

The test article is in a 483 km (260.79 nmi), 35° inclination orbit and has a spin rate of 765°/sec. The rectenna is located at 35°N latitude. For this case the test article will pass through the zenith point of the rectenna every 15th orbit. Twenty tests are required.

Subsequent to completion of the electronic test phase, the tension cable system geometry can be replaced with a system representative of the future prototype design and a proof test to the limit loads of the future prototype structure (33-1/3% increase in test article loads) can be performed.



ARTICLE I HEXAGONAL FRAME STRENGTH/STABILITY REQUIREMENTS

The strength/stability requirements applicable to any construction utilized in the hexagonal frame are summarized below.

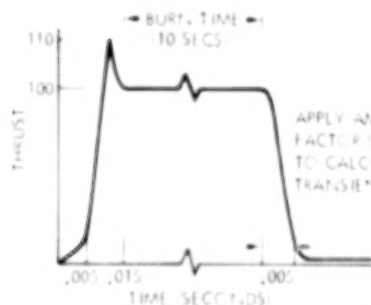
Requirement (1) applies to the frame construction phase in which the frame is attached to and constructed from a fixture (SOC or equivalent). The system is in a free-drift mode with the lowest orbit altitude at the end of construction being 500 km (270 nmi). Libration damping maneuvers are required for orbiter docking to the fixture prior to material delivery. The drag and thermal loads, which are construction dependent, are determined from the mission description.

Requirement (2) applies to the installation phase. The test article is at an altitude of 482 km (260 nmi) and in a quasi-inertial mode. Structurally, significant installations during this phase are cable tensioning, microwave sub-array panel mounting, APS pods attachment, and orbiter docking to the frame.

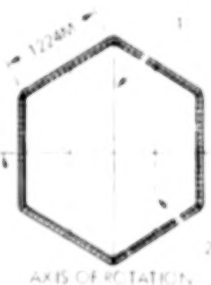
Requirements (3) and (4) present the dominant frame axial compression loading resulting from the associated cable configuration tension loads. The cable tension is determined to maintain the required flatness for the respective microwave antenna designs for the test article and prototype use. The primary cable geometry in both cases produces no primary frame shear or bending moments. Secondary loads will occur, however, due to fabrication deviations and deflections.

For the test article design the APS thruster versus thrust time characteristics and centripetal loads model are provided.

- (1) SUSTAIN FREE-DRIFT MODE CONSTRUCTION LOADS (500 KM ORBIT)--THERMAL, LIBRATION DAMPING, FRAME CLOSURE
- (2) SUSTAIN TENSION CABLE & SYSTEMS INSTALLATION LOADS (483 KM ORBIT)--THERMAL, LIBRATION DAMPING, ORBITER DOCKING
- (3) TEST ARTICLE USE (SAFETY FACTOR = 2.0)-SUSTAIN LIMIT AXIAL COMPRESSION = 63.4 KN (14,250 LBS) WITH THERMAL, CENTRIPETAL, APS FIRING (142 AND 22 N THRUST)



APS THRUSTER LOAD VERSUS TIME



CENTRIPETAL LOADS MODEL

- SPIN RATE .765° SEC
- CABLE 1 AE 18×10^6 N
- CABLE 2 AE 9×10^6 N
- FRAME MASS, EI & GJ UNIQUE TO CONSTRUCTION

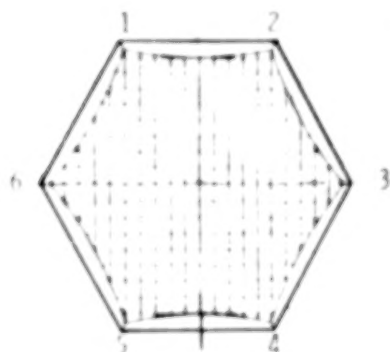
- (4) SPS PROTOTYPE USE (SAFETY FACTOR = 1.5)-SUSTAIN LIMIT AXIAL COMPRESSION = 84.3 KN (18,950 LB) WITH THERMAL LOADS

ARTICLE 1 HEXAGONAL FRAME MODAL/FIGURE CONTROL REQUIREMENTS

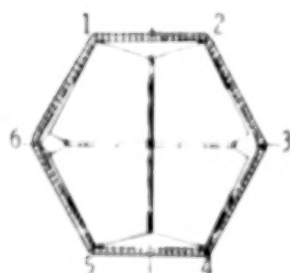
The hexagonal frame requirements pertaining to modal frequency and figure control are shown below.

The frame stiffness must be sufficient to provide adequate frequency separation between the structure, control system, and disturbances. The highest disturbance frequency is due to the combination of gravity gradient and article spin rate of $0.765^\circ/\text{sec}$ and is 0.00425 Hz . The conservative approach, compatible with a classical control system of requiring a minimum structure frequency that is 10 to 20 times that of the disturbance frequency, is prohibitive for this application. Instead, an acceptable structure frequency is automatically provided by the frame in order to preclude buckling due to the axial compression. This is demonstrated by the analysis in the study final report.²

Of the dimensional stability criteria listed below, the most critical requirement is the restriction of frame deflection to no more than 15 cm for SPS prototype use. This is necessary to limit the total 1700 m antenna microwave deviation from flatness to 21 cm. While 15 cm represents a deflection/aperture diameter ratio of 0.00013, structural analysis of the prototype frame³ indicated this is achievable (without active control) for an open truss structure constructed of a material with a coefficient of expansion of $0.36 \times 10^{-6} \text{ m/m/}^\circ\text{C}$. However, active control to obtain the same end result is certainly appropriate. It is pertinent to note the 15 cm deflection restriction is for a frame supported at three points by the SPS structure with removal of all fabrication deviations by a system of adjustable supports at the corners.



SPS PROTOTYPE DESIGN
(Supports at 1, 3, 5)



TEST ARTICLE

- (5) STIFFNESS (MINIMUM MODAL FREQUENCY) FOR SEPARATION FROM TEST MANEUVER / GRAVITY GRADIENT DISTURBANCE (0.0042 Hz) - SATISFIED BY FRAME E1 / GJ REQUIRED FOR OVERALL FRAME STABILITY

- (6) DIMENSIONAL STABILITY REQUIREMENTS - INITIAL ADJUSTMENT CAPABILITY AT CABLE ATTACHMENT INTERFACES

SPS PROTOTYPE USE

- Passive Control - Maximum deflection of Points 2, 4, 6 from plane of supports - 15 cm
- Active Control - Attachment adjustment to within 15 cm

TEST ARTICLE USE

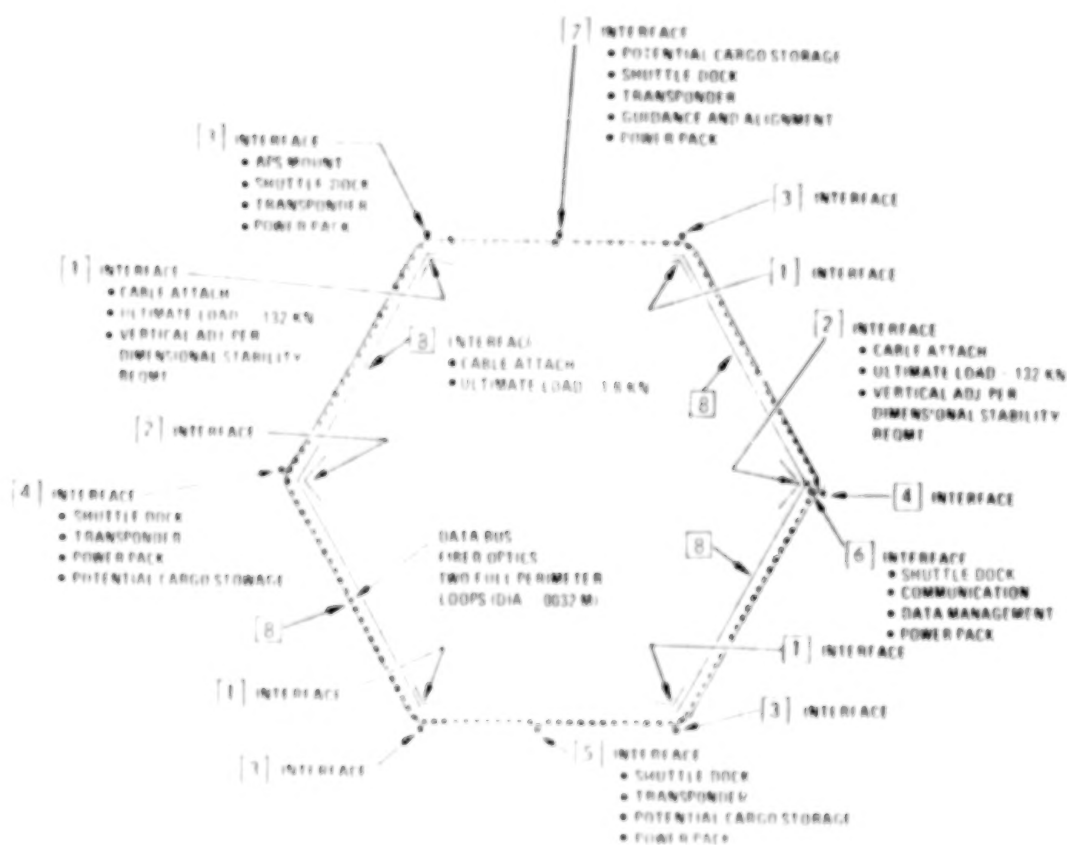
Maximum relative deflection between any three points, normal to plane through other three points, - 24 cm

ARTICLE 1 HEXAGONAL FRAME INTERFACES AND UTILITIES

Interfaces 1 and 2 receive the fitting that supports the pair of intersecting antenna array support tension cables. The interface must sustain the resultant delivered ultimate radial tension load of 132 kN (including centripetal forces). The structural design must also provide for adjustment normal to the plane of the frame that is compatible with the dimensional stability requirements.

Interface 3 (four required) is located as shown and contains a male/female docking device for attachment of the APS pod to the structure and another device to permit orbiter docking for future removal of this pod. The data bus for the APS pod is also shown. This interface must be capable of sustaining the loads occurring during APS installation, orbiter docking, APS firing, and during spin (centripetal loads). The APS thruster loads need not be concurrent.

Interfaces 4, 5, 6, and 7 contain the male and female components of docking ports and must be capable of sustaining the transient loads incurred during docking of the orbiter during the systems installation and post-test mission phases. The orbiter/payload contact conditions shall be used in the loads analysis. Interfaces 4, 5, and 7 also contain provisions for equipment storage during construction. Interfaces 4, 5, and 6 contain solar cells to be supported from the basic structure. The ACCS equipment is located at Interface 7. Interface 8 receives the secondary tension cables.



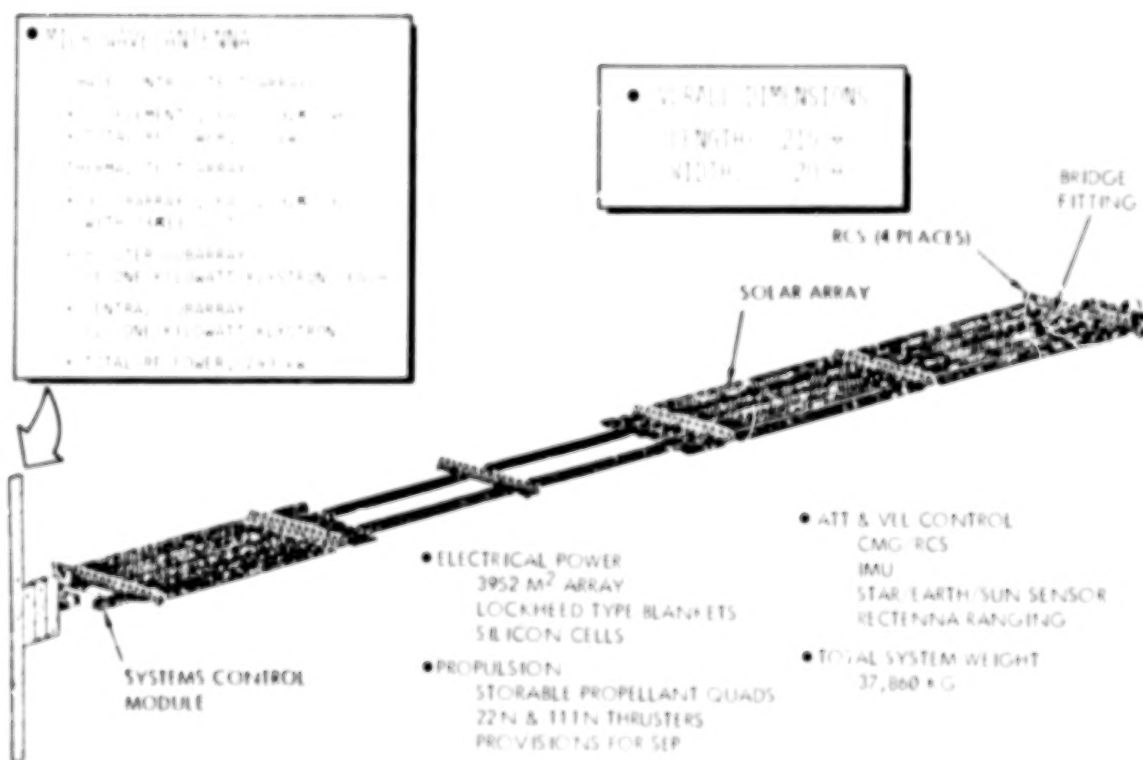
ARTICLE II CONFIGURATION

This SPS test article consists of a microwave antenna and its power source, a 20 by 200 m array of solar cell blankets, both of which are supported by the solar blanket array support structure. The microwave antenna is attached to a rotary joint on the systems control module. A control moment gyro/auxiliary propulsion system (CMG/APS) attitude control stationkeeping concept is used. The four APS modules are at the corners of the configuration. A system control module contains the CMG's; tracking, telemetry, and control (TT&C); and power storage batteries. A bridge fitting at the opposite end provides the support for the solar electric propulsion module retrofit for GEO transfer.

The solar array consists of twenty-five 4 by 40 m solar blankets tensioned to a minimum of 17.5 N/M (0.10 lb/in.) and attached to the transverse beams. Power leads will plug into individual switching boxes. For each of the switch gear boxes, power lines will run along the longitudinal beams to interface with the systems control module and continue on to the power slip ring of the rotary joint. This arrangement provides voltage control for each of the 25 blankets.

The test article structure, a ladder, is comprised of two longitudinal beams (215 m long) spaced 10 m apart and interconnected by six lateral beams. The system control module structure and bridge fitting provide bending and torsional stiffness, and supplement the in-plane Vierendeel structure behavior.

The APS modules, system control module, and bridge fitting are attached to berthing ports on the structure with the orbiter RMS.

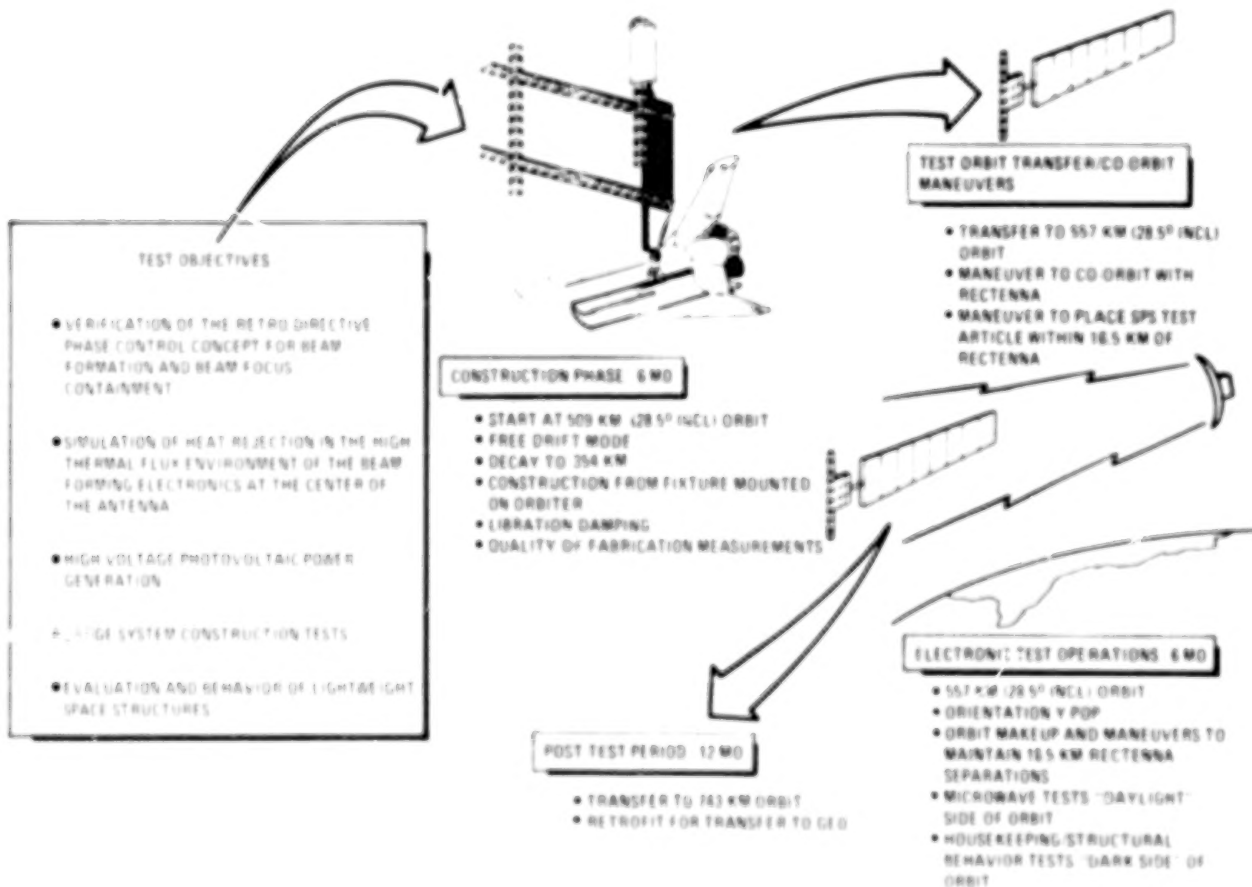


ARTICLE II MISSION DESCRIPTION

The SPS Test Article II mission scenario highlights are discussed below.

Construction is from a fixture attached to the orbiter and starts at an altitude of 509 km (375 nmi). The system is in a free-drift mode, and at the end of six months is at an altitude of 354 km (191 nmi). The mission profile calls for the orbital delivery of a rectenna vehicle following construction and check-out of SPS Test Article II. The rectenna is the receiving element of the space-to-space microwave beam performance test and is a separate vehicle. Once the rectenna vehicle is suitably placed in the test orbit, SPS Test Article II would be maneuvered to the same orbit with the appropriate standoff distance.

The first mode for the microwave tests requires precision pointing of the antenna toward the rectenna receiving system. Further, the solar array area must be sun oriented. Thus, a rotary joint is provided between the antenna and the solar array to provide their respective viewing requirements. An orbit altitude of 555 km (300 nmi) was selected for the microwave tests. This was deemed the lowest feasible altitude consistent with the large area, low W/CpA characteristics of the configuration. A six-month mission duration was estimated to be adequate for the performance of the planned microwave tests. This provides over 2700 orbit revolutions with nearly four full cycles of sun/orbit geometries.



ARTICLE 11 SOLAR BLANKET SUPPORT STRUCTURE STRENGTH/STABILITY REQUIREMENTS

The strength/stability requirements applicable to any construction utilized in the solar blanket support structures are summarized below.

Requirement (1) pertains to the solar blanket support structure construction phase which occurs in a free-drift mode, with construction from a fixture attached to the orbiter. The drag, thermal, and gravity-gradient loads which are dependent on the specific construction are determinable from the mission definition. For a deployable structure, deployment loads will be peculiar to the particular concept.

Requirements (2), (3), and (4), respectively, pertain to the installation of the solar blankets, equipment modules, and power/data lines. The installation of equipment modules will be accomplished by the RMS for each SPS pod (1800 kg), the bridge fitting (1500 kg), and system control module (5000 kg). The RMS capability and rates are specified in the study.²

Requirements (5) and (6) are interrelated. Requirement (5) provides a minimum blanket structural frequency several times that of the overall structure and is consistent with Requirement (6). The specified tension is to be maintained despite differential thermal expansion between the blanket and structure.

- (1) SUSTAIN FREE-DRIFT MODE CONSTRUCTION LOADS (354 KM ORBIT)--THERMAL, GRAVITY GRADIENT, LIBRATION DAMPING (PRIOR TO BLANKET INSTALLATION)
- (2) SUSTAIN WORST COMBINATION OF INSTALLATION BLANKET TENSION LOADS, THERMAL GRAVITY GRADIENT, LIBRATION DAMPING
- (3) SUSTAIN INSTALLATION LOADS OF APS PODS, BRIDGE FITTING, SYSTEM CONTROL MODULE (RMS FOR PLACEMENT)
- (4) SUSTAIN INSTALLATION OF POWER / DATA MANAGEMENT UTILITIES (ACCOMMODATE STRUCTURE / UTILITY DIFFERENTIAL EXPANSION)
- (5) MAINTAIN MINIMUM SOLAR BLANKET TENSION (17.5 N/M)--DIFFERENTIAL THERMAL EXPANSION
- (6) SOLAR BLANKET / STRUCTURE INTEGRATION TO PRECLUDE BLANKET DAMAGE DUE TO APS THRUSTER FIRING

ARTICLE II SOLAR BLANKET SUPPORT STRUCTURE ADDITIONAL REQUIREMENTS

The additional strength/stability and minimum modal frequency requirements applicable to the solar blanket support structure are shown below.

Requirement (1) pertains to the loads applied during APS thruster firing for attitude control, stationkeeping, or orbit transfer. The loads conditions shown in the table are not concurrent.

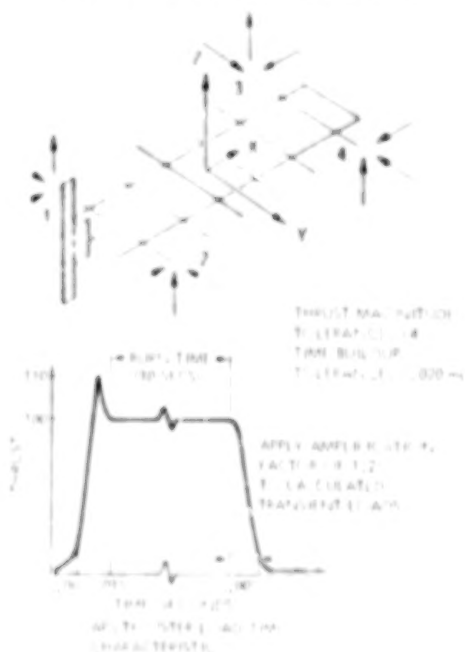
The typical thrust transient shown is for low-thrust APS thrusters. The data are based on test firings of low-thrust bipropellant thrusters with relatively slow acting valves. These data are applicable to the range of thrust values and burn times used in the study.

The time build-up tolerance is between thrusters. The amplification of 1.25 to be applied to calculated transient loads is based on the ability of the control system to limit load magnification.

Requirement (2) provides frequency separation between the highest frequency disturbance and that of the structure in excess of 14, and permits a classical control approach.

There is no significant requirement for dimension stability of the solar blanket support structure.

(1) SUSTAIN WORST COMBINATION OF APS ORBIT TRANSFER, STATIONKEEPING, & ATTITUDE CONTROL LOADS (WITH THERMAL GRADIENT AND BLANKET TENSION LOADS)



LOAD CONDITIONS (N)

CASE (LOAD)	STATIONKEEPING								ATTITUDE			
	1	2	3	4	5	6	7	8	9	10	11	12
1 _x	???											
1 _y			111							111		
1 _z							??		-??			??
2 _x	???											
2 _y				111							111	
2 _z							??		-??			-??
3 _x		???										
3 _y					111						111	
3 _z								??	??			??
4 _x		???										
4 _y						111				111		
4 _z								??	??			-??

(2) STIFFNESS

MINIMUM MODAL FREQUENCY
TO BE GREATER THAN 0.001 Hz

(3) DIMENSIONAL STABILITY

NONE

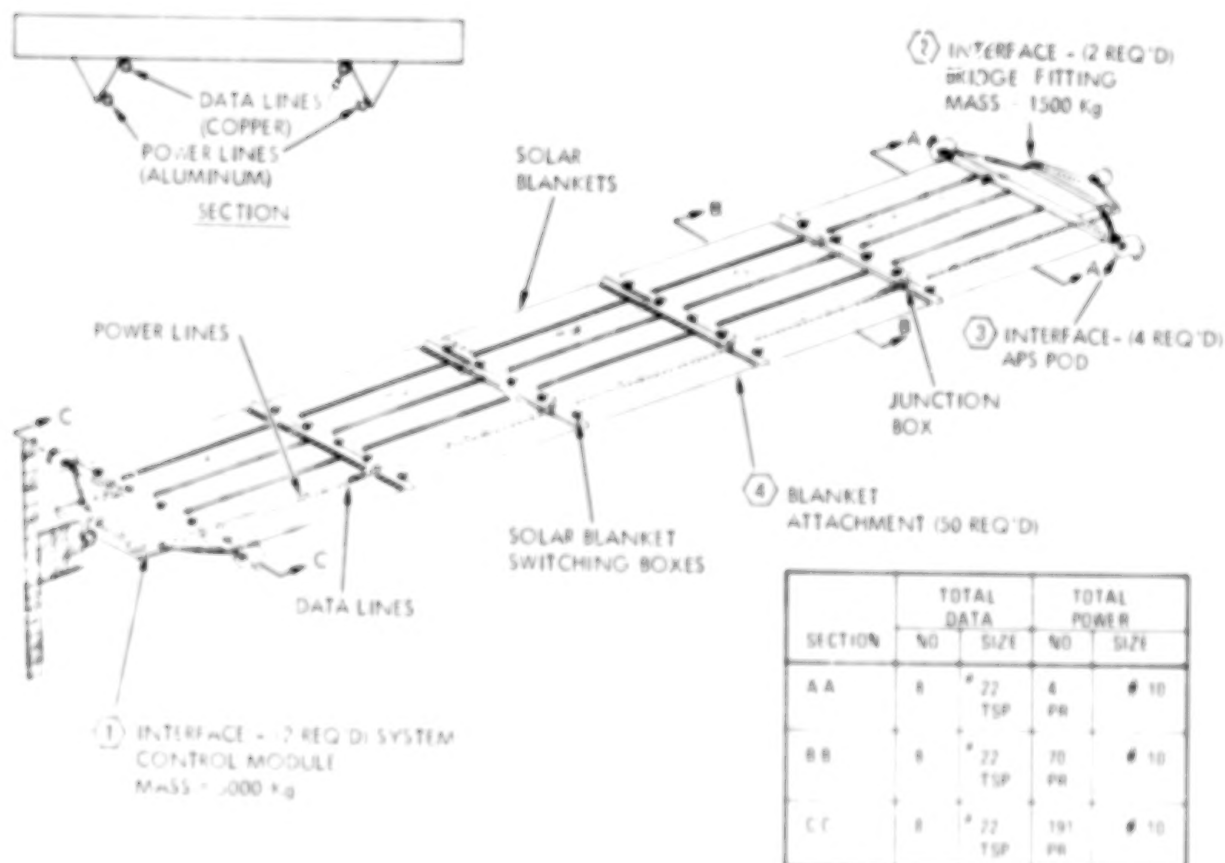
ARTICLE II SOLAR BLANKET SUPPORT STRUCTURE INTERFACES AND UTILITIES

Interface 1 is the attachment for the system control module. The system control module contains the control moment gyroscope, TT&C unit, electrical power conditioning unit, EPD panels, battery packages, and docking port for attachment of the rotary joint and microwave antenna. 191 pairs of No. 10 and four pairs of No. 22 TSP lines for power and data lines, respectively, are provided across the interface. The total mass of the structure and contained equipment is 5000 kg.

Interface 2 is the attachment for the bridge fitting. The bridge fitting assembly mass is 1500 kg. No power and data lines cross this interface until retrofit for GEO.

Interface 3 is the attachment for each of the APS pods. This interface must sustain the transient loads occurring during berthing and during thruster firing. Two pairs each of No. 10 and No. 22 TSP for power and data lines, respectively, cross each interface.

Interface 4 is between the edge of the 4 m by 40 m solar blanket arrays and the supporting solar blanket structure, and contains the blanket tension devices. The integrated tension device system, solar blanket system, and solar blanket support structure shall maintain a minimum limit tension of 17.5 N/m throughout all mission phases. Also, the tension device system shall introduce no loads (at the attachment) detrimental to the solar blanket support structure.



CONCLUSIONS

While the study was directed toward determination of the structural requirements for each of the two test articles, the significant differences in the character of the structures are apparent from the conclusions listed below.

Test Article I represents an order of magnitude more significant challenge than Test Article II. The major challenge for Article I is in the construction (from orbiter) of the fixture to be used for the frame construction and in the guidance and control system design which does not have the luxury of high frequency separation.

While Test Article II is amenable to deployable, erectable, and space fabrication constructions, Test Article I is not amenable to the first. Further, Test Article I is highly loaded and will represent 20 to 75% of the satellite mass (depending on construction) with frame construction primarily driven by structural efficiency considerations. In direct contrast, SPS Test Article II is lightly loaded and represents only 2-1/2% of the satellite mass, with construction driven by systems installation requirements.

TEST ARTICLE I

- TEST ARTICLE IS SIGNIFICANT BUT "DO-ABLE" CHALLENGE
- HEXAGONAL FRAME STRUCTURE HIGHLY LOADED (LARGE SPACE STRUCTURE STANDARDS)--ULTIMATE STRESS = 117 MPa (17,000 PSI)
- CONSTRUCTION DRIVEN MOST BY LOAD / DIMENSIONAL STABILITY CRITERIA RATHER THAN EQUIPMENT MOUNTING
- DOCKING LOADS CAN BE MINIMIZED TO CAPABILITY OF STRUCTURE
- HEXAGONAL FRAME STRUCTURE WEIGHT 50 TO 75% OF TOTAL SATELLITE DRY MASS

TEST ARTICLE II

- TEST ARTICLE AMENABLE TO DEPLOYABLE, ERECTABLE, SPACE FABRICATION CONSTRUCTIONS
- STRUCTURE IS LIGHTLY LOADED (ULTIMATE STRESS, 21 MPa (3000 PSI))
- CONSTRUCTION DRIVEN MOST BY FABRICATION & EQUIPMENT SUPPORT ACCOMMODATIONS
- DOCKING LOADS (USING RMS) NOT EXPECTED TO HAVE SIGNIFICANT DESIGN IMPACT
- SOLAR BLANKET BASIC SUPPORT STRUCTURE MASS--2-1/2% OF TOTAL SATELLITE

CONTENTS

VOLUME I - SYSTEMS TECHNOLOGY

PREFACE	iii	1/A7
1. LARGE SPACE SYSTEMS TECHNOLOGY OVERVIEW	1	1/A13
Robert L. James, Jr.		

SUPPORTING ACTIVITIES

2. LSST CONTROL TECHNOLOGY	9	1/B7
A. F. Tolivar		
3. ADVANCED CONTROL TECHNOLOGY FOR LSST ANTENNAS	19	1/C3
Y. H. Lin		
4. ADVANCED CONTROL TECHNOLOGY FOR LSST PLATFORM	31	1/D1
R. S. Edmunds		
5. CONTROL TECHNOLOGY DEVELOPMENT	49	1/E5
G. Rodriguez		
6. INTEGRATED ANALYSIS CAPABILITY (IAC) DEVELOPMENT	65	1/F7
J. P. Young		
7. INTEGRATED ANALYSIS CAPABILITY PILOT COMPUTER PROGRAM	73	1/G1
R. G. Vos		
8. AN ECONOMY OF SCALE SYSTEM'S MENSURATION OF LARGE SPACECRAFT	87	2/A4
L. J. DeRyder		
9. RADIATION EXPOSURE OF SELECTED COMPOSITES AND THIN FILMS	105	2/B8
Wayne S. Slomp and Beatrice Santos		
10. THERMAL EXPANSION OF COMPOSITES: METHODS AND RESULTS	119	2/C8
David E. Bowles and Darrel R. Tenney		

SPACE PLATFORMS

11. SPACE PLATFORM REFERENCE MISSION STUDIES OVERVIEW	129	2/D4
James K. Harrison		
12. ADVANCED SCIENCE AND APPLICATIONS SPACE PLATFORM	133	2/D8
Jack White and Fritz Runge		

13. STRUCTURAL REQUIREMENTS AND TECHNOLOGY NEEDS OF GEOSTATIONARY PLATFORMS	149 2/E10
G. R. Stone	
14. SUMMARY OF LSST SYSTEMS ANALYSIS AND INTEGRATION TASK FOR SPS FLIGHT TEST ARTICLES	167 2/F14
H. S. Greenberg	
15. ERECTABLE CONCEPTS FOR LARGE SPACE SYSTEM TECHNOLOGY	183 3/A5
W. E. Agan	
16. SPACE ASSEMBLY METHODOLOGY	199 3/B7
J. W. Stokes and H. H. Watters	
17. CONSTRUCTION ASSEMBLY AND OVERVIEW	217 3/C11
Lyle M. Jenkins	
18. SPACE PLATFORM ADVANCED TECHNOLOGY STUDY	229 3/D9
G. C. Burns	
19. A DOCUMENT DESCRIBING SHUTTLE CONSIDERATIONS FOR THE DESIGN OF LARGE SPACE STRUCTURES	243 3/E9
John A. Roebuck, Jr.	

SPACE ANTENNAS

20. ELECTROSTATIC MEMBRANE ANTENNA CONCEPT STUDIES	259 3/F11
J. W. Goslee	
21. ELECTROSTATIC ANTENNA SPACE ENVIRONMENT INTERACTION STUDY	271 3/G9
Ira Katz	
22. ENVIRONMENTAL EFFECTS AND LARGE SPACE SYSTEMS	279 4/A6
H. B. Garrett	
23. JPL ANTENNA TECHNOLOGY DEVELOPMENT	287 4/A14
R. E. Freeland	
24. OFFSET WRAP RIB ANTENNA CONCEPT DEVELOPMENT	295 4/B8
A. A. Woods, Jr.	
25. ANALYTICAL PERFORMANCE PREDICTION FOR LARGE ANTENNAS	325 4/D10
M. El-Raheb	
26. JPL SELF-PULSED LASER SURFACE MEASUREMENT SYSTEM DEVELOPMENT	339 4/E10
Martin Berdahl	
27. ANTENNA SYSTEMS REQUIREMENTS DEFINITION STUDY	349 4/F6
C. T. Golden	

28. HOOP/COLUMN ANTENNA TECHNOLOGY DEVELOPMENT SUMMARY	357	4/F14
Thomas G. Campbell		
29. DEVELOPMENT OF THE MAYPOLE (HOOP/COLUMN) DEPLOYABLE REFLECTOR CONCEPT FOR LARGE SPACE SYSTEMS APPLICATIONS	365	4/G8
D. C. Montgomery		
30. RADIO FREQUENCY PERFORMANCE PREDICTIONS FOR THE HOOP/COLUMN POINT DESIGN	407	5/C12
Thomas G. Campbell		
31. OFFSET FED UTILIZATION OF FOUR QUADRANTS OF AN AXIALLY SYMMETRICAL ANTENNA STRUCTURE	431	5/E8
P. Foldes		
32. SURFACE ACCURACY MEASUREMENT SENSOR FOR DEPLOYABLE REFLECTOR ANTENNAS	439	5/F2
R. B. Spiers, Jr.		
SECOND ANNUAL TECHNICAL REVIEW ATTENDEES	449	5/F12

REFERENCES

1. SSD 80-0108-5, Volume V, Satellite Power Systems (SPS) Concept Definition Study, Exhibit D, Final Report (August 1980).
2. SSD 80-0102, LSST Systems Analysis and Integration Task for SPS Flight Test Article, Exhibit E, Final Report (August 1980).
3. SSD 79-0077, Space Construction Systems and Mission Descriptions, Task I, Final Report (April 26, 1979).
4. Structural Analysis of Large Hexagonal Compression Frame/Tension Cable Array Structure for SPS Microwave Antenna, H. S. Greenberg, SAWE 1980 Convention, St. Louis, May 12, 1980.

ERECTABLE CONCEPTS FOR LARGE
SPACE SYSTEM TECHNOLOGY

W. E. AGAN
VOUGHT CORPORATION
DALLAS, TEXAS

Large Space Systems Technology - 1980
Second Annual Technical Review
November 18-20, 1980

OUTLINE

The outline of the presented material defines and coordinates the various subjects to be addressed. The objective and background establish the purpose and point of departure for the effort. The schedule shows the scope and order of the work performed. The engineering design effort is then described. The test plan established the purpose and content of the test activities. Photographs of the test hardware are shown. A seven minute sound film is presented of typical test operations. Stowage in Orbiter, deployment, translation, joining, retraction, and RMS/EVA activities are shown for deployable module testing. The film sound track is recorded in this text. The detailed timeline results of the test procedures are presented in Reference (1). Conclusions of the design and test effort are summarized.

- **OBJECTIVE**
- **BACKGROUND**
- **TASK SCHEDULE**
- **DESIGN FEATURES**
- **TEST PLAN**
- **TEST HARDWARE**
- **NEUTRAL BUOYANCY TEST FILM**
- **CONCLUSIONS**

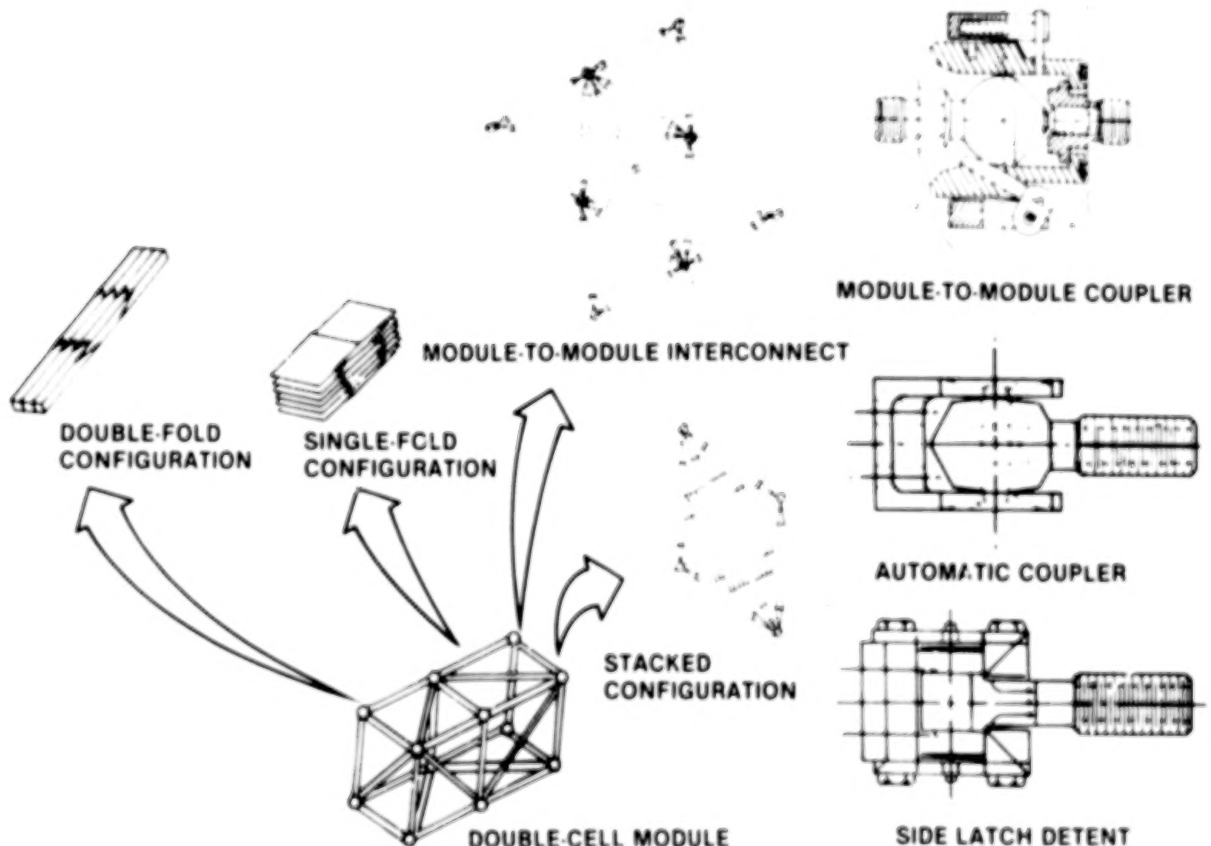
OBJECTIVE

As stated, the objective of this contract was to contribute to the overall technical data base for various programs using deployable structures. The requirements and resultant configurations are generic and are intended to provide general information and data to emerging space programs employing erectable/deployable structural concepts.

**CONTRIBUTE TO THE OVERALL TECHNICAL
DATA BASE FOR VARIOUS PROPOSED
MISSIONS/PROJECTS USING
ERECTABLE/DEPLOYABLE STRUCTURES
THROUGH DESIGN ANALYSIS AND
HARDWARE TESTING**

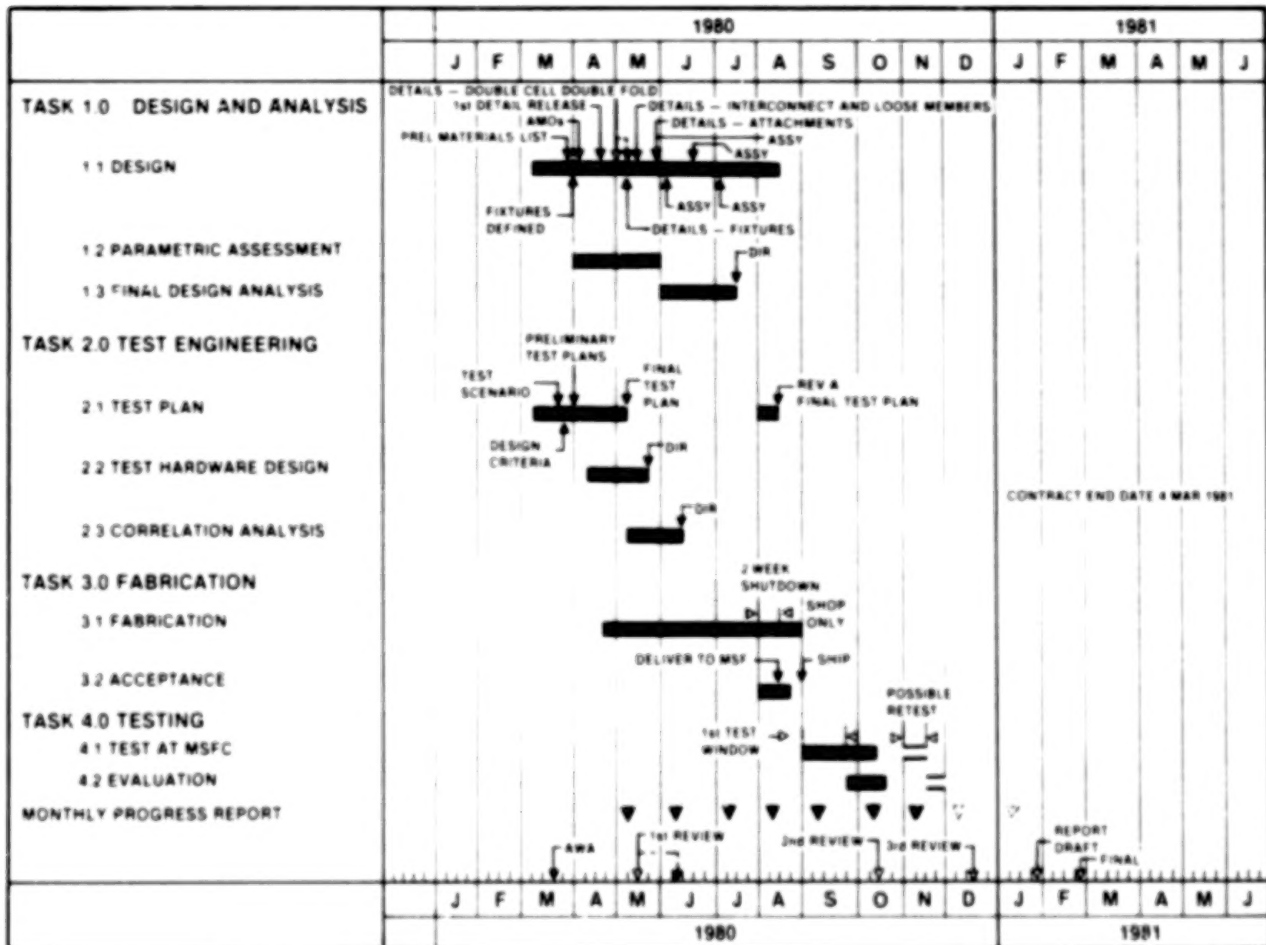
BACKGROUND

In the previous year's effort, a multitude of ideas and concepts were reviewed and/or developed for structural erectable/deployable considerations including joining and packaging. Shown below are the concepts selected from that study for further development into full scale neutral buoyancy test hardware. The basic structural configuration is a double cell double folding cubic module. It is 3 meters by 3 meters in crosssection by 6 meters long. The first folding operation results in a 3 meter by 6 meter planar configuration. The second folding operation results in a 9 meter linear configuration. Folding (deployment) is achieved by single and double pivoting joints and telescoping diagonal members. Deployment and retraction is accomplished by an external force. The stacked configuration shown was a stowage option which was not exercised in the design or test program. The module-to-module interconnect is one way of joining two modules without having adjacent or redundant bulkhead members at the joint interface. Two joining devices, the module-to-module coupler and the automatic coupler, were designed and fabricated for test. The module-to-module coupler features angular and axial locking compliances of 10° and 2.5 mm, respectively. It also has a linear zero free play stiffness characteristic.



TASK SCHEDULE

The program schedule identifying all tasks and their logical sequence of completion is presented. The initial contract consisted of Tasks 1 through 4. The neutral buoyancy testing of the deployable modules was completed 15 October 1980. Tasks 5 and 6 were added to the contract for the purpose of reviewing and generating automatically deployable concepts.

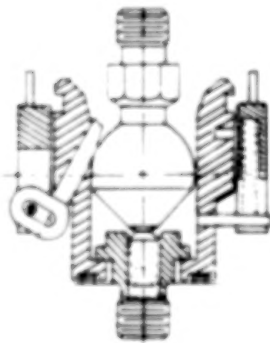


		1980												1981					
		J	F	M	A	M	J	J	A	S	O	N	D	J	F	M	A	M	J
TASK 5.0	REVIEW OF CANDIDATE CONCEPTS																		
	TASK 6.0																		
PRELIMINARY LAYOUT DESIGN																			

DESIGN FEATURES

Three design features of the deployable module are described. The module-to-module couplers are used to connect the structural modules at the four joint interface. It is a quick connect automatically locking probe/drogue device. It will capture and lock with an angular misalignment of 10° . Three radial fingers capture the probe 2.5 mm before seating which is equivalent to a permissible out-of-plane tolerance between the four joints. The coupler can be released and locked open for demating.

The telescoping member lock also operates automatically. The forward flange provides a shear blockage between two cylindrical members. The aft or larger flanges indicate a locked status and may be depressed to initiate release. The joint may be locked in the released position. Power and communication have been incorporated into an internal and external folding joint using clamps and guide bars. The power bundle comprised 4-1/0 cables, 2-8 AWG, and 4-12 AWG wires. The communication bundle comprised 20 twisted pair shielded and 4 coax cables.

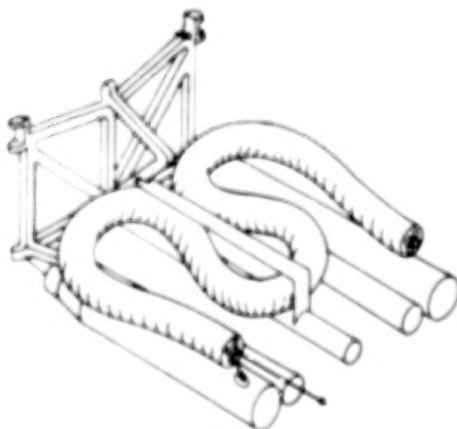
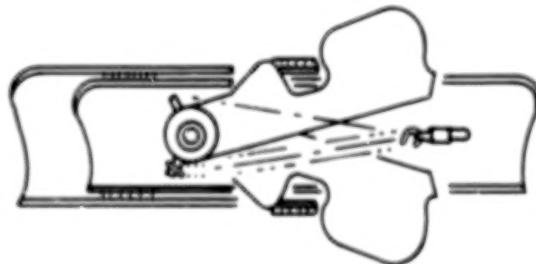


COUPLERS

- QUICK CONNECT
- LOCKOUT FOR RELEASE
- 1-INCH DIAMETER CAPTURE RANGE (1 INCH = 2.54 CM)
- 0.08-INCH DIAMETER TOLERANCE ACCOMMODATION
- 0.10-INCH AXIAL CAPTURE TOLERANCE
- RELEASE LEVER

TELESCOPING TUBE LOCKS

- AUTOMATIC LATCH
- SQUEEZE RELEASE
- LOCKOUT DEVICE FOR STOWING

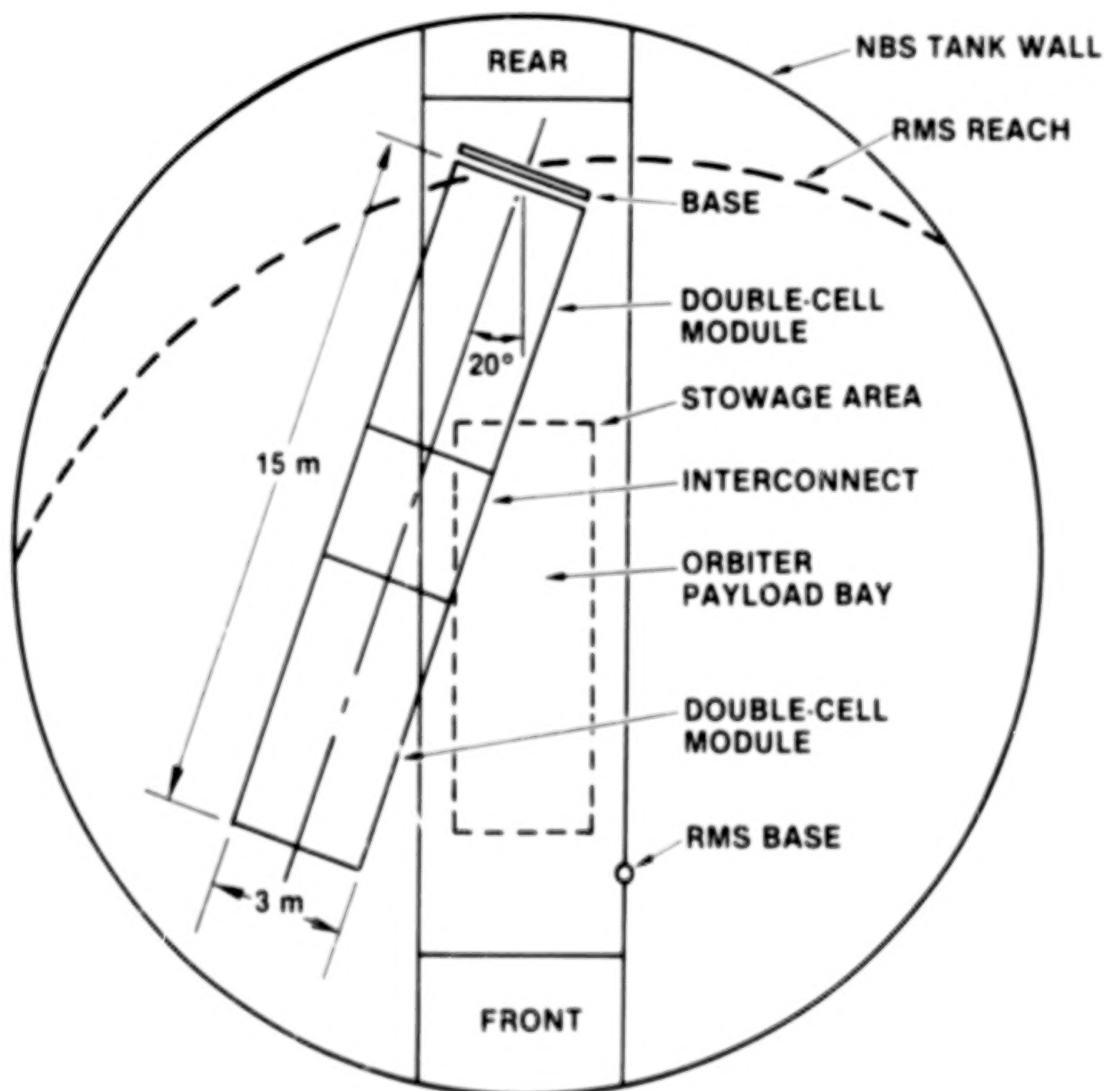


UTILITIES

- MINIMAL EFFECT ON DEPLOYMENT
- POWER AND COMMUNICATION TO MULTIPLE NODE
- ROUTING INTERNAL OR EXTERNAL TO STRUCTURE

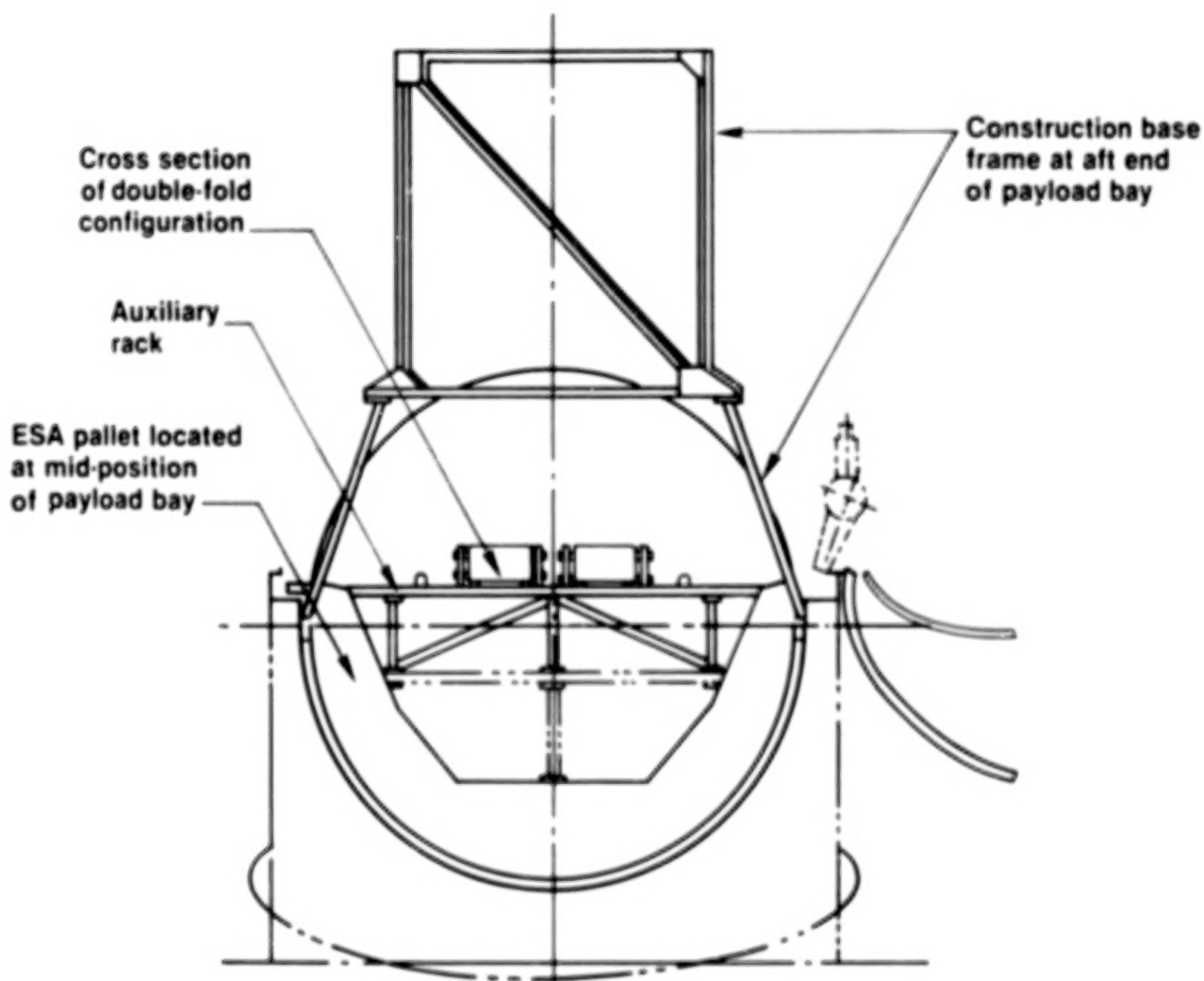
TYPICAL TEST LAYOUT IN NEUTRAL BUOYANCY SIMULATOR

A plan view of the 23 meter diameter Neutral Buoyancy Simulator (NBS) shows the full size mockup of the Orbiter payload bay and 15 meters of deployed structure. The 15 meters comprises 2-6 meter modules and a 3 meter interconnect. The structure is attached to the rigid base frame at the aft end of the payload bay and oriented at 20° with respect to the Orbiter centerline to avoid interference with the stowage area. The RMS is located at the forward end of the payload bay and can reach the base frame. It was discovered during testing that the RMS could not maneuver the end 6 meter module into position because of interference with the NBS wall.



STOWED DOUBLE FOLDED MODULES

This is a cross section of the test setup. A simulated ESA pallet is located midway of the payload bay. An auxiliary fixture was mounted to the ESA pallet to allow stowage of the 3 meter wide single fold configuration within the payload bay. A double folded configuration is shown positioned in the fixture ready for deployment. The modules are held in the fixtures by bar linkages which are actuated by EVA subjects prior to deployment. The construction base frame is located at the aft end of the payload bay. Its purpose is to provide a rigid starting point, possibly a space platform for construction. The RMS is responsible for deployment and translation of the modules from the payload bay to the construction frame. Module release alignment and joining were the responsibility of the EVA subjects.



SUMMARY TEST MATRIX

Nineteen tests were proposed during the test planning period. Test numbers 9 and 14, which were RMS operation only, were deleted because the toggle switch control of the RMS did not provide enough control to align and mate the joining couplers without EVA assistance. Test numbers 3 and 19 could not be completed because the structure deployed vertically from the Orbiter was 12 meters long and protruded through the NBS water level.

A total of 15 NBS sessions were conducted with a total of 24 test runs completed. Some tests were repeated to investigate learning curve factors. Three-two man EVA teams participated in the testing.

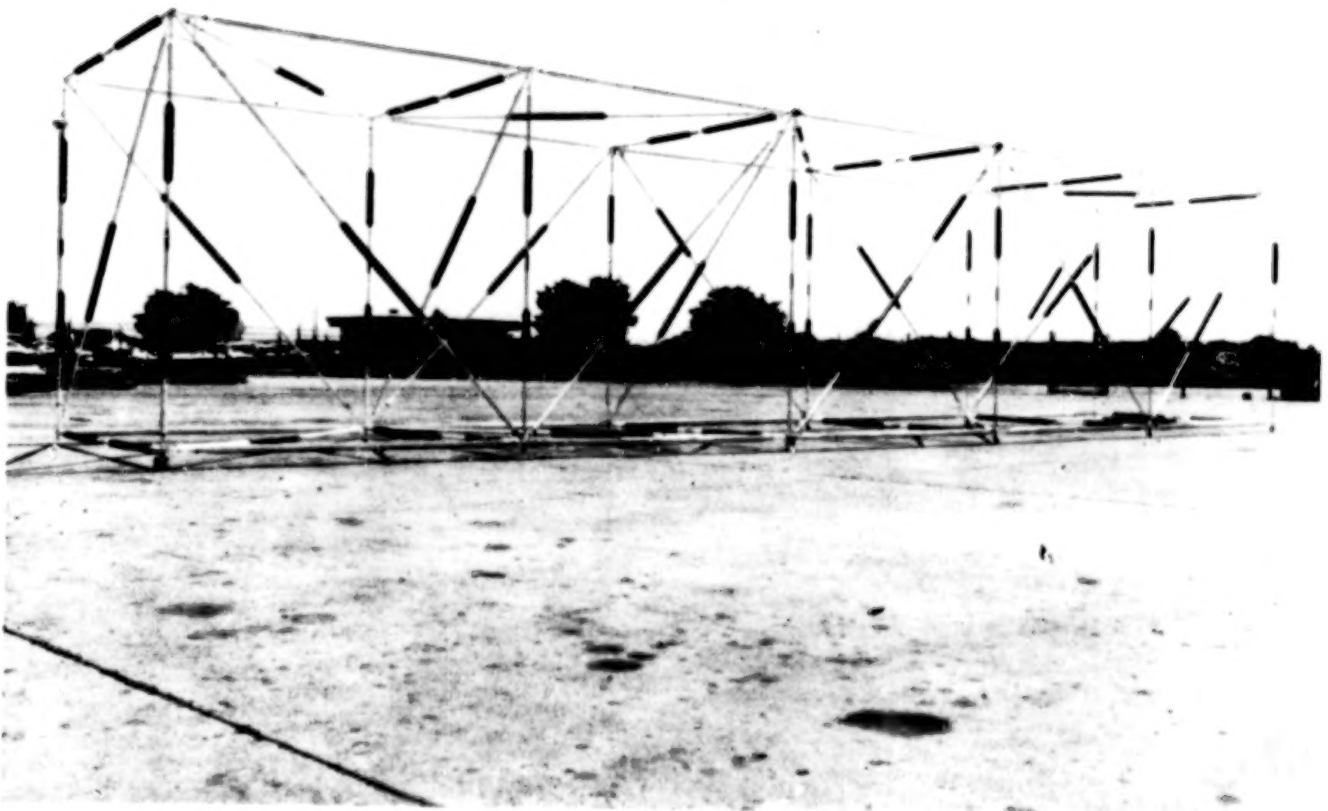
Testing was done in either the single folded or double folded configuration with deployment occurring at either the Orbiter or construction base frame. For example, in the test number 1, two 6 meter single folded modules were translated separately from the Orbiter to the base frame where they were deployed. The operation employed the RMS and two EVA subjects.

TEST NO CONDITION	SEPARATE DOUBLE CELL MODULE		INTER CONNECT MODULE	EVA	RMS	DEPLOY		RETRACT	
	DOUBLE FOLD CONFIGURATION	SINGLE FOLD CONFIGURATION				BASE	ORBITER	BASE	ORBITER
1		2		2	X	X			
2		2		2	X		X		
3		1		2	X	X			
4		2		2	X			X	
5		2		1	X	X			
6		2		1	X			X	
7		2		1	X		X		
8		1		1	X	X			
9		1*		0	X	X			
10	2			2	X	X	X		
11	2			2	X			X	X
12	2			1	X	X	X		
13	2			1	X			X	X
14	1*			0	X	X	X		
15	1			2	X	X	X		
16	1			1	X	X	X		
17		2	X	2	X	X	X		
18		2	X	2	X			X	X
19		2	X	1	X	X	X		

* SINGLE UNIT ONLY

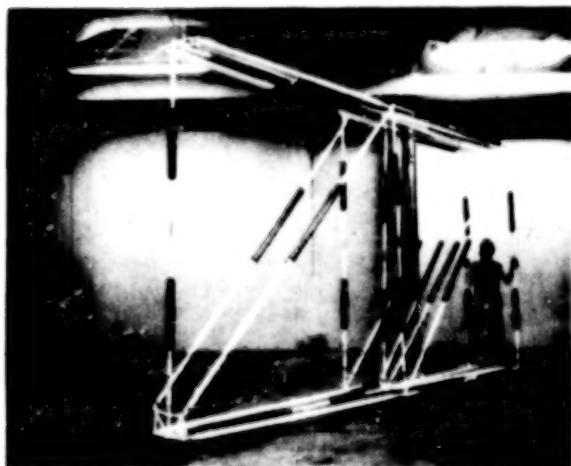
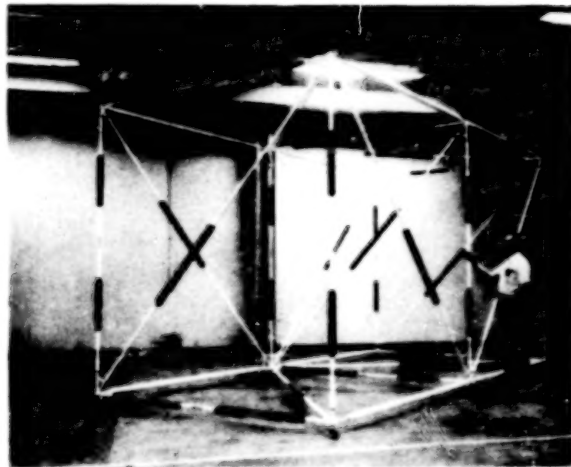
TEST HARDWARE

The fully assembled 15 meter test structure is shown below. The crosssection is 3 meters by 3 meters. The members are 6061-T6 aluminum to reduce fabrication cost and to increase ruggedness in the test environment. The blue cylindrical items located near the mid-point of the members provide neutral buoyancy. Solid aluminum inserts are placed at mid-point of the bulkhead members for the RMS to grip the modules.



TEST HARDWARE

A three step folding sequence and deployable module are shown.



NEUTRAL BUOYANCY TEST FILM

The sound track of a 6 1/2 minute film of neutral buoyancy testing is reproduced below.

The Vought Corporation under NASA contract has produced generic deployable space structure modules for simulated zero "g" testing in the Marshall Space Flight Center's Neutral Buoyancy Simulator. Two 3 meter by 3 meter by 6 meter cubic modules will be removed from the stowage fixture by a specially built Remote Manipulator System or RMS.

The RMS end effector clamps the solid portion of the structural member for translation to the construction base frame at the aft end of the payload bay mockup.

The 6 degrees-of-freedom of the RMS allow translation and rotation of the structure into position for final attachment at the base frame by the suited EVA subjects. The construction base frame used in these tests represents a space platform to which the structural modules may be attached. The test structure has been fabricated from aluminum tubing for resistance to the water corrosion and to provide general ruggedness. Flight hardware is expected to be a composite material. Neutral buoyancy of the module is attained by integral flotation chambers on the members and are shown in blue. A total of 15 separate tests were performed over a five week period. The main function of the RMS was to move the modules from the Orbiter to the base frame where the EVA subjects performed the final alignment and joining operations. Deployment of the structure was accomplished by the RMS. The integrated RMS/EVA activity worked satisfactorily.

The structure is guided into its final position when the module is within reaching distance of the EVA subject. The final joining activity is easily accomplished by EVA and was necessary because of sensitivity constraints of the RMS in the neutral buoyancy simulator. The module is attached to the base frame by an auto-lock coupler. The design of this probe/drogue device permits joining at an angular misalignment in excess of 10 degrees. The coupler automatically locks when joined to the probe. It can be locked in the released position for demating.

With one corner joined at the base frame, the EVA subject proceeds to the other locations to complete the joining operation.

Looking out of a window from the Orbiter Aft Flight Deck presents a different perspective of the activities. This is indicative of the view that operators in the Orbiter will have when performing operations that are being simulated in these tests.

The RMS now performs its second function of deploying the 6 meter module to the extended rigid position. The module is held rigid in the deployed position by telescoping diagonal members which lock upon full extension.

The telescoping member is shown in the locked position as indicated by the protruding flanges. Depressing the flanges inward to the member unlocks the joint and retains it in the unlocked position.

The second 3 meter by 3 meter by 6 meter module is deployed at the payload bay by the RMS and will then be translated to the first module for joining. Positioning the RMS at an exact location on the structure requires skill and practice. Remote operation and visual distortion due to the water presents a challenge for the RMS operators.

The module is deployed vertically in the payload bay. Hold down restraints are released by the EVA subjects standing at the aft end of the module. The Neutral Buoyancy Simulator is 23 meters in diameter and 13 meters deep. The deployment of one 6 meter module in the vertical direction from the payload bay mockup approaches the water level in the neutral buoyancy simulator. Once the module is deployed and automatically locked into its rigid position, translation to the first module may begin.

The RMS brings the module out of the payload bay area for the joining operation. Interference between the RMS operational envelope and the Neutral Buoyancy Simulator wall prevented final translation of the module. The module was maneuvered into final position and alignment by the EVA subjects with assistance from the utility scuba divers as required.

The modules are joined at four corners using the auto-lock couplers. Angular misalignment and out-of-plane tolerances will not preclude a successful joining of the two modules. Two to three pounds of axial force is required for joining.

The two modules are now retracted for return and stowage in the Orbiter. Release of the telescoping member locking features allow easy retraction. The RMS/EVA integrated testing of these deployable modules is providing machine data as well as EVA data useful for studies leading to the development of automatically deployed systems.

CONCLUSIONS

Two major conclusions are that the program objective has been achieved and the deployable modules performed satisfactorily. Supporting comments are presented. The data and experience gained from this program concerning EVA, RMS, and deployment are the first steps in the justification and evaluation of automatically deployed space systems.

- **Program objective has been achieved by obtaining experience and data on RMS and EVA operations**
 - ✓ EVA - Final aligning, locking/unlocking and joining was easily accomplished
 - ✓ RMS - Translation and general orientation of modules successfully achieved
 - ✓ TIMELINES - Average time to remove, deploy, retract, and restow 12 meters of subject test structure with 2 EVA subjects and 1 RMS was approximately 1 ¼ hours
- **Deployable modules performed satisfactorily**
 - ✓ Components withstood harsh environment
 - ✓ Couplers and telescoping members operated satisfactorily - isolated binding due to paint and corrosion
 - ✓ Joint roll pins removed free play but worked free after multiple rotations - need positive retention

SYMBOLS

EVA - Extra Vehicular Activity
RMS - Remote Manipulator System
NBS - Neutral Buoyancy Simulator
ESA - European Space Agency

REFERENCE

(1) Stokes, J. W.: and Watters, H. H.: Space Assembly Methodology. Large Space Systems Technology - 1980, Volume I - Systems Technology, Frank Koprivier III, compiler, NASA CP-2168, 1981. (Paper 16 of this volume.)

SPACE ASSEMBLY METHODOLOGY

J. W. Stokes

and

H. H. Watters

National Aeronautics and Space Administration
George C. Marshall Space Flight Center
Marshall Space Flight Center, Alabama

Large Space Systems Technology - 1980
Second Annual Technical Review
November 18-20, 1980

FOREWORD

This summary reviews our activities during the past year. We have been actively developing our assembly analysis techniques, conducting underwater and other simulations, and applying the results to the assembly of three particular Large Space System concepts.

We would like to acknowledge the valuable support of many organizations; from across our center, from across the agency, from the academic community (notably Massachusetts Institute of Technology), and from several contractors. Special recognition is in order for the Essex Corporation, Huntsville Facility, whose enthusiastic people contributed substantially to each phase of our effort.

MAN/MACHINE SPECTRUM FOR ASSEMBLY

We will quickly review with you our interest and goals in Large Space Systems (LSS) assembly. We have felt all along that assembly of structures can be performed by man, by automated assembly, or by any mixture of the two (fig. 1). Man has proven that he is capable of assembly activities. However, as space systems become larger or assembled in higher orbits, we must push technology to develop automated assembly methods. Interim assembly may be performed via remote assembly devices.

In developing an acceptable assembly methodology for any space system, these three assembly variations should be integrated or mixed to provide the most efficient assembly technique. Factors to be considered in mixing are the economics of the assembly, as well as the nature of the assembly tasks. Economics will be governed by the availability of technology, skills, energy, time, materials appropriate for man or machine, etc. The nature of the assembly tasks to be considered include degree of repetition of the task, amount of real time judgment required, the manipulative complexity of the structure components, the degree of precision required, the degree of hazard of the test, and the scale of the space system.

SPACE ASSEMBLY METHODOLOGY

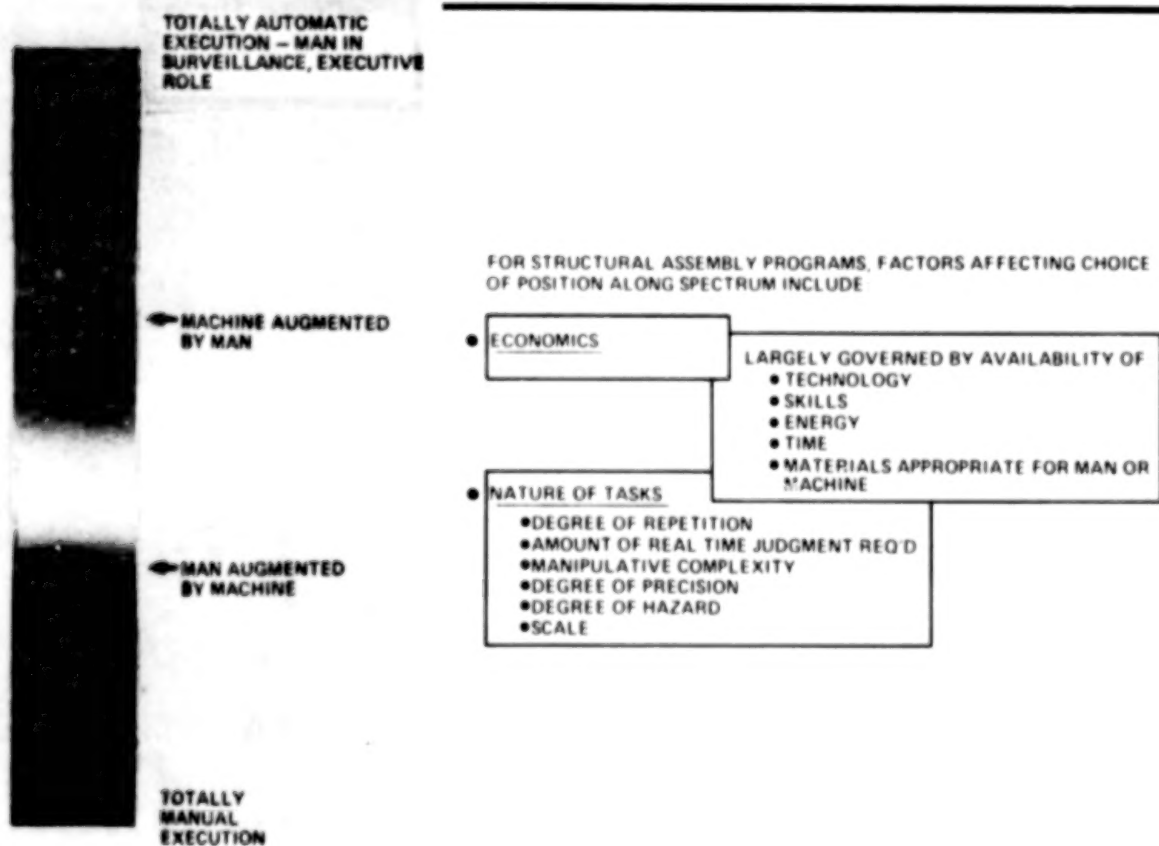


Figure 1

LSS ASSEMBLY ANALYSIS

In an attempt to develop a methodology which will define LSS assembly operations and determine its efficiency in mixing man and machine, Marshall Space Flight Center (MSFC) has divided its assembly activity into three parts or phases. The first part delves into the definition and development of a LSS assembly analysis. The purpose of the assembly analysis is to develop a technique for defining assembly requirements, criteria, and guidelines and to minimize assembly costs for LSS. The assembly requirements, design criteria, and guidelines will address manual, remote, and automated assembly, concentrating on operational aspects, hardware, and personnel. Assembly cost definition and reduction will be aimed at flight operations, labor, LSS hardware, and support equipment.

In order to gather valid estimates on required assembly time (which can be converted into Shuttle flights), assembly task definition and task times must be calculated. Since we are presently not flying space missions we must use previous flight data or data collected from assembly simulations. As described in figure 2, these include assembly tasks performed underwater (neutral buoyancy), in the zero-gravity aircraft (KC-135), in multiple-degrees-of-freedom simulations, and through computerized simulations.

SPACE ASSEMBLY METHODOLOGY MAN/MACHINE ASSEMBLY ANALYSIS

MSFC ASSEMBLY ACTIVITY MAY BE BROKEN INTO THREE PARTS :

ASSEMBLY ANALYSIS DEFINITION AND DEVELOPMENT

- SCENARIOS
- FUNCTIONAL ANALYSIS
- ASSEMBLY REQUIREMENTS
- ASSEMBLY COSTS

ASSEMBLY SIMULATION ACTIVITY TO SUPPORT ANALYSIS

- NEUTRAL BUOYANCY
- KC 135
- MULTIPLE DEGREES OF FREEDOM
- COMPUTERIZED SIMULATION

ASSEMBLY ANALYSIS APPLICATION

- MDAC ADVANCED SASP
- RI SATELLITE POWER SYSTEM
- GDC GEOSTATIONARY PLATFORM

Figure 2

LSS ASSEMBLY ANALYSIS (Continued)

As the analysis becomes more defined, it should be applied to currently envisioned LSS proposals including the Advanced Science and Applications Space Platform (SASP), the Satellite Power System, and the Geostationary Platform in order to evaluate both the LSS and the analysis as a tool. Application of the assembly analysis should define, for any structure, hardware design and assembly requirements. Additionally, development of the assembly technique may be verified by an on-orbit demonstration prior to the LSS mission.

This is precisely what MSFC is currently doing (fig. 3). The assembly analysis is still being defined and remains in preliminary form. A large amount of data has been collected for manual assembly. A major push is now in work for establishing a remote assembly data base. As assembly requirements direct, automated assembly methods will be defined and evaluated. Results will be incorporated into the assembly analysis. As holes are determined in the data base, new simulations are defined and performed in order to provide data to fill the voids.

The assembly analysis was portrayed in a detailed flow diagram as part of the MSFC exhibit at the LSST Technical Review. Several iterations are required to investigate assembly by manual, remote, and automated methods.

Once the assembly analysis has been developed, it must be verified. This can be accomplished by application to proposed LSS proposals. Therefore, the analysis has been, or is being, applied to the previously referenced large systems. To date, the analysis has been able to demonstrate, within the assumptions made for the study, a cost-effective suggested approach to assembly for the Advanced SASP and Satellite Power System.

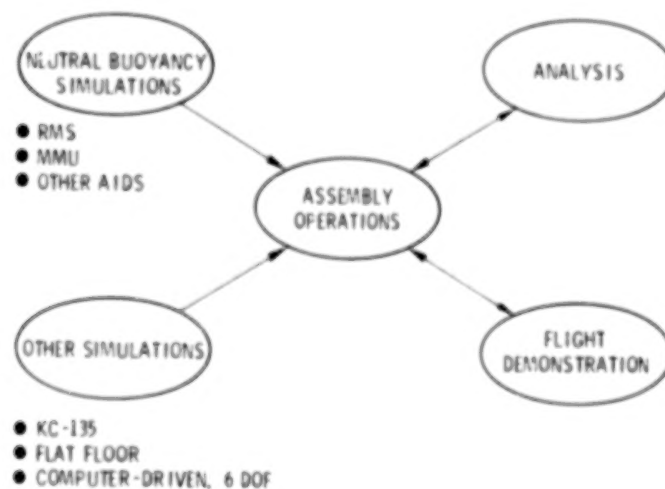


Figure 3

SIMULATION ACTIVITIES

In FY80, we conducted four major simulation series, the results of which fed back into the analysis data base and provided a wealth of information in their own right. These were:

- o An Extravehicular Activity (EVA) assembly simulation with Massachusetts Institute of Technology (MIT) faculty and graduate students;
- o A fabricated beam assembly series using MSFC/Grumman "beam machine" beam, Rockwell/Essex end caps, and Essex-designed cross-beam brackets;
- o Deployment of a Vought-designed deployable truss, using our neutral buoyancy Remote Manipulator System (RMS) with EVA crewman assistance; and
- o A series aboard the KC-135 zero-g aircraft, where, among other objectives, we examined the effects of water "drag" on assembly performance.

EVA ASSEMBLY NEUTRAL BUOYANCY TEST

The first neutral buoyancy simulation (fig. 4) was conducted by MIT with MSFC personnel monitoring assembly operations. The assembly task consisted of mating 36 elements into a tetrahedron-based area structure. The assembly was performed manually. One assembly sequence required the use of a manned maneuvering unit as a translation aid.



SPACE ASSEMBLY METHODOLOGY NEUTRAL BUOYANCY TESTS

TITLE UNDERWATER SIMULATION OF EVA ASSEMBLY

SPONSOR MASSACHUSETTS INSTITUTE OF TECHNOLOGY

DATES JULY 7-31, 1980

OBJECTIVES
1) EVALUATION OF LSS ASSEMBLY VIA EVA
2) EVALUATION OF CREW MANEUVERING UNIT AS
EVA AID IN ASSEMBLY

APPARATUS
• 36 3-METER COLUMNS
• A 9-POINT CONNECTOR CLUSTER
• 12 PERIMETER CLUSTERS
• STOWAGE HARDWARE
• PERSONAL UNDERWATER MANEUVERING APPARATUS
(PUMA)
• CARGO BAY

TEST SUMMARY
1) ASSEMBLY OF AREA STRUCTURE VIA EVA
2) ASSEMBLY OF AREA STRUCTURE VIA EVA WITH PUMA

Figure 4

EVA ASSEMBLY TEST RESULTS

The results of the test (fig. 5) included the verification of the assembly task by one and two subjects. The maneuvering unit proved unreliable, with minor redesign planned for future trials. Typical assembly times were 1:37 for a single subject and 00:50 for a two-subject team.

SPACE ASSEMBLY METHODOLOGY

NEUTRAL BUOYANCY TESTS

UNDERWATER SIMULATION OF EVA ASSEMBLY (CON'T)

RESULTS: ● EVA ASSEMBLY TECHNIQUE FEASIBLE

● MINOR HARDWARE PROBLEMS COMPROMISED PUMA UTILITY

● TYPICAL ASSEMBLY TIMES:

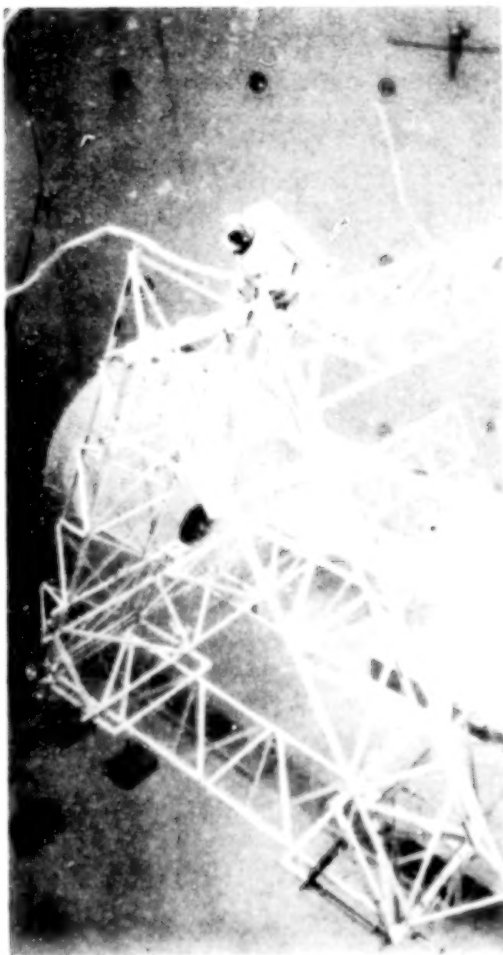
● ASSEMBLY BY SINGLE SUBJECT 1 HOUR,37 MINUTES

● ASSEMBLY BY TWO SUBJECTS 50 MINUTES

Figure 5

FABRICATED BEAM ASSEMBLY NEUTRAL BUOYANCY TEST

The next neutral buoyancy test was a combined effort between MSFC and the Essex Corporation to evaluate techniques for assembling beams fabricated by the MSFC beam machine (fig. 6). Lap joints and end caps interfacing with the Rockwell ball/socket unions were designed and evaluated. Assembly tasks included the attachment of the end caps and lap joints to the beam extruding from the machine, and the assembly of the beams into a truss structure. Future plans call for a vertical truss assembly.



SPACE ASSEMBLY METHODOLOGY NEUTRAL BUOYANCY TESTS

TITLE	FABRICATED BEAM ASSEMBLY
SPONSOR	MSFC/EP 13/E E ENGLER
DATES	AUGUST 11-27, 1980
OBJECTIVE	1) EVALUATION OF LSS ASSEMBLY VIA EVA 2) EVALUATION OF LAP JOINT, END CAP, AND BALL/SOCKET UNIONS WITH FABRICATED BEAMS
APPARATUS	• FABRICATED BEAMS OF VARIOUS LENGTHS • LAP JOINTS • END CAPS WITH BALL/SOCKET UNIONS • BEAM MACHINE WITH CREW RESTRAINTS • CARGO BAY
TEST SUMMARY	1) PHASE I (COMPLETED) - EVA CREWMEN ATTACH END CAPS AND LAP JOINTS TO BEAM PROTRUDING FROM BEAM MACHINE 2) PHASE II (COMPLETED) - ASSEMBLE FABRICATED BEAMS TOGETHER AS HORIZONTAL TRIANGULAR TRUSS 3) PHASE III (TBD) - ASSEMBLE VERTICAL TRIANGU- LAR TRUSS

Figure 6

FABRICATED BEAM ASSEMBLY TEST RESULTS

Results (fig. 7) verified that the hardware design is acceptable with minor modifications. The beams were, as expected, found to be fragile and suffered some damage due to crew activity and structure loading during assembly. Typical assembly time for installing two lap joints and two end caps for a beam was 35 minutes. This time estimate does not include beam extrusion time. Assembly of the triangular truss structure was typically 43 minutes.

As an aside, the low mass of these beams, combined with their relatively high "sail area" led to comparatively difficult manual manipulation in the underwater environment. This simulation artifact probably accounted for several of the instances where beams were damaged. Another reason for damage (not peculiar to the water medium) was the unforgiving need for rather precise alignment. Misalignments tended to build up so that at final "closure," deforming stresses were introduced into the fabricated beams.

SPACE ASSEMBLY METHODOLOGY

NEUTRAL BUOYANCY TESTS

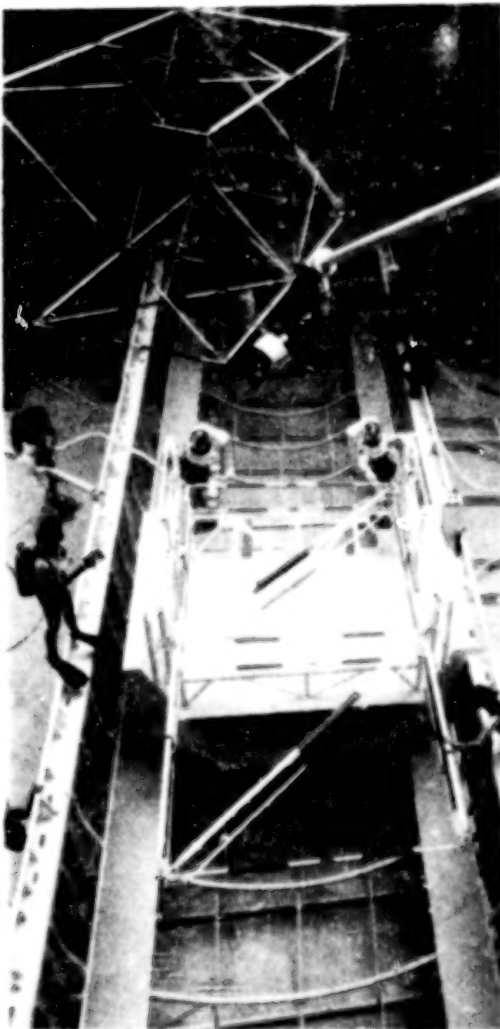
FABRICATED BEAM ASSEMBLY (CON'T)

- RESULTS:
- ASSEMBLY DESIGN/TECHNIQUE FEASIBLE
 - BASIC HARDWARE DESIGN ACCEPTABLE WITH MINOR MODIFICATIONS
 - FABRICATED BEAMS FRAGILE AND SUSCEPTIBLE TO DAMAGE FROM ASSEMBLY OPERATIONS
 - TYPICAL ASSEMBLY TIMES:
 - INSTALLATION OF TWO LAP JOINTS AND TWO END CAPS-35 MINUTES
 - ASSEMBLY OF NINE BEAMS WITH ATTACHED END CAPS AND LAP JOINTS INTO TRIANGULAR TRUSS-43 MINUTES.

Figure 7

ERECTABLE/DEPLOYABLE CONCEPTS NEUTRAL BUOYANCY TEST

The last neutral buoyancy test was a MSFC/Vought study to evaluate a deployable structure concept (fig. 8). EVA test subjects assisted the RMS as it withdrew the two modules from their stowage rack, attached each to the assembly fixture, and deployed them. Incorporation of an interconnect cell between the two modules was demonstrated.



SPACE ASSEMBLY METHODOLOGY NEUTRAL BUOYANCY TESTS

TITLE: ERECTABLE/DEPLOYABLE CONCEPTS

SPONSOR: MSFC/VOUGHT

DATES: SEPT 2 - OCT 8, 1980

OBJECTIVES

- DEVELOP DESIGN AND PROCEDURE REQUIREMENTS FOR PACKAGING, DEPLOYING, ASSEMBLING, AND STOWING STRUCTURES FOR NEAR-TERM SPACE PLATFORM SYSTEMS

APPARATUS

- TWO DOUBLE-CELL STRUCTURE MODULES, EACH WITH SINGLE-FOLD OR DOUBLE-FOLD CAPABILITY
- THREE "CARD TABLE" LEGS AND TWO SINGLE MEMBERS USED TO MAKE INTERCONNECT CELL
- SUPPORT FIXTURES - STOWAGE AND ERECTABLE
- CARGO BAY WITH PALLET AND REMOTE MANIPULATOR

TEST SUMMARY

- DEPLOYMENT OF SINGLE MODULE FROM STOWAGE FIXTURE
- DEPLOYMENT OF SINGLE AND/OR DOUBLE MODULE FROM ERECTABLE SUPPORT FIXTURE
- DEPLOYMENT OF DOUBLE MODULES MATED WITH INTERCONNECT

Figure 8

ERECTABLE/DEPLOYABLE TEST RESULTS

Results (fig. 9) indicate the module deployment was feasible, by RMS, but required EVA assistance for attachment tasks, etc. In several respects, the neutral buoyancy RMS does not replicate the flight version, but the concept was demonstrated.

SPACE ASSEMBLY METHODOLOGY

NEUTRAL BUOYANCY TESTS

ERECTABLE/DEPLOYABLE CONCEPTS (CON'T)

- RESULTS:
- DEPLOYMENT OF A MODULE BY RMS IS FEASIBLE. HOWEVER, THE ACTIVITY IS BEST PERFORMED BY A COMBINATION OF RMS AND EVA CREWMEN; RMS PERFORMING GROSS TRANSPORTATION AND ORIENTATION, EVA CREWMAN PERFORMING DEXTEROUS TASKS.
 - CREW WORK STATIONS WERE NOT OPTIMALLY LOCATED
 - DIFFICULTY IN OPERATING LOCKING DROGUES, REDESIGN AND CREW ACCESS CONSTRAINTS RECOMMENDED
 - OPPOSED JAW END EFFECTOR (SPECIAL END EFFECTOR) LESS THAN OPTIMAL FOR HANDLING DUE TO ROTATIONAL FORCES
 - TYPICAL ASSEMBLY TIMES:
 - FOR 2 SINGLE-FOLD MODULES, 2 EVA CREWMEN - 45 MINUTES
 - FOR 2 SINGLE-FOLD MODULES WITH INTERCONNECT MODULE, 2 EVA CREWMEN - 39 MINUTES
 - FOR 2 DOUBLE-FOLD MODULES, 1 EVA CREWMAN - 48 MINUTES

Figure 9

LSS PART TASK ASSEMBLY TEST

One other simulation mode was used to provide support or clarification data to the neutral buoyancy test data. The NASA KC-135 Zero-Gravity Aircraft provided a test bed to better evaluate assembly activities by MSFC and MIT which were previously affected by water drag (fig. 10). The MIT test continued to attempt to define body reaction to simple assembly. The MSFC test further defined the capability of the manual EVA crewman to assemble the Rockwell ball/socket union with a 9.1-meter (30-foot) column.



SPACE ASSEMBLY METHODOLOGY ZERO-G AIRCRAFT TESTS

TITLE LSS PART TASK ASSEMBLY TEST	
SPONSOR:	MSFC & MIT
DATES:	(A) MAY 6-7, 1980 (B) JUNE 9-13, 1980
OBJECTIVES	1) EVALUATE HANDLING AND ATTACHMENT OF RI-30 FT. COLUMNS AND BALL/SOCKET JOINT WITH EMU PRESSURE SUIT 2) MEASURE QUANTITATIVELY THE REACTION OF HUMAN BODY TO SIMPLE ASSEMBLY MOTION
APPARATUS	(A) • 30-FT. COLUMN WITH CENTER SLEEVE LOCK, BALL ENDS • 30-FT. COLUMN WITH CENTER LATCH LOCK, BALL ENDS • PEDESTAL - MOUNTED SOCKET • FOOT RESTRAINTS, HARDWARE RESTRAINTS (B) • TEST MASS SPHERES • EXO SKELETON • TAPE RECORDER, STRIP CHART RECORDER, POWER SUPPLY
TEST SUMMARY	(A) • ATTACHMENT OF FOLDED BEAMS TO EVALUATE CENTER LATCH • MANEUVERING OF 30 FT. COLUMN FOR PRECISION POSITIONING • ATTACHMENT OF 30 FT. COLUMN WITH BALL/SOCKET UNION • TRANSLATION ALONG ATTACHED 30 FT. COLUMN

Figure 10

LSS PART TASK ASSEMBLY TEST RESULTS

Results (fig. 11) demonstrated the ease of accomplishment of both test objectives. The 9.1-meter (30-foot) beam was easily maneuvered and positioned by the pressure-suited subject.

SPACE ASSEMBLY METHODOLOGY

ZERO-G AIRCRAFT TESTS

LSS PART TASK ASSEMBLY TEST (CON'T)

TEST SUMMARY (CON'T)

- (B) • HAND-HELD SPHERES SWUNG THROUGH 90° ARC BY FREE-FLOATING CREWMAN WITH EXOSKELETON
- POSITIONED HIGH MOMENT-OF-INERTIA BEAM WITH SUBJECT RESTRAINED AND FREE FLOATING

RESULTS

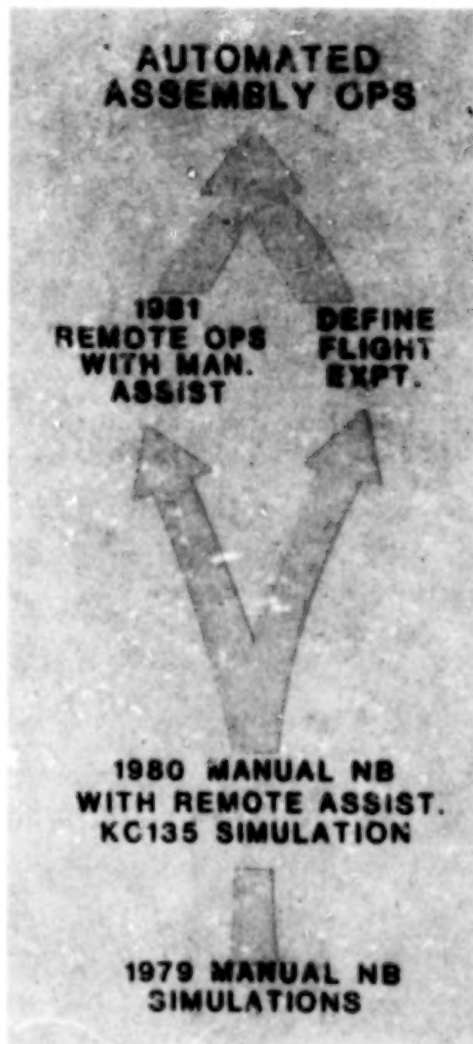
- (A) • 30-FT COLUMN CENTER HINGE JOINTS EQUALLY EASY TO LATCH. SLEEVE LOCK PREFERRED. BETTER VISUAL VERIFICATION
- 30-FT COLUMN MANIPULATION EASY. TIP PLACEMENT WITHIN ± 1 INCH POSSIBLE
- BALL SOCKET LATCHING POSSIBLE. FORE/AFT TIP PLACEMENT DIFFICULT AT 15-FT DISTANCE. SUGGEST BALL GUIDE ON SOCKET
- EMU CHEST-MOUNTED TOOL KIT PROVIDED NO VISIBILITY OR OPERATIONAL PROBLEMS
- CREW TRANSLATION ALONG COLUMN EASILY ACCOMPLISHED
- (B) • DATA STILL IN ANALYSIS. PRELIMINARY DATA INDICATES PREDICTABLE MOVEMENTS BY BODY

Figure 11

1 foot = 0.3048 meter; 1 inch = 2.54 centimeters.

THE NEXT LOGICAL STEP

In summary, we have pursued the definition and development of a man/machine assembly analysis to be applied to any large orbital structure (fig. 12). We have accumulated a large amount of data on manual assembly operations. We are now pursuing the development of a remote assembly operations data base. In 1981, we will further develop this latter assembly approach, with emphasis upon remote assembly with manual assist, and ultimately define, as best possible, automated assembly requirements and costs.



SPACE ASSEMBLY METHODOLOGY THE NEXT LOGICAL STEP

FOR 1981 MSFC WILL DO THE FOLLOWING
IN PURSUIT OF DEFINING ASSEMBLY
TECHNOLOGY:

- FURTHER DEVELOP MAN/MACHINE ASSEMBLY ANALYSIS WITH EMPHASIS UPON REMOTE ASSEMBLY WITH MANUAL ASSIST
- BEGIN DEFINITION OF A LOW-COST EARLY-MISSION FLIGHT EXPERIMENT DIRECTLY CORRELATED TO NEUTRAL BUOYANCY TESTS

Figure 12

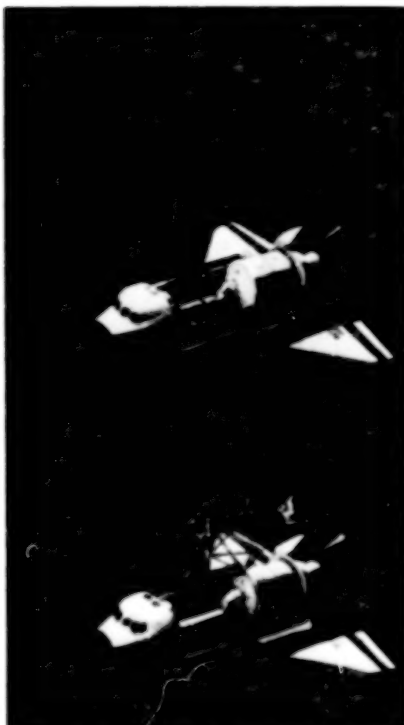
FLIGHT VALIDATION EXPERIMENT

Parallel to this effort we believe that an orbital flight validation experiment is in order (fig. 13 and 14). We have extracted much information from our simulation program. However, each simulation mode, though having direct relationships to flight, has inherent individual shortcomings, prohibiting the attainment of flight-replicative data. What is required is a correction factor that can be applied to the test results to make them closely approximate orbital results. The most obvious technique for obtaining such a correction factor would be to replicate on-orbit a simulation performed on earth, then compare detailed tasks and associated times to establish the differences. Statistical analysis applied to the results should produce a correction factor capable of producing ground-based test results very similar to those occurring on orbit.

This approach is proposed for comparison between spaceflight and neutral buoyancy simulation. An on-orbit assembly of one of the concepts tested in the MSFC neutral buoyancy simulator would provide an inexpensive and easily-prepared experiment. The hardware (e.g., MIT structure or Vought deployable module) would be the same for both parts of the experiment, as would be the procedure and possibly the test subjects. The only new hardware would appear to be that required to support the equipment in the flight payload bay. The experiment could be flown on any early Shuttle flight on a space-available, "piggyback" basis.

Interfaces would be limited to the mechanical interface required for launching and assembling the structure. Data would be collected via video tape and crew comments.

The advantage of this experiment is that it can be flown early for little cost or planning, and produce needed data. Our 1981 plans include initial planning toward this goal.



The Next Logical Step..... -Flight Validation Experiment

- TIME: Target for early shuttle mission
- LOCATION (STOWED/DEPLOYED) IN SHUTTLE
Forward of pressurized module, around tunnel
- TEST HARDWARE: ● Erectable cell using MMU
(e.g. MIT structure)
or
● Deployable cell using RMS
(e.g. Vought structure)
- HARDWARE MODIFICATIONS: Minimal, to extent
necessary to fly on shuttle
- SHUTTLE REQUIREMENTS: Two EVA crewmen, two
MMU's, RMS
- DATA REQUIREMENTS: Video photography, time-
annotated voice recording/transcript, crew
debriefing transcript
- PROCEDURE: Identical to ground based
simulations, modified only to extent necessary
to accommodate orbital constraints

Figure 13

SPACE ASSEMBLY METHODOLOGY THE NEXT LOGICAL STEP

FLIGHT VALIDATION EXPERIMENT

- SKYLAR OFFERED LAST FLIGHT ASSEMBLY DATA THERMAL PROTECTION FIX
- GROUND BASED ZERO - G SIMULATIONS WHICH PROVIDE LSS ASSEMBLY DATA
 - KC 135 PARABOLIC FLIGHTS
 - NEUTRAL BUOYANCY
 - 6 D O F SIMULATION
 - AIR BEARING (5 D O F) SIMULATION
 - ONE - G SIMULATION
- EACH SIMULATION MODE HAS
 - DIRECT RELATIONSHIP TO FLIGHT
 - INHERENT SHORTCOMINGS IN SIMULATING ZERO - G
- CORRECTION FACTOR (CONSTANT) REQUIRED TO VALIDATE EACH SIMULATION MODE TO
ZERO - G OBTAINABLE THROUGH FLIGHT EXPERIMENT
- LSS ASSEMBLY OPERATIONS HARDWARE DESIGN VALIDATED THROUGH EARLY, SIMPLE
FLIGHT DEMONSTRATIONS
 - MANUAL EVA - MMU
 - REMOTE - RMS

Figure 14

BLANK PAGE

BLANK PAGE

CONSTRUCTION ASSEMBLY AND OVERVIEW

Lyle M. Jenkins
Program Development Office
Lyndon B. Johnson Space Center
Houston, Texas

Large Space Systems Technology - 1980
Second Annual Technical Review
November 18-20, 1980

GRAPHITE COMPOSITE FORMING AND WELDING TECHNOLOGY

One of the LSST activities related primarily to space fabrication has been conducted by General Dynamics-Convair under contract to JSC. The objective has been the continued development of forming and welding the composite material planned for use in a beam builder concept. The material is a composite of graphite fibers in a polysulfone resin matrix which is also under development. In addition to component tests, a truss segment was fabricated for test at JSC.

- CONTRACTOR - GENERAL DYNAMICS-CONVAIR
- OBJECTIVES
 - CONTINUE DEVELOPMENT OF FORMING AND WELDING METHODS FOR GR/TP COMPOSITE MATERIALS
 - CONTINUE GR/TP MATERIALS TECHNOLOGY DEVELOPMENT
 - FABRICATE AND TEST A LIGHTWEIGHT TRUSS SEGMENT

CAP FORMING OPERATIONS

Summary

The photograph shows the formed cap strip emerging from the bench test forming machine. A flat strip of material enters the machine, is heated above the thermoplastic transition temperature, then rolled into the desired shape. Cooling platens reduce the strip temperature to hold the final shape.



RUN NO.	DATE	CAP LENGTH	END USE	RESULTS & ACTION
1	14 MAY	2.74m (9 FT)	TEST RUN ONLY	POOR - HEATING ELEMENTS ADJUSTED - SUPPORT GUIDES ADDED
2	9 MAY	2.74m (9 FT)	TEST RUN ONLY	FAIR - MINOR ADJUSTMENTS MADE
3	13 MAY	6.1m (20 FT)	TEST RUN - CRIPPLING SPECIMENS	GOOD - MINOR IRREGULARITIES - INSULATED SUPPORT BRACKETS
4	14 MAY		COLUMN TEST SPECIMEN	GOOD
5	14 MAY		PROTOTYPE TRUSS CAP	GOOD
6	15 MAY		PROTOTYPE TRUSS CAP	GOOD
7	15 MAY	6.1m (20 FT)	PROTOTYPE TRUSS CAP	GOOD

TOTAL 38m (118 FT)

FINAL WELDING TEST SETUP

The welding approach was based on a commercial ultrasonic welding machine. Vibrations induced by the machine create friction heating of the faying surfaces of the material. This melts the thermoplastic resin to produce a spot weld. Space conditions were simulated in a vacuum chamber. Potential effects of gravity on the weld nugget were evaluated by welding flat, at 45° and at 90° angles.

• INSTRUMENTATION AND CONTROLS

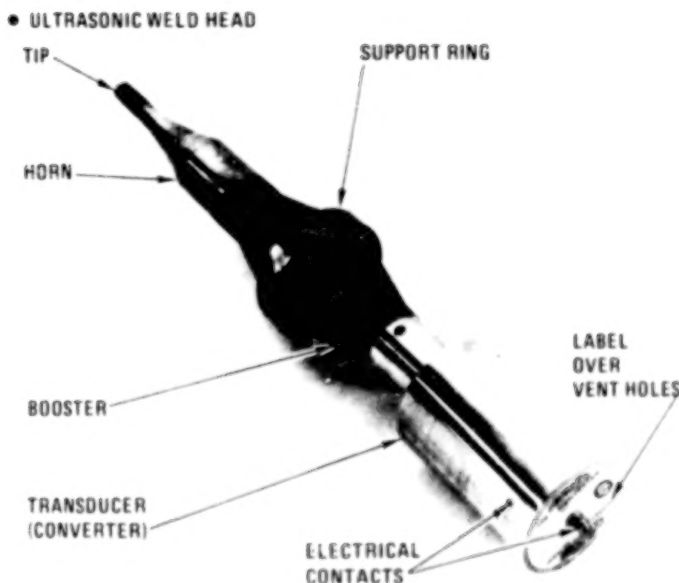


• VACUUM CHAMBER 6" SET-UP



WELDER PROBLEM INVESTIGATION/RESOLUTION

Initial tests in the vacuum chamber produced a puzzling situation. Although the welder was not designed for vacuum operation, there was no technical reason to expect that it would not work properly. During the first tests the welder would not weld in the vacuum chamber. Trouble-shooting and detailed examination discovered a label covered vent holes in the transducer. This apparently trapped sufficient gas to produce a corona. Satisfactory welds were produced in vacuum after clearing the vent holes.



PROBLEM

- WELDER WOULD NOT WELD IN VACUUM
 - ERRATIC POWER
 - WELD AND HOLD TIME CHANGED
 - ERRATIC FREQUENCY
 - NO WELD OR MELT

ACTION/RESULTS

- TROUBLESHOOT ELECTRONICS AND ACTUATOR
 - INCONCLUSIVE
- REPAIRED ELECTRONICS AND REPLACED TRANSDUCER
 - NO EFFECT
- REMOVED AMPLIFIERS FROM CHAMBER
 - WIRING PROBLEMS
- REMOVED POWER AND CONTROL PACKAGE FROM CHAMBER
 - INTERMITTENT WELDS
- REMOVED LABEL FROM TRANSDUCER
 - WELDS NORMALLY

CONCLUSIONS

- CORONA EFFECT IN TRANSDUCER
- UNIDENTIFIED ELECTRONIC COMPONENTS MALFUNCTION IN VACUUM

VACUUM AND GRAVITY EFFECTS

Specimens were examined for evaluation of gravity effects. There were no detectable differences in tip penetration, rear face abrasion or resin flow patterns. Strength test results showed a slight degradation for specimens welded on an angle. This is attributed to the weight of the machine and can be compensated by changing the weld schedule.

VISUAL COMPARISONS

● EXAMINATIONS

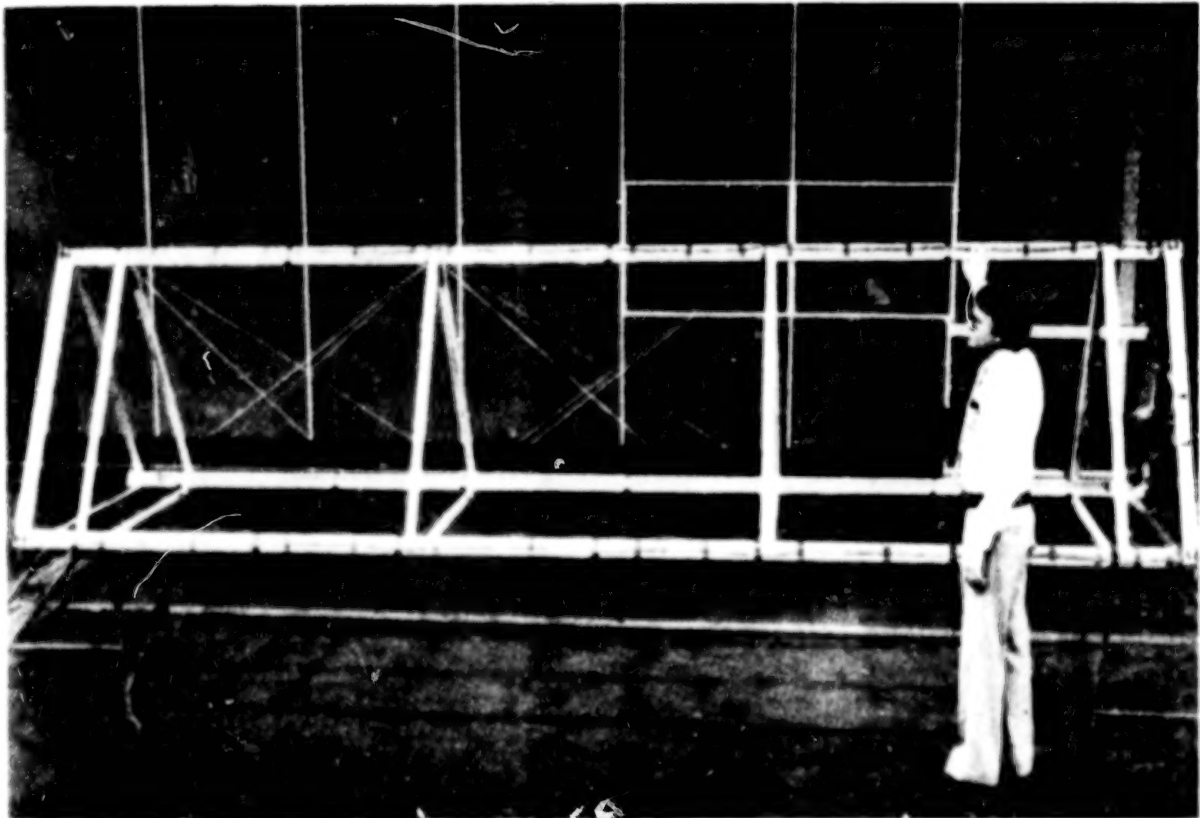
- ▲ FIVE SPECIMENS FROM EACH TEST
- ▲ LAP SHEAR SPECIMENS
- ▲ PEEL SPECIMENS

● RESULTS

- ▲ NO DETECTABLE DIFFERENCE
 - TIP PENETRATION
 - REAR FACE ABRASIONS
 - RESIN FLOW PATTERNS
 - & CHARACTERISTICS

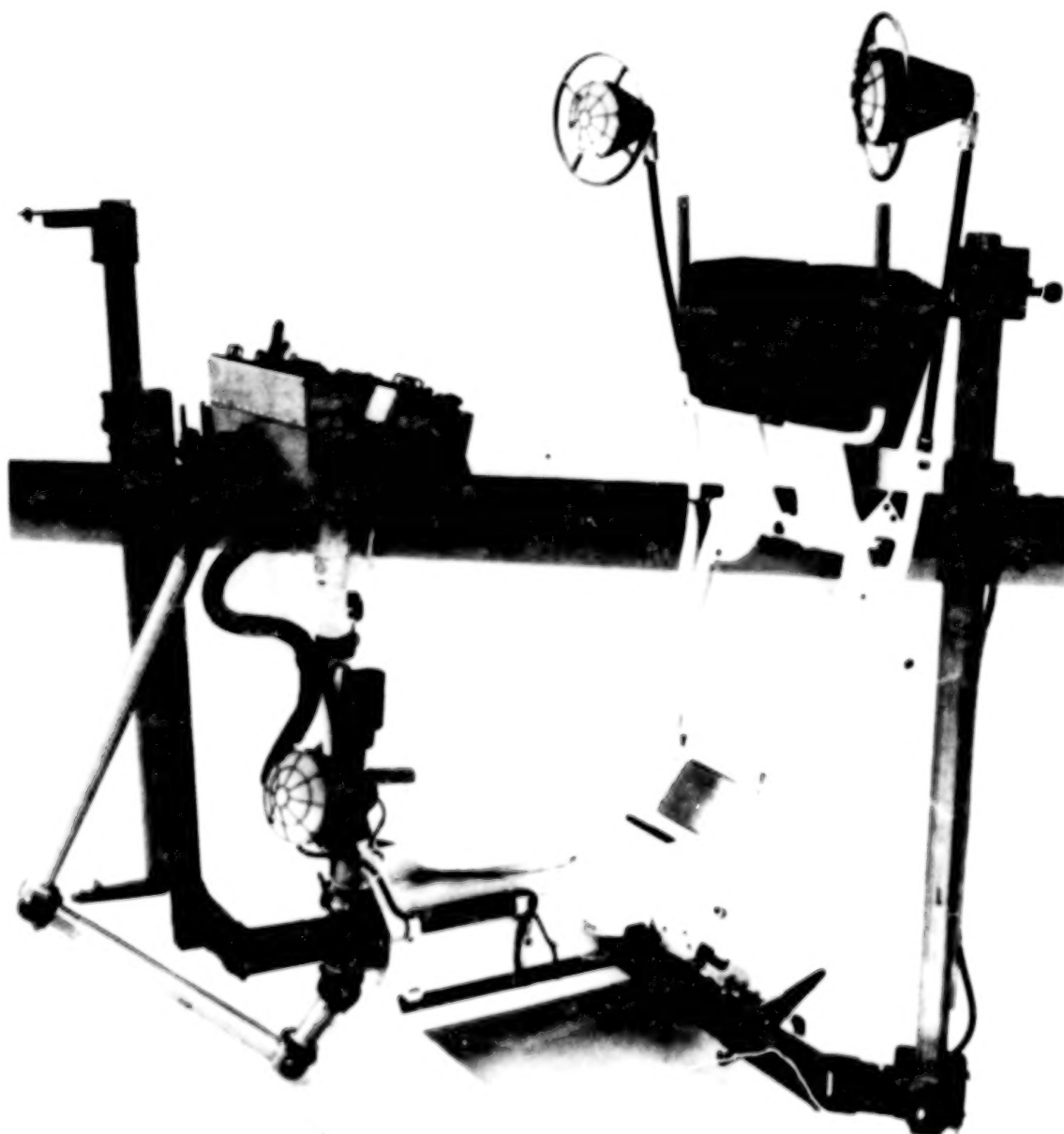
PROTOTYPE TRUSS SEGMENT

Roll-formed cap strips were ultrasonically welded to cross members and cords to produce the prototype truss segment. A number of tests were run on the truss at JSC. Unfortunately an inadvertent actuation of the hydraulic load cylinder ruptured the truss without obtaining compressive strength data. The final report on this study will be distributed early in December.



SATELLITE SERVICES

The photograph shows the development test article of an open cherry picker-type of manned remote work station. This will be a valuable piece of support equipment for use in construction operations to position the EVA astronaut. Tests have been conducted by Grumman Aerospace Company on their Large Amplitude Space Simulator. Tests are planned in the coming year in the JSC Manipulator Development Facility and Water Immersion Facility, as well as in the Neutral Buoyancy Facility at MSFC.



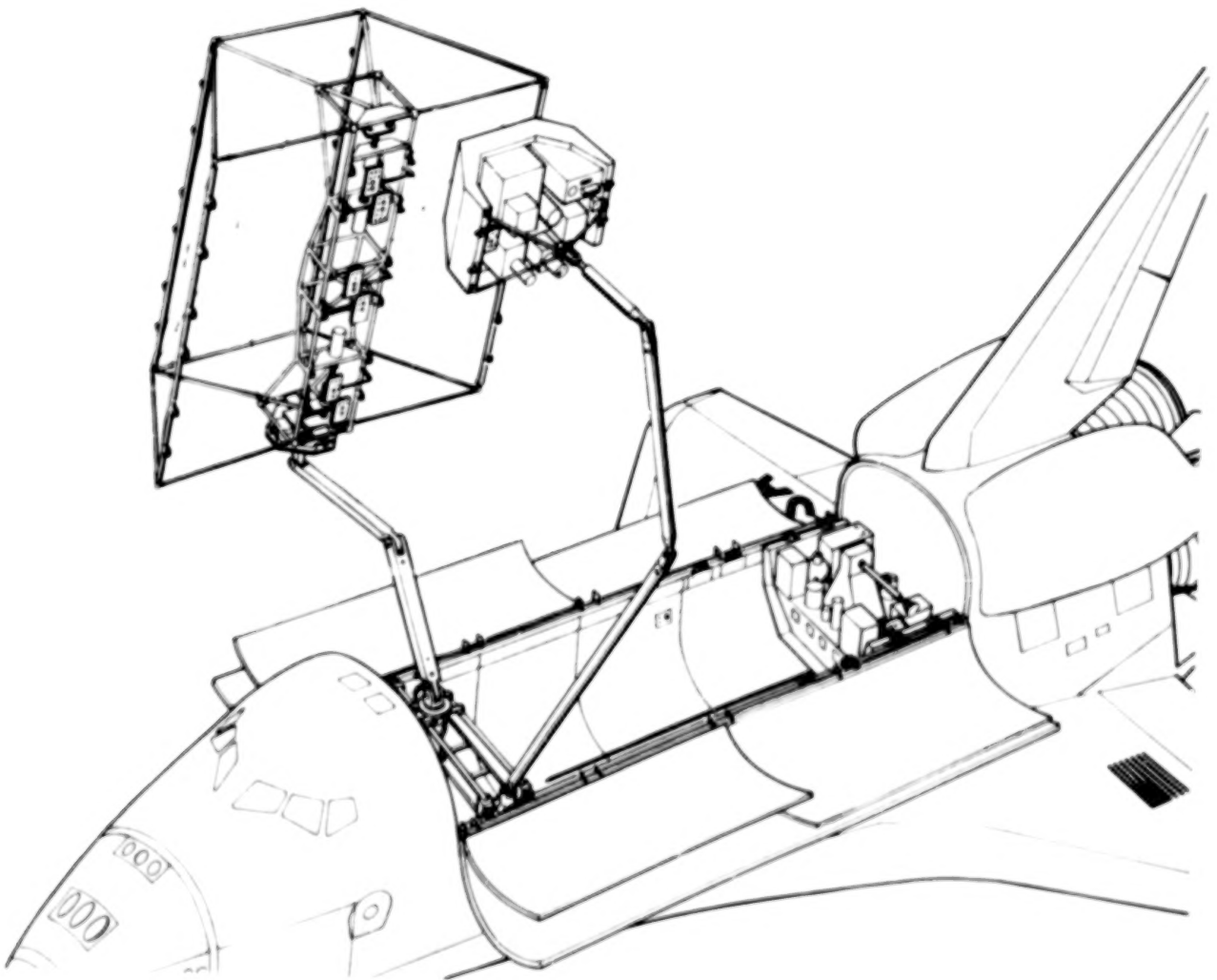
ORBITER-BASED CONSTRUCTION EQUIPMENT STUDY

The contractor for this study has not yet been selected. A study task will examine requirements for Orbiter-based construction equipment concepts. The principal thrust of the study will be the Holding and Positioning Aid concept. It will permit greater use of the RMS by supporting and indexing the work. An engineering test article will be fabricated for evaluation in the MDF.

- CONTRACTOR - TO BE SELECTED
- OBJECTIVES
 - REQUIREMENTS FOR CONSTRUCTION EQUIPMENT
 - DESIGN HOLDING AND POSITIONING AID CONCEPT, FABRICATE ENGINEERING TEST ARTICLE.

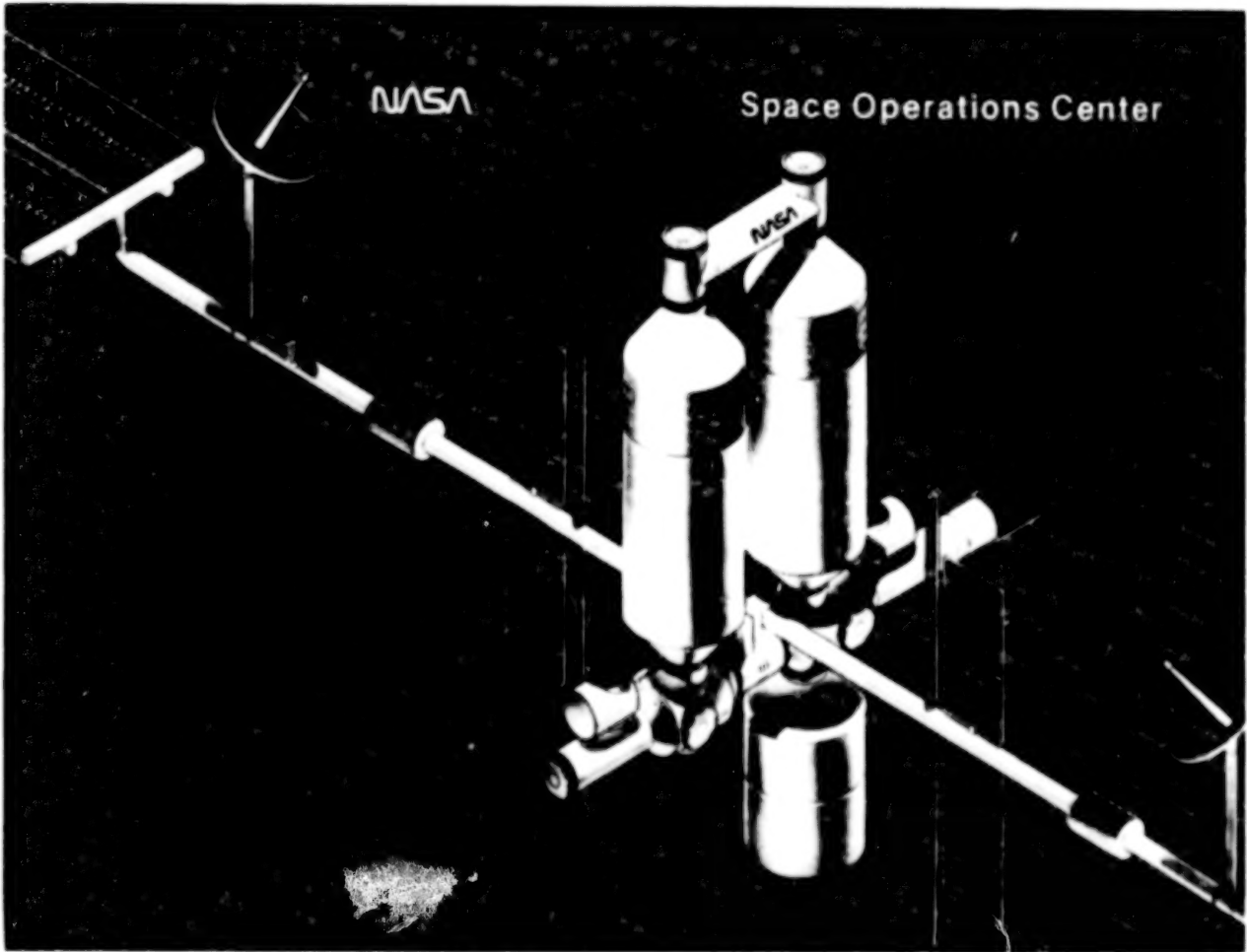
HOLDING AND POSITIONING AID

A concept for the Holding and Positioning Aid (HPA) is illustrated in a platform servicing function. Because it has only six degrees, the RMS is limited in its ability to reach certain locations. The fundamental job of the HPA is to berth the work to the Orbiter and index to positions for access by the RMS. The Berthing Latch Interface Mechanism, to be described by MDAC in the Platform Advanced Technology review, will be integrated with the HPA design.



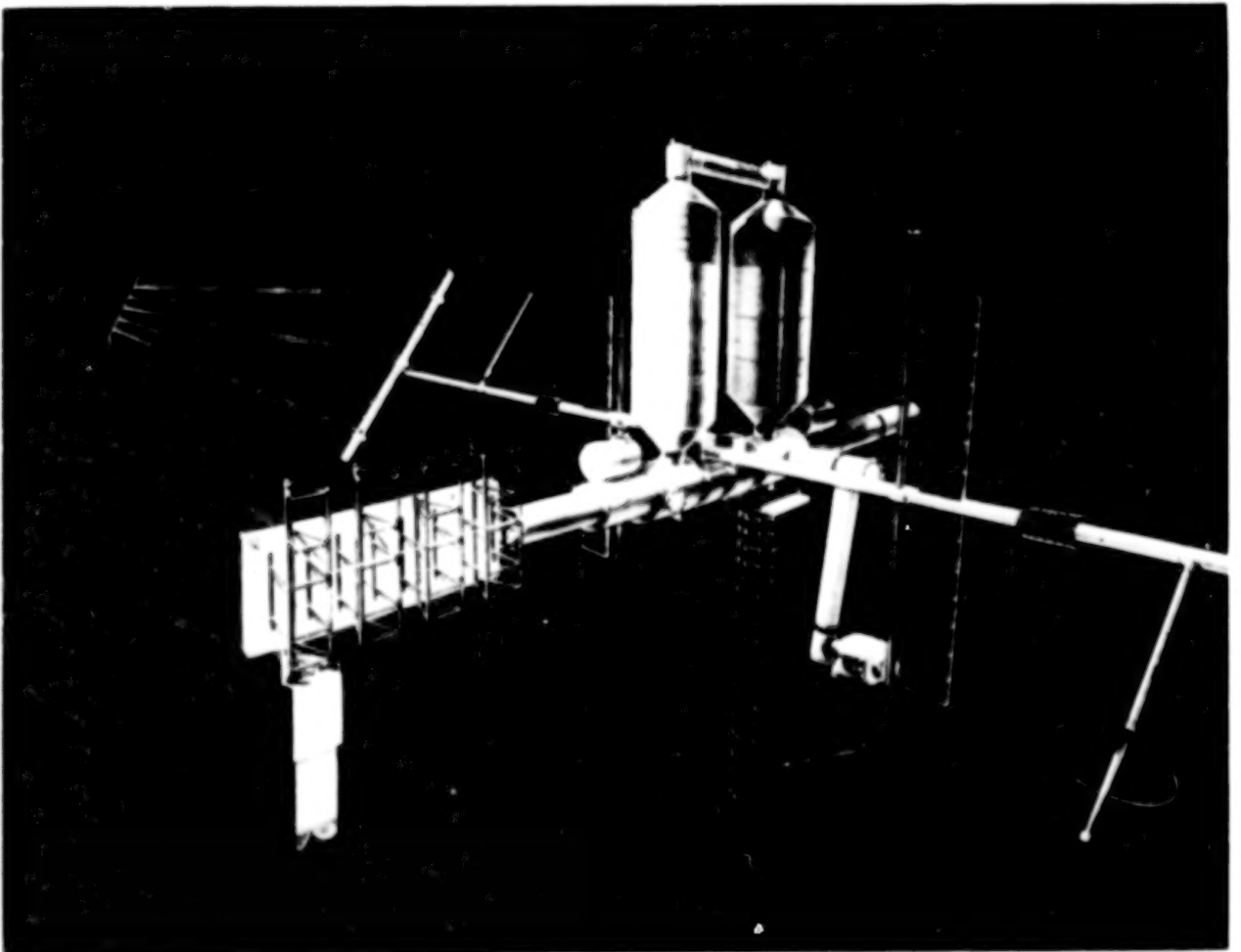
SPACE OPERATIONS CENTER

The Space Operations Center (SOC) represents the next level of manned construction capability beyond Shuttle sortie mode. The assembly of the SOC will pose a major construction challenge with deployment of solar arrays, radiators and antennas as well as berthing of modules. This buildup will undoubtedly be phased over several years in an evolutionary program. Module interfaces will have to be established early or the ability to make modifications on-orbit developed.



SOC CONSTRUCTION OPERATIONS

The mission-oriented role of the SOC will include construction, assembly, and servicing of large space systems. It is expected that current studies can indicate the beneficial combinations of man and machine. The SOC may utilize much of the support equipment developed for the Orbiter as well as new items such as a closed cherry picker and beam builder.



SPACE PLATFORM
ADVANCED TECHNOLOGY STUDY

G. C. Burns
McDonnell Douglas Astronautics Company
Huntington Beach, California

Large Space System Technology - 1980
Second Annual Technical Review
November 18-20, 1980

OBJECTIVE

The objectives of the Space Platform Advanced Technology Study are examination of the requirements for and partial development of mechanisms which would have application regardless of which of many space platform configurations is finally selected to be built. The study consists of five tasks as follows:

1. Space Platform Technology Review
2. Orbiter Berthing System Requirements
3. Berthing Latch Interface Requirements, Design and Model Fabrication
4. Berthing Umbilical Interface Requirements and Design
5. Adaptive End Effector Requirements, Design and Model Fabrication

Task Number 1 consisted of reviewing prior studies of: science and applications space platforms, power modules, large space structures and space stations. The objective of this review was to select those mechanical systems, for further development, which would have universal application to platform-type structure buildup in space. The typical space platform will consist of a power system, structural support arms, palletized payloads, gimbals and potentially pressurized and manned habitability modules. All of these elements must be handled and structurally attached together. They must also provide a variety of functions such as electrical power, communications and thermal control loops across the mating interfaces. These elements and functions will exist regardless of space platform configuration. Figure 1 illustrates a

ORBITER-PLATFORM-POWER MODULE BERTHED ORBITING CONFIGURATION

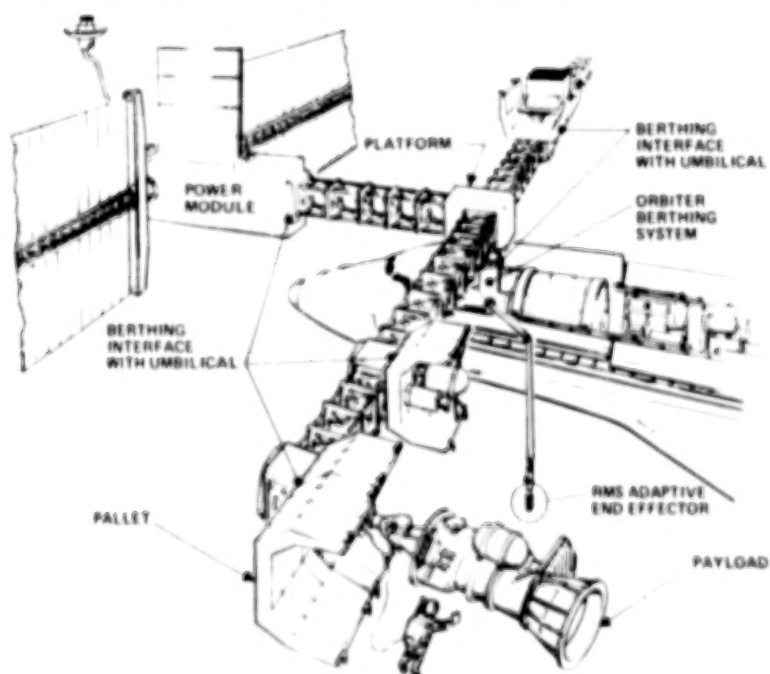


Figure 1

typical space platform orbiting configuration with palletized payloads attached. Because of their universal adaptability, the Orbiter Berthing System, Berthing Latch Interface, Berthing Umbilical Interface and the Adaptive End Effector for the Orbiter RMS were selected for further development in Tasks 2 through 5 of this study.

The object of Task 2 was to establish the requirements for an Orbiter Berthing System. These requirements were derived by analyzing the positioning requirements of the various configuration platforms for deployment servicing and payload changeout. Orbiter bay volume available for stowage of the berthing fixture was defined.

Task 3 had the objective of developing a full scale working model of a Berthing Latch Interface Mechanism. In order to accomplish this development the requirements had to be established; a trade study of various mechanism configurations was conducted, a concept was selected, design layouts and detail drawings were prepared and a model was fabricated.

The requirements for the Berthing Latch Mechanism were derived based on the use of the Orbiter RMS to position and hold the payload in berthing position and to guide the two bodies until a structural latch is accomplished. A total of six Berthing Latch Interface configurations were evaluated and the hexagonal frame configuration was selected based on envelope and lack of mechanical complexity. A full scale model of the mechanism was designed and the fabrication of the model is now 90% complete.

Task 4 has the objective of establishing requirements for and preparing a preliminary design layout for the umbilical to be used in conjunction with the Orbiter Berthing System and the Berthing Latch Interface mechanism. The requirements were derived based on payload needs, compatibility with the Berthing Latch Interface and platform requirements. Accommodations were provided for electrical power, data and coolant fluid transfer across the umbilical interface.

The objective of Task 5 is to develop a full scale working model of an Adaptive End Effector to be used in conjunction with the Orbiter RMS. The requirements for the end effector were derived based on projected usage in conjunction with future space platform assembly, deployment, maintenance and payload changeouts. A full scale working model is being fabricated and is to be used in conjunction with the RMS simulator at NASA/JSC.

STUDY OUTPUTS

Berthing System

The Berthing System requirements were derived based on Orbiter constraints and performance, platform characteristics and RMS performance.

Berthing System Key Requirements

- Object - Provide a berthing interface and a structural bridge between the Orbiter and a free-flying space platform or a power module.
- Stowage Volume - The Berthing System shall be installed in the forward portion of the Orbiter cargo bay and be compatible with the installation of Spacelab module, short access tunnel, airlock, MMU, Ku antenna and left- and/or right-hand installation of RMS.
- Deployed Berthing Interface - The Berthing System shall deploy from the Orbiter bay and provide the structural mounting for a berthing latch mechanism. The centerline of the deployed interface shall be located at $Y_0 = 0$, Z_0 515 minimum, X_0 633 maximum.
- Orbiter Structural Interface - The Berthing System shall structurally attach to the Orbiter through the use of standard Orbiter keel and longeron bridge fittings attach points.
- Structural Stiffness - The structural stiffness of the Berthing System shall be 5.4×10^6 N-m/rad (4×10^6 ft-lb/rad) in both bending and torsion. In the deployed position the system shall exhibit no looseness or backlash in joints or drive actuators.
- Structural Loads - The structural design bending and torsion loads applied at the berthing interface mechanism shall be 21 000 N-m (16 000 ft-lb).

The Berthing System must be designed to be stowed in the Orbiter cargo bay between Stations X_0 637 and X_0 748.8 as illustrated by Figure 2.

BERTHING SYSTEM STOWED MAXIMUM DYNAMIC ENVELOPE

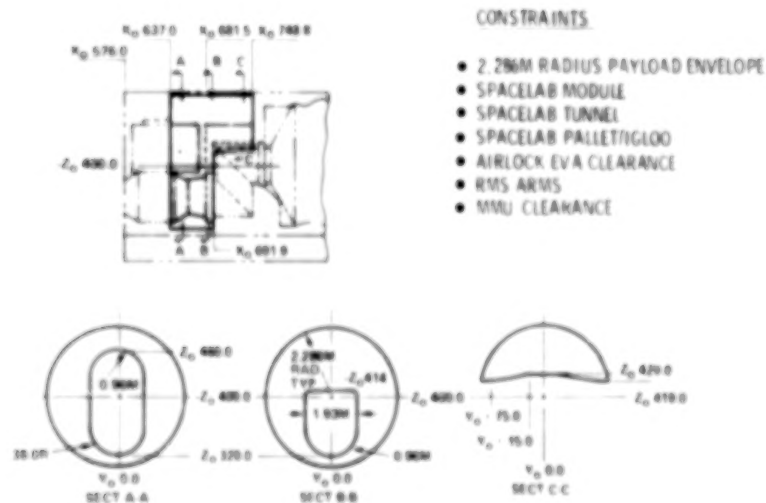


Figure 2

The forward constraint is determined by MMU clearance. The 2.3-m (90-in.) radius payload envelope, Spacelab module, Spacelab short tunnel, the air-lock and RMS installations also bound the volume available for the system installation.

The Berthing System, in contrast to a docking system, assumes that one side of the interface is attached to the Orbiter and the other side is under control and being positioned by the RMS. Because of the fluidity of platform design and wide variations in mass and MOI, the condition of two Orbiters berthed together was examined to establish load ranges. As illustrated by Figure 3, the interface moment produced from the RCS system would be 60 703 N-m (44 775 ft-lb).

The interface moment produced by berthing the two Orbiters, with an impact velocity of 0.03 m/sec (0.1 ft/sec) and a structural spring constant of 4.69×10^6 N-m/rad (3.46×10^6 ft-lb/rad), would be 20 972 N-m (15 469 ft-lb).

For the purposes of this study and preliminary design, an interface moment of 21 000 N-m (16 000 ft-lb) in pitch and yaw was selected.

The platform studies assume that during the period when the Orbiter and platform are berthed, the stabilization of the pair will be accomplished by the platform using CMGs. The control system frequency response dictates that structural natural frequencies should be above 0.1 Hz.

BERTHING SYSTEM LOADS

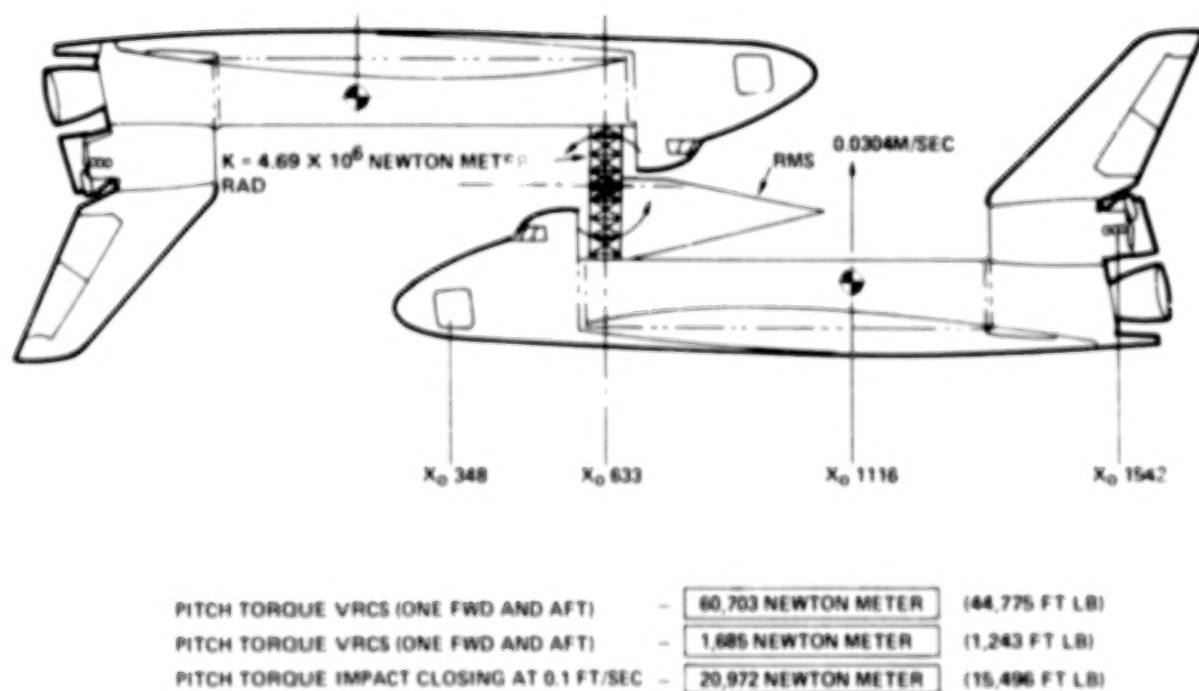


Figure 3

The plots in Figure 4 show that as the platform MOI increases the structural natural frequency becomes almost constant for a given spring rate. The structural stiffness for the berthing system was established at 5.4×10^6 N-m/rad (4×10^6 ft-lb/rad) which maintains the structural natural frequency above 0.1 Hz for any platform regardless of MOI. The MOI of 23.88×10^6 kg-m² (17.62×10^6 slug-ft²) represents two Orbiters berthed together.

Berthing Latch Interface Mechanism (BLIM)

Although the requirements for the BLIM were based on a berthing operation, i.e., RMS-controlled, the implementation of these requirements into a design concept did not lose sight of the potential of the BLIM being used for a docking interface.

Contact velocities and mismatch are based on RMS performance. The one-meter clear access requirement is derived from future potential use on habitability modules. The envelope for the passive half is established by the geometry of a standard pallet.

- Object - Capture and structurally attach together two bodies in space, one of which is being maneuvered by the RMS; the other is fixed to the Orbiter.
- Contact Velocities - Closing 0.03 m/sec (0.1 ft/sec) lateral and forward
1 deg/sec pitch, roll and yaw
- Mismatch - Lateral 10 cm (4 in.)
Angular pitch, roll and yaw 10 deg
- Clear Access - A clear access opening 1.0-meter in diameter shall be provided through the center of the berthing latch interface mechanism (BLIM).

STRUCTURAL NATURAL FREQUENCY VERSUS PLATFORM MOI

CENTERLINE DOCKING STA $X_0 = 633$

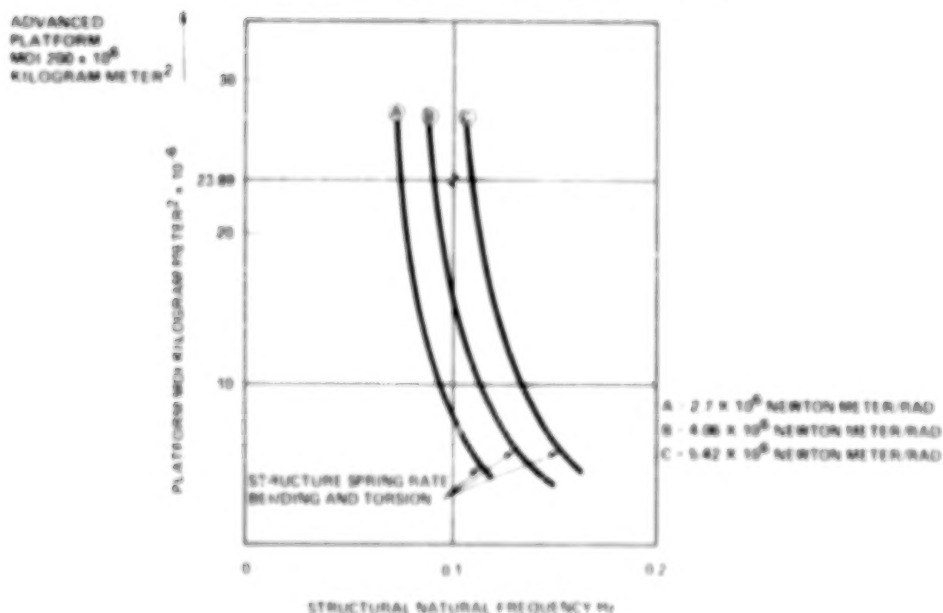


Figure 4

- Envelope - The envelope for the passive half and the active half of the BLIM will be defined separately. The physical size limits of the passive half are defined by the pallet cargo bay clearance.
- Loads - The BLIM shall be designed for a thrust load in both directions of 88 000 N (20 000 lb) and moments in pitch, roll and yaw of 21 000 N-m (16 000 ft-lb). These loads shall be applied both in the capture mode and the rigidized mode.
- Alignment - After mating and rigidizing any active and passive halves of the BLIM, the angular alignment in pitch, roll and yaw of one half relative to the other shall be within ± 1.32 arc min.
- Capture Latches - The capture latches shall be designed for simultaneous operation, i.e., a single capture latch of a multiple array of latches shall not provide a structural tie between the two halves of the BLIM until all latches are engaged.
- Umbilicals - The BLIM shall provide mounting provisions for fixed umbilical plates on the passive side of the mechanism and actuated plates on the active side of the mechanism.
- Mechanism Arrangement - The BLIM shall have one active side and one passive side. No electrical signal or power transfer will be required on the passive side of the interface to capture, rigidize or release the two sides.
- Androgynous - The design of the BLIM shall allow for the mating and structural attachment of any two active halves of a mechanism.

Six BLIM configurations were evaluated as illustrated by Figure 5. The evaluation also consisted of an evolutionary process in that Configuration 6 evolved from the initial selection of Configuration 4 and modifying it to reduce

BERTHING LATCH INTERFACE CONFIGURATIONS EVALUATED

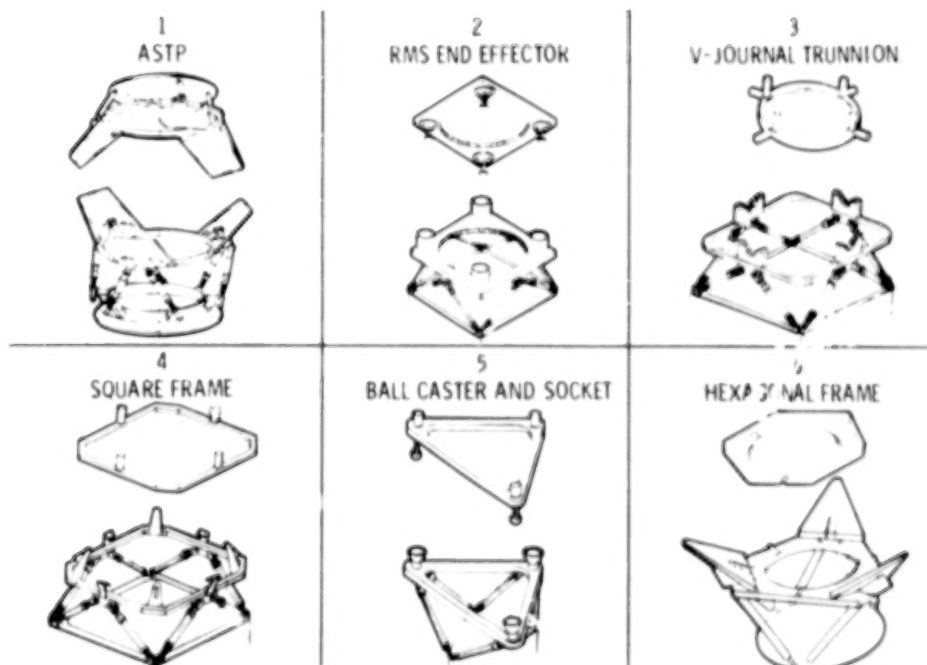


Figure 5

the inactive half. As a result of the evaluation, Configuration 6, the hexagonal frame was selected for design and model fabrication. This configuration is the only one of the six evaluated which will meet the envelope restriction imposed by its use on the bottom of a standard Spacelab pallet while maintaining the one-meter clear opening through the center of the mechanism.

Figure 6 illustrates the selected Berthing Latch Interface Mechanism. The passive half of the BLIM consists of a simple hexagonal frame with three alignment grooves in the face. The active side of the BLIM consists of a hexagonal frame with three alignment keys to match the grooves in the passive frame. On three sides triangular capture guides provide guidance for the passive frame to be nested with the active. Contoured within the capture guide is the capture and structure latch mechanism.

Solenoids in each latch are activated by proximity switches in the face of the active frame. The actuation of the solenoids release the capture/structural latches to contain and hold the passive frame. Dual motor actuators retract the latches to provide structural rigidity and alignment. The frames are structurally supported by six struts. These struts are rigid for berthing but can be exchanged for shock struts if energy attenuation is required. The shock struts would contain latches to rigidize them after capture.

HEXAGONAL FRAME — BERTHING LATCH INTERFACE MECHANISM (BLIM)

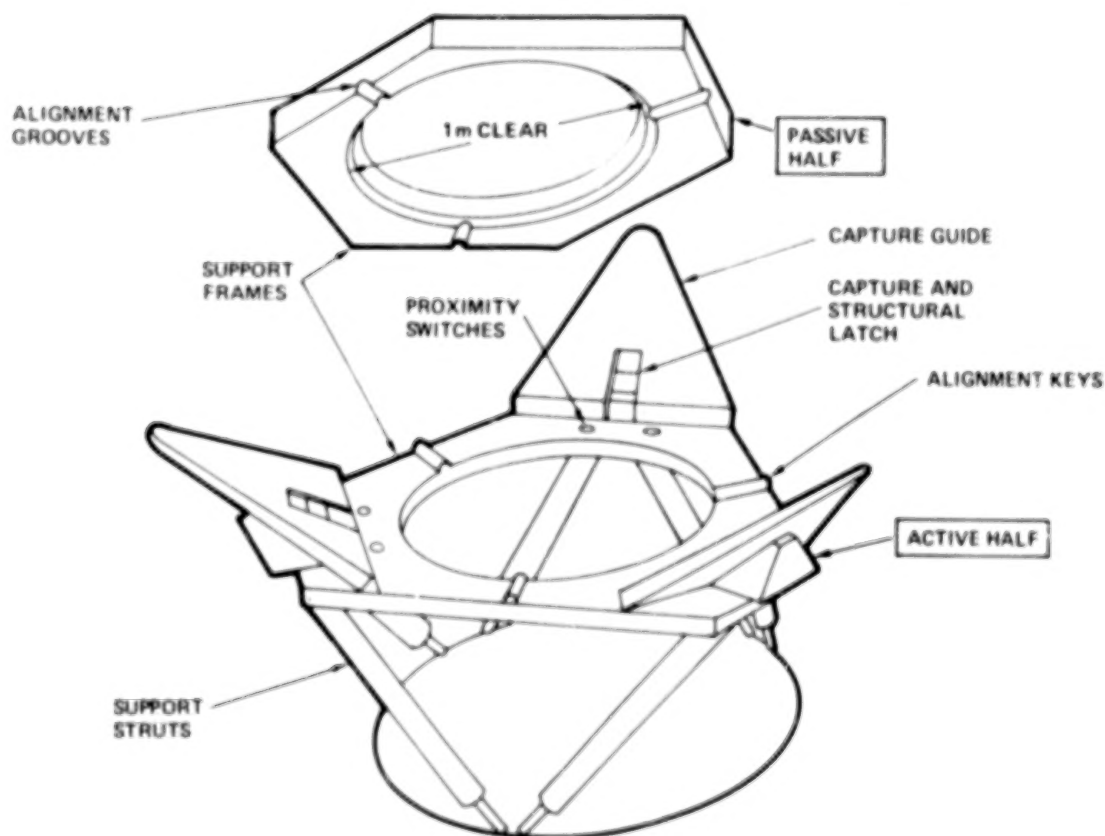


Figure 6

Figure 7 shows the capture latch mechanism in three states; ready, capture and structure latch. In the ready position the spring-loaded latch is retracted below the surface of the capture guide. When the passive frame activates three or more of the six proximity switches the frame is within the capture range of latches. The capture solenoids are actuated and the latches, driven by springs, move to the capture position. The latch drive actuators pull the latch drive link down and clamp the two frames together and engage the alignment keys. The drive actuators springs and solenoids are dual to provide operation after one failure. The mechanism may also be driven manually by rotating the eccentric with a crank.

Berthing Umbilical Interface

The Berthing Umbilical Interface requirements were derived based on power, data and coolant fluid transfer across the Orbiter interface with a 25 kW power module.

Umbilical Requirements

- Object - The umbilical shall provide the transfer of electrical power, data and coolant fluid across the mated active and passive halves of the Berthing Latch Interface Mechanism (BLIM).
- Stowage Volume - The active half of the umbilical shall be installed on the back face of the active side of the BLIM. The umbilical package when retracted shall not preclude the mechanical mating of two active halves of the BLIM and shall not protrude into the one meter diameter clear area of the BLIM.
- Engagement Rate - The active half of the umbilical shall travel from its stowed position to complete engagement with the passive half in no more than 20 seconds. The disengagement time shall not be greater than 20 seconds.

CAPTURE AND LATCH MECHANISM

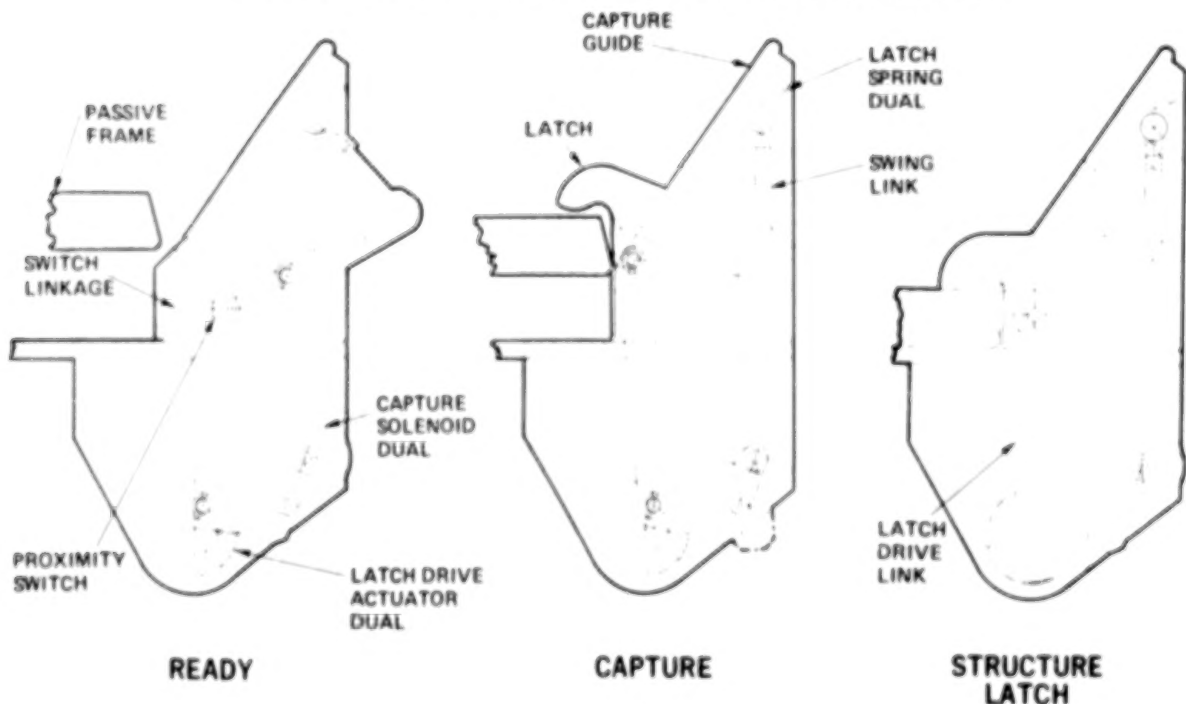


Figure 7

- Redundancy - All drive mechanisms shall incorporate redundant power sources arranged so that failure of one will allow operation of the other. Reduced performance in the single failure mode is acceptable.
- Manual Override - All drive mechanisms shall incorporate the ability to be operated manually by an EVA astronaut in the event of failure of both power sources.
- Position Indication - Instrumentation in the form of switch shall be provided to signal when the umbilical is fully engaged and fully stowed.
- Electrical Power Transfer - The umbilical system shall transfer electrical power at the berthing interface. The electrical power wiring will consist of three circuits each with the capacity for 8 kW at 28 to 33 VDC.
- Data Transfer - The umbilical system shall transfer data at the berthing interface. The data circuits shall consist of the following:
 1. Payload scientific data at rates to 5 MBPS
 2. Control and display functions (20 circuits)
 3. Caution and warning (two circuits)
 4. Bidirectional data bus (1.024 MHz)
 5. Hardware command circuit (1 KBPS)
 6. Telemetry (4 KBPS)
- Coolant Fluid Transfer - The umbilical system shall transfer coolant fluid at the berthing interface. Two coolant circuits (four lines) shall be provided. Each line shall be capable of flowing 2175 lb/hr of Freon 21 with a pressure drop of 5 psi maximum.
- Umbilical Controls - The engagement and retraction of the umbilical will be controlled from the RMS operator's station. The controls are to be located on the RMS display and control panel No. A8.

Figure 8 illustrates the arrangement of the umbilical panels on both the active and passive halves of the BLIM. The active half of the BLIM contains the

BERTHING UMBILICAL INTERFACE

Plan Views

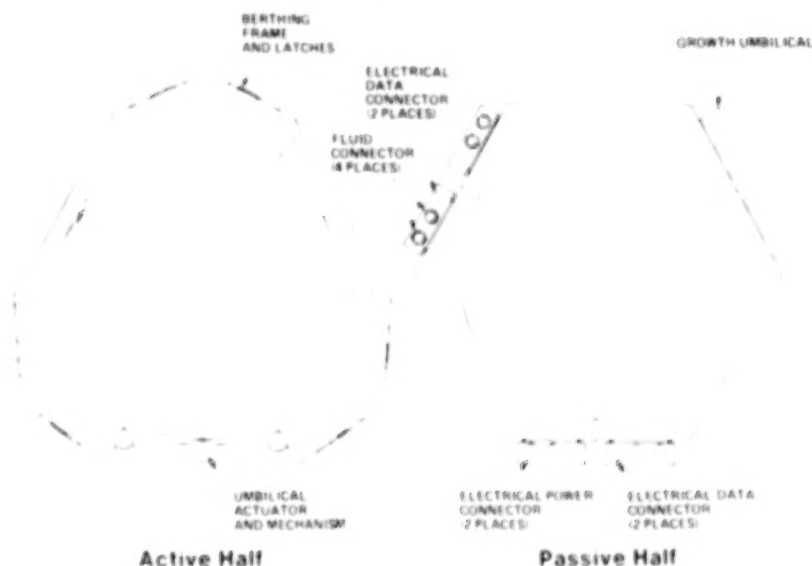


Figure 8

active half of the umbilical. The carrier plates are retracted behind the hexagonal frame until the two halves are structurally mated. After mating the umbilical actuator drives the carrier plates outboard and down to engage the fixed connectors of the passive half of the BLIM. The umbilical engagement sequence is shown in Figure 9.

Adaptive End Effector (AEE)

The requirements for the Adaptive End Effector were based on RMS capabilities and geometry and anticipated uses such as: handling structural elements for space construction; instrument/equipment exchange; stabilize spacecraft for EVA operations; vent cryogen tanks; contingency handling of payload pallets. Operator force feedback is incorporated to aid in the handling of fragile objects.

Adaptive End Effector Requirements

- Object - Provide an end effector for the RMS with the capability to grasp, hold and maneuver objects which are not equipped with a grapple fixture and have no preplanned interface for mating with the RMS.
- RMS Interface - The Adaptive End Effector (AEE) shall mate with the Special Purpose End Effector (SPEE) of the RMS.
- Grasp - The grasp of the AEE shall have the capability of holding cylindrical, spherical, flat and irregular shaped objects up to a dimension of 15 cm (6 in.). The fully open span of the grasping mechanism shall be 18 cm (7 in.) minimum.
- Visibility - The gripping mechanism of the AEE shall be within the field of view of the wrist CCTV camera and light mounted on the RMS.

BERTHING UMBILICAL INTERFACE ENGAGEMENT SEQUENCE

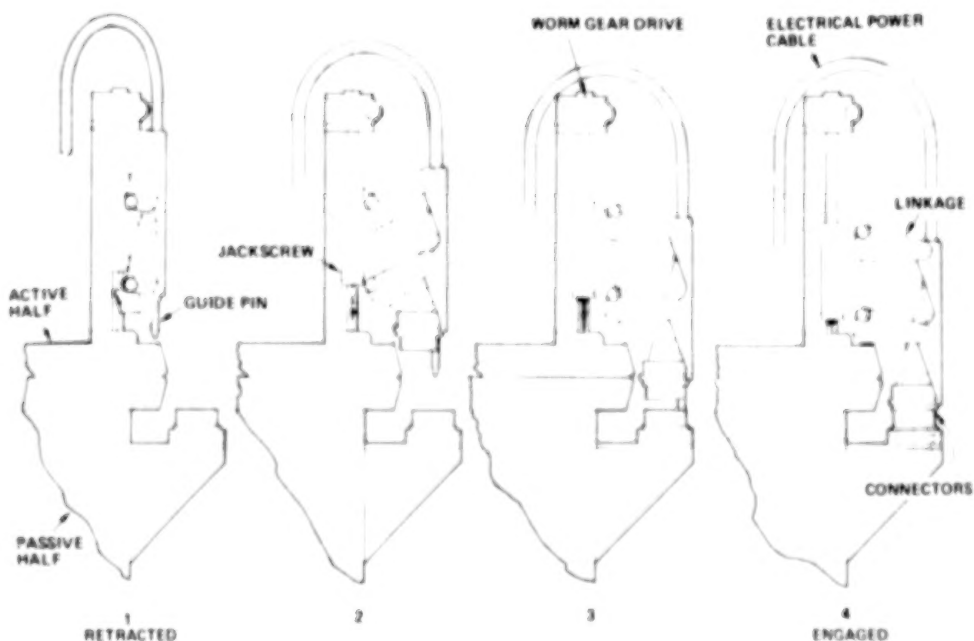


Figure 9

- Kinematics - Grasping mechanism jaws shall remain parallel during operation and not translate in the plane of the jaws during grasping or release operation.
- Jaw Compliance - The jaws of the grasping mechanism are to have a compliant surface. The coefficient of friction between the surface of the jaws and anodized aluminum shall be as high as possible but not less than 0.8.
- Power - The AEE shall be powered by 28-33 VDC electrical power. The limit on system wattage is to be determined.
- Stowage - The AEE shall be stowed in a container or rack within the Orbiter cargo bay and within the reach envelope of the RMS. The grapple fixture of the AEE shall be exposed to allow capture by the RMS SPEE. The AEE shall be secured to the stowage provisions to prevent disengagement during the launch and descent environments imposed by the Orbiter. The securing mechanism shall be operated by the drive system of the AEE jaws.
- Control - The grasping mechanism of the AEE shall be operated by a hand controller integrated with or in close proximity to the RMS controls. Displacement of the controller shall cause a proportional displacement of the grasping mechanism of the AEE. The grasping force encountered by the mechanism shall cause a proportional resisting force at the hand controller. A hand controller lock will be provided to allow the grip at the AEE to be maintained with hands off the controller.
- Grasping Force - The jaws of the AEE shall have sufficient force to impart a torque of 270 N-m (200 ft-lb) to an 8 cm (3-in.) diameter cylinder with a coefficient of friction between the jaws and cylinder of 0.8.
- Grasping Rate - The no load rate of the grasping mechanism shall provide for full open to close or close to full open time of 7 seconds maximum.

Figure 10 illustrates the arrangement of the RMS end effector, viewing light and TV camera. The Adaptive End Effector (AEE) will be offset from the RMS wrist centerline to provide visibility for the TV camera.

ADAPTIVE END EFFECTOR (AEE) GEOMETRY

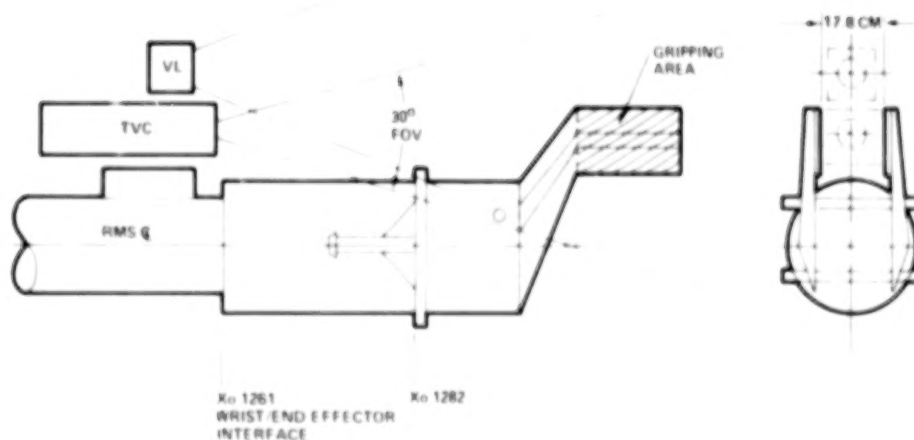


Figure 10

Figure 11 illustrates the AEE system consisting of an electrically driven jaw moving with respect to a fixed jaw. The jaws have elastic surface pads and the fixed jaw contains force sensors. A jaw position potentiometer tracks the moving jaw position.

The controller consists of a lever attached to a position command potentiometer and a torquer. Movement of the control lever causes a corresponding movement of the jaw. The gripping force encountered by the jaw produces a proportional force on the control lever allowing the operator to determine how tightly the object is being gripped.

ADAPTIVE END EFFECTOR SCHEMATIC

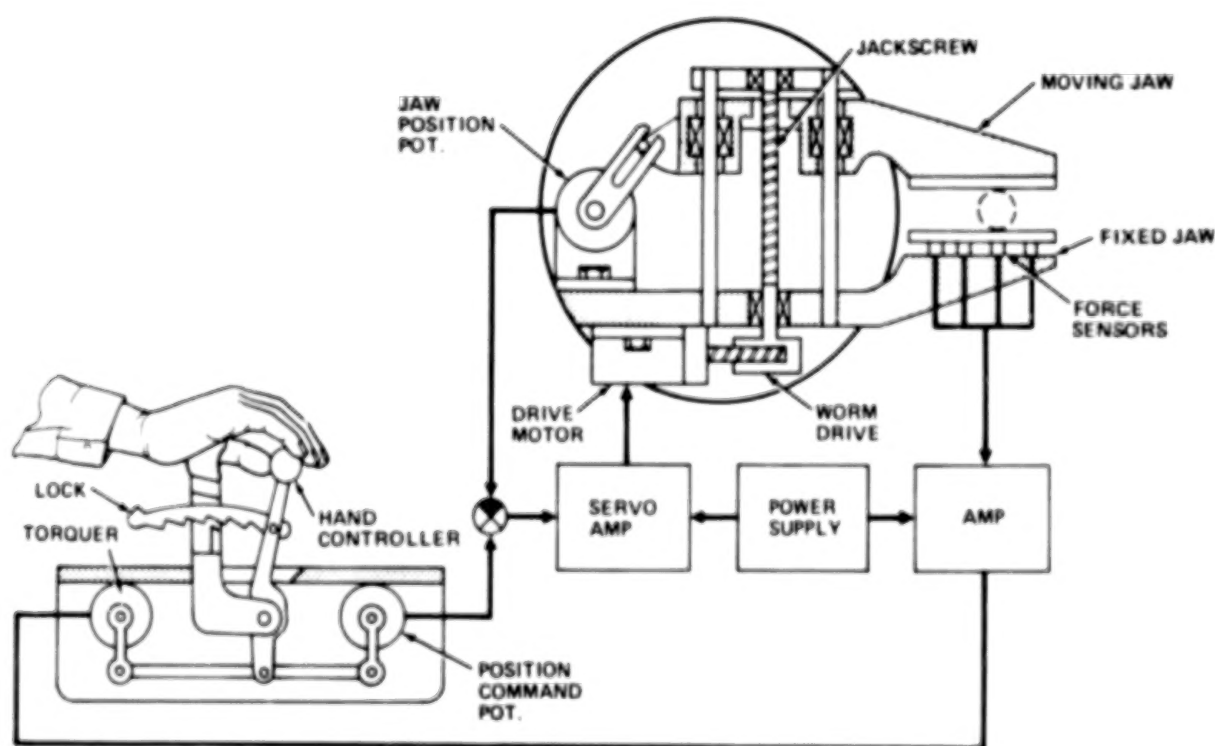


Figure 11

MODEL FABRICATION

The full scale working models of the Berthing Latch Interface mechanism, the Adaptive End Effector and the End Effector controller are currently being fabricated. The models will be complete in December of this year. Figures 12 and 13 illustrate the models being assembled during November 1980.

BERTHING LATCH INTERFACE MECHANISM

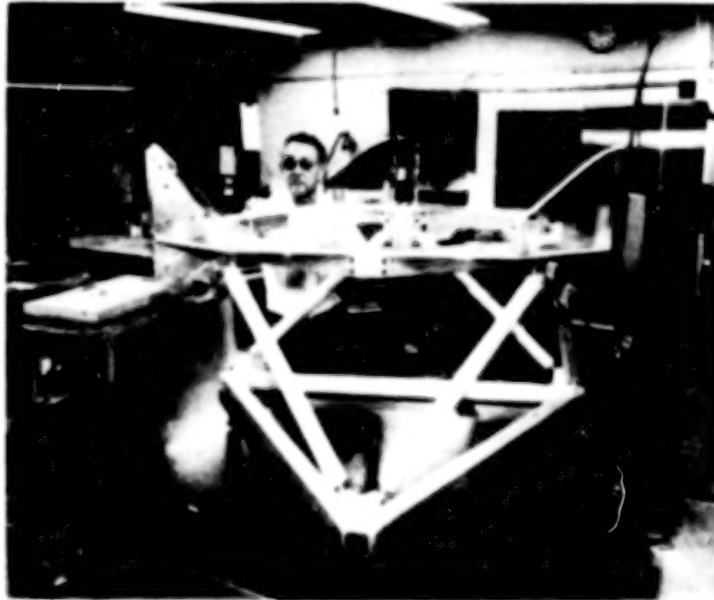


Figure 12

ADAPTIVE END EFFECTOR AND CONTROLLER

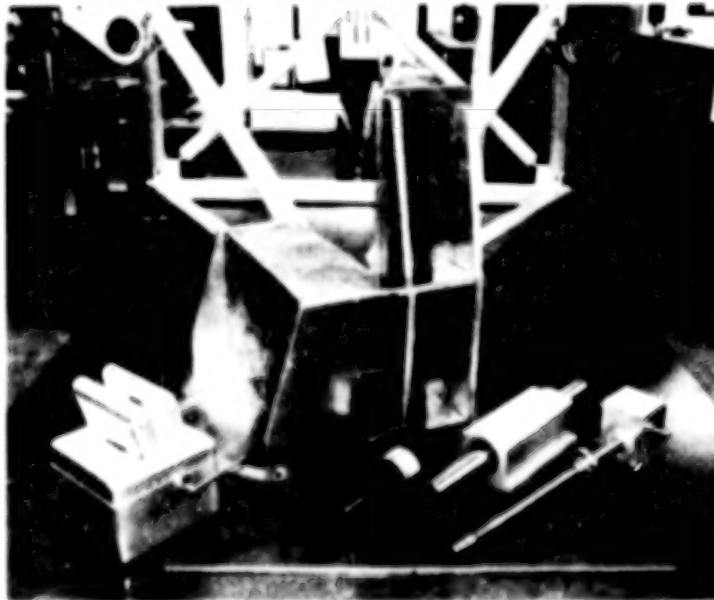


Figure 13

A DOCUMENT DESCRIBING SHUTTLE CONSIDERATIONS
FOR THE DESIGN OF LARGE SPACE STRUCTURES

John A. Roebuck, Jr.
Space Operations and
Satellite Systems Division
Rockwell International
Downey, California

Large Space Systems Technology - 1980
Second Annual Technical Review
November 18-20, 1980

INTRODUCTION

The purpose of this paper is to introduce and describe to potential users a new document, published in November 1980, as an aid to designers of large space systems. This paper begins with a discussion of some key concerns in preparation of the document and then outlines the scope of included subject matter, and explains key features of the document format. The remainder of this paper provides overviews and examples of the technical contents, approximately in their order of appearance in the document.

The contract for preparation of the document was administered under the technical direction of Mr. Lyle Jenkins, Spacecraft Systems Office, Spacecraft Design Division, Lyndon B. Johnson Space Center. It was a portion of the Space Construction System Analysis Study contract (NAS9-15718) performed by Rockwell International. Funding for the document preparation was provided through the office of the Large Space Systems Technology Program.

During the document preparation period, selection of material for inclusion was largely based on the author's recent experience in systems analyses of large space structures construction. In addition, material of special interest was included as a result of inquiries to other contractor personnel active in studies of large space systems. A preliminary draft of the document has been reviewed by NASA personnel at JSC, MSFC and Langley Research Center, and by payload integration personnel at Rockwell International. Their resulting comments are currently being incorporated.

INPUTS AND REVIEWER'S COMMENTS

Figure 1 briefly notes document material related to three major issues of concern to a sample of potential document users and reviewers of the draft document.

An example of one major technical concern was attitude control of the orbiter and its attached space construction project. In answer to this query, considerable space was devoted to the inclusion of data on reaction control systems and the digital autopilot. Also, some example study results were included describing results of analyses of gravity-gradient motions during a construction project.

Reviewers pointed out that timeliness is a serious concern as the Space Shuttle development is a dynamic program, undergoing frequent changes. Despite these problems, it was felt that the available information, as of the time of publication, is valuable as general background and as an indication of the kinds of information which should be considered in design. It was suggested that such a document should, like many other Shuttle-related documents, be periodically updated in order to be of maximum usefulness.

The level of detail included in the draft was also controversial. Some reviewers preferred very brief, "bare bones" lists of constraints and associated references. However, the author and several other reviewers felt more comfortable with added illustrative and narrative data, even though much of it is taken directly from orbiter specifications, user guides, and drawings.

ISSUES	DOCUMENT MATERIAL
<u>ATTITUDE CONTROL</u> <ul style="list-style-type: none"> * DOCKING/BERTHING (REVISIT) * ATTACHED TO STRUCTURE * FREE-DRIFT MODE * RUNAWAY JET 	<ul style="list-style-type: none"> * RCS & VRCS THRUSTERS LOCATION/ORIENTATION * DIGITAL AUTOPILOT DATA * EXAMPLE: EFFECTS OF ASSEMBLY MOTIONS IN GRAVITY-GRADIENT MODE * REFERENCES TO OTHER STUDIES
<u>UPDATING OF INFORMATION</u> <ul style="list-style-type: none"> * REFERENCES TO OLDER DOCUMENTS, SPECIFICATIONS, USER GUIDES * FUTURE TRENDS FOR SPACE STRUCTURE DESIGN 	<ul style="list-style-type: none"> * CAUTIONARY NOTES IN TEXT * POSSIBLE LATER UPDATES * EXAMPLES FROM STUDIES OF SPACE CONSTRUCTION
<u>LEVEL OF CONTENTS</u> <ul style="list-style-type: none"> * REFERENCES * DISCUSSION—NARRATIVE/ART FROM EXISTING SPECIFICATIONS/GUIDES * STUDY RESULTS, EXAMPLES * TECHNICAL VS. ADMINISTRATIVE AND PROCEDURAL 	<ul style="list-style-type: none"> * CONTAINS BROAD SPECTRUM OF NARRATIVE, GRAPHICS, CHECK LISTS, REFERENCES * OMITS DATA IRRELEVANT TO DESIGN OF SPACE STRUCTURES AND ORBITER DELIVERY IMPACTS * EMPHASIZES TECHNICAL INFORMATION

Figure 1

SCOPE

This paper briefly describes the purpose, format, and scope of a recently prepared document entitled "Shuttle Considerations for the Design of Large Space Structures" (ref. 1). This document was prepared under NASA Contract NAS9-15718, Amendment/Mod 4S, as an aid for preliminary designers and managers of Phase A and early Phase B studies involved with use of the Space Shuttle orbiter. It describes what can and cannot be done with the orbiter as regards construction of the class of large space systems depending upon direct use of the orbiter for assembly, construction, and servicing. In contrast to design specifications and currently available user guides emphasizing sortie modes and small satellite handling (for example, "Space Shuttle System Payload Accommodations", "Space Transportation System User Handbook", and "Shuttle EVA Description and Design Criteria"), this document includes considerations of future and long-term uses related to space construction. In creating this document, the general approach was to selectively compile information on orbiter interfaces and impacts — not to create new engineering data.

The document contents are divided into six major sections plus appendixes as shown in Figure 2. Four of the sections are related to orbiter operations regimes. Section 1.0 introduces the format, subject matter, and organization. It relates the reader's interest in design considerations for large space structures to applicable general capabilities, constraints, and guidelines inherent in the Space Shuttle orbiter.

<u>SECTION NO.</u>	<u>TITLE</u>	<u>MAJOR CONTENTS</u>	<u>NO. OF PAGES</u>
1.0	INTRODUCTION—SCOPE	<ul style="list-style-type: none"> • DOCUMENT ORGANIZATION • CONSTRUCTION INTERFACE ISSUES • SHUTTLE ACCOMMODATIONS • PAYLOAD INTEGRATION 	22
2.0	SHUTTLE FLIGHT CONSTRAINTS ON LARGE SPACE STRUCTURES DESIGN	<ul style="list-style-type: none"> • ORBIT DECAY • ASCENT • DESCENT 	34
3.0	PACKAGING CONSTRUCTION EQUIPMENT & MATERIALS FOR SHUTTLE DELIVERY	<ul style="list-style-type: none"> • VOLUME AVAILABLE • INTERFACES TO ORBITER 	94
4.0	DESIGNING FOR SHUTTLE ORBIT OPERATIONS CAPABILITIES	<ul style="list-style-type: none"> • DOCKING/BERTHING • ATTITUDE CONTROL • PAYLOAD HANDLING (CONSTRUCTION) • EQUIPMENT CHARACTERISTICS • EVA OPERATIONS • TV & ILLUMINATION • SYSTEMS INTERFACES 	232
5.0	CREW PRODUCTIVITY AND SAFETY CONSIDERATIONS	<ul style="list-style-type: none"> • CABIN ACCOMMODATIONS • WORK-REST CYCLES • HOUSEKEEPING REQUIREMENTS 	14
6.0	SPACE SHUTTLE GROUND OPERATIONS	<ul style="list-style-type: none"> • KSC GROUND OPERATIONS FLOW • GROUND TURNAROUND OPERATIONS • VAFB SUPPORT SYSTEM 	6
APPENDIX A.	ACRONYMS		3
B.	GLOSSARY		7
C.	BIBLIOGRAPHY		6
ALPHABETICAL	SUBJECT INDEX		8
TOTAL PAGES			385

Figure 2

FORMAT

The document is prepared in the form of a manual with explanatory text, tables, graphs, and illustrations as appears appropriate to explain Shuttle hardware and geometry features. A balance in content was sought between simply listing data sources and providing a full set of instructive information for readers unfamiliar with the orbiter.

A key feature of the document format is the use of checklists such as shown in Figure 3. These checklists provide a systematic means to present baseline, factual constraints and capabilities, as well as suggested guidelines and occasional speculations which may be of concern to space construction. Each major statement in the checklists is supported by a reference (denoted by author and year) which qualifies the source of information and which provides opportunity to seek further data. Specific exceptions and qualifications are listed below each statement. Such qualifications may also call out explanatory art work or tabulated data which follow the appropriate checklist or are included in other text material. Where judged appropriate, potential impacts to design of large space structures are briefly suggested in the column at the right.

A rating figure appears in parentheses at the end of each statement. The purpose of this number is to indicate the relative validity of the statement in terms of whether implementing hardware or procedures are actually available or are under development (R-1), or only in a planning (R-2) or study (R-3) or conceptual stage (R-4 or R-5).

Table 4.4-5. Checklist: Detail Constraints on Support Attachments, Payload Deployment Clearances and Equipment Configurations for Shuttle Operations

(CONSTRAINTS - Qualifications)	REFERENCES (IMPLICATIONS)	SOURCE REFERENCE
<p>1. Clearance shall be provided for deployment and operation of the Ku-Band antenna(s). (R-1)</p> <p>Normal installation is right hand starboard side, mount centerline on station 589.</p> <p>Port side installation is (TRD).</p> <p>See Section 4.11.4.</p> <p>See Figure 4.4-5 for deployment envelope.</p> <p>See Section 4.4.2.1 for clearance envelope details.</p>	<p>Ruckwell 1978 (a): RC 409-0025</p> <p>Location forward of radiators ardon poses configuration constraints, but analysis is required.</p>	<p>BRIEF COMMENT ON IMPLICATIONS TO SPACE CONSTRUCTION</p>
<p>2. Clearance shall be provided for deployment and operation of the Remote Manipulator System (RMS) arm when the latter is extended.</p> <p>RMS should be located as far forward outboard as possible to provide added clearance for large payload extraction and -up while in orbit.</p> <p>See Section 4.5 for RMS details.</p>	<p>NASA 1980 (a): JSC-07700, Vol. 80V LICD 2-190011</p> <p>Affects design of assembly fixtures attached to improms.</p>	<p>AVAILABILITY RATING OR FIRMNESS OF REQUIREMENT</p>

Figure 3

OVERVIEW OF SHUTTLE PAYLOAD ACCOMMODATIONS/CONSTRAINTS

Section 1.0 includes an overview of payload accommodations, an introduction to the general subject of Shuttle payload accommodations in terms of orbiter services, as indicated in Figure 4.

The "good news" is that the extent and range of services represent a truly remarkable technology advancement. The obverse is that the potential number and complexity of interfaces with the orbiter are also significant. Such information is not readily learned from available user guides and documents dealing mainly with sortie missions and small satellite delivery and retrieval operations. Therefore, this document emphasizes information specific to large space construction. In general, it is usually advisable to reduce the connections and interfaces for orbiter services to a minimum, in order to save costs of payload integration. However, a particular space construction project may involve a unique and extensive combination of these accommodations and constraints. Space construction may use the orbiter as a truck, an office, a construction control base, a crane, a housing and food service facility, a communications facility, and a power generation unit.

Section 2.0 describes some significant issues of flight mode concerns which affect mission planning and the orbiter height and inclination selected for space construction. These include ascent and descent times, orbit decay considerations, ionizing radiation in the orbital environment, and orbiter thermal conditioning concerns prior to descent.



Figure 4

PACKAGING FOR DELIVERY

Section 3.0 deals with the highly important problem of efficient and safe packaging for delivery. Building large structures in space is similar in some respects to the old trick of building a model ship in a large bottle with a small neck. All the materials must pass through the neck of the bottle, which is somewhat analogous for the Space Shuttle set of constraints—particularly the cargo bay. In addition to restrictions on physical sizes of payloads, there are limitations on reach of the RMS, on power, on energy, on crew habitation volume, and on many other Shuttle system parameters which affect the size and configuration of structures built out of the orbiter.

Figure 5 provides a visual reminder of a few major considerations for packaging payloads in the orbiter payload bay. Some will be limited by total volume, while others will be limited by weight. All must be arranged so the center of gravity of the load is within certain geometrical constraints. Also, package designs must consider a finite set of location points for attachments to the orbiter structure.

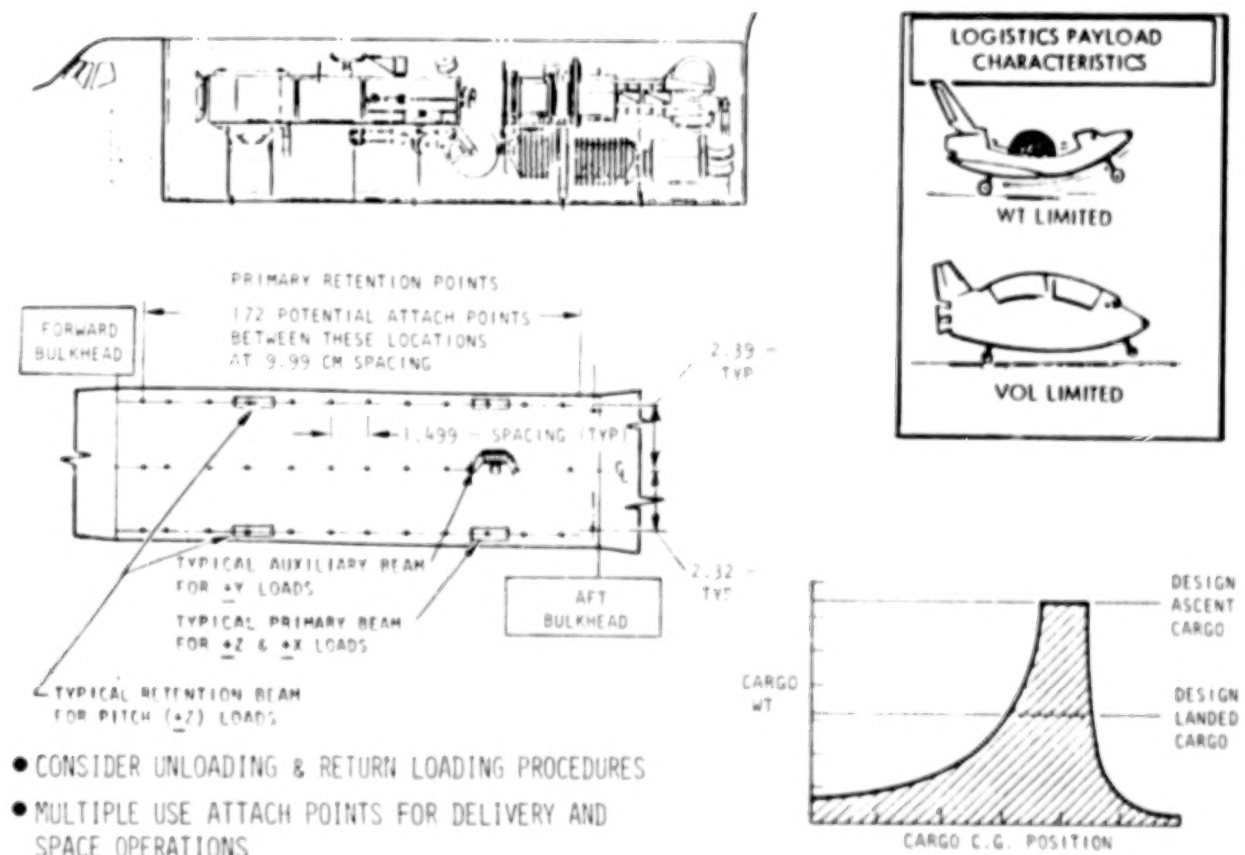


Figure 5

POTENTIAL INTRUSIONS INTO PAYLOAD VOLUME

There is a small number of potential intrusions into the nominal 4.57 km (15 ft) diameter by 18.29 km (60 ft) long cargo volume in the payload bay, according to special payload requirements. These intrusions are indicated in Figure 6. The major concerns are the orbital maneuvering system (OMS) fuel supply kits and the considerations for contingency EVA. All others are relatively small intrusions into the nominal clearance space or dedicated volume for payloads.

- DELIVERY/RETURN PHASE

- ON-ORBIT OPERATIONS

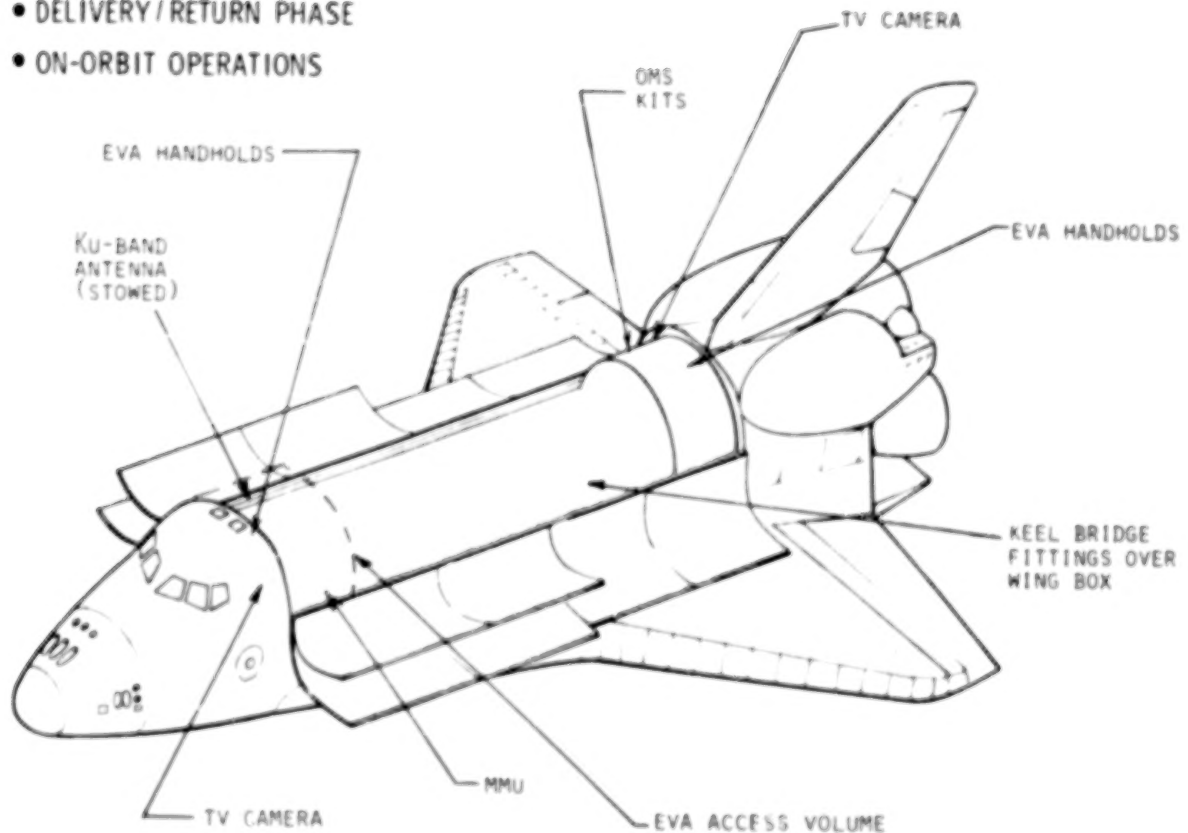


Figure 6

CONNECTIONS FOR ORBITER SERVICES/CONSTRUCTION FIXTURES

If orbiter services are used, such as electrical power or signal/control lines to the crew cabin, there are recommended locations for connections to the orbiter systems such as indicated in Figure 7.

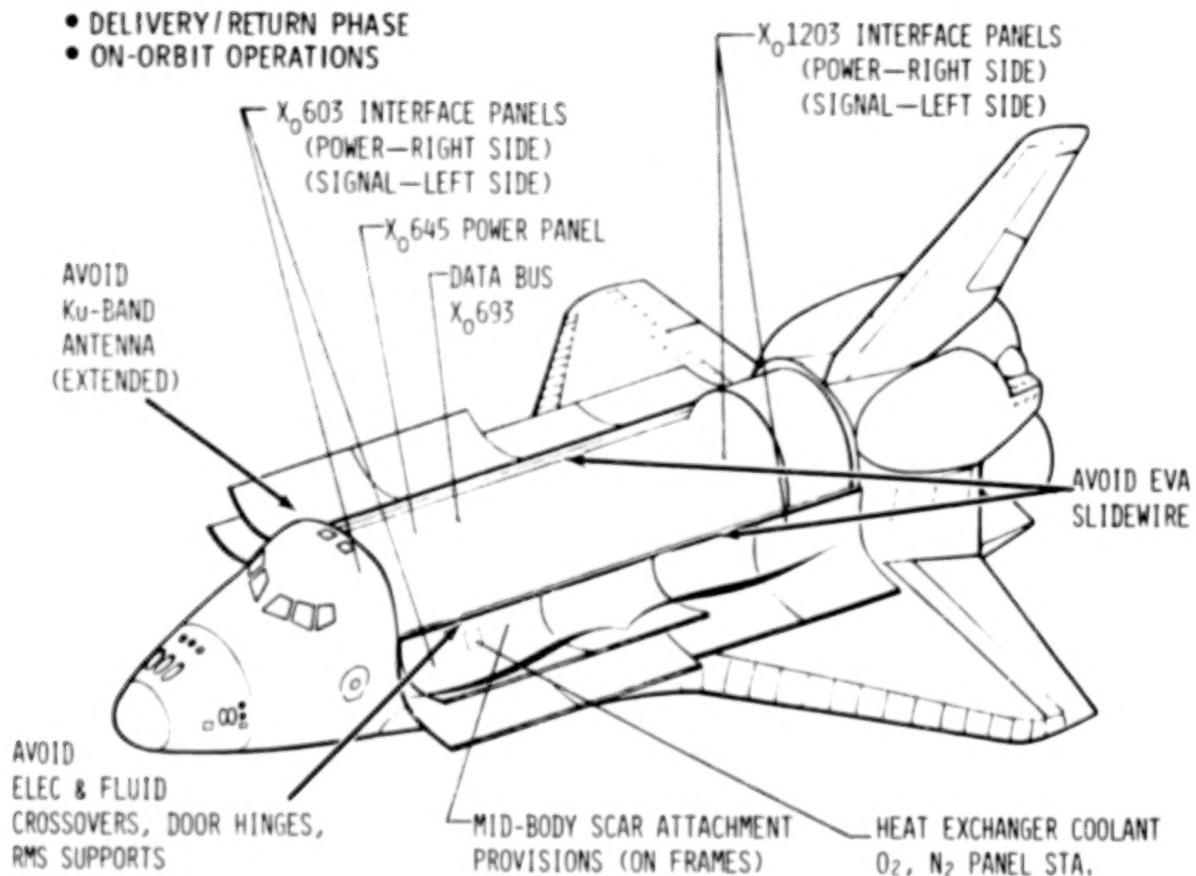


Figure 7

CONSTRUCTION SPACE GEOMETRY

Section 4.0, which is the largest, deals with the majority of on-orbit interface concerns. Obvious examples include such geometric constraints as illustrated in Figure 8: configuration, visual fields for the crew, standard TV cameras, and star trackers. Section 4.0 also describes considerations of docking or berthing, plume impingement, attitude control of combined orbiter and construction project, payload handling, power and energy availability, and extravehicular operations. In addition, Section 4.0 contains material on communications, thermal environment, and various orbiter subsystems which may be involved in construction or maintenance/checkout operations.

- ORBITER CONFIGURATION
- EVA ACCESS SPACE
- RMS REACH CLEARANCE
- VISION FIELDS OF VIEW
 - WINDOWS, TV CAMERAS
 - STAR TRACKERS
- SUPPORT EQUIPMENT OBSTRUCTIONS
- EQUIPMENT ATTACH POINTS ON ORBITER
- PALLETS, CRADLES, OMS KITS, DOCKING MODULES, ETC.

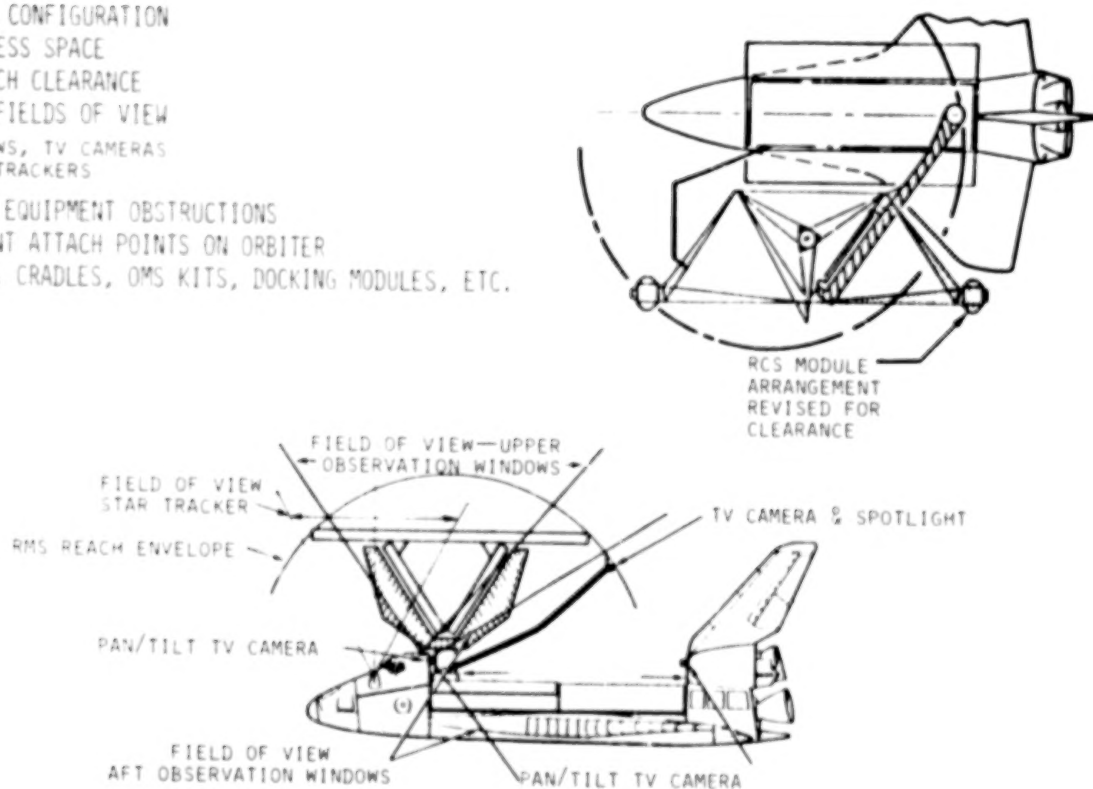


Figure 8

THERMAL CONSIDERATIONS

Figure 9 presents an example of a thermal issue of particular concern to space construction. The issue is the potential for solar ray concentration by the orbiter payload bay doors. In general, a structure should not be located where it is exposed to solar heat concentration input above the doors, or else the attitude of the orbiter needs to be controlled to avoid such solar reflections. Also included in Section 4.0 are considerations of reduced orbiter heat rejection capability due to large surfaces (e.g., solar arrays) located above the payload bay doors. These data are presented in parametric graphical form for convenience of use.

SOLAR REFLECTIVITY

• SUNLIGHT CONCENTRATION BY PAYLOAD BAY DOORS

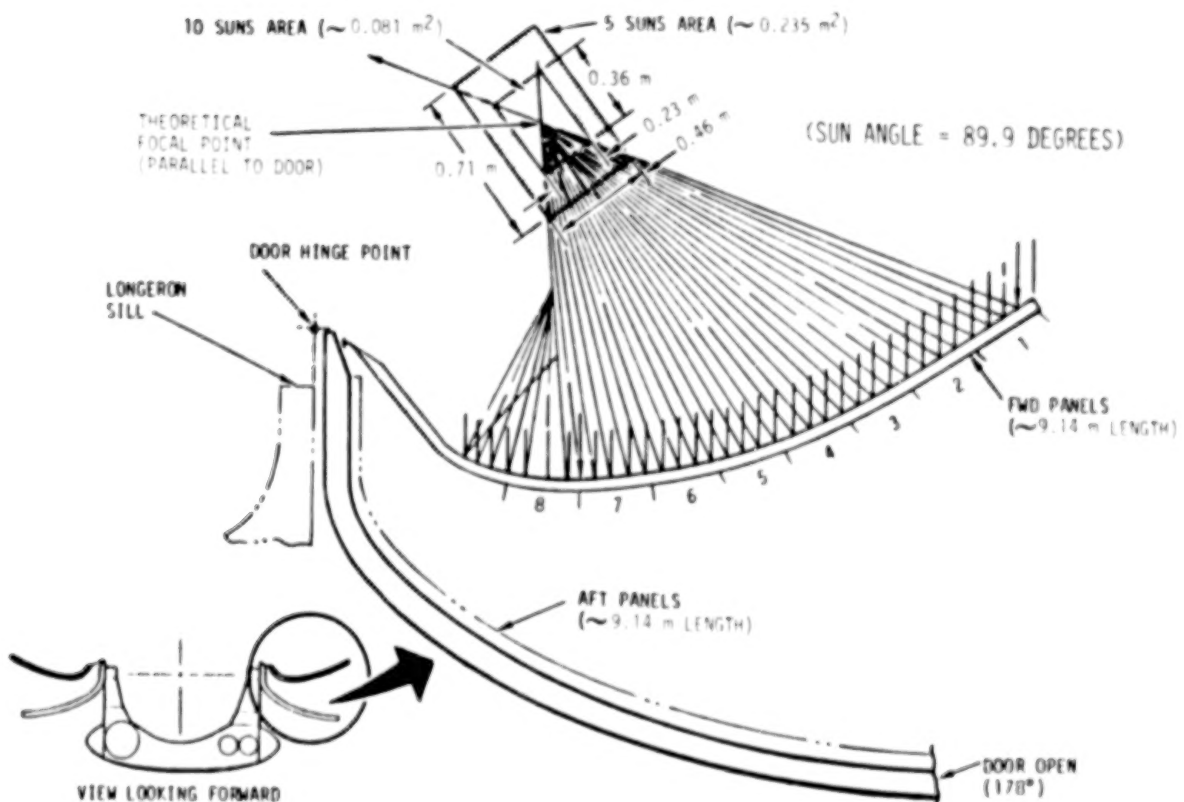


Figure 9

CREW STATION CONSIDERATIONS

Section 5.0 is dedicated to description of crew considerations, which are of continuous concern from the time of crew ingress prior to launch until post-landing egress. Included in this section are work-rest cycle data, work and habitation space and arrangements data, and orbiter housekeeping requirements. Selected concerns of crew operations are highlighted in Figure 10. Included are the limited space available on the flight deck for simultaneous activity by the payload handler and payload specialist, the limited sleeping space, limited stowage space, and special time requirements for donning and doffing EVA gear. While detail requirements cannot be foreseen for particular missions, it is pointed out that crew stowage space and habitation space could easily become a constraint on extended construction schedules.

- WORKSPACE FOR PAYLOAD HANDLER VS. PAYLOAD SPECIALIST
- CREW VISIBILITY, CONTROLS, & DISPLAYS ACCESS
- CREW SKILLS MIX
- HOUSEKEEPING SCHEDULE

- MULTI-SHIFT OPERATIONS
 - LIGHT, SOUND, DISTURBANCE OF SLEEP
 - CREW SIZE VS. SLEEP STATION
 - WORK-REST CYCLES
- STOWAGE VOLUME
 - EXTRA PRESSURE SUITS & EVA EQUIP.
- AIRLOCK OPERATIONS

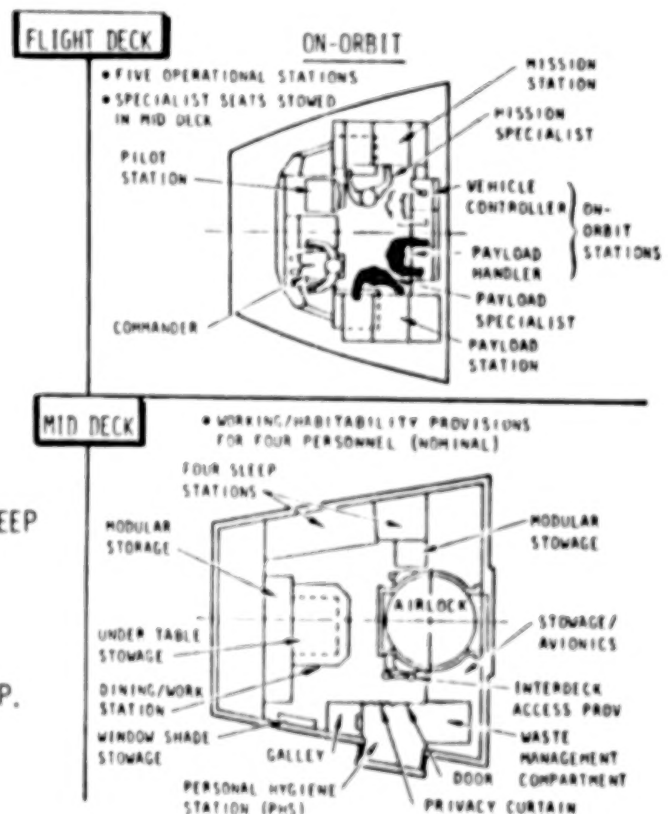


Figure 10

GROUND OPERATIONS

The last section of the document (Section 6.0) presents a brief description of ground turnaround operations considerations at KSC and Vandenberg Air Force Base. Detail constraints on loading the orbiter were not included in Section 6.0, even though they are indeed related to ground turnaround operations. Rather, they are included in Section 3.7 because of their close relationship to the other details of physical geometry constraints of the orbiter cargo bay. Figure 11 is an example of particular interest. The payload ground handling mechanism (PCHM) equipment design constrains the distances between trunnions on adjacent individual payload items. When many separate items are stowed in the payload bay, this constraint may be a driving factor in design of cradles or pallets.

- GROUND TURNAROUND PROCESS BRIEFLY DESCRIBED IN SECTION 6.0
 - KSC
 - VAFB
- DETAILS AFFECTING PACKAGING AND LOADING APPEAR IN SECTION 3.7 (REFERENCED IN SECTION 6.0)

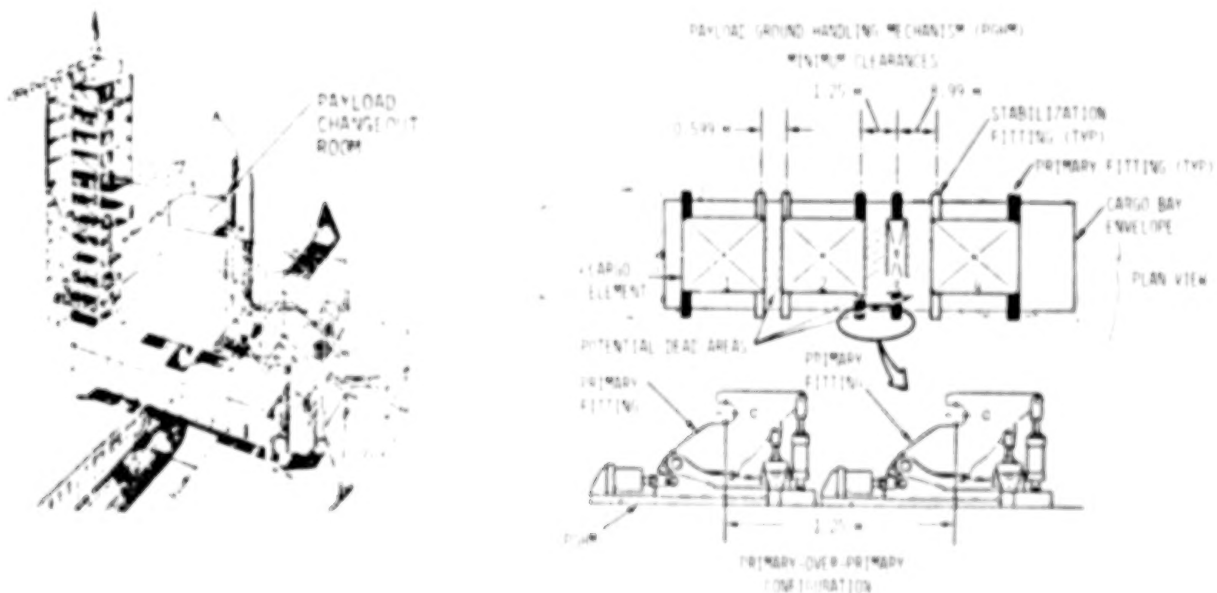


Figure 11

SUMMARY
(Figure 12)

A Shuttle user guide document has been prepared to aid designers and analysts associated with large space structures projects. Reviewer comments to date indicate the document satisfies the desired objectives and that it will be useful.

The format and contents are a compromise designed to satisfy the needs of several levels of users. Special features include checklists and references to source documents as a convenience to very knowledgeable readers. In addition, general, introductory and explanatory text, and art work are included for the reader less familiar with Shuttle systems. Also, there are a subject index, glossary, list of acronyms, and many cross-references. Throughout the document, there are suggested implications or references to the importance of the included orbiter interfaces material as it pertains to designing and planning large space structures projects.

It has been noted that such a document is inherently subject to obsolescence over a period of time, as underlying source documents change and technology advances. Therefore, it is recommended that this document be periodically updated to incorporate such changes.

- DOCUMENT PROVIDES INTRODUCTION AND CONVENIENT ACCESS TO CURRENT DATA ON SHUTTLE CONSIDERATIONS INFLUENCING DESIGN OF LARGE SPACE STRUCTURES
 - CURRENT SPECIFICATIONS & USER GUIDES FOR STS
 - CURRENT DESIGN THINKING ON ORBITER
 - EXAMPLE ANALYSES AFFECTING SPACE CONSTRUCTION
- FORMAT & CONTENTS ARE COMPROMISE FOR SEVERAL LEVELS OF USER
 - CHECKLISTS & REFERENCES
 - NARRATIVE & ART
 - INDEXES, CROSS REFERENCES, GLOSSARY, ACRONYMS
- PERIODIC REVISIONS RECOMMENDED
 - UPDATE TO AGREE WITH SPEC CHANGES
 - INCORPORATE LATER STUDY RESULTS OF LARGE SPACE STRUCTURES STUDIES

Figure 12

SYMBOLS AND ABBREVIATIONS

C.G.	Center of Gravity
CM	Centimeters
ECLS	Environmental Control/Life Support
EVA	Extravehicular Activity
FSS	Flight Support System
GN&C	Guidance, Navigation and Control
GO ₂	Gaseous Oxygen
HPA	Holding-Positioning Aid
H ₂ O	Water
JSC	Lyndon B. Johnson Space Center
KSC	John F. Kennedy Space Center
Km	Kilometers
LEO	Low Earth Orbit
LSS	Large Space Structures/Systems
m	Meters (Unit of Length)
MMU	Manned Maneuvering Unit
NASA	National Aeronautics and Space Administration
OCP	Open Cherry Picker
OMS	Orbital Maneuvering System
O ₂	Oxygen
PGHM	Payload Ground Handling Mechanism
PIDA	Payload Installation and Deployment Aid
PRCS	Primary Reaction Control System
RCS	Reaction Control System
RMS	Remote Manipulator System
SMCH	Standard Mixed Cargo Harness
STS	Space Transportation System
TV	Television
VAFB	Vandenberg Air Force Base
VRCS	Vernier Reaction Control System
Δ (Delta)	Additional (Supplies, equipment, capacity)

REFERENCE

1. Roebuck, J.A., Jr.; Shuttle Considerations for the Design of Large Space Structures. NASA Contractor Report 160861, prepared by Rockwell International, Space Operations and Satellite Systems Division, Downey, CA 90241, November 1980.

ELECTROSTATIC MEMBRANE ANTENNA
CONCEPT STUDIES

J. W. Goslee
NASA Langley Research Center
Hampton, Virginia

Large Space Systems Technology - 1980
Second Annual Technical Review
November 18-20, 1980

4.88-m (16-Foot) Diameter Test Fixture

A 4.88-m (16-foot) diameter test fixture has been fabricated for testing electrostatically formed membranes. The fixture was designed to permit adjustment of the membrane tension and also adjustment of the back electrode position. The electrode configuration was made of concentric circles, each of which was powered by a separate power supply. Figure 1 shows the electrostatic concept where the electrostatic force applied varies with the distance of the membrane from the back electrode. Figure 2 shows the five concentric electrode rings, each ring being connected to a separate power supply.

SCHEMATIC OF 4.88-m (16-foot) $f_N = 3.5$ ELECTROSTATIC
MEMBRANE REFLECTOR

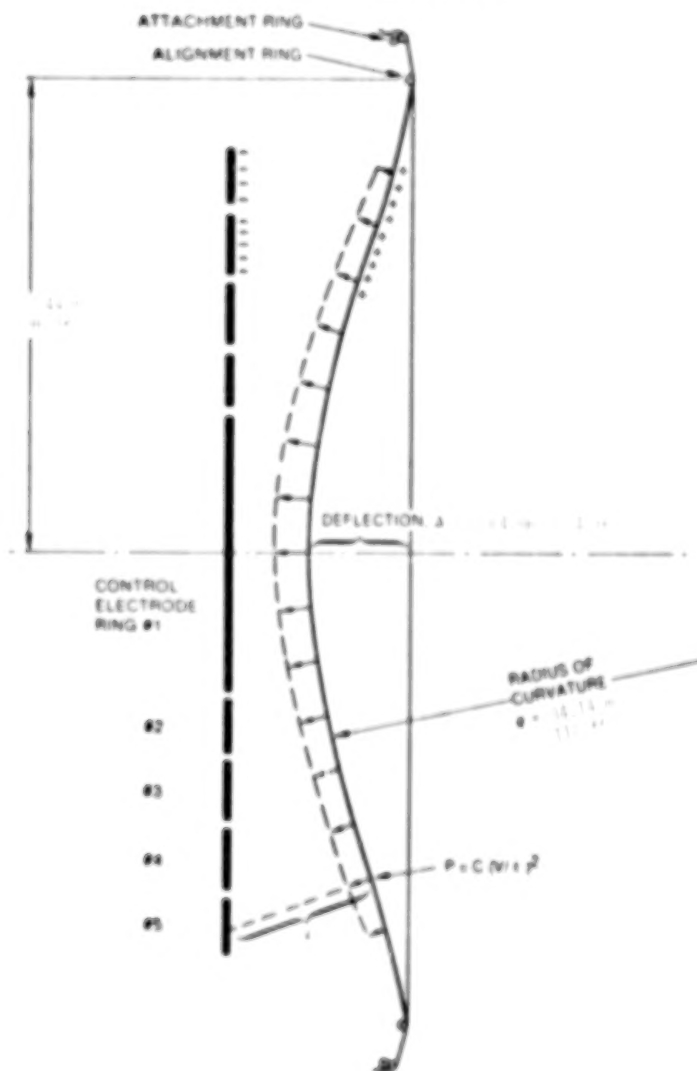


Figure 1

4.88-m (16-foot) DIAMETER TEST FIXTURE BACK ELECTRODE CONFIGURATION

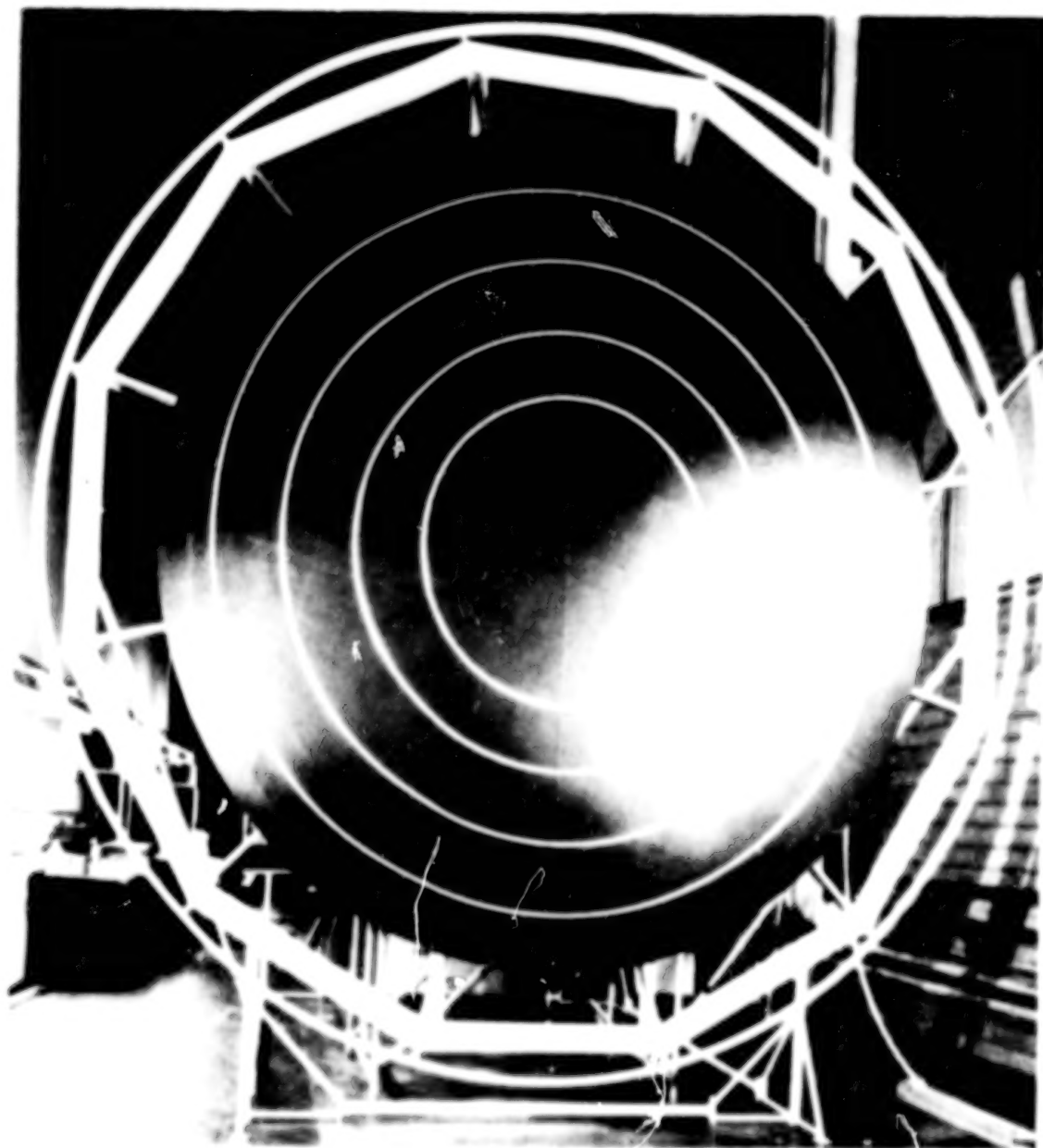


Figure 2

INSTALLATION OF 0.3 MIL ALUMINIZED KAPTON

Problems have been encountered in fabricating 4.88-m (16-foot) diameter thin film membranes. We have been using commercially available 0.5 mil Mylar and 0.3 mil Kapton as initial material candidates. We have been seeing both wrinkles at the seams of the panels as well as wrinkles or surface imperfections on the individual panels. With the types of wrinkles being seen, the electrostatic force is not strong enough to pull all of them out. A typical 0.3 mil Kapton membrane installed on the ring is shown both with and without the electrostatic force being applied (figs. 3 and 4).

0.3 mil KAPTON WITH ELECTROSTATIC FORCE APPLIED

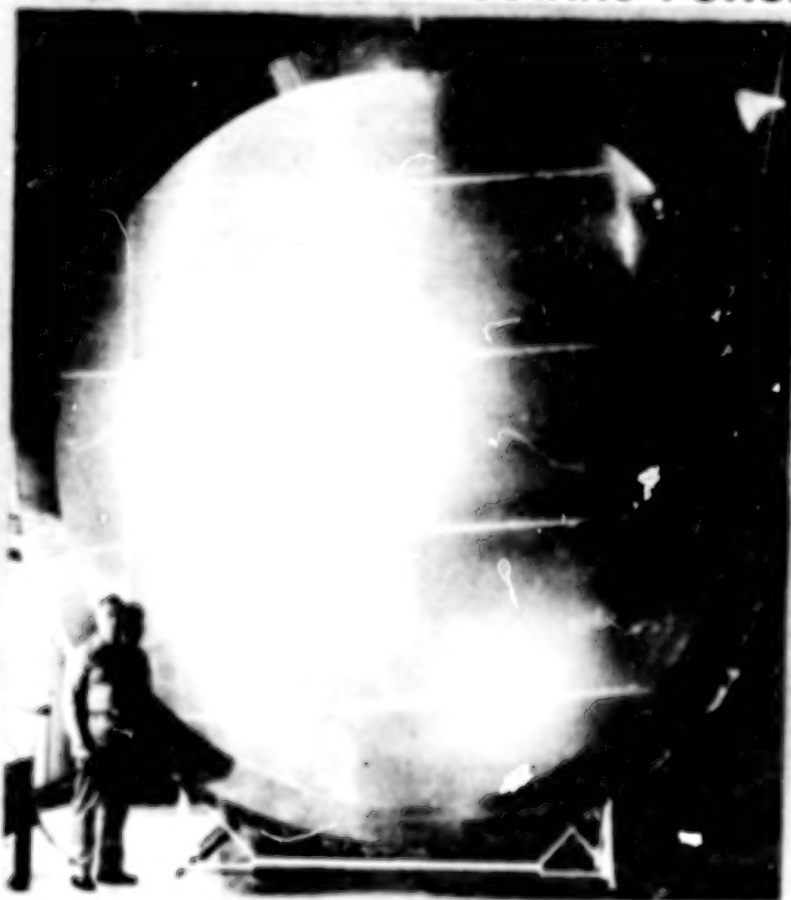


Figure 3

**0.3 mil KAPTON INITIAL INSTALLATION
WITHOUT ELECTROSTATIC FORCE**

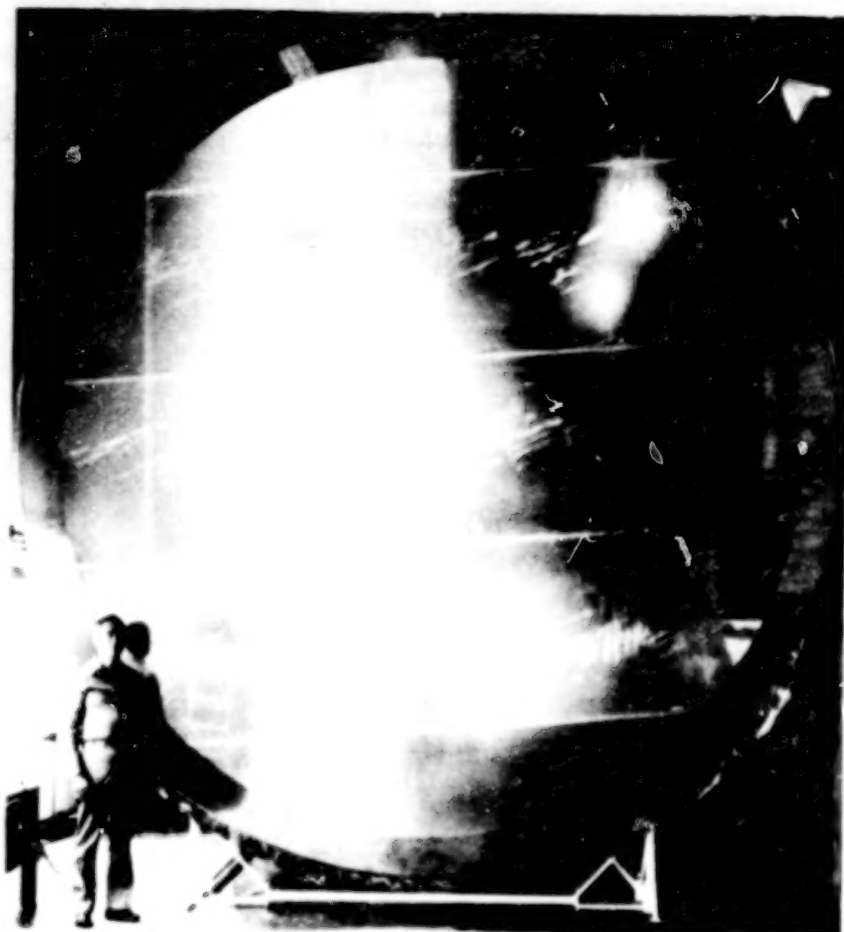
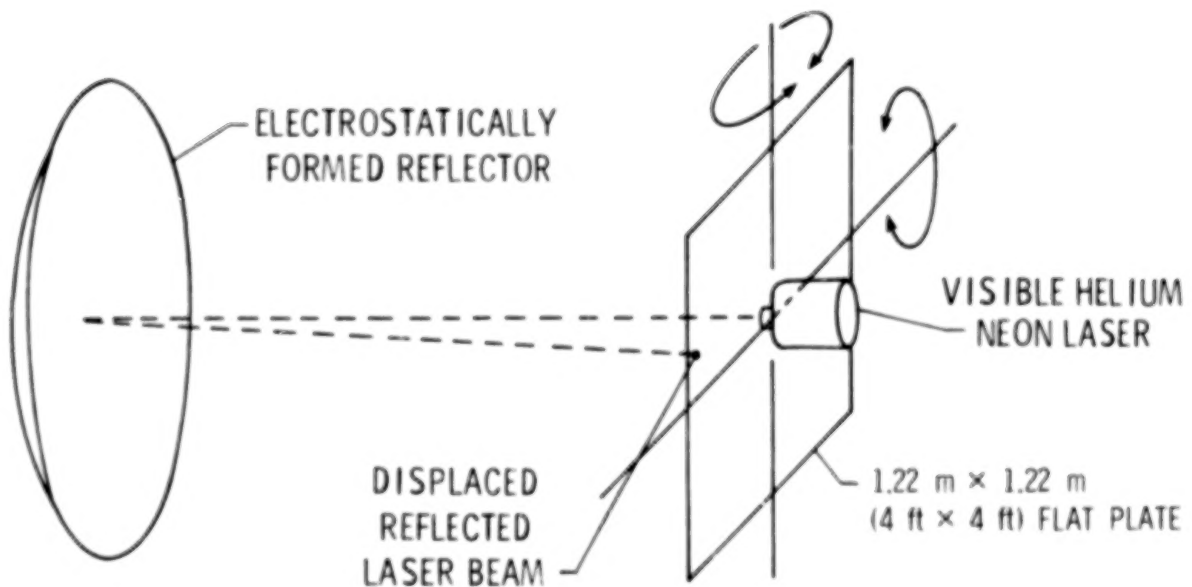


Figure 4

SURFACE MEASUREMENT SYSTEMS

Several surface measurement systems are being evaluated. The system shown in figure 5 uses a reflected laser beam and a modified foucault equation appears to be a system that will become more useful as the surface becomes smoother and more wrinkle-free. When the laser beam hits an area with wrinkles or distortions, the reflected beam cannot be measured on the flat plate. The theodolite system shown in figure 6 reads the elevation and azimuth digitally and inputs the readings into the 4052 which calculates the X, Y, Z coordinates of a series of 61 points on the surface of the membrane. The coordinates are then used to produce a contour map of the surface. This technique using three theodolites is used by the Harris Corporation in measuring the surfaces of their antennas. The photogrammetric system shown in figure 7 uses multiple camera images in calculating the X, Y, Z coordinates on the points on the surface. This technique has been used by the Harris Corporation and many other industrial firms when exact locations of surfaces or points are required. The single most important disadvantage with this system is the length of time required to derive the X, Y, Z coordinates after the pictures are taken.

VISIBLE LASER SURFACE SENSING DEVICE



MEASUREMENT OF DISPLACEMENT OF REFLECTED BEAM AND USE
IN MODIFIED FOUCAULT EQUATION PRODUCES CONTOUR OF
SURFACE IN VERTICAL AND HORIZONTAL PLANES

Figure 5

DIGITAL THEODOLITE METROLOGY SYSTEM

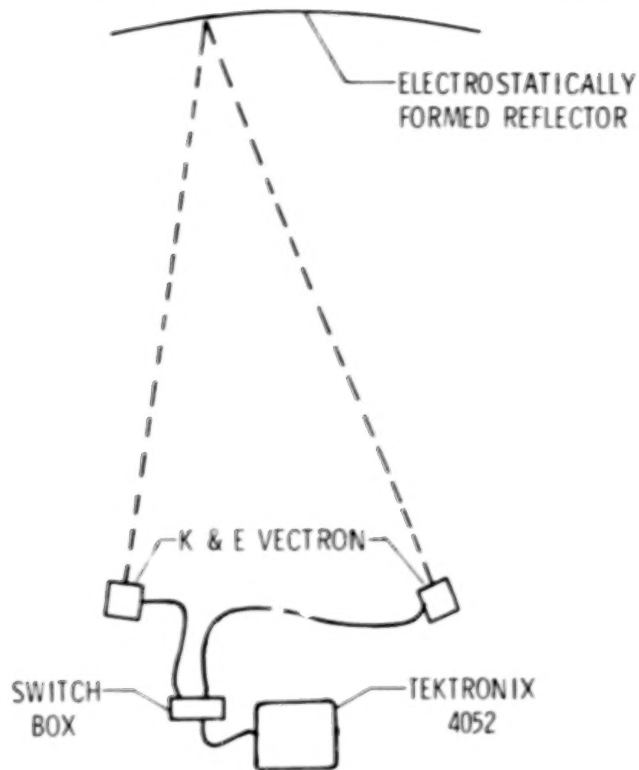


Figure 6

PHOTOGRAMMETRIC SURFACE MEASUREMENT SYSTEM

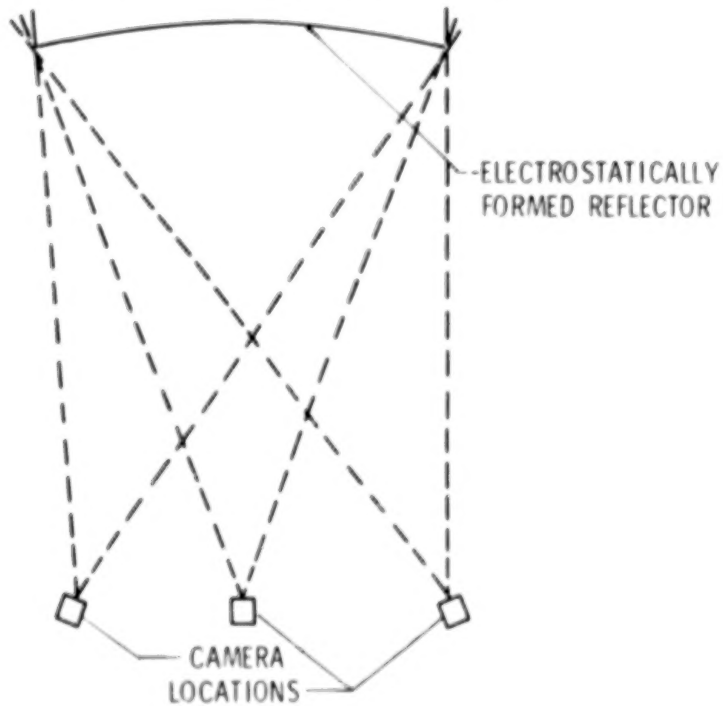


Figure 7

INITIAL TEST RESULTS

Typical results from two of the three surface sensing methods are shown in figures 8 and 9. The theodolite data has not been reduced yet. These curves represent the variation of the horizontal diameter from a perfect spherical curve measured under two different humidity conditions. The voltages used are those required to get an approximate 8.64-mm (3.4 in.) deflection in the center, except for the second case on the photogrammetric curves, and that series of voltages was recommended by GRC and produced a 11.58-mm (4.56 in.) center deflection.

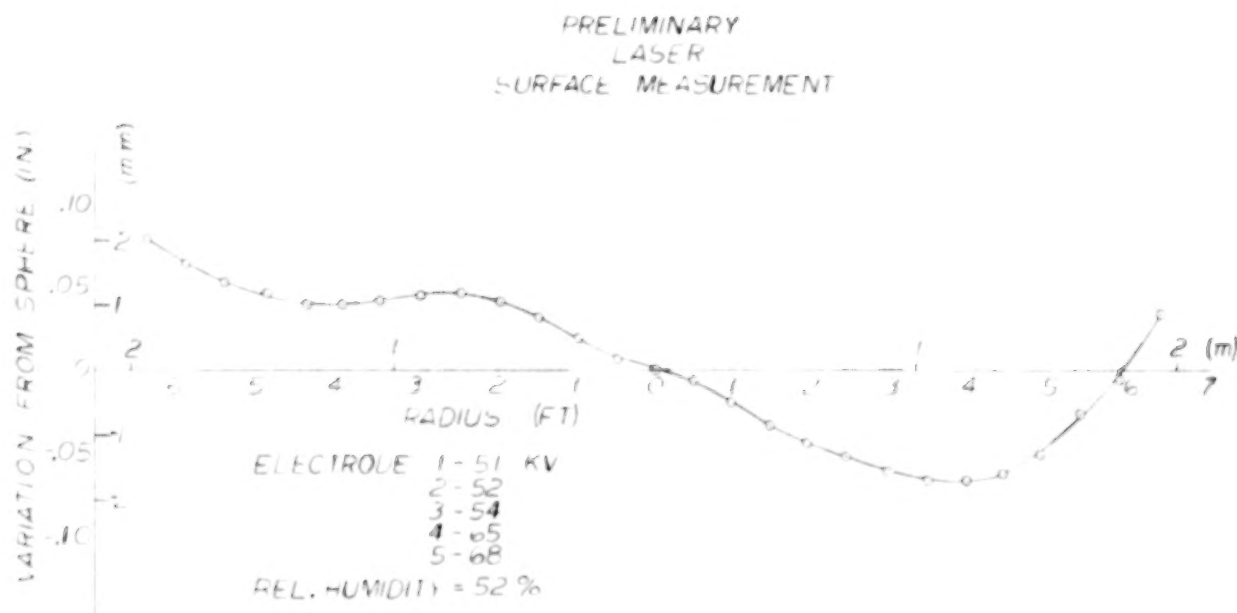


Figure 8

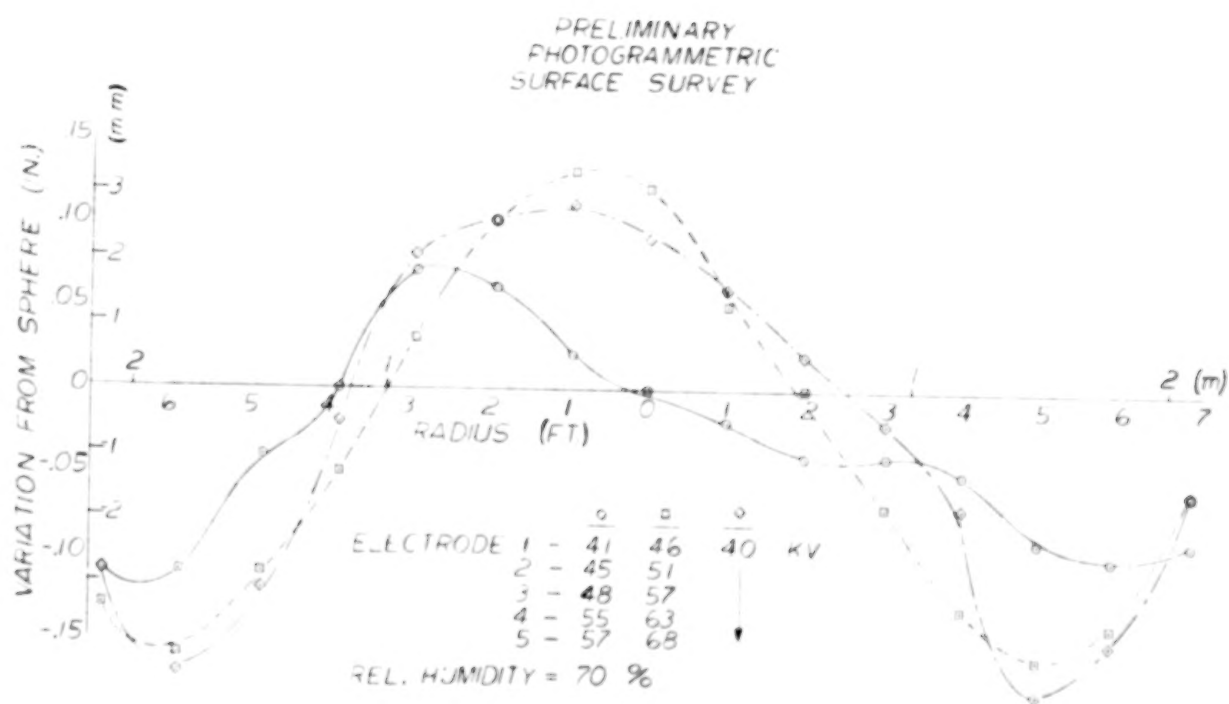


Figure 9

F.Y. 1981 SCHEDULE

The initial tests were made on 0.3 mil aluminized Kapton. 0.5 Mylar was tried but problems were encountered due to wrinkling, and attempts to smooth it were not too successful. The space charging study has been completed and is reported in this publication. The advanced space systems analysis study is underway. Other materials are being considered as well as other configurations of the black electrode. The proposed F.Y. 1981 schedule is shown in figure 10.

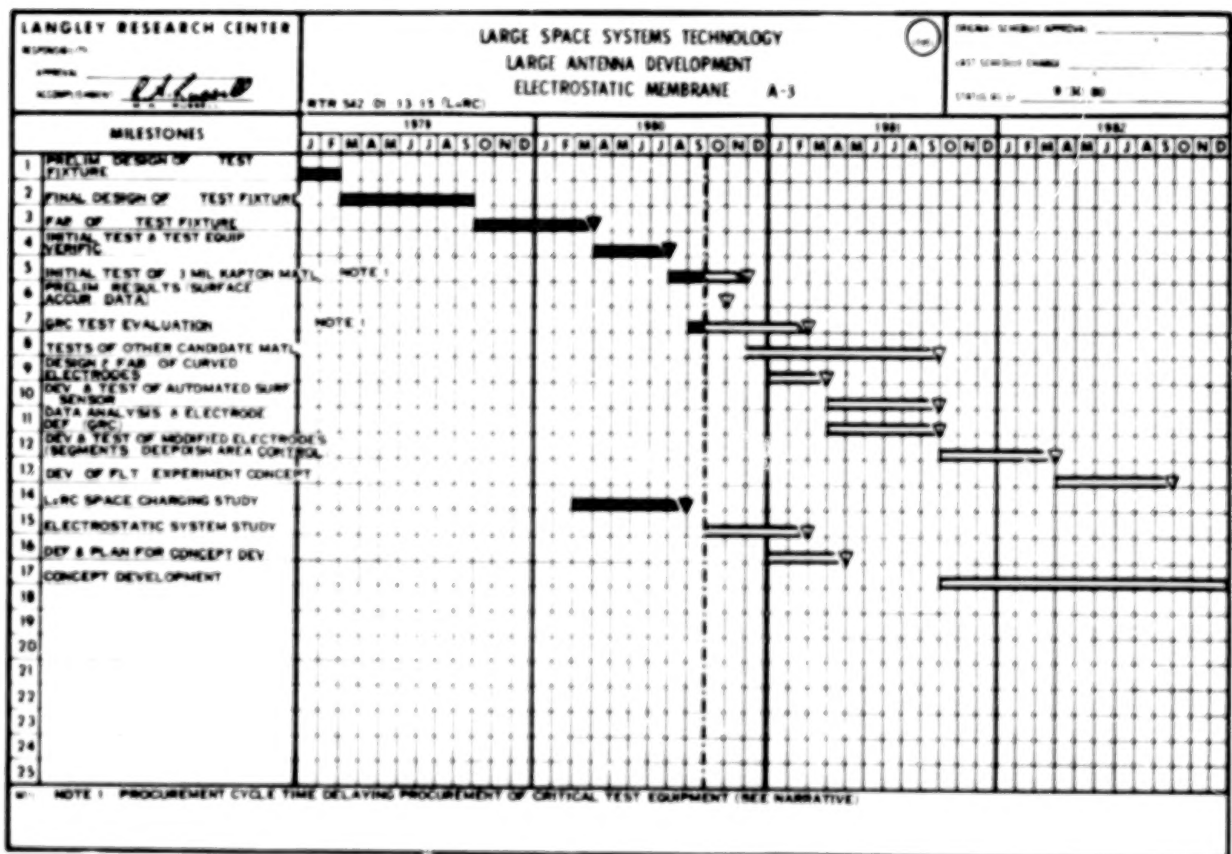


Figure 10

COMMENTS ON THE TESTING TO DATE

- o The fabrication of large surfaces using commercially available thin film plastics needs to be refined in order to produce consistent smooth surfaces in the seam areas.

- o Ambient conditions such as noise (aircraft, heavy machinery), air currents and humidity may limit the size of large thin films that can be tested on the ground.

- o Surface measuring techniques may be most useful when related to specific types of tests and surfaces, i.e.:

- The laser reflection technique may be more practical and quicker if the surface is a smooth, high precision, mirror-like reflective surface without targets and results are needed quickly.

- The theodolite system may be more useful in lower precision non-reflective surfaces where targets can be applied to the surface and results are needed in real time.

- The photogrammetric system may be most useful in ground tests where targets can be applied to the surface and where real time analysis is not required.

BLANK PAGE

BLANK PAGE

ELECTROSTATIC ANTENNA SPACE
ENVIRONMENT INTERACTION STUDY

Ira Katz
Systems, Science and Software
La Jolla, California

Large Space Systems Technology - 1980
Second Annual Technical Review
November 18-20, 1980

SPACE ENVIRONMENT PARAMETERS

We have studied the interactions of the electrostatic antenna with the space environment in both low earth orbit (LEO, ~200 km altitude) and geosynchronous orbit (GEO, ~7 R_E altitude). We did not consider polar orbits. While the ambient^e plasma in space is very tenuous, it is not negligible. In GEO, where the density is about 10^6 m^{-3} , the plasmas may be sufficiently energetic to create thousand volt differences in potential across spacecraft surfaces. The plasma in GEO may be characterized at times by temperatures as high as 10,000 electron volts. The LEO plasma has a density maximum of 10^{11} - 10^{12} m^{-3} in the range of 300 to 500 km. It drops off sharply below 250 km, but varies slowly with altitude above 500 km, maintaining a value of 10^{10} - 10^{11} m^{-3} . This plasma has a temperature of around 0.1 eV. Spacecraft also generate their own plasma from photoelectrons emitted by absorbing solar ultraviolet radiation. While characterized by only a few electron volts of energy the photocurrent densities are larger than those of the ambient plasma in GEO.

SPACE PLASMA ENVIRONMENT

● GEO

LOW DENSITY

HIGH TEMPERATURE

● LEO

HIGH DENSITY

LOW TEMPERATURE

● PHOTO ELECTRONS

INTERACTION MECHANISMS

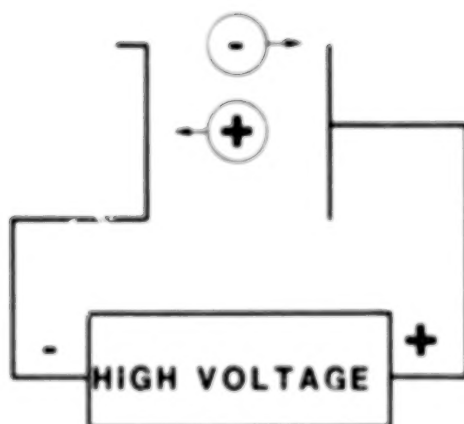
The major interaction mechanisms between the electrostatic antenna and the ambient space environment fall into three major categories. The first, spacecraft charging, is an effect which occurs fairly frequently at GEO when a satellite encounters a magnetospheric substorm. During such events a very hot (~ 10 keV) plasma can cause kilovolt electrical potentials to develop on the spacecraft which may lead to arcing. To prevent differential charging, the electrostatic antenna is designed to be conducting over its entire surface. The second interaction category is the mechanical effects of electrical interactions with the space environment. These turn out to be extremely small. For example, the electric fields due to uniform spacecraft charging create forces more than six orders of magnitude less than the membrane control forces. The third type of interaction, parasitic current losses, may be design limiting. These interactions are examined on the next chart.

SPACE-ELECTROSTATIC ANTENNA INTERACTIONS

- SPACECRAFT CHARGING
- ELECTROMECHANICAL EFFECTS
- PARASITIC CURRENT LOSSES

LOSSES DUE TO PARASITIC CURRENTS

The two membranes of the electrostatic antenna can be thought of as two electrodes in an enormous vacuum diode. With 50 kV across a 10 cm gap and a 10,000 square meter plate area, the power capabilities of such a device would be clearly limited by the rate of emission of charged particles from the electrodes. The system impact of charges flowing between the electrodes is in the design load of the high voltage power supply. Every milliampere of current demands 50 watts from the HV supply. Space plasma which enters the high field region acts as a source of charged particles which then act as current flowing through electrode - HV supply circuit.



**CIRCUIT REPRESENTATION OF POWER LOSSES
DUE TO PARASITIC CURRENTS**

LOSSES DUE TO PLASMA ENTERING APERTURES

The magnitude of the plasma currents is substantial, particularly in regard to the area of the antenna membranes. Below we indicate the power loss which would occur if the parasitic current was equal to the plasma thermal current. We see that power loss for a few square meters of holes or gaps in the antenna structure would not cause much problem in GEO ($n_e \sim 10^6 \text{ m}^{-3}$).

However, in LEO ($10^{10} \text{ m}^{-3} \leq n_e \leq 10^{12} \text{ m}^{-3}$) the entire structure must be plasma tight since power losses may exceed a kilowatt per square meter of opening. Sunlight coming through outgassing holes or around the periphery may also cause substantial power losses if care is not taken to minimize the surface area exposed. Consequently the design of the membrane support structure must include as few gaps and holes as is absolutely possible.

PLASMA CURRENT POWER LOSS (W/m^2) AT 50 KV

DENSITY (m^{-3})	TEMPERATURE (eV)	ELECTRONS	PROTONS
10^6	1	1.3×10^{-3}	3.1×10^{-5}
10^6	10^3	4.3×10^{-2}	1.0×10^{-3}
10^6	10^4	0.13	3.1×10^{-3}
10^{10}	1	13.0	0.31
10^{12}	1	1300.0	31.0
(SUNLIGHT)		~ 1	

POWER LOSSES USING METALLIZED CLOTH

One immediate consequence of the plasma loss figures presented is that only solid membrane materials are acceptable. It has been suggested that metallized cloth be used as an alternative for the aluminized plastic. Metallized cloth has been flown successfully; for example, the ATS-6 antenna was made of 70 percent transparent copper-clad Dacron. Suitability for rf applications does not, however, imply adequate blockage of very high dc fields or plasma electrons. In fact the effective transparency for plasma particles is substantially higher than the nominal transparency. Metallized cloth would require an antenna HV supply with a power handling capability of kilowatts.

RESULTS OF CLOTH POTENTIAL AND PARTICLE TRACKING CALCULATIONS

SPACING/DIAMETER	8 / 1	4 / 1
NOMINAL TRANSPARENCY	77%	56%
FIELD LEAKAGE	4%	1%
PARTICLE TRANSPARENCY	98%	77%

CONTENTS

VOLUME I - SYSTEMS TECHNOLOGY

PREFACE	iii	1/A7
1. LARGE SPACE SYSTEMS TECHNOLOGY OVERVIEW	1	1/A13
Robert L. James, Jr.		

SUPPORTING ACTIVITIES

2. LSST CONTROL TECHNOLOGY	9	1/B7
A. F. Tolivar		
3. ADVANCED CONTROL TECHNOLOGY FOR LSST ANTENNAS	19	1/C3
Y. H. Lin		
4. ADVANCED CONTROL TECHNOLOGY FOR LSST PLATFORM	31	1/D1
R. S. Edmunds		
5. CONTROL TECHNOLOGY DEVELOPMENT	49	1/E5
G. Rodriguez		
6. INTEGRATED ANALYSIS CAPABILITY (IAC) DEVELOPMENT	65	1/F7
J. P. Young		
7. INTEGRATED ANALYSIS CAPABILITY PILOT COMPUTER PROGRAM	73	1/G1
R. G. Vos		
8. AN ECONOMY OF SCALE SYSTEM'S MENSURATION OF LARGE SPACECRAFT	87	2/A4
L. J. DeRyder		
9. RADIATION EXPOSURE OF SELECTED COMPOSITES AND THIN FILMS	105	2/B8
Wayne S. Slomp and Beatrice Santos		
10. THERMAL EXPANSION OF COMPOSITES: METHODS AND RESULTS	119	2/C8
David E. Bowles and Darrel R. Tenney		

SPACE PLATFORMS

11. SPACE PLATFORM REFERENCE MISSION STUDIES OVERVIEW	129	2/D4
James K. Harrison		
12. ADVANCED SCIENCE AND APPLICATIONS SPACE PLATFORM	133	2/D8
Jack White and Fritz Runge		

13. STRUCTURAL REQUIREMENTS AND TECHNOLOGY NEEDS OF GEOSTATIONARY PLATFORMS	149 2/E10
G. R. Stone	
14. SUMMARY OF LSST SYSTEMS ANALYSIS AND INTEGRATION TASK FOR SPS FLIGHT TEST ARTICLES	167 2/F14
H. S. Greenberg	
15. ERECTABLE CONCEPTS FOR LARGE SPACE SYSTEM TECHNOLOGY	183 3/A5
W. E. Agan	
16. SPACE ASSEMBLY METHODOLOGY	199 3/B7
J. W. Stokes and H. H. Watters	
17. CONSTRUCTION ASSEMBLY AND OVERVIEW	217 3/C11
Lyle M. Jenkins	
18. SPACE PLATFORM ADVANCED TECHNOLOGY STUDY	229 3/D9
G. C. Burns	
19. A DOCUMENT DESCRIBING SHUTTLE CONSIDERATIONS FOR THE DESIGN OF LARGE SPACE STRUCTURES	243 3/E9
John A. Roebuck, Jr.	

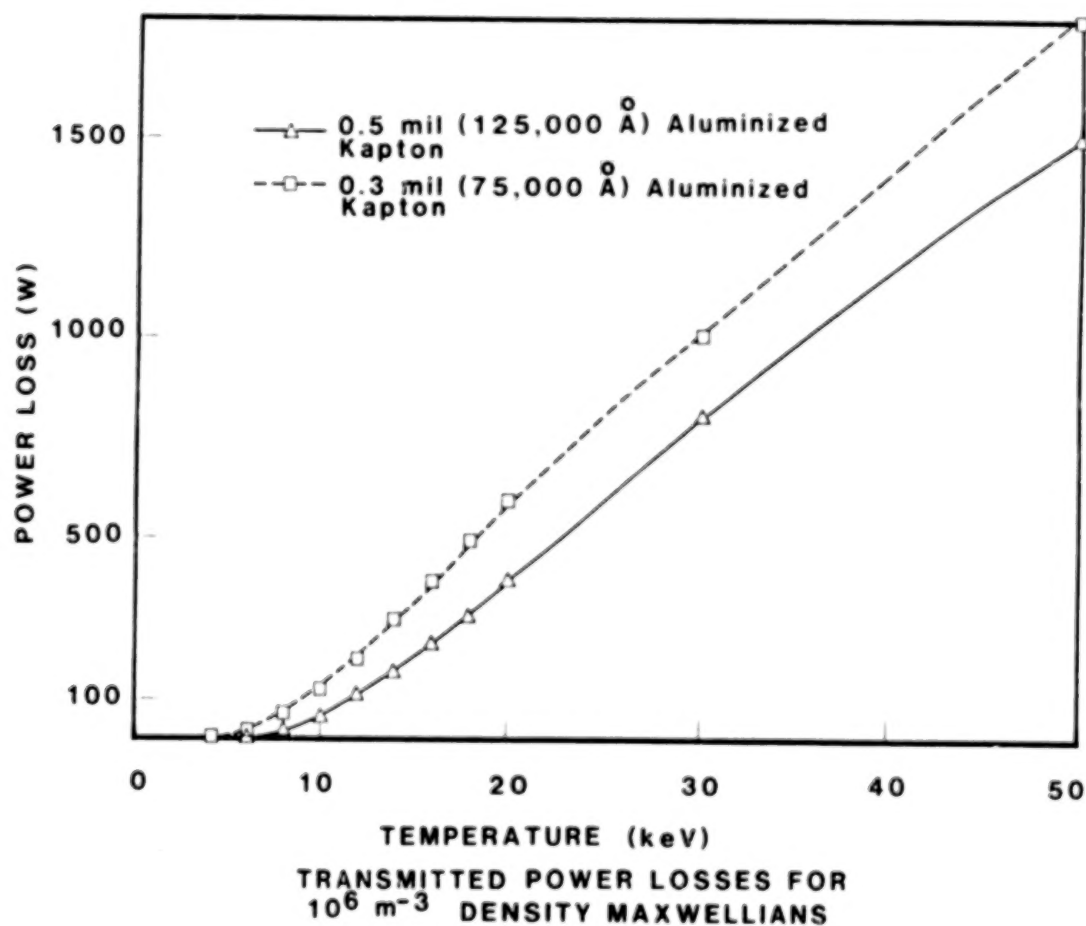
SPACE ANTENNAS

20. ELECTROSTATIC MEMBRANE ANTENNA CONCEPT STUDIES	259 3/F11
J. W. Goslee	
21. ELECTROSTATIC ANTENNA SPACE ENVIRONMENT INTERACTION STUDY	271 3/G9
Ira Katz	
22. ENVIRONMENTAL EFFECTS AND LARGE SPACE SYSTEMS	279 4/A6
H. B. Garrett	
23. JPL ANTENNA TECHNOLOGY DEVELOPMENT	287 4/A14
R. E. Freeland	
24. OFFSET WRAP RIB ANTENNA CONCEPT DEVELOPMENT	295 4/B8
A. A. Woods, Jr.	
25. ANALYTICAL PERFORMANCE PREDICTION FOR LARGE ANTENNAS	325 4/D10
M. El-Raheb	
26. JPL SELF-PULSED LASER SURFACE MEASUREMENT SYSTEM DEVELOPMENT	339 4/E10
Martin Berdahl	
27. ANTENNA SYSTEMS REQUIREMENTS DEFINITION STUDY	349 4/F6
C. T. Golden	

28. HOOP/COLUMN ANTENNA TECHNOLOGY DEVELOPMENT SUMMARY	357	4/F14
Thomas G. Campbell		
29. DEVELOPMENT OF THE MAYPOLE (HOOP/COLUMN) DEPLOYABLE REFLECTOR CONCEPT FOR LARGE SPACE SYSTEMS APPLICATIONS	365	4/G8
D. C. Montgomery		
30. RADIO FREQUENCY PERFORMANCE PREDICTIONS FOR THE HOOP/COLUMN POINT DESIGN	407	5/C12
Thomas G. Campbell		
31. OFFSET FED UTILIZATION OF FOUR QUADRANTS OF AN AXIALLY SYMMETRICAL ANTENNA STRUCTURE	431	5/E8
P. Foldes		
32. SURFACE ACCURACY MEASUREMENT SENSOR FOR DEPLOYABLE REFLECTOR ANTENNAS	439	5/F2
R. B. Spiers, Jr.		
SECOND ANNUAL TECHNICAL REVIEW ATTENDEES	449	5/F12

HIGH ENERGY ELECTRON PENETRATION

High energy electrons ($e \geq 20$ keV) in the GEO plasma can penetrate the very thin (0.3-0.5 mil) membranes proposed for the electrostatic antenna. While this sounds high for a plasma temperature, half the current in a Maxwellian has energy exceeding 1.7 times the temperature. Furthermore, a thermal characterization of the GEO plasma tends to underestimate the high energy electron current. Calculations show that for the 0.3 mil membrane the power loss reaches 100 watts at a plasma temperature of 10 keV. Thus the system design must allow for a greater than 100 watt power loss approximately 10 percent of the time in orbit. The situation for the 0.5 mil membrane is only slightly better. These losses are, of course, in addition to those due to plasma or sunlight leaking into the high field region.



SUMMARY

We conclude that, insofar as spacecraft-environment interactions are concerned, the electrostatically controlled membrane mirror is a viable concept for space applications. However, great care must be taken to enclose the high voltage electrodes in a Faraday cage structure to separate the high voltage region from the ambient plasma. For this reason, metallized cloth is not acceptable as a membrane material. Conventional spacecraft charging at geosynchronous orbit should not be a problem provided ancillary structures (such as booms) are given non-negligible conductivity and adequate grounding.

Power loss due to plasma electrons entering the high-field region is a potentially serious problem. In low earth orbit any opening whatever in the Faraday cage is likely to produce an unacceptable power drain. At geosynchronous altitude, where current levels are lower, a gap of ~ 1 cm at the membrane point-of-attachment may be tolerable. However, a geosynchronous antenna will occasionally encounter high energy plasma capable of penetrating a thin membrane to produce power drains of 100 watts or more.

ELECTROSTATIC ANTENNA SPACE ENVIRONMENT INTERACTIONS SUMMARY

- ELECTROMECHANICAL EFFECTS ARE SMALL
- CHARGING MAY BE IMPORTANT, BUT PROBABLY
CAN BE ALLEVIATED
- POWER DRAIN MAY LIMIT SOME DESIGNS

ENVIRONMENTAL EFFECTS AND LARGE SPACE SYSTEMS

H. B. Garrett
Jet Propulsion Laboratory
Pasadena, California

Large Space Systems Technology - 1980
Second Annual Technical Review
November 18-20, 1980

ENVIRONMENTAL EFFECTS AND LARGE SPACE SYSTEMS

With the growth in size, power, and complexity of space systems, the interactions between space systems and the environment will become of increasing concern to the satellite designer. This talk will briefly discuss some of the more important of these interactions. Although some effects may limit the full utilization of specific systems, careful consideration of these causes should greatly reduce the more severe problems. Thus this paper should be viewed as a check list of concerns rather than as a source of dire warnings.

INTERACTIONS

There are a number of interactions that are of concern to the designer of large space systems. These range from the well-known effects of radiation damage to the less well-known effects of spacecraft charging. Whereas these effects and those of contamination are common to all space systems, the related issues of high power and large size are peculiar to the next generation of vehicles. Likewise, the effects of large space systems on the environment will become a new area of concern. These areas are considered in more detail in the following pages.

- RADIATION
- SPACECRAFT CHARGING
- CONTAMINATION
- HIGH POWER, SIZE
- ENVIRONMENTAL IMPACT

RADIATION

Although most people are aware of the deleterious effects of radiation dosage on spacecraft systems, few are aware that the new systems, as they have grown in complexity, have also grown in sensitivity. For example, sophisticated optical sensing systems can be confused by light flashes due to the passage of high energy particles through glass. Material damage, such as to solar cells, due to high dosage rates are well known. Hard errors, actual physical destruction of integrated circuits, are also understood by most designers. With the advent of LSI and VLSI circuitry, however, a new problem--soft errors--has become equally important. Soft errors, the resetting rather than destruction of individual memory bits, are difficult to prevent and detect. They represent a particularly severe threat to the complex control systems proposed for large space systems.

- FALSE SIGNALS
- MATERIAL DEGRADATION
- HARD ERRORS
- SOFT ERRORS

SPACECRAFT CHARGING

The last decade has seen growing concern for the effects of spacecraft charging. Spacecraft charging is the result of nature's attempt to balance currents to and from space vehicles. These currents arise from the ambient electron and ion fluxes, secondary and back scattered fluxes generated by these fluxes, photoelectrons, artificial sources (plasma beams, etc.), radiation deposition, and currents induced by movement across the Earth's magnetic field. Except for radiation deposition, these currents deposit charge on spacecraft surfaces. These surfaces, particularly for dielectrics, cause potentials which can distort particle trajectories in the vicinity of the vehicle. Not only can this lead to distortions in plasma measurements, but it can enhance contamination by attracting ions or by arc discharge. Arc discharge can also apparently be caused by charge deposition in dielectrics. That is, high energy particles can penetrate into dielectrics and deposit charge. As the particles have energies in excess of 1 MeV, fields of 10^6 V/cm are required to significantly reduce the particle fluxes. These fields are greatly in excess of the breakdown potential of most materials.

- INSTRUMENT EFFECTS
- ARCING
- ENHANCED CONTAMINATION

CONTAMINATION

The changes in satellite surface properties due to contamination are well known. Contamination sources abound and range from the launch environment to the environment induced around the satellite by thruster operations. There is even evidence that the Shuttle bay may be another major contamination environment. Contamination can significantly alter thermal properties. The use of a multitude of control thrusters on large structures will, however, be the worst source of contamination.

- SURFACE PROPERTY CHANGES
- THERMAL CONTROL

HIGH POWER, SIZE

A major use of large structures will be as solar cell platforms. These systems will be characterized by high voltages and high power. Large currents will also flow through the satellite surface. The ambient plasma, particularly at Shuttle altitudes, can lead to current loss and enhanced arcing. The Earth's magnetic field can likewise interact with the magnetic moments generated by the surface currents (these torques can be of benefit in stabilizing the satellite). The large size of the planned systems means that effects which were previously ignored for small satellites may become significant. These range from the increased effects of gravitational gradients and atmospheric drag, which could deform the satellite surface, to the increased likelihood of collisions at hypervelocity with man-made debris.

- POWER LOSS
- MAGNETIC TORQUES
- ARCING
- DEFORMATION

ENVIRONMENTAL IMPACT

With the advent of truly large scale operations in space, the issue of environmental impact has surfaced as a new concern. First there is the obvious issue of pollution. Pollution of the atmosphere and space is caused by rocket effluents, photoelectron pollution (photoelectrons are generated in large amounts by sunlight falling on satellite surfaces), and even light pollution (the SPS may reflect so much light as to be a nuisance to astronomers). Large (100 Km²) structures also will absorb the high energy particles that impinge on them (as the refill rate is not well known, it is difficult to assess this effect). Altogether, these effects may drastically alter the Earth's magnetosphere. This already happened in the case of the nuclear tests in outer space which altered the radiation belts for over 11 years. Even so, it is not clear if these alterations will in any way affect the Earth's surface climate. Finally, large structures will generate large plasma wakes and waves. These plasma waves may cause interference with communications to the vehicle. Similarly, a high energy, microwave beam from the SPS will cause ionospheric turbulence, affecting UHF and VHF communications. Although none of these effects may ultimately prove critical, they must be considered in the design of large structures.

- POLLUTION
- ABSORPTION
- PLASMA WAKE AND WAVES

JPL ANTENNA TECHNOLOGY DEVELOPMENT

R. E. Freeland
Jet Propulsion Laboratory
Pasadena, California

Large Space Systems Technology - 1980
Second Annual Technical Review
November 18-20, 1980

LONG TERM OBJECTIVE

The basic objective of the LSST Program is to provide systems-level technology for evolving cost-effective, STS compatible antennas that will be automatically deployed in orbit to perform a variety of missions in the 1985 to 2000 time period. For large space-based antenna systems, the LSST Program has selected deployable antennas for development. The maturity of this class of antenna, demonstrated by the success of smaller size apertures, provides a potential capability for satisfying a significant number of near-term space-based applications. Two specific antenna concepts selected for development are the offset wrap-rib and the maypole (hoop/column) configurations. The offset wrap-rib concept development is the basis of the JPL LSST Antenna Technology Development Program. Supporting technology to the antenna concept development includes analytical performance prediction and the capability for measuring and evaluating mechanical antenna performance in the intended service environment.

TO DEVELOP THE TECHNOLOGY NEEDED TO EVALUATE,
DESIGN, FABRICATE, PACKAGE, TRANSPORT, AND DEPLOY
COST EFFECTIVE AND STS COMPATIBLE ANTENNA
SYSTEMS UP TO 300 METERS IN DIAMETER FOR
POTENTIAL APPLICATIONS.

- MOBILE COMMUNICATIONS
- EARTH RESOURCES
- ORBITING VLBI

JPL PROGRAM ELEMENTS

The offset wrap-rib antenna conceptual development program at LMSC is intended to result in technology that will accommodate the application of reflectives up to 100 meters in diameter and larger. The program benefits from an extensive heritage of demonstrated technology for axisymmetric reflector structures that is directly applicable to the offset reflector. The offset deployable feed support structure development is expected to be a new configuration design for the large size antennas.

Analytical estimates of antenna performance are essentially estimates of reflector surface precision and feed structure alignment in the intended service environment. Such analyses are under development at JPL to (a) understand the fundamental wrap-rib antenna, (b) accomplish an independent assessment of potential antenna performance, and (c) determine the applicability of this concept for a number of different applications.

The determination of antenna interface requirements and constraints, as a consequence of specific applications, is under development at the Boeing Co. These interfaces will result from the development of system level configuration designs for classes of applications. The interface characterizations will then be used to guide the conceptual antenna development.

Remote measurement of antenna reflector surfaces and feed structure alignments in space is needed to (a) validate the mechanical design of precision surfaces, (b) characterize dynamic and thermal performance for verification of analytical performance prediction models, and (c) to accommodate active control basic structural elements. Such a system is currently under development at JPL.

- OFFSET WRAP-RIB ANTENNA CONCEPT DEVELOPMENT
- ANALYTICAL PERFORMANCE PREDICTION FOR LARGE ANTENNAS
- ANTENNA SYSTEM REQUIREMENTS
- SURFACE MEASUREMENT SYSTEM DEVELOPMENT

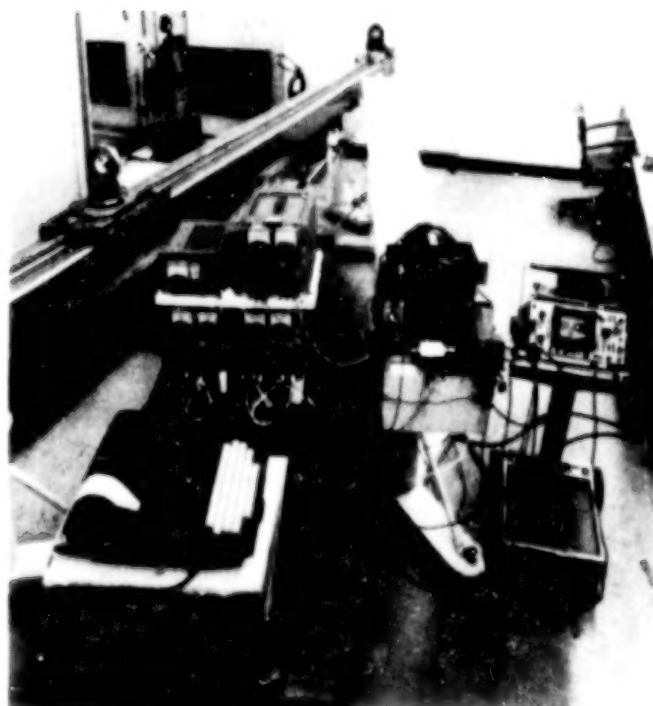
JPL PROGRAM FUNCTIONAL RELATION

The functional diagram delineates the relationship between the four major elements on the JPL Program. The focal point of the program is the LMSC offset wrap-rib antenna conceptual development. This antenna development is driven by the LSST focus mission requirements, which are the basis for system level configuration designs, to be developed by the Boeing Co., as part of the Antenna Subsystem Requirements Study. The results of this study, which is another level of refinement of the LSST focus mission requirements, will be used to characterize the antenna subsystem requirements and constraints for specific classes of applications. These subsystem requirements will provide the focus needed to guide the detail design of the offset antenna concept. The analytical performance prediction capability development at JPL will augment the LMSC analytical capability for estimating cost and functional antenna performance for a variety of applications. The JPL surface measurement system, intended for large mesh deployable antenna applications will be demonstrated and validated as part of the antenna ground based demonstration program. Results of the offset wrap-rib deployable antenna technology development will include, (a) high confidence structural designs for antennas up to 100 meters in diameter, (b) high confidence estimates of functional performance and fabrication cost for a wide range of antenna sizes (up to 300 meters in diameter), (c) risk assessment for fabricating the large size antennas, and (d) 55 meter diameter flight quality hardware that can be cost effectively completed to accommodate a flight experiment and/or application.

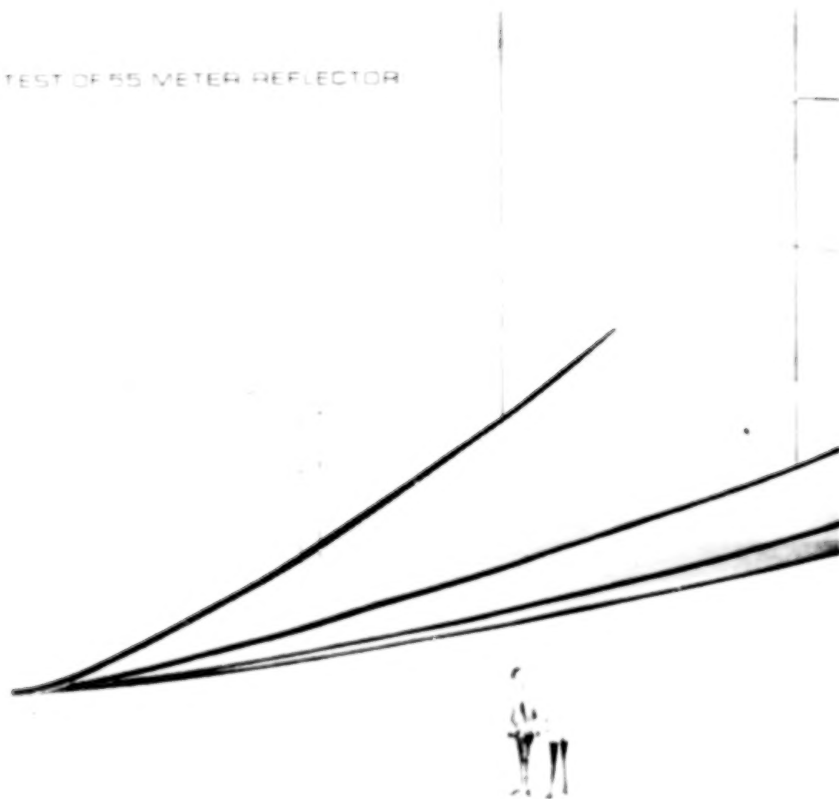
LSST OFFSET WRAP-RIB TECHNOLOGY DEVELOPMENT PLAN



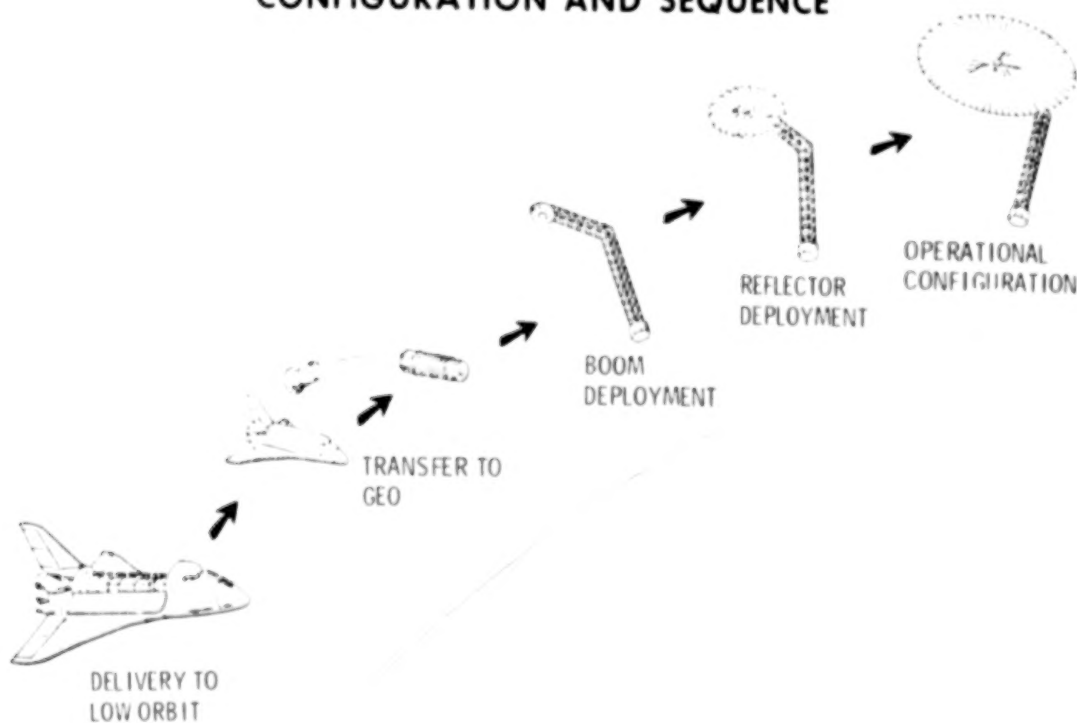
JPL SELF-PULSED LASER RANGING SYSTEM BREADBOARD MODEL

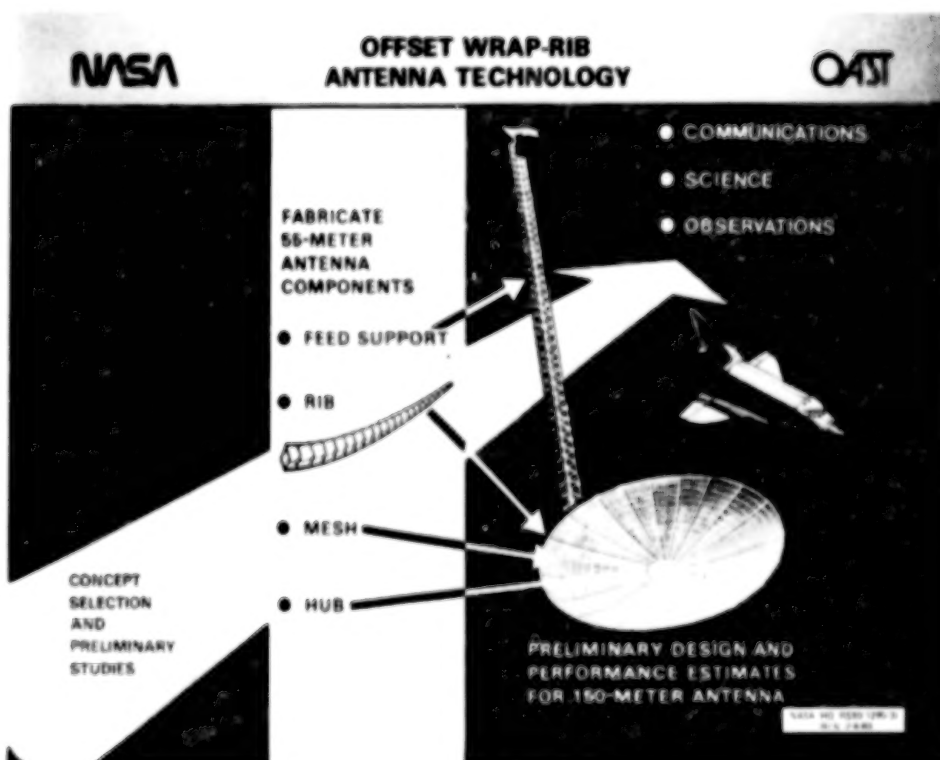


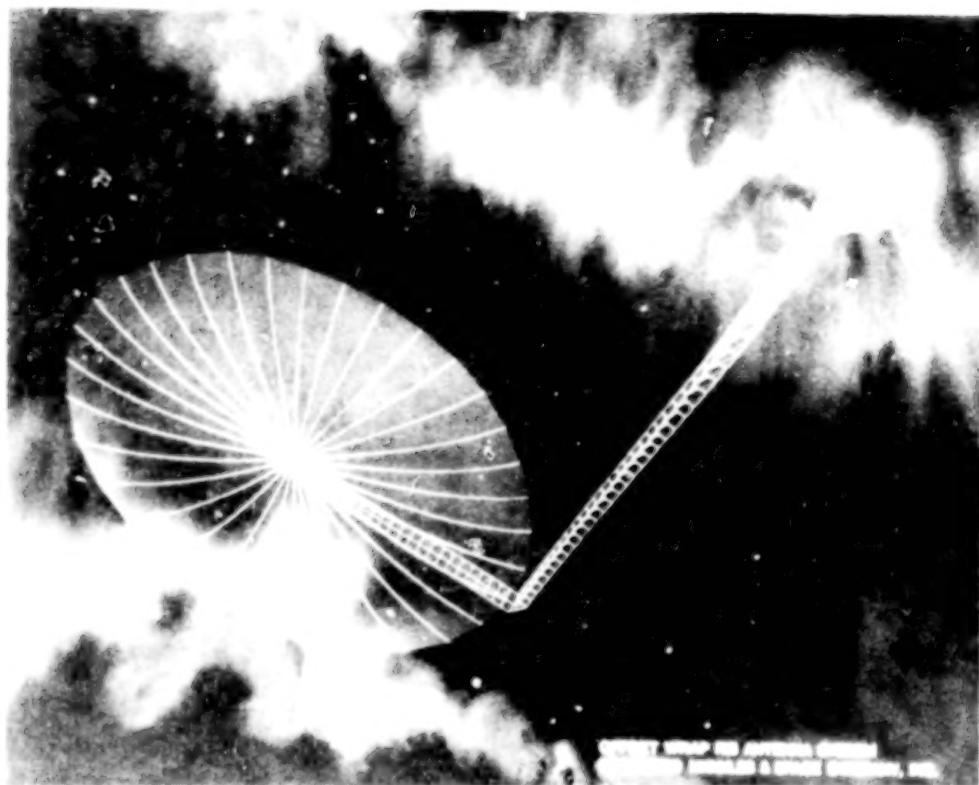
GROUND TEST OF 55 METER REFLECTOR



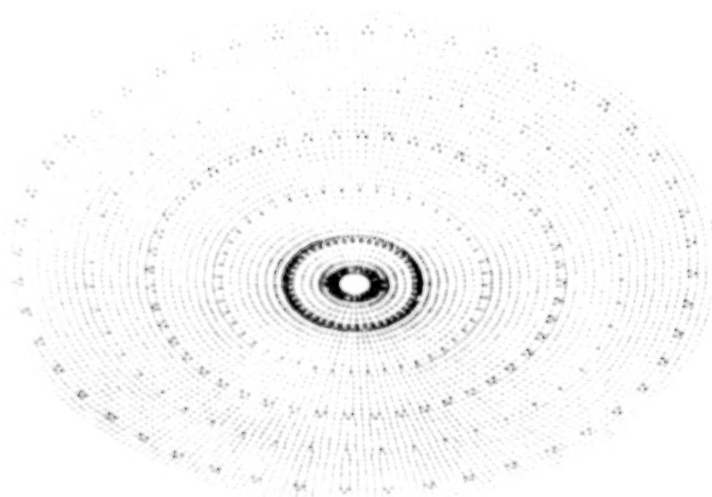
OFFSET FEED ANTENNA SYSTEM OPERATIONAL CONFIGURATION AND SEQUENCE







ANTENNA REFLECTOR STRUCTURES
55 METER DIAMETER —
25.000 DEGREE OF FREEDOM



OFFSET WRAP RIB ANTENNA
CONCEPT DEVELOPMENT

A. A. Woods, Jr.
Lockheed Missiles and Space Company
Sunnyvale, California

Large Space Systems Technology
Second Annual Technical Review
Langley Research Center
Hampton, VA

November 20, 1980

BACKGROUND AND STUDY OBJECTIVES

A three year hardware design and demonstration program was initiated in March of 1980. This contract, originated by Jet Propulsion Laboratory in support of the Large Space Systems Technology Program, was designed to demonstrate large diameter offset reflector technology readiness through development of ground testable, flight representative full size hardware. The program was also designed to provide a basis of data which will allow confirmation of cost, performance and size growth projections for the offset Wrap Rib antenna design. The contract objectives are summarized in Figure 1.

<p>ESTABLISH A 55-M DATA BASE OFFSET REFLECTOR</p> <ul style="list-style-type: none">• MANUFACTURE AND TEST COMPONENTS/PROCESSES• ASSEMBLE I-G TESTABLE SEGMENT• DEMONSTRATE DEPLOYMENT AND RETRACTION• MEASURE DEPLOYED CONTOUR WITH OFFLOADING TEST AID• UPDATE DESIGN AND DESIGN ALGORITHM
<p>DESIGN A COMPATIBLE FEED SUPPORT STRUCTURE</p> <ul style="list-style-type: none">• EVALUATE CANDIDATES• SELECT CONCEPT WHICH EXPLOITS LSST TECHNOLOGY• CHARACTERIZE DESIGN• UPDATE DESIGN ALGORITHM
<p>EVALUATE BENEFITS OF INCORPORATING ACTIVE FIGURE CONTROL</p> <ul style="list-style-type: none">• ONE TIME ADJUSTMENT• CONTINUOUS ADJUSTMENT• COSTS

Figure 1

STUDY TASKS

The specific study tasks are overviewed in Figure 2. This schedule presents the full program activity segmented by the four funding phases of the contract. Phase II which is the subject of this report will yield the design basis for the data base reflector and offset feed support tower as well as the first hardware component, a 25 meter long rib. In the subsequent phases the remainder of the hardware will be fabricated, assembled and finally demonstration tested.

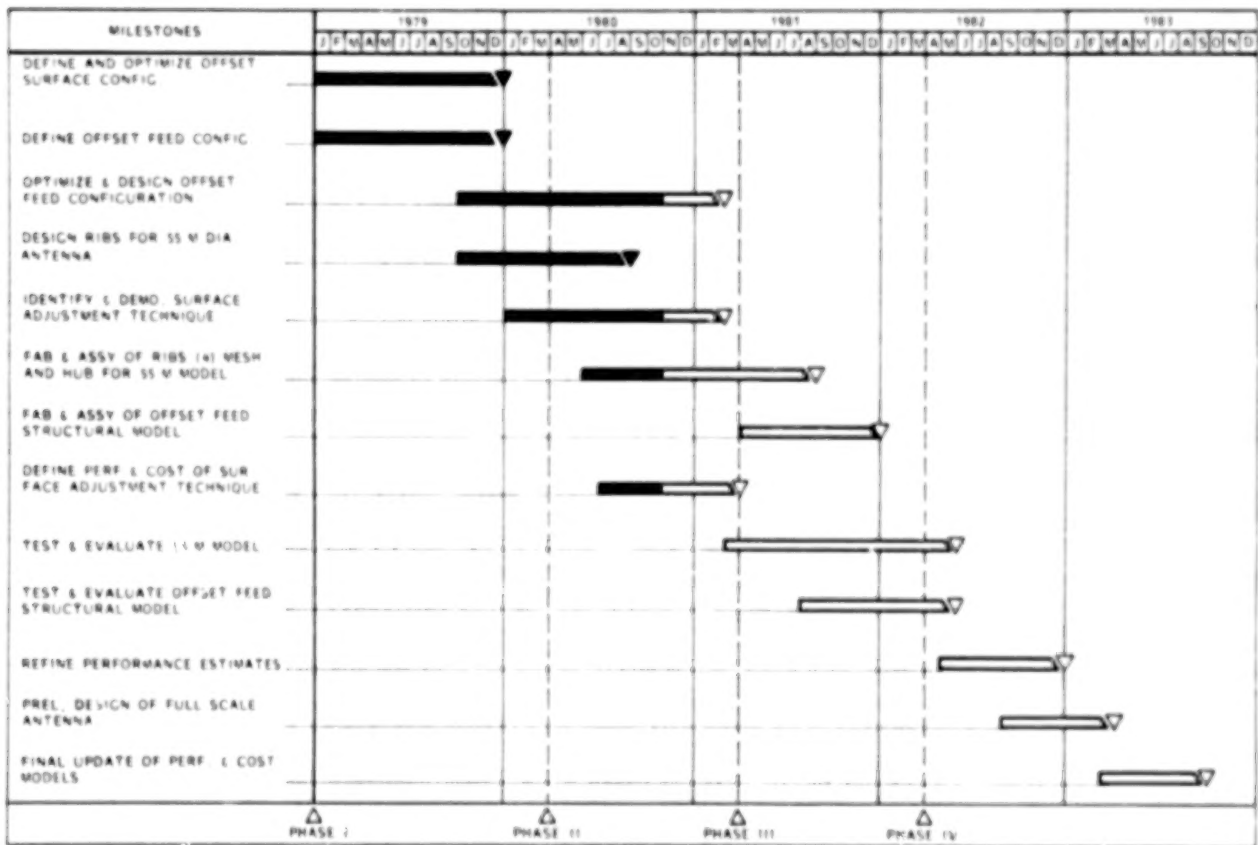


Figure 2

OFFSET ANTENNA SYSTEM OVERVIEW

The system under study is presented in Figure 3 which depicts a 100 m diameter communication antenna. The reflector is of the offset Wrap Rib design with the hub structure located at the center of the offset section. The cantilevered rib surface support structure can be seen radiating from this central hub. The spacecraft which contains the control, communications and power subsystems is located in the focal point area but out of the microwave aperture to assure optimum performance. A deployable truss mast connects the reflector to the spacecraft and maintains system alignment. The mast is also configured to remain outside of the microwave path.

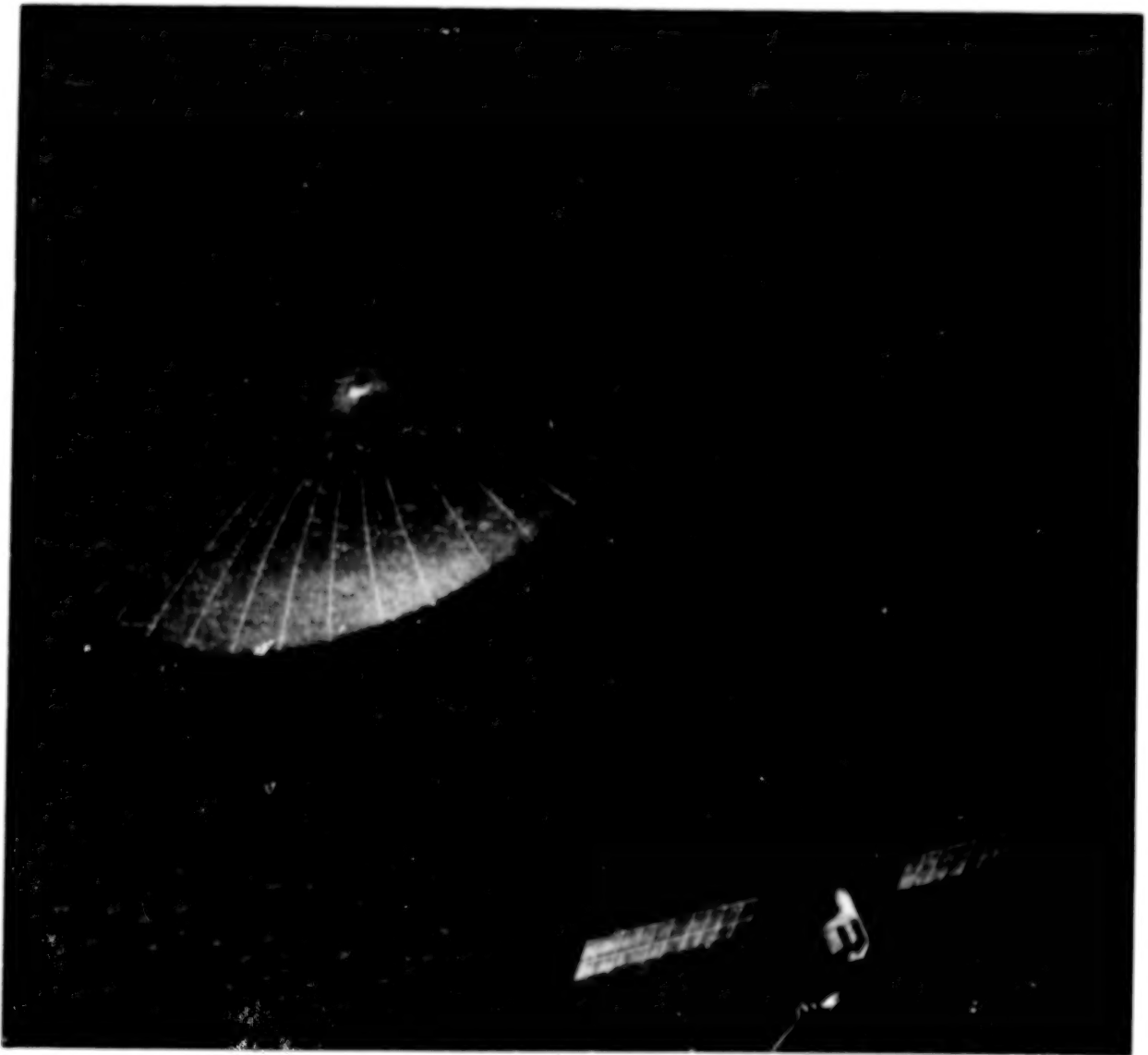


Figure 3

OPERATIONAL DEPLOYMENT SEQUENCE

Figure 4 presents the stowed spacecraft configuration as it is being deployed from the shuttle. The stowed reflector seen as a flat cylinder is shown at one end of the spacecraft and the IUS, used for orbit transfer, on the opposite end. The spacecraft segment is depicted next to the IUS with the feed system and solar array panels folded forward toward the reflector. In this configuration the mast is stowed in the triangular section hidden by the spacecraft equipment.

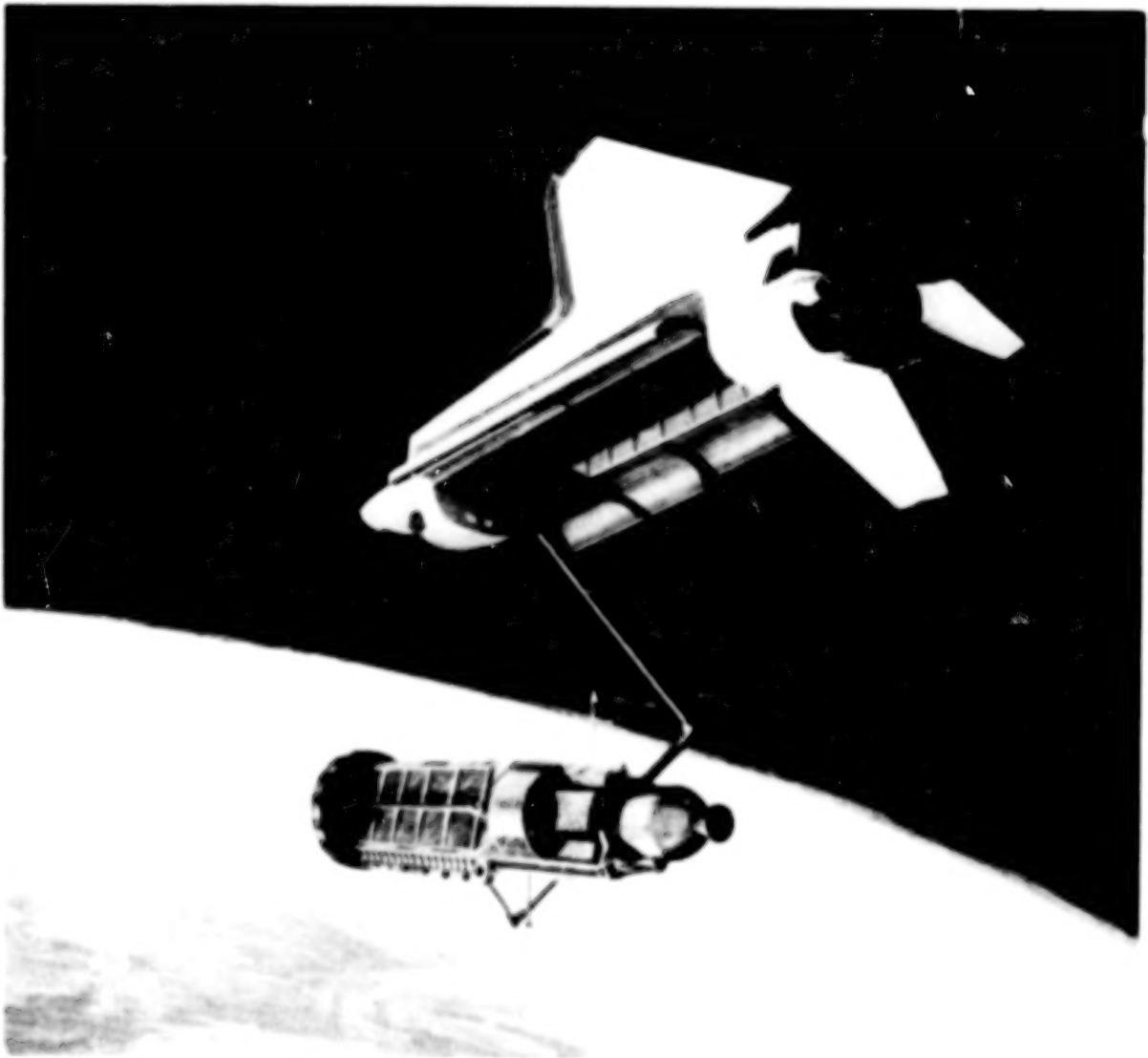


Figure 4

After the spacecraft has achieved operational orbit (Figure 5), the IUS is separated and the deployment sequence initiated. The first deployment is that of the mast. This activity can be seen in the figure as the reflector is being moved away from the spacecraft segment.

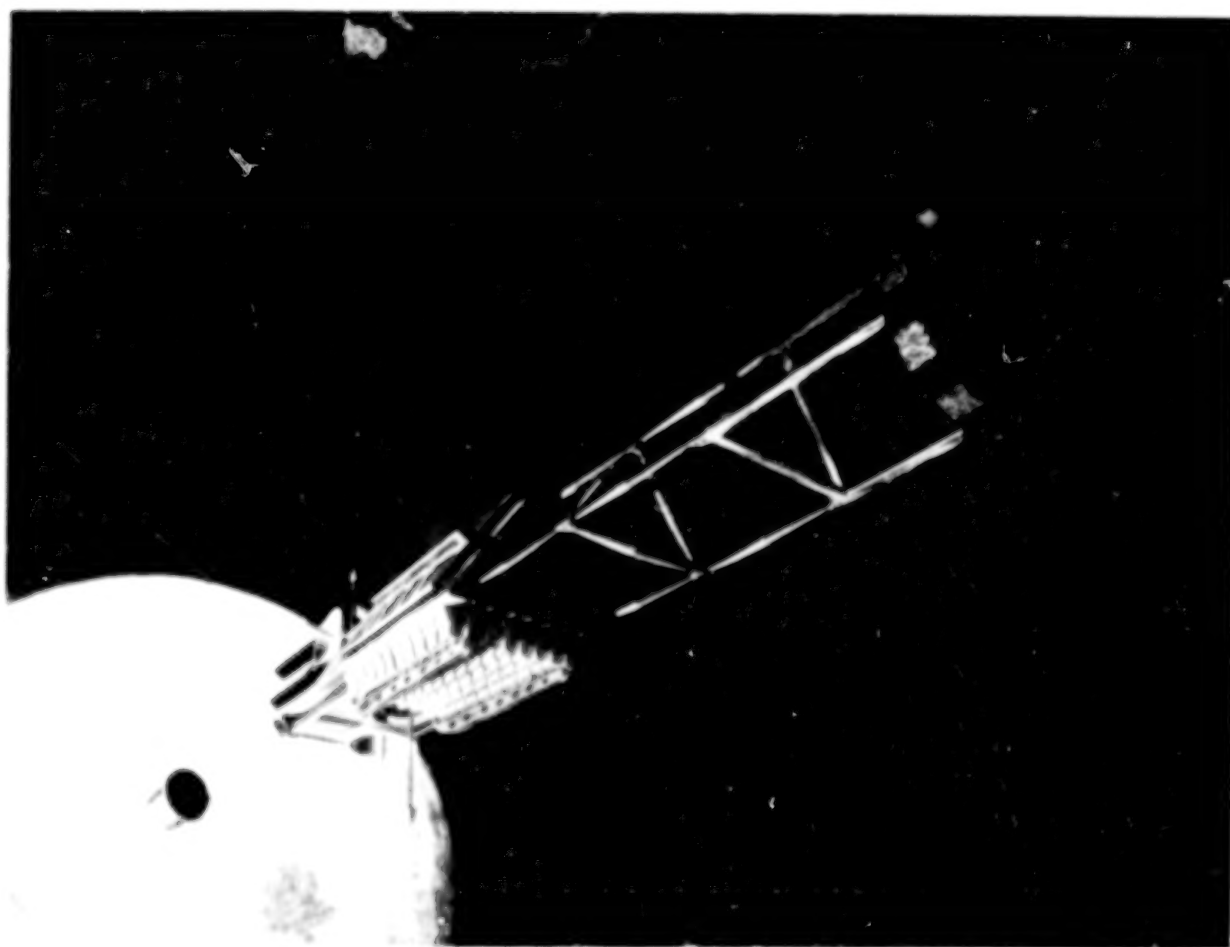


Figure 5

The final operation is that of reflector deployment. Figure 6 depicts this event at about the one-third point. The reflective surface and ribs can be seen unwrapping off the hub at the end of the fully deployed mast.

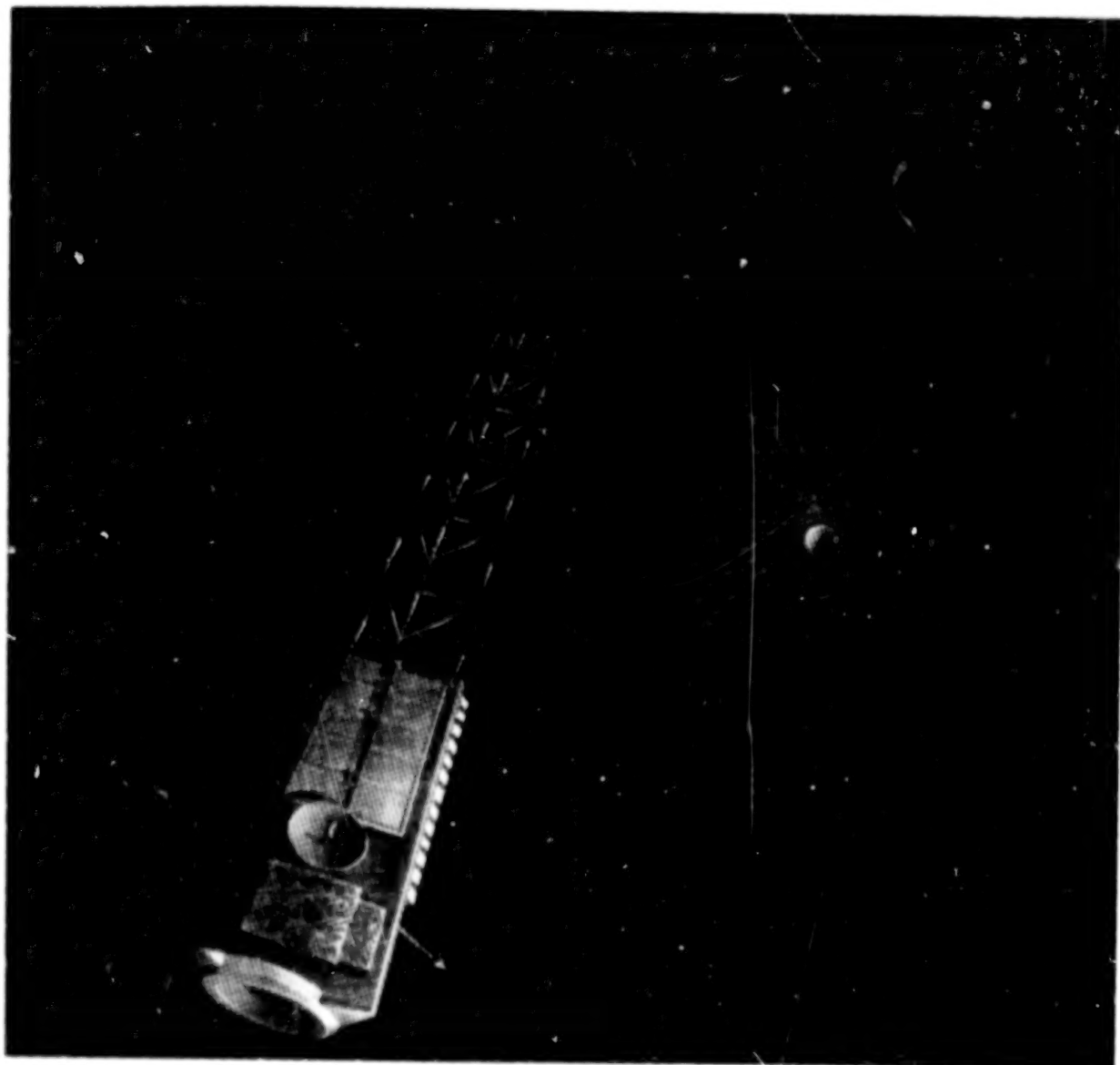


Figure 6

DESIGN/MISSION COMPATIBILITY

The previous study activity identified the growth limits of the offset Wrap Rib design. These limits are presented in Figure 7 along with the data point which locates the 55 m data base design. The three major mission regions of interest are also presented to provide an appreciation for the projected design capability with respect to the defined mission models. The results show that the design potential comfortably envelops the defined near term mission zones as well as the projected far term missions (dotted projections).

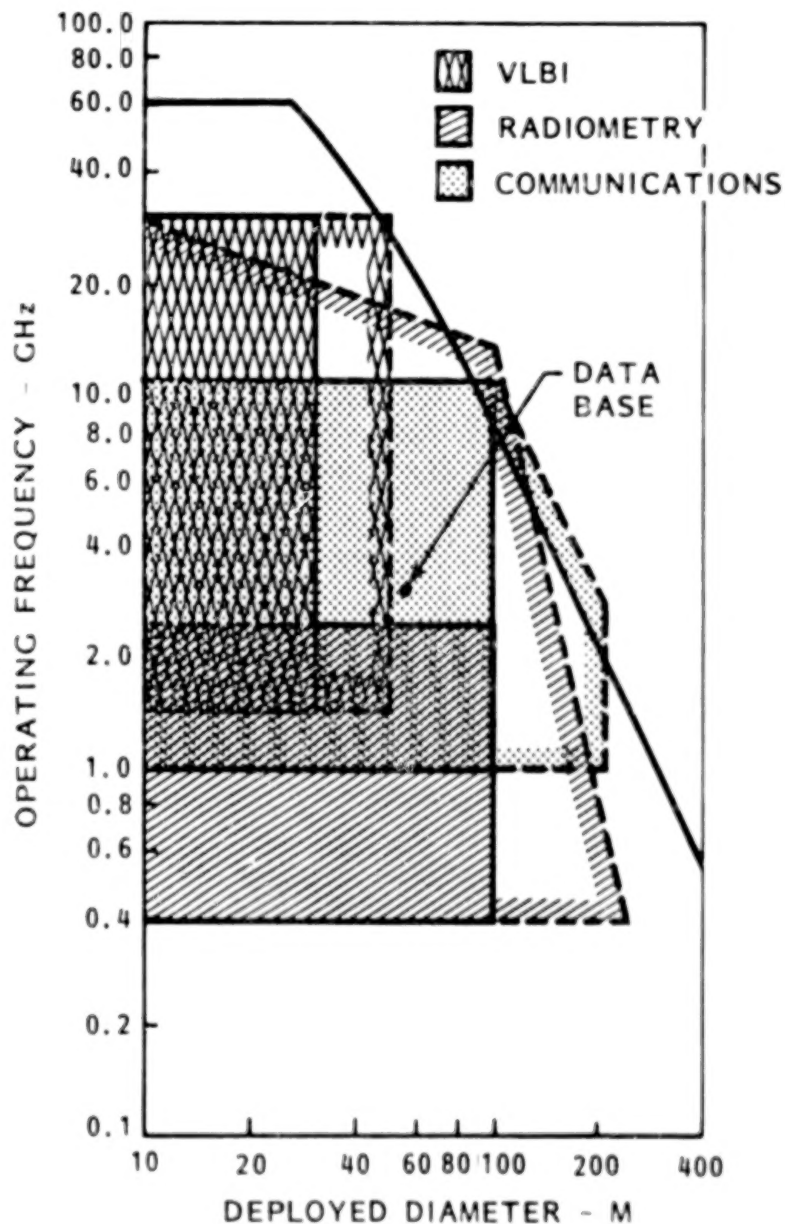


Figure 7

REFLECTOR DATA BASE CONCEPT SELECTION (REF 1)

The antenna hardware model selected as the basis for a new data base should: extend the current and proven data base of 16 meters to the largest practical size, address the same basic set of problems to be faced by building full-size antennas, be large enough so that extrapolation from the new data base to full-size antennas can be done with confidence, be representative enough of full-scale designs to accommodate direct scaling, lend itself to ground-based evaluations, and be of sufficient hardware quality to accommodate the completion of fabrication for a flight demonstration and/or application article.

The criteria established for defining the new data base hardware suggest that the selection of the largest practical diameter (partial offset reflector antenna) structure that can be accommodated by current funding and technology limitations is 55-meters in diameter. The partial antenna would be composed of four full-size ribs, three mesh gores, a hub structure, and a deployable feed support structure. The selection of 55-meter diameter for the hardware represents an increase in size by a factor of 3.4 with respect to current wrap-rib antenna hardware demonstrations. The development of this size hardware will address the same basic problems associated with fabricating full-scale antennas (i.e., 100 meters in diameter).

Figure 8 overviews this process of definition and highlights the technology items to be influenced by the development model activity.



Figure 8

DESIGN OBJECTIVES FOR DEMONSTRATION (REF 1)

The specific objectives and goals established for the new data base over-viewed in Figure 9 include:

- o Demonstration and evaluation of deployment of a 55-meter diameter antenna;
- o Demonstration and verification of large size antenna fabrication, assembly, and alignment techniques and procedures;
- o Verification of the stability and durability of the mesh, rib, deployment mechanisms, and feed-support structure by repeated deployments;
- o Development and verification of tooling for rib and mesh gore assembly;
- o Verification of the predicted packaging densities of the ribs and mesh gore assemblies;
- o Verification of the deployment envelope of the reflector and feed support structure; and
- o Verification of analytical models used to predict full-scale antenna performance.

RIBS	<ul style="list-style-type: none">• JOINING/SPLICING• ROOT ATTACHMENT• STOW/DEPLOY
MESH	<ul style="list-style-type: none">• RIB ATTACHMENT• PANEL SPLICING• PRE-STRAIN/INSTALLATION
ASSEMBLY	<ul style="list-style-type: none">• DEPLOYMENT• STABILITY• CONTOUR REPEATABILITY

Figure 9

RIB TOOL DESIGN AND DEFINITION

The rib layup tool design, engineering and manufacturing definition was accomplished using CADAM (Computer Graphics Augmented Design And Manufacturing System). Engineering tool definition (reflector shape, three-dimensional tool contour and tool segments) was created on CADAM. CADAM then produced numerical control (N/C) tapes which defined the flat pattern part to be scribed, contour templates to be used in bump forming and bump-forming guide lines.



Figure 10

N/C TOOL SCRIBING

The N/C tapes generated by CADAM were then used to drive an N/C plotter, which scribed directly on the invar. The plotter scribed the rib centerline, rib bond and trim lines, flat pattern tool definition, bump forming guide lines and contour checking stations.

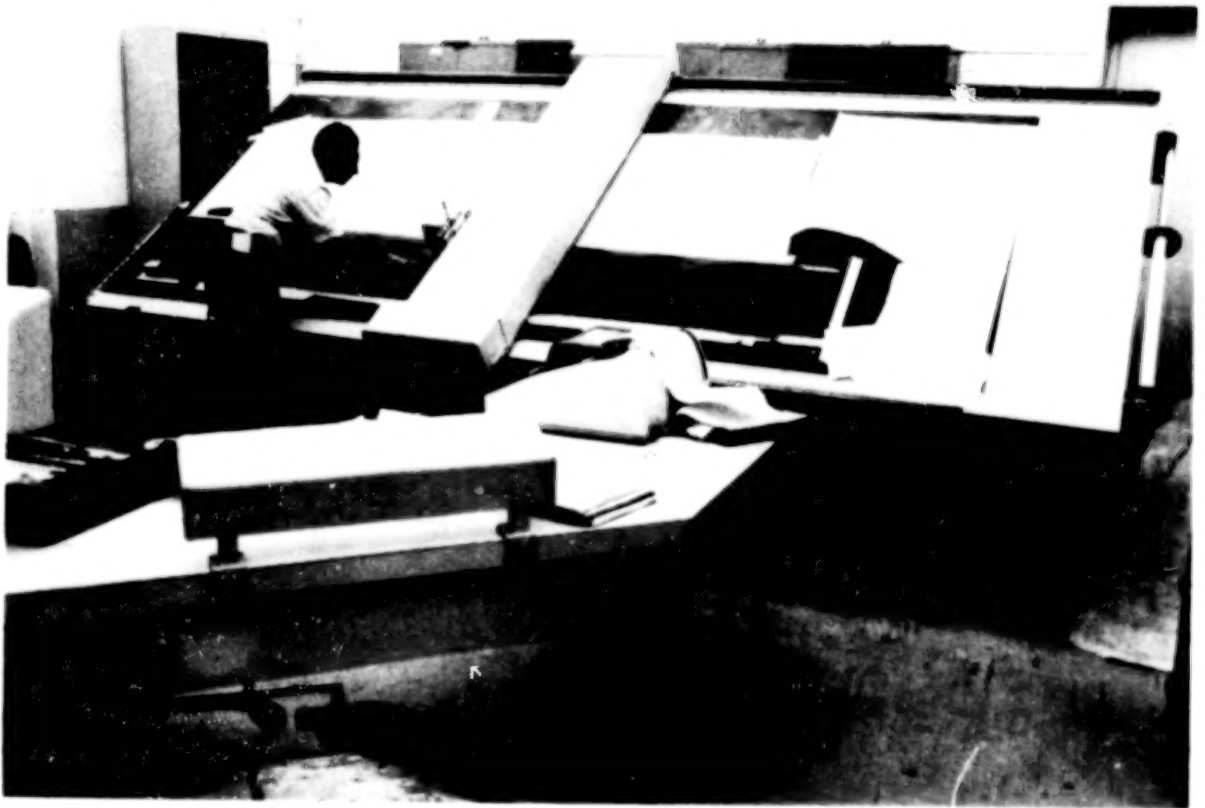


Figure 11

BUMP FORMING

The graphite epoxy layup surface of the tool (semi-lenticular shape) was generated by bump forming. A hydraulic brake with steel dies and a hard rubber reactor was used.



Figure 12

SHAPE CONTROL

The three-dimensional variation of the tool layup surface was generated using the bump forming guide lines for rib reflector curvature and cross-sectional rib contour templates at intervals along the length of the tool.



Figure 13

TOOL MATING

The bump formed semi-lenticular top is then mated to the base. The two parts are aligned, final contour checked and clamped together.



Figure 14

SPOT SEAM WELDING

The mated parts are then spot welded together to create a temporary assembly of the layup tool. The tool is then seam welded on both edges to create both a structural attachment and an air-tight joint.



Figure 15

RIB MANUFACTURING

Manufacturing of the rib is then accomplished by laying up the graphite epoxy directly on the rib layup tool.



Figure 16

GROUND TEST OF DATA BASE MODEL (REF 1)

The ground test of the 55-meter diameter proof-of-concept model will represent the largest ground-based demonstration for this concept. The ground test program will include: deployment and refurling of single rib structures, deployment and repeated refurling of the 4-rib partial antenna, measurement of rib stiffness and surface contour for comparison with analytical predictions. The reflector ribs will be supported during deployment and furling operation: (Figure 17). The rib support system consists of four sets of balance beam/carriage assemblies for each rib. These assemblies ride on fixed rails that are located radially with respect to the antenna. The deployment displacements of the ribs will be tracked by the carriage assemblies in the radial direction and by the balance beams in the vertical and lateral directions. This passive support system progressively offloads the weight of the ribs and mesh as they unfold from the central hub. To maintain the rib positions approximately colinear with the overhead support rails, the hub will be mounted on a platform that rotates during deployment. The three degrees of freedom accommodated to the ribs during deployment by the support system results in a controlled deployment sequence where the unfolding mesh is not affected by the rib support system. Since the effect of gravity loading on the mesh will tend to force the mesh against the deployment control devices, the ground demonstration of mesh management with respect to identifying snagging problems is considered conservative.

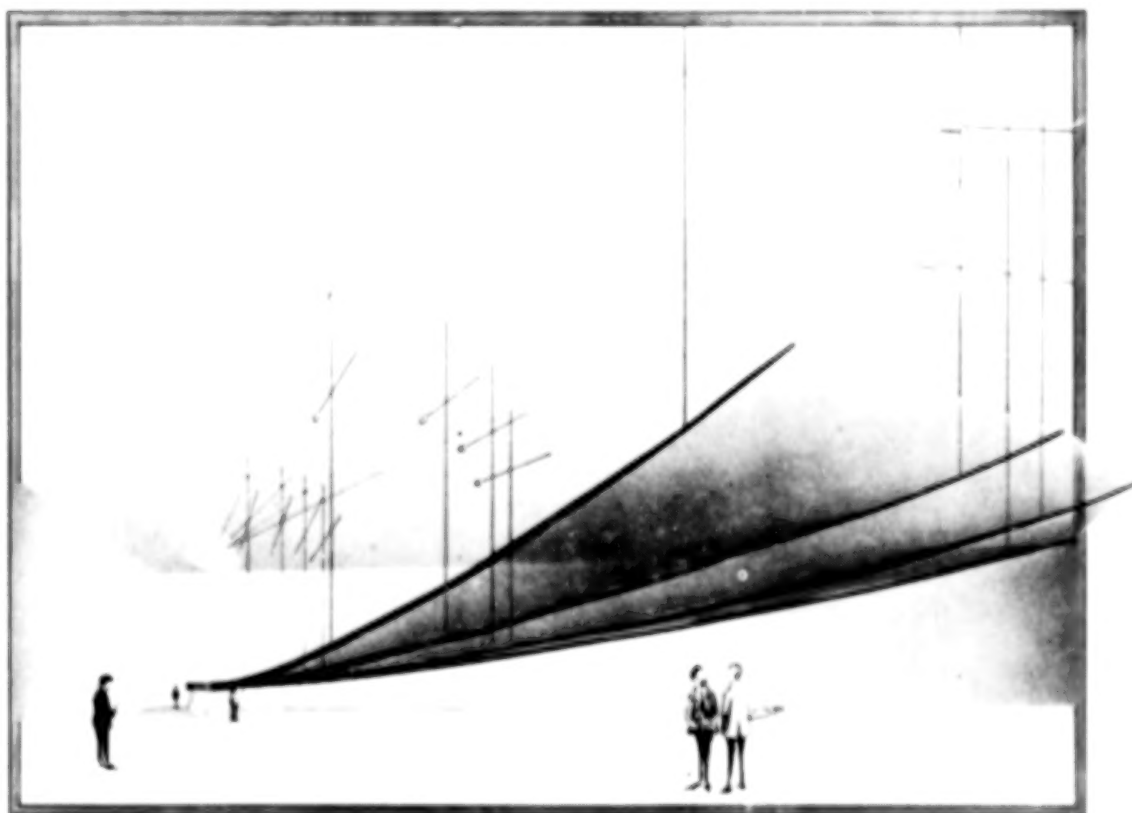


Figure 17

DEPLOYABLE MAST DEVELOPMENT ACTIVITY

The previous years activity concentrated on the development of the off-set Wrap Rib reflector characteristics. With the credibility of the concept established it became necessary to place emphasis on the deployable mast technology and a mast evaluation task was included in this years activity. To accomplish this task the initial step was to define critical requirements and an approach toward concept evaluation. This flow which led to the development of comparative performance data and evolved a new concept is overviewed in Figure 18. As suggested in the figure the concept which evolved borrowed heavily from approaches developed by several companies involved in deployable boom technology.

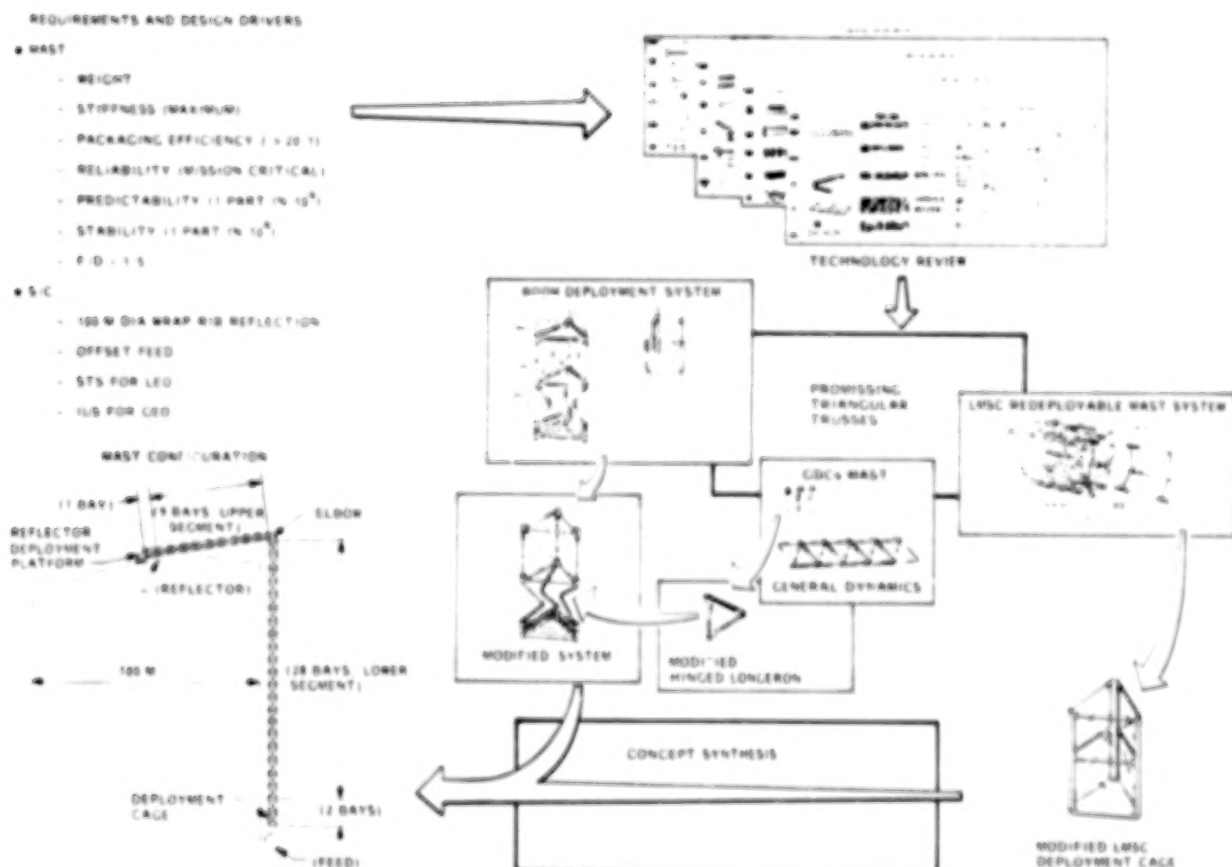


Figure 18

MAST CONCEPT COMPARATIVE CHARACTERISTICS

The results of the mast concept evaluation study are indicated in Figure 19. These data were obtained by equating stiffness and applying the design formulae as available in open literature. In all cases graphite epoxy construction was assumed. The results indicate that the hybrid tapered tube mast afforded the minimum weight approach and with the exception of the coilable longeron, the minimum stowed length. Since technical concerns exist with the compatibility of graphite epoxy and the coilable longeron approach, the tapered tube concept was selected for further study and characterization.

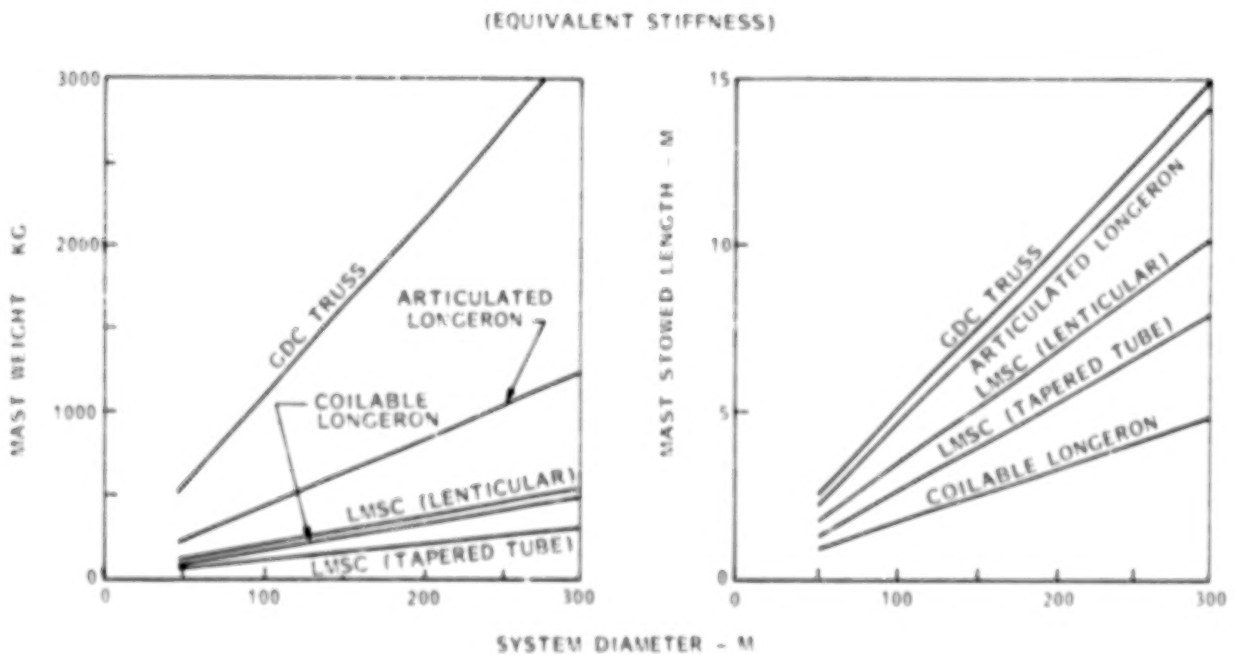


Figure 19

TAPERED TUBE DESIGN APPROACH

The tapered tube mast design, as implied in the name, is constructed with tapered graphite epoxy tubes as the major structural elements. These tubes are used as both longeron and batten members as shown in Figure 20. The longerons are hinged with a prestressed joint in the center which allows them to be folded so that the battens can be stowed next to each other for ascent. In the folding operation the longerons fold adjacent to the battens so that a maximum length can be used and the central area of the stowed package is open and available for equipment. The diagonal stiffeners are small diagonal high modulus graphite epoxy rods. The stowed package is completely contained within a rigid deployment cage which houses the deployment control device and can be used to mount spacecraft components. Deployment is accomplished one bay at a time so that stiffness is maintained throughout the event.

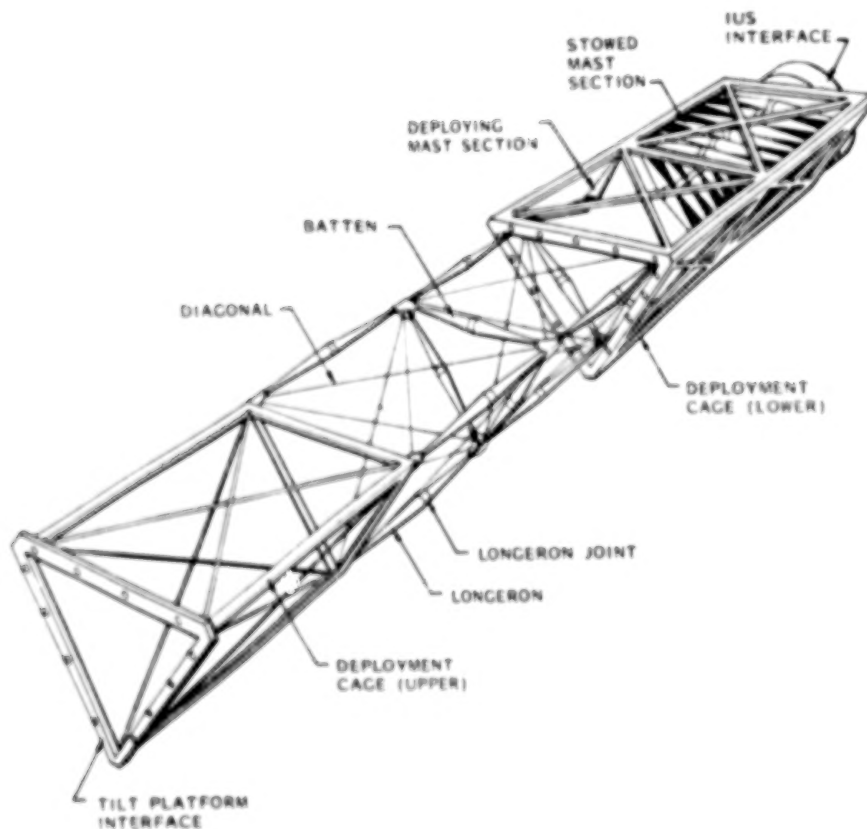


Figure 20

APPROACH TOWARD DESIGN CHARACTERIZATION

The approach taken to develop the parametric design characteristics of the deployable tapered tube mast focussed on the construction of a computer aided design package. The design package was constructed to accept basic material and structural element characterization and develop design solutions which satisfied these inputs and the mission constraints of weight, stowed diameter and antenna system geometry. The developed designs were then analyzed to determine the system stiffness, load carrying capability and thermal stability. This characterization sequence is overviewed in Figure 21.

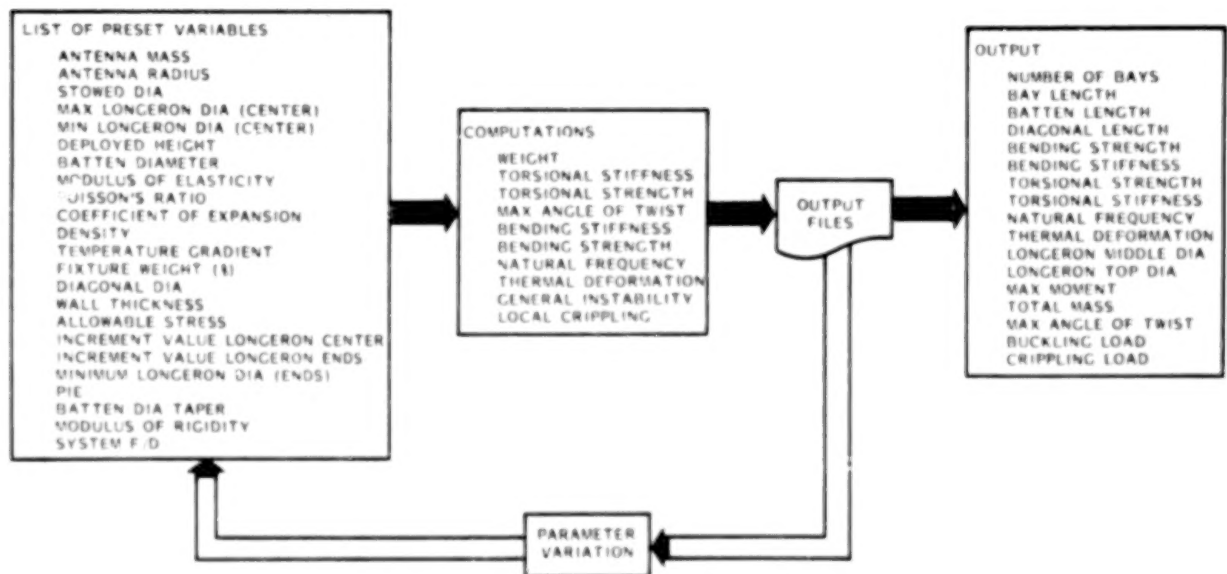


Figure 21

SYSTEM STIFFNESS CHARACTERISTICS

The characterization activity yielded the stiffness information presented in Figure 22. The bounds on the data include a mast bay aspect ratio (bay length/bay foot print) of 1.0 with 10 cm diameter longerons and an aspect ratio of 1.8 with a longeron diameter of 2.5 cm. These present reasonable bounds on the design as indicated during data development. The STS/IUS and STS limits indicated on the curve show the design as constrained by available cargo bay length. This data indicates that the mast stiffness characteristics, as defined by the minimum system natural frequency of the combined bending-torsional mode of the L-shaped structure, will be between 0.01 and 0.3 Hz. Mass allocation for the structure in the 200 to 400 Kg region will not be a limiting factor.

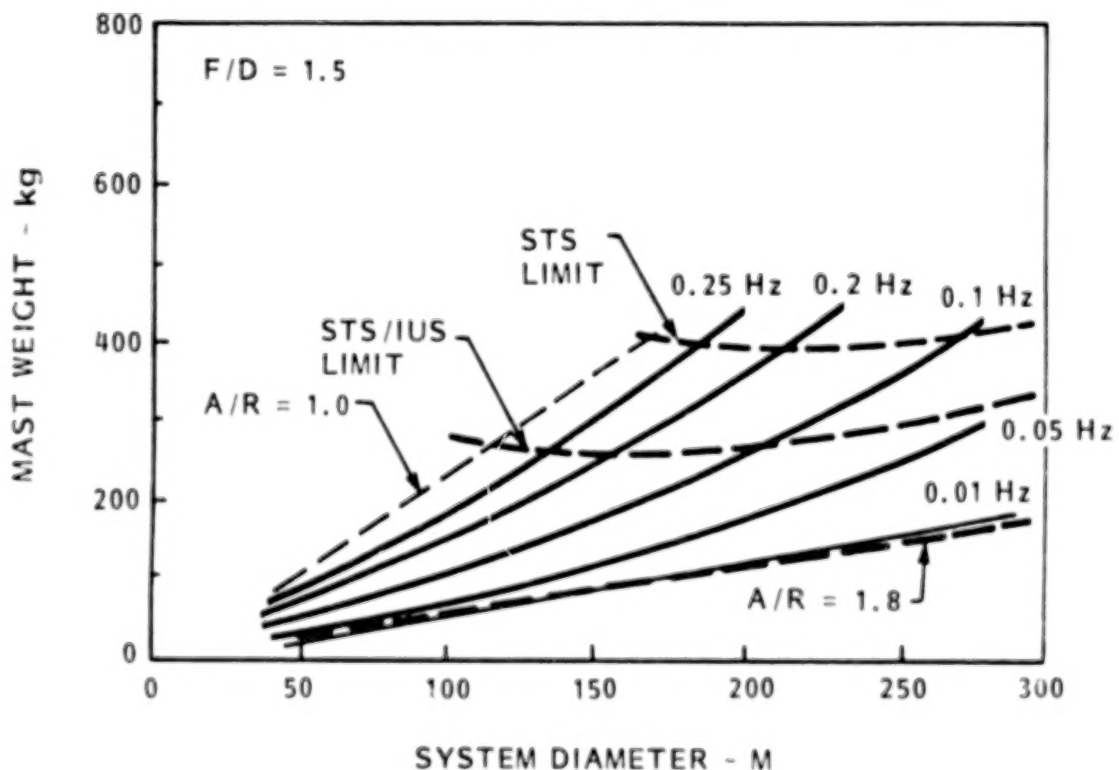


Figure 22

STOWED CHARACTERISTICS

Although the previous figure indicates a potential excess in stowed length requirements, Figure 23 shows that a reasonable stowed length is available for 50 to 150 m class antennas. In fact stowed lengths of as little as 2 m can be obtained for the 150 m structure if the low natural frequency is acceptable.

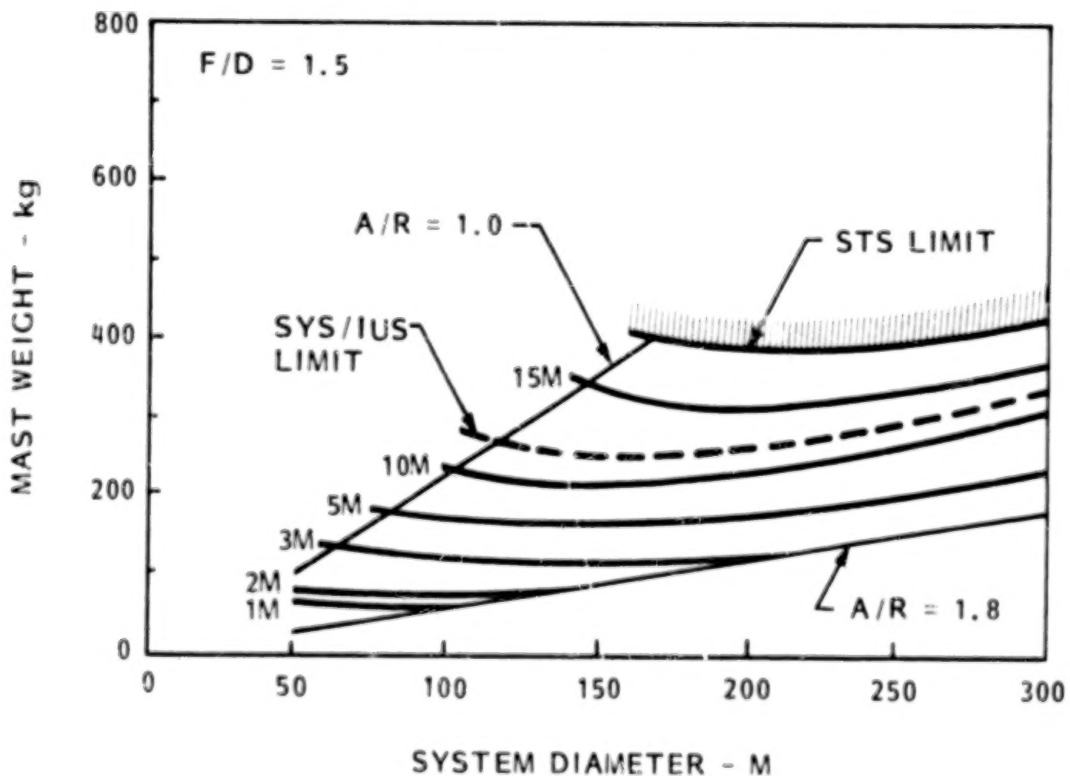


Figure 23

CONCLUSIONS

The conclusions which can be drawn at this interim point in the development program are shown in Figure 24. Sufficient activity has been accomplished to assure the ability to manufacture multiple segment ribs and the expected costly tooling has been successfully redesigned to reduce cost. The mast design which has evolved is potentially superior to previous concepts and will provide adequate stiffness and minimum stowed volume. This concept should provide a firm ground from which to embark on a mast development activity.

- RIB SPLICING AND JOINING CAN BE ACCOMPLISHED
- REFLECTOR COSTS CAN BE REDUCED THROUGH REVISED TOOLING APPROACH
- HIGH STIFFNESS MASTS CAN BE DESIGNED COMPATIBLE WITH OFFSET GEOMETRY AND STS CONSTRAINTS
- FURTHER ACTIVITY SHOULD BE DIRECTED TOWARD A MAST DATA BASE DESIGN/TEST PROGRAM

Figure 24

REVISED COST PROJECTIONS

The most significant program impact can be seen in the effect of the revised tooling design. The new tooling requirements were used to update the cost algorithm in the antenna design package. This revised program was executed for the same set of parametric designs used in last years presentation. The results shown in Figure 25 indicate that the reduction in tooling expense and part count has a significant cost benefit.

OFFSET ANTENNA COST PROJECTIONS

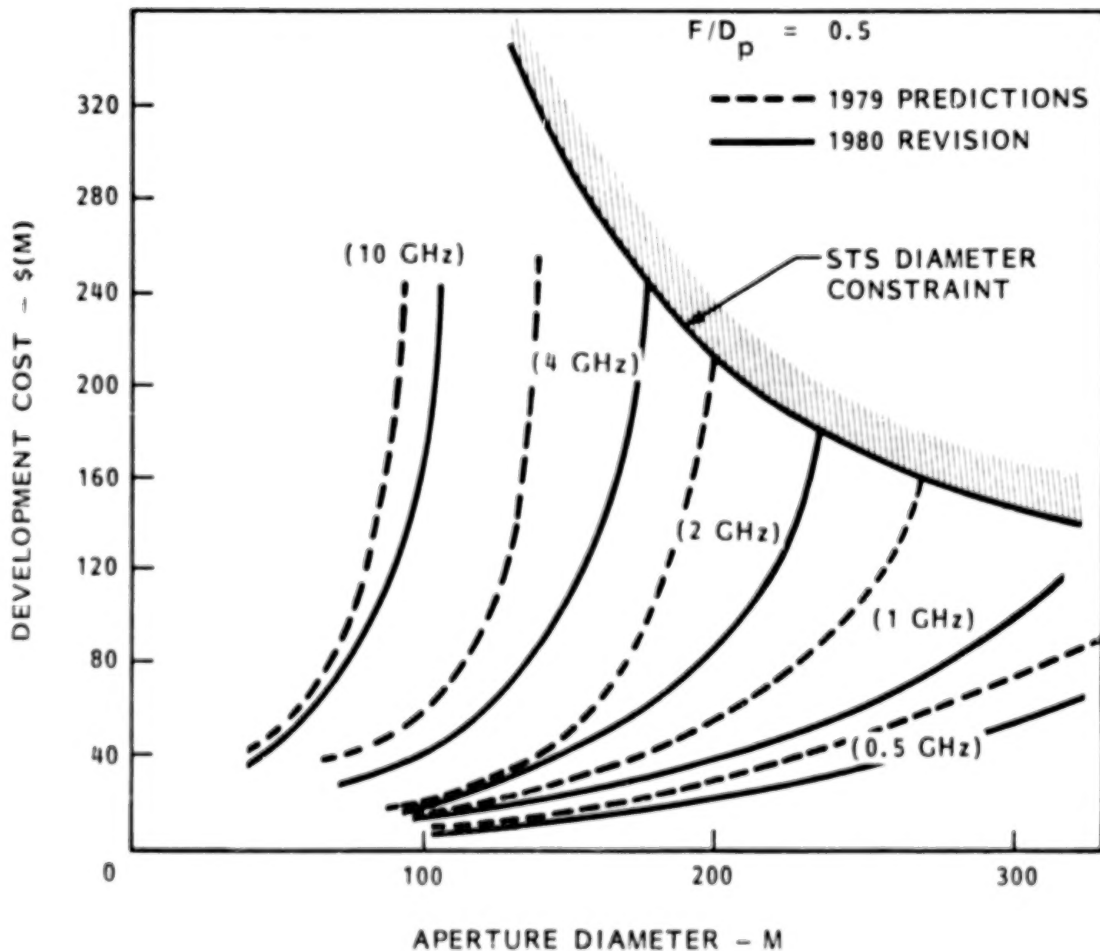


Figure 25

TECHNICAL CONCERNS

Even though we are deeply involved in the present development program and have yet to uncover a major technology limit these remain substantial technical concerns. The reflector concerns stated in Figure 26 will be gradually removed in the course of the present program. The mast activity and corresponding concerns are now about one year behind the reflector activity. Removal of these concerns will be required prior to a flight program undertaking and this can only be accomplished through a hardware program.

REFLECTOR

- ASSEMBLY/ALIGNMENT FACILITY REQUIREMENTS
- MESH MANAGEMENT
- VEHICLE STABILITY DURING DEPLOY/RETRACT
- OPERATIONAL CONTROL SYSTEM INTERACTION/STABILITY

MAST

- ACCURACY OF ANALYSIS OVER RANGE
- DEVELOPMENT OF JOINTS
- DEVELOPMENT OF DEPLOYMENT CONTROL DEVICE
- ASSEMBLY AND ALIGNMENT
- I-G TESTABILITY
- CONTROL SYSTEM INTERACTION/STABILITY

Figure 26

PROGRAM PLAN

The success of the current program indicates continuation will yield substantial technological and cost benefits. The success in the reflector development should encourage definition of a similar activity in the deployable mast design and proof-of-concept development. In addition sufficient analytical capability now exists to provide detailed, credible design information to emerging programs. It is suggested that an exchange of this design information be initiated. Figure 27 summarizes recommended activities and key objectives.

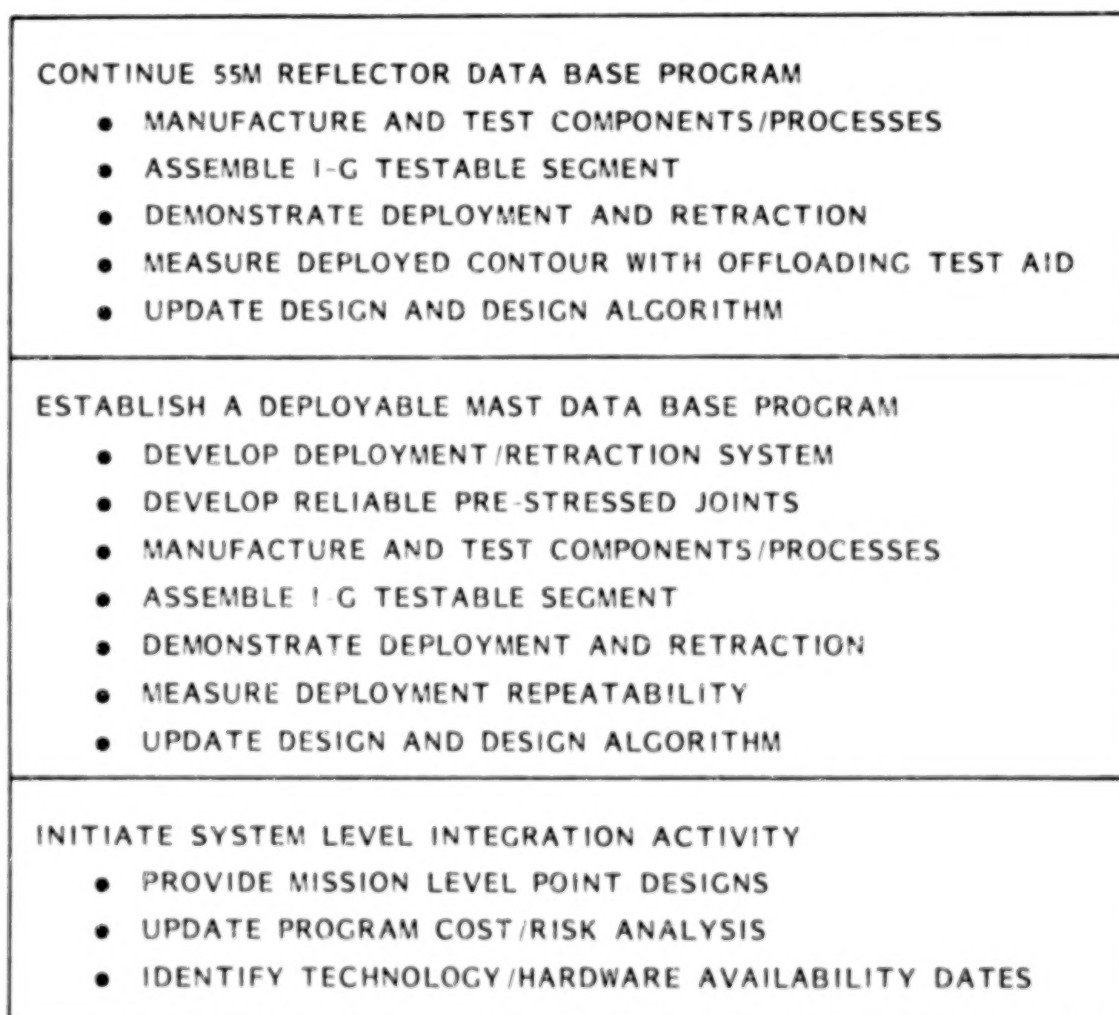


Figure 27

REFERENCE

1. Russell, Campbell and Freeland; A Technology Development Program for Large Space Antennas; Paper Number IAF-80 A33, Thirty-first International Aeronautical Congress of the International Astronautical Federation, September 1980.

BLANK PAGE

BLANK PAGE

ANALYTICAL PERFORMANCE PREDICTION
FOR LARGE ANTENNAS

M. El-Raheb
Jet Propulsion Laboratory, California Institute of Technology
Pasadena, California

Large Space Systems Technology - 1980
Second Annual Technical Review
November 18-20, 1980

STRUCTURAL DESIGN CONCEPT AND OBJECTIVES

Reflectors ranging in size between 50 and 100 meter in diameter are presently in the process of conceptual design. The operational radio frequency of these antennas lies between 3 and 10 GHz. One of the suggested design concepts is the Lockheed Missile and Space Corporation wrap-rib mesh deployable antenna (ref. 1). This particular reflector consists of a central hub around which are wrapped the graphite epoxy ribs that form the skeleton supporting structure. The rib cross section is of lenticular type and is specifically designed to elastically collapse while furling the reflector for storage. The reflective surface is a moly-gold woven mesh which is attached eccentrically to the concave surface of the ribs. The criterion for rib design is based on column collapse under its own weight in a one g environment. The direction and number of orthotropic graphite laminates in the rib construction are chosen to optimize thermal and shear carrying properties. The mesh is attached to the rib skeleton in a pretensed condition sufficient to provide out-of-plane membrane stiffness but always below the pretension that might cause pillowling. Such a pretension is comparatively small and leads, in most situations, to small but finite coupling between the different ribs. The mesh pretension and the elasticity of the central hub are the only two mechanisms through which the rib motions can be coupled in the linear sense.

The principal aim of this study is to numerically simulate the surface distortion resulting from thermal loading and transient oscillations from control. The discrete finite element nodal displacements can be fitted by continuous (zeroth and first derivative) surfaces using splines. These surfaces then form the basis for the evaluation of radio frequency performance in the different stages of the static and dynamic response.

An essential requirement in the process of modelling is to construct efficient (inexpensive) numerical algorithms while retaining the accuracy of the results. Hopefully, these programs will be used by the designer and analyst for parametric decisions in the conceptual stage of the design of this class of structures.

ANALYTICAL APPROACH

A linear mathematical modeling of the static and dynamic characteristics of this type of structure was first attempted using small amplitude motions. Although the ribs can be modeled as slender beams of varying cross sections and equivalent linear material properties, the mesh poses a problem since its equivalent stress strain relations are highly nonlinear and sensitive to the biaxial prestressed state. Consequently, the macroscopic material properties are measured experimentally in the neighborhood of the design prestress. An equivalent tangent modulus technique is then adopted about this equilibrium state and assumed to be valid within a small range of incremental stresses. The range of validity of the adopted linearized theory is yet to be determined using a more exact nonlinear analysis where material properties are allowed to change with instantaneous strain level. Since the structure possesses cyclic symmetry about the reflector axis, only one of many segments is modelled using finite elements. The succeeding segments satisfy continuity of displacement and slope at the interface between two consecutive segments. This process enables us to solve $(N/2 + 1)$ static or dynamic problems of substantially smaller order and bandwidth where N is the number of segments. The solutions of each of the $(N/2 + 1)$ transformed problems lead to motions having a distinct circumferential wave number " n ". This technique substantially decreases computational cost.

The technique described above is valid whenever the structure possesses cyclic symmetry. Since only the reflector belongs to this class, the dynamic coupling to the feed support structure is studied by adopting modal synthesis, thus retaining the useful qualities of cyclic symmetry. The eigenvalue problem of the reflector is determined in the usual efficient way with the hub clamped. A separate eigenvalue problem is solved for the truss-like feed support structure with the same fixity conditions at the interface connections to the reflector. The combined eigenfunction and mass matrices are then divided into rigid body and elastic parts. The size of the new eigenvalue problem reduces to the total number of combined modes of the reflector and feed support.

THE 15 METER EXPERIMENTAL REFLECTOR

The geometric characteristics of this reflector are listed below:

Outside radius	7.6 m (300 in.)
Hub radius	1.1 m (43 in.)
Focal length	7.6 m (300 in.)
Number of equidistant ribs	18 (graph. epoxy 0/90/90/0)
Mesh prestress	$N_r = 1.8 \text{ N/m (0.01 lb/in.)}$, $N_c = 3.6 \text{ N/m (0.02 lb/in.)}$
Mass of reflector excluding hub	5.67 kg (0.3886 slugs, 150 lbs on earth)

The finite element simulation has the following characteristics:

No. of elements per segment	27 rib elem. + 184 mesh elem.
Total number of nodes	3276 nodes
Total number of degrees of freedom	11178 D.O.F.
Cost on CDC-7600 for 16 frequencies	\$92.

The mesh mass constitutes less than 5% of the reflector mass excluding the hub. It is therefore anticipated that the mesh will have a negligible dynamic effect on the attitude control of the antenna. For the present simulation, the mesh dynamic modes were suppressed by lumping the mesh mass onto the supporting ribs. Note however that the mesh modes might be important in the evaluation of "surface quality" as affecting radio frequency performance.

Some representative mode shapes are shown in figures 1 to 7, while resonances in hertz are given in table I.

TABLE I

	n = 0	n = 1	n = 2	n = 3	n = 4	n = 5
1	3.9613	3.9603	3.9588	3.9581	3.9585	3.9587
2	3.7590	3.7813	3.8440	3.9367	4.0465	4.1594
3	4.7815	4.7819	4.7832	4.7855	4.7888	4.7932
4	5.7357	5.7358	5.7360	5.7364	5.7368	5.7373
5	6.6103	6.6102	6.6101	6.6099	6.6095	6.6092
6	6.7259	6.7251	6.7227	6.7191	6.7146	6.7100
7	7.4559	7.4559	7.4559	7.4559	7.4560	7.4566
8	8.0872	8.0867	8.0853	8.0831	8.0805	8.0778
9	8.2621	8.2621	8.2622	8.2622	8.2622	8.2622
10	9.0221	9.0221	9.0219	9.0217	9.0215	9.0212
11	9.1701	9.1696	9.1683	9.1665	9.1645	9.1626
12	9.4938	9.4980	9.5102	9.5293	9.5534	9.5802
13	9.7454	9.7454	9.7455	9.7457	9.7458	9.7463
14	10.100	10.099	10.096	10.090	10.081	10.070
15	10.211	10.209	10.205	10.199	10.191	10.184
16	10.526	10.526	10.526	10.526	10.526	10.526

Some Resonances of the 15m. WRAP Rib Reflector (mesh modes included)

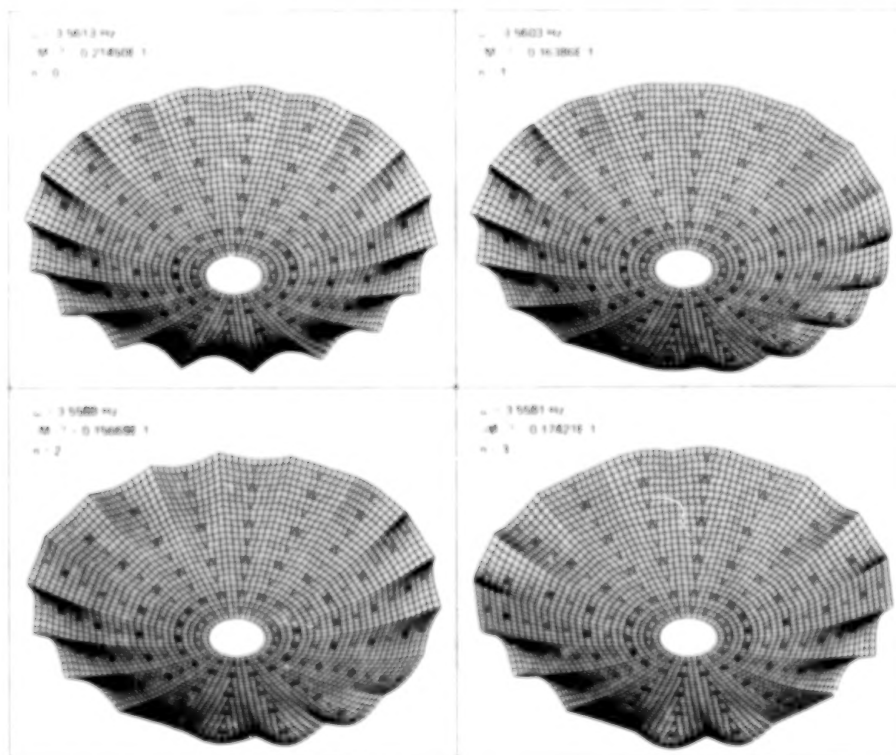


Figure 1. Clamped Wrap-Rib Reflector (15 M. Dia., 18 Ribs)
(Mesh Modes Included)

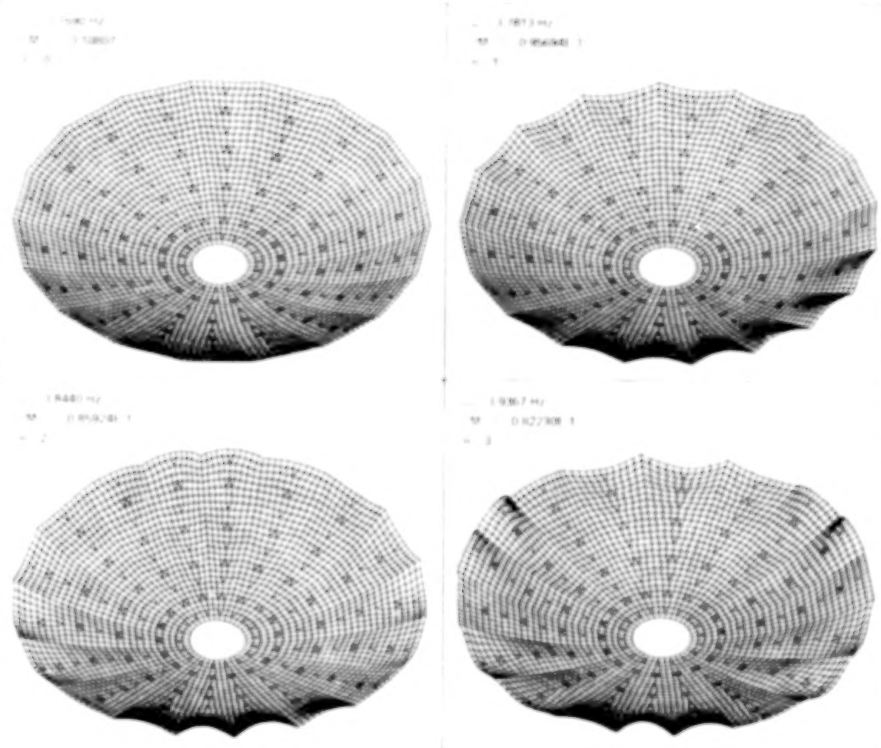


Figure 2. Clamped Wrap-Rib Reflector (15 M. Dia., 18 Ribs)
(Mesh Modes Included)

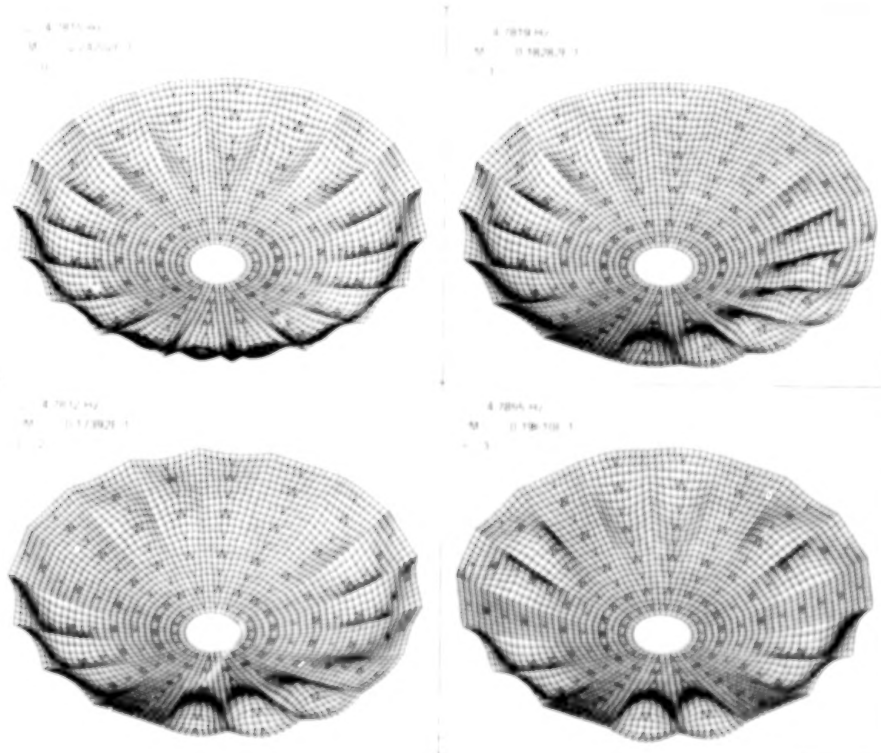


Figure 3. Clamped Wrap-Rib Reflector (15 M. Dia., 18 Ribs)
(Mesh Modes Included)

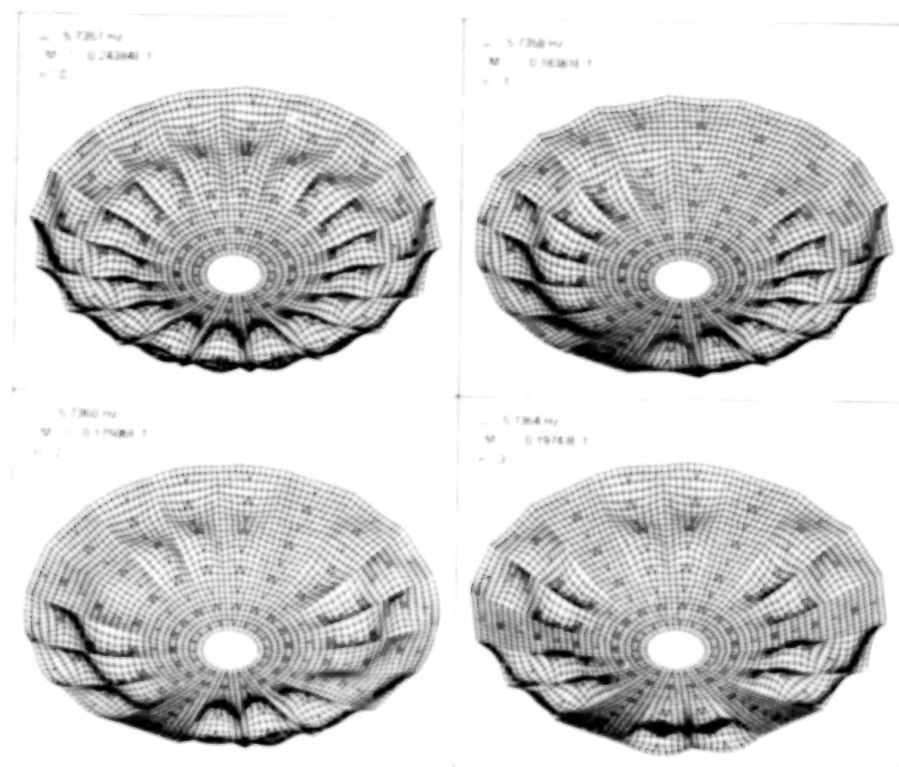


Figure 4. Clamped Wrap-Rib Reflector (15 M. Dia., 18 Ribs)
(Mesh Modes Included)

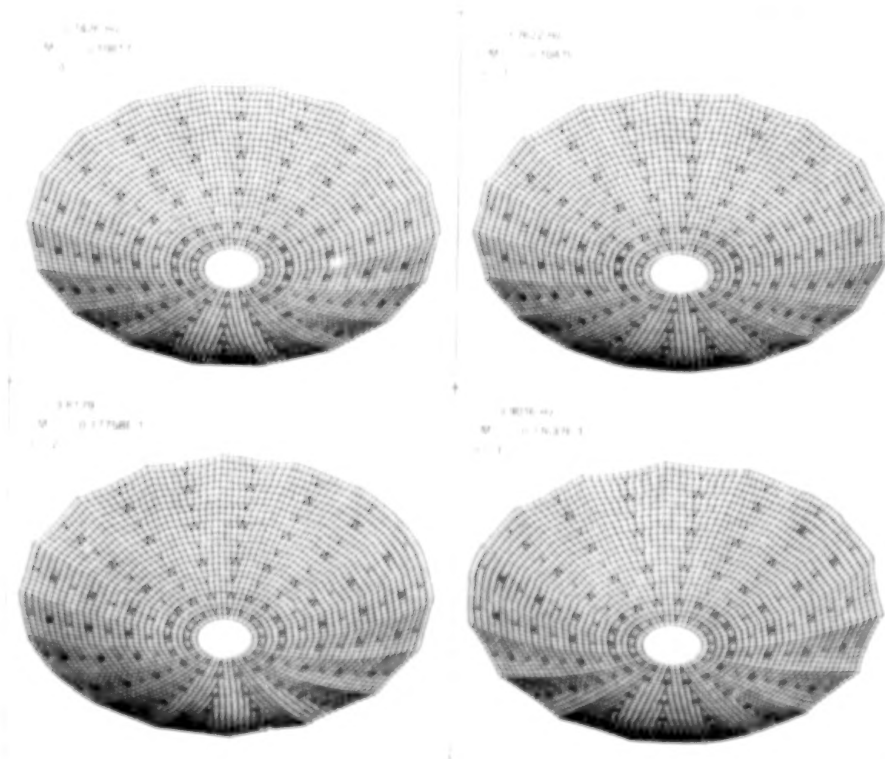


Figure 5. Clamped Wrap-Rib Reflector (15 M. Dia., 18 Ribs)
(Suppressed Mesh Modes)

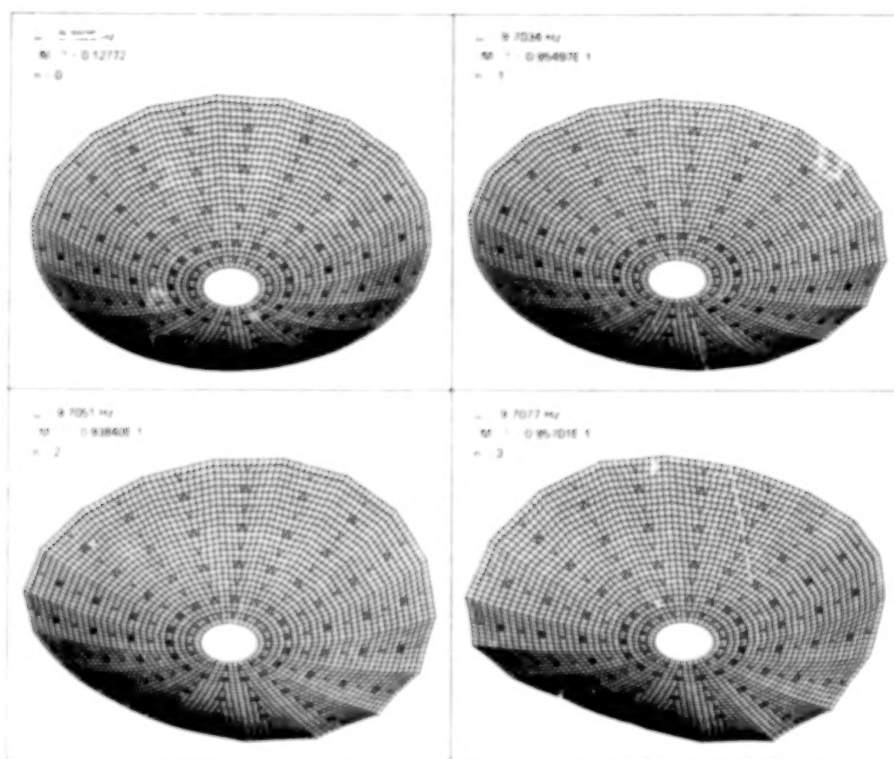


Figure 6. Clamped Wrap-Rib Reflector (15 M. Dia., 18 Ribs)
(Suppressed Mesh Modes)

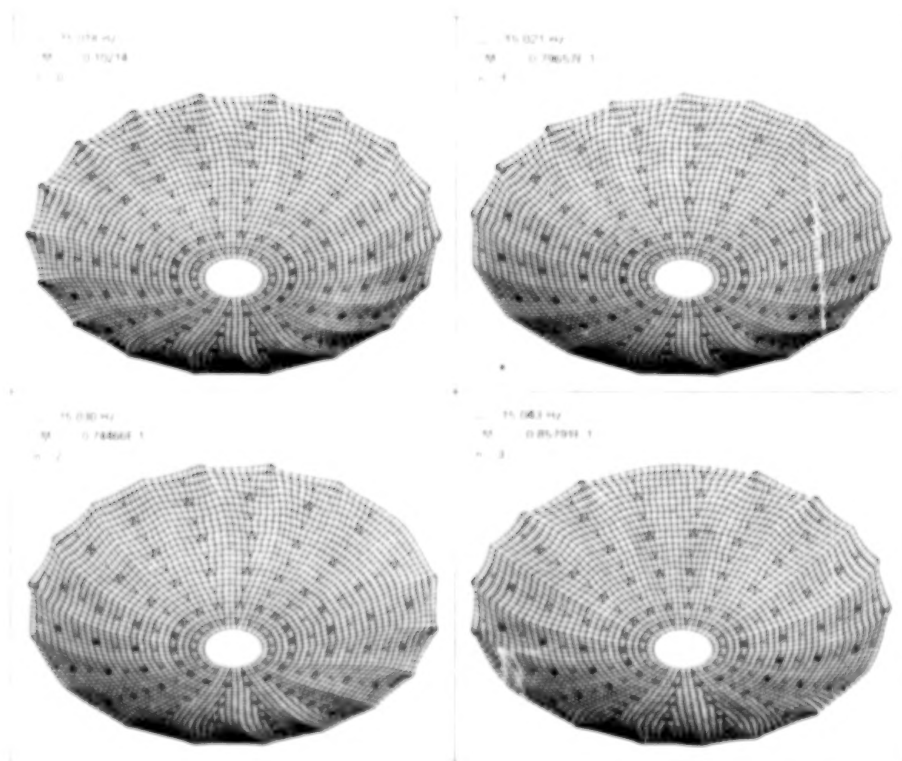


Figure 7. Clamped Wrap-Rib Reflector (15 M. Dia., 18 Ribs)
(Suppressed Mesh Modes)

THE 3 GHz 55 METER REFLECTOR

The geometric characteristics of this reflector are listed below:

Outside radius	27.5 m (1083 in.)
Hub radius	1.2 m (46 in.)
Focal length	83.8 m (3300 in.)
Number of equidistant ribs	48 (graph. epoxy 45/0/45)
Mesh prestress	$N_r = 0.18 \text{ N/m (0.001 lb/in.)}$, $N_c = 0.36 \text{ N/m (0.002 lb/in.)}$
Mass of reflector excluding hub	38.38 kg (2.63 slugs, 1015 lbs on earth)
Mass of mesh	2.09 kg (0.143 slugs)

The finite element simulation has the following characteristics:

No. of elements per segment	40 rib elem. + 140 mesh elem.
Total number of nodes	6624 nodes
Total number of degrees of freedom	25488 D.O.F.
Cost on CDC-7600 for 16 frequencies	\$103.

This reflector exhibits rib bending modes coupled to mesh modes suggesting that the rib was optimally designed.

Representative mode shapes are shown in figures 8 to 10.

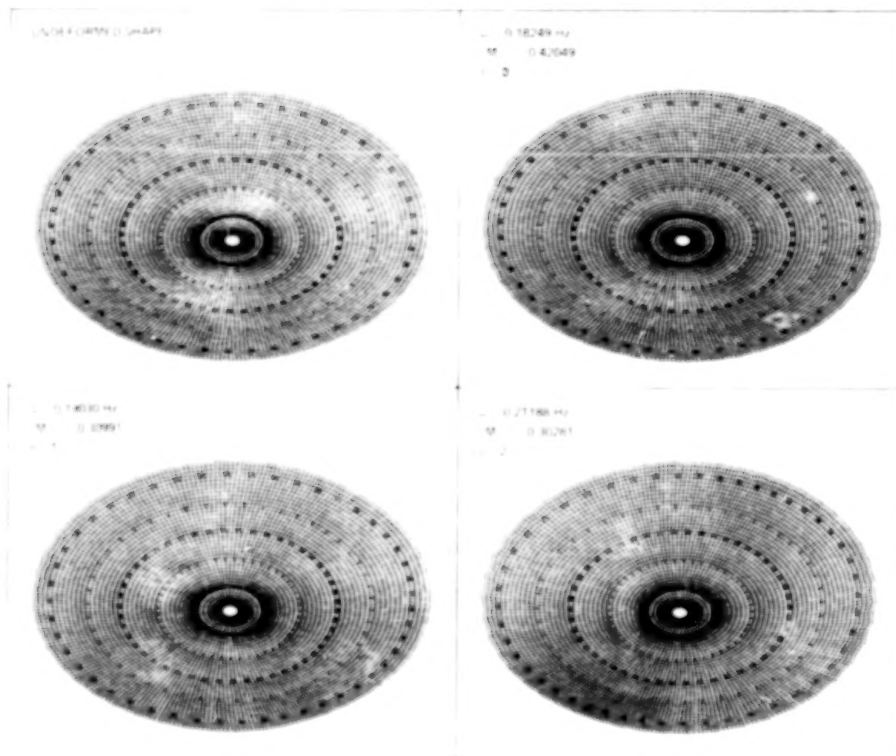


Figure 8. 55 Meter Rigid Hub Reflector with 48 Ribs
(Mesh Modes Included)

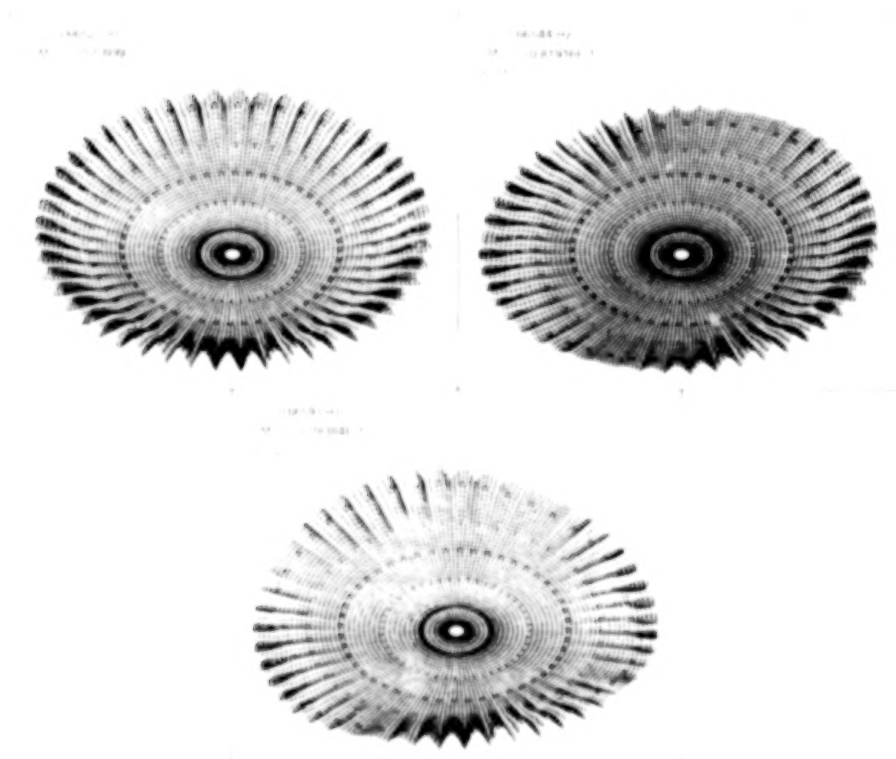


Figure 9. 55 Meter Rigid Hub Reflector with 48 Ribs
(Mesh Modes Included)

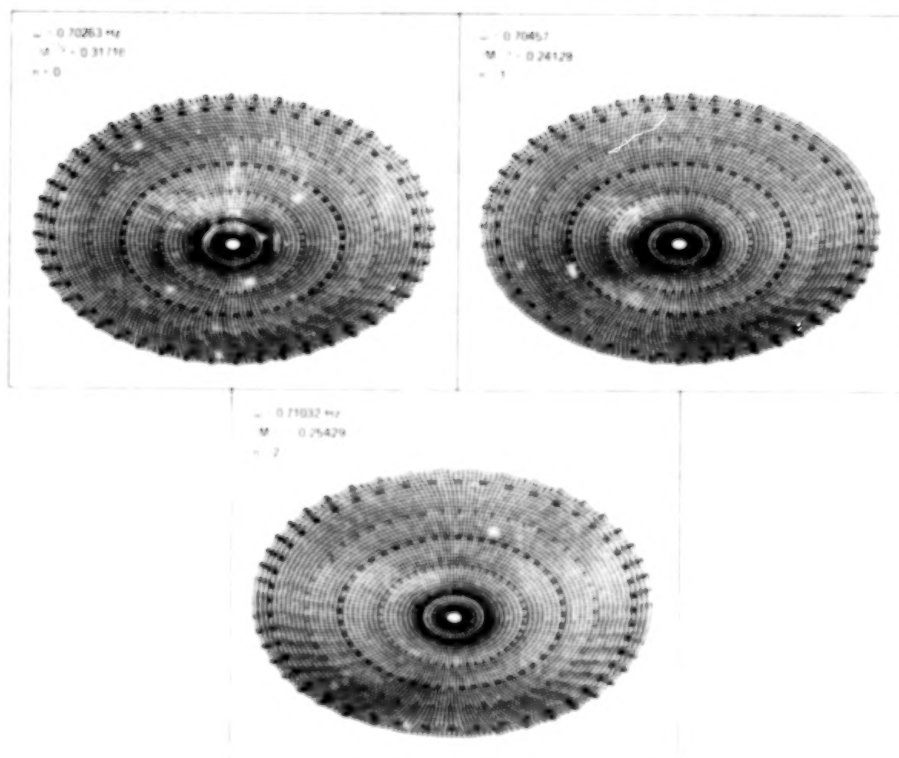


Figure 10. 55 Meter Rigid Hub Reflector with 48 Ribs
(Mesh Modes Included)

A simplified model of the reflector and feed support structure was analysed with no cyclic symmetry or modal synthesis. The total number of degrees of freedom was 342 and the cost was comparable to the 25000 degree of freedom model of the reflector alone. This example demonstrates the necessity of the proposed technique (use of cyclic symmetry and modal synthesis) for parametric analysis of this class of structures.

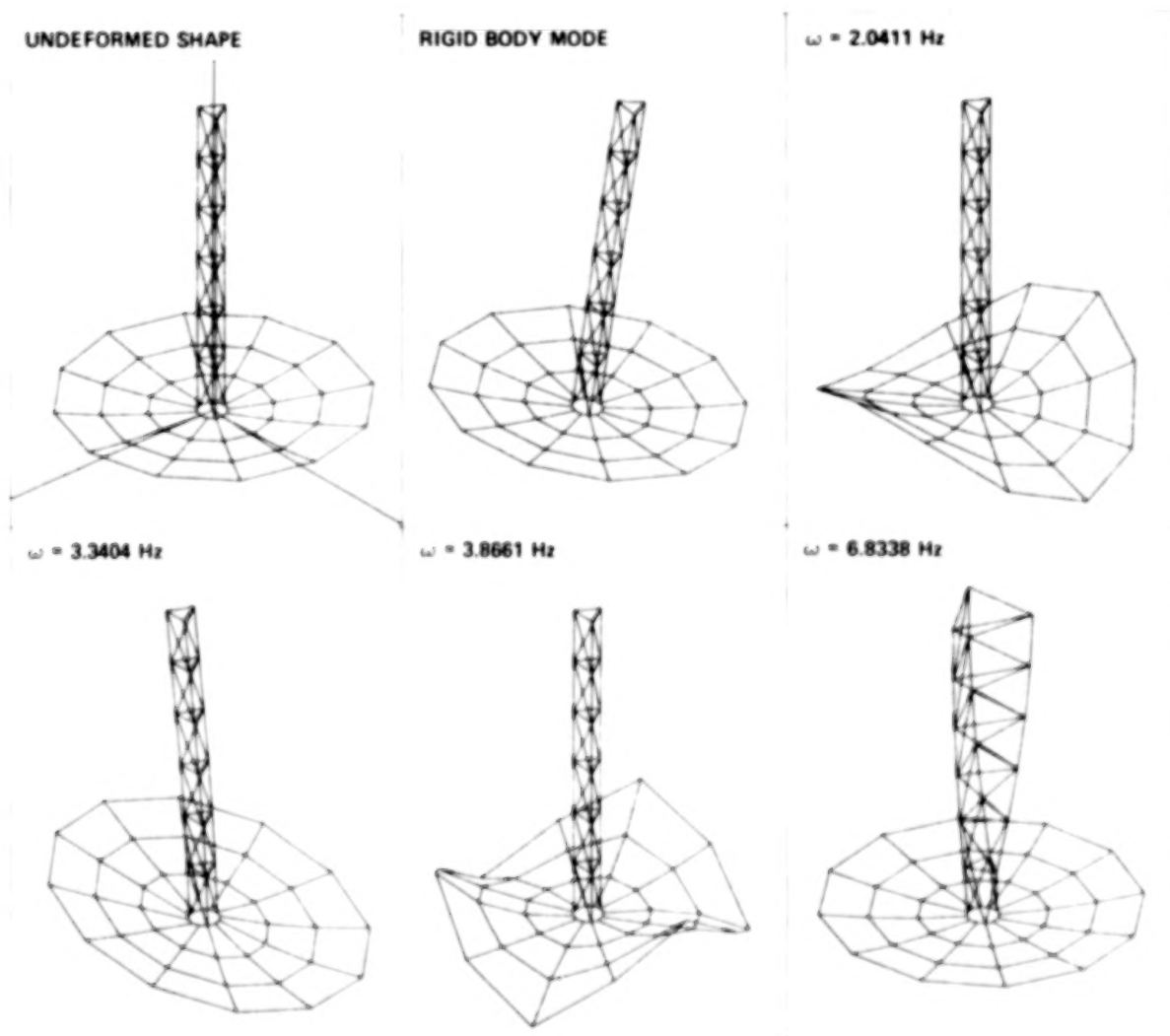


Figure 11.- Simplified Model (342 Degrees of Freedom).

Reference

1. Woods, A.: Final Report for Study of Wrap-Rib Antenna Design. Lockheed Missiles & Space Company, Inc.

BLANK PAGE

BLANK PAGE

JPL SELF-PULSED LASER SURFACE MEASUREMENT
SYSTEM DEVELOPMENT

Martin Berdahl
Jet Propulsion Laboratory
Pasadena, California

LSST 2ND ANNUAL TECHNICAL REVIEW

November 18, 19, 20, 1980

INTRODUCTION AND BACKGROUND

JPL recently made a study of several methods and systems for measurement of antenna surface curvature. The investigation covered the use of methods varying from comparatively simple to extremely complex, high resolution systems using phase comparison and optic interferometry. A system of intermediate complexity which is of suitable capability for measuring early deployed antennas was demonstrated by Lockheed Missiles and Space Corp. under Contract No. 955130 to JPL. Some systems used angular measurement techniques rather than distance measurement to determine surface distortion. Most of the promising systems are presently in the development stage. Some have the projected capability of satisfying the requirements of future conceptual designs. The measuring system now under development at JPL is intended to satisfy requirements of early deployable concepts such as the LMSC offset wrap rib antenna.

SURFACE MEASUREMENT ACCURACY REQUIREMENTS FOR LARGE SPACE ANTENNAS

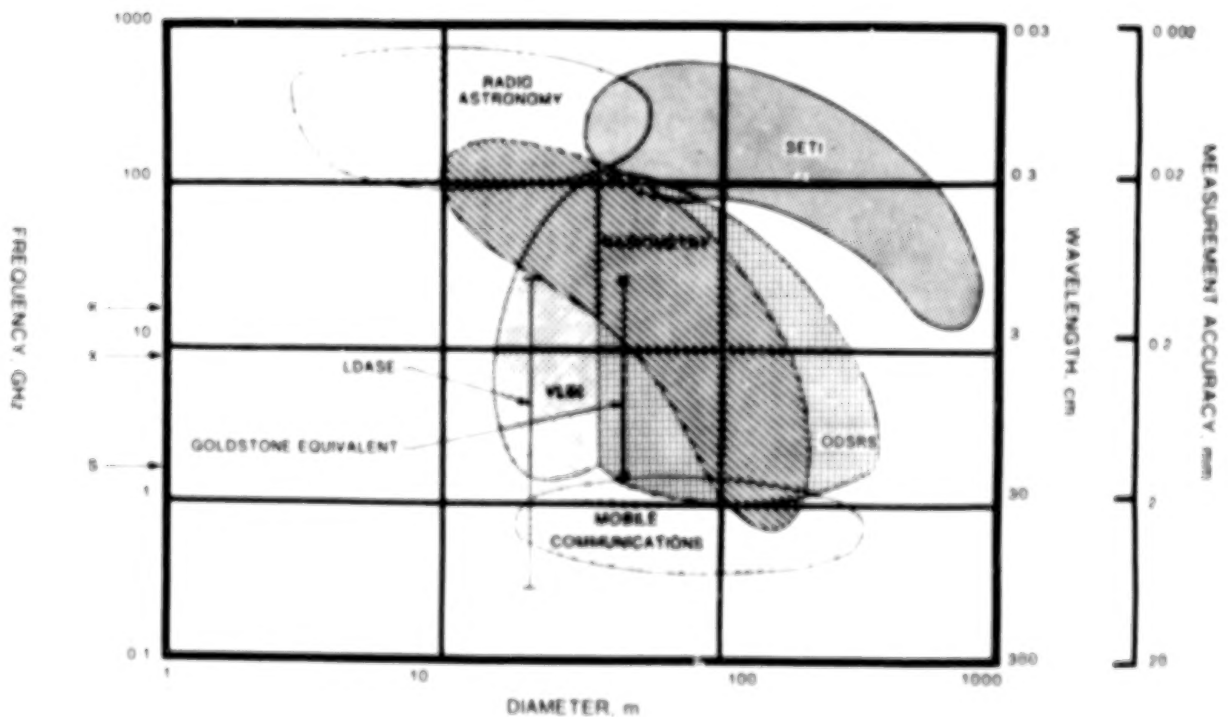


Figure 1

SELF-PULSED LASER RANGING SYSTEM

The self-pulsed laser ranging system is used for measuring distances from a fixed reference or scan position to several locations on the surface of an antenna reflector. Processing the information thus obtained is used to define the "figure" or shape of the surface upon which antenna operational efficiency is directly dependent.

Operation of the system consists of initiating a pulse from the laser emitter which is pointed at the scan mirror. The emitted pulse strikes the scan mirror, is reflected and sent to one of several targets located on the surface of the antenna. Upon reflection from the target, the pulse returns to a detector via the scan mirror. The detected pulse is amplified and used to trigger the next emitted pulse. After the first pulse is emitted, received and used to trigger another pulse the process becomes repetitive with a repetition rate uniquely determined by the distance traveled to the target and back. A measure of the repetition rate or frequency thus created provides the means required for determining range since the total distance traveled is inversely proportional to the frequency.

During its round trip travel, the emitted pulse traverses the distance from the laser to the target and back to the detector at the speed of light. It then proceeds through electronic circuitry with some delay until it triggers another light pulse. A distance equivalent to the time delay realized by the travel time of the returning pulse from the scan mirror to the detector, through the electronics, and back to the scan mirror may be subtracted from the total distance to provide a precise measure of the round trip distance from the scan mirror to the target.

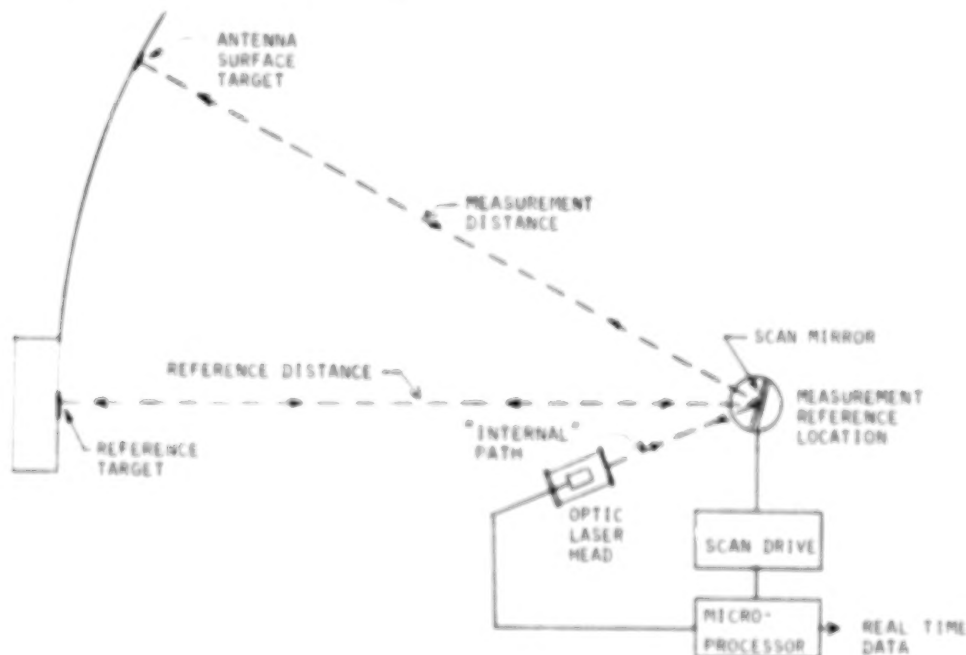


Figure 2

OBJECTIVES OF FY80 EFFORT

During FY79 the concept of electro-optically measuring a distance using a self pulsed laser oscillator was tested. Results conclusively verified the concept and projected the feasibility of making long distance absolute measurements with an expected accuracy and resolution in the order of a few millimeters or less. Out of this success came several objectives for the FY80 effort.

1. Develop a breadboard hardware system.
2. Test and upgrade
3. Project performance capability.

APPROACH

Improve hardware to the point where realistic performance tests could be made with simulated antenna measurement geometry.

HARDWARE DEVELOPMENT

Hardware development in FY80 consisted of completion of the "optic head", insertion of a fiber optic delay line, purchase and modification of a microprocessor/computer, and iterative improvements of electronic components. As a result of this process a background of information has been acquired for use as a guide to the design of an improved engineering prototype system.

A block diagram of the system is shown in the figure below. The hardware consists of an optic head, a fiber optic delay line, a scan mirror, a target retroreflector, a microprocessor/computer, and a power supply. Since midyear FY80 the system has been operational and provides a printout of distance measurements in meters in real time.

SYSTEM BLOCK DIAGRAM

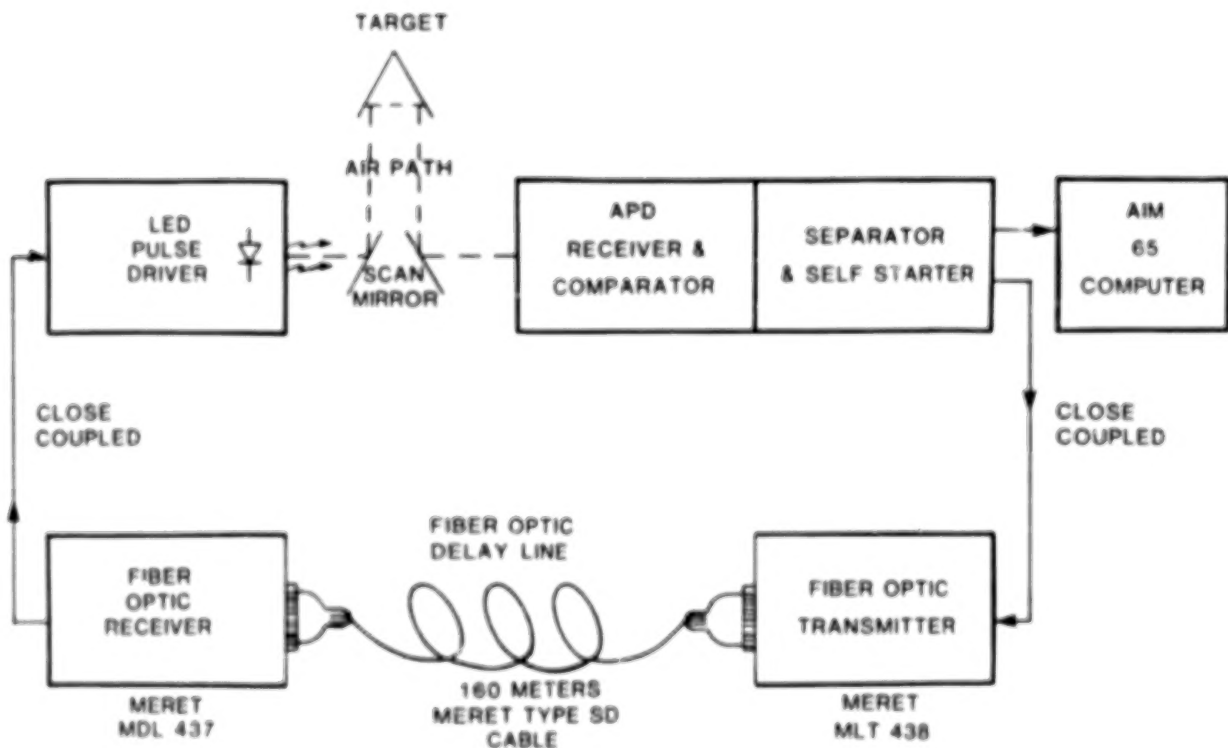


Figure 4

HARDWARE DEVELOPMENT OPTIC HEAD

The optic head, which was started in FY79, has been completed, modified and used in FY80 for many hours of testing. The optic head is used to generate, transmit, receive, and detect short light pulses from a Light Emitting Diode (LED) or a solid state laser. The head consists of a 14 cm diameter by 25.4 cm long (5.5 in. by 10 in.) cylinder to which optical and electronic components are mounted. A central axially located tube houses the LED transmitter and collimating lens in one end and receiving optics in the opposite end. The return signal is collected by a 10.2 cm (4 in.) diameter primary mirror and reflected into the receiving optics. The primary mirror diameter requirement is determined by the maximum path length of the required antenna measurement as well as transmitter light collimation and will be different for measuring various sizes of antenna concepts.

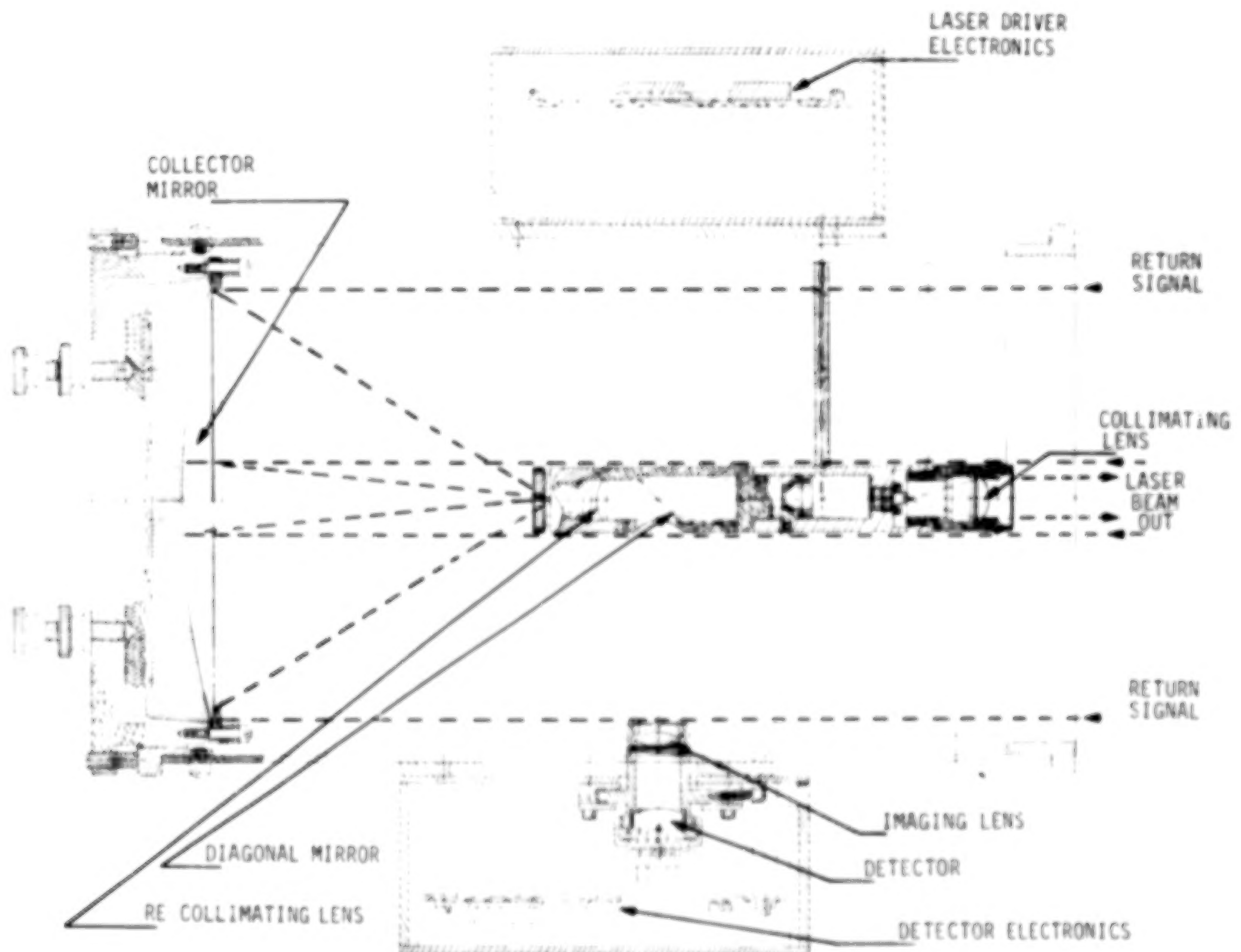


Figure 5

BREADBOARD SYSTEM TEST LAYOUT

This photo shows a laboratory distance measuring set up. The optic head, power supplies and computer-printer are located at one end of an optical bench. Light pulses to and from the optic head are directed along the length of a second optical bench. A movable target on the second bench allows several range distances to be optically measured and checked against accurate physical measurement. System performance tests were made using this set up.

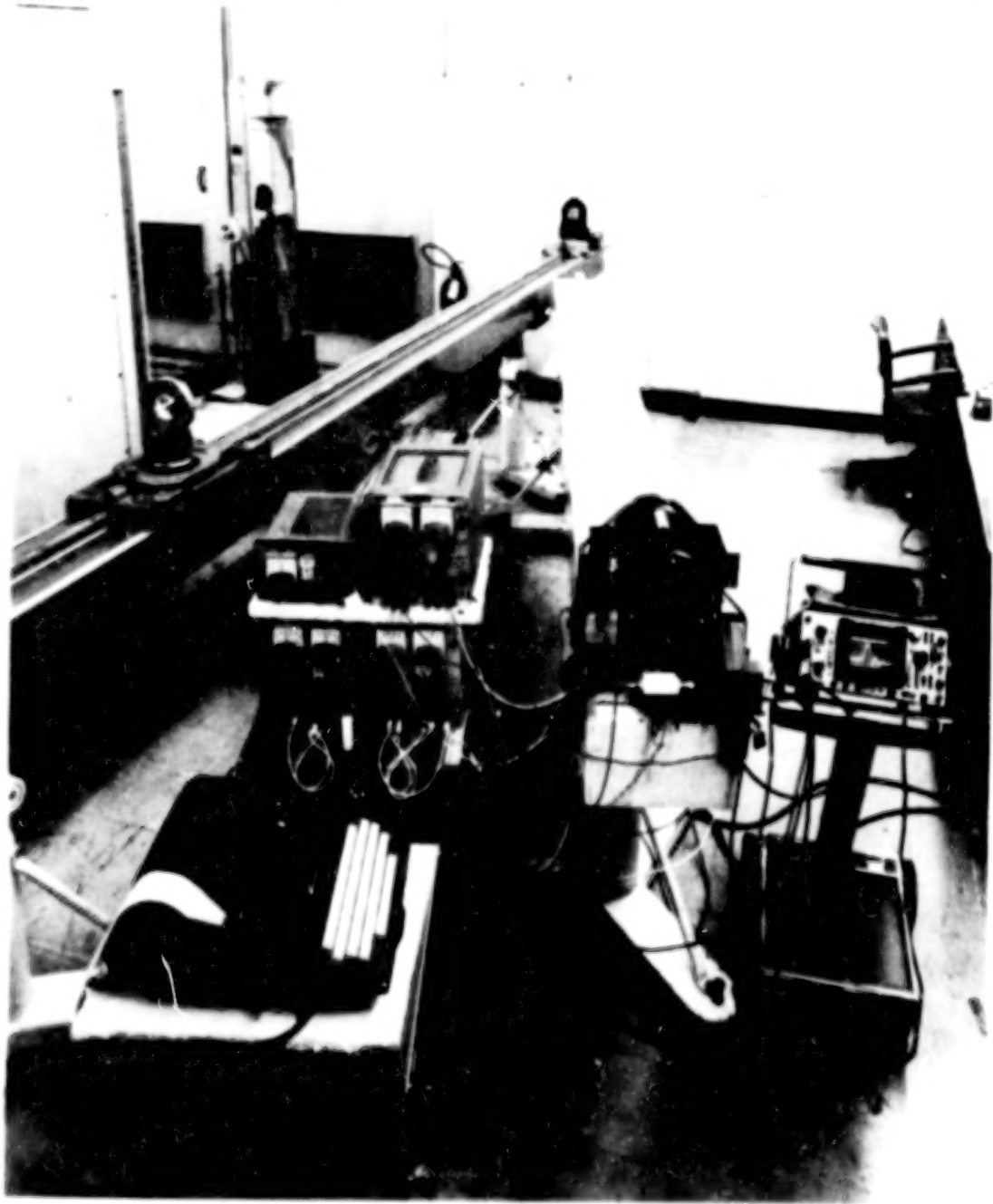


Figure 6

TEST RESULTS SUMMARY

Data from six runs using four targets spaced one meter apart were taken after a six hour warm-up time. No attempt was made to correct for amplitude changes and for systematic noise caused by component recovery time and cross talk. This type of noise contributes to the error in absolute distance measurement but not to scatter and repeatability.

In order not to have to rotate the scan mirror from the optic head to target locations, five in-line targets were used in which the measurement to the closest target was used for determining the "internal path" distance. This distance was subtracted from itself to provide a zero distance and successively from the four in-line targets. Data from these runs are used for determination of the breadboard system performance.

JPL SELF-PULSED LASER RANGING SYSTEM BREADBOARD SYSTEM PERFORMANCE

<u>TOTAL PHYSICAL DISTANCE METERS</u>	<u>MEAN MEASURED TOTAL DISTANCE METERS</u>	<u>MEAN SCAN RANGE (METERS)</u>	<u>MEAN RELATIVE ERROR(MM)</u>	<u>σ DEVIATION MM</u>
141.3619	141.3619	0.0000	0.0	1.8*
142.3619	142.3692	1.0073	7.3	1.9
143.3619	143.3665	2.0046	4.6	2.3
144.3619	144.3692	3.0073	7.3	0.9
145.3619	145.3735	4.0116	11.6	0.6

BASED ON 6 SCANS OF 4 TARGETS EACH
TAKING 5 READINGS ON EACH TARGET PER SCAN

* AVERAGE OF ZERO SCAN RANGE ZERO RETURN

Figure 7

TEST RESULTS GRAPHICAL DISPLAY

When scanning the surface of a large space antenna where many measurements are required it is desirable to take only one reading for each target. This means that each measurement must be within the tolerance limit. The graphical presentation of test results allows performance evaluation based on individual measurement error.

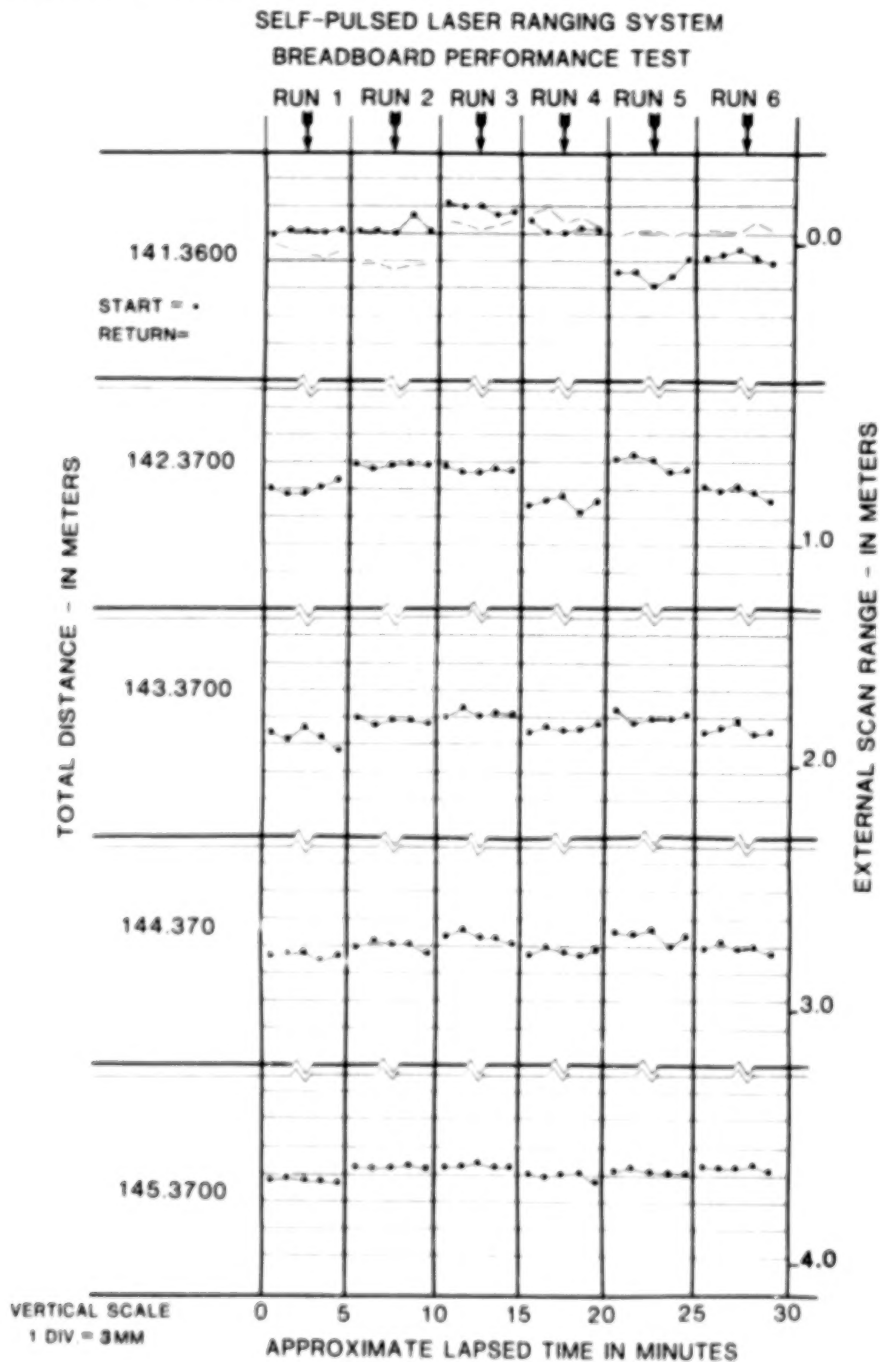


Figure 8

PERFORMANCE ANALYSIS

Test results indicate satisfactory operational performance as a distance measuring system. Range may be read out as printed data in meters to the fourth decimal place. Measuring time is on the order of one second with additional time required for printing. Absolute accuracy, precision and range capability still leave something to be desired. Weakness together with corrective plans to be incorporated in the prototype engineering model are listed below. Incorporation of the improvements together with use of the best known construction techniques is expected to produce a system capable of making consistent absolute range measurements with an absolute accuracy on the order of 2 or 3 millimeters and a precision of a small fraction of one millimeter.

<u>Weakness</u>	<u>Correction</u>
Range Limitation	Use of a laser diode and improved optics in place of an LED.
Absolute Measurement Error	Increase pulse rise rate. Reduce electrical cross talk. Match signal amplitude.
Precision	Use of faster detector and circuitry.
Drift Rate	Use of optical chopper. Improve power supply regulation.

CONCLUSIONS

Hardware modifications can result in significant performance improvement.

Projected performance capability is satisfactory for measurement of large mesh deployable antenna structures.

The system simplicity and development maturity is such that early deployment is feasible.

Antenna Systems Requirements Definition Study

C. T. Golden
Boeing Aerospace Company
Kent, Washington

Large Space Systems Technology - 1980
Second Annual Technical Review
November 18-20, 1980

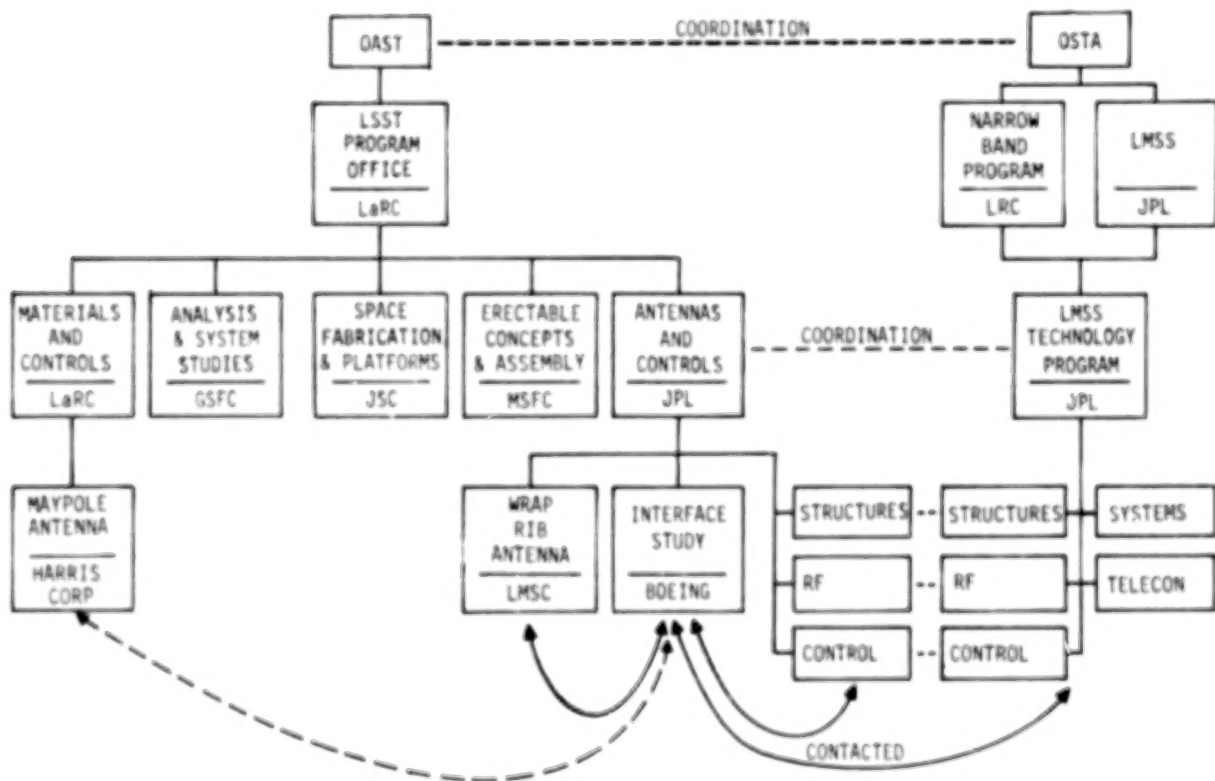
ANTENNA SYSTEMS REQUIREMENTS DEFINITION STUDY

The Antenna Systems Requirements Definition Study was initiated to define System Interfaces associated with specific missions using LSST elements. The goal is to define technology requirements related to interfaces and performance requirements among subsystems. These levy requirements on the system design (e.g. power requirements size solar panels that affect solar pressure torque that places requirements on the control subsystem).

- JPL CONTRACT 955807, STUDY OF SUBSYSTEM INTERFACES OF DEPLOYABLE ANTENNAS FOR THE LARGE SPACE SYSTEMS TECHNOLOGY (LSST) PROGRAM
- STATEMENT OF WORK
 - REVIEW LSST FOCUS MISSION DEFINITIONS
 - REVIEW LSST ANTENNA CONCEPTS
 - DEFINE THE ANTENNA MECHANICAL SUBSYSTEM
 - DEVELOP THE SPACECRAFT SYSTEM CONFIGURATION
 - DEFINE THE ANTENNA SUBSYSTEM INTERFACES
 - DEVELOP AND DESCRIBE THE ANTENNA SUBSYSTEM MODEL
- STUDY OBJECTIVE
THRU ANALYSIS OF SPECIFIC MISSION REQUIREMENTS, SYSTEM LEVEL CONFIGURATION DESIGNS WILL BE DEVELOPED TO CHARACTERIZE THE SUBSYSTEMS INTERFACES AND REQUIREMENTS

LSST INTERFACE STUDY

The chart relates our understanding of the LSST Program relative to the Land Mobile Satellite Service (LMSS) Program. Our approach is to use a 55m wrap rib antenna in a second generation LMSS application as a specific mission to define an LSST System and its interfaces. The maturity of the wrap rib reflector design currently is ahead of the other subsystems. Boeing has discussed the antenna status with Lockheed and the controls development with both the LSST and LMSS Managers at JPL. Other areas discussed at JPL include the LMSS Structures, RF, Systems and Telecons. This combined with previous LSST study results and the data developed as of this Annual Review will be used in conducting the study. We will meet with the Harris Corporation in the future to fully understand the Maypole Antenna Reflector.



MOBILE COMMUNICATION MISSION REQUIREMENTS

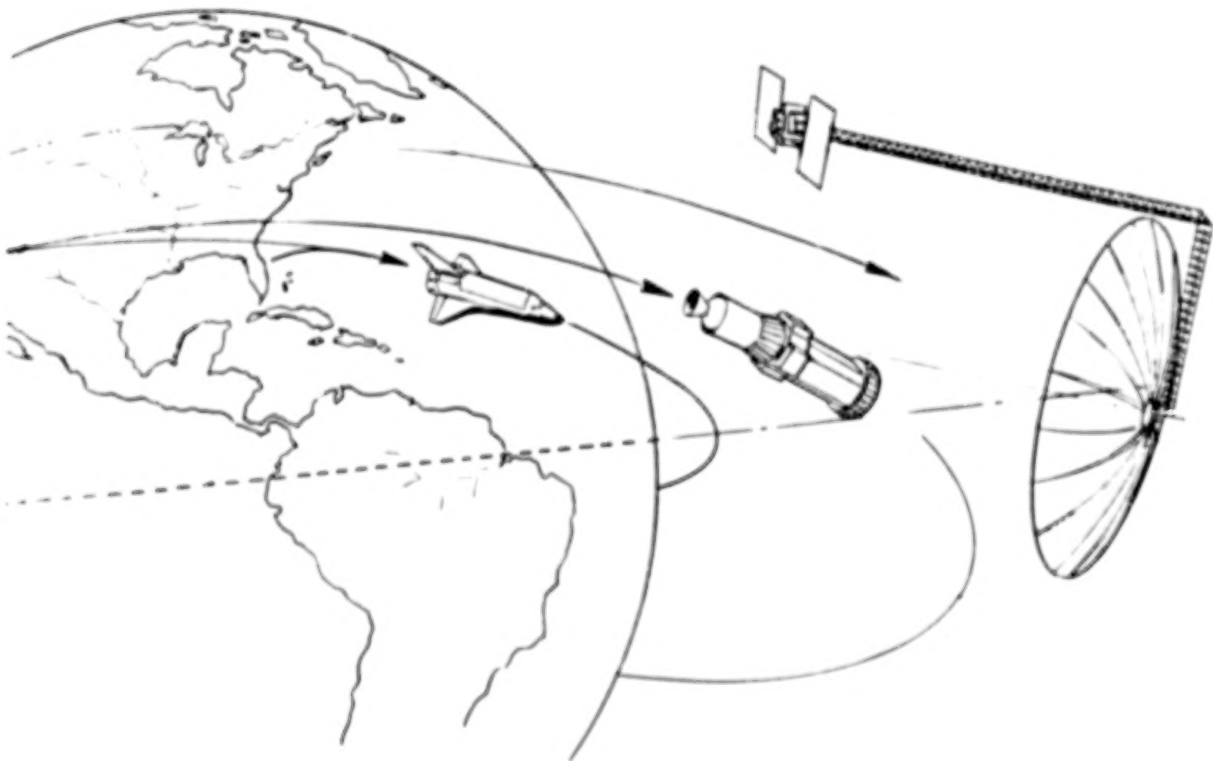
The antenna characteristics to be used in the initial system Requirements Definition Study are shown below for the Land Mobile Satellite Service (LMSS). The mission description and system design will be based on these data. Interface definition and requirements will be developed to describe the system.

<u>ANTENNA</u>	<u>LMSS</u>	<u>LSST FOCUS MISSION</u>
DIAMETER, METERS	55	100
FREQUENCY, MHz	806-890	806-890
F/DP	~0.458	~0.4
BEAMS	30	250
SURFACE ACCURACY (RMS)	$\sigma = \lambda / 30 = 12\text{MM}$	$\sigma = \lambda / 30 = 12\text{MM}$
FEED	OFFSET CLUSTER	OFFSET CLUSTER
BEAM SIDE LOBE LEVEL	-35 dB	-35 dB
BEAM TO BEAM ISOLATION	-30 dB	-30 dB
BEAMWIDE (-3dB) ($v=0.54$)	0.4 TO 0.5	0.25
ORBIT	GEO	GEO
MISSION LIFE, YEARS	10	10
TECHNOLOGY READINESS	1990	1990
LAUNCH YEAR	1995	1995
BOL TOTAL POWER KW	20	20

OFFSET FED ANTENNA SYSTEM

LAUNCH AND SYSTEM DEPLOYMENT

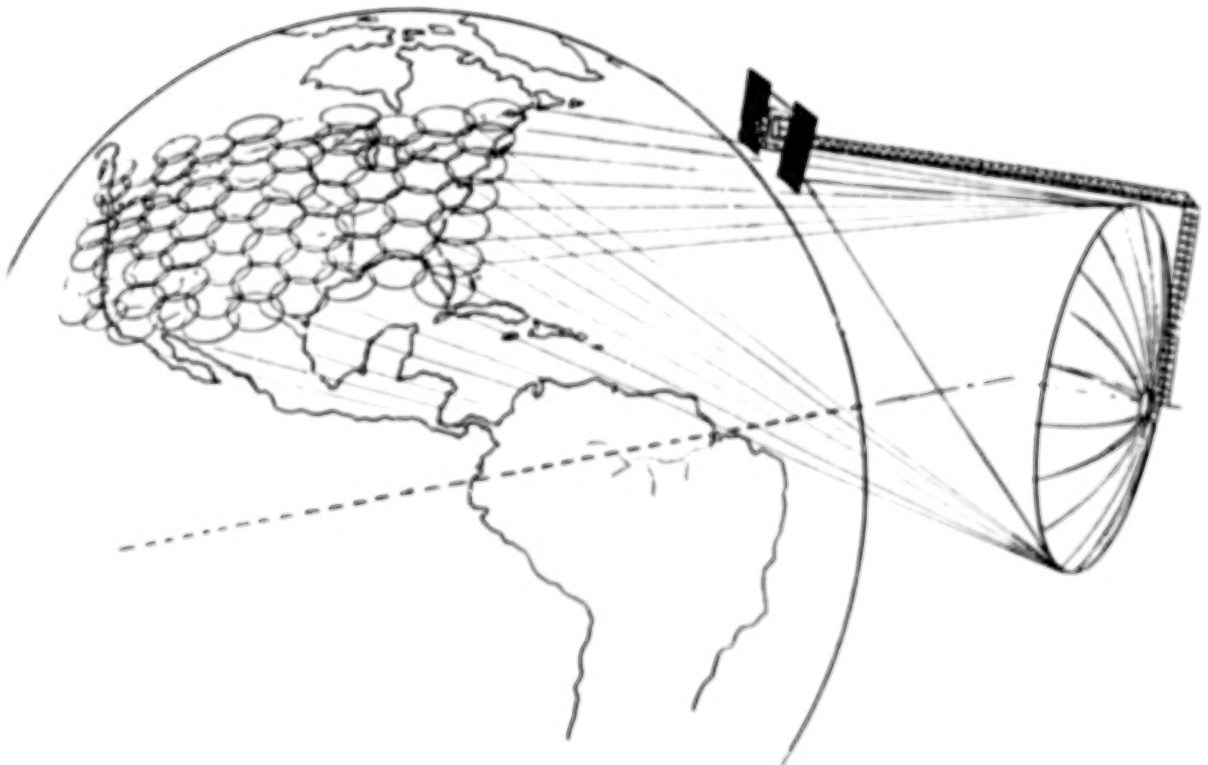
The System design will examine the launch phase of the mission including the interface with the Space Transportation System (STS), the orbital transfer vehicle and the deployment from the spacecraft of the boom, antennas and solar panels. As depicted below the "Spacecraft" is located at the antenna feed. This undoubtedly makes the RF to feed interface optimum. Other interfaces such as a boom deployment, pointing and control, solar pressure torque, shadowing (solar panels and reflector interaction) and others may be adversely affected. The study will include system configuration analyses and describe the interface requirements associated with each. We do not propose to produce an optimum system design but to characterize the effect of system configuration on the interfaces.



OFFSET FED ANTENNA SYSTEM

OPERATIONAL CONFIGURATION

In addition to the launch/deployment phase, we will assess the effects of the space environment and the operational events on the system and its subsystem interfaces.



INTERFACES TO BE ASSESSED

Within the limits of the mission, system and subsystem definition, the study will assess the interfaces and establish their requirements. Hopefully this can be done to a level of detail that will permit finite requirements development. This can then lead to requirements allocations, design solutions and identifying areas requiring technology development.

TO INCLUDE BUT NOT BE LIMITED TO:

- WEIGHT (SHUTTLE / IUS CAPABILITY)
- PACKAGING CONFIGURATION (STS INTERFACE)
- TRANSFER STAGE INTERFACE
- POINTING (CONTROLS)
- STRUCTURAL INTERFACE (DYNAMICS / CONTROL)
- FEED (TYPE AND LOCATION)
- CONFIGURATION (SOLAR TORQUE)
- POWER (SOLAR ARRAY AND BATTERIES)
- RF (SWITCHING AND ELECTRONICS)
- DATA MANAGEMENT (SPACECRAFT SYSTEM)
- THERMAL
- ORBIT CORRECTION
- SPACECRAFT COMMUNICATIONS

SCHEDULE

[illegible]

HOOP/COLUMN ANTENNA TECHNOLOGY
DEVELOPMENT SUMMARY

THOMAS G. CAMPBELL
NASA LANGLEY RESEARCH CENTER
HAMPTON, VIRGINIA 23665

LARGE SPACE SYSTEMS TECHNOLOGY - 1980
SECOND ANNUAL TECHNICAL REVIEW
NOVEMBER 18-20, 1980

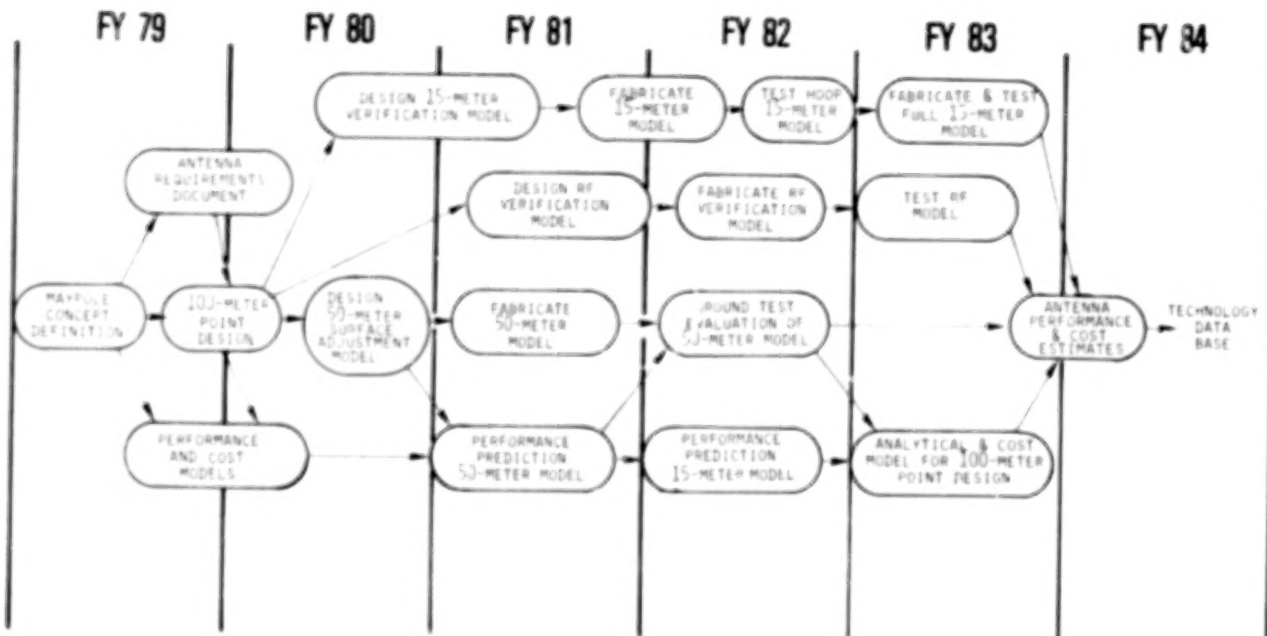
HOOP/COLUMN TECHNOLOGY DEVELOPMENT
MAJOR ACCOMPLISHMENTS DURING FY 80

The Hoop/Column Technology Development Program at Langley Research Center has made significant accomplishments during the past year. Basically, the entire program has been redirected and now includes the fabrication and test of much larger models such as the 4-gore segment of a 50-meter antenna and the 15-meter diameter fully deployable antenna. Significant results have been obtained in the point design that includes a quad-aperture reflector system for multiple beam applications. Accomplishments have been made in the specific task areas listed below as well as the in-house support activities at Langley.

- 0 REDIRECTED HOOP/COLUMN TECHNOLOGY PROGRAM TO INCLUDE FOLLOWING ENGINEERING MODELS.
 - 4-GORE SEGMENT OF 50-METER DIAMETER ANTENNA
 - 15-METER DEPLOYABLE ANTENNA
 - RADIO FREQUENCY VERIFICATION MODEL
- 0 COMPLETED BASIC DESIGN OF QUAD APERTURE ANTENNA CONFIGURATION
- 0 SIGNIFICANT ACCOMPLISHMENTS IN SPECIFIC TASK AREAS.
 - ECONOMIC ASSESSMENT
 - MATERIALS TECHNOLOGY
 - DESIGN VERIFICATION MODELS OF HINGE JOINT, DEPLOYABLE MAST AND DEMONSTRATION MODELS.
- 0 EXPANDED INHOUSE ACTIVITIES IN SUPPORT OF HOOP/COLUMN ACTIVITIES.
 - DESIGNED AND FABRICATED ALTERNATIVE HINGE JOINT CONCEPTS
 - DEVELOPED MASH MANAGEMENT MODEL
 - RF TESTING AND EM ANALYSIS
 - DEVELOPMENT OF MEASUREMENTS LABORATORY FOR SURFACE MEASUREMENT

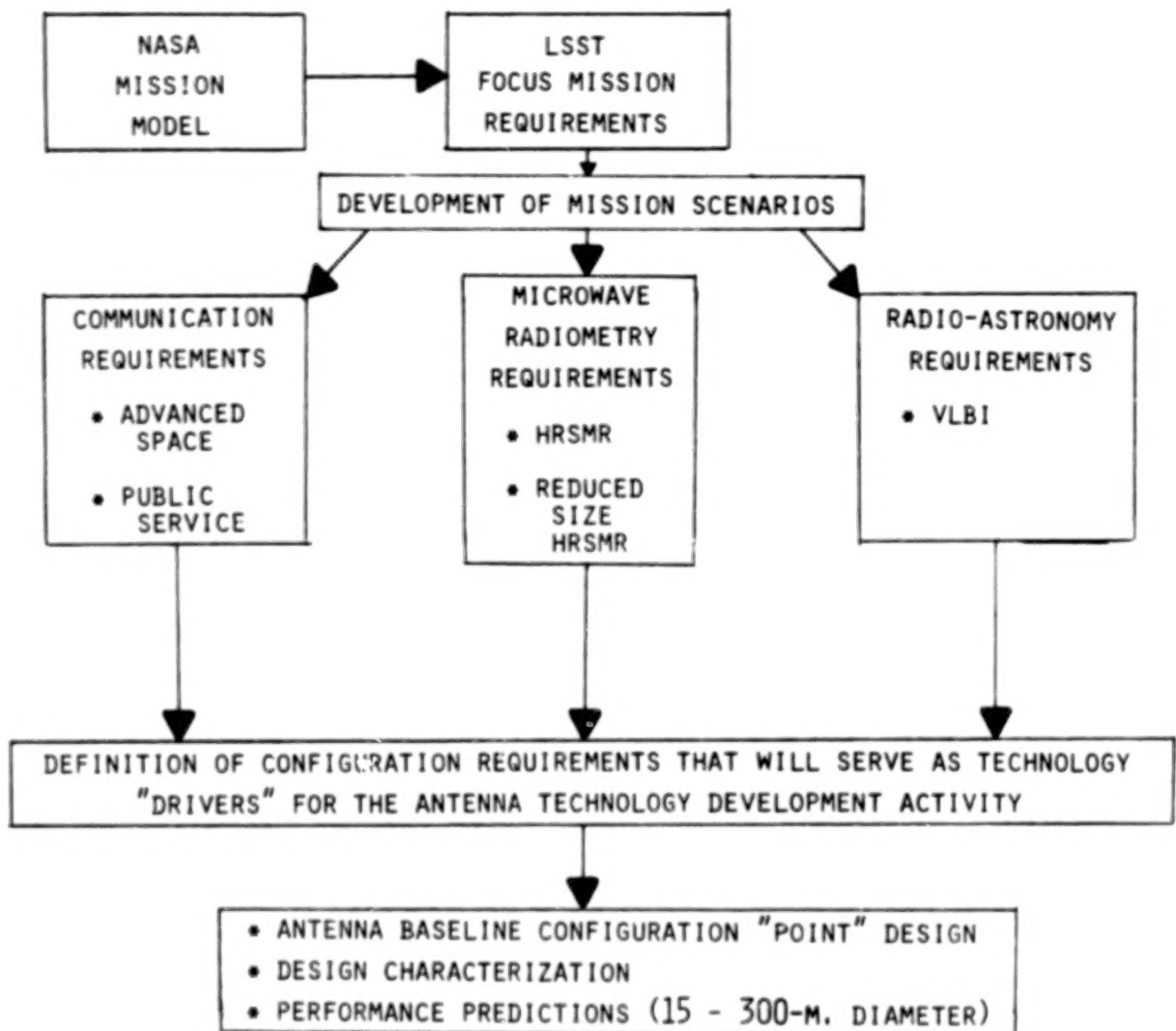
HOOP/COLUMN TECHNOLOGY DEVELOPMENT PLAN

The Hoop/Column technology development plan is shown below. Basically, the Phase-I effort through FY 80 has been completed and the Phase-II will begin early CY 81. The development of the 50-meter model and the 15-meter antenna will be completed during the Phase-II activity.



LSST CONFIGURATION DEFINITION

In order to define the configuration for the Hoop/Column development effort, the technology drivers for the communication, radiometry, and radio astronomy mission were reviewed. The multiple beam requirements (100 - 200 beams) were adjudged to be one of the most challenging technology drivers associated with the mission. Therefore the configuration for the Hoop/Column was chosen on that basis.



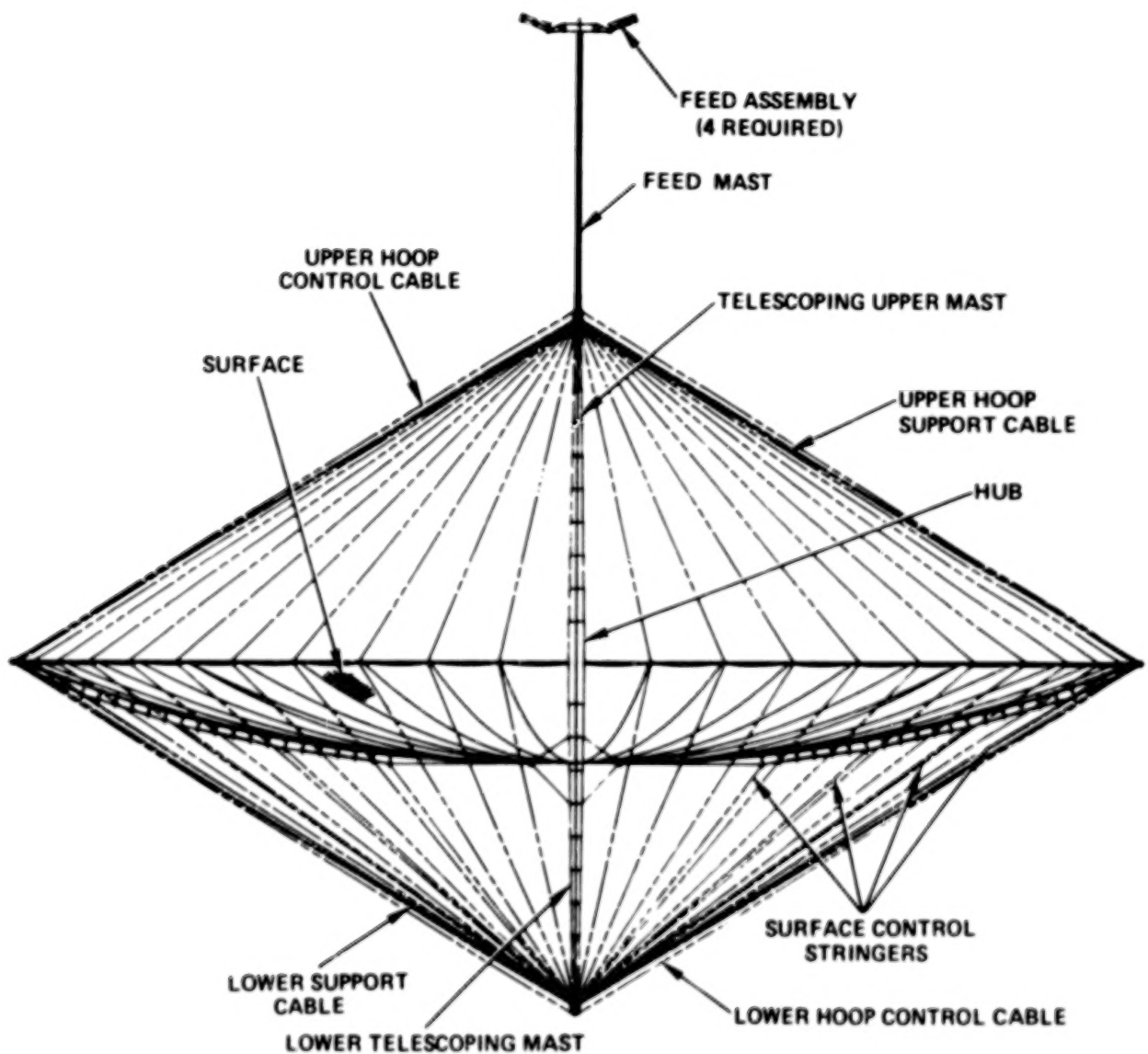
ANTENNA REQUIREMENTS SUMMARY

The antenna requirements for the point design that would provide multiple beam capability are presented below. The objective of the Hoop/Column program is to verify that this technology can be used for different frequencies and reflector diameters.

PARAMETER	REQUIREMENTS
• CONFIGURATION	• 100 METER DIAMETER QUAD-APERTURE
• f/D	• 1.53
• STOWED ENVELOPE	• MAXIMUM ALLOWABLE ENVELOPE IS <ul style="list-style-type: none">- 4.56 METERS (15 FEET) DIAMETER- 12 METERS (30.4 FEET) LENGTH
• OPERATING FREQUENCY	• 2.0 GHz
• CONTOUR ACCURACY	• $\lambda/20$ MAXIMUM (7.5mm RMS)
• GAIN	• 55.4 dB
• NO. BEAMS	• 219 (55 BEAMS/APERTURE)
• HPBW	• 0.256°
• BEAM-TO-BEAM ISOLATION	• 30 dB
• POINTING ACCURACY	• 0.03°
• SURFACE ADJUSTMENT	• ADJUSTMENT CAPABILITY ON ORBIT

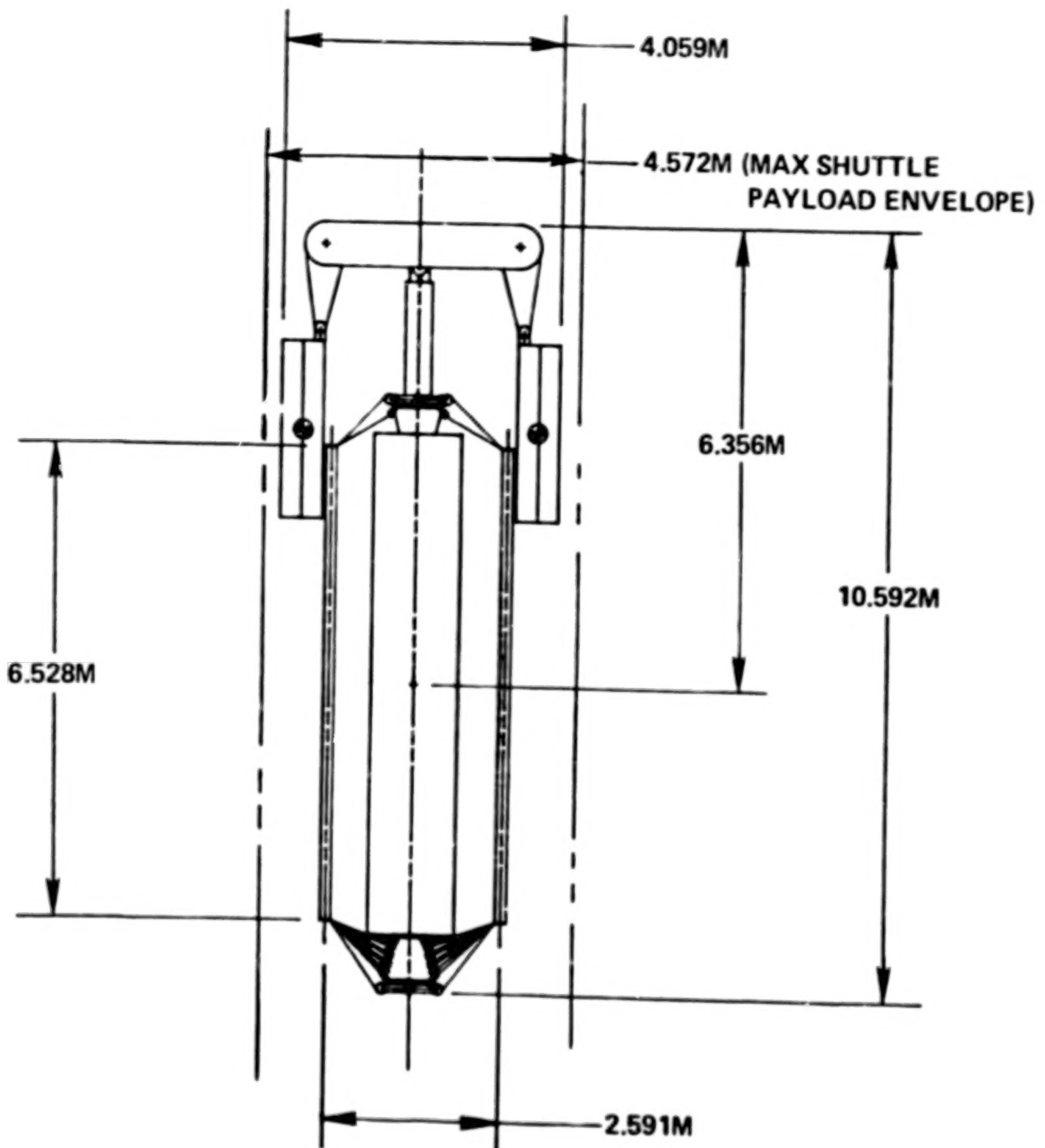
CONFIGURATION OF HOOP/COLUMN
POINT DESIGN - DEPLOYED CONFIGURATION

The deployed configuration of the Hoop/Column point design is shown below. A 100-meter point design has been selected that provides the quad aperture reflector system.



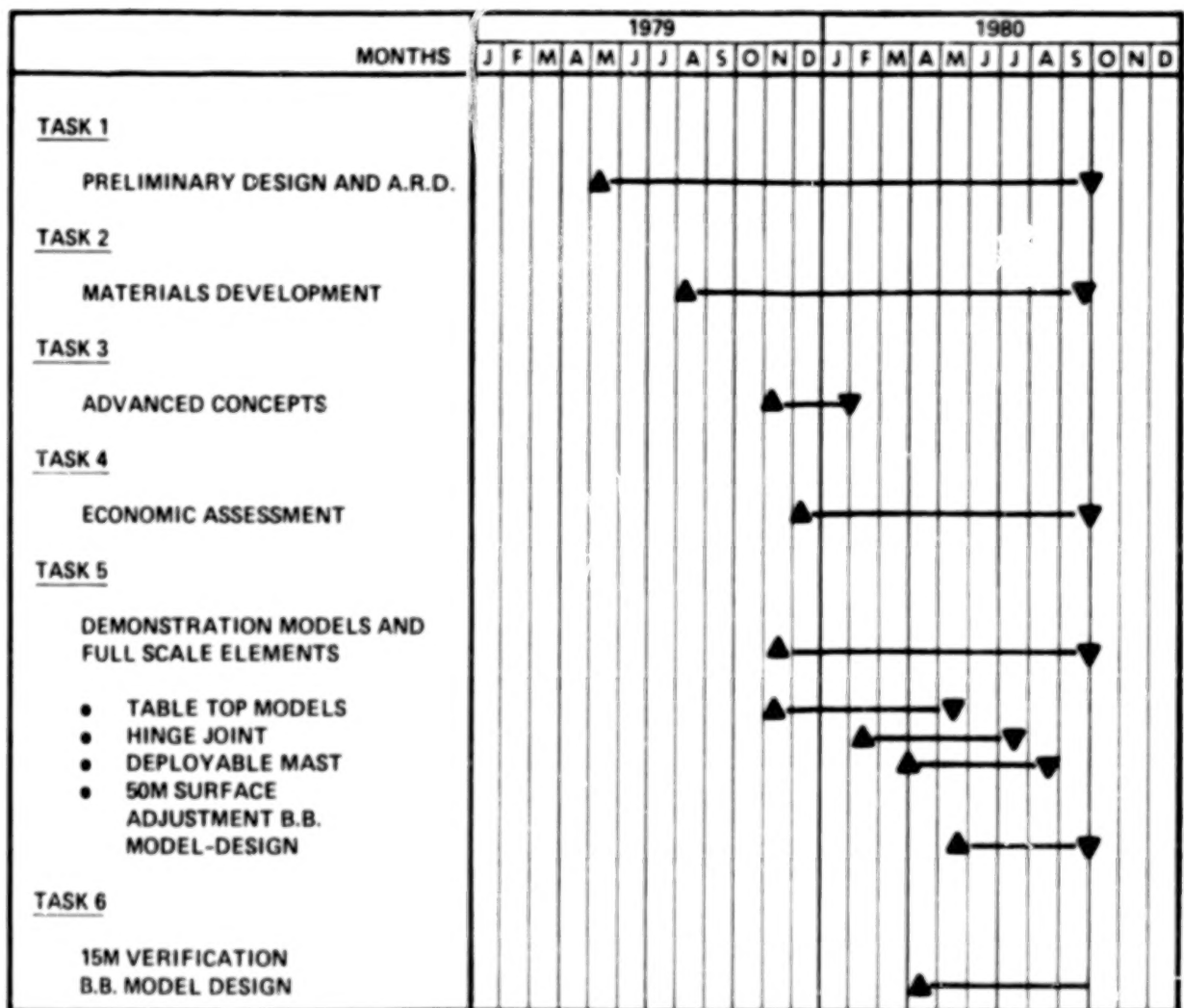
STOWED CONFIGURATION OF THE
HOOP/COLUMN POINT DESIGN

The stowed configuration for the 100-meter point design is shown below.



PHASE-I SCHEDULE

Don Montgomery of the Harris Corporation discusses the Phase-I activity in detail in the next paper. The specific task headings scheduled during Phase-I are listed below.



DEVELOPMENT OF THE MAYPOLE (HOOP/COLUMN)
DEPLOYABLE REFLECTOR CONCEPT FOR LARGE SPACE
SYSTEMS APPLICATIONS

D. C. Montgomery
Harris Corporation
Government Systems Group

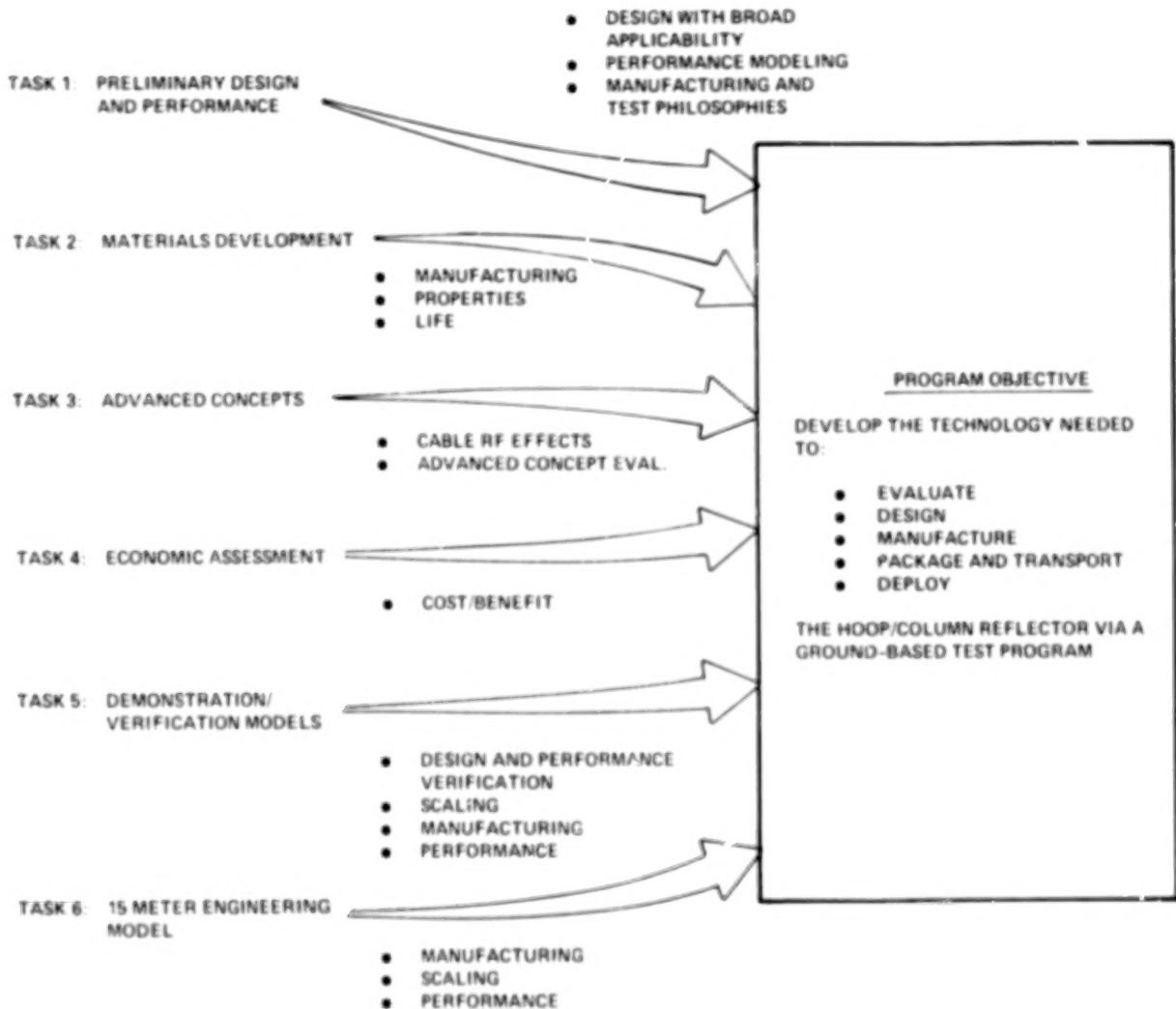
NAS1 - 15763

LSST 2ND ANNUAL TECHNICAL REVIEW

November 18-20, 1980

TASK DESCRIPTIONS & PROGRAM OBJECTIVES

The Hoop/Column Antenna development program is divided into 6 Tasks. All support the main objective of the program which is the technology development necessary to evaluate, design, manufacture, package, transport and deploy the Hoop/Column reflector by means of a ground based test program.



PHASE I PROGRAM SUMMARY

The program was initiated with a review of the NASA supplied mission scenarios for the communications, radiometry and radio astronomy missions. The study of these mission scenarios led to specific Hoop/Column antenna configurations for each mission. The mission configurations were then evaluated to identify specific technology items requiring further development. The compilation of these technology drivers resulted in a specification of an artificial or "point" design. The point design then, is the design element around which all design and performance estimates for the rest of the program were made.

REVIEW MISSION SCENARIOS:

COMMUNICATIONS

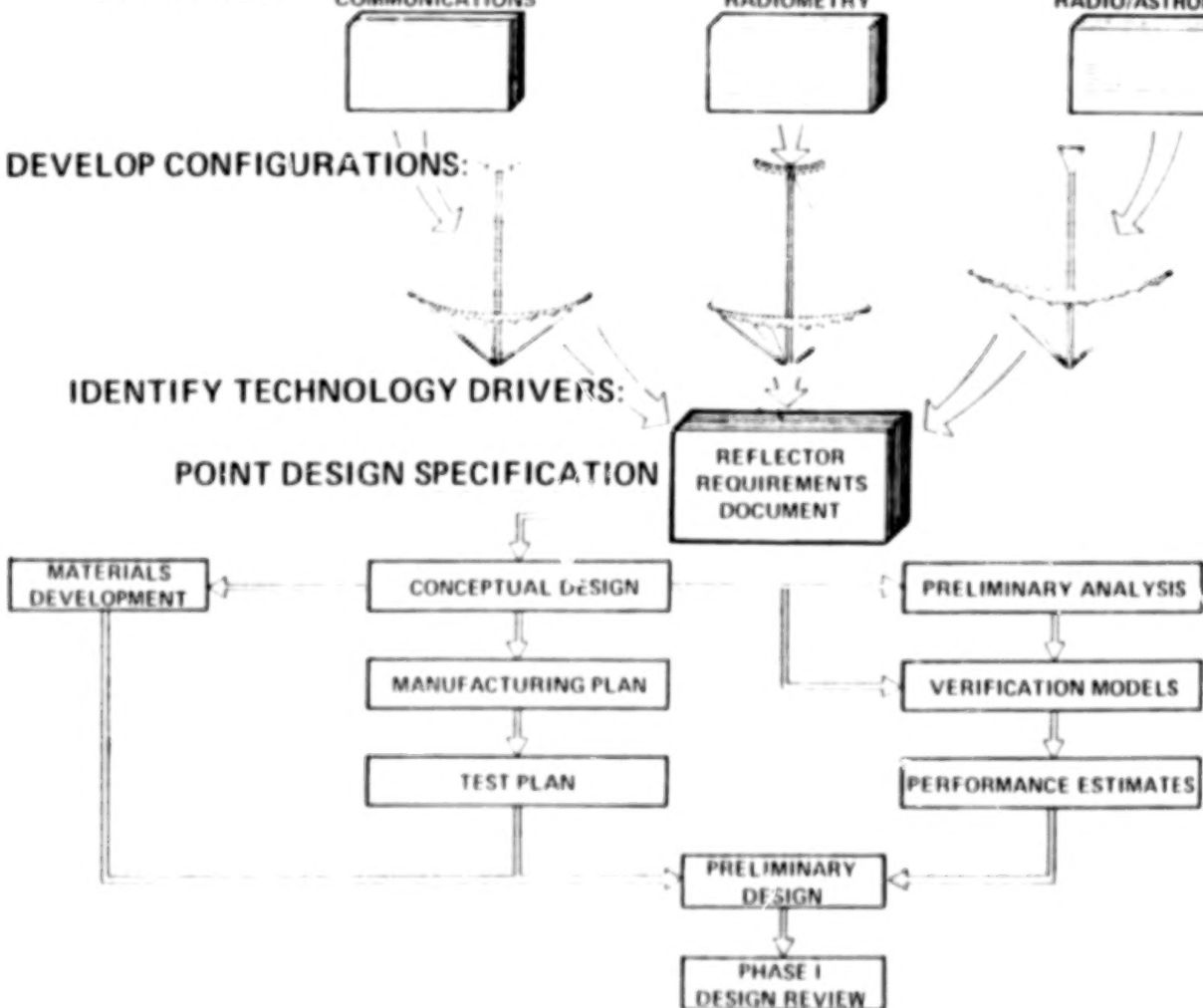
RADIOMETRY

RADIO/ASTRONOMY

DEVELOP CONFIGURATIONS:

IDENTIFY TECHNOLOGY DRIVERS:

POINT DESIGN SPECIFICATION



POINT DESIGN SELECTION FLOW

This chart describes in more detail the flow that led to the point design selection. The missions requirements of the three identified missions were reviewed, with specific technology drivers being identified for each mission. These technology drivers were traded-off to define those elements that were realizable and those that were categorized as being far term or not within reasonable advanced state-of-the-art. These far term items were discarded. The resulting technology drivers were combined to define the requirements about which all design and development work was done. This design element is referred to as the point design and the document which describes the antenna specifications is called the Antenna Requirements Document.



ANTENNA REQUIREMENTS SUMMARY

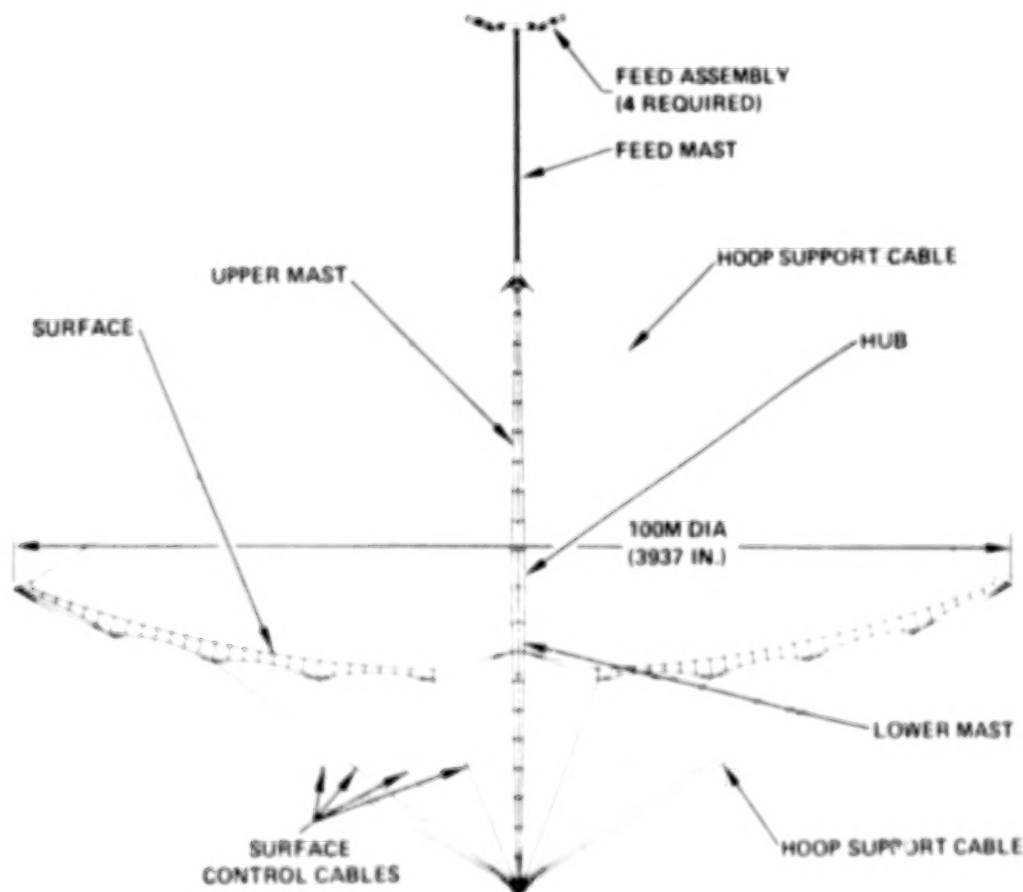
The following two viewgraphs identify the specific performance parameters that were selected to be design goals for the Point Design.

PARAMETER	REQUIREMENTS
• CONFIGURATION	• 100 METER DIAMETER QUAD-APERTURE
• f/D	• 1.53
• STOWED ENVELOPE	• MAXIMUM ALLOWABLE ENVELOPE IS <ul style="list-style-type: none"> - 4.56 METERS (15 FEET) DIAMETER - 12 METERS (30.4 FEET) LENGTH
• OPERATING FREQUENCY	• 2.0 GHz
• CONTOUR ACCURACY	• λ /20 MAXIMUM (7.5mm RMS)
• GAIN	• 55.4 dB
• NO. BEAMS	• 219 (55 BEAMS/APERTURE)
• HPBW	• 0.256°
• BEAM-TO-BEAM ISOLATION	• 30 dB
• POINTING ACCURACY	• 0.03°
• SURFACE ADJUSTMENT	• ADJUSTMENT CAPABILITY ON ORBIT
• DEPLOYMENT	• CONTROLLED, AUTOMATIC (NO EVA) <ul style="list-style-type: none"> • 60 MINUTES MAXIMUM • MICROSWITCHES FOR DEPLOYMENT VERIFICATION AND STOP
• RETRIEVABILITY	• AUTOMATIC, CONTROLLED <ul style="list-style-type: none"> • MICROSWITCHES TO STOP AND VERIFY STOWAGE • MESH SURFACE IS EXPENDABLE
• LAUNCH & LANDING LOADS	• COMPATIBLE WITH STS ENVIRONMENTS
• ORBITAL ENVIRONMENT	• COMPATIBLE WITH LEO AND GEO

POINTY DESIGN DEPLOYED CONFIGURATION

The specific elements of the Hoop/Column are identified in the figure below. The main structural element of the antenna concept is the mast, which is made up of the hub in the center and the two extendable portions, one above and one below called the upper and lower mast. The periphery of the reflector is a hoop made of rigid articulating segments. The hoop is controlled by a series of cables emanating from both the lower portion of the lower mast and the top of the upper mast and attached to each hoop joint. These cables serve to support the hoop and determine its location. The reflector surface is attached to both the hoop and a lower mast section and is shaped by a series of catenary cord elements which supports and shapes the reflective mesh surface. The cord elements are high stiffness/low coefficient of thermal expansion graphite material which provide a very stable structure to which the gold-plated molybdenum reflective mesh is attached. Control cords are attached to the edges of each catenary element to provide adjustment points for in-orbit surface enhancement. The feed mast is an independent, expandable mast which supports the four separate feed array elements.

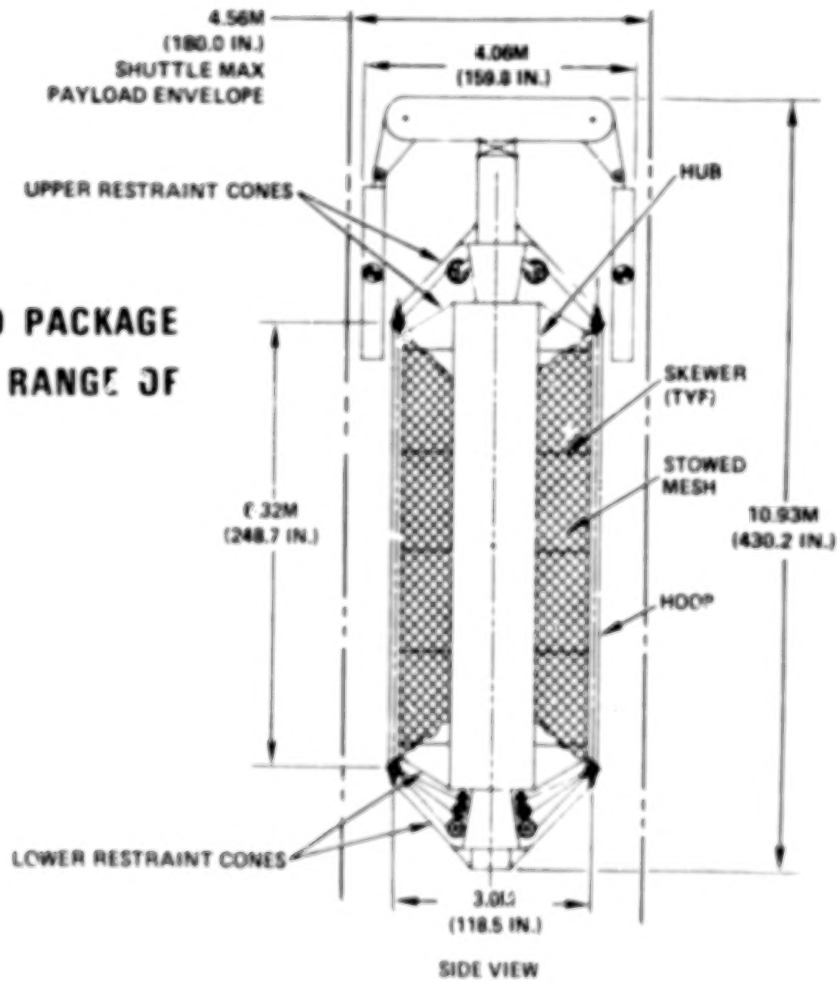
THE ENVIROMENTALLY STABLE DEPLOYED CONTOUR CAN BE ADJUSTED



POINT DESIGN STOWED CONFIGURATION

The stowed Hoop/Column antenna packages very efficiently within the constraints of the shuttle bay. The configuration selected for the point design, which is a 100 meter dia. deployed reflector, utilizes 48 articulating hoop segments. This constraint dictates the aspect ratio or length to diameter of the stowed package. This aspect ratio can be modified for any given deployed diameter by changing the number, and hence, the length of each of the hoop segments.

**THE EFFICIENT STOWED PACKAGE
CAN BE TAILORED TO A RANGE OF
REQUIREMENTS**



CONTENTS

VOLUME I - SYSTEMS TECHNOLOGY

PREFACE	iii	1/A7
1. LARGE SPACE SYSTEMS TECHNOLOGY OVERVIEW	1	1/A13
Robert L. James, Jr.		

SUPPORTING ACTIVITIES

2. LSST CONTROL TECHNOLOGY	9	1/B7
A. F. Tolivar		
3. ADVANCED CONTROL TECHNOLOGY FOR LSST ANTENNAS	19	1/C3
Y. H. Lin		
4. ADVANCED CONTROL TECHNOLOGY FOR LSST PLATFORM	31	1/D1
R. S. Edmunds		
5. CONTROL TECHNOLOGY DEVELOPMENT	49	1/E5
G. Rodriguez		
6. INTEGRATED ANALYSIS CAPABILITY (IAC) DEVELOPMENT	65	1/F7
J. P. Young		
7. INTEGRATED ANALYSIS CAPABILITY PILOT COMPUTER PROGRAM	73	1/G1
R. G. Vos		
8. AN ECONOMY OF SCALE SYSTEM'S MENSURATION OF LARGE SPACECRAFT	87	2/A4
L. J. DeRyder		
9. RADIATION EXPOSURE OF SELECTED COMPOSITES AND THIN FILMS	105	2/B8
Wayne S. Slomp and Beatrice Santos		
10. THERMAL EXPANSION OF COMPOSITES: METHODS AND RESULTS	119	2/C8
David E. Bowles and Darrel R. Tenney		

SPACE PLATFORMS

11. SPACE PLATFORM REFERENCE MISSION STUDIES OVERVIEW	129	2/D4
James K. Harrison		
12. ADVANCED SCIENCE AND APPLICATIONS SPACE PLATFORM	133	2/D8
Jack White and Fritz Runge		

13. STRUCTURAL REQUIREMENTS AND TECHNOLOGY NEEDS OF GEOSTATIONARY PLATFORMS	149 2/E10
G. R. Stone	
14. SUMMARY OF LSST SYSTEMS ANALYSIS AND INTEGRATION TASK FOR SPS FLIGHT TEST ARTICLES	167 2/F14
H. S. Greenberg	
15. ERECTABLE CONCEPTS FOR LARGE SPACE SYSTEM TECHNOLOGY	183 3/A5
W. E. Agan	
16. SPACE ASSEMBLY METHODOLOGY	199 3/B7
J. W. Stokes and H. H. Watters	
17. CONSTRUCTION ASSEMBLY AND OVERVIEW	217 3/C11
Lyle M. Jenkins	
18. SPACE PLATFORM ADVANCED TECHNOLOGY STUDY	229 3/D9
G. C. Burns	
19. A DOCUMENT DESCRIBING SHUTTLE CONSIDERATIONS FOR THE DESIGN OF LARGE SPACE STRUCTURES	243 3/E9
John A. Roebuck, Jr.	

SPACE ANTENNAS

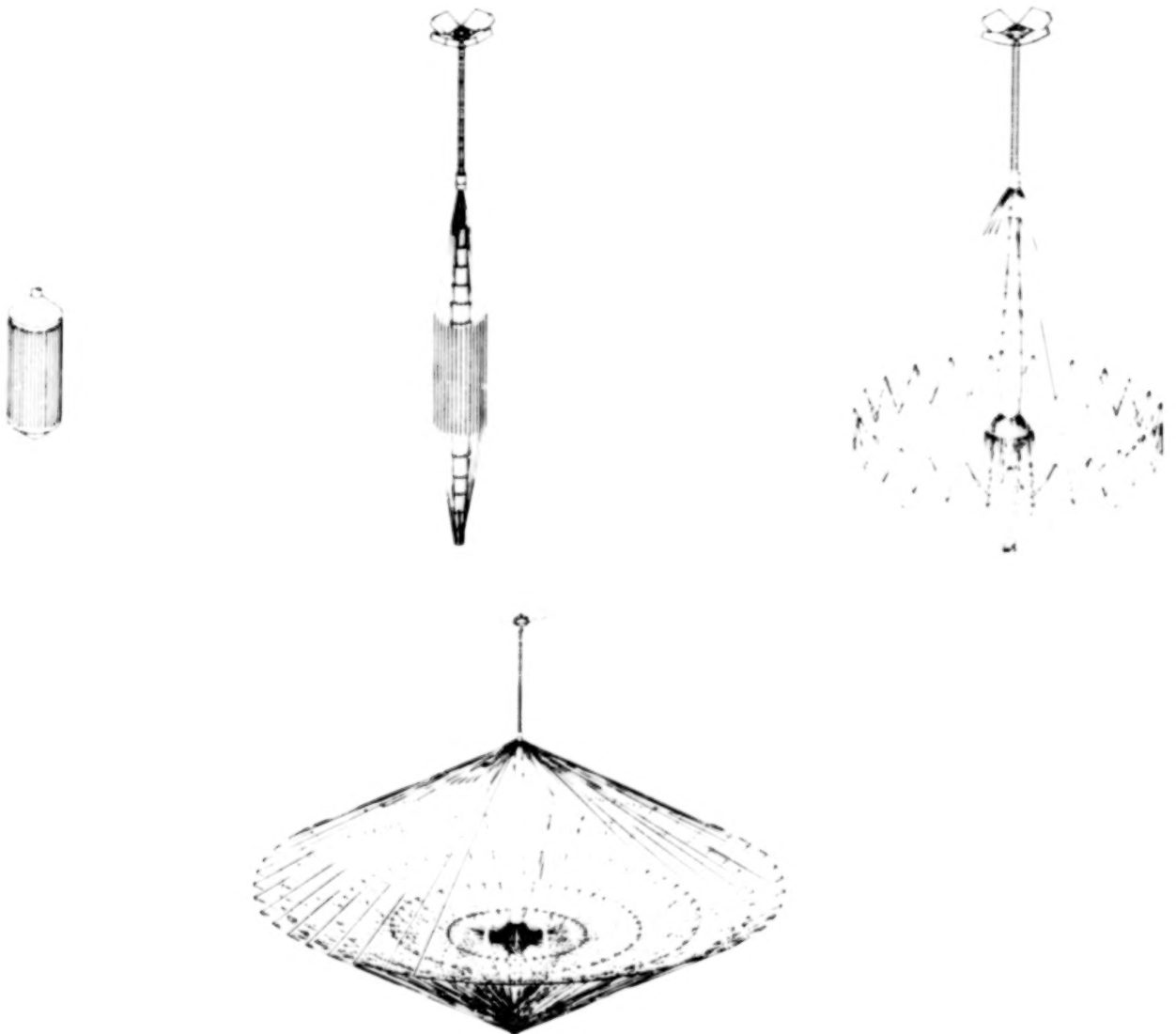
20. ELECTROSTATIC MEMBRANE ANTENNA CONCEPT STUDIES	259 3/F11
J. W. Goslee	
21. ELECTROSTATIC ANTENNA SPACE ENVIRONMENT INTERACTION STUDY	271 3/G9
Ira Katz	
22. ENVIRONMENTAL EFFECTS AND LARGE SPACE SYSTEMS	279 4/A6
H. B. Garrett	
23. JPL ANTENNA TECHNOLOGY DEVELOPMENT	287 4/A14
R. E. Freeland	
24. OFFSET WRAP RIB ANTENNA CONCEPT DEVELOPMENT	295 4/B8
A. A. Woods, Jr.	
25. ANALYTICAL PERFORMANCE PREDICTION FOR LARGE ANTENNAS	325 4/D10
M. El-Raheb	
26. JPL SELF-PULSED LASER SURFACE MEASUREMENT SYSTEM DEVELOPMENT	339 4/E10
Martin Berdahl	
27. ANTENNA SYSTEMS REQUIREMENTS DEFINITION STUDY	349 4/F6
C. T. Golden	

28. HOOP/COLUMN ANTENNA TECHNOLOGY DEVELOPMENT SUMMARY	357	4/F14
Thomas G. Campbell		
29. DEVELOPMENT OF THE MAYPOLE (HOOP/COLUMN) DEPLOYABLE REFLECTOR CONCEPT FOR LARGE SPACE SYSTEMS APPLICATIONS	365	4/G8
D. C. Montgomery		
30. RADIO FREQUENCY PERFORMANCE PREDICTIONS FOR THE HOOP/COLUMN POINT DESIGN	407	5/C11
Thomas G. Campbell		
31. OFFSET FED UTILIZATION OF FOUR QUADRANTS OF AN AXIALLY SYMMETRICAL ANTENNA STRUCTURE	431	5/E7
P. Foldes		
32. SURFACE ACCURACY MEASUREMENT SENSOR FOR DEPLOYABLE REFLECTOR ANTENNAS	439	5/F1
R. B. Spiers, Jr.		
SECOND ANNUAL TECHNICAL REVIEW ATTENDEES	449	5/F11

HOOP/COLUMN ANTENNA DEPLOYMENT SEQUENCE

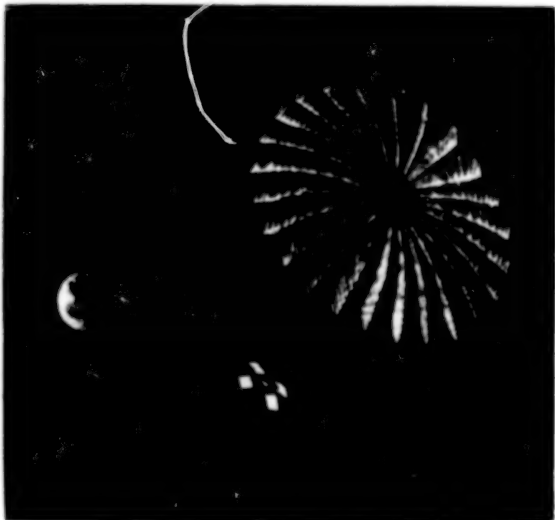
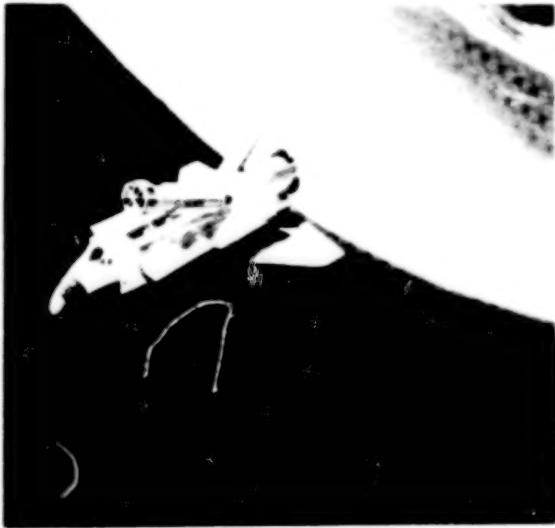
The deployment sequence of the Hoop/Column antenna is initiated by the extension of both the feed mast and the main structural mast. Once this mast extension is completed, the hoop begins to deploy outward. The energy for deployment is provided by four separate drive units located on joints 90° apart around the hoop. Once the hoop is deployed to its full circular approximation, a separate section of the mast called the preload section is deployed. This motion tensions all of the hoop support cables and thus preloads the system.

DEPLOYMENT IS CONTROLLED AND UNIT CAN BE AUTOMATICALLY RESTOWED



POINT DESIGN MISSIONS SCENARIO

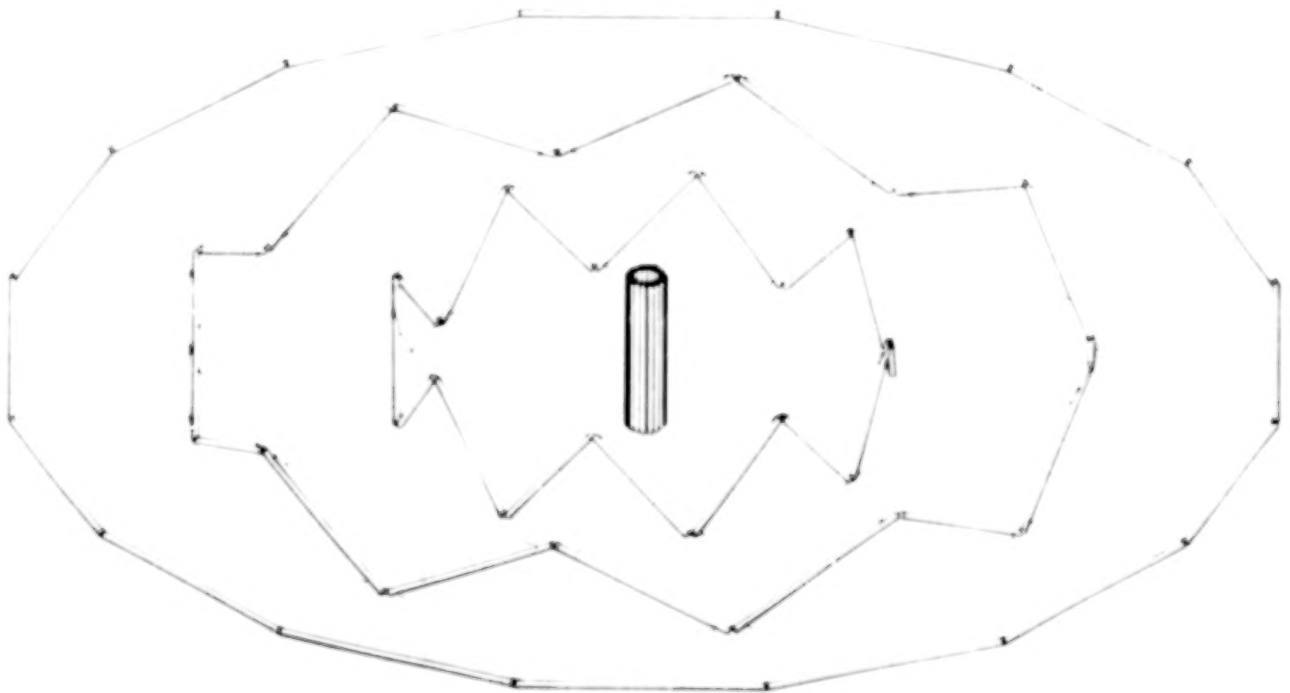
The artist depiction represents the various stages of the mission for the point design. The first stage is orbit insertion by the STS and deployment out of the orbiter bay with the IUS attached. Second phase is a boost from LEO to geosynchronous orbit where deployment initiation takes place. Finally, the spacecraft is oriented earth looking and the operational phase of the antenna begins.



SINGLE STAGE HOOP DEPLOYMENT SEQUENCE

The deployment sequence is shown in the figure below. The approach developed utilizes a double hinge at each joint which permits rotation without any torsional wrap-up in the hoop members. The single stage deployment refers to the motion of the hoop throughout its deployment. The joints of the hoop describe a right circular cylinder at all stages of deployment. The individual hoop segments simply rotate from vertical to horizontal about an axis through the center of each member. These axes are radial lines forming a plane normal to the axis of the mast.

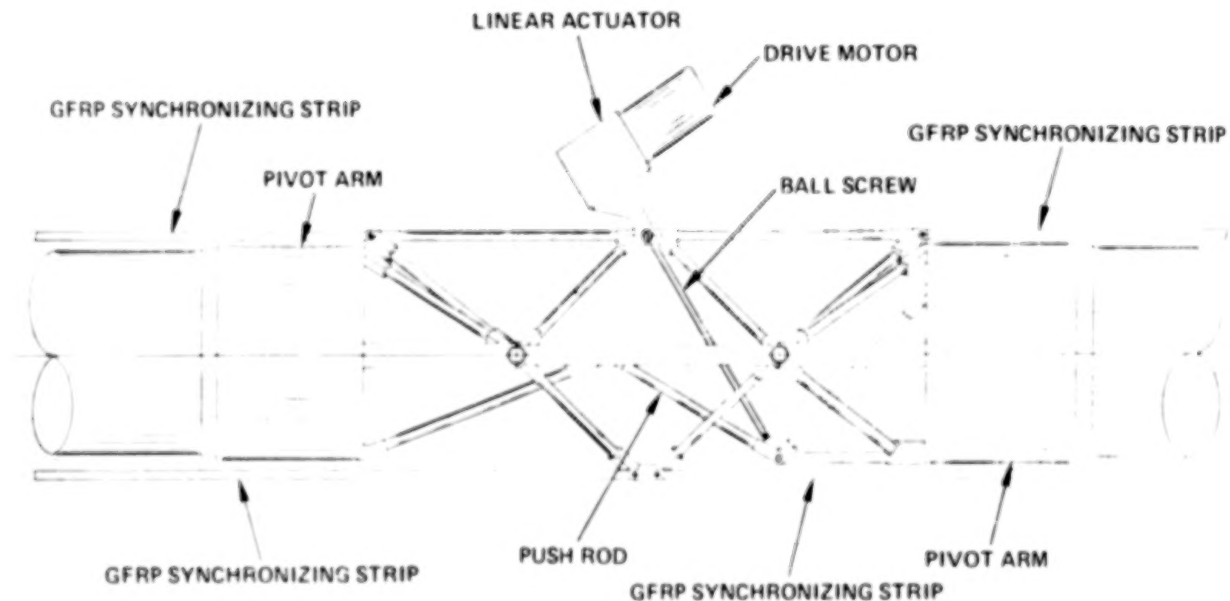
Advantages of this hoop deployment method include control system simplification, good mesh handling characteristics, and no toggling action as the hoop completes its deployment.



SINGLE STAGE HOOP SIDE VIEW

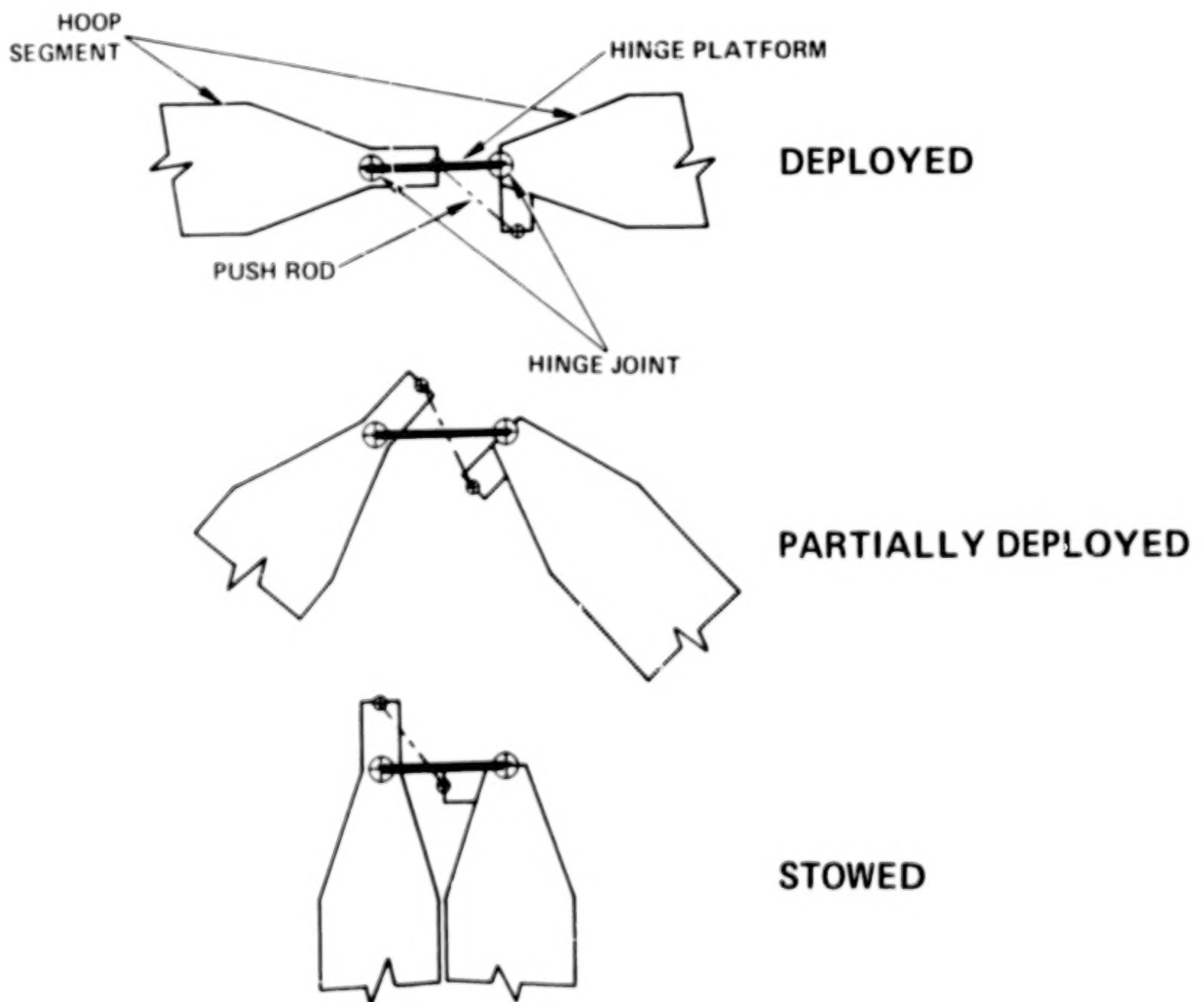
This figure shows detailed layouts of the hinge joint. The hinge platform is a truss structure which exhibits high efficiency from a strength and stiffness to weight standpoint. The tubular hoop segments are terminated with bonded fittings transitioning from a tubular section to a truss section which mates with the hinge platform. The pushrod can be seen connecting the adjacent hoop segments. The synchronization strips can also be seen attaching to the hinge platform. A linear actuator is used to drive one section which in turn drives the adjacent section.

DEPLOYED POSITION



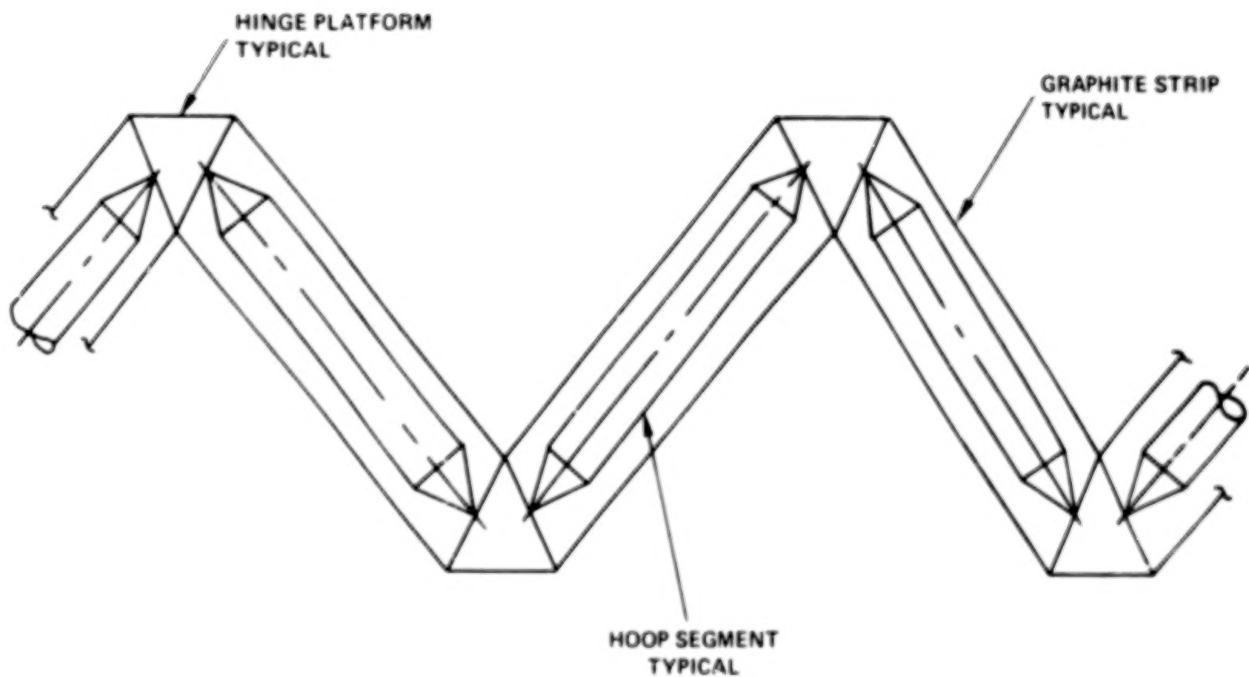
SINGLE STAGE HOOP

This figure shows a schematic of the joint required for the single stage hoop and how one member is coupled to another in different stages of deployment. The hinge platform supports the two hinge points required of this concept. Each hinge axis is along a radial line through the center of the mast and in a plane normal to the mast central axis. Uniform motion is achieved by means of a pushrod connected to offset attach points. Synchronization of this hoop is realized by keeping all hinge platforms parallel during deployment. This occurs by means of strips or cables (not shown) connecting one platform to the next. The system works similarly to a pantograph.



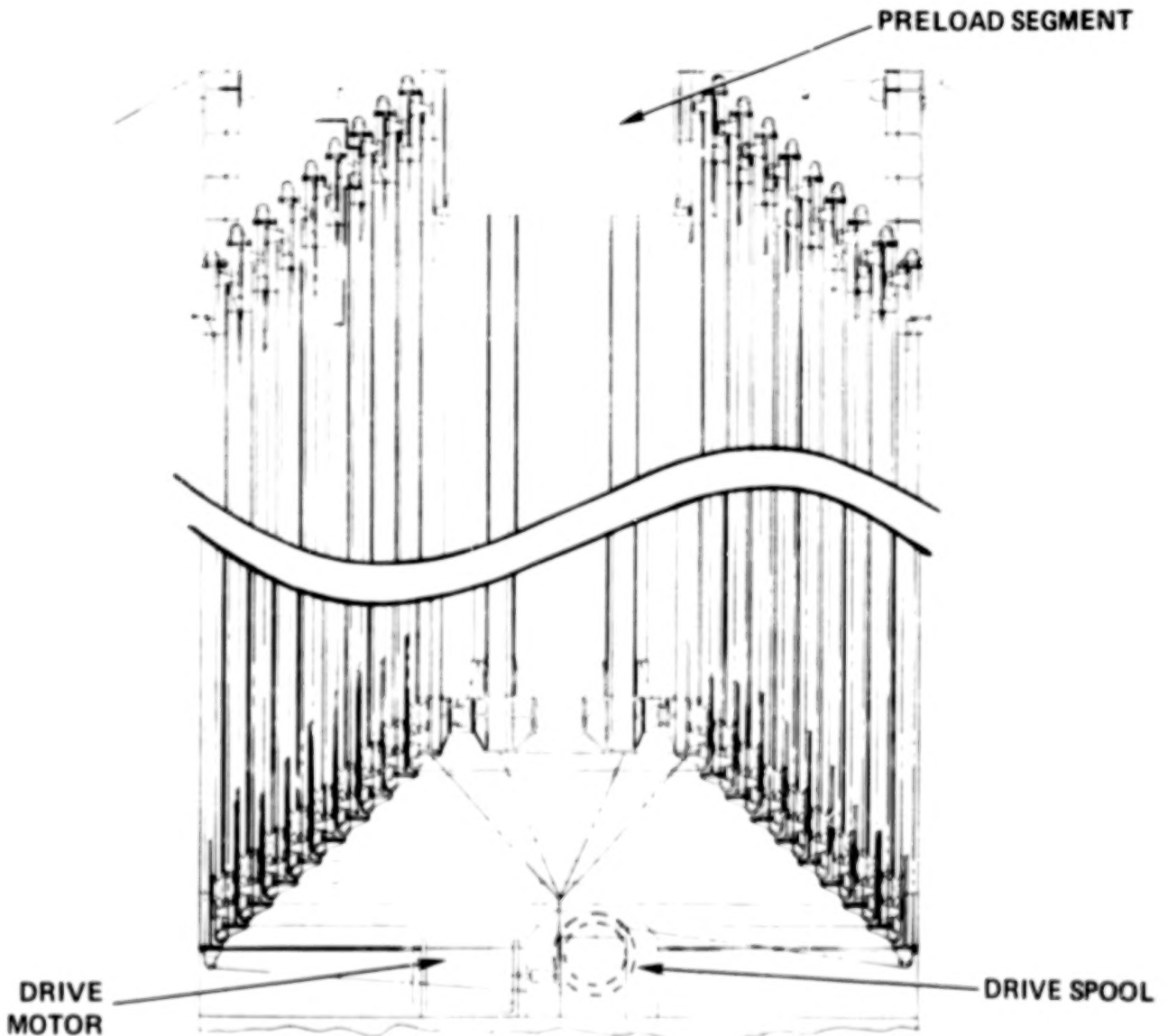
HOOP SYNCHRONIZATION APPROACH

The hoop synchronization approach is one of pantograph or parallelogram type action, the philosophy of synchronization being that if all hinge planforms remain parallel throughout the deployment motion, then synchronization is accomplished.



CABLE DRIVEN MAST

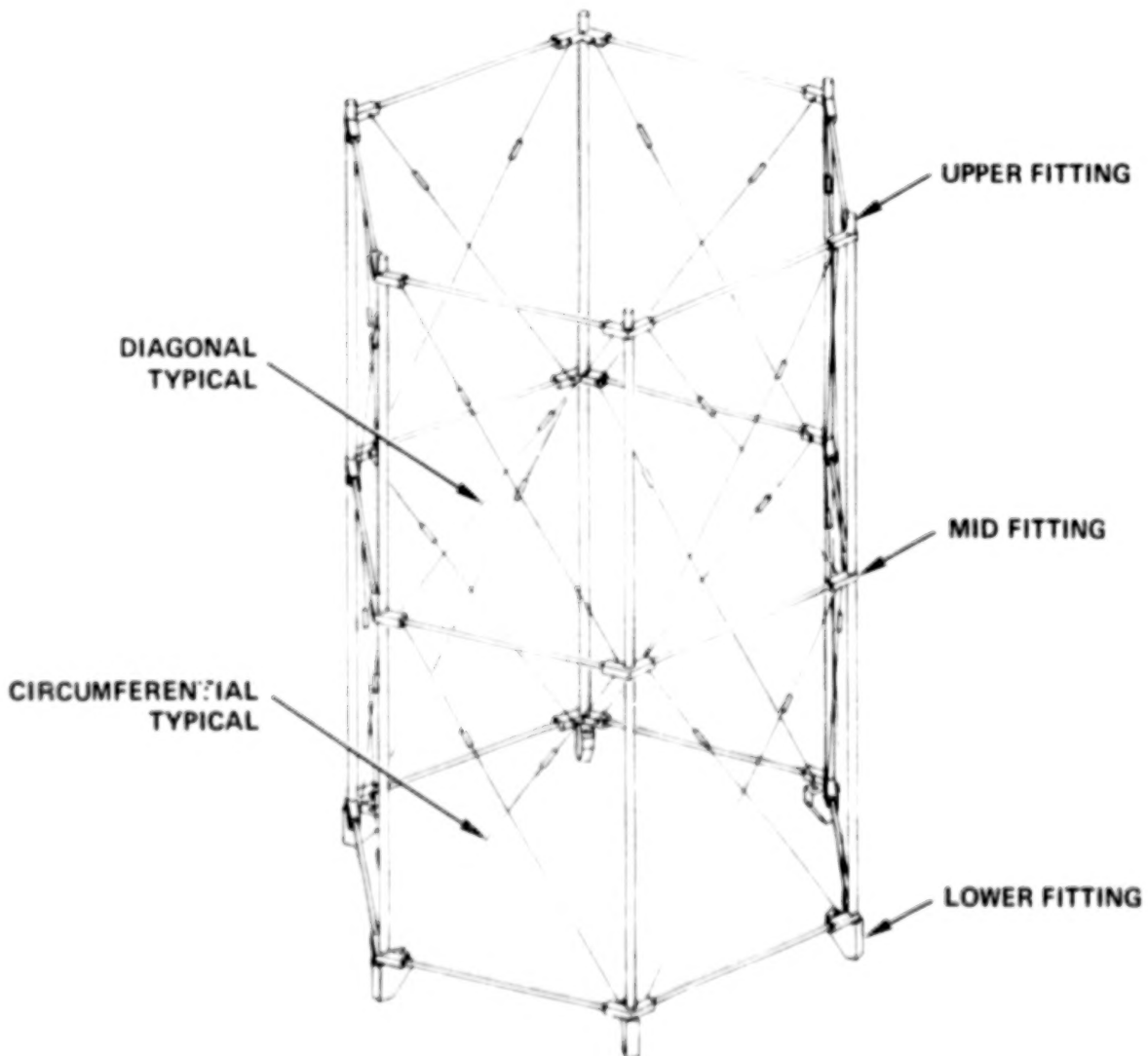
After many trade-off exercises, the cable driven mast was selected as the candidate approach which offered the most advantages. The deployment mechanism design consists of a cable that emanates from a drive spool and extends to the outer-most section of the telescopic mast. The cable runs over a pulley at the outer-most section, up the full length of the section, over a pulley at the top of that section and back down the adjacent section. It continues this way until it reaches the innermost section, at which time the cable crosses over to the opposite side of that section and returns to the drive spool by an identical circuit to that just described. Deployment is initiated by activating the drive spool which takes up the cable and thus forces the sections to expand outward.



TELESCOPIC MAST DESIGN

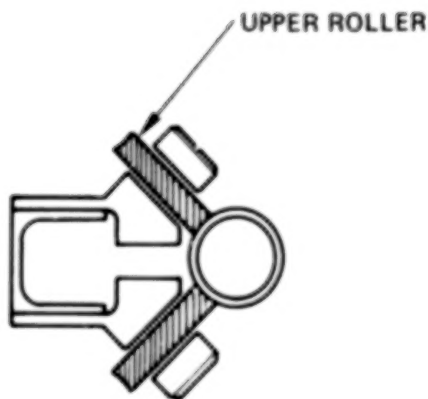
A typical mast section shown in the figure below is designed with an open lattice truss-type structure. This configuration was selected for high structural efficiency and very low weight.

TYPICAL MAST SEGMENT

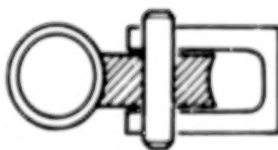


LATCH-PULLEY-ROLLER

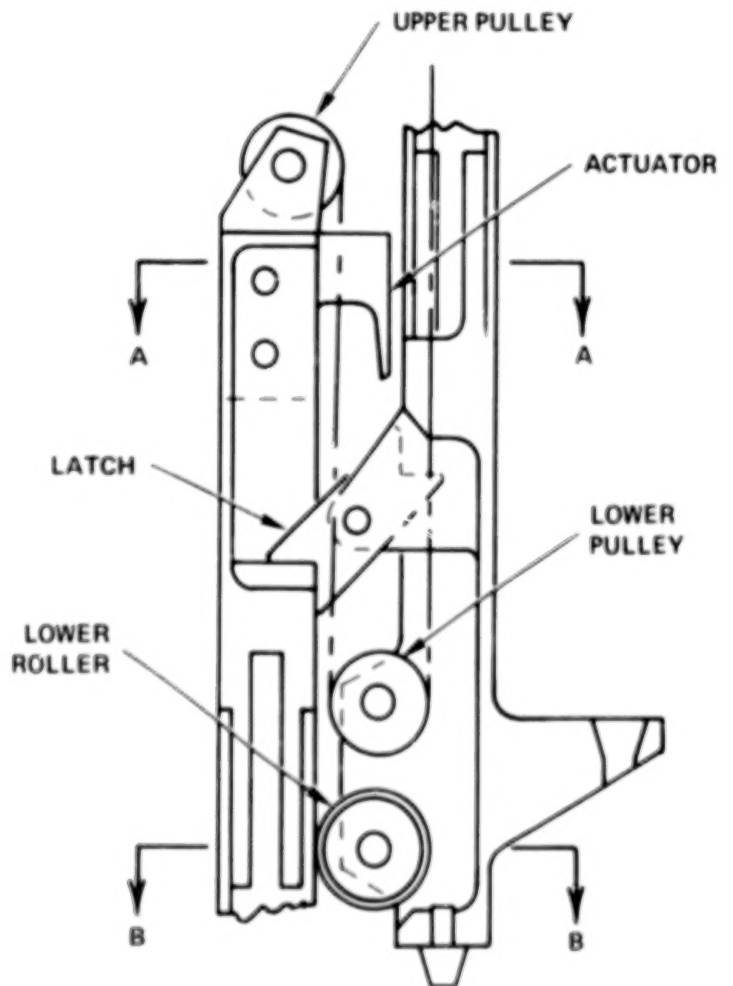
One of the unique features of this design results from the requirement of restowability. A latch design had to be developed which would provide the means for reliably deploying and restowing the mast repeatedly without having to use electro-mechanical devices to de-actuate the latch upon the restowed cycle. The latch shown is a simple ratchet type device that is triggered upon an over-deployment of the mast. Once the mast is compressed, the latch engages against the adjacent fitting which provides a structural load path through the vertical elements of the mast. These structural members also serve as guides for rollers to ride on during the mast deployment.



SECTION A-A

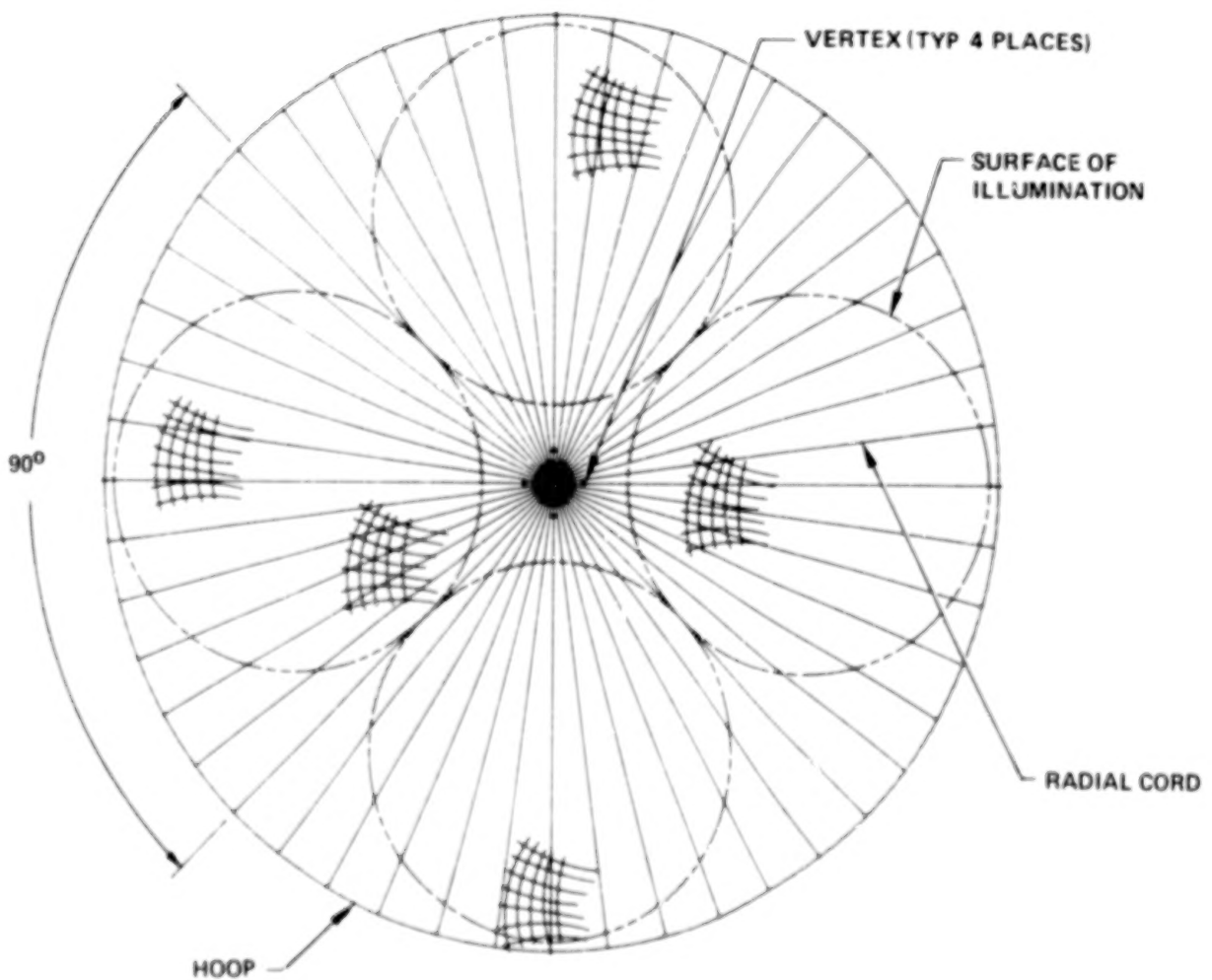


SECTION B-B



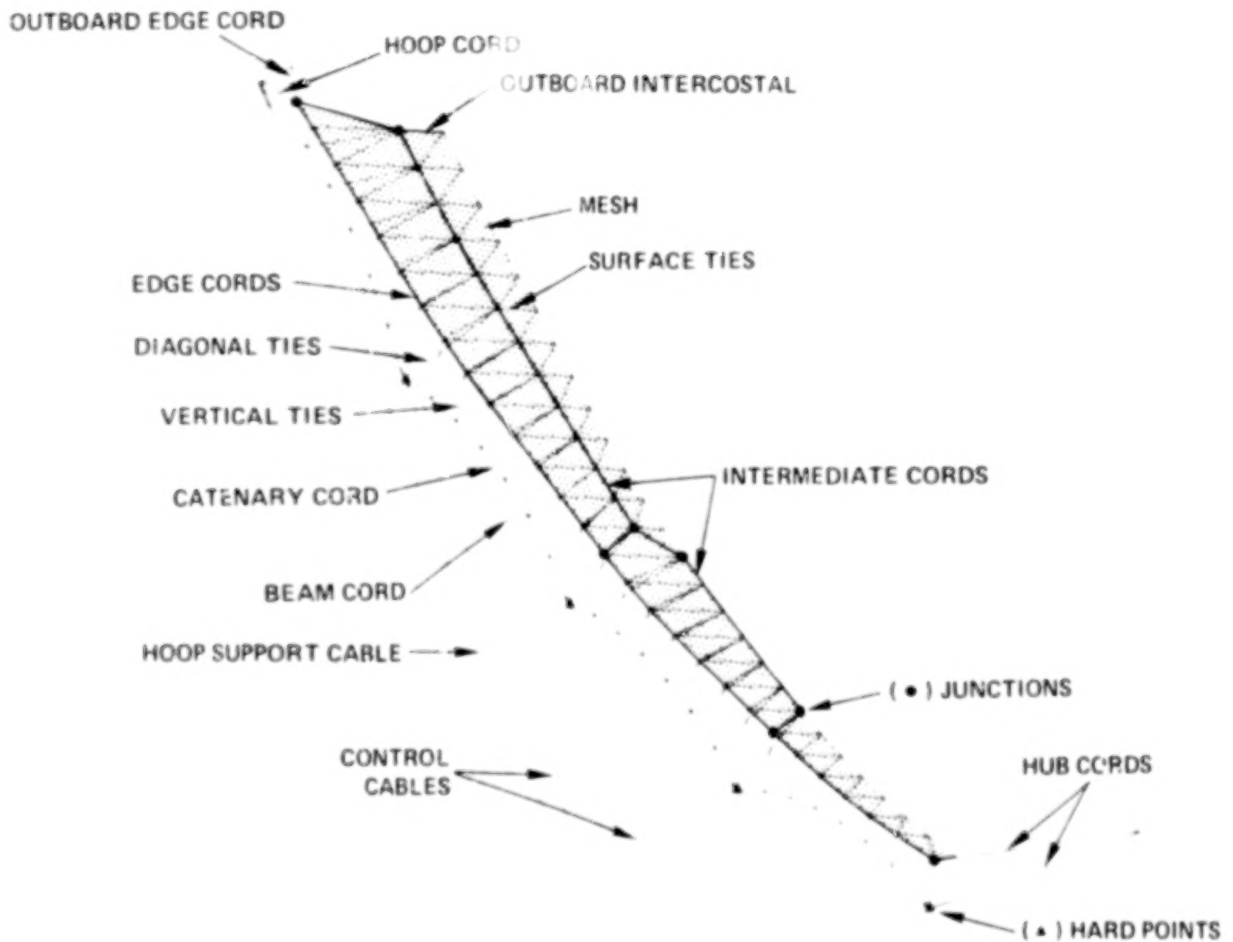
SURFACE PLAN VIEW

The point design is a multiple beam/multiple quadrant offset reflector system. Four separate areas of illumination or aperture areas on the parent reflector are shown. The surface is shaped as if it were four offsets; thus the parent reflector is cusped.



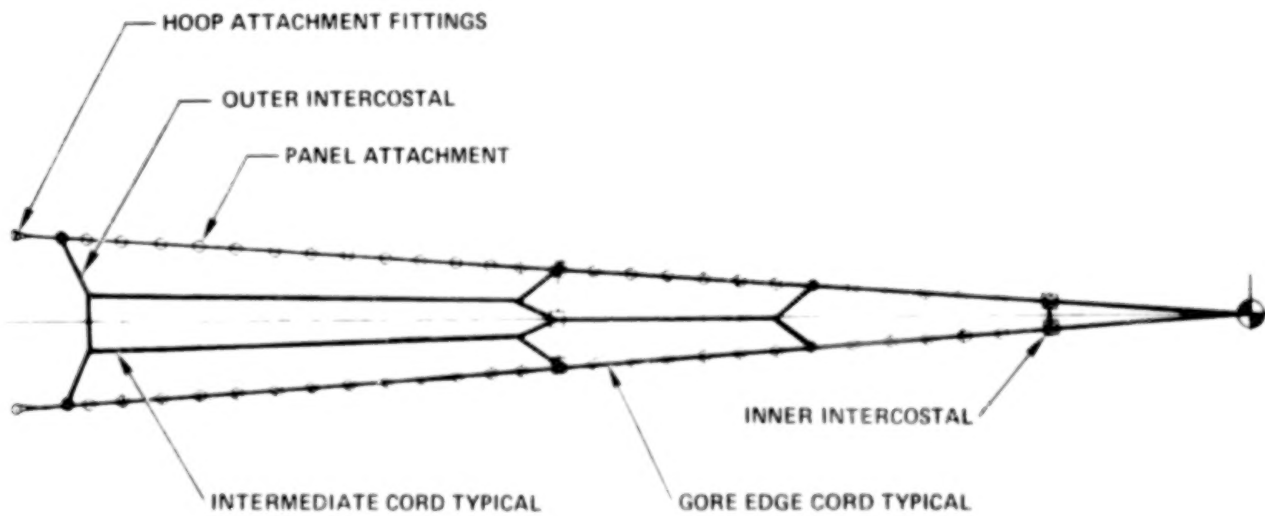
SURFACE ELEMENTS

This figure shows an isometric view of a one-half gore analytical model with the major elements of the design identified. The surface is shaped by a catenary cord and tie members and a series of radial front cord elements. Diagonal ties are also used to position points on the surface between the edges of the gore.



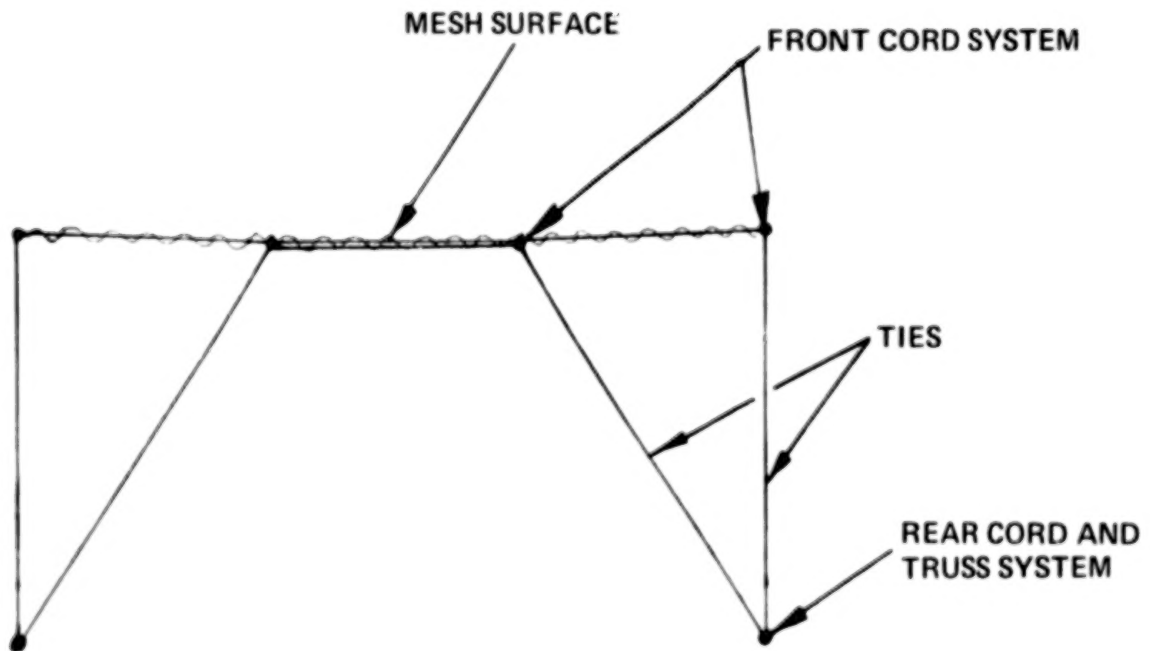
FRONT CORD SYSTEM

The front cord system which makes up the main load carrying structure of the cord dominated antenna concept is shown in this figure.



DIAGONAL CIRCUMFERENTIAL MEMBERS

This viewgraph represents a section cut through the outboard 1/3 of a single gore. It shows the position of both the vertical and diagonal ties and their role in positioning surface elements.



TASK 2 MATERIALS DEVELOPMENT

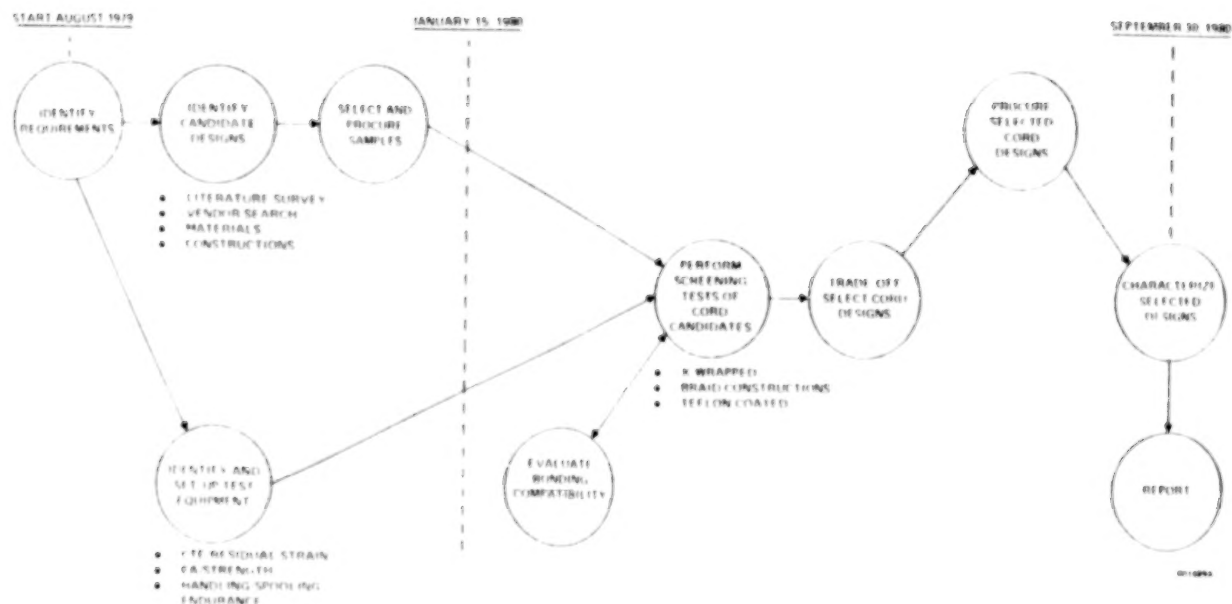
Because of the large number of cords and cable elements involved with the Hoop/Column concept, this task was devoted entirely to the development of key materials for the various cord applications. The objectives of the task are defined in the figure below.

OBJECTIVES

- DEFINE CABLE REQUIREMENTS, STRUCTURAL, THERMAL, ENVIRONMENTAL
- PERFORM DATA RESEARCH
- EVALUATE CANDIDATE MATERIALS AND CONFIGURATIONS
- FABRICATE SAMPLES OF SELECTED CABLE MATERIAL/ CONFIGURATION COMBINATIONS
- DETERMINE MATERIAL PROPERTIES OF SELECT CONFIGURATIONS VIA APPROPRIATE TESTS
- PROVIDE DESIGN DATA AS INPUT TO OTHER TASKS

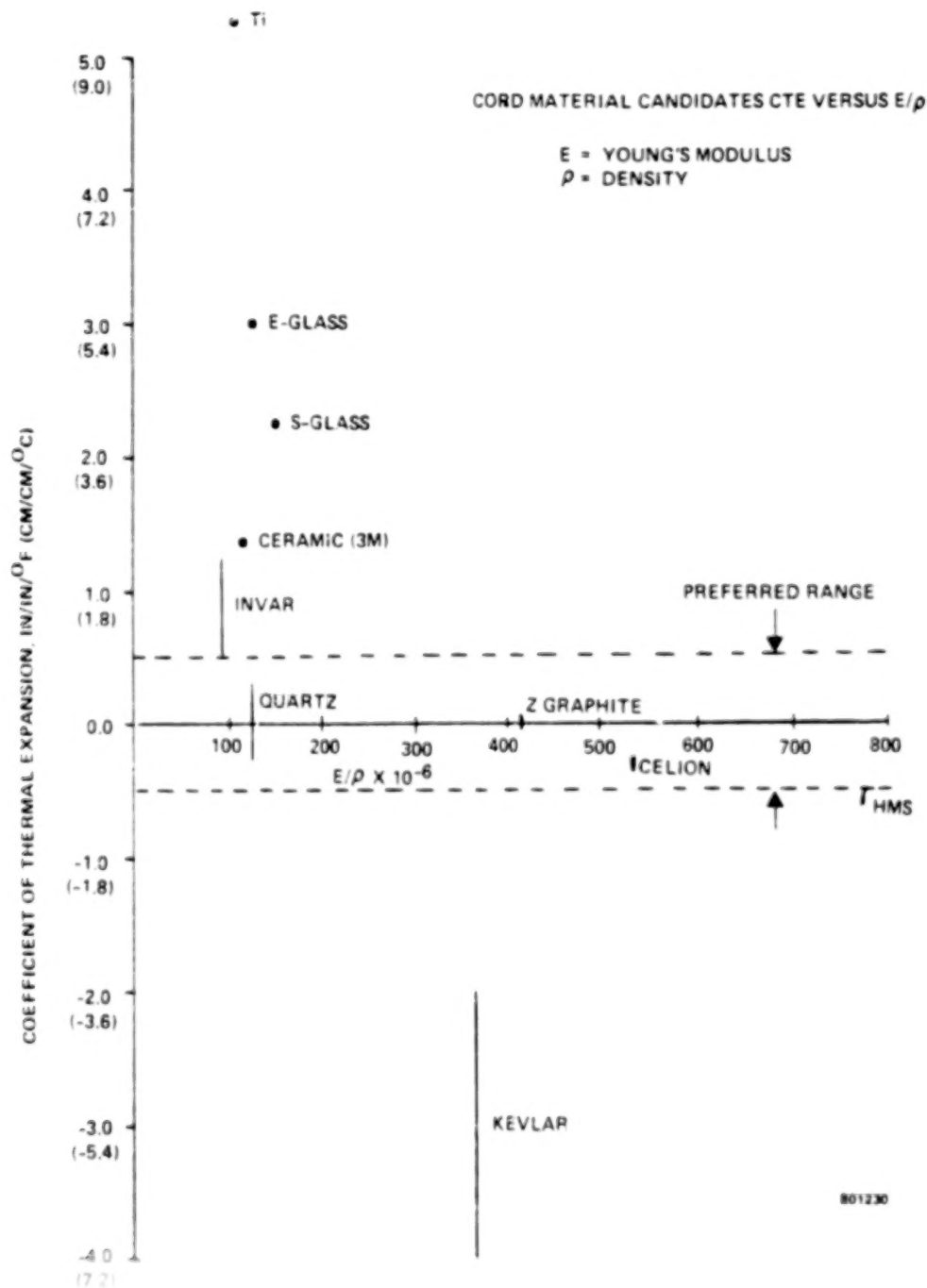
TASK 2 FLOW

The chart below shows the basic flow the materials development task took from its initiation to the present time.



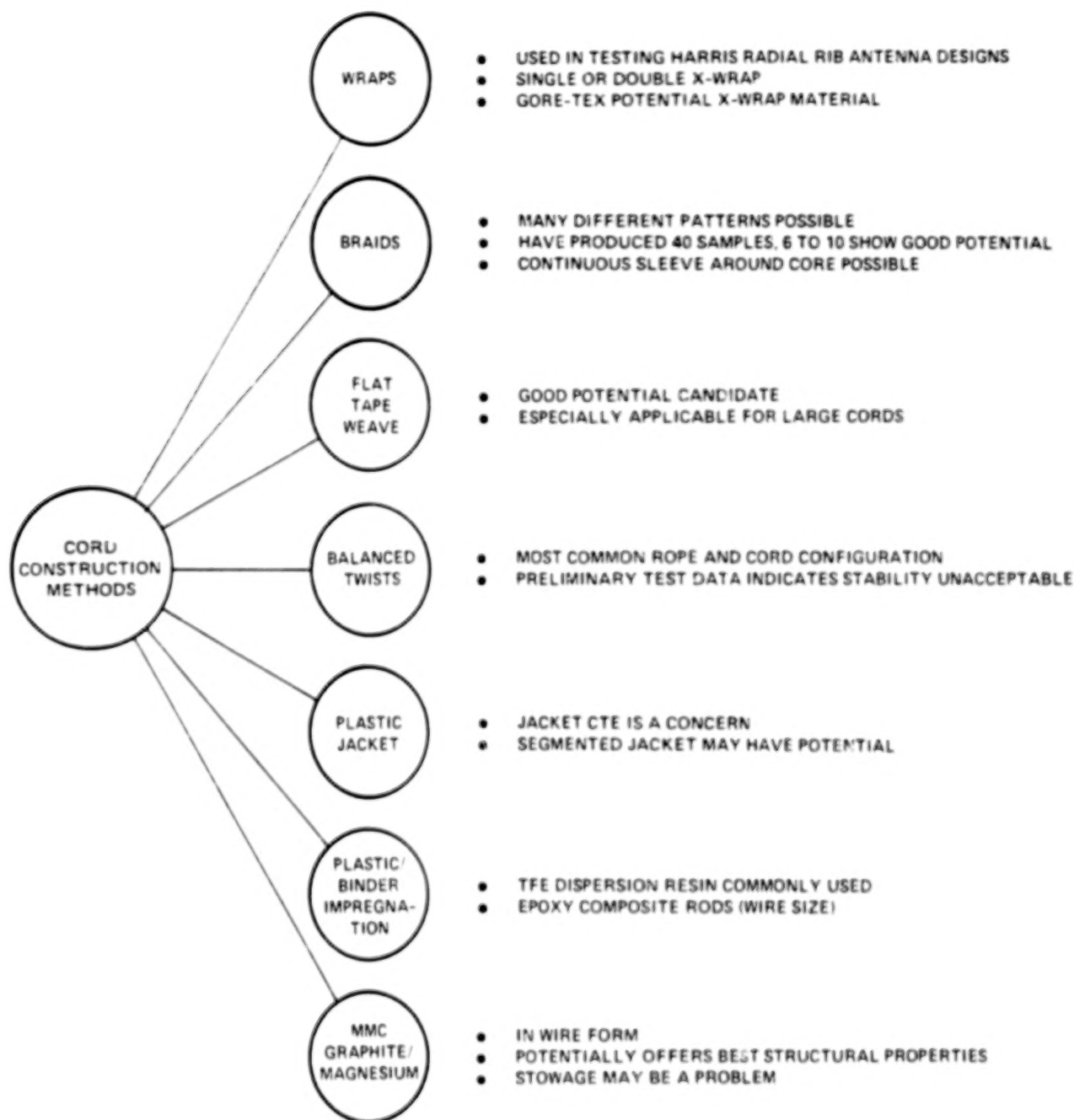
CTE VS SPECIFIC MODULUS FOR VARIOUS MATERIALS

One of the critical parameters used to evaluate different material configurations under consideration was the coefficient of thermal expansion (CTE). In the chart below, values of the CTE are plotted against specific modulus. The candidates that fall within a preferred range of $\pm .9 \times 10^{-6}$ cm/cm/°C (graphite and quartz) show highly desirable thermal elastic properties. The graphite, however, shows a significant advantage in terms of the specific modulus. This led to most of the evaluation work being performed on the Celion fiber.



CORD CONSTRUCTION METHODS

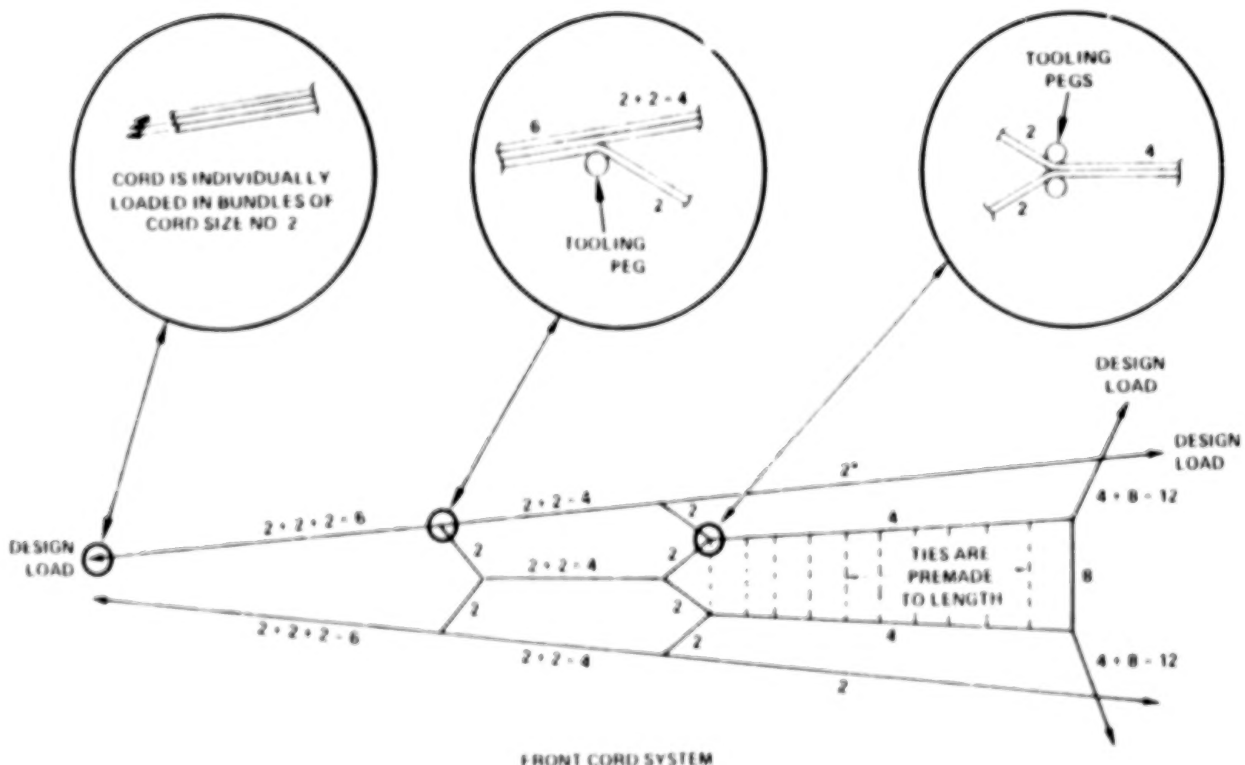
Various techniques were evaluated for making cords. The chart below describes the basic types that were considered and comments on each. For most of the Hoop/Column cord applications, the teflon impregnated cord offers the greatest promise.



CORD JOINT MANUFACTURING

The unique configuration of cords coming into a junction presented problems in joining techniques. After various trade studies were completed, the following joint concept was selected as being the most readily implementable and providing uniform structural properties. In order to meet the primary goal of build to dimension for the point design, an assembly method had to be devised which would yield the lowest manufacturing tolerances. The method selected involved the use of maintaining both geometry control and preload control during the manufacturing process. Individual cords are loaded and positioned over accurately placed tooling pegs at each junction on the panel. The appropriate regions of teflon coating on the cords are stripped-off and adhesive applied. A graphite epoxy board fitting is placed over the tool pegs and bonded to the cords. Finally, separate graphite fittings having the same thickness as the cords are bonded in position and a top cover placed in a sandwich fashion over the top. The result is a very high strength joint for transitioning load around the corner in the cable while still maintaining full cable properties. The various joints and cord quantities per panel are shown in the following three figures.

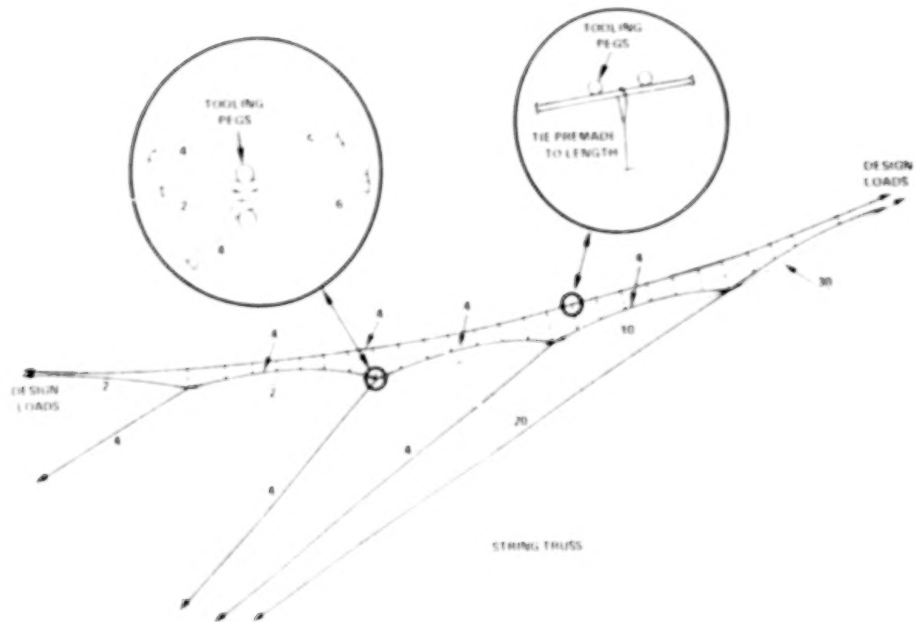
CORD JOINT DESIGN MANUFACTURING CRITERIA



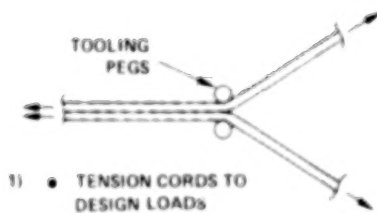
*NUMBERS INDICATE CORD SIZE

801437A

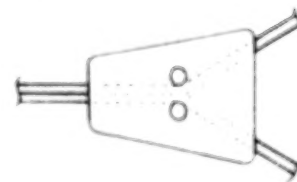
CORD JOINT DESIGN
MANUFACTURING CRITERIA (CONTINUED)



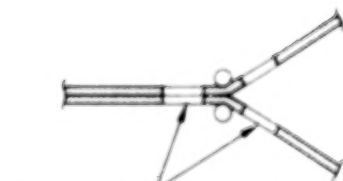
CORD JOINT MANUFACTURING PROCESS



- 1) • TENSION CORDS TO DESIGN LOADS



- 3) • TO APPLY EPOXY ADHESIVE TO GRAPHITE/EPOXY FITTING
- PLACE FITTING OVER TOOLING PEGS WITH ADHESIVE IN CONTACT WITH CORDS
- ALLOW 24 HOURS FOR ADHESIVE CURE



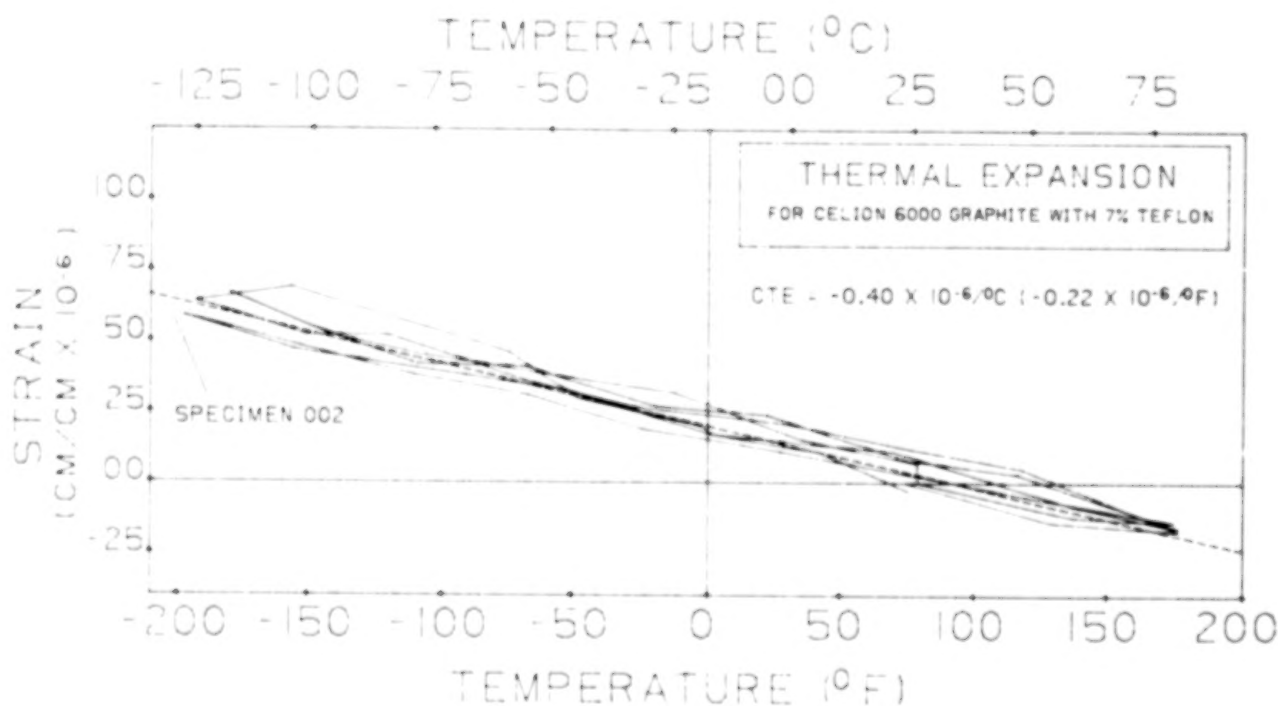
- 2) • REMOVE TEFLON WITH MINIATURE BUTANE TORCH
- APPLY EPOXY ADHESIVE TO CORD AREAS



- 4) • REMOVE FITTING AND CORDS FROM TOOLING PEGS AND BOND LAMINATE CAP TO EXPOSED CORD SIZE OF FITTING

COEFFICIENT OF THERMAL EXPANSION DETERMINATION

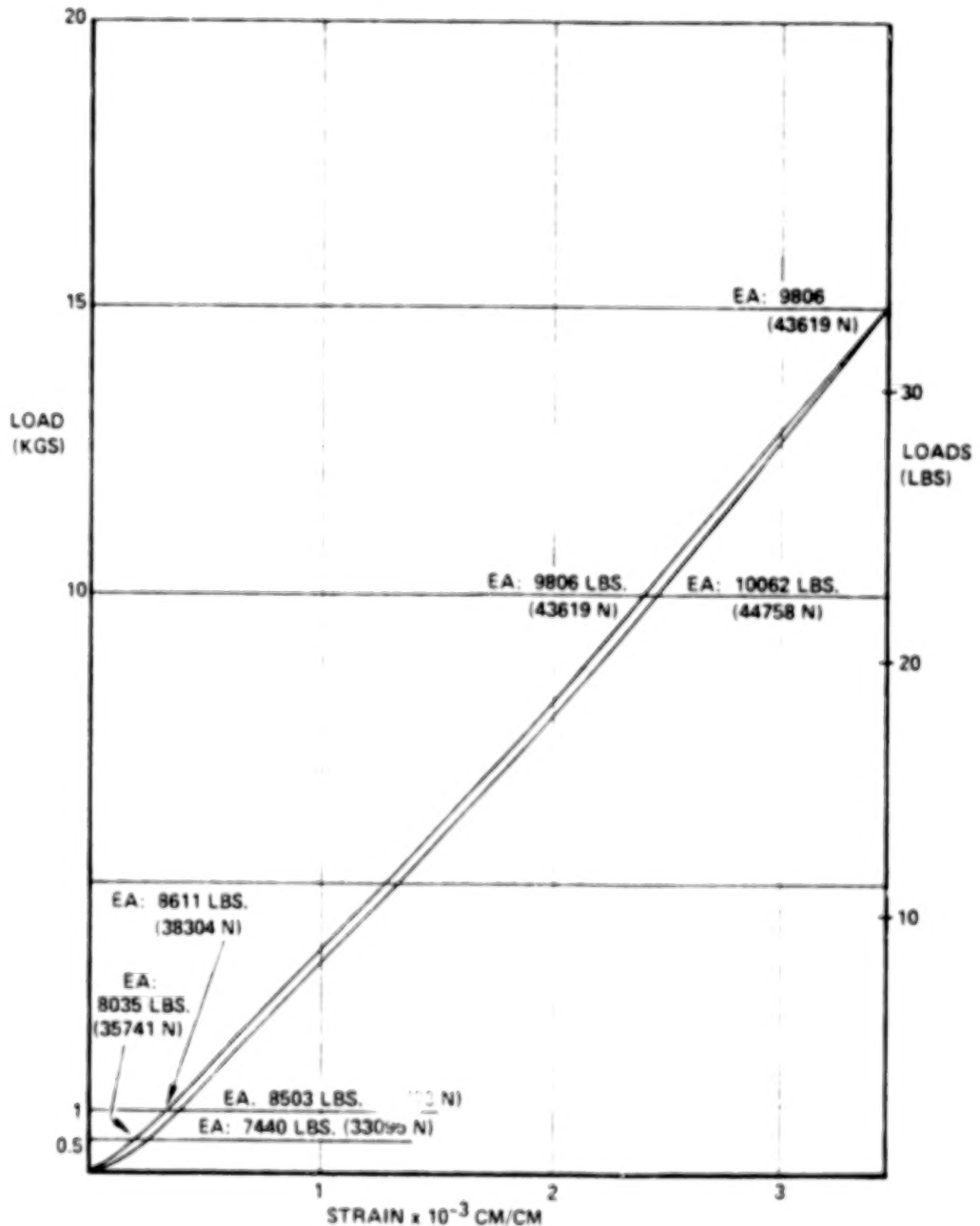
The coefficient of thermal expansion is determined by means of a deflection test set-up using a long cord specimen which is heated and cooled over the appropriate temperature range. Deflection is measured at various temperature increments. It can be seen by the curve below that good repeatability of strain verses temperature occurs, and the resulting CTE is very low. (Approximately -0.4×10^{-6} cm/cm/°C)



GRAPHITE CORD STIFFNESS

The figure below shows the results of load/strain tests for a number two cord (Celion 6000 graphite fiber) with a 7% teflon coating. The curve shows the relatively linear characteristics of the graphite material over the load range indicated. The analytical value of EA of 40 000 N (9000 lbs) is an average number that was reproducible within the range of the curve. As can be seen, the EA value varies slightly with load.

**LOAD VS. STRAIN FOR CELION 6000 GRAPHITE WITH 7 % TEFLON
(NO. 2 CORD)**



RESULT SUMMARY

The chart below highlights some of the results of the cord & cable development task. Results for the teflon coated graphite cords were very encouraging from a structural, thermal-elastic, residual strain and manufacturing sense. Further work is still required to develop statistical basis allowables, but the results to date are very promising.

- TEFLON COATED GRAPHITE CORD MATERIAL WAS SELECTED. COMPARED TO QUARTZ, IT HAS:
 - THREE TIMES HIGHER MODULUS (E)
 - TWICE THE STRENGTH
 - EXHIBITS NO RESIDUAL STRAIN (AVERAGE OF FOUR SAMPLES)
 - MEASURED CTE OF $-0.41/^{\circ}\text{C}$ ($-0.23/^{\circ}\text{F}$) AND OTHER FIBERS FROM MANUFACTURERS WITH PREDICTED ZERO CTE
 - 30% LOWER WEIGHT
 - GOOD HANDLING TOUGHNESS
- TEFLON COATING ON CORDS FACILITATED THE DEVELOPMENT OF IMPROVED JOINT DESIGNS
- DEVELOPED LSST CORD MANUFACTURING PHILOSOPHY
- DEVELOPED TEST PROCEDURES AND EQUIPMENT

TASK 5

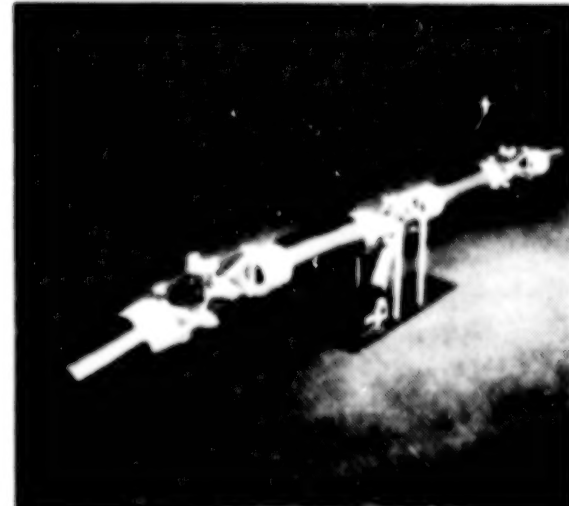
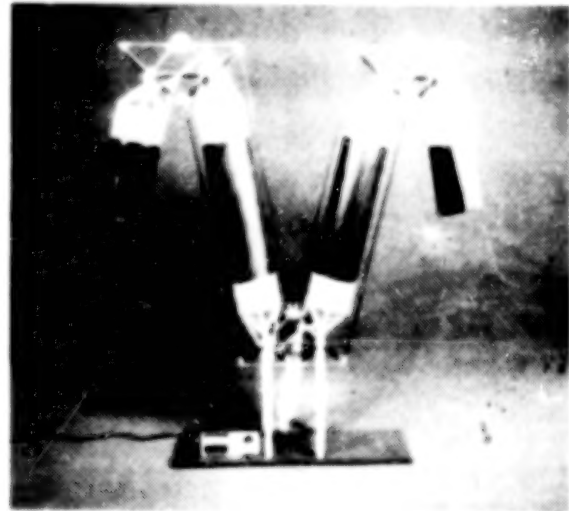
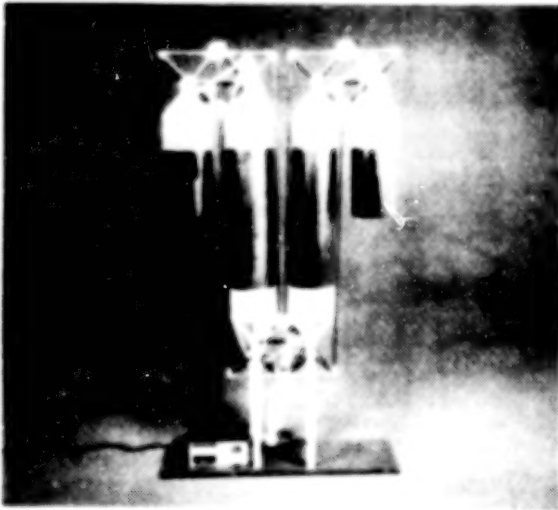
DEMONSTRATION MODELS AND FULL SCALE ELEMENTS

OBJECTIVES

- PROVIDE HOOP/COLUMN DISPLAY MODELS WHICH SATISFY FOCUS MISSION CONFIGURATION REQUIREMENTS
- IDENTIFY CRITICAL COMPONENTS AND FABRICATE FULL OR PARTIAL SCALE VERIFICATION MODELS
- BUILD ACTIVE SURFACE CONTROL BREADBOARD MODEL CAPABLE OF INCORPORATING S.A.M.S.
- BUILD ENGINEERING BREADBOARD MODELS REQUIRED TO SUPPORT DESIGN TRADE-OFFS

HOOP HINGE JOINT MODEL

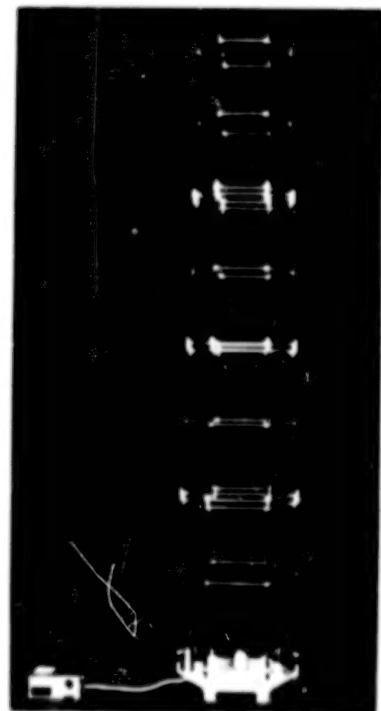
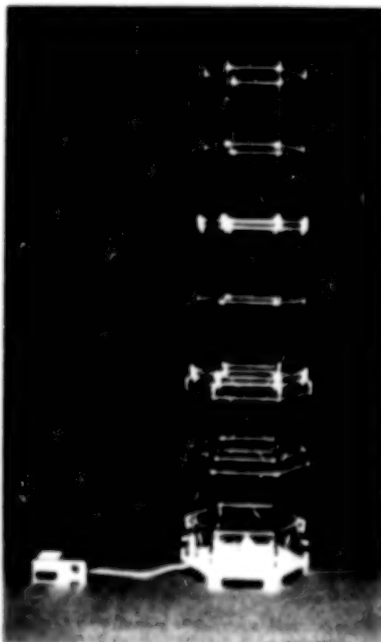
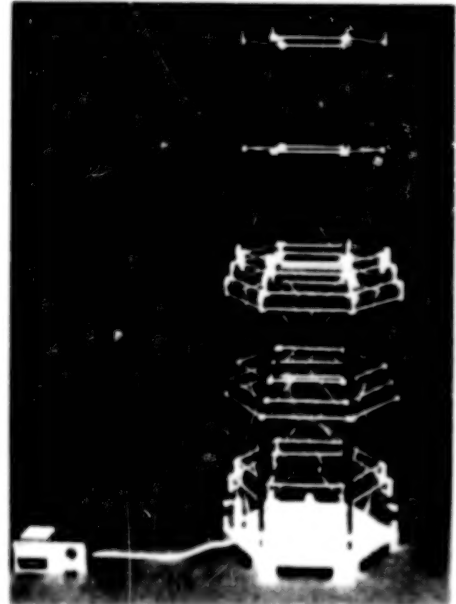
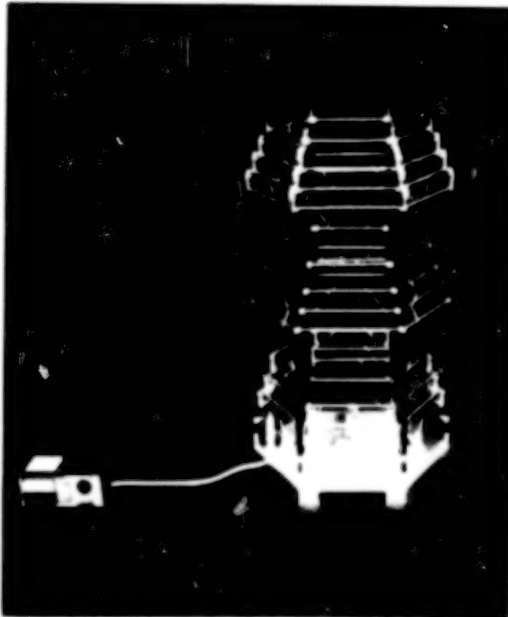
One critical element of the design is the hoop and its deployment method. A model of three full-scale hinge joints with truncated hoop members was fabricated to evaluate the hoop's deployment, synchronization, and repeatability. A single drive unit deploys the model with synchronization being accomplished by means of synchronizing strips connecting adjacent hinge platforms and drive motion accomplished by means of a pushrod link.



**THE HOOP HINGE JOINT MODEL HAS
VERIFIED THE HOOP DEPLOYMENT
MECHANISM DESIGN**

DEPLOYABLE MAST MODEL

Design verification of the mast was accomplished by means of a deployment model. This model represents an approximate 1/5 scale of the point design.



THE MAST MODEL HAS VERIFIED MAST DEPLOYMENT

50 M SURFACE ADJUSTMENT BREADBOARD

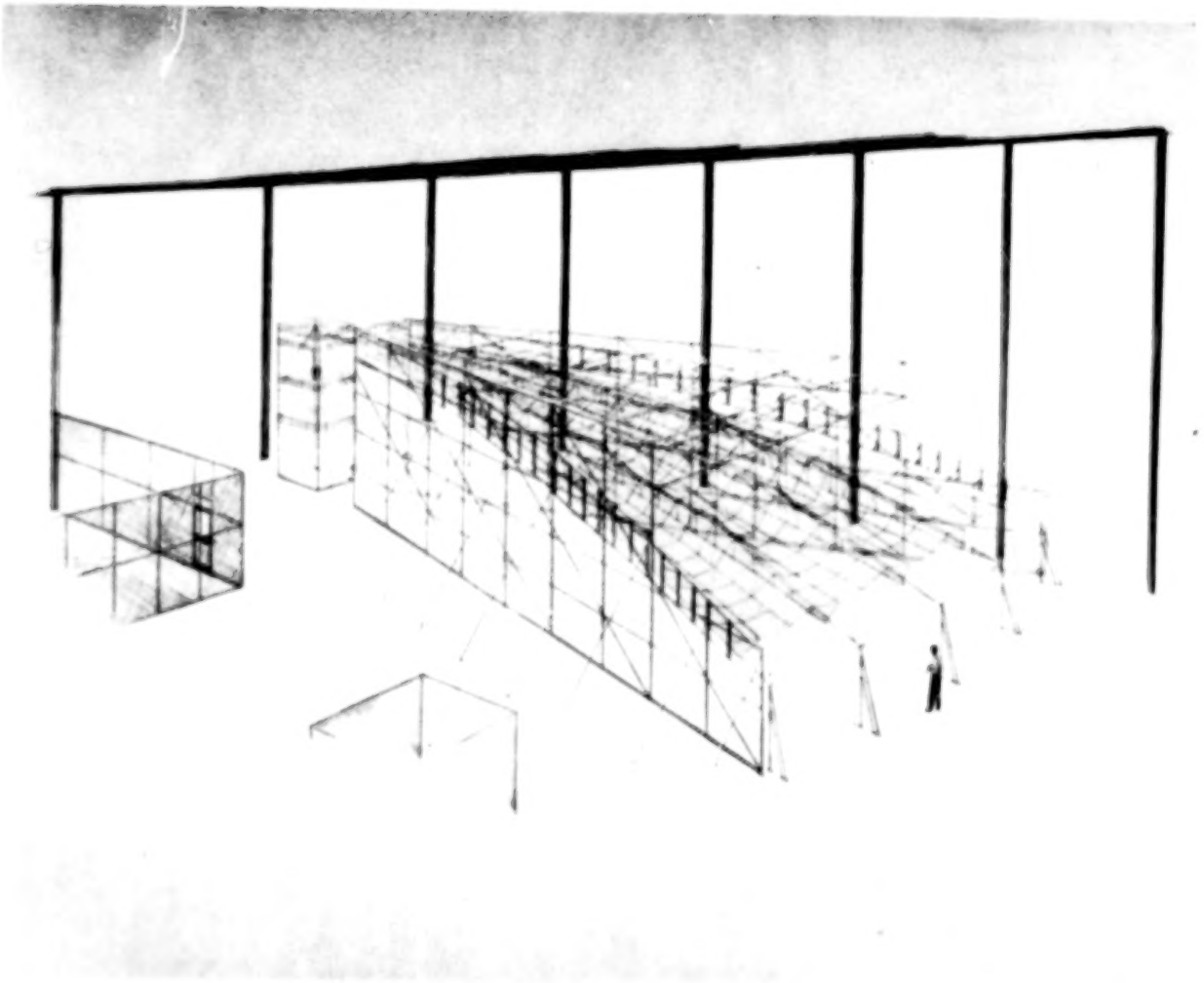
The size of the surface adjustment breadboard model was selected at 50 M for the parent reflector. This size was selected in order to provide a realistic assessment of the manufacturing techniques, analytical models and the ability to adjust the contour. The present phase of the program has completed the design and analysis efforts associated with the configuration. The procurement, fabrication, assembly, and test operations will be accomplished during the second phase of the program in FY'81 & '82. Upon completion of the fabrication and assembly operations, the model will incorporate an engineering model of the Surface Accuracy Measurement System to evaluate the integrated performance.

- TASK OBJECTIVES

- DEMONSTRATE SURFACE ADJUSTMENT CAPABILITY
- VERIFY ANALYTICAL MODELS
- EVALUATE FABRICATION AND ASSEMBLY TECHNIQUES
- PROVIDE TEST-BED FOR OPERATIONAL DEMONSTRATION OF SAMS
- PROVIDE DATA AS INPUT TO SCALING LAWS

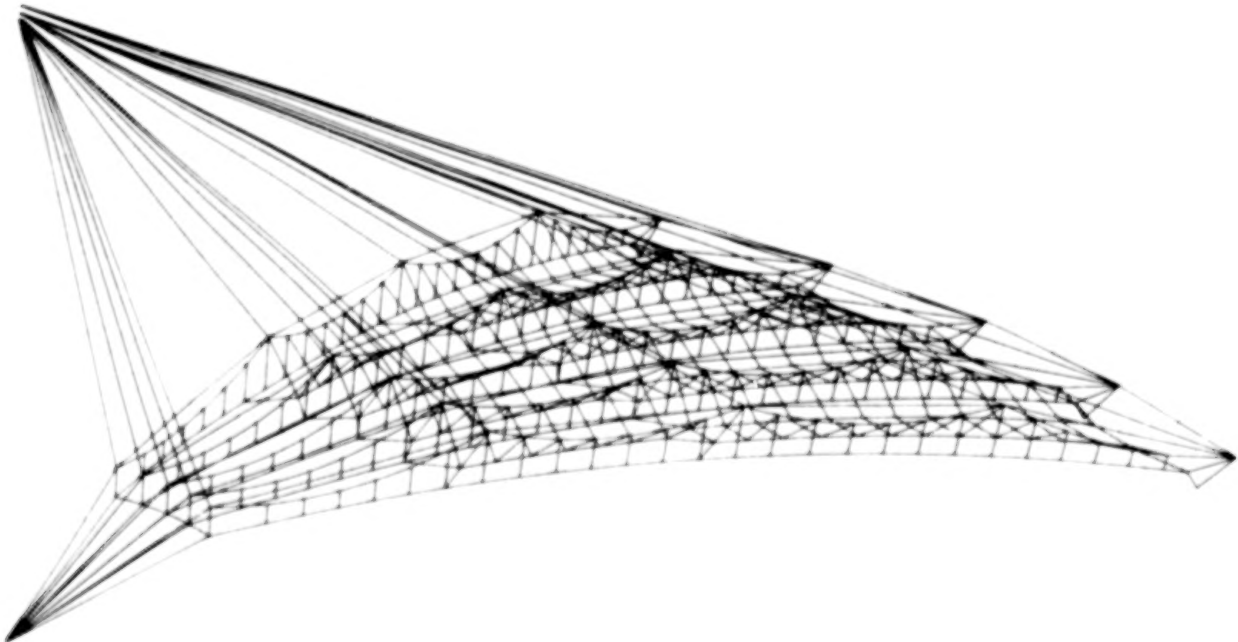
50 M MODEL CONFIGURATION

This artist depiction of the 50 M surface adjustment model shows the four gores which comprise the test article along with the boundary tooling required to support it. The boundary tooling is designed to provide high stiffness and therefore, predictable boundary conditions.



CORD STRINGER ELEMENTS

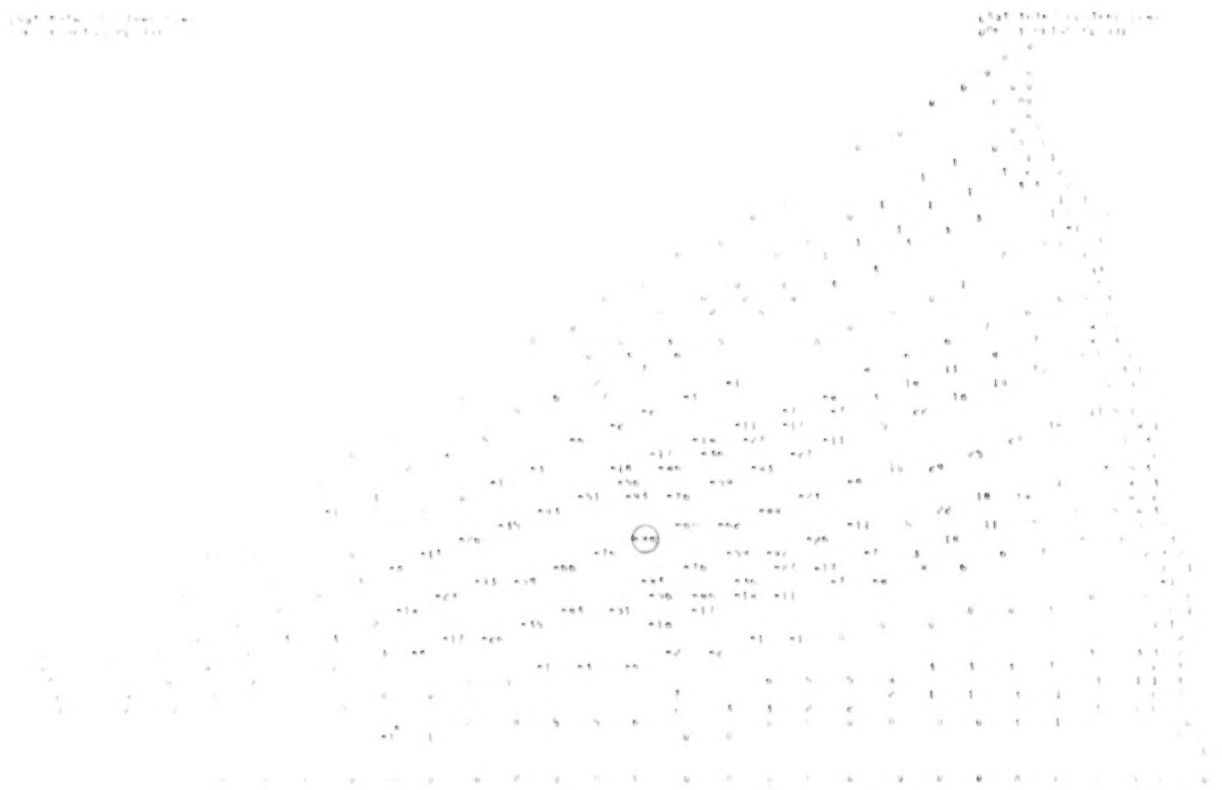
Detailed analytical models were made to assess the performance of the 50 M breadboard model. The figure below is a graphic representation of the four-gore finite element model used in the analysis. Artificial displacements were induced in each control cord to determine the extent of the resulting surface perturbation. This data then permitted an evaluation of the overall adjustment capability of the entire model. The next figure displays the results of this analysis.



SURFACE EFFECTS OF CONTROL CORD DISPLACEMENT

The figure below shows the surface effects of a 2.5 mm (1/10 in.) displacement along the number three control cord. The displacements of surface node points are indicated by the numbers on the figure which represent normal surface displacements in 0.025 mm (1/1000 in.).

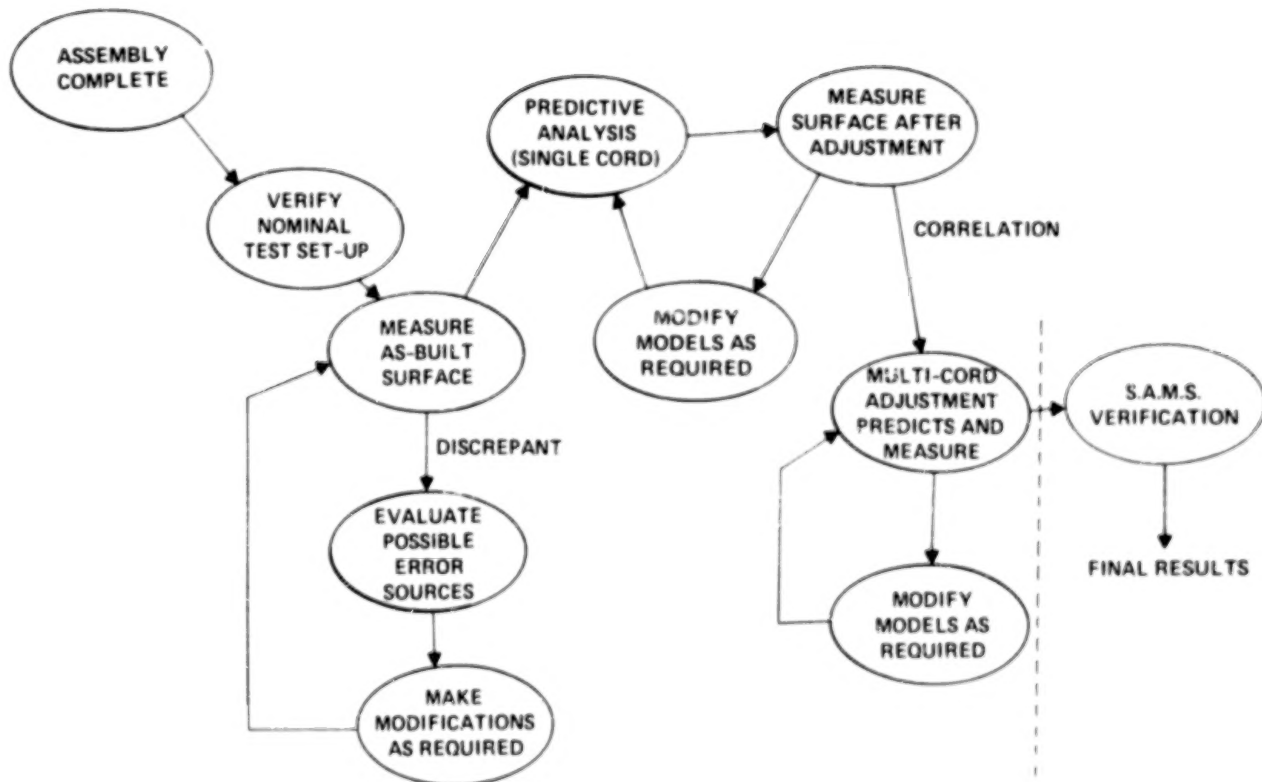
THIRD CONTROL CORD



**MICROFILMED FROM
BEST AVAILABLE COPY**

50 M SURFACE ADJUSTMENT BREADBOARD TEST FLOW

The test flow for the surface adjustment breadboard involves iterative measurements and adjustments of either the model or analytical software. The influence coefficients of each adjustment will be determined analytically and correlated by test. This method will result in a full interaction model capable of predicting cable displacements required to enhance the surface in orbit.



TASK 6 - 15 M MODEL

A 15 M model will be designed and fabricated to evaluate system level performance. The objectives of the task are stated below. The present state of the program is approximately through 1/2 of the design phase. The completion of the model will take place during phase II.

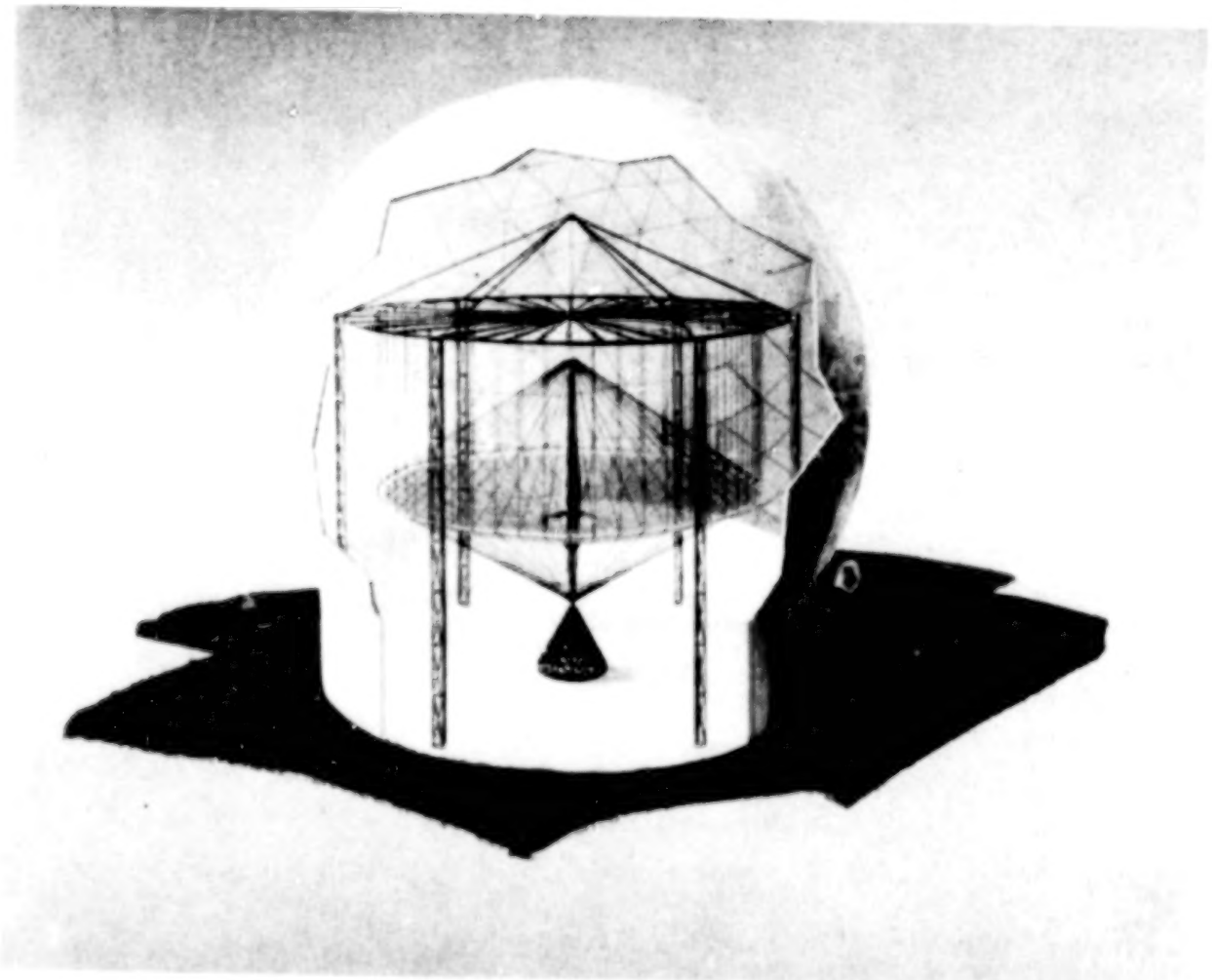
OBJECTIVES

VERIFY THE 100 METER POINT DESIGN IN TERMS OF:

- DEPLOYMENT KINEMATICS
 - HOOP
 - MAST
- DEPLOYMENT RELIABILITY AND REPEATABILITY
- FAILURE MODES INVESTIGATION
- SURFACE INTERACTION
- MANUFACTURING TECHNIQUES
- SCALING

15 M BREADBOARD MODEL

The artist's depiction shows the configuration of the 15 M model. The model will be capable of deployment and stow cycles, repeatability measurements, cup-up/cup-down contour measurements and a series of deployment and failure modes testing.



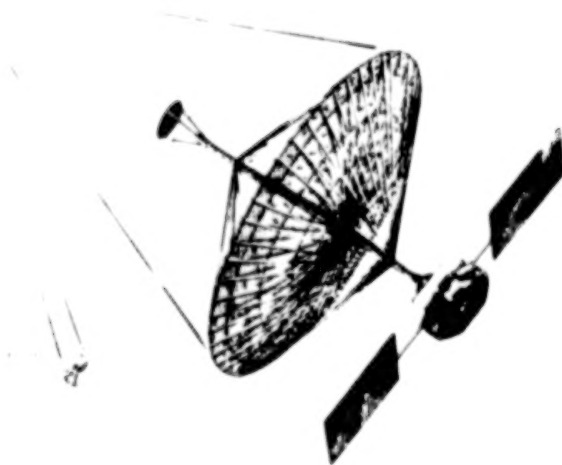
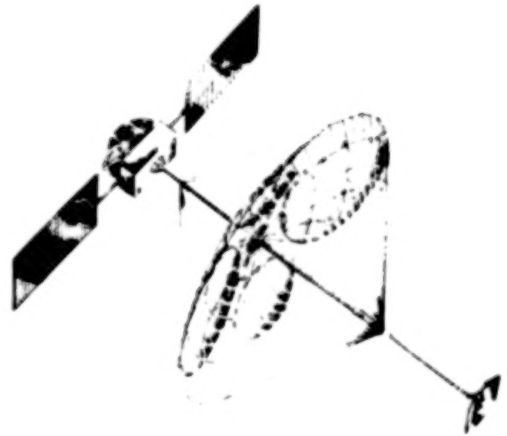
HOOP/COLUMN PERFORMANCE SUMMARY

The following two charts summarize the results of the program to date in terms of the concept's ability to meet the specification established early in the program.

PARAMETER	REQUIREMENTS	PERFORMANCE PROJECTION
• CONFIGURATION	• 100 METER DIAMETER QUAD-APERTURE	• FOUR 40.6 METER APERTURES
• I/D	• 1.53	• COMPLY
• STOWED ENVELOPE	• MAXIMUM ALLOWABLE ENVELOPE IS - 4.56 METERS (15 FEET) DIAMETER - 12 METERS (30.4 FEET) LENGTH	• COMPLY, 4.06M DIAMETER; 10.93M LENGTH
• OPERATING FREQUENCY	• 2.0 GHz	• COMPLY, DESIGN FREQUENCY
• CONTOUR ACCURACY	• $\lambda / 20$ MAXIMUM (7.5mm RMS)	• $\lambda / 27$
• GAIN	• 55.4 dB	• 55.5 dB
• NO. BEAMS	• 219 (55 BEAMS/APERTURE)	• COMPLY
• HPBW	• 0.256°	• COMPLY
• BEAM-TO-BEAM ISOLATION	• 30 dB	• TBD
• POINTING ACCURACY	• 0.03°	• TBD
• SURFACE ADJUSTMENT	• ADJUSTMENT CAPABILITY ON ORBIT	• COMPLY
• DEPLOYMENT	• CONTROLLED, AUTOMATIC (NO EVA) • 60 MINUTES MAXIMUM • MICROSWITCHES FOR DEPLOYMENT VERIFICATION AND STOP	• COMPLY
• RETRIEVABILITY	• AUTOMATIC, CONTROLLED • MICROSWITCHES TO STOP AND VERIFY STOWAGE • MESH SURFACE IS EXPENDABLE	• COMPLY
• LAUNCH & LANDING LOADS	• COMPATIBLE WITH STS ENVIRONMENTS	• COMPLY, ENVIRONMENTS BEING UPDATED
• ORBITAL ENVIRONMENT	• COMPATIBLE WITH LEO AND GEO	• COMPLY, GEO PROVIDES WORST CASE

HOOP/COLUMN DESIGN HAS BROAD APPLICABILITY

The results of the program to date indicate the versatility of the generic concept to be applied to many varying missions. Performance evaluations of the Hoop/Column concept have determined its capabilities to meet the requirements of future identified large antenna missions.



BLANK PAGE

BLANK PAGE

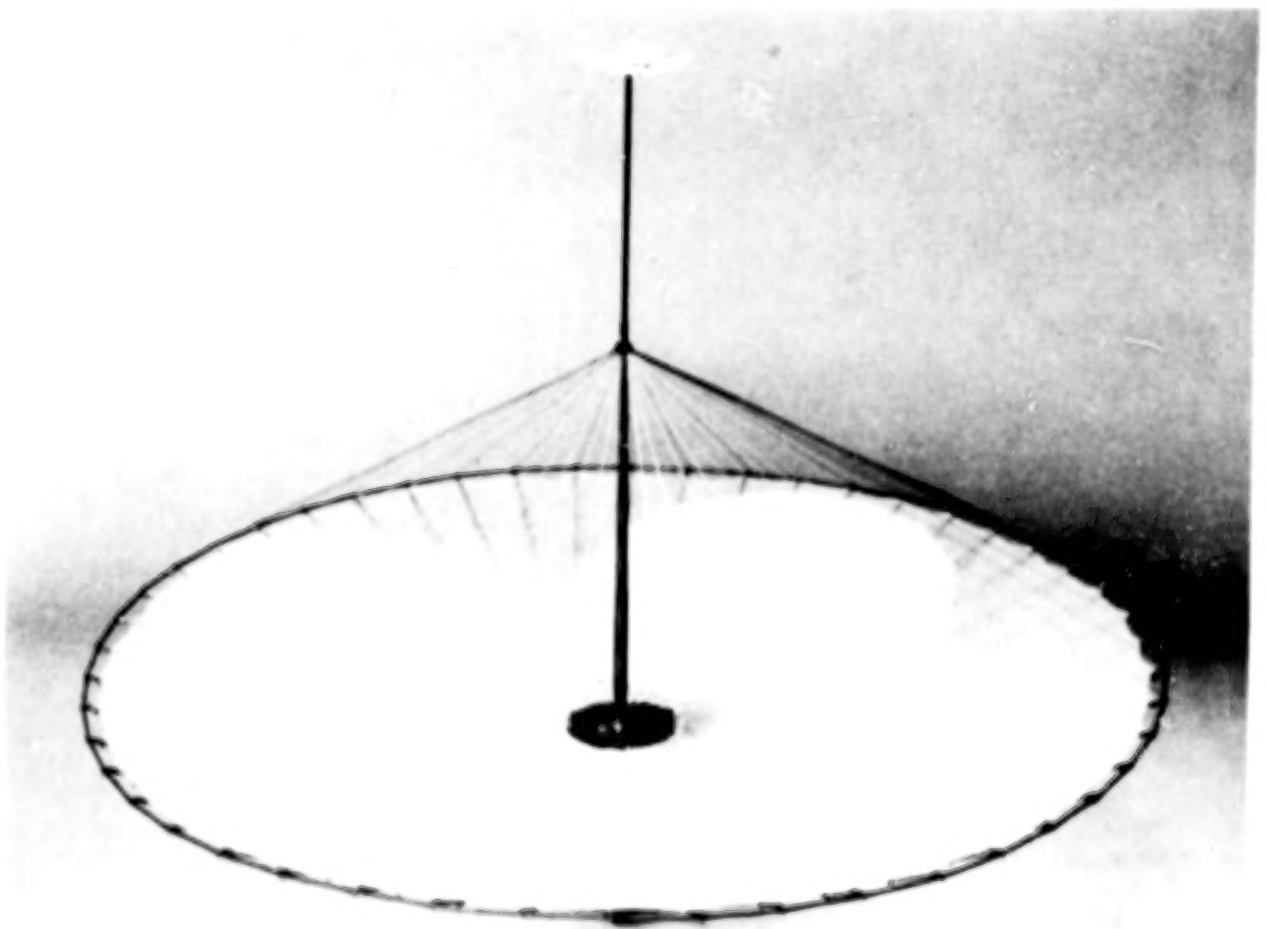
RADIO FREQUENCY PERFORMANCE
PREDICTIONS FOR THE HOOP/COLUMN
POINT DESIGN

THOMAS G. CAMPBELL
NASA LANGLEY RESEARCH CENTER
HAMPTON, VIRGINIA 23665

LARGE SPACE SYSTEMS TECHNOLOGY - 1980
SECOND ANNUAL TECHNICAL REVIEW
NOVEMBER 18-20, 1980

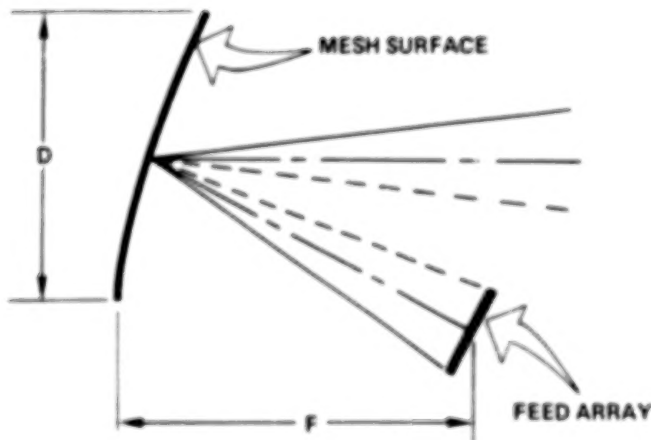
QUAD APERTURE POINT DESIGN
FOR THE HOOP/COLUMN ANTENNA

Shown below is the quad aperture point design for the 100-meter diameter point design. The four 40-meter diameter offset reflectors are indicated. Utilizing multiple offset apertures is an approach for producing asymmetrically illuminated reflectors within a symmetrical structural configuration.



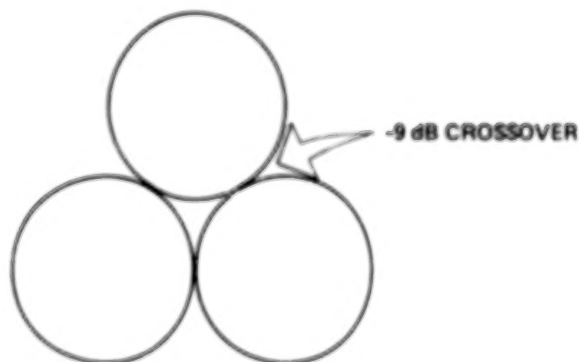
MULTIPLE BEAM PERFORMANCE USING SINGLE OFFSET REFLECTOR

The multiple beam performance using a single offset reflector is limited by the space allowable for the corresponding feed arrays in producing the number of beams required. Typically a -9dB crossover level is achievable using a moderate number of beams. But as the number of beams is increased and a higher crossover level is desired, then a single offset reflector can not be used effectively.



- $F/D > 1.0$ REDUCES COMA
- CLOSE BEAM PACKING ACHIEVED BY UTILIZING TRIANGULAR LATTICE

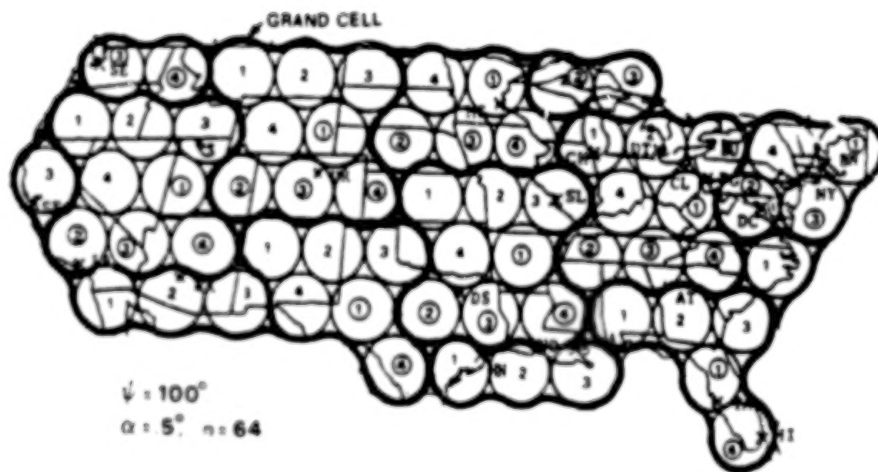
OFFSET REFLECTOR
ANTENNA



FAR-FIELD BEAM CONTOUR

STUDY BEAM PLAN

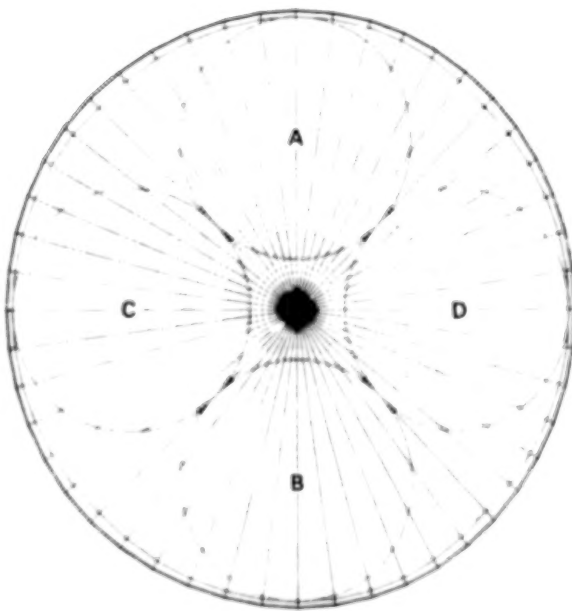
The multiple beam antenna requirements presently being considered will produce beam topologies similar to one shown below. This beam study plan is presently under contract with General Electric and Mr. Peter Foldes.



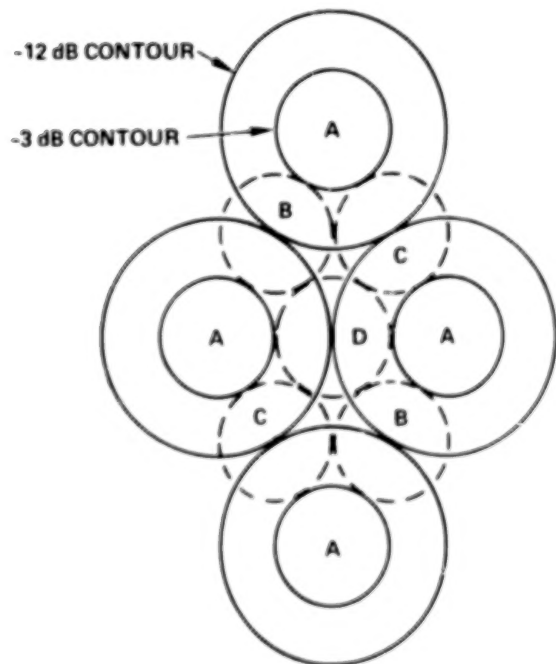
QUAD APERTURE ANTENNA

Improved beam crossover levels and the feed "real estate" problem can be solved by using multiple offset reflectors. Shown below, the beam crossover level can be improved to -3dB by interleaving the beam from four separate offset reflectors.

FOUR OFFSET REFLECTORS



FOUR REFLECTOR BEAM INTERLEAVING



- -12 dB BEAMWIDTH 0.52°
- -3 dB BEAMWIDTH 0.26°
- 3° N-S BY 6° E-W CONTIGUOUS COVERAGE BY 219 BEAMS

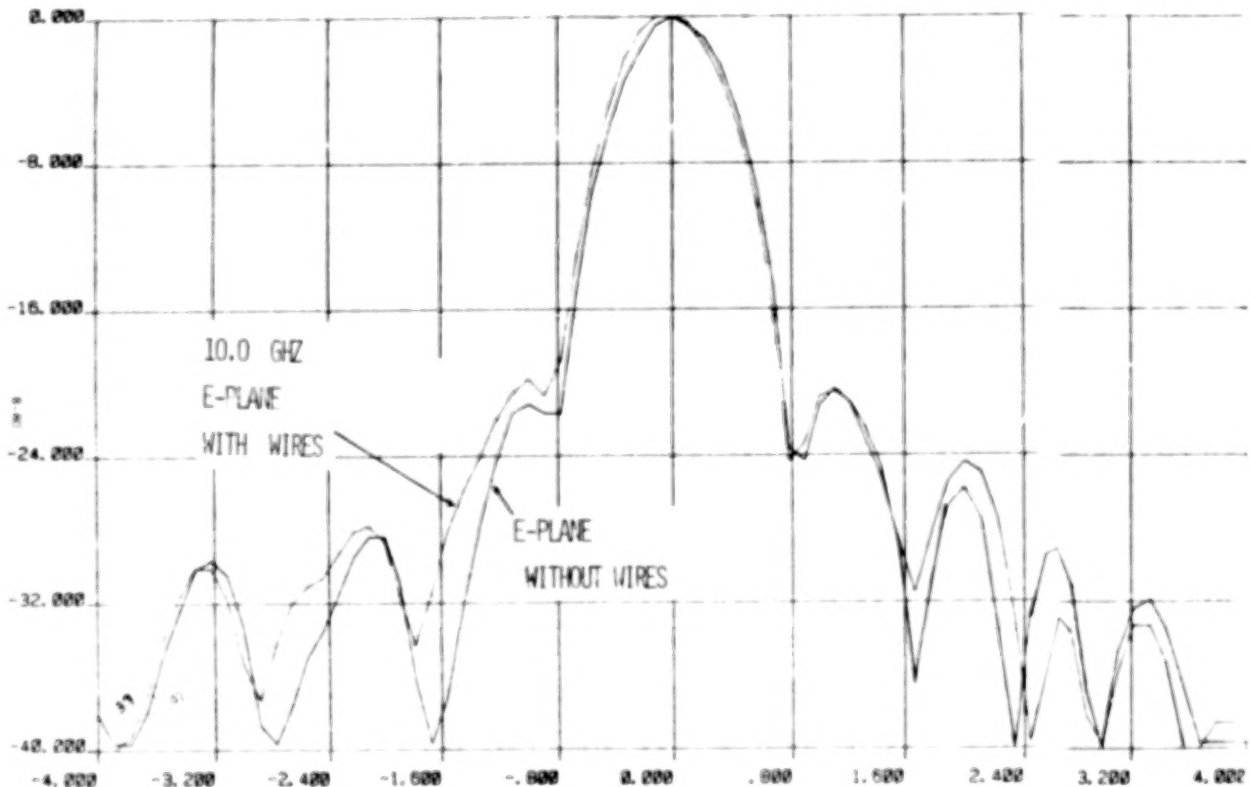
PROJECTED GAIN BUDGET
FOR THE QUAD APERTURE HOOP/COLUMN
ANTENNA

The projected gain budget for the 100-meter quad aperture antenna is shown below. The loss associated with cable blockage is based on task results using the AAFE Hoop/Column configuration. Analysis methods are being developed that will predict the scattering and blockage effects caused by the hoop control cables in front of the aperture. But, until this analysis is completed, experimental tests are and will be conducted to better understand the effect.

LOSS MECHANISM	LOSS (dB)
AMPLITUDE ILLUMINATION (20-dB TAPER)	1.27
PHASE EFFICIENCY	0.05
AMPLITUDE SPILLOVER	0.46
FEED BLOCKAGE	0.00
FEED OHMIC LOSS	0.15
FEED VSWR (1.2:1)	0.04
CABLE BLOCKAGE (CABLE DIA. = 5.6 mm (0.22 IN.))	0.13
SURFACE REFLECTIVITY (MESH OPENING SIZE 6.3 mm (0.25 IN.))	0.20
REFLECTOR ROUGHNESS (RMS ϵ = 6.6 mm (0.22 IN.))	0.47
REFLECTOR CROSS POLARIZATION	0.01
DEFOCUS (ΔF = 173.2 mm (6.82 IN.))	0.08
SCAN LOSS (13 BEAMWIDTHS SCAN)	<u>0.25</u>
TOTAL LOSSES (dB)	3.1
ANTENNA EFFICIENCY	49%
100% GAIN (dBi)	58.6
NET GAIN (dBi)	55.5

RESULTS OF BLOCKAGE TESTS

Preliminary antenna pattern tests were conducted early in the program to determine if catastrophic effects were produced by cables (conducting) in the aperture. This test consisted of an apex feed illuminating a 3-meter solid reflector. The hoop/column configuration developed during the AAFE program was used in positioning the various wires and cables. Radiation patterns were measured at 7 GHz and 10 GHz. No catastrophic effects were observed for the AAFE configuration, but additional tests are required to determine the effects for more precision multiple beam applications.



E - PLANE COMPARISON

CONCLUSIONS BASED ON PRELIMINARY TESTS RESULTS

- ° GAIN DEGRADATION DUE TO METALLIC CABLE BLOCKAGE SHOULD BE MINIMAL (LESS THAN 0.10 dB FOR 100 - METER DISH)
- ° MAXIMUM ANTICIPATED SIDELobe IMPACT DUE TO CABLE BLOCKAGE 1.0 dB
- ° AGREEMENT BETWEEN MEASUREMENTS AND ANALYTICAL PREDICTIONS VALIDATE ANALYSIS FOR APPLICATION TO SIMILAR DESIGN
- ° FURTHER TESTS RESULTS WILL BE AVAILABLE BY NOV. 1980 OF CABLE EFFECTS FOR QUAD APERTURE CONFIGURATION.

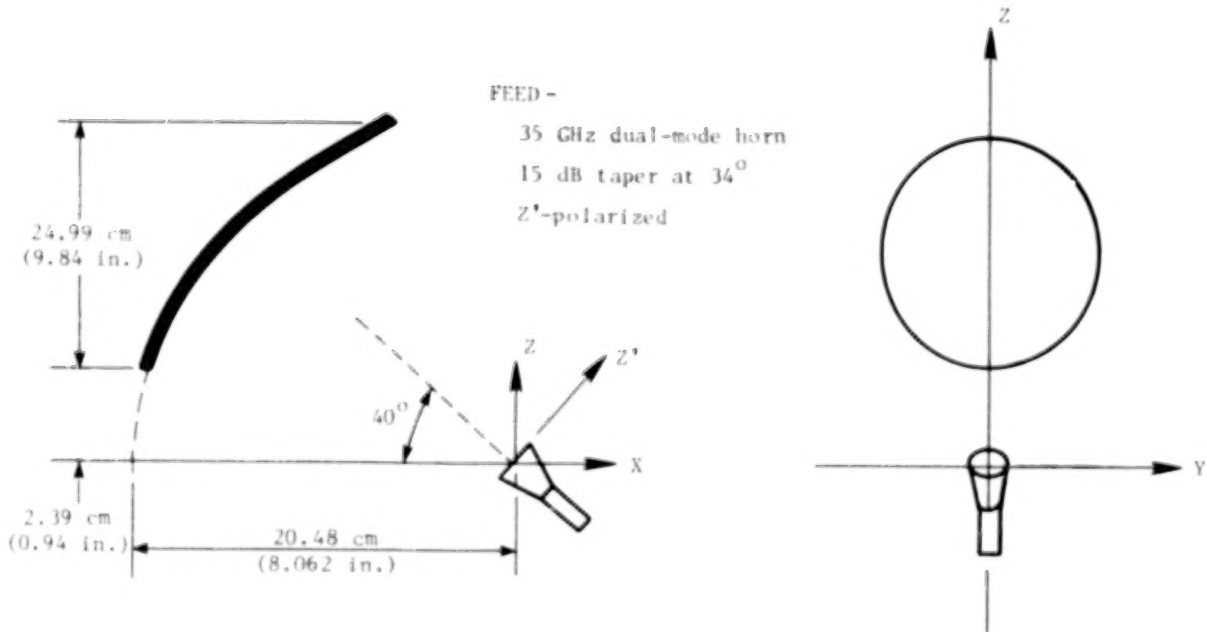
PHOTOGRAPH OF BLOCKAGE MODEL

The 3-meter reflector used for the blockage test is shown below.



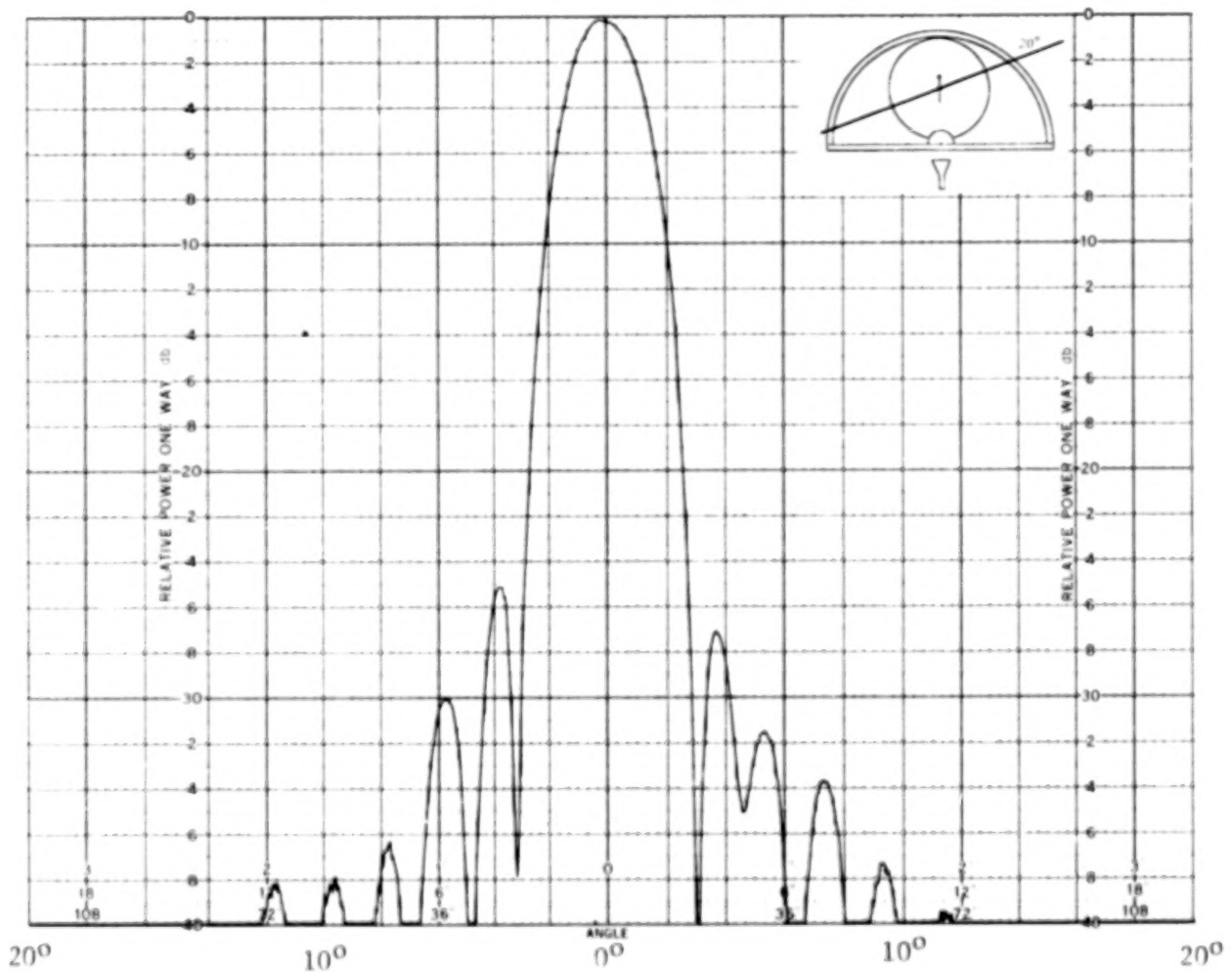
OFFSET PARABOLOIDAL REFLECTOR

In order to better understand the scattering and blockage effects on multiple beam performance, a 35 GHz model was used to model somewhat a single quad aperture configuration. The geometry for this model is shown below.



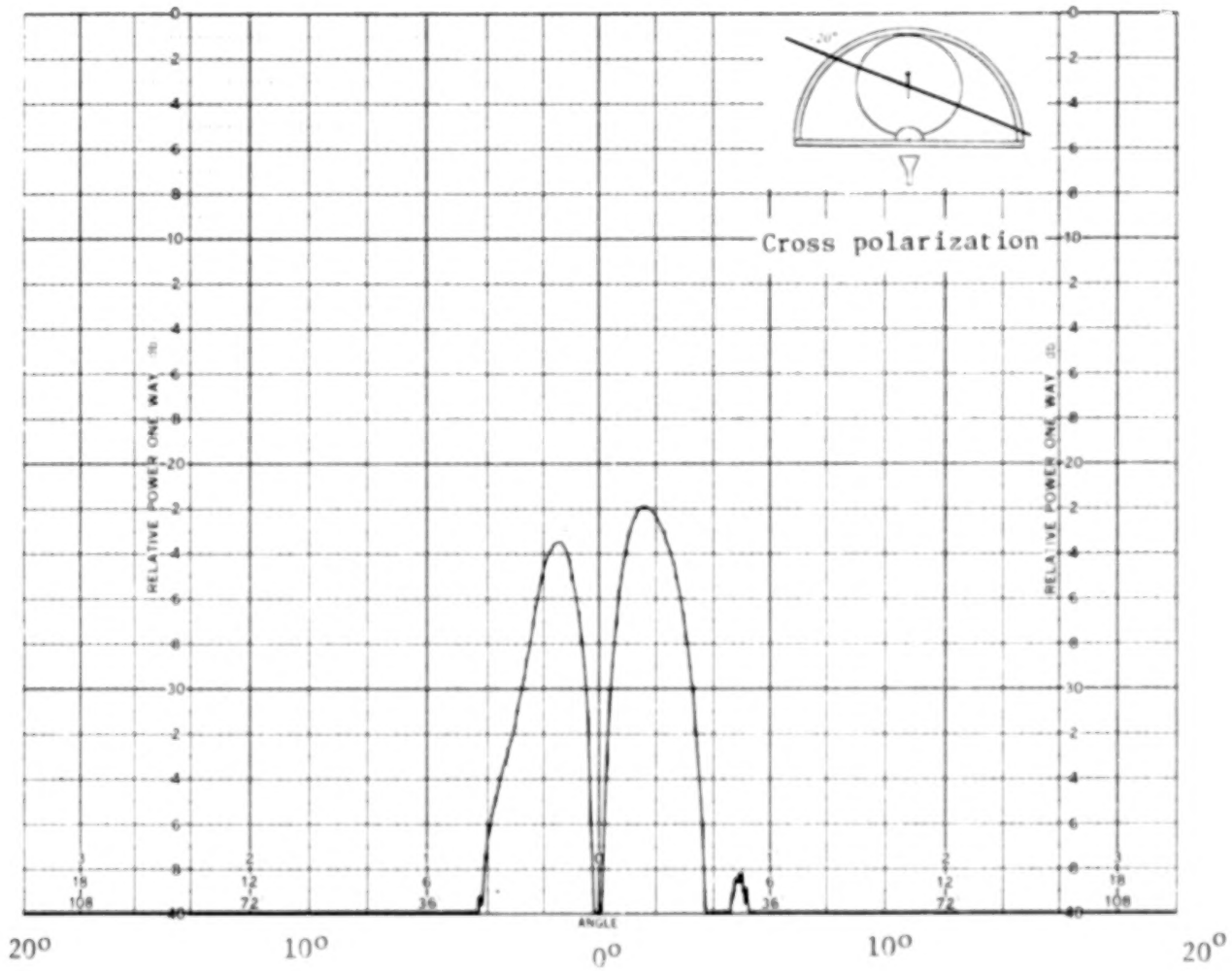
EXPERIMENTAL RESULTS USING 35-GHz MODEL

The experimental results using the 35-GHz model simulating the quad aperture reflector begin with the following figure. This pattern is for the case of no cables in the aperture and vertical polarization.



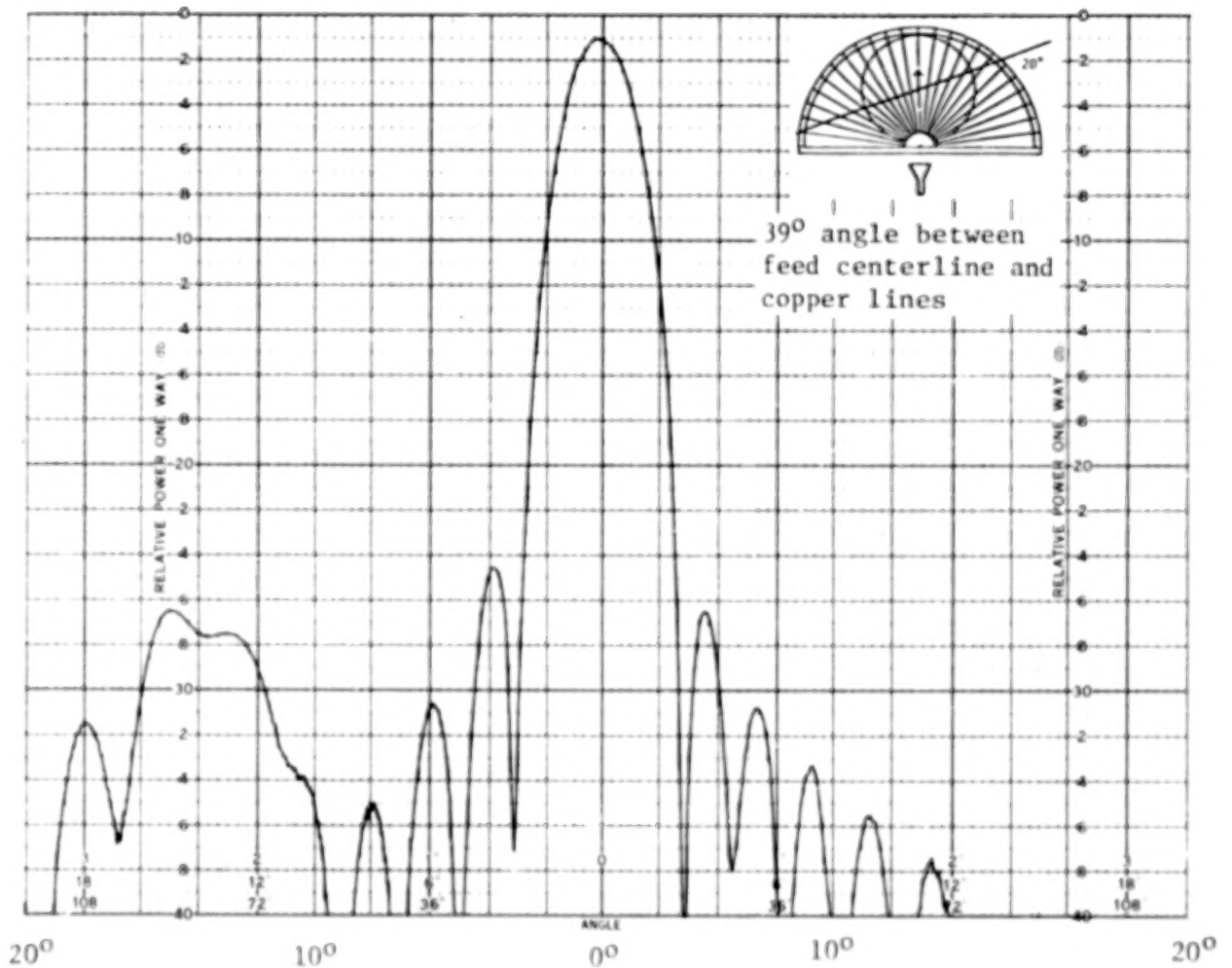
EXPERIMENTAL RESULTS USING
35-GHz MODEL

The following pattern is for cross polarization and no cables.



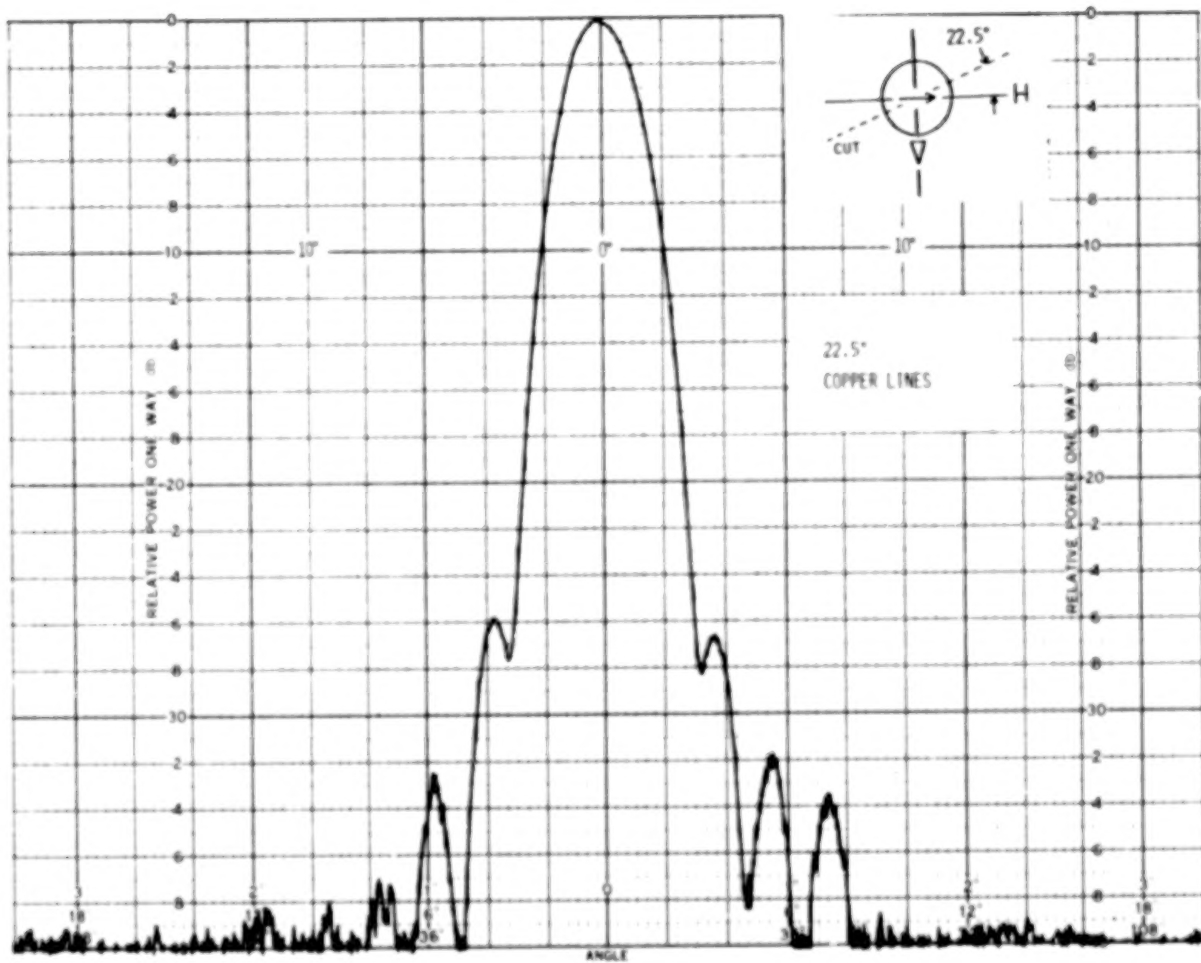
EXPERIMENTAL RESULTS USING 35-GHz MODEL

The following pattern is for vertical polarization and conducting wires in aperture.



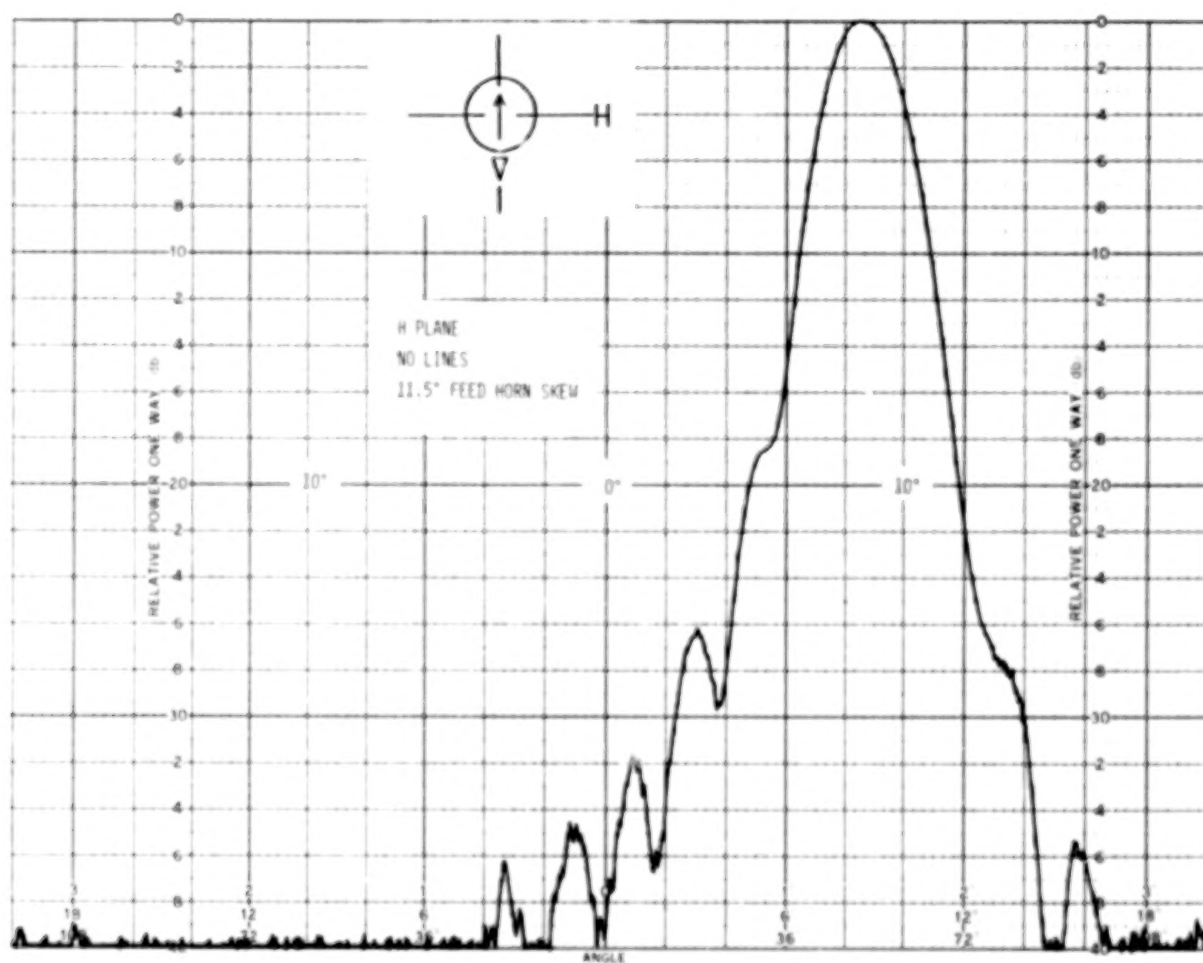
EXPERIMENTAL RESULTS USING 35-GHz MODEL

The following pattern is for horizontal polarization (orthogonal to wires) and with wires in aperture.



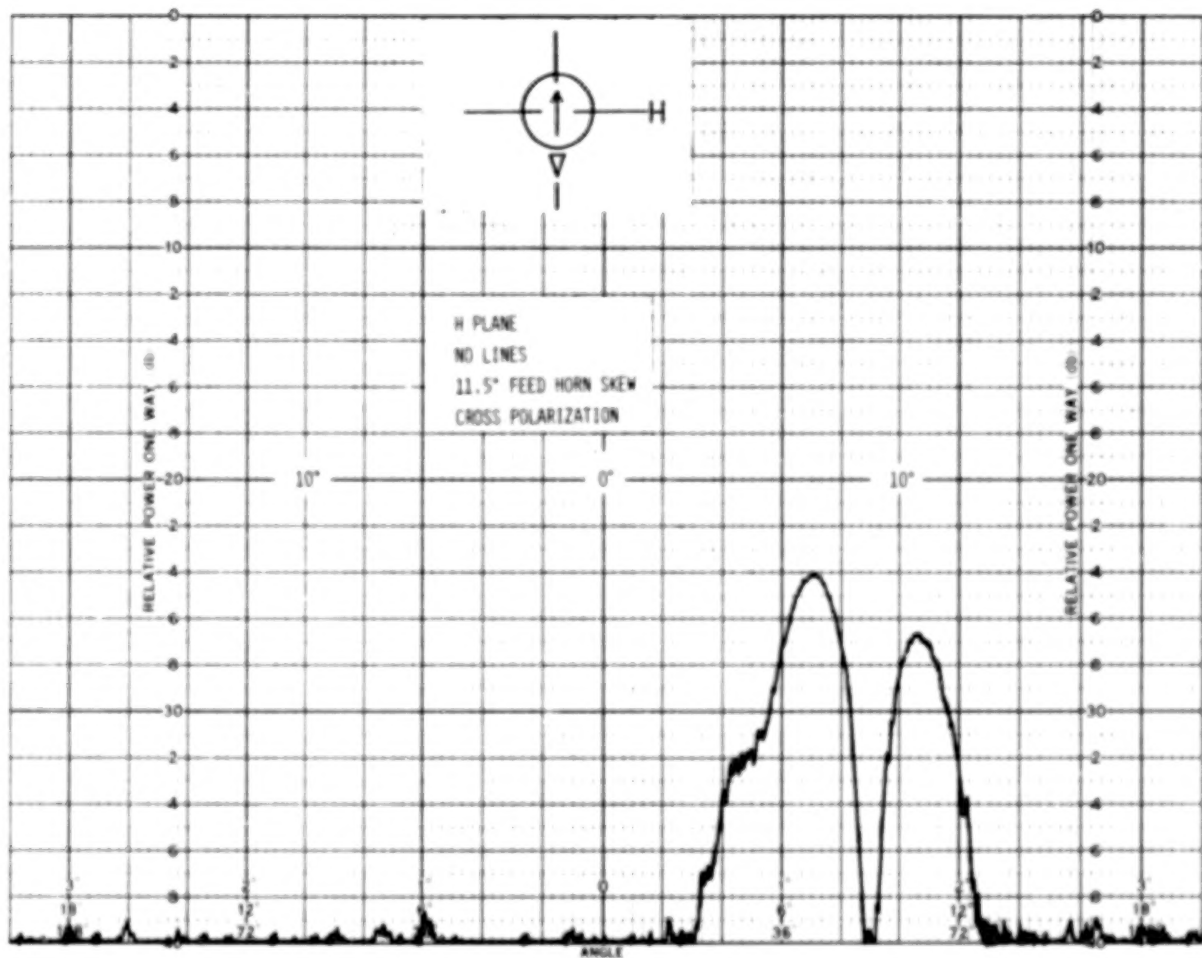
EXPERIMENTAL RESULTS USING 35-GHz MODEL

The following pattern is for horn scan angle of 11.5-degrees, no wires in aperture, and vertical polarization.



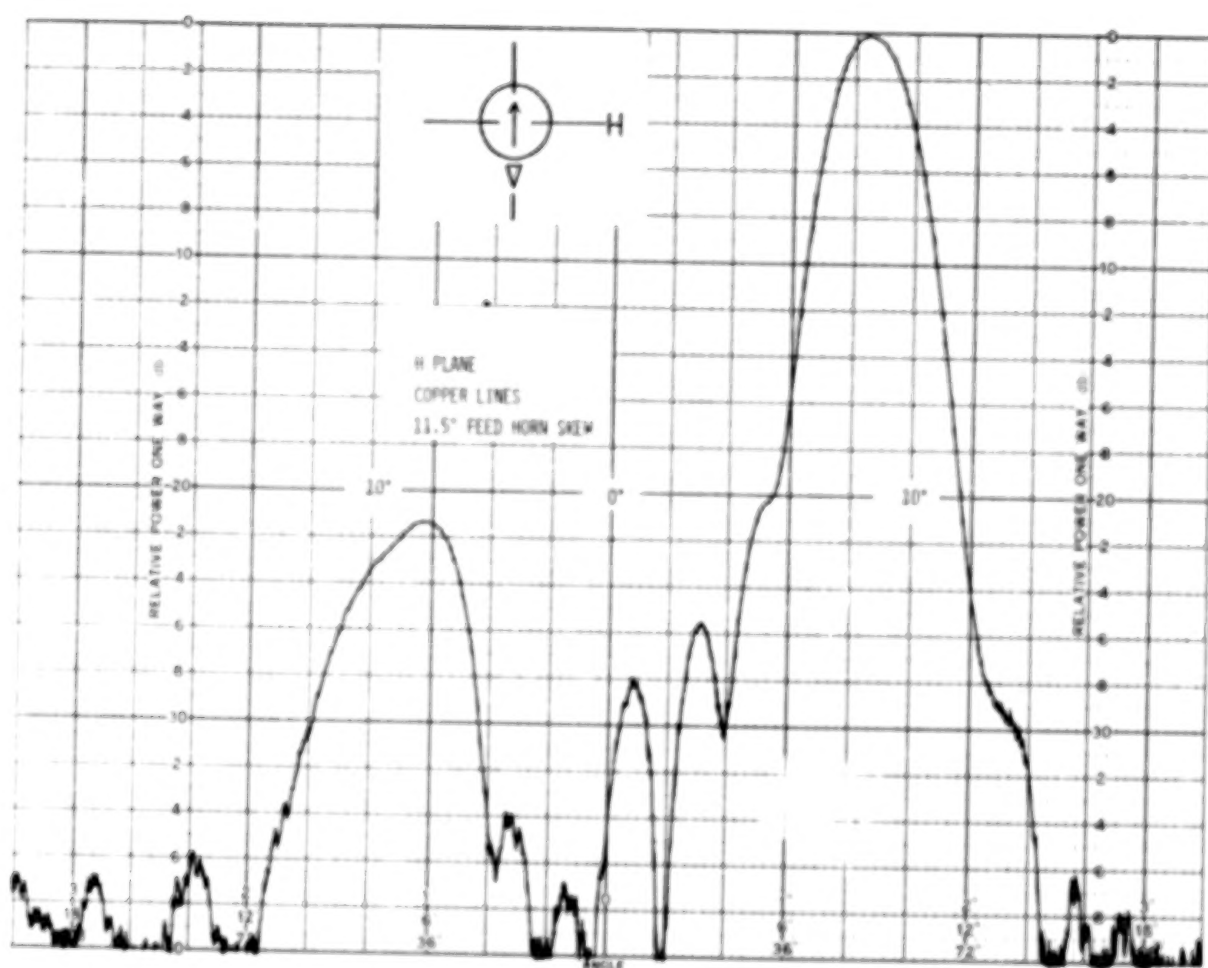
EXPERIMENTAL RESULTS USING 35-GHz MODEL

The following pattern was measured for cross polarization, 11.5-degree scan angle, and no lines in the aperture.



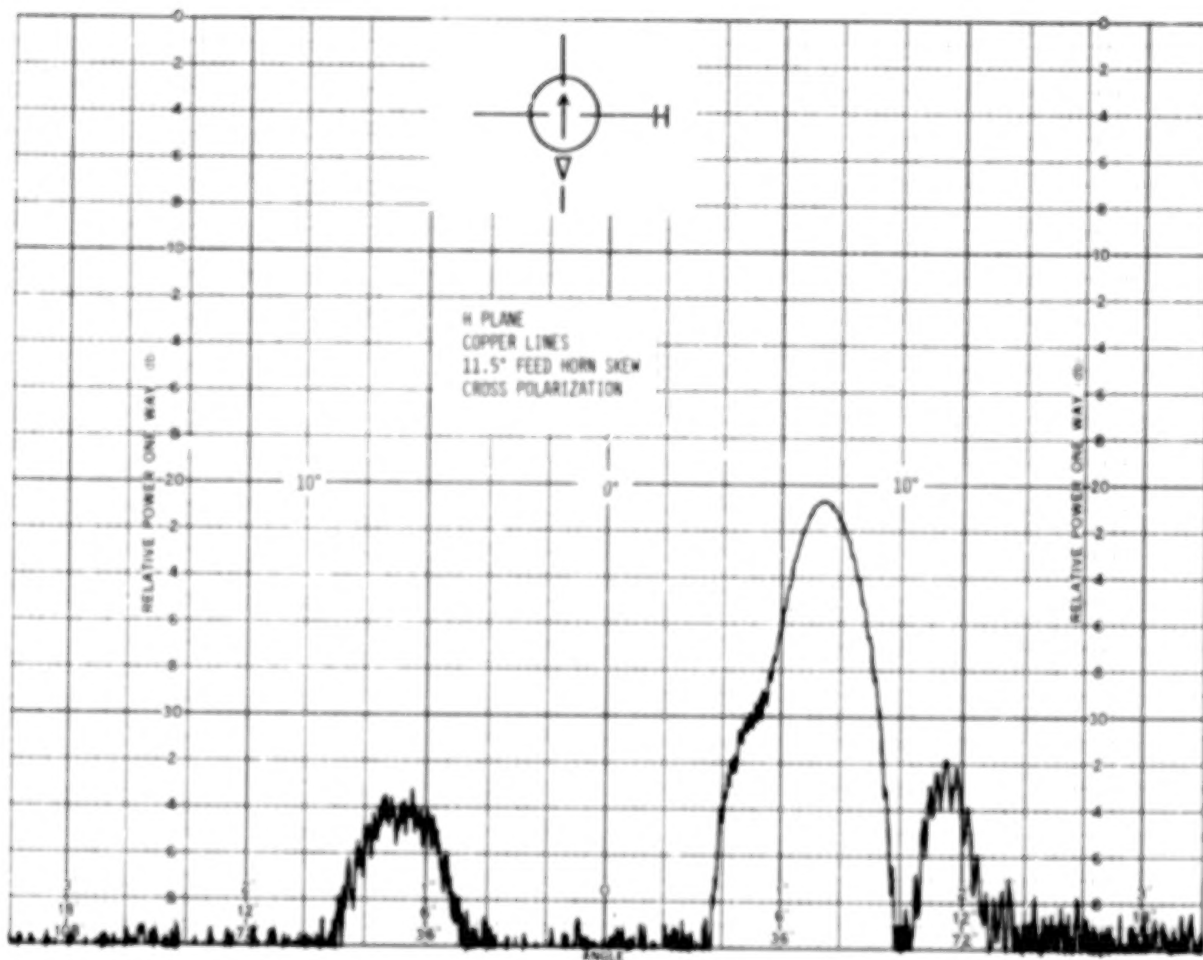
EXPERIMENTAL RESULTS USING 35-GHz MODEL

The following pattern was measured with the 11.5-degree scan angle with wires in the aperture and vertical polarization.



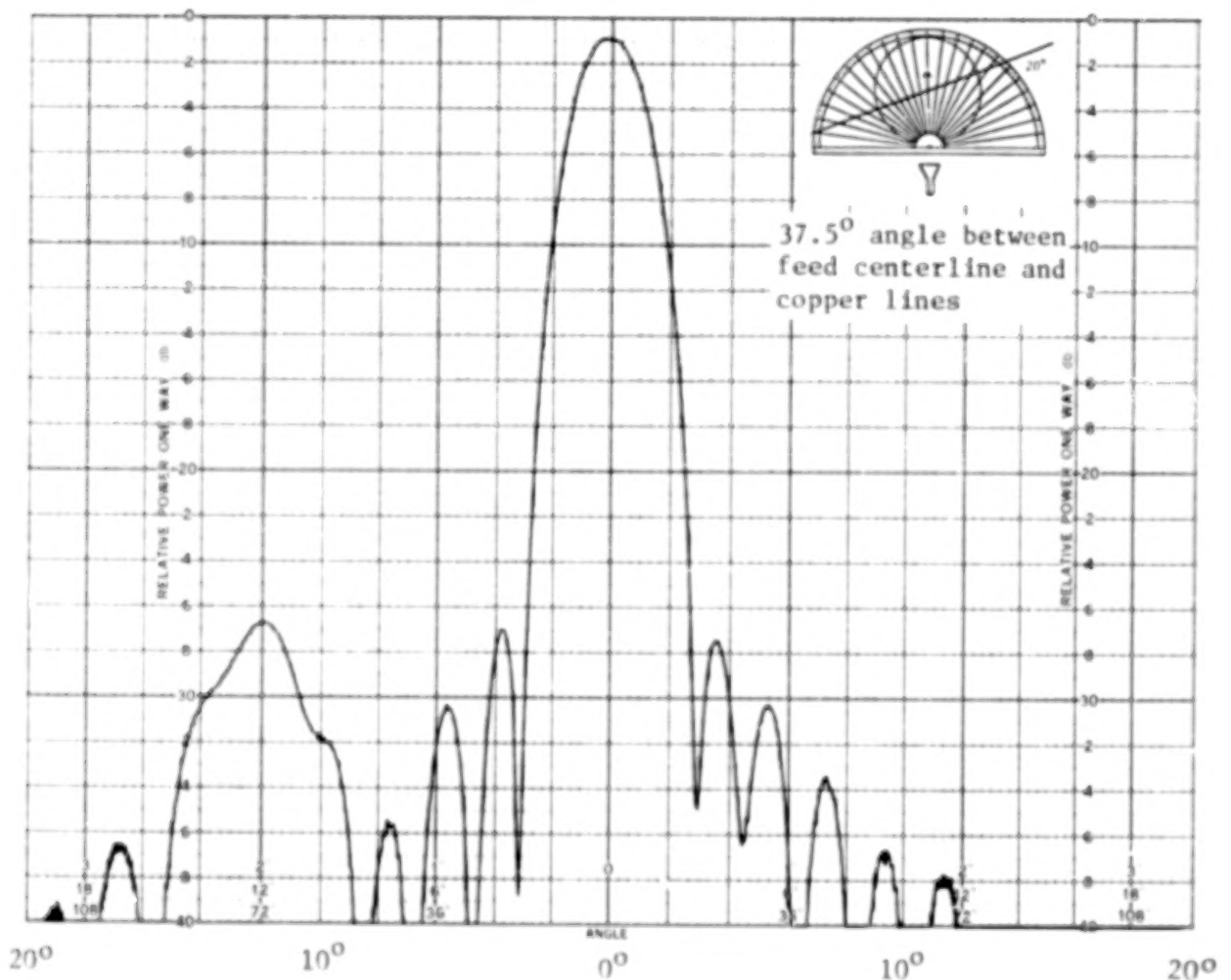
EXPERIMENTAL RESULTS USING 35-GHz MODEL

The following pattern was measured for the cross polarization and the 11.5-degree scan angle with wires in the aperture.



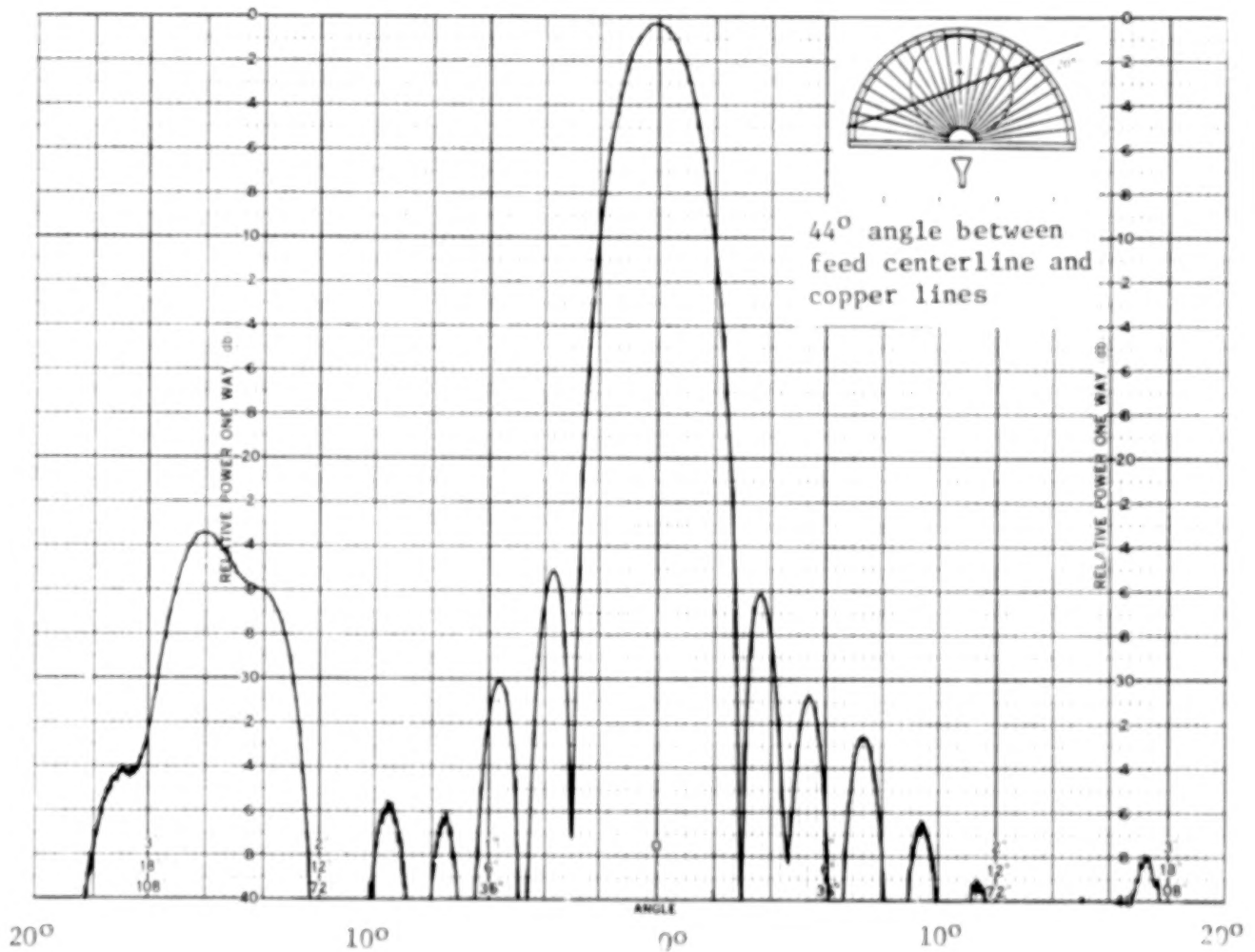
EXEPRIMENTAL RESULTS USING 35-GHz MODEL

The following pattern is for a $\theta = 37.5$ degree which represents an increased wire cone angle. The scattering lobe was observed to shift toward the main lobe.



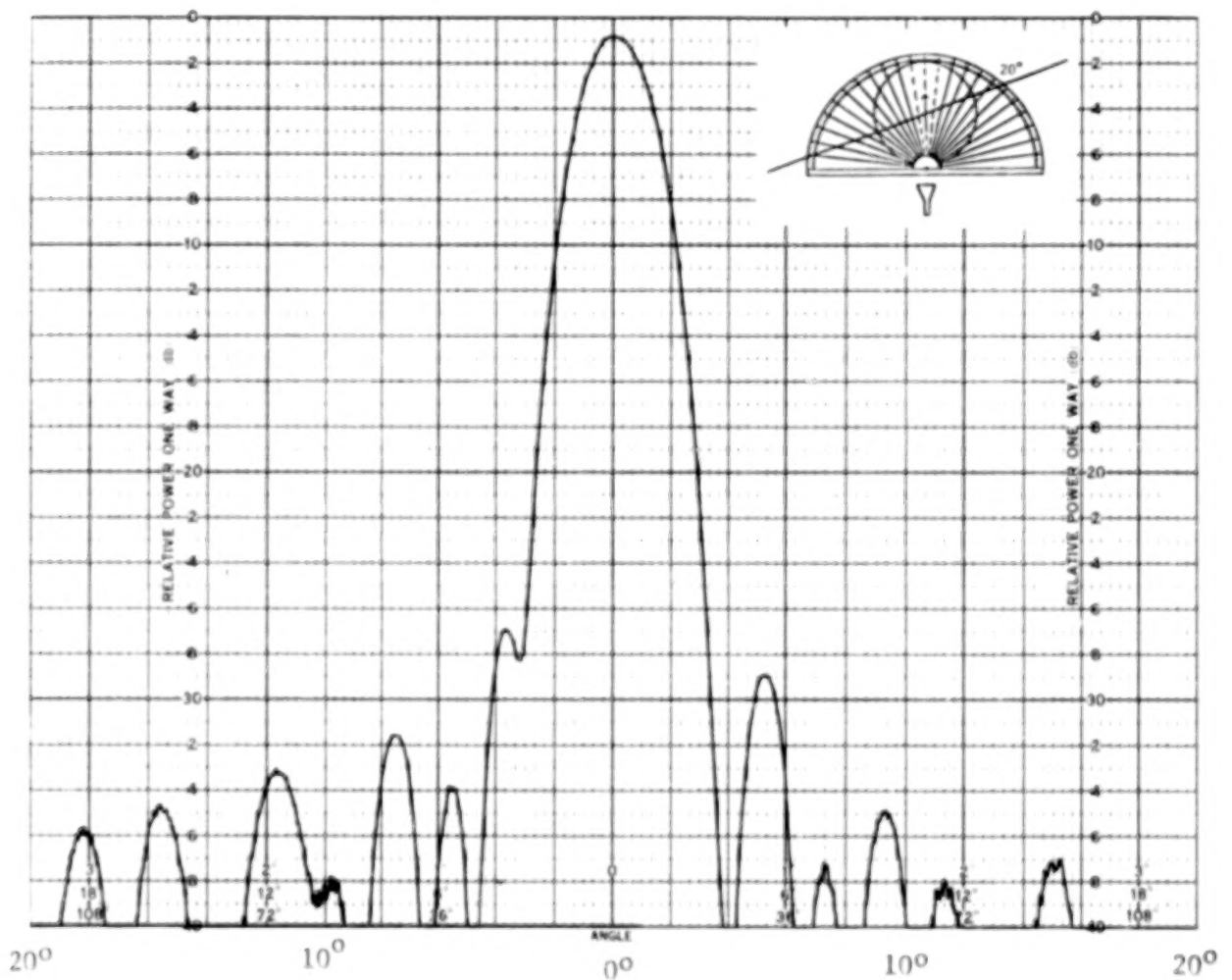
EXPERIMENTAL RESULTS USING 35-GHz MODEL

The following pattern was measured for a $\phi = 44$ degree wire cone angle. This is a decreased wire cone angle and the scattering lobe was observed to shift away from the main lobe.



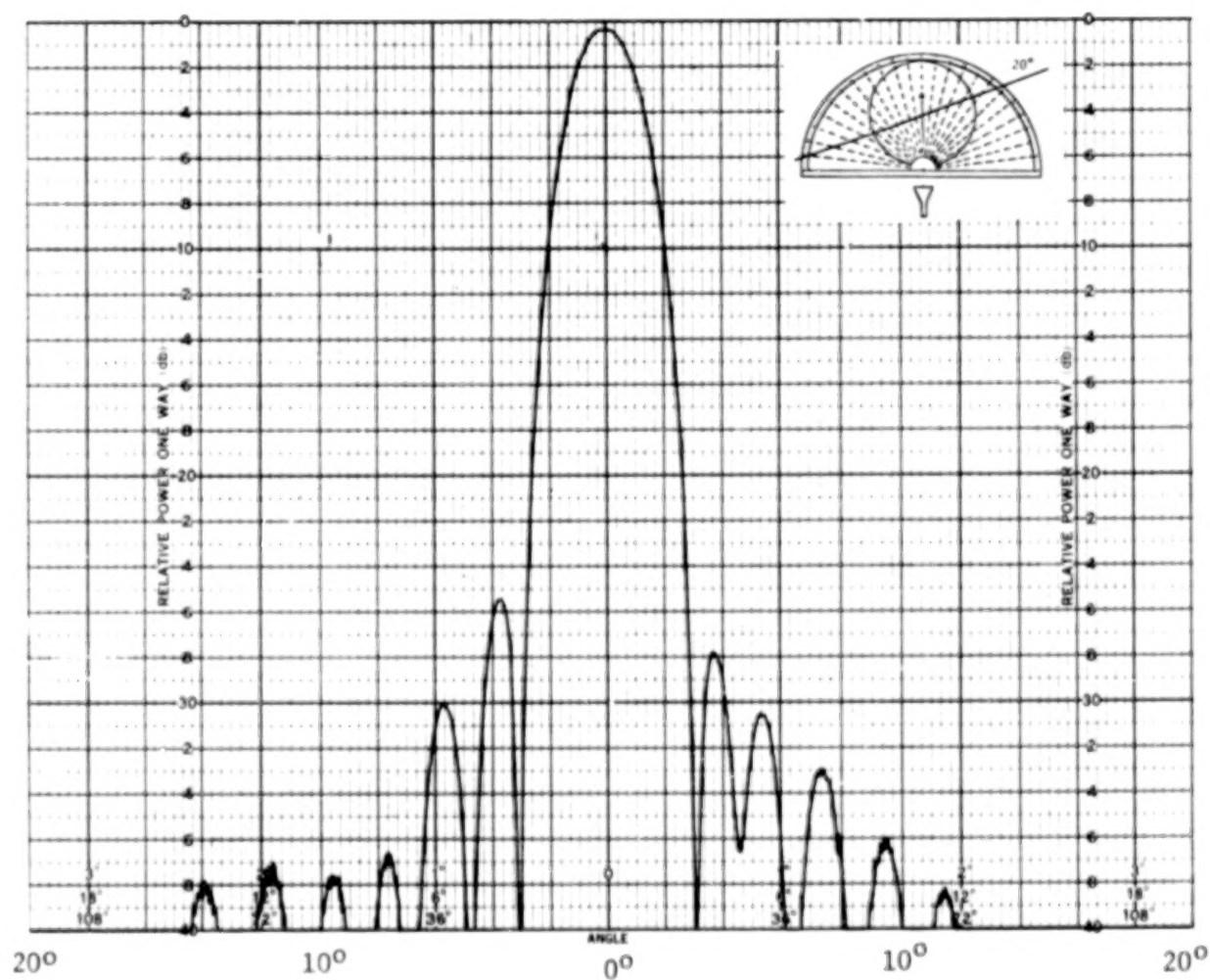
EXPERIMENTAL RESULTS USING 35-GHz MODEL

The following pattern was measured when three conducting wires in the center of the reflector were removed and replaced with dielectric cords. The scattering lobe measured previously with the conducting wires is greatly reduced.



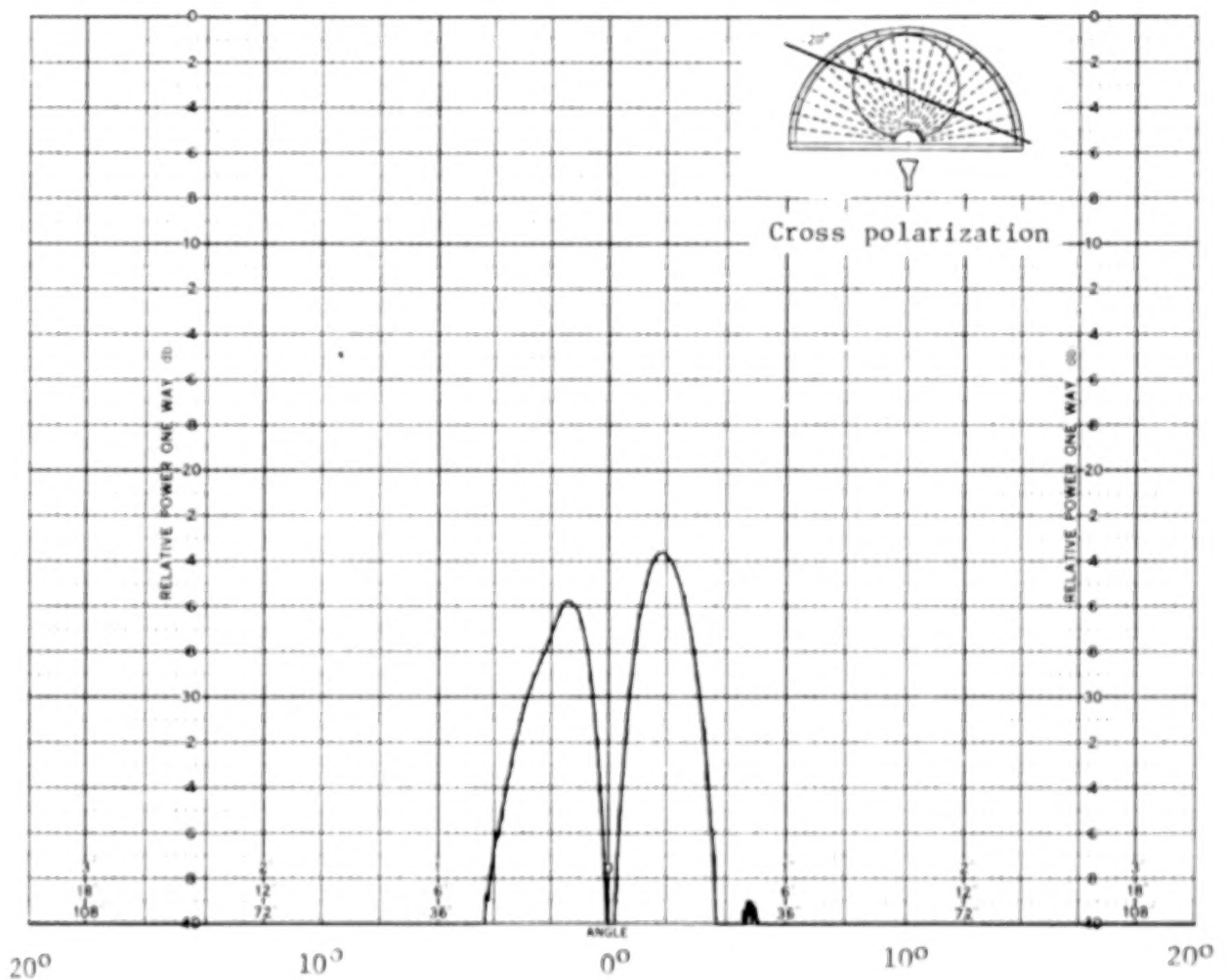
EXPERIMENTAL RESULTS USING 35-GHz MODEL

The following pattern was measured for dielectric cords in the aperture. The scattering lobe is essentially removed.



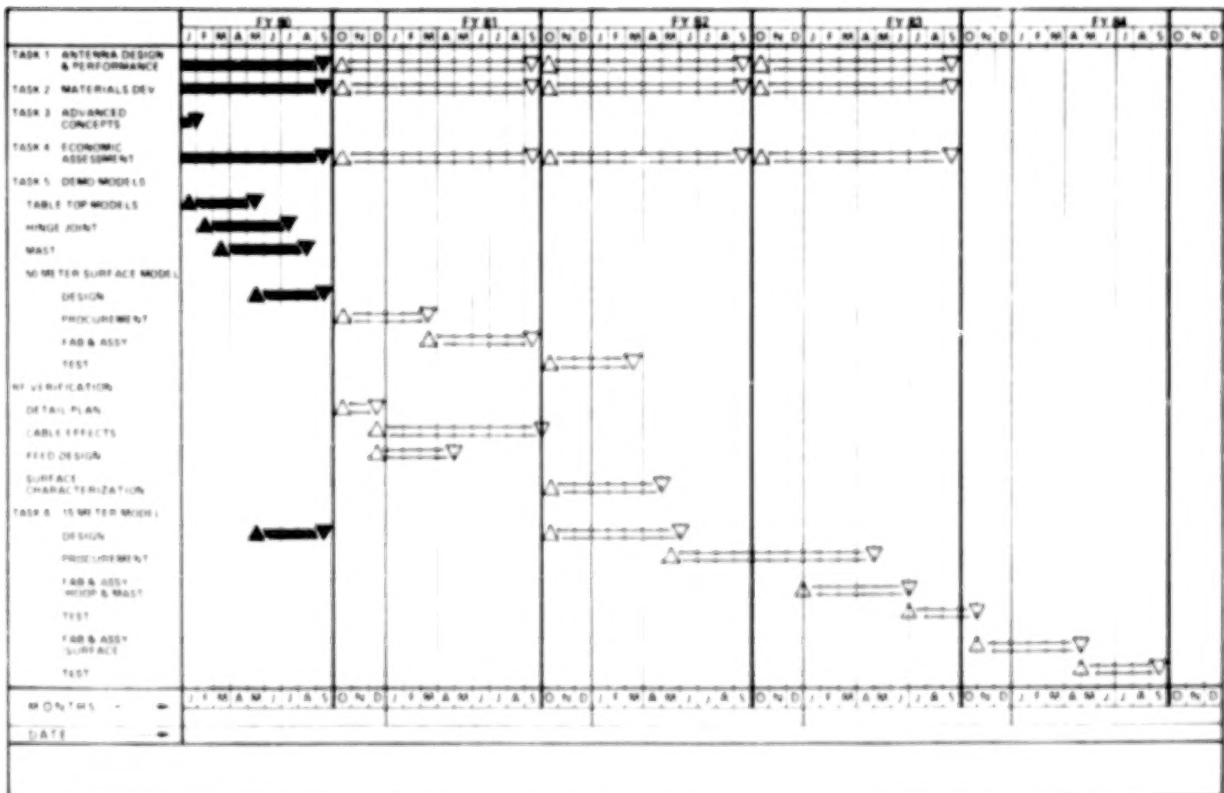
EXPERIMENTAL RESULTS USING 35-GHz MODEL

The following pattern was measured for dielectric cords in the aperture and for cross polarization.



ALTERNATE PHASE II PLAN SCHEDULE

In order to better understand the scattering and blockage effects, a specific task will address this problem during the Phase-II effort. The following schedule indicates when this activity will be completed.



BLANK PAGE

BLANK PAGE

OFFSET FED UTILIZATION OF FOUR QUADRANTS OF AN AXIALLY SYMMETRICAL ANTENNA STRUCTURE

P. Foldes
GENERAL ELECTRIC CO., VALLEY FORGE CENTER, PHILADELPHIA, PA.

1. Introduction

Satellite communication is one of the most important present utilizations of space technology. Table 1 shows the up and downlink frequency bands allocated for communication satellites. The antenna size for each of the indicated communication links is usually characterized by the minimum frequency, f_m . When the beam cross section for the up and downlink must be equal then the easiest way to achieve this is by using separate up and downlink antennas with an aperture diameter ratio corresponding to the ratio of minimum frequencies for the up and downlinks (f_m^U/f_m^D). It can be seen that for the C and Ka-bands this ratio is relatively large, while for the other bands it is smaller. Thus most C and Ka-band satcom antennas use separate antenna apertures for the up and downlink.

Communication traffic generally is unevenly distributed within the overall coverage region. With the use of multibeam antennas it is possible to provide different communication capacities by using different frequency band assignments for different shape beams. As a minimum the traffic can be divided into heavy route and thin route categories carried by spot beams and contiguous coverage area beams respectively. While these beams can be provided by a single antenna aperture this needs either a duplexer or an orthogonal coupler at each radiating element for the combination of the two types of traffic. The first method may be quite complicated while the second restricts the freedom of beam topology planning.

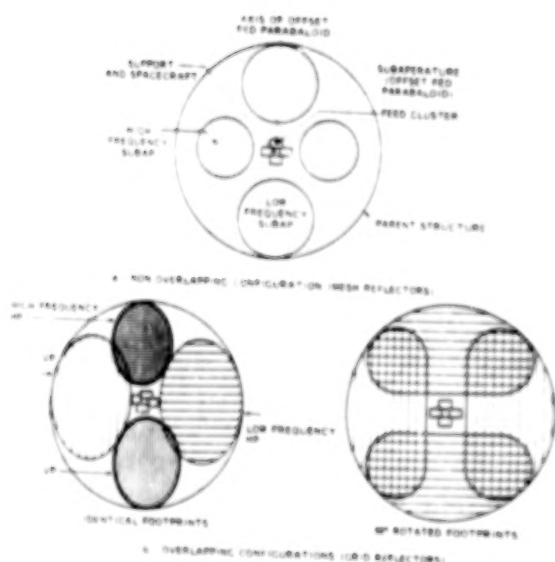


Figure 1 - OFFSET FED ANTENNA

Table 1 - UP AND DOWNLINK FREQUENCY BANDS ALLOCATED FOR COMMUNICATION SATELLITES

Band Designation	Link	Band (f _m - f _M) MHz	f _c	f _m ^U /f _m ^D	f _M ^U /f _M ^D
C (MHz)	Down	800-840	825	1.053	1.055
	Up	850-890	870		
C (Frequency Used)	Down	3700-4200	3950	1.563	1.601
	Up	5925-6425	6175		
C (Authorized by WARC '79)	Down	3600-4200	4100		
	Up	4500-4800		1.573	1.713
K _a	Down	5925-7075	6500		
	Up	7200-7700	7450		
K _a	Down	7900-8400	8150	1.094	1.097
	Up	10200-11700	11200		
K _a	Down	12750-13250	13000	1.16	1.308
	Up	14000-14500			
K _a	Down	17700-20200	18950		
	Up	22500-28000	25250	1.517	1.554

The feed complexities and/or restrictions can be eliminated if the spot and area coverage beam are generated by separate antenna apertures.

The above discussion intended to show that in many satcom systems it is desirable to use 4 antenna apertures (up/down, spot/area) provided that the weight and complexity of such a 4 aperture system (quad-antenna) is less than the eliminated complexity in the feed.

Figure 1 shows the concept of such a quad antenna. The 4 subapertures are placed within a single, symmetrical overall structure. The figure shows two basic classes of such antennas: a) The subapertures are not overlapping each other and may use mesh reflecting surfaces, b) The subapertures are overlapping and use frequency or polarization dependent reflecting surfaces. In the indicated configurations the feeds and their supports occupy the center of the overall (parent) structure and illuminate the subapertures in an offset fed manner. The 4 subapertures are realized by offset fed paraboloid sections with axes parallel to each other and going through the center of the corresponding illuminating feed cluster aperture. When this configuration is realized by a deployable hoop column structure nearly blockage free operation can be expected, provided the structure supporting cables between the hoop and the column in the front of the offset fed paraboloids can be made with negligible blockage or scatter.

In the following a brief review will be given of the necessary beam topologies and geometries to accomplish acceptable operational performance with this type antenna.

2. Beam Topology

The beam topology design for a multibeam antenna is concerned with the assignment of bandwidth and polarization to the component beams of the system in such a manner that a given traffic requirement in a given allocation bandwidth can be provided with the minimum antenna and overall system complexity.

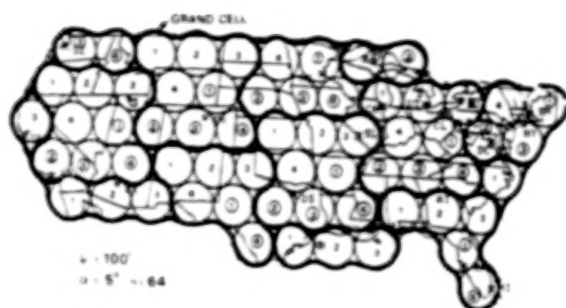


Figure 2 BEAM TOPOLOGY PLAN (CONT.) (1) 100 MILES AND 4-WAY CHANNELIZATION OF THE ALLOCATION BANDWIDTH FOR THE AREA BEAMS. (2) 100 MILES AND 4-WAY CHANNELIZATION.

The present paper concerns itself with the coverage of the US 48 states by a C-band Comsat system, which operates in the 3.7 - 4.2 GHz downlink and 5.925 - 6.425 GHz uplink frequency band, provides most of its coverage toward major cities (10 or 18 spot beams) and the rest of its coverage on a contiguous basis for the remaining of the country. $\lambda = .5'$ and $.3'$ cell size (approximate component bandwidth) is assumed. Among the practically infinite possible beam topologies only 1 plan will be analyzed for the area coverage and 3 plans for the spot beam coverage.

Figure 2 shows the beam topology for the area coverage case, using $\lambda = .5'$ and a 4-way channelization of the available frequency band. If 72 MHz is available for the area coverage traffic then 18 MHz can be assigned for each of the vertically polarized channels 1, 2, 3 and 4. Similarly 18 MHz is available for the horizontally polarized channels 1, 2, 3 and 4. Assuming adequate polarization isolation in the system these 8 channels are isolated from each other. Arranging the 8 channels into the "grand cell" as indicated in Figure 2 the closest identically polarized identical frequency band channels are separated by approximately 2 "empty" cells, while the oppositely polarized identical frequency band channels are separated by 1 empty cell. This assures the potential for relatively large beam isolation even for the maximally scanned beam. (This corresponds to Channel 1 covering Houston in the example shown on Figure 2.) The plan for $\lambda = .5'$ provides $n = 64$ cells (component beams) and 8 times reuse of the 72 MHz spectrum allocated for the area beams.

Table 2 shows a beam topology plan for the spot beams covering the indicated 10 major cities. In this plan each spot beam has the same (maximum available) bandwidth and both polarizations are utilized. The plan provides $\lambda = 1.2'$ separation between identically polarized and $\lambda = .37'$ separation between orthogonally polarized spot beams, where λ refers to beam center to beam center angles for a 100°W located geosynchronous satellite. Figure 3 shows distribution of the spot beams and the corresponding area coverage beams for $\lambda = .3'$. The grand cells of the area coverage topology have the same internal distribution as for the $\lambda = .5'$ case. Assuming that $10 \times 36 \text{ MHz} = 360 \text{ MHz}$ is allocated for the spot beams the total spot beam system has 3600 MHz reused spectrum. The area beam segment of the system utilizes

Table 2 BEAM TOPOLOGY PLAN (MAJOR CITIES)

SATELLITE: TRISTAR NO. OF CITIES: 10 NO. OF BANDS: 12
BAND 1: 3.7 - 4.2 GHz
SATELLITE LONGITUDE: 100°W

List of Cities			Polarization	Band
No.	Name	Symbol		
1	New York	NY	V	1
2	Washington	DC	H	1
4	San Francisco	SP	V	1
6	Chicago	CR	V	1
7	Los Angeles	LA	H	1
8	Denver	DB	V	1
9	Minneapolis	MS	H	1
10	Atlanta	AT	V	1
11	Dallas	DS	H	1
12	Houston	HN	V	1

List of Closest City Pairs and Their Angular Separation

City Pairs		Polarization	λ	Note
No.	Symbol			
1-2	NY-DC	V-H	.57	Notes for cross polarization isolation.
11-12	DS-HN	H-V	.67	
4-7	SP-LA	V-H	.57	Notes for main polarization isolation. (3 empty cells for $\lambda = .3'$)
4-9	CR-MS	V-H	.66	
2-10	DC-AT	H-V	.96	
6-10	CR-AT	V-V	1.20	

$n = 160$ cells thus allowing 20 times reuse of the $2 \times 36 \text{ MHz} = 72 \text{ MHz}$ allocation bandwidth yielding 1440 MHz reused bandwidth. The total usable bandwidth of the system is 5040 MHz employing the 500 MHz allocation bandwidth.

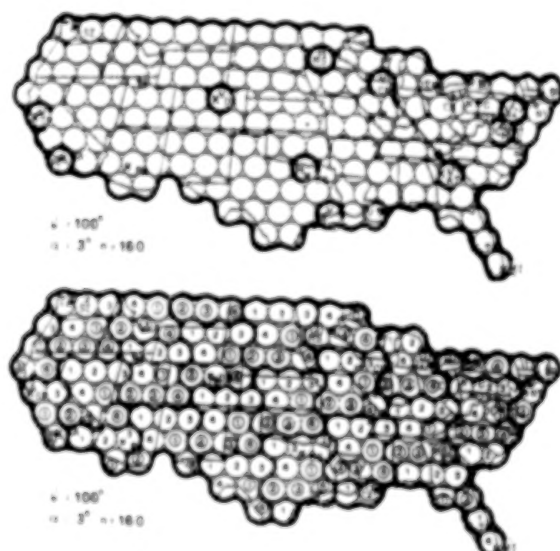


Figure 3 BEAM TOPOLOGY PLAN (CONT.) (1) 100 MILES AND 4-WAY CHANNELIZATION OF THE ALLOCATION BANDWIDTH FOR THE AREA BEAMS. (2) 100 MILES AND 4-WAY CHANNELIZATION OF THE ALLOCATION BANDWIDTH FOR THE AREA BEAMS. (3) 100 MILES AND 4-WAY CHANNELIZATION OF THE ALLOCATION BANDWIDTH FOR THE AREA BEAMS. (4) 100 MILES AND 4-WAY CHANNELIZATION OF THE ALLOCATION BANDWIDTH FOR THE AREA BEAMS.

Table 3 BEAM TOPOLOGY PLAN: MAIN ALLOCATION
(FREQUENCY PLANS 1 AND 2)

STATION: TRENK, NO. OF CITIES: 18, NO. OF BANDS:
BAND 1: 1.7-4.2 GHz, BAND 2: 1.7-4.2 GHz, ALT: 1100
BAND 1: 1.7-4.2 GHz, BAND 2: 1.7-4.2 GHz, ALT: 1100
SATELLITE: (UNDESIGNATED) 100 W

List of Cities			Polarization	Band
No.	Name	Symbol		
1	New York	NY	V	1
2	Washington	DC	H (H ₁₁)	1 or 11
3	Boston	BN	H (H ₁₂)	1 or 12
4	San Francisco	SP	H	1
5	Seattle	SE	V	1
6	Chicago	CH	H	1
7	Los Angeles	LA	V	1
8	Denver	DN	H	1
9	Minneapolis	MS	V	1
10	Atlanta	AT	V	1
11	Dallas	DS	H	1
12	Houston	HN	V	1
13	Detroit	DT	V	1
14	Buffalo	BU	H (H ₁₂)	1 or 12
15	St. Louis	SL	V	1
16	Phoenix	PH	H	1
17	New Orleans	NO	H	1
18	Miami	MI	H	1

FIGURE 4: BEAM TOPOLOGY PLAN AND BEAM ANGLE
SEPARATION, FREQUENCY PLANS 1 AND 2

City Pairs		Polarization	α^*	Note
No.	Symbol			
1-3	NY-DC	V-H	.23	Worst for cross polarization isolation in Alt. 1 and 2
1-2	NY-DC	V-H	.33	
6-13	CH-SL	H-V	.40	
11-12	DS-HN	H-V	.48	
13-14	DT-BU	V-H	.48	
6-13	CH-DT	H-V	.49	
2-3	DC-BN	H-H	.55	Worst for main polarization isolation in Alt. 1.
	or H ₁₁ -H ₁₂			
2-14	DC-BU	H-H	.61	
	or H ₁₁ -H ₁₂			
4-17	SP-LA	H-V	.62	
1-14	NY-BU	V-H	.72	
12-17	HN-NO	V-H	.75	
13-14	BN-BU	H-H	.79	Worst for main polarization isolation in Alt. 2.
	or H ₁₁ -H ₁₂			
10-17	AT-NO	V-H	.82	
13-15	DT-SL	V-H	.82	
7-16	LA-PH	V-H	.85	
2-10	DC-AT	H-V	.88	
6-9	CH-MS	H-V	.89	
9-15	MS-SL	V-H	.90	

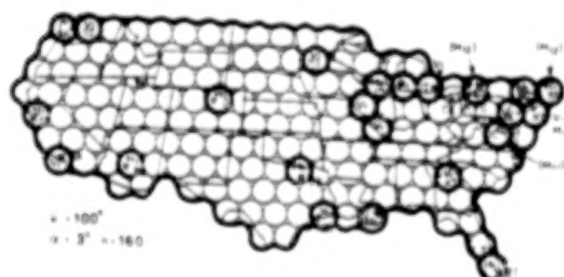


Figure 4 BEAM TOPOLOGY PLAN: MAIN ALLOCATION
(FREQUENCY PLANS 1 AND 2)

Table 3 shows 2 frequency plans for the spot beams covering 18 cities. Plan No. 1 allows the total allocation bandwidth for each of the spot beams. Plan No. 2 provides the same except for DC, BN and BU which have only half of the bandwidth relative to the other spot beams. The worst case main polarized beam separation is .55° and .79° for Plan 1 and 2 respectively. Figure 4 shows the beam topology for the spot beams. The beam topology for the area coverage beams is the same as for Figure 3.



Figure 5 BEAM TOPOLOGY PLAN: MAIN ALLOCATION
(FREQUENCY PLANS 1 AND 2)

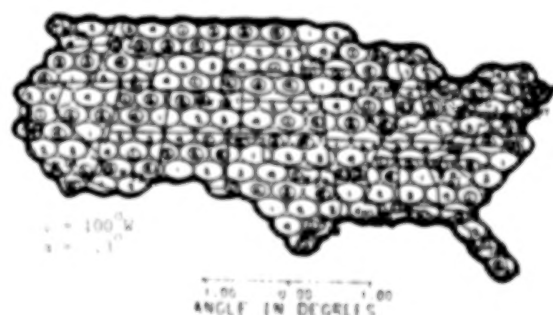


Figure 6 BEAM TOPOLOGY PLAN: MAIN ALLOCATION
(FREQUENCY PLANS 1 AND 2)

Figures 5 and 6 show the modification of the area coverage plan given on Figure 3 by using elliptical instead of circular component beam cross sections. For $\alpha_{av} = .5^\circ$ and $.1^\circ$ still the same $n = 64$ and 160 component beams are employed but the maximum beam scan in terms of beam width is reduced by the square root of the major to minor axis ratio r of the beam cross section. For instance with circular beam cross section the realization of the Houston beam requires 12 beamwidth of 1K plane beam scan. With the elliptical beam cross section only 9 beamwidth scan is necessary. This reduces the beam scan caused beam distortion and improves the achievable beam isolation.

3. Geometry and Weight

Figure 7 shows the main geometrical characteristics of the quad antenna. The figure assumes that the up and downlink subaperture sizes are different and the subaperture shapes are elliptical. This allows a reduction of the discussed beam distortion with beam scan and results in a better utilization of the available parent structure aperture. It may be noted that for $r = f_m^2 / f_0^2 D$ the corresponding subaperture diameter ratio is also r for identical solid angle component beam cross sections. Additionally the major to minor axis ratio of the subapertures is also r if maximum utilization of the aperture is desirable and no subaperture overlap is desirable. For the investigated cases the subaperture area of the circular and elliptical realizations is identical so the peak gain of the unscanned beam is the same.

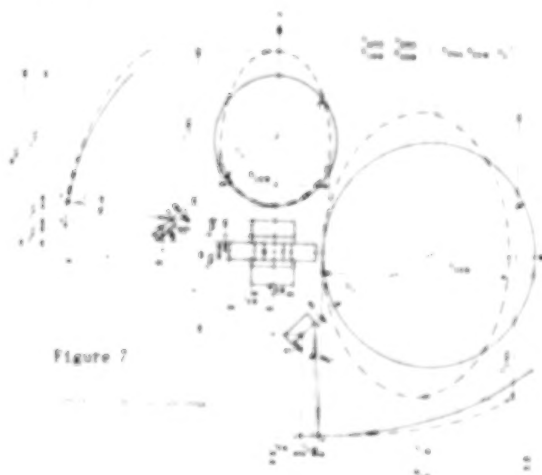


Figure 7

Table 4 shows the dimensions of the investigated cases. These cases included $\alpha = .5^\circ$ and $.3^\circ$, $r = 1$ (circular beam) and 1.6 (elliptical beam), downlink reflector in the EW or in the NS plane of the parent structure and EW plane or NS plane elongated beam cross sections. Figure 8 shows how the utilization of the parent structure aperture varies as a function of these parameters. It can be seen that for the considered C-band application with $r = 1.6$ and EW plan elongation of the component beam beamwidth the downlink reflector must be in the EW plane for a utilization u better than 66%. Figure 9 exhibits the geometry of the hoop column structure for the quad antenna for $\alpha = .3^\circ$. In this case the parent structure requires 33.7 m diameter and the total system length is 38.3 m.

Table 4

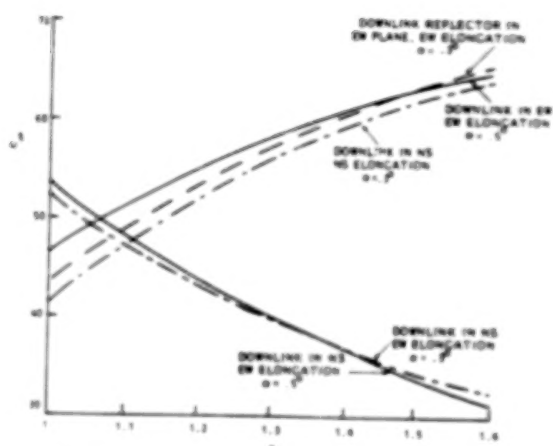


Figure 8

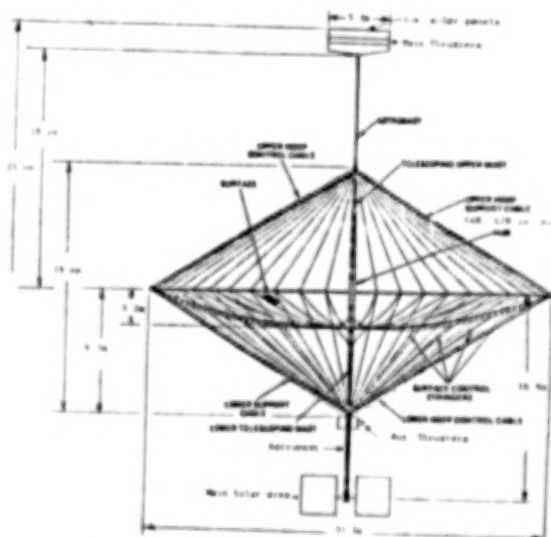


Figure 9 SYSTEM CONFIGURATION (1000000)

Table 5 exhibits the weight breakdown for $\alpha = .5^\circ$ (20.3 m structure diameter) and $\alpha = .3^\circ$ (13.7 m structure diameter). It is interesting to note that the hoop-column structure (reflector and East) represents only 17.3% and 1% of the overall system weight.

Table 5. (Continued)

[illegible]

4. Radiation Characteristics

One basic characteristic of any multibeam antenna is the beam distortion introduced by beam scan. Figures 10 and 11 show gain contours of the singlet used for the $\lambda = .5^\circ$ cell diameter system for a beam in the center of the country and for a beam scanned to the extreme (Boston) location. It can be seen that two empty cells away from the coverage region of the BN beam the sidelobe level is only about -28 db with a singlet beam. Better sidelobe level for such an extreme scan will require the use of more complex beams formed by using main and auxiliary (sidelobe cancelling) component beams.

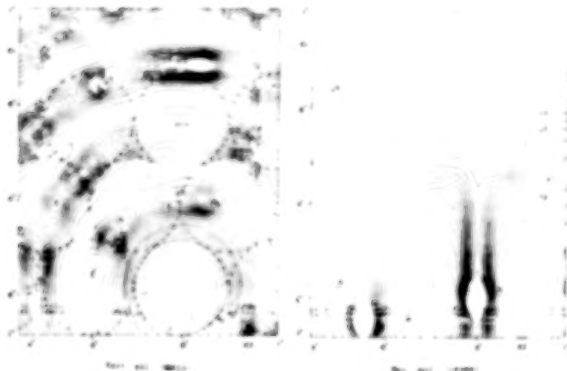


Figure 10

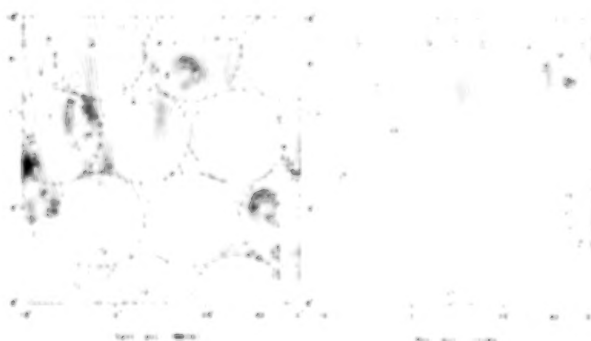


Figure 11

Figure 12 exhibits another typical characteristic of the multibeam system. In this case more than one beam contributes to interference at a given location. The example shows the gain contour of the spot beams for $\lambda = .1^\circ$ when BN, DC-NY and BN beams use the same frequency band and polarization as the AI beam which is located in a central position. The lower right figure shows the resultant sidelobe level of the 3 spot beams in the vicinity of AI verifying that the selected antenna geometry and beam topology plan is compatible with the desired beam isolation. (AI is illuminated by lower than -40 db resultant interfering power level in the exhibited example.)

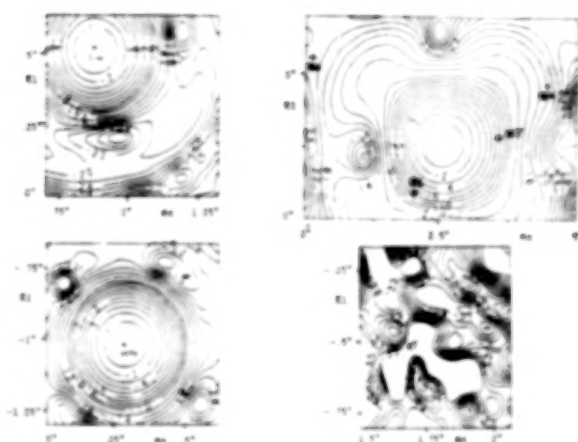


Figure 12

Figure 13 shows the gain contour of the unscanned beam for $\lambda = .3^\circ$ at 3.95 GHz. Figure 14 shows the gain contours when the beam is scanned to BN (9 beamwidth away from the center). The beam distortion is considerably less than feasible with the circular cross section singlet. Figure 15 shows the same beam at the center of the uplink frequency band. Note that the beam cross section in the coverage region is very similar to the 4 GHz band case and the sidelobe levels at the closest applicable cell are comparable.

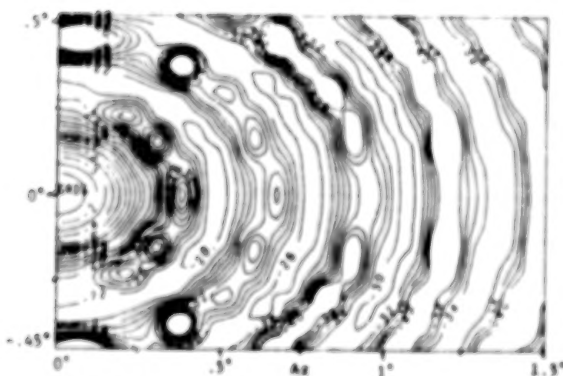


Figure 13 GAIN CONTOURS FOR ELLIPTICAL CROSS SECTION SINGLET, $r = 1.6$, $\lambda = .3^\circ$, $f = 3.95$ GHz, $\theta_{\text{max}} / \lambda = 0.3$

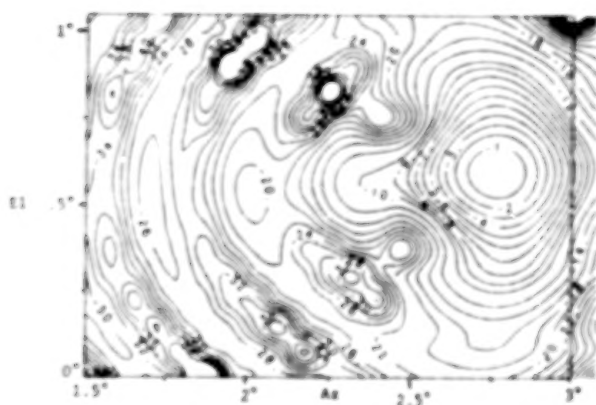


Figure 14 GAIN CONTOURS FOR ELLIPTICAL CROSS SECTION SINGLET, $r = 1.45$, $(\alpha = .3^\circ)$, $f = 6.175$ GHz, $a/a_0 = 0$, $\sigma = .13$ cm (.05 in.) rms, 32 blockage, $D_{EW} = 10.25$ m, $D_{NS} = 14.86$ m, $F = 19.83$ m, $G = 54.96$ DB.

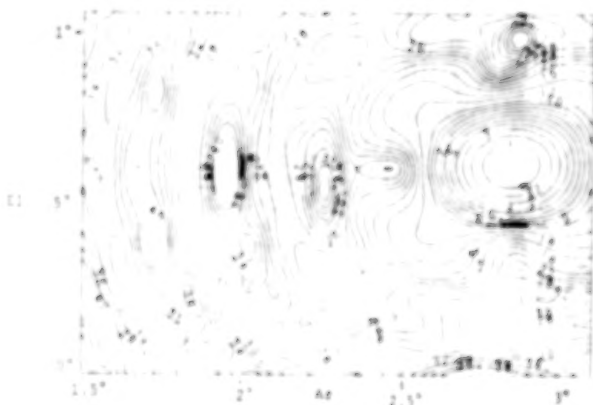


Figure 15 GAIN CONTOURS FOR ELLIPTICAL CROSS SECTION SINGLET, $r = 1.45$, $(\alpha = .3^\circ)$, $f = 6.175$ GHz, $a/a_0 = 0$, $\sigma = .13$ cm (.05 in.) rms, 32 blockage, $D_{EW} = 10.25$ m, $D_{NS} = 14.86$ m, $F = 19.83$ m, $G = 54.96$ DB.

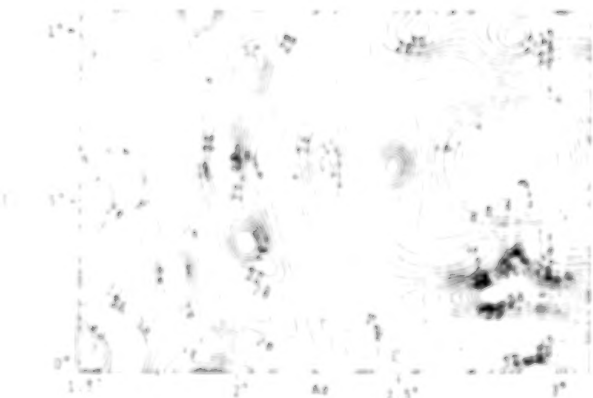


Figure 16 GAIN CONTOURS FOR ELLIPTICAL CROSS SECTION SINGLET, $r = 1.45$, $(\alpha = .3^\circ)$, $f = 6.175$ GHz, $a/a_0 = 0$, $\sigma = .13$ cm (.05 in.) rms, 32 blockage, $D_{EW} = 10.25$ m, $D_{NS} = 14.86$ m, $F = 19.83$ m, $G = 54.96$ DB.

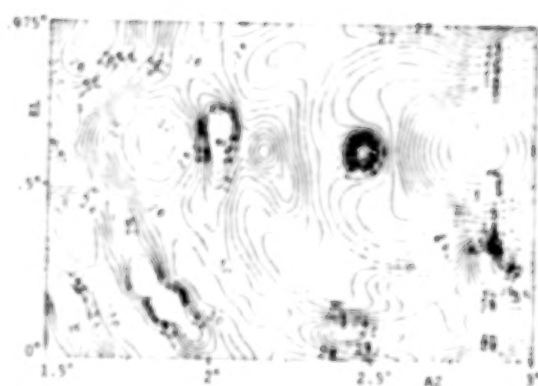


Figure 17 GAIN CONTOURS FOR ELLIPTICAL CROSS SECTION SINGLET, $r = 1.45$, $(\alpha = .3^\circ)$, $f = 6.175$ GHz, $a/a_0 = 0$, $\sigma = .13$ cm (.05 in.) rms, 32 blockage, $D_{EW} = 10.25$ m, $D_{NS} = 14.86$ m, $F = 19.83$ m, $G = 54.96$ DB.

Up to now ideal implementation conditions were assumed. In the following the effect of reflector surface inaccuracy and supporting cable blockage will be demonstrated.

Figure 16 shows the effect of $\sigma = .05$ in. rms surface inaccuracy at 6.175 GHz for the Boston beam. A comparison with Figure 15 reveals considerable sidelobe level degradation at $2.82^\circ = .846^\circ$ away from the center of the Boston cell. This angular separation corresponds to the nearest identical band-identical polarization cell for the area coverage case using the selected beam topology plan. Due to the surface error the sidelobe level in this cell drops to -27 db from the -30 db level achievable with ideal surface accuracy.

Figure 17 displays the gain contour if additional to the .05 inch surface inaccuracy 32 cable blockage is also included. It can be seen that the peak sidelobe levels could reach -22 db in regions where the sidelobe level was -28 db down in the presence of .05 inch rms surface errors.

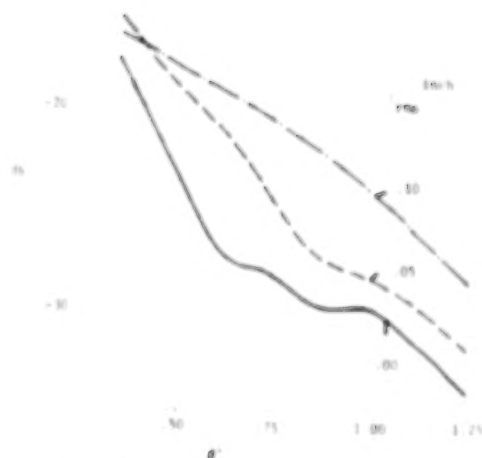


Figure 18 GAIN CONTOURS FOR ELLIPTICAL CROSS SECTION SINGLET, $r = 1.45$, $(\alpha = .3^\circ)$, $f = 6.175$ GHz, $a/a_0 = 0$, $\sigma = .13$ cm (.05 in.) rms, 32 blockage, $D_{EW} = 10.25$ m, $D_{NS} = 14.86$ m, $F = 19.83$ m, $G = 54.96$ DB.

Figure 18 exhibits the effect of surface errors on the sidelobe level as a function of the angle from the center of the main beam. Figure 19 gives the sidelobe level within the closest applicable cell as a function of the σ surface error and blockage, B . It can be seen that 30 db sidelobe level is feasible for $\sigma = 0$ and $B = 0$. .25% blockage or .017 rms surface accuracy at 6.175 GHz can deteriorate the sidelobe level performance by 1 db each. For an initial sidelobe performance of 30 db and beam isolation of 27 db the resultant isolation is only 25 db for such a condition. An improvement relative to these values requires the use of more complicated BFN (clustered feeds), lower blockage, better surface accuracy or less sidelobe sensitive beam topology plans.

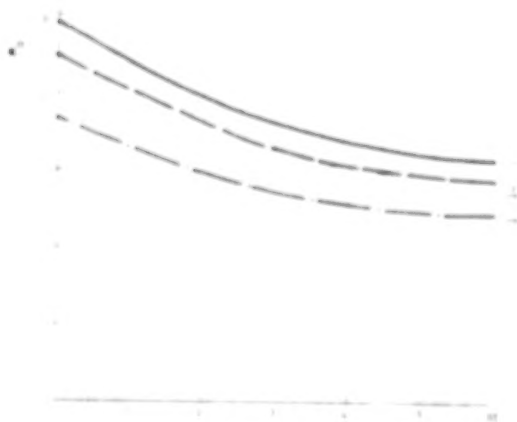


Figure 19

5. Conclusions

On the basis of theoretical calculations conducted for the use of the hoop-column structure in a quad antenna configuration the following conclusions can be drawn:

1. It is possible to utilize, near blockage free, a symmetrical antenna structure.
2. Such utilization leads to the availability of 4 subapertures.
3. Elliptical subaperture shape improves surface utilization and reduces beam scan distortion.
4. 20.3 m parent structure diameter allows $\sigma = .5''$ cell size for a C-band communication system and results in approximately 116000 telephone channels in 500 MHz frequency allocation band on a traffic density distributed manner covering the US 48 states.
5. 33.7 m parent structure diameter allows $\sigma = .3''$ cell size and approximately 220000 telephone circuits.
6. At 6.175 GHz .017 in rms surface inaccuracy causes 1 db degradation of beam isolation at 27 db level.
7. At 6.175 GHz .125 in diameter (metal or graphite) support cables (Qty 48 for the entire system) causes 1 db degradation of beam isolation at 27 db level.

BLANK PAGE

BLANK PAGE

SURFACE ACCURACY MEASUREMENT SENSOR
FOR DEPLOYABLE REFLECTOR ANTENNAS

R. B. Spiers, Jr.
NASA Langley Research Center
Hampton, VA 23665

Large Space Systems Technology - 1980
Second Annual Technical Review
November 18-20, 1980

INTRODUCTION

The breadboard Surface Accuracy Measurement Sensor for Deployable Reflector Antennas (SAMS-DRA) has been designed, built and tested by TRW Systems and Energy Group (ref 1). The program objectives, sensor concept and proof of concept was reported at the First Annual LSST Technical Review (ref. ?). The sensor is an optical angle sensor which provides continuous line-of-sight position measurements of infrared source targets placed strategically about the antenna surface. Measurements of target coordinates define the surface figure relative to a reference frame on the antenna. The breadboard (see fig. 1 and 2) which was delivered to the Langley Research Center is being tested to determine its performance under laboratory simulated flight conditions. A brief description of the sensor operation, tests and test results to date is presented.

ANTENNA DISTORTION SENSOR PRINCIPAL UNITS RECEIVER

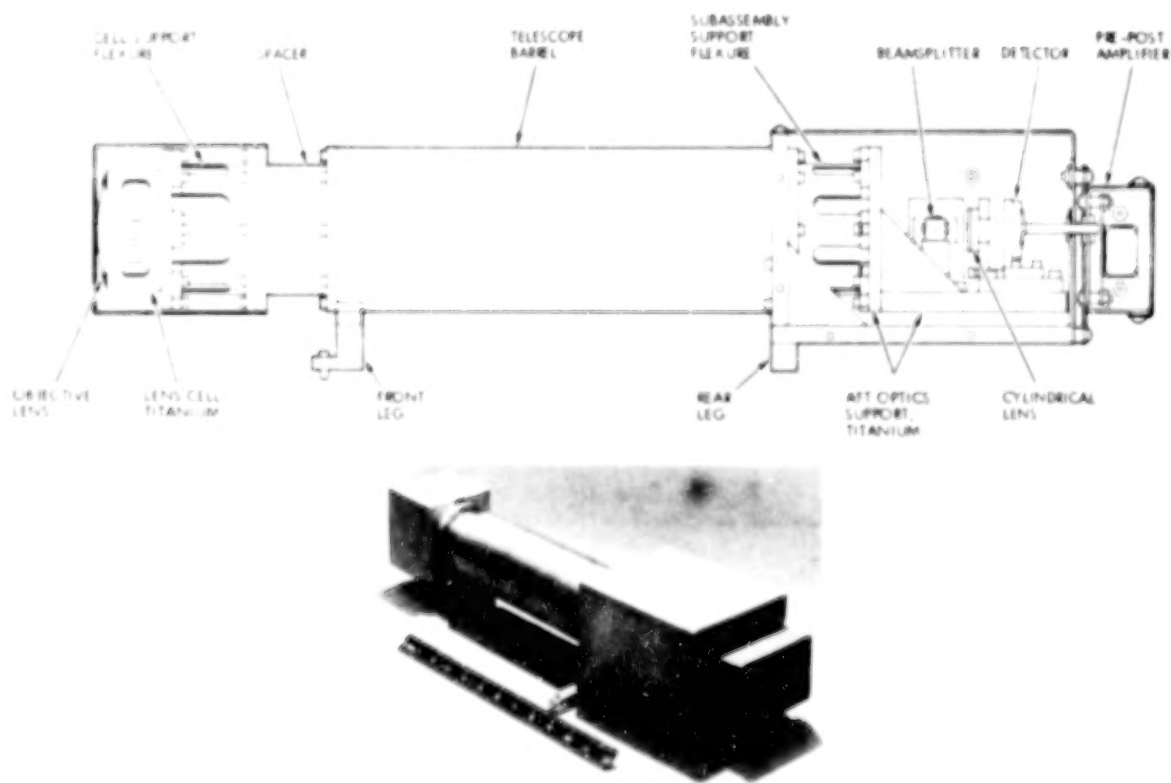


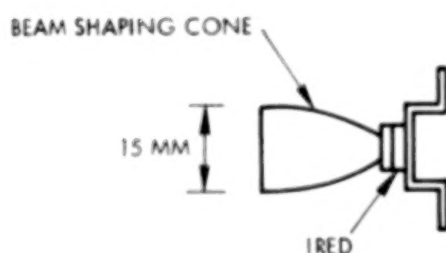
Figure 1

BREADBOARD SENSOR

Receiver - The receiver (see fig. 1) has an objective lens which receives radiation from target sources and images the targets on a pair of lateral effect planar diffuse silicon photodiode detectors via a beam splitter and two cylindrical lenses with orthogonal axes to perform coordinate separation of target motions. The detectors sense the positions of the images along their lengths, and convert this information into electrical signals which are amplified by the pre-post amplifiers and fed to a signal processor.

Target Sources - The infrared (.9 μm) emitting diodes (IRED) (see fig. 2) are powered by a square wave modulated (40 Hz) d.c. power supply. Parabolic cone reflectors collect and direct the radiation into a solid angle radiation pattern toward the receiver. Two types of target sources are used, an active source of 20° diameter solid angle and a passive retrodirective reflector illuminated by a source of 4° diameter solid angle. The retroreflector has an optical wedge over half its aperture to efficiently direct the reflected radiation to the receiver which is located slightly off the IRED optical axis.

ACTIVE LED TARGET, 20° CONE



ILLUMINATED RETROREFLECTOR

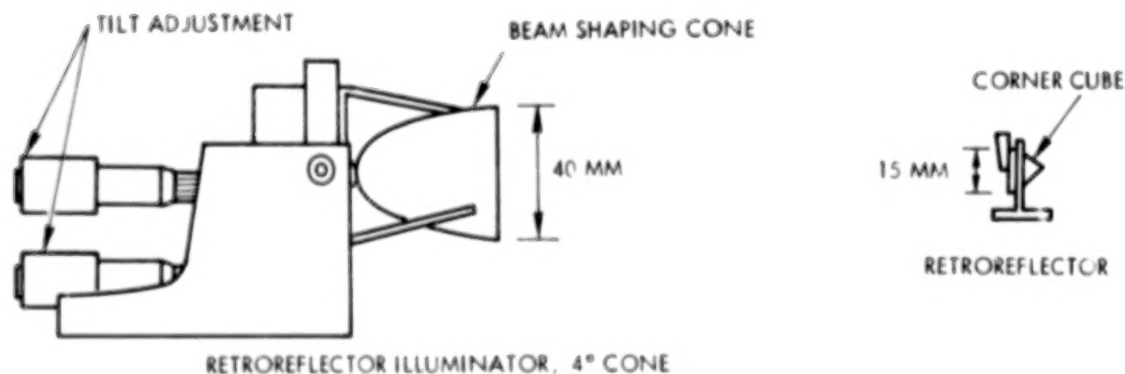


Figure 2

SIGNAL PROCESSING

The receiver collects light from the targets to form small spot images on the position sensing detectors. The beamsplitter and relay lenses perform coordinate separation producing X-axis only image motion at the X-detector and Y-axis only image motion at the Y-detector. Electronic signal processing for the X coordinate detector is shown in figure 3. The image position on the detector generates two square wave modulated signals due to the IRED source modulation. Each signal from the detector has an amplitude proportional to the image distance from the respective end electrodes of the detector. Both signals are amplified and fed into a multiplexer where samples are taken at the square peaks (e.g. X_1^+) and troughs (e.g. X_1^-) and then digitized. The signals are then processed in a microprocessor using an algorithm (see fig. 3) to compute the measured image coordinate X . Identical processes are carried out on the Y-detector to find the image coordinate-Y. These coordinates are converted to angular target excursions by a conversion constant, k , and then to target displacements x, y , by multiplying by the receiver to target range, z .

DETECTOR SIGNAL PROCESSING

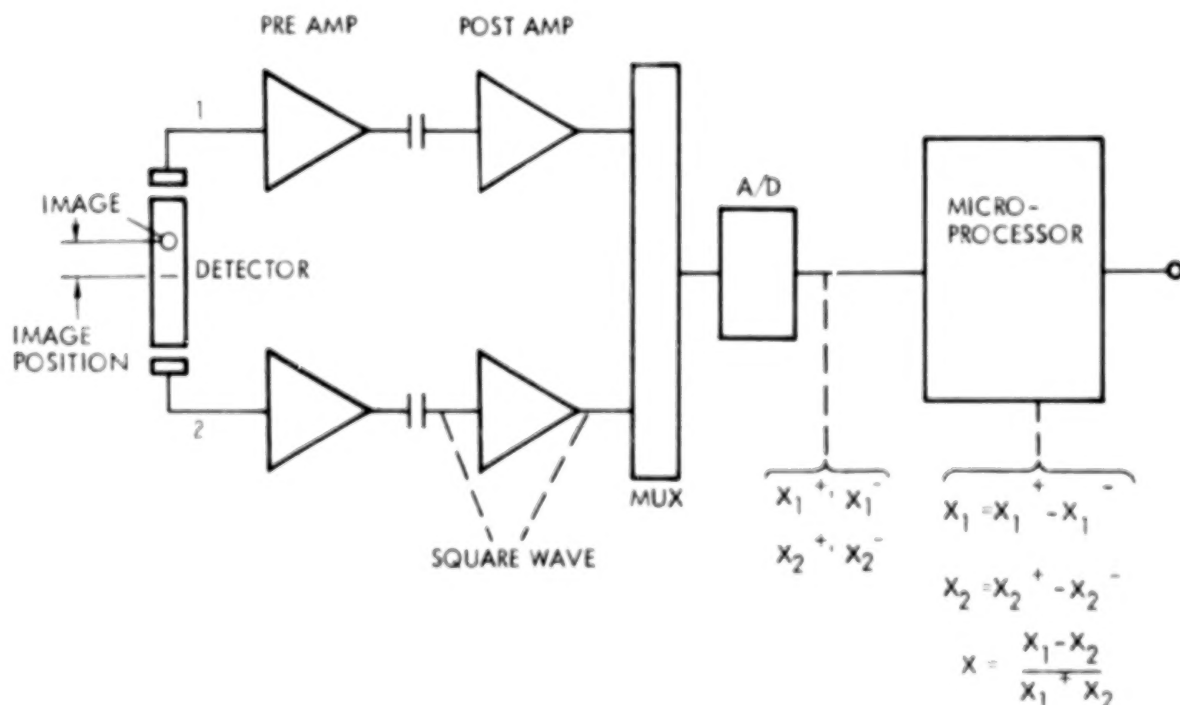


Figure 3

TEST FACILITY

Evaluation of the SAMS breadboard requires a highly stable platform of approximately full scale antenna dimensions (≈ 50 m). The facility being used (see fig. 4) is two flat steel-topped tables (1.8 by 2.4 m area), 13 m apart on concrete piling foundations which are anchored into the ground and isolated from the building structure. The receiver and source targets are mounted on opposite tables giving a 13 m single pass separation or a 39 m triple path separation through the use of folding mirrors. A dark tunnel (0.6 by 0.6 m cross section) reduces ambient light and atmospheric scintillation effects in the light path between tables. Auto-collimations measurements indicate atmospheric scintillation causes random angular deflections of the optical path with peak values of approximately 3 arc seconds due primarily to air turbulence from the air conditioning system. The dark tunnel isolates the optical path from most of the air turbulence but does not eliminate the effect completely. Relative vibrations between tables have been below the threshold sensitivity of presently available vibration measuring equipment. Equipment is being purchased to make these measurements. At the receiver bench (see fig. 5) are the receiver microprocessor, power supplies and peripheral equipment. At the target bench (see fig. 6) the sources, either IRED or the retroreflector, are mounted on the X-Y lateral transverse having a range of ± 0.25 cm and a resolution of 2.5 micrometers. The retroreflector illuminator is located at the receiver bench.

SAMS CALIBRATION FACILITY SCHEMATIC

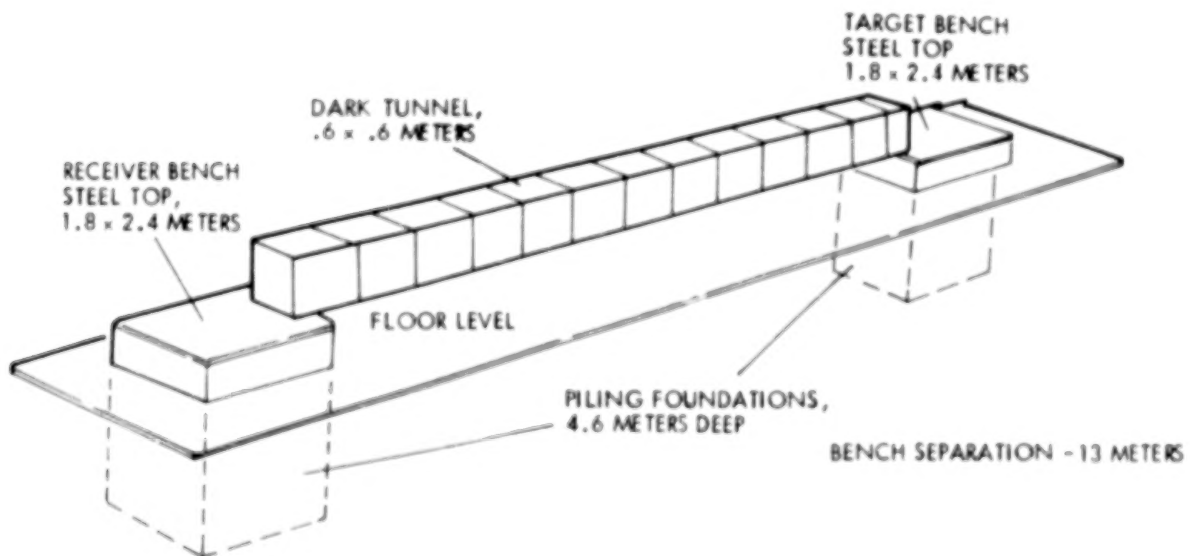


Figure 4

TEST AND RESULTS

The tests to date include (1) the SAMS response and response linearity to limited target displacements (± 0.25 cm), (2) the noise limited resolution of the system, and (3) short-term stability of the system.

Response to target displacements - In this test, each target, the active IRED target and the retroreflector target, is moved across the field in incremental steps. The IRED target at a range of 39 meters was moved in increments of .254 mm (.01 inch) with a positional accuracy of 2.54 micrometers (.0001 inch). The retroreflector was moved in increments of 25.4 micrometers (.001 inch) at a range of 13 meters. These actual displacements (x) are compared to the target position (x') indicated by the sensor. The dimensionless computed coordinates (X), (see fig. 3) are linearly transformed to the measured value (x') by

$$x' = m X + b$$

where the slope (m) depends upon the target range (z) and the center offset (b) is zero if the initial alignment of the sensor center and target is perfect. Typical responses comparing x' and x for the two targets is given in figures 7 and 8. The maximum error at 39 meters is less than 150 micrometers (.006 inch) and at 13 meters is less than 30 micrometers (0.001 inch). These errors are random and reduce with target range giving reason to suspect they are due to atmospheric scintillation effects.

CALIBRATION FACILITY RECEIVER BENCH

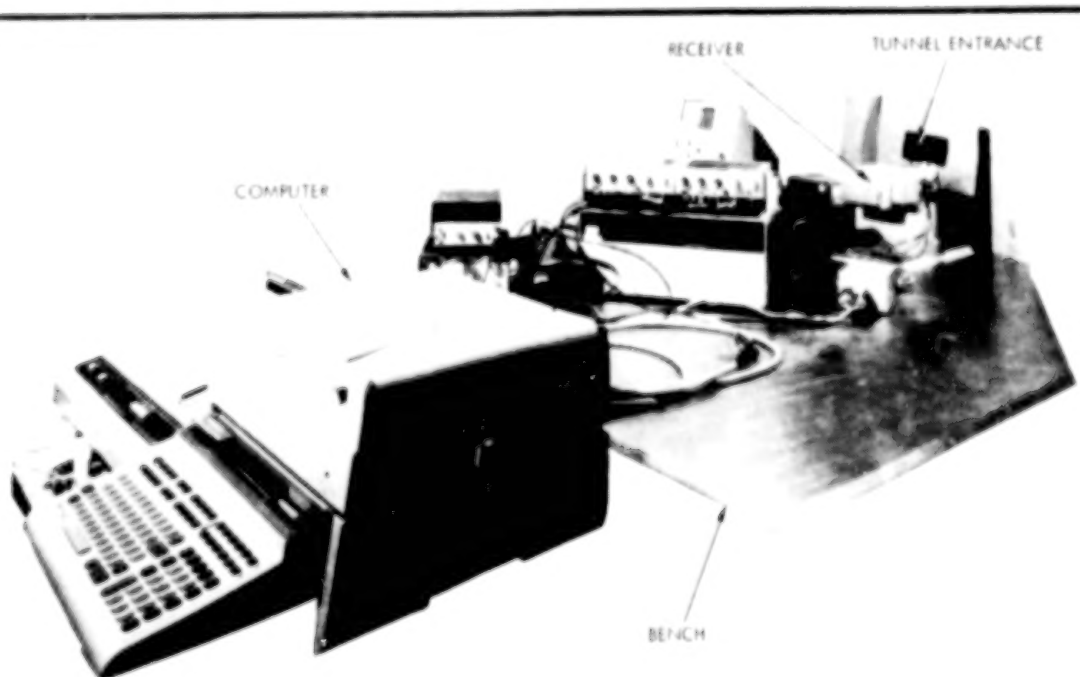


Figure 5

TEST AND RESULTS (CONT.)

Noise limited resolution - For large structures in space, modal vibration frequencies would be expected to be much less than 1 Hz, so significant sources of noise at the sensor signals would be generated (1) by target source noise, and (2) by internal noise at the sensor detector and pre-amplifier. If the source is an IRED driven by a noise-free current, then its contribution to the observed noise is insignificant (photon pattern noise at the detector can be ignored).

Noise Test A

Target:	Retroreflector
Range:	13 meters (43 feet)
Noise:	
In-Band Channel Voltage:	1.4 millivolts, rms
Smoothed, Processed:	1.6×10^{-4} (X-value)
Equivalent Error:	14.5 micrometers, rms (5.7×10^{-4} inches)

Noise Test B

Target:	IRED with 4° Beam Shaping Cone
Range:	39 meters (129 feet)
Noise:	
• In-Board Channel Voltage	1.4 millivolts, rms
• Smoothed, Processed:	1.6×10^{-4} (X-value)
• Equivalent Error	44 micrometers (1.7×10^{-3} inches)

CALIBRATION FACILITY TARGET BENCH

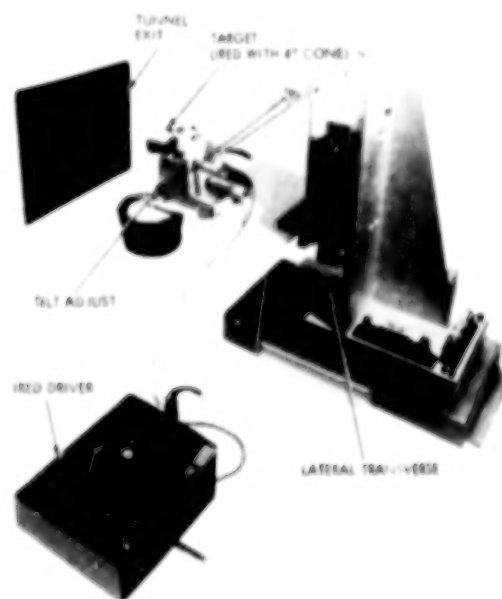


Figure 6

TEST AND RESULTS (CONT.)

Noise Test B (cont.)

These noise contributions are small compared to the goal measurements accuracy of 200 micrometers. Also note that the noise is invariant with target range, indicating that it is primarily internally generated at the receiver. In fact the measured channel noise is essentially that expected from a 15 K ohm detector, and a 50 M ohm feedback transimpedance amplifier.

The measured noise values are substantially smaller than the error fluctuations in the overall responses (see figs. 7 and 8), implying that substantial low frequency beam jitter may exist.

Short Term Stability - Although long term stability testing will demand ancillary, stable measurements of vibration, drift, and atmospheric effects, short term tests of stability with the existing test setup can provide clues to the nature and magnitude of the errors.

For this test, the target (retroreflector) was fixed at a range of 13 meters, the sensor system activated and left running for 6.5 hours. During the first 30 minutes, the warmup drift amounted to 76 micrometers (0.003 inches) (equivalent motion of the target). For the following six hours, the

RESPONSE TEST INFRARED EMITTING DIODE TARGET

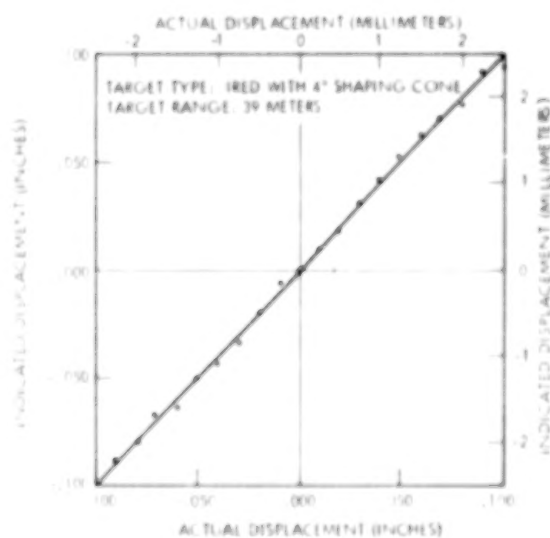


Figure 7

TEST AND RESULTS (CONT.)

total change was 150 micrometers (.006 inches).

After warmup, the total drift was less than the allowable error (150 micrometers drift compared to 200 micrometers allowed), and most of the short term stability appeared to be associated with the setup. During the course of the test, the ambient air temperature increased from 18°C to 24°C, and the error approximately tracked the temperature change. Possible sources of drift (about 2 arc-seconds at the line of sight) are bench motion, laminar air refraction and receiver mount changes.

MEASUREMENT ERROR RETROREFLECTOR TARGET

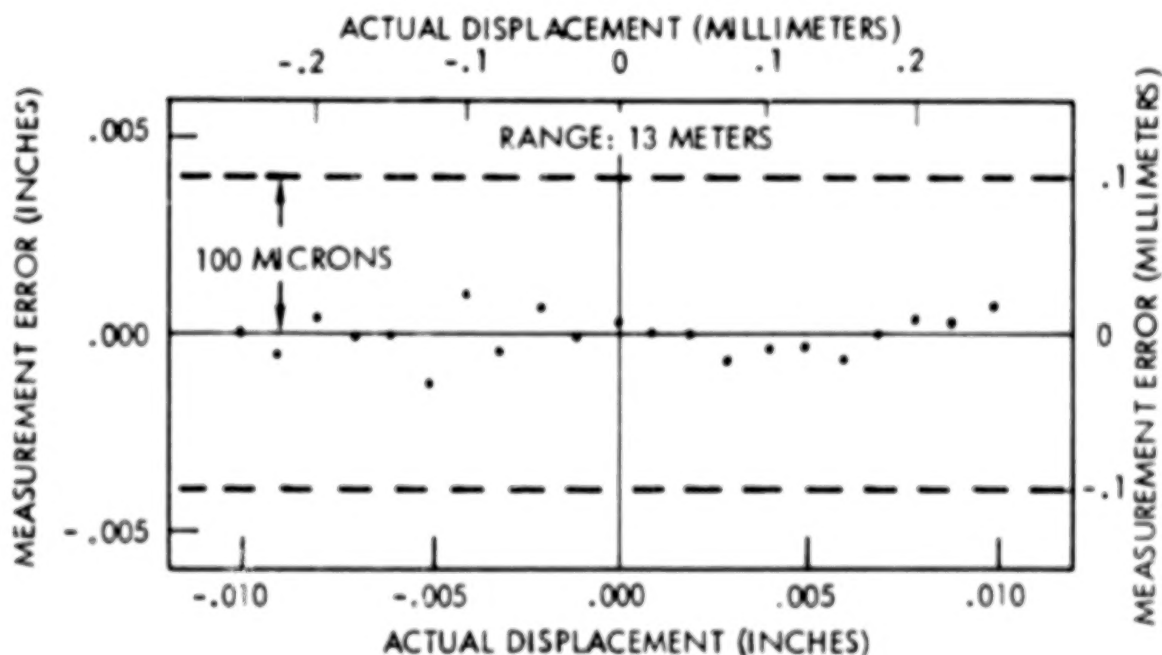


Figure 8

REFERENCES

1. Neiswander, Robert S.: Surface Accuracy Measurement Sensor for Deployable Reflector Antennas, NASA CR-159263, 1980.
2. Neiswander, R. S. : Surface Accuracy Measurement Sensor For Deployable Reflector Antennas (SAMS-DRA). Large Space Systems Technology - 1979, NASA CP-2118, 1979, pp. 157-171.

SECOND ANNUAL TECHNICAL REVIEW ATTENDEES

NASA Headquarters Washington, DC

R. F. Carlisle
J. D. DiBattista
F. D. Kochendorfer
S. V. Manson

NASA Langley Research Center Hampton, VA

I. I. Akpan (ODU)
J. L. Allen, Jr.
Dr. M. S. Anderson
E. S. Armstrong
M. C. Bailey
H. T. Banks (ICASE)
L. J. Bement
D. E. Bowles
W. J. Boyer
M. L. Brumfield
Dr. J. D. Buckley
H. G. Bush
T. G. Campbell
J. E. Canady
Dr. M. F. Card
C. W. Coffee
S. R. Cole
L. J. DeRyder
R. S. Dunning
J. R. Elliott
Dr. L. B. Garrett
J. W. Goslee
W. M. Hall
H. A. Hamer
W. L. Heard, Jr.
B. B. Hefner, Jr.
W. F. Hinson
R. B. Holt
Dr. G. C. Horner
Dr. E. K. Huckins, III
R. L. James, Jr.
L. S. Keafer
C. R. Keckler
F. Koprivier III (Syst. Management Assoc.)
E. B. Lightner
M. J. Long
U. M. Lovelace
R. C. Montgomery
A. K. Noor (CMU)

NASA Langley Research Center Hampton, VA (Continued)

B. L. Overman
J. C. Robinson
M. T. Russell
R. A. Russell
A. A. Schy
Dr. J. D. Shaughnessy
W. S. Slomp
R. B. Spiers
Dr. O. O. Storaasli
L. W. Taylor, Jr.
J. E. Walz
Dr. D. J. Weidman
T. M. Weller

NASA Goddard Space Flight Center Greenbelt, MD

J. Eckerman
J. P. Young

NASA Johnson Space Center Houston, TX

L. M. Jenkins

NASA Lewis Research Center Cleveland, OH

C. E. Provencher, Jr.
F. J. Shaker
O. F. Spurlock

NASA Marshall Space Flight Center Huntsville, AL

Dr. J. Blair
H. J. Buchanan
E. C. Hamilton
J. K. Harrison
J. F. Macpherson
K. Smith
J. Stokes
H. H. Watters

Jet Propulsion Laboratory
Pasadena, CA

C. N. Berdahl
R. S. Edmunds
M. El-Raheb
R. E. Freeland
J. A. Garba
Dr. H. B. Garrett
Dr. E. Heer
Yu-Hwan Lin
G. Rodriguez
Dr. J. G. Smith
S. Z. Szirmay
A. F. Tolivar
W. J. Weber, III

Wright Patterson Air Force Base
WPAFB, OH

J. Pearson
Dr. L. C. Rogers
N. D. Wolf
Lt. C. J. Worsowicz

Naval Research Center
Washington, DC

K. T. Alfriend
F. L. Markley

SAMSO
Los Angeles, CA

Maj. R. Gajewski

Edwards Air Force Base
EAFB, CA

R. Preston

Howard University
Washington, DC

P. N. Bainum
P. Bofah
A. Choudhury
V. K. Kumar
A. S. S. R. Reddy

Rensselaer Polytechnic Institute
Troy, NY

A. A. Desrochers
C. G. Rubeiz

Massachusetts Institute of Technology
Lincoln Laboratory
Lexington, MA

M. Floyd
D. C. Hyland
A. N. Madiwale
G. Sarver

Massachusetts Institute of Technology
Cambridge, MA

Prof. E. F. Crawley
Dr. J. H. Lang

University of Cincinnati
Cincinnati, OH

A. H. Nayfeh

Harris Corporation
Melbourne, FL

H. L. Deffebach
J. W. Mays
D. C. Montgomery
J. W. Shipley
W. B. Stevens
M. Sullivan

Aerospace Corporation
Los Angeles, CA

G. N. Smit

Aerospace Corporation
El Segundo, CA

E. M. Polzin

Vought Corporation
Dallas, TX

W. E. Agan
G. S. Bumgarner
R. J. French
J. J. Pacey

Kentron Incorporated (LaRC)
Hampton, VA

E. P. Brien
R. E. Calleson
J. K. Jensen
R. W. LeMessurier
A. Taylor
R. E. Wallson

Bendix Field Engineering
Corporation (GFSC)
Greenbelt, MD

G. T. Foote

The Boeing Company
Seattle, WA

C. T. Golden
E. E. Spear
R. G. Vos
W. J. Walker

The Boeing Company
Hampton, VA

W. E. Parker

Vigyan Research Associates
Hampton, VA

S. M. Joshi

INTELSAT
Washington, DC

Dr. B. N. Agrawal
W. W. Dorsey

TRW Systems
Redondo Beach, CA

J. S. Archer
J. T. Bennett
Dr. R. Gluck
R. S. Neiswander
R. Van Vooren

Grumman Aerospace
Bethpage, NY

F. Austin
L. H. Hennerdinger
C. A. Paez
J. L. Schultz
W. E. Simpson

Martin Marietta
Denver, CO

A. L. Brook
J. Bunting
J. V. Coyner, Jr.
C. E. Farrell
A. Fehr
W. J. Gardner
R. B. Rice, Jr.
F. R. Schwartzberg

General Dynamics/Convair
San Diego, CA

J. W. Beatty
R. H. Thomas

Lockheed Missiles and Space Company
Sunnyvale, CA

G. G. Chadwick
H. Cohan
Dr. J. Y. L. Ho
R. R. Johnson
W. B. Pruitt
R. M. Vernon
A. A. Woods

Barnes Engineering
Stamford, CT

P. W. Collyer
S. C. Spielberger
K. A. Ward

Honeywell
Minneapolis, MN

T. B. Cunningham
C. W. Farnham
C. S. Greene

Honeywell
St. Petersburg, FL

R. P. Singh

C. S. Draper Laboratories
Cambridge, MA

E. Fogel
J. G. Lin
K. Soosaar

Rockwell International
Downey, CA

H. S. Greenberg
J. A. Roebuck

Astro Research
Carpinteria, CA

J. M. Hedgepeth

MRJ, Incorporated
Fairfax, VA

R. D. Jones

The Analytic Sciences Corporation
Reading, MA

L. E. Mabus

Systems, Science and Software
La Jolla, CA

I. Katz

Systems & Applied Sciences
Riverdale, MD

J. Forbush

McDonnell Douglas
Huntington Beach, CA

F. C. Junge

General Research Corporation
Santa Barbara, CA

D. J. Nihora

General Electric
Philadelphia, PA

H. A. Brust
W. J. Downs
P. Foldes
R. V. Greco
J. J. McClinchey
A. Monfort
B. N. Ordonio

Essex Corporation (MSFC)
Greenbelt, MD

N. Shields

Scientific-Atlanta
Crofton, MD

R. Mauck

Palo Alto Research Laboratory
Lockheed Missiles and Space Company
Palo Alto, CA

M. G. Lyons

1 Report No. NASA CP-2168		2 Government Accession No.		3 Recipient's Catalog No.	
4 Title and Subtitle LARGE SPACE SYSTEMS TECHNOLOGY - 1980 Volume I - Systems Technology				5 Report Date February 1981	
				6 Performing Organization Code 506-62-43-05	
7 Author(s) Frank Kopriver III, compiler				8 Performing Organization Report No. L-14219	
				10 Work Unit No.	
9 Performing Organization Name and Address NASA Langley Research Center Hampton, VA 23665				11 Contract or Grant No.	
				13 Type of Report and Period Covered Conference Publication	
12 Sponsoring Agency Name and Address National Aeronautics and Space Administration Washington, DC 20546				14 Sponsoring Agency Code	
15 Supplementary Notes Frank Kopriver III: Systems Management Associates, Hampton, Virginia					
16 Abstract <p>This document is a compilation of the papers presented at the Second Annual Large Space Systems Technology (LSST) Review at the Langley Research Center. The research was supported in Fiscal Year 1980 by the LSST Program Office and the Materials and Structures Section, Research and Technology Division, of the Office of Aeronautics and Space Technology. The review provided government, university, and industry personnel with an opportunity to exchange information, to assess the present status of technology developments in large space systems, and to plan the development of new technology for large space systems. These papers were divided into three major areas of interest: (1) technology pertinent to large antenna systems, (2) technology related to large space platform systems, and (3) base technology applicable to both antenna and platform systems. Design studies, structural testing results, and theoretical applications are presented with accompanying validation data. These research studies represent state-of-the-art technology that is necessary for the development of large space systems. A total systems approach including controls, platforms, and antennas is presented as a cohesive, programmatic plan for large space systems.</p>					
17 Key Words (Suggested by Author(s)) Large space systems Space platform systems Large antenna systems			18 Distribution Statement Unclassified - Unlimited Subject Category 15		
19 Security Classif. (of this report) Unclassified	20 Security Classif. (of this page) Unclassified	21 No. of Pages 460	22 Price A20		

END

APRIL 27, 1981